# Polypyrrole modified with sulfonated β-cyclodextrin: Controlled release of DA and host-guest complexation properties.

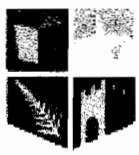

NUI MAYNOOTH

Ollscoil na hÉireann Má Nuad

**Gillian. M. Hendy BSc. (Hons)**

**Department of Chemistry**

**National University of Ireland Maynooth**

**March 2009**

**Thesis submitted to the National University of Ireland in Fulfilment of the requirements for the Degree of Doctor of Philosophy**

**Supervisor: Professor Carmel B. Breslin**

**Head of Department: Professor John Lowry**

# Table of contents

Title page ..... - i -
Table of contents ..... - ii -
Declaration ..... - x -
Acknowledgements ..... - xi -
Dedication ..... - xiii -
Abstract ..... - xiv -
List of Abbreviations ..... - xvi -

**Chapter 1 – Introduction and literature review**

1.1 INTRODUCTION ..... - 2 -
*1.1.1 Controlled drug release* ..... - 3 -
*1.1.2 Conducting polymers* ..... - 7 -
1.1.2.1 Polymerisation methods ..... - 10 -
1.1.2.2 Polypyrrole ..... - 11 -
1.1.2.2.1 Historical background of polypyrrole ..... - 11 -
1.1.2.2.2 Polymerisation mechanism of pyrrole ..... - 12 -
1.1.2.2.3 Biocompatibility ..... - 14 -
1.1.2.2.4 Electroactivity of polypyrrole ..... - 15 -
1.1.2.2.5 Polypyrrole and drug delivery ..... - 16 -
1.1.2.2.6 The application of nanotechnology in drug delivery ..... - 18 -
1.1.2.2.7 The application of electrospinning to drug delivery ..... - 19 -
*1.1.3 Cyclodextrins* ..... - 22 -
1.1.3.1 History and structural properties of cyclodextrins - 22 -
1.1.3.2 Inclusion complexation ..... - 26 -
1.1.3.3 Driving forces in the inclusion complexation process ..... - 28 -
1.1.3.4 Applications of CDs in DDS ..... - 31 -
*1.1.4 Drug release: Controlled release of dopamine* ..... - 32 -
1.2 REFERENCES ..... - 35 -

**Chapter 2 – Experimental- Techniques and related theories**


2.1 INTRODUCTION ..... - 41 -

2.2 ELECTROCHEMICAL SET UP ..... - 42 -

*2.2.1 Electrochemical apparatus* ..... - 42 -

*2.2.2 The electrochemical cell* ..... - 42 -

*2.2.3 Electrode materials and preparation* ..... - 43 -

2.3 CHEMICALS AND PURIFICATION ..... - 44 -

2.4 PREPARATION OF POLYMER SAMPLES ..... - 48 -

*2.4.1 Potentiostatic techniques* ..... - 48 -

*2.4.2 Galvanostatic techniques* ..... - 49 -

*2.4.3 Cyclic voltammetry* ..... - 49 -

*2.4.4 Vapour phase polymerisation* ..... - 50 -

*2.4.5 Electrospinning* ..... - 50 -

2.5 CHARACTERISATION OF SAMPLES ..... - 51 -

*2.5.1 EQCM measurements* ..... - 52 -

*2.5.2 UV-visible spectroscopy* ..... - 53 -

*2.5.3 Cyclic voltammetry* ..... - 54 -

*2.5.4 Rotational disc voltammetry* ..... - 56 -

*2.5.5 Nuclear magnetic resonance* ..... - 59 -

*2.5.6 Optical and scanning electron microscopy* ..... - 60 -

*2.5.7 Solution properties* ..... - 60 -

2.6 THEORY OF EXPERIMENTAL TECHNIQUES AND EQUATIONS USED ..... - 61 -

*2.6.1 Complexation studies* ..... - 61 -

2.6.1.1 Job's method ..... - 61 -

2.6.1.2 Formation constants ..... - 62 -

2.6.1.2.1 UV-visible studies ..... - 63 -

2.6.1.2.2 Electrochemical studies .....

2.6.1.2.3 NMR studies ..... - 65 -

2.7 REFERENCES ..... - 66 -

**Chapter 3 – PPy doped with an anionic CD: formation and characterisation**


3.1 INTRODUCTION ..... - 68 -

3.2 EXPERIMENTAL ..... - 69 -

*3.2.1 Materials* ..... - 69 -

3.2.1.1 Reagents ..... - 69 -

3.2.1.2 Electrodes and Instruments ..... - 70 -

*3.2.2 Procedure* ..... - 71 -

3.2.2.1 Polymer film preparation ..... - 71 -

3.2.2.2 Film characterisation ..... - 72 -

3.2.2.3 Electrochemical quartz crystal microgravimetry ..... - 73 -

3.3 RESULTS AND DISCUSSION ..... - 74 -

*3.3.1 Polymer synthesis* ..... - 74 -

3.3.1.1 Investigations on the growth of PPy in various dopant electrolytes ..... - 76 -

3.3.1.2 Polymer synthesis using constant potential ..... - 85 -

*3.3.2 Film characterisation* ..... - 89 -

3.3.2.1 Probing the redox properties using CV ..... - 89 -

3.3.2.3 Probing the redox properties using EQCM measurements ..... - 92 -

*3.3.3 Analysis of the PPy/Sβ-CD films* ..... - 107 -

3.3.3.1 SEM and optical images ..... - 107 -

3.3.3.2 EDAX ..... - 110 -

3.4 SUMMARY OF RESULTS ..... - 111 -

3.5 REFERENCES ..... - 113 -


**Chapter 4 – The investigation into the incorporation and release of DA from electrochemically synthesised PPy films**


4.1 INTRODUCTION ..... - 115 -

4.2 EXPERIMENTAL ..... - 116 -

*4.2.1 Materials* ..... - 116 -

4.2.1.1 Reagents ..... - 116 -

4.2.1.2 Electrodes and Instruments..... - 117 -
*4.2.2 Procedures*..... ..... - 117 -
4.2.2.1 Polymer film preparation..... - 117 -
4.2.2.2 Incorporation of drug..... - 118 -
4.2.2.3 Release of drug..... - 118 -
4.2.2.4 Influence of varying parameters for the PPy/$SO_4$ system..... - 119 -
4.2.2.4.1 Influence of varying the growth potential and charge..... - 119 -
4.2.2.4.2 Influence of varying the incorporation step..... - 120 -
4.2.2.4.3 Influence of varying the release step..... - 120 -
4.2.2.4.4 Influence of the nature of the dopant anion..... - 120 -
4.2.2.5 Influence of varying parameters for the PPy/Sβ-CD system..... - 121 -
4.2.2.5.1 Influence of varying the growth potential and charge..... - 121 -
4.2.2.5.2 Investigations into the oxidation of DA at thicker PPy/Sβ-CD films..... - 121 -
4.2.2.5.3 Influence of varying the incorporation step..... - 122 -
4.2.2.5.4 Influence of varying the release step..... - 123 -
4.2.2.6 EQCM measurements..... - 123 -
4.3 RESULTS AND DISCUSSION..... - 124 -
*4.3.1 Dopamine, a cationic model drug*..... - 124 -
*4.3.2 Polymer preparation*..... - 128 -
*4.3.3 Influence of varying parameters for PPy/$SO_4$ system*..... - 129 -
4.3.3.1 Influence of varying the growth potential and charge of PPy/$SO_4$ film..... - 133 -
4.3.3.2 Influence of varying the incorporation step..... - 134 -
4.3.3.2.1 Influence of varying the incorporation

potential..... - 135 -
4.3.3.2.2 Influence of varying the pH of the incorporating DA solution..... - 136 -
4.3.3.3 Influence of varying the release step..... - 138 -
4.3.3.3.1 Influence of varying the release potential..... - 138 -
4.3.3.4 Influence of varying electrolyte..... - 139 -
*4.3.4 Influence of varying parameters for PPy/Sβ-CD system*... - 141 -
4.3.4.1 Influence of varying the PPy film growth conditions - 142 -
4.3.4.1.1 Influence of varying potential applied upon growth of the polymer..... - 142 -
4.3.4.1.2 Influence of varying polymer thickness..... - 144 -
4.3.4.1.3 Uptake and release of DA from PPy/Sβ-CD films synthesised in the presence of a supporting electrolyte..... - 152 -
4.3.4.2 Influence of varying the incorporation step..... - 154 -
4.3.4.2.1 Influence of varying the incorporation potential..... - 154 -
4.3.4.2.2 Influence of varying incorporating time..... - 157 -
4.3.4.2.3 Influence of varying supporting electrolyte concentration..... - 158 -
4.3.4.3 Influence of varying the release step..... - 159 -
4.3.4.3.1 Influence of the release potential..... - 159 -
4.3.4.3.2 Kinetics of the release process..... - 161 -
4.3.4.3.3 Electrochemical stimulation..... - 162 -
*4.3.5 EQCM*..... - 165 -
4.3.5.1 EQCM measurements for the incorporation of DA - 165 -
4.3.5.2 EQCM data for the release of DA..... - 168 -
*4.3.6 Comparing PPy/$SO_4$ to PPy/Sβ-CD*..... - 172 -
4.4 SUMMARY OF RESULTS..... - 172 -
4.5 REFERENCES..... - 174 –

**Chapter 5 – Host-guest complexation studies between Sβ-CD and DA**

5.1 INTRODUCTION..... - 177 -

5.2 EXPERIMENTAL ..... - 178 -
*5.2.1 Materials* ..... - 178 -
5.2.1.1 Reagents ..... - 178 -
5.2.1.2 Electrodes and Instruments ..... - 178 -
5.2.1.3 Buffer solutions ..... - 178 -
*5.2.2 Procedures* ..... - 179 -
5.2.2.1 Determination of the stoichiometry of Sβ-CD and DA ..... - 179 -
5.2.2.2 Determination of the stability constant of Sβ-CD and DA ..... - 181 -
5.2.2.3 NMR analysis ..... - 181 -
5.2.2.4 Varying the pH ..... - 183 -
5.2.2.5 Varying the electrolyte ..... - 183 -
5.2.2.6 Varying the size of the cavity ..... - 184 -
5.2.2.7 Complexation studies of levodopa and tyrosine with Sβ-CD ..... - 185 -
*5.2.3 Evaluation of the stability constants* ..... - 185 -
5.3 RESULTS AND DISCUSSION ..... - 187 -
*5.3.1 Determination of the stoichiometry of Sβ-CD and DA* ..... - 187 -
5.3.1.1 UV data ..... - 187 -
5.3.1.2 CV data ..... - 189 -
*5.3.2 DA-Sβ-CD complex stability constant* ..... - 196 -
5.3.2.1 Determination of $K_f$ by UV ..... - 196 -
5.3.2.2 Determination of $K_f$ by CV ..... - 198 -
5.3.2.3 Determination of $K_f$ by RDV ..... - 204 -
*5.3.3 Analysis of the DA-Sβ-CD complex by NMR* ..... - 211 -
5.3.3.1 Determination of the DA-Sβ-CD complex molecular structure by NMR ..... - 211 -
5.3.3.2 Determination of complex stoichiometry by NMR - 215 -
5.3.3.3 Determination of the $K_f$ value by NMR ..... - 217 -
*5.3.4 Factors that influence DA-Sβ-CD Complexation* ..... - 220 -
5.3.4.1 Influence of pH ..... - 220 -
5.3.4.2 Influence of counter ions ..... - 228 -

5.3.4.3 Varying the size of the cavity ..... - 236 -
*5.3.5 Complexation studies of a related structure to DA* ..... - 240 -
5.3.5.1 Levodopa ..... - 240 -
5.3.5.2 Tyrosine ..... - 245 -
5.4 SUMMARY OF RESULTS ..... - 248-
5.5 REFERENCES ..... - 250 –

**Chapter 6 – An investigation into the presence of electrospun PLGA fibers coated with PPy for the uptake and release of DA**

6.1 INTRODUCTION ..... - 254 -
6.2 EXPERIMENTAL ..... - 255 -
*6.2.1 Materials* ..... - 255 -
6.2.1.1 Reagents ..... - 255 -
6.2.1.2 Electrodes and Instruments ..... - 256 -
*6.2.2 Procedures* ..... - 257 -
6.2.2.1 Formation of PLGA nanofibers by electrospinning - 257 -
6.2.2.2 Formation of electrospun fibers containing DA..... - 258 -
6.2.2.3 Optical microscopy and SEM sample preparation and imaging ..... - 258 -
6.2.2.4 Electrochemical analysis ..... - 259 -
6.2.2.5 Polymerisation of pyrrole ..... - 259 -
6.2.2.6 Incorporation and release of DA ..... - 260 -
6.3 RESULTS AND DISCUSSION ..... - 261 -
*6.3.1 Electrospinning of PLGA fibers* ..... - 261 -
6.3.1.1 Varying the voltage applied ..... - 262 -
6.3.1.2 Varying the solvent and solution concentration..... - 265 -
6.3.1.3 Varying the feeding rate ..... - 270 -
6.3.1.4 Varying the distance from needle tip to collector - 271 -
6.3.1.5 Varying the substrate ..... - 272 -
*6.3.2 Incorporation of DA into the polymer solution prior to electrospinning* ..... - 274 -
*6.3.3 Electrochemical Characterisation* ..... - 278 -

*6.3.4 Polymerisation of pyrrole onto the nanofibers* ..... - 286 -
6.3.4.1 Polymerisation using electrochemical methods ..... - 286 -
6.3.4.2 Polymerisation using CV ..... - 288 -
6.3.4.3 Vapour phase polymerisation of pyrrole ..... - 293 -
6.3.4.3.1 Incorporation of the oxidant prior to electrospinning ..... - 293 -
6.3.4.3.2 VPP on previously electrospun PLGA fibers .... - 295 -
*6.3.5 Incorporation and release of DA* ..... - 298 -
6.3.5.1 Uptake and release of DA using electrochemical means ..... - 299 -
6.3.5.2 Comparison of applying a potential for release ..... - 302 -
6.3.5.3 Comparing the release of DA ..... - 304 -
6.4 SUMMARY OF RESULTS ..... - 305 -
6.5 REFERENCES ..... - 306 –

**Chapter 7 - Conclusions**

7.1 CONCLUSIONS ..... - 309 -
7.2 CONFERENCE PRESENTATION ..... - 312 -
7.3 PAPERS IN PREPARATION/SUBMITTED ..... - 314 -
7.4 REFERENCES ..... - 315 -

# Declaration

I hereby certify that this thesis, which I now submit for assessment on the programme of study leading to the award of PhD, has not been submitted, in whole or part, to this or any other University for any degree, and is, except where otherwise stated is the original work of the author.

Signed: Gillian Hendy

# Acknowledgements

A special and heart felt thank you to my supervisor Prof. Carmel Breslin for her continuous support in my PhD program. Carmel has been a friend and a mentor. She has showed me how to approach my research problems and the need to be persistent with my goal. She gave me the encouragement to indulge in all aspects of a research program, that every student should have the opportunity to accomplish. She was always there to proofread and correct my chapters, and to ask me questions to help me think through my problems. Carmel has made me a better scientist, had confidence in me when I doubted myself, and brought out the good ideas in me. Without her support and constant guidance, I could not have finished this thesis.

Also thank you to Dr. Denise Rooney, Dr. Johnny Colleran, Dr. John Stephens, Dr. Martin Collier, Dr. Niall Finnerty and Dr. Fiachra Bolger, all of your help and support was invaluable. To the technical staff of the chemistry department, Ken, Ollie, Ria, Barbara and Ann, thank you for your expertise and time. A special thanks to Noel Williams for teaching me Human-Computer interactions techniques with out him I would not be here, he has the patience of a saint and all his help was much appreciated. I would also like to thank the Tyndall institute and the National access programme (NAP) for some of the SEM and EDAX data shown in this thesis. Thanks also to Prof. Gordon Wallace, Dr. Simon Moulton, Dr. Dan Li and all at IPRI in Wollongong for a incredible experience.

Claire the memories we have shared through this journey especially our trip to Australia will remain with me always. We have been through it together and I wish you every success in the future. Likewise, thank you to my lab colleagues, Catherine, Eimear, Valeria, Sinead, Adelaide, Richard, Enrico, Paul, Ursula and Anita. To my fellow postgraduate students both past and present, a special mention to Linda, Rob, Owen, Declan, John, Patrick and Denis it's been a great few years best of luck to you all. Thanks also to Declan and Ciaran for your expertise in NMR and quantum calculations. And to the 'newbies' especially

Roisin, Conor and Lynn and to all postgrads and postdocs it is hard to mention everyone, but thanks for being fun to be with and the great nights out. I wish you all every success in the future.

During the course of this work I was supported by the Irish Research Council for Science Engineering and Technology (IRCSET), John and Pat Hume scholarship and the European Endeavour programme which funded my work in Australia.

Nobody has been more important to me through all of this than my family and friends: My parents Robin and Mary, for their unconditional love and support. My brothers Damien, Graham and Garry and extended family Linda, Karen and Ciara. To all my friends, especially Edel, Grainne, Karina, Suzanne and Emer thanks for keeping me sane and for all the phone calls they were well needed breaks. To John, Lucy and family thanks for all your love and support.

And finally, Liam, through thick and thin you have been there since day one and stood by me, I can't imagine it was easy and for that, I thank you.

**Dedicated to my parents, with love**

# Abstract

This thesis originates with the synthesis and characterisation of conducting polypyrrole (PPy) films, deposited in the presence of various electrolytes, predominantly, a large anionic cyclodextrin (Sβ-CD). The presence of the Sβ-CD dopant was confirmed using SEM/EDAX. It was shown that the Sβ-CD-doped PPy films have cation exchange properties and the oxidation and reduction of the polymer is accompanied by solvent, $H_2O$, exchange. Once characterised, these materials were used for the incorporation and release of an important pharmaceutical compound, dopamine (DA). It was found that the sulfonated β-cyclodextrin (Sβ-CD) dopant enhanced the delivery of the DA by ~ 90 %, in comparison to a PPy film doped with sulfate. It was demonstrated that the thickness of the Sβ-CD-doped PPy, as well as the application of appropriate incorporation and release potentials were the most important factors controlling the release profiles. The electrical stimulation applied during release of the drug was a significant factor and in comparison to diffusion, the rate of release of DA was increased by ~ 80 % on the application of an oxidation stimulus. These promising results lead to an investigation into the host-guest complexation properties of the Sβ-CD with DA.

A detailed analysis, using electrochemistry and spectroscopy, was performed on complexation of Sβ-CD with the DA host molecule. The formation of an inclusion complex between the Sβ-CD and DA was proven using UV, CV, RDV and NMR techniques. It was also established that a 1:1 complex was formed between the Sβ-CD and the DA, where the inclusion occurred predominantly through the aromatic ring of the DA and the hydrophobic CD cavity.

Finally, a study into the use of poly($_{D,L}$ – lactide-*co*-glycolide) (PLGA) nanofibers as a mat for the deposition of PPy films, was carried out, to determine if the presence of nanofibers enhanced the delivery of the DA. The PLGA fibers were deposited onto a conducting gold mylar surface using electrospinning. SEM analyses verified the presence of the nanofiber mat. Sβ-CD-doped PPy was

successfully deposited onto the insulating fibers using vapour phase chemical polymerisation and electropolymerisation. CV was confirmed to be the best electrochemical technique for the deposition of the PPy films, enabling the formation of uniform conducting films, while still maintaining the nano-fibrous structure of the PLGA fibers. DA was again effectively incorporated and delivered from these new materials using electrical stimulation.

# List of abbreviations

| | |
|---|---|
| Å | angstrom |
| A | absorbance |
| ΔA | absorbance change |
| Ag | silver |
| ATP | adenosine-tri-phosphate |
| Au | gold |
| β | beta |
| c | concentration |
| C | complex |
| CB | conduction band |
| CD | cyclodextrin |
| CE | counter electrode |
| CP | conducting polymer |
| CT | charge transfer |
| CV | cyclic voltammetry |
| δ | chemical shift |
| $\delta_{obs}$ | observed chemical shift |
| $\delta_{lim}$ | chemical shift at equilibrium |
| d | doublet |
| DA | dopamine |
| DBS | **dodecyl** benzene sulfonate |
| DEX | dexamethasone |

| | |
|---|---|
| dd | doublet of doublets |
| DDS | drug delivery system |
| DMF | N,N-**dimethylformamide** |
| DMSO | dimethylsulfoxide |
| $D_20$ | deuterated water |
| ε | molar absorptivity coefficient |
| $E_{1/2}$ | half-wave potential |
| EQCM | electrochemical quartz crystal microgravitmetry |
| F | Faraday's constant |
| G | guest |
| GC | glassy carbon |
| H | host |
| h | hour |
| $J$ | coupling constant |
| $k_B$ | Boltzmann constant |
| K | Kelvin |
| $K_f$ | the formation, binding or stability constant |
| L-dopa | levodopa |
| λ | wavelength |
| m | multiplet |
| MHz | megahertz |
| min | minute |
| ml | millilitre |
| MS | mass spectroscopy |
| mV | millivolt |

| | |
|---|---|
| NMR | nuclear magnetic resonance |
| PD | Parkinson's disease |
| PLA | poly(lactic) acid |
| PLGA | poly(lactic-co-glycolic) acid |
| ppm | parts per million |
| Py | pyrrole |
| PPy | polypyrrole |
| PSS | poly(styrenesulfonate) |
| Pt | platinum |
| PTS | poly(toluene)sulfonic acid |
| q | quartet |
| r | radius |
| R | gas constant |
| RDV | rotational disc voltammetry |
| s | singlet or second |
| SA | surface area |
| Sα-CD | sulfonated α-cyclodextrin |
| Sβ-CD | sulfonated β-cyclodextrin |
| SCE | saturated calomel reference electrode |
| t | triplet |
| TOF | time of flight |
| Tyr | tyrosine |
| UV | UV-visible spectroscopy |
| VB | valence band |
| VPP | vapour phase polymerisation |

| | |
|---|---|
| WE | working electrode |

## 1.1 Introduction

The initial aim of this work was to examine the use of polypyrrole (PPy), a well-known conducting polymer, for the uptake and release of a cationic species, dopamine (DA). DA was chosen as it represents a large family of amine-based drugs. Therefore, if appropriate PPy films could be electrosynthesised and used in the controlled delivery of DA, then the concept could be used more widely in the field of controlled drug delivery.

In Chapter 3, the growth of PPy films in the presence of various dopant anions, including a large anionic cyclodextrin (CD), sulfonated β-cyclodextrin (Sβ-CD) is explored. Although Sβ-CD doped PPy films have been reported in the recent literature, there has been very little work devoted to the characterisation of these films. Accordingly, much of Chapter 3 is devoted to the unique redox properties of the Sβ-CD doped PPy films.

With the growth of the PPy films achieved, Chapter 4, shows the drug release profiles of the protonated DA and reveals that in the case of the polymer films doped with the anionic Sβ-CD, there is a substantial increase in the amount of DA released in comparison to other polymer films. In order to explain the enhanced release profiles, the well-known supramolecular complexation properties of cyclodextrins were considered. However, on searching the literature no reports on the complexation of DA with anionic cyclodextrins were found and consequently this was studied in detail. These findings are presented in Chapter 5, where the host-guest interactions between DA and the anionic Sβ-CD are examined using a variety of techniques, both spectroscopic and electrochemical.

In Chapter 6 the technique of electrospinning is introduced. Details on how it is used to fabricate nanostructured biodegradable polymer films with a high surface area are provided. The approaches used to deposit the Sβ-CD doped PPy films onto the nanostructured biodegradable film are then considered and discussed. It is shown that cyclic voltammetry was the most successful

approach. Moreover, it was possible to control the amount of PPy deposited and to maintain the nanostructured fiber substrate by varying the number of cycles. These high surface area Sβ-CD doped PPy films are promising for the uptake and liberation of DA.

In this introductory chapter, the concept of controlled drug release is firstly introduced. This is then followed with information on conducting polymers, particularly PPy and the current state-of-art in using PPy in drug delivery. The technique of electrospinning is then introduced and linked to DDS. The next section is devoted to cyclodextrins, as it is the Sβ-CD doped PPy films that give the best controlled release properties. Finally, the chapter ends with a short account of the properties of DA and its delivery.

### 1.1.1 Controlled drug release

In the early 1970s, controlled release systems first materialised. Since then, the number and the areas in which a controlled release system is utilised have significantly increased. These systems have been used in areas such as cosmetics[1], food[2], and pesticides[3]. Controlled release systems are focused on obtaining the release of the proposed material, over a certain time without an external influence from any other potential release factor.[4] Polymeric materials have been previously investigated for controlled release as they can be easily manufactured and their composition can be finely tuned.[5] Polymers used in controlled release systems can be natural or synthetic and release can be achieved through the engineering of the polymer substrates, i.e., the degradation of poly($_{D,L}$ – lactide-*co*-glycolide) (PLGA) can be controlled through the polymer composition, higher ratios of PLA lead to a higher degradation rate.[6]

Another important research area under consideration is the development of controlled drug delivery systems (DDS).[7, 8] In 1980, controlled DDS were virtually unknown, yet in 2005, almost 100 million people globally were using some form of polymer based DDS.[8] The aim of a DDS is to supply the drug in its

therapeutically active form to a specific target in the body when the drug is required. In the current administration process there is a critical concentration needed in order to achieve the drug's maximum therapeutic effect. If the concentration goes beyond the maximum level, toxicity problems come into play. Conversely, if the concentration administered is below the minimum level the effect of the drug is not observed. The use of these DDS could potentially eliminate these problems as the release would be of a controlled manner.

Santini *et al.*[7] compared the release profiles of both conventional and controlled methods, as illustrated in Figure 1.1. With conventional methods of drug delivery, outlined in Figure 1.1(A), i.e., oral administration or injections, drug levels rise after initial administration, which could lead to potential toxicity problems, and then decrease until the next dosage, which has consequences on the efficiency of the dosage. The other schematic, Figure 1.1(B), demonstrates the effectiveness of a controlled release system. After dosage, the drug level in the blood remains constant, between the maximum and minimum levels, for a certain period of time.

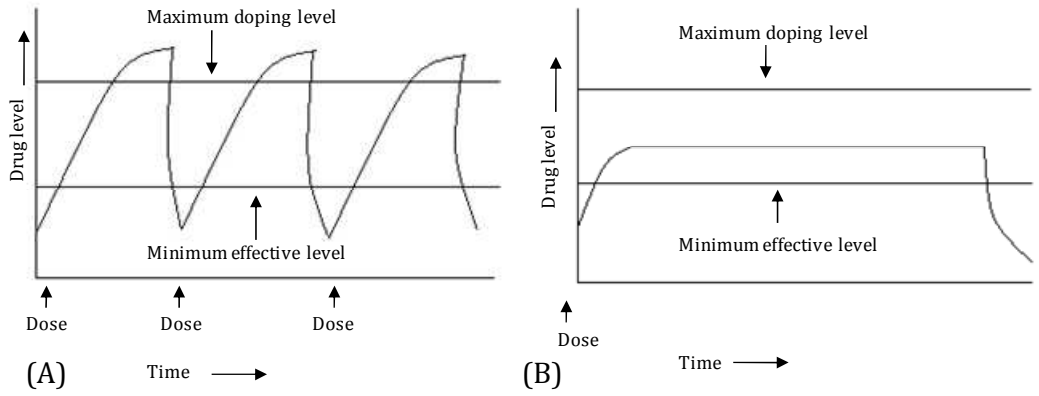


**Figure 1.1:** Drug levels in the blood with (A) conventional drug dosage (B) controlled delivery dosage, taken from Santini *et al.*[7]

In recent years, polymeric materials have been examined and shown to provide an alternate means of delivering drugs. Implanted polymeric pellets or microspheres localise therapy to specific anatomic sites, providing a continuous sustained release of drugs while minimising systemic exposure.[9] Polymers that display a physiochemical response to stimuli have been broadly researched for controlled release systems. Various stimuli include pH, temperature and the application of an electrical field.[10] According to Langer[11], polymeric DDS should i) maintain a constant drug level ii) reduce harmful side effects iii) minimise the amount of drug needed and iv) decrease the amount of doses which will have a pronounced effect on the patient.

The original polymeric controlled DDS was based on a non-biodegradable polymer, silicone rubber, which was designed and tested by Folkman and Long.[12] They loaded a silicone capsule (Silastic*) with a number of different drugs for the treatment of heart block and successfully implanted and monitored their effects over a number of days.

In more recent years there has been considerable interest in the development of new and efficient DDS, particularly with the growth of sophisticated drugs that are based on DNA and proteins.[5, 13] Currently, there are several materials under consideration in drug delivery, for example dendrimers[14], nanoparticles[15] and hydrogels[16]. The most promising opportunities in controlled DDS are in the area of responsive polymeric materials, with the possibility of implantable devices being used to deliver drugs. Murdan[17] exhaustively reviewed the use of hydrogels as 'smart' drug delivery devices. He showed that hydrogels could be engineered for various medicinal treatments depending on the patients needs, for example, pain relief. In the body, drug release can only be accomplished if the drug carrier responds to some class of stimuli, be it chemical, physical or biological. Conversely, an implanted 'smart' drug delivery device should be non-responsive to all other types of stimulus, once inside the body. A way of achieving this form of control is through an electrical stimulus.[17] A number of *in vivo* devices, in the form of iontophoresis, have already been used for this type of controlled release.[17, 18] Murdan presented a case where hydrogels loaded

with a bioactive compound, were implanted at a target site and the drug liberated through the application of an electrical field. In utilising such a system, many advantages including, minimal drug usage and lowering toxicity problems can be achieved. However, a problem arising with the application of an electrical stimuli to polymeric materials like, hydrogels, is that they experience deswelling or bending, which affects the drug release.[17]

To overcome these problems, conducting polymers (CPs) are also receiving much attention in the field of biomedical research, for the application of controlled DDS, due to their light weight, good biocompatibility and ability to function at body temperature. In particular, conducting polymers exhibit a reversible electrochemical response. These reversible oxidation-reduction reactions are attractive for a responsive DDS, as a change in the net charge on a conducting polymer film during its reduction or oxidation requires ions to flow into or out of the film. This, in turn, allows the polymer film to bind and expel ions in response to electrical signals. Controlled release of drugs from polymers offers many advantages over conventional methods including better control of the drug level administered resulting in fewer side effects, local drug delivery, decreased requirements for the total amount of drug and protection of drugs which are rapidly destroyed by the body. However, in order to devise a suitable technology, the polymeric material must be responsive, i.e., it must be capable of altering so that the drug is released in a controlled fashion when needed.

### 1.1.2 Conducting polymers

A polymer is a large molecule made up of smaller repeating units. The name comes from the Greek *poly*, meaning 'many', and *mer*, meaning 'part'. They are built up from simple molecules called *monomers* 'single part'. Polymers are produced through a method known as polymerisation. This polymerisation step can be achieved through chemical or electrochemical methods. Originally polymers with the basic carbon chains were considered only as insulators.[19] The first real interest in conducting polymers can be attributed to Walatka *et al*.[20] in 1973 with the report of highly conducting polysulfur nitride $(SN)_x$. Meanwhile

and towards the late 1970s , MacDiarmid, Shirakawa and Heeger enhanced the discovery of the semi-conducting and metallic properties of the chemically synthesised organic polyacetylene.[21-24] As is well known, the Nobel Prize in Chemistry was awarded to Alan J.Heeger, Alan G. MacDiarmid and Hideki Shirakawa in 2000 for the discovery and development of conducting polymers (CPs).[21-24] In the following years, a wide range of polymeric organic species have been prepared as stable inherent films on inert electrodes via both chemical oxidation and electropolymerisation from aqueous and organic solution.[25]

CPs are organic materials, which generally are comprised simply of C, H and simple heteroatoms such as N and S. Common examples include PPy, polyaniline and polythiophene which are shown in Figure 1.2. These and a number of other conducting polymers have been used in a variety of applications ranging from corrosion protection of materials, sensors to many biomedical applications, such as tissue engineering, nerve cell regeneration and drug delivery.[26-29]

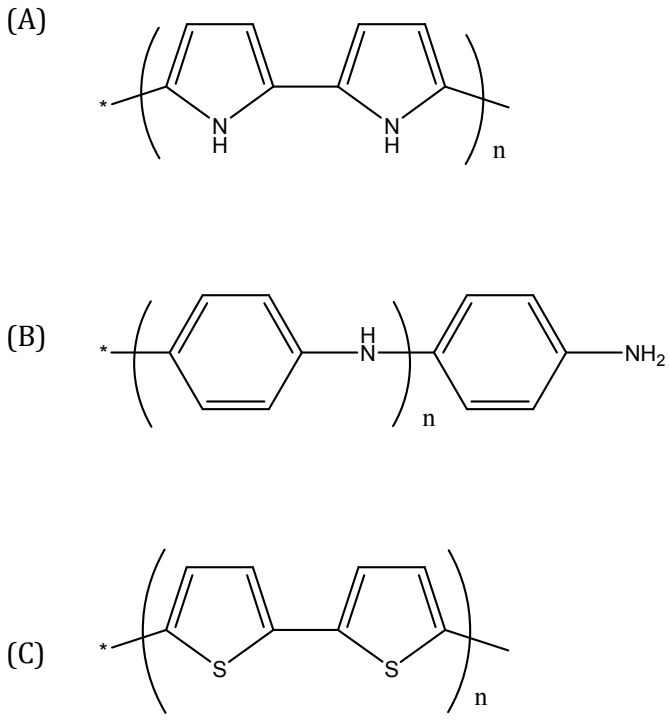


**Figure 1.2:** Chemical structures of (A) polypyrrole (B) polyaniline and (C) polythiophene. All polymers are shown in the dedoped state.

In, general materials are classed depending on their electrical conductivity, κ, where the electrical conductivity of insulators < semiconductors < conductors. Bredas and Street[30] explained this phenomenon in terms of the band gap structure. Figure 1.3 illustrates the difference in each material using the band gap theory. The highest occupied molecular orbital is equivalent to the valence band (VB), while the lowest unoccupied molecular orbital may be equated to the conduction band (CB). The difference between each band is known as the band gap energy ($E_g$) and it is this energy gap that establishes the electrical properties of a material. If $E_g$ > 10 eV, it is difficult to excite electrons into the conduction band and an insulator is formed. If $E_g \sim 1.0$ eV then thermal energy is sufficient to promote the electrons into the conduction band and a semiconductor is formed. If the gap vanishes, with overlap of the valence and conduction band, as shown in Figure 1.3, metallic conduction is observed. For most doped CPs the band gap energy is generally close to 1.0 eV, and consequently, CPs can be classified as semi-conductors.

As pointed out by Bredas and Street[30], the conductivity observed upon doping of the CPs was originally thought to be from the formation of unfilled electronic bands, however this idea was quickly dissipated upon experimental analysis of PPy and polyacetylene and now it is recognised that the conductivity is due to the formation of polarons and bipolarons, which are more energetically favoured.[30, 31]

The π-bonded system of CPs, which comprises of alternating single and double bonds, enabling the delocalisation of electrons along the polymer backbone, is related to the conductivity of the system. The conductivity of these materials arises from a state of relative oxidation or reduction. In these states the polymer either loses (oxidation) or gains (reduction) an electron. Generally, it is said that this process occurs in 1 in every 4 monomer units.[32] In this state the polymer is electronically charged and requires the introduction of counter ions (dopants) to compensate and reform the charge neutrality. The oxidation of the polymer in which an electron is removed from a π-bond, gives rise to a new energy state, which leaves the remaining electron in a non-bonding orbital. This energy level

is higher than the valence band and behaves like a heavily doped semiconductor.[32] The extent of doping can be controlled during the polymerisation of the polymers.

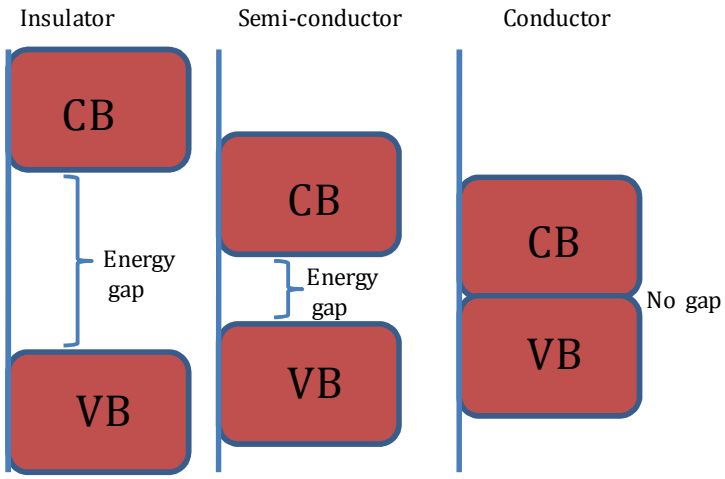


**Figure 1.3:** Schematic of the difference in band gap for Insulators, semi-conductors and metals (conductors).

### *1.1.2.1 Polymerisation methods*

CPs are synthesised through a method known as oxidative polymerisation. This can be generated chemically or electrochemically. Chemical polymerisation involves the use of a chemical oxidant, such as ammonium peroxydisulfate (APS), ferric ions, permanganate, dichromate anions or hydrogen peroxide. The oxidants not only oxidise the monomer but provide dopant anions to neutralise the positive charges formed on the polymer backbone.[33] In the presence of these oxidants, the monomers are oxidised and chemically active cation radicals are formed which further react with the monomer and generate the desired polymer. An advantage of vapour phase chemical polymerisation of CPs is that the polymerisation occurs almost exclusively on the preferred surface and a higher surface area can be attained.[34] Vapour phase chemical polymerisation of

pyrrole leads to further doping after polymerisation and this gives rise to an increase in conductivity.[35]

The electrochemical deposition is a simple and reproducible technique where the dopant is present in the electrolyte during polymerisation. It is generally performed in a conventional three electrode set up, described later in Chapter 2, where current is passed through a solution containing the monomer in the presence of a dopant (electrolyte). The CP is deposited at the positively charged working electrode or anode.[27] Polymerisation is initiated through the oxidation of the monomer which forms a mobile charge carrier known as a polaron (radical cation), that can react with another monomer or polaron to form a bipolaron (radical dication) which leads to the formation of the insoluble polymer chain and deposition of the polymer onto the working electrode.[36]

In his book 'Conducting Polymers' published in 1986, Alcacer commented on the possibility of using CPs to make artificial muscles or perhaps even modification for the brain; little did he realise the extent to which these materials have been extensively researched, over the past 20 years.[32] Since their discovery, the preparation and characterisation of these materials has evolved substantially through the use of electrochemistry. The majority of research is significantly based in this area due to the ease and control of synthesis of these electronically CPs.[19] Reviews on the development of CPs show the various areas to where they can be applied. The applications are ongoing.[37-40] However, in the case of DDS, CPs, in particular PPy, are widely researched for the controlled release of therapeutically active compunds.[41-45] During oxidative polymerisation, a dopant molecule, with an overall anionic charge, is used to compensate for the positive charges originating from the oxidation of the monomer. It is during this process that the concept of drug delivery originated. Burgmayer and Murray[46] observed changes in the ionic permeability of PPy redox membranes using a voltage-controlled electrochemical reaction. This led to further investigations into the application of CPs in DDS.

### *1.1.2.2 Polypyrrole*

#### 1.1.2.2.1 Historical background of polypyrrole

In 1968 Dall'Olio and colleagues prepared black films of an oxypyrrole on platinum by the electrochemical polymerisation of pyrrole from a solution of sulfuric acid.[47] In 1979 Diaz with the help of colleagues modified Dall'Olio's approach and demonstrated that polymerising pyrrole onto platinum in acetonitrile led to a black, adherent film.[48] Elemental analysis showed that the monomer unit was retained in the polymer. PPy in general, was poorly crystalline, and its ideal structure was a planar (α-ά)-bonded chain in which the orientation of the pyrrole molecules alternate.[25]

The monomer unit, pyrrole, is shown in Figure 1.4. PPy is an organic material comprised simply of C, H and a simple N heteroatom, but is highly conducting. It is an inherently conductive polymer due to interchain hopping of electrons. PPy can be synthesised both chemically[49] and electrochemically[48]. The electrochemical synthesis method is a one step synthesis method and allows the simple deposition of polymer films where its surface charge characteristics can easily be modified by changing the dopant anion (A-) that is incorporated into the material during synthesis. In a cell containing an aqueous or non-aqueous solution of the monomer, PPy forms a (semi) conducting film on the working electrode; the film grown is in the oxidised form and can be reduced to the non-conducting insulating form by stepping the potential to more negative values. The potential cycling can be repeated many times between the insulating and (semi) conducting forms without a loss of the electroactivity of the film.[25]

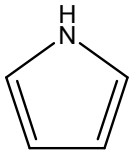


**Figure 1.4:** Schematic illustration of a monomer unit of pyrrole.

PPy in its neutral form is weakly coloured while the oxidised form is a deep blue/black. The switching of the state of the film not only changes its conductivity but it is also accompanied by a marked colour change, termed electrochromism.[36] Materials such as PPy are important in terms of future technological impact as it may be possible to develop them to replace more expensive, often toxic, metallic conductors commonly employed in the electronics industry.[25]

#### 1.1.2.2.2 Polymerisation mechanism of pyrrole

Although there are still various opinions on the mechanistic features of the electropolymerisation of pyrrole, the mechanism proposed by Diaz and his colleagues[48] and later used by Baker and Reynolds is in good agreement with many experimental reports.[50] The mechanism is demonstrated in Figure 1.5.

The initial step is the generation of the radical cation. This cation has different resonance forms, as shown in Figure 1.5. In the next step in the chemical case, the radical cation then attacks another monomer molecule, generating a dimer radical cation. In the electrochemical case, the concentrations of radical cations is much larger than that of neutral monomers in the vicinity of the electrode where reactions are occurring, and radical-radical coupling leads to a radical dication. This coupling between the two pyrrole radicals results in the formation of a bond between the two $\alpha$ positions to give the radical dication, as highlighted in Figure 1.5. This is then followed by the loss of two protons, generating a neutral dimer. This dimer is then oxidised into a radical cation, where the unpaired electron is delocalised over the dimer. The radical dimer then couples with the radical monomer to form a trimer. The polymerisation thus progressing in this fashion to completion.

The controversy in the mechanism of electropolymerisation is not surprising given that many factors, such as the nature of the electrolyte, ionic strength, pH, temperature and potential are important and can influence the mechanism of the reaction.

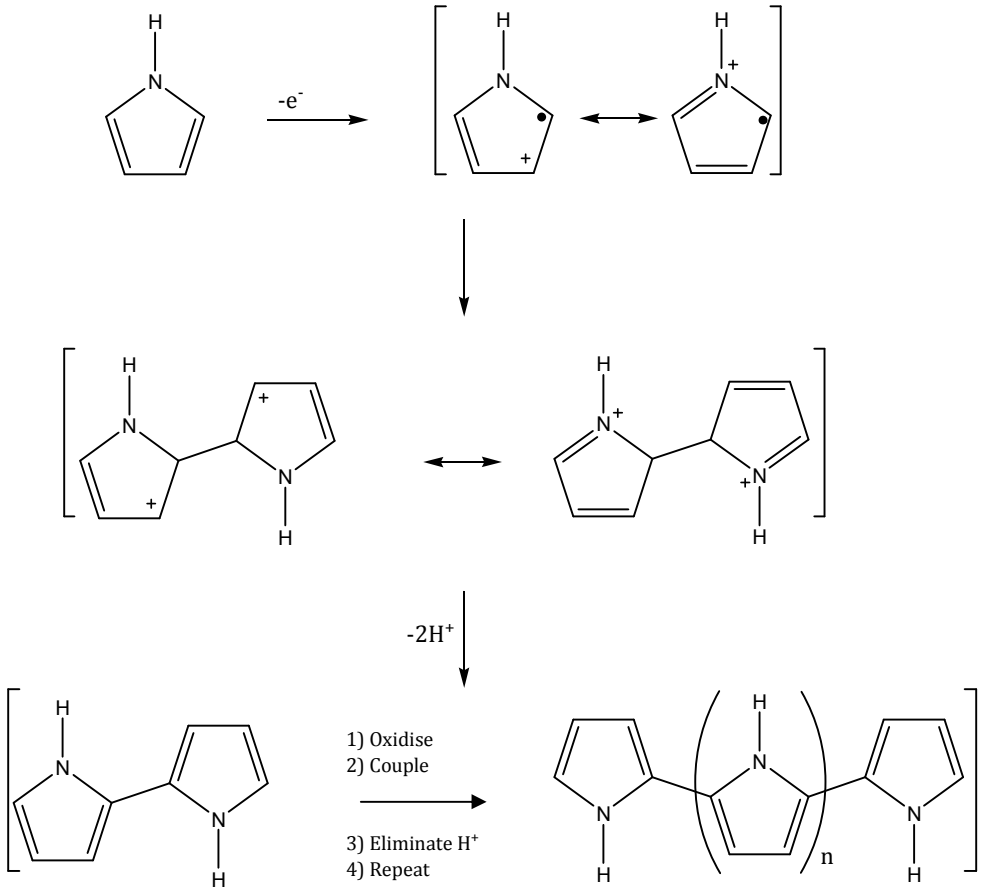


**Figure 1.5:** Mechanism of electrochemical polymerisation of pyrrole.[50]

#### 1.1.2.2.3 Biocompatibility

PPy is one of the most widely researched conductive polymers. The fact that it can form biologically compatible matrices is one of the prominent reasons for the extensive research on the use of PPy in the field of biological applications.[51] Wang *et al.*[52] acknowledged the reality that PPy had showed very good *in vitro* biocompatibility,[29, 53, 54] but they wanted to evaluate further the *in vivo* biocompatibility prospects. They demonstrated that in comparison to no PPy, the presence of PPy/biodegradable composites stimulated no abnormal tissue response and had no affect on the degradation behaviour of the biodegradable materials. In 1994, PPy was one of the first conducting polymers investigated for its effect on mammalian cells.[55] Since then, PPy is known to be

biocompatible, so it can be placed in the body without having adverse effects. It has been shown, in particular, to support cell growth and adhesion of endothelial cells.[29, 55-57] Schmidt *et al*.[29] also demonstrated that PPy was a suitable material for both in vitro nerve cell culture and in vivo implantation. PPy was electrochemically deposited onto ITO-conductive borosilicate glass. Moreover, the application of an external electrical stimulus through the polymer film resulted in enhanced neurite outgrowth. The median neurite length for PC-12 cells grown on PPy film subjected to an electrical stimulus increased nearly two-fold compared with cells grown on PPy without the application of a constant potential. The group also investigated PPy in vivo and their studies showed that PPy promotes little negative tissue and inflammatory response. Due to the good biocompatible factor, studies on the application of an electric field to the PPy have also shown cell compatibility.[29] In some important applications, such as biological sensors and actuators for medical devices it is a very attractive trait and some recent applications show that PPy can enhanced nerve cell regeneration and tissue engineering.[27]

#### 1.1.2.2.4 Electroactivity of polypyrrole

PPy can be easily switched between the neutral, partially oxidised and fully oxidised states, as shown in Figure 1.6. In its neutral state PPy exists as an insulator where the conduction band is empty as all the electrons remain in the valence band. Upon oxidation, an electron is removed from a π-bond (valence band) and a polaron is formed. The separation of the positive charge and the unpaired electron decreases during continual oxidation as the number of polarons increases. This in turn gives rise to the formation of a bipolaron, as depicted in Figure 1.6(C), and the polymer is now in its fully oxidised state.

During oxidation and the generation of positive charge an influx of anions into the polymer matrix is observed in order to maintain charge balance. This can be represented in Equation 1.1, where $PPy^{o}$ refers to the neutral (reduced) polymer, $PPy^{+}$ refers to the oxidised polymer and $A^{-}$ refers to the anionic dopant.

$$PPy^0 + A^- \rightarrow PPy^+A^- + e^- \quad 1.1$$

Typical anionic dopants are chlorides, bromides, iodides, perchlorates, nitrates, sulfates and para-toluene sulfonates.[58-64] The extent of oxidation/reduction is given by the doping level and this is generally expressed as the ratio of dopant anions, $A^-$, incorporated per monomer unit. For example, 1 $A^-$ per 4 monomer units gives a doping level of 0.25 or 25%. The maximum doping level achievable with PPy is 0.33 or 33%, i.e., 1 $A^-$ per 3 pyrrole units. It is important to point out that doping may not always be uniform; there can be islands with high doping levels surrounding by regions with a much lower doping level.

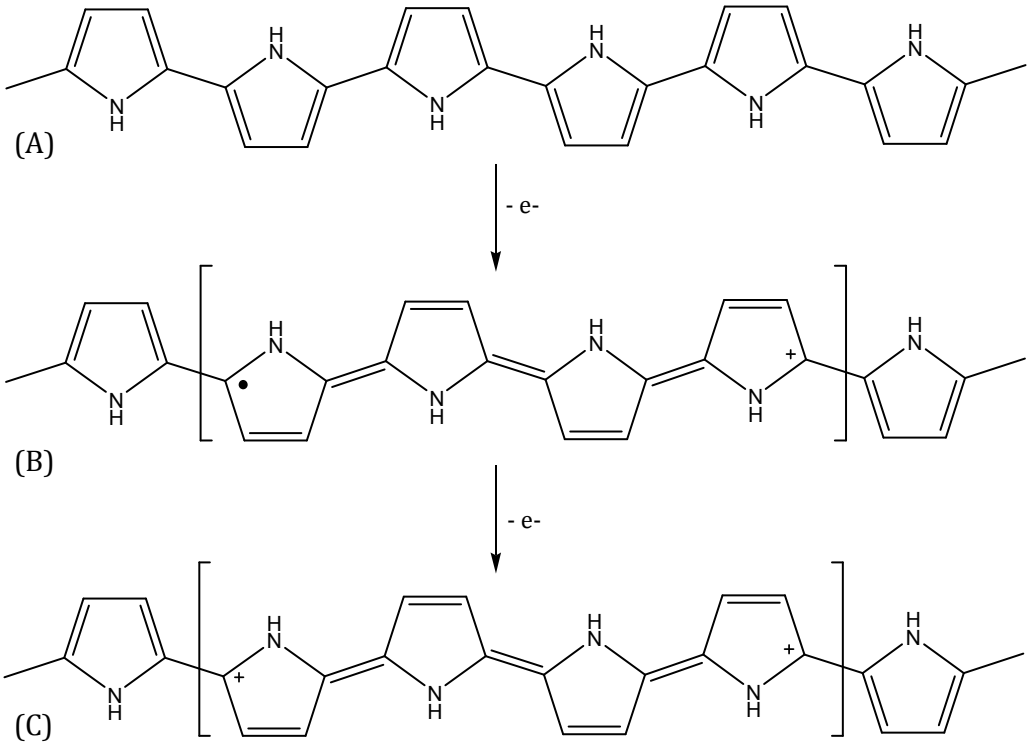


**Figure 1.6:** Electronic structures of (A) neutral PPy, (B) polaron in partially doped PPy and (C) bipolaron in fully doped (oxidised) PPy.[36]

**1.1.2.2.5 Polypyrrole and drug delivery**

The electrochemical switching of PPy films is accompanied by movement of counter or dopant ions in and out of the polymer matrix to maintain the charge neutrality, as shown in Section 1.1.2.3.4. Consequently, PPy films are attractive for the controlled release of drug molecules. The concept of using PPy membranes for the uptake and release of ions was introduced, in the early 1980s, by Burgmayer and Murray[46]. They demonstrated that these polymeric films could be exchanged from their oxidised state to their neutral state. PPy has been seriously considered for drug delivery due to these unique redox properties. PPy gives a responsive material needed in order for the uptake and release of the drug to be controlled; in its oxidised state anions are electrostatically bound to the polymer film. These properties allow the controlled transport of ions. The uptake of these ions can occur in two ways. The first is where the bioactive molecule exists as an anion and is involved in the doping process of the polymeric material during polymerisation, Figure 1.7 (A). Some anions that have been researched include adenosine tri phosphate (ATP)[65], salicylate[26], and dexamethasome[26]. These anions are electrostatically entrapped into the polymer matrix during the growth process upon application of an anodic potential. The anions are consequently liberated during the reduction of the polymer.

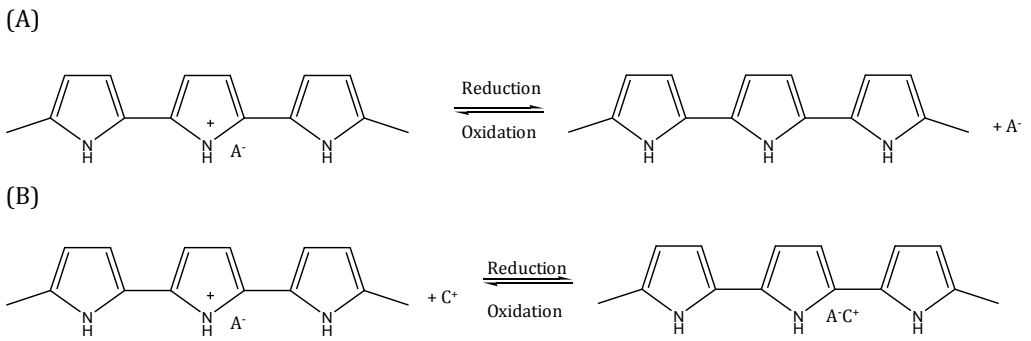


**Figure 1.7:** Interconversion between oxidation and reduction states of PPy (PPy). (A) Anion (A-) incorporation and release which is notably observed in small mobile anions (e.g. Cl-) while, (B) Cation (C+) insertion and liberation from polymer films doped with larger anions (e.g. $DDS^-$) which remain entrapped in the polymer matrix.

In the second case, cations can be incorporated into the system, Figure 1.7 (B), if the properties of the polymer film are modified.[66] This is achieved through the

initial inclusion of a large anion which remains entrapped in the polymer matrix and thus the polymer behaves as a cation exchanger, where, the charge of the polymer system can only be compensated through the uptake of cations. The cations are therefore, taken in during the reduction of the polymer and released upon oxidation. Figure 1.7 demonstrates both these concepts.

Miller and Zhou[67] previously reported the release of dopamine from a poly(*N*-methlypyrrole)/poly(styrenesulfonate) (PNMP/PSS) polymer based on the properties of these redox polymers. Immobilisation of PSS, a large anion, allows the uptake and release of the cation upon appropriate application of a potential. They achieved the release of dopamine using potential control, while more recently, Hepel and Mahdavi[66] demonstrated the controlled release of a cationic species, chloropromazine, from a composite polymer film based on the same principles. They reported the development of a new composite conducting polymer, PPy/melanin, which performed as a cation binder and releaser. The modification of the polymer films, to enable the predominant cationic exchange properties of the CP, is an interesting way of improving the uptake and release of cationic species from these attractive materials.

New ways of improving the controlled release of drugs are continually being sought after. Lately, Abidan *et al*.[41] reported on a method to prepare conducting-polymer nanotubes that can be used for controlled drug release. They introduced a method known as electrospinning to fabricate a nanofibrous mat in which the drug to be delivered had previously been incorporated; followed by electrochemical deposition of PPy films around the drug-loaded, electrospun biodegradable polymers. The drug release was achieved through the electrical stimulation of the PPy nanotubes.

#### 1.1.2.2.6 The application of Nanotechnology in drug delivery

Nanotechnology, although dating back to much earlier times, gained considerable attention in the early 1990s and has been the focus of much research over the last number of years. The introduction of nanotechnology into a controlled DDS has been shown to enhance many physical and chemical properties and overall has been used to increase the surface area of materials. This, in turn, leads to an increase in the amount of drug released from various materials. Many groups have introduced nanotechnology in various forms to improve on the drug delivery of a number of bioactive compounds, including nanoparticles[15], micellar systems[68] and nanofibers[69]. Polymeric nanofibers are gaining substantial interest for various applications including drug delivery[69, 70]. Several techniques have been employed for the production of nanofibers such as template synthesis[71], self assembly[72] and drawing[73]. One technique, in particular that is receiving considerable interest in this field, is electrospinning.[74-77] Electrospinning has been introduced to achieve nanoscale membranes and fibres from various polymeric materials.[78]

**1.1.2.2.7 The application of Electrospinning to drug delivery**

Although electrospinning was first reported by Formhals[79] in 1934 it has only been explored further in recent times.[80, 81] In 1996, Reneker and Chun restored interest in the electrospinning technique by demonstrating the possibility of electrospinning a wide range of organic polymers.[81] Since then the technique of electrospinning has become extremely useful in a variety of applications.[82-85] Electrospinning is a simple and inexpensive means for the formation of nano- to micron polymer fibers.

This technique involves the application of a high electric field between a polymer fluid and a grounded electrode. When the polymer solution is subjected to an external electric field at a critical point the forces overcome the surface tension of the polymer solution to form a droplet with a conical shape, i.e., the Taylor cone.[83, 86] The fluid is drawn into a jet which undergoes a whipping motion. Volatile solvents are used to dissolve the polymer as the subsequent evaporation from the liquid jet results in solid fibers. A more detailed

description of this technique is provided in Chapter 2, Section 2.4.5. In the majority of cases the fibers deposit randomly on the grounded collector. However, many groups have investigated the use of rotating collector plates to produce aligned nanofibers.[87] Figure 1.8 illustrates a typical SEM micrograph of an electrospun fiber mat of PLGA fibers.

This production of nanofibers allows these polymers to be used in a wide variety of applications including, tissue engineering (muscles, skin, cartilage and bones), wound healing and sutures, biosensors and DDS. Shin *et al.*[88] studied the use of PLGA nanofiber scaffold for cartilage reconstruction, while, Kim and colleagues incorporated antibiotics in the fibrous matrix for use in wound dressings.[89] Other groups have also prepared ultrafine polymers via electrospinning for skin regeneration.[74]

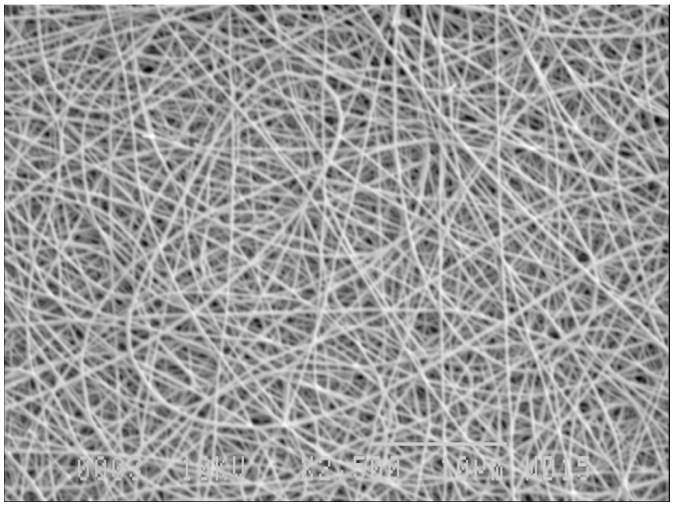

**Figure 1.8:** A typical SEM image of electrospun PLGA nanofibers.

Another attractive feature of using this electrospinning technique is that biodegradable polymeric materials, such as poly(lactic acid) (PLA) and poly($_{D,L}$ – lactide-*co*-glycolide) (PLGA) can be used as a biomedical controlled release system. These biodegradable polymers can be electrospun in the presence of varying amounts of the required medication. They can then be placed in the

body and the drug release achieved through the modification of the polymer matrix's morphology, porosity and composition.[89] These biodegradable polymers have FDA approval for biomedical and drug delivery use.[90-93] In comparison to other delivery forms, the electrospun nanofibers can conveniently incorporate the therapeutic compound during the electrospinning process.[94] Many drugs have been incorporated into PLGA electrospun polymer matrices, in order to achieve delivery of the therapeutic drug, including, tetracycline hydrochloride[95] and mefoxin[89]. In these cases, the drug release was monitored and a burst release was observed and was attributed to the high surface area-to-volume ratio of the electrospun material. This is a disadvantage. In the last few years a small number of groups have deposited electroactive polymers, such as PPy, onto previously electrospun fibers in order to enhance the electrochemical properties[57] of the material. Also, electrospun fibers have been used as a template in order to obtain a high surface area in the hope of achieving a greater uptake and release of drugs.[41]

Another method of improving the DDS of conducting polymers is the use of various dopants during polymerisation of the polymer films. The functionalisation of PPy films with large anionic dopants is not new to this field of research. It has been well reported that the use of large anionic dopants during the electrochemical polymerisation of monomers leads to these bulky negatively charged groups being immobilised within the polymer matrix.[96] In fact, these polymers, with their cationic exchange properties, have been used to incorporate various cationic groups for various applications. For example Fan and Bard in the late 1980s demonstrated the uptake of a positively charge $Ru(NH_3)_6^{3+}$ and methylviologen in PPy/Nafion films.[97]

However, the generation of PPy films in the presence of negatively charged cyclodextrins is a new concept.[98-100] There has been very little work reported on the electropolymerisation of pyrrole in the presence of anionic cyclodextrins. Indeed, much of the current published work is unreliable as very high potentials in the vicinity of 1.8 V vs. SCE were used to form the polymers.[100, 101] It is very well known that these high potentials give rise to the overoxidation of PPy and a

considerable loss in its conductivity.[59] The incorporation of cyclodextrins into conducting polymers provides a unique way of combining the unique host-guest complexation properties of cyclodextrins with the stability, high conductivity and ease of preparation of conducting polymers.

## 1.1.3 Cyclodextrins

### *1.1.3.1 History and structural properties of cyclodextrins*

Cyclodextrins (CD) are macrocyclic oligosaccharides composed of α-D-glucopyranoside units linked by α-(1,4) bonds. They were first discovered by Villiers in 1891[102], while in 1904, Schardinger[103] further developed the cyclic structures hence; CDs are sometimes referred to as Schardinger dextrins. However, it was only in the mid 1970s that the structure and chemical properties of natural cyclodextrins were fully characterised.[104] Cyclodextrins have developed quickly over the past two decades and have become an important branch of host-guest chemistry, specifically due to their ability to be involved in several practical applications.[105] The main interest in cyclodextrins lies in their ability to form inclusion complexes with a variety of compounds. Host-guest chemistry is the study of these inclusion phenomena, where the 'host' molecules are capable of including smaller 'guest' molecules through non-covalent interactions.

CDs are obtained through enzymatic degradation of starch in the presence of a glycosyl transferase, a type of amylase.[106] Many organisms contain glycosyl transferase, however, in general it is obtained from *Bacillus megaterium, Bacillus stereothermophilus and Bacillus macerans.*[106, 107] They are generally made up of glucopyranoside units of $^4C_1$ chair conformation which leads to a truncated cone shape encasing a cavity.[108] Figure 1.9 shows the structures of the most common CD members; α-, β- and γ-CD, which include 6, 7 and 8 repeating glucopyranoside units, respectively. These units orientate themselves in a cyclic manner offering a typical conical or truncated cone structure with a relatively hydrophobic interior and hydrophilic exterior.[109] This structural property gives cyclodextrins good water solubility and the ability to hold appropriately sized

guests, such as amines and ferrocenes[110], through non-covalent interactions such as hydrogen bonding, hydrophobic interactions, and electrostatic interactions.[111] Table 1.1 demonstrates the approximate geometries of the most common CDs.[109]

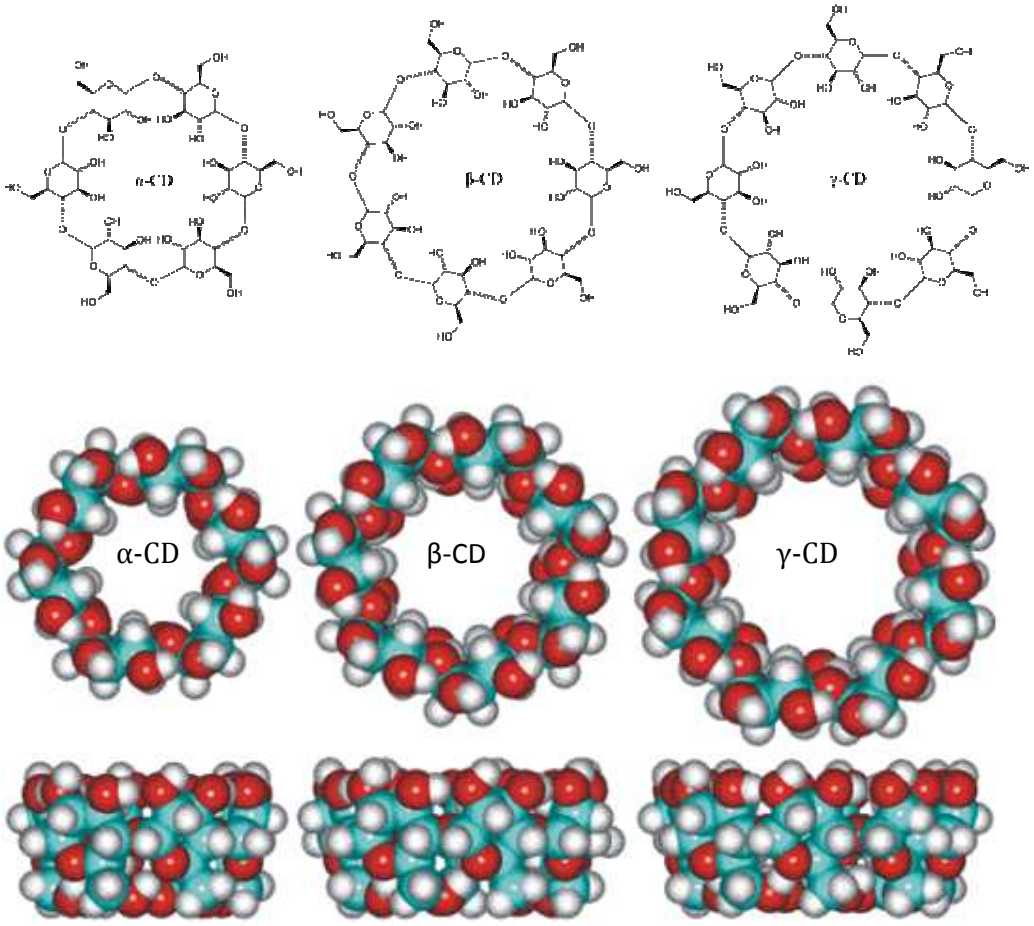


**Figure 1.9:** Structures of α-, β- and γ-cyclodextrin taken from Szjetli.[109]

Due to their exceptional host-guest complexation abilities, CDs have been used in a variety of fields, such as environmental protection through immobilising toxic compounds in their cavities and in the food industry.[104] In fact one of the commercially available applications for CDs is Febreze®, which is an aqueous solution of modified β-cyclodextrins. Febreze® is based on the host-guest chemistry of the CDs, with molecules that produce aroma forming inclusion complexes with the modified CDs. In the pharmaceutical industry, CDs are also

used for many applications including, drug delivery to enhance the solubility, stability and bioavailability of drug molecules.[108, 112]

**Table 1.1:** Approximate geometric dimensions of the three common CDs.[106]

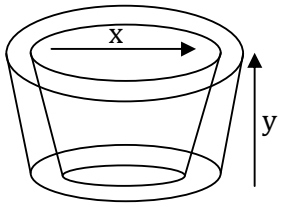


| Cyclodextrin | x / nm | y / nm | Cavity volume / Å$^3$ |
|---|---|---|---|
| **α** | 0.49 | 0.78 | 174 |
| **β** | 0.62 | 0.78 | 262 |
| **γ** | 0.79 | 0.78 | 427 |

Cyclodextrins can also be chemically modified to replace the hydroxyl groups on both the primary and secondary rims of the CDs, with a variety of appropriate alkyl groups (R). It has been reported that this can improve binding affinity.[108] In the research presented here, a negatively charged cyclodextrin with a number of sulfonated groups present on the outer rims was used, sulfonated β-CD (Sβ-CD). Sβ-CD is obtained by substitution of either primary or secondary hydrogen of the hydroxyl group of β-CD with a sulfonate group. Sβ-CD has an average of 7-11 substituents per CD and, therefore, has between 7-11 negative charges associated with it, which are counterbalanced with sodium ions, as illustrated in Figure 1.10.[113] It is reported that β-CD and Sβ-CD have the same ring structure, differing only in the substituent located on the rims of the CD ring.[14] Although Sβ-CD has the same ring structure as other derivativsed CDs the presence of the substituent on the ring contributes to its chiral discrimination properties.[114] A major area in which these sulfonated CDs are being utilised is chromatography, or more specifically capillary electrophoresis, for the enantiomeric separation of acidic and basic compounds. In enantiomeric separation, using neutral CDs, they are not appropriate for neutral racemates as the complex has no electrophoretic mobilities.[115] Therefore, the use of charged

CDs is now been widely researched for the separation of neutral compounds. It has been reported that the use of these sulfonated CDs for the enantiomeric separation of chiral compounds is highly effective as a result of the anionic charges.[116, 117]

A number of groups have also characterised the Sβ-CD.[115, 117] Figure 1.11 illustrates a single glucose unit of an Sβ-CD (comprised of 7 units). On the primary ring there are 7 potential substitution sites corresponding to the C-6 positions, while, on the secondary rim there are 14, represented by the C-2 and C-3 positions. Amini and co-workers[117] reported that substitution of these CDs is predominantly at the C-2 and C-6 positions, while, Chen *et al.*[115] confirmed nearly complete sulfation at the C-6 position of the primary hydroxyl groups and partial sulfation at the C-2 secondary hydroxyl groups. They also reported no substitution at the C-3 positions. From these reports it can be stated that almost the entire primary rim is sulfonated and some of the secondary rim. Due to this phenomenon and the fact that the sulfation brings with it negative charges these CDs are good candidates for the doping of CPs.

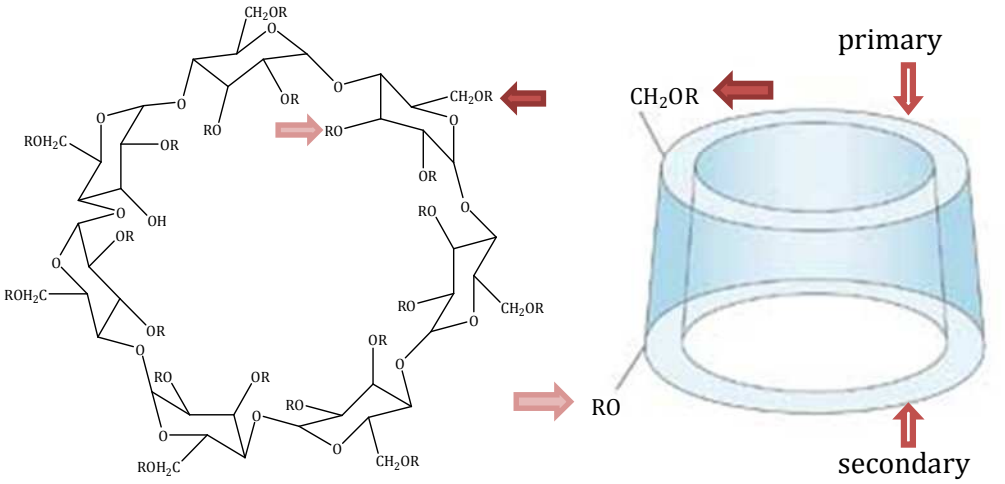


R = $SO_3^-Na^+$ or H ~ 7-11 $SO_3^-Na^+$ groups.

**Figure 1.10:** Structural and schematic representation of sulfonated β-cyclodextrin (Sβ-CD). The arrows point to the primary and secondary rims, respectively.[118]

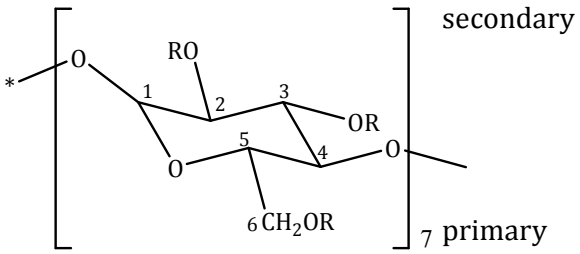


**Figure 1.11:** Chemical structure of Sβ-CD, depicting the numbering carbons.

### *1.1.3.2 Inclusion complexation*

Cyclodextrins (CD) form a group of cyclic oligosaccharides that contain cavities in which guest molecules can be encapsulated.[108, 109] It is well known that the size of the compounds are important and compounds are only capable of including into the cavity of the CD if they are within the dimensions of the CD cavity.[119] In aqueous media, the cavity is filled with water molecules, which becomes displaced by the guest through complexation, as illustrated in Figure 1.12. The guest molecule, xylene, displaces the water molecules and forms an inclusion complex with the CD.

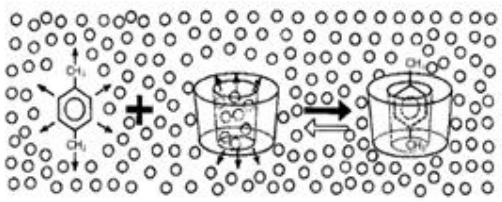

**Figure 1.12:** Schematic representation of xylene forming a complex with a β-cyclodextrin. The small circles represent water molecules taken from Szjetli.[109]

During the formation of an inclusion complex the chemical and the physical properties of the guest molecule change and can be monitored using a number of techniques. Various spectroscopic and electrochemical techniques can be used to confirm complexation, including fluorescence, UV-visible spectroscopy (UV), Nuclear magnetic resonance (NMR) and electrochemical studies. These changes attributed to the complexation can be used to evaluate the apparent

binding or formation constant ($K_f$). However, prior to the determination of the $K_f$ value the stoichiometry of the host-guest complex must be established.[120] This is obtained by the well known continuous variation or Job's method which is described in more detail in Chapter 2, Section 2.6.1.1.[121] Generally, inclusion complexes form a ratio of 1:1, 1:2 and sometimes 2:1 (CD:guest).[122]

NMR is also a useful tool for the study of complexation due to its quantitative information and assuming the guest enters the cavity, NMR, can be also used to locate the protons involved in complexation.[87] Many groups have studied the complexation properties with the neutral β-CD and monitored the changes in the chemical shifts for both the CD, and the guest. However, in the case of the modified CD used in this research, the NMR spectral data are too difficult to differentiate so the chemical shift of the guest is followed.[120, 123-126] Bratu and colleagues[125] studied the chemical shift changes observed when Fenbufen was in the presence of a neutral β-CD. They noticed an up-field shift of the guest protons, some more pronounced than others, and suggested that the complexation was initiated through the benzene moiety of the guest. Cruz *et al*.[127] also used NMR to quantitatively evaluate the binding constant of the complexation of doxepin and a neutral β-CD.

If a guest absorbs light in the UV or visible region then the inclusion phenomenon can be followed and subsequently, evaluated by UV.[106] This technique can be used to confirm complexation and indeed obtain the formation constant associated with the inclusion complex. In the majority of cases the guest that absorbs in the UV-vis region experiences changes in the intensity and the position of the absorption bands in the presence of the CD. These spectral changes can be used to determine the $K_f$ constants. Generally, a Hiedlebrand-Benesi modified equation is used to evaluate the $K_f$ constants.[119, 128, 129] Ramaraj and co-workers[130] monitored the changes attained during the complexation formation of a number of aromatic amines and nitro compounds in the presence of a neutral β-CD. They observed an increase in the intensity of the bands in all cases. Dang *et al*.[119] observed shifts of the absorption bands to longer

wavelengths in the case of 1,4 benzoquinone (BQ) and 9,10 anthraquinone (AQ) in the presence of a neutral β-CD.

Electrochemical techniques can also be performed on the complexation properties of CDs. If the guest is electroactive the peak current and potential can be followed for the free state and compared to the complexed state of the guest in question. Two features are generally observed during these electrochemical observations if an inclusion complex is found. Firstly, a decrease in the peak current can be seen, and, attributed to a decrease in the diffusion of the bulky CD complex as opposed to the more mobile free guest. Secondly, a shift in the peak potential is observed if the complexed species is included in the cavity, as it is harder to oxidise or reduce while located in the cavity. Once again based on these variations a number of equations can be used to verify the formation constant.[129, 131, 132] Coutouli-Argyropoulou and his group[133] reported the effect of complexation on the electrochemical properties of ferrocence derivatives and showed shifts, in both the peak current and peak potential, when higher concentrations of a neutral β-CD were added. Yanez *et al*.[131] showed similar observations for nifedipine (NF) and nicardipine (NC) and estimated apparent formation constants of 135 and 357, respectively.

Complexation studies of DA have been previously demonstrated in the presence of a neutral β-CD by Zhou *et al*.[134] using UV and fluorescence spectroscopy. From the fluorescence technique, utilising a Hiedlebrand-Benesi modified equation, a $K_f$ value of 95.06 was estimated. The degree of the complexation can vary over a wide range due to the stability of the complex, as it depends on a number of factors. In the next section a discussion on the main driving forces, involved in this complexation process are dealt with.

#### *1.1.3.3 Driving forces in the inclusion complexation process*

There are many reviews and books written on the driving forces behind the inclusion complexation abilities of cyclodextrins, not all agree, some refer to the predominantly hydrophobic affects while others state that it is a collection of a

number of weaker interactions (H-bonding, van der Waals, electrostatic interactions).[106, 108, 111, 135, 136] Either way the majority agree that the size of the cavity and shape of the guest are important factors in the complexation process. The most widely studied possible driving forces include

- Hydrogen bonding
- Electrostatic interaction
- Van der Waals
- Hydrophobic effect

Hydrogen bonding is an interaction between an electronegative donor, a hydrogen and an electronegative acceptor.[136] Various groups have demonstrated the importance of hydrogen bonding in the solid state, illustrating crystal structures defining the hydrogen bonding between the guest and the hydroxyls of the CDs.[137] However, during the complexation of the CD and guest, in aqueous solution, the subject is still arguable as few direct measurements of hydrogen bonding have been made, as water molecules can compete with CDs to form hydrogen bonding with guest molecules. However, many groups will still argue over the significance of hydrogen bonding.

Electrostatic interaction occurs when molecules of opposite charges interact. There are three types of electrostatic interactions, ion-ion interaction, ion-dipole interaction and dipole-dipole interaction.[136] Matsui and Okimoto[138] reported that ion-ion interaction is only eligible in the case of modified CDs, where as ion-dipole is considered more favourably due to the fact that CDs are polar molecules however as with hydrogen bonding, in aqueous media, the interaction between the guest and water will also be strong.[136] Therefore, it is the case of dipole-dipole interaction that is mostly considered during complexation.

Van der Waals forces or London dispersion forces are made up of dipole induced dipole contributions or the coordination of the electronic motion in the CD and guest. As CDs are known to have large dipole moments it is logical that

these induction forces are important in complexation. Experimental evidence has shown that the stability of the complex increases with an increase in polarisability. Also, as the polarisability of water is lower than the organic components of the CD cavity, van der Waals forces have an encouraging donation to the stability of the complex due to a stronger interaction of the CD and guest over the water and guest.[136] CDs have also been reported to form stable inclusion complexes in organic solvents like DMF and DMSO confirming the importance of van der Waals forces.[139]

The hydrophobic interaction which is entropically favourable, due to the expulsion of water, leads to the aggregation of non-polar solutes in aqueous solution.[136] As reviewed by Connors[135] the 'classical' hydrophobic interaction is said to be 'entropy driven' and a positive entropy and enthalpy is associated for the interaction between two non polar molecules. However, experimental studies in the complexation of CD and guests, show negative enthalpy and entropy changes,[111] which have been suggested to indicate that these interactions are not a dominant force.

Mosinger *et al*.[122] reported that the formation of an inclusion complex is based on the electrostatic, van der Waals and π-π interactions, where, steric affects and Hydrogen bonding are inevitable. Chao and co-workers[124] investigated the formation of an inclusion complex with β-CD and caffeic acid, they reported that the weak forces of hydrogen bonding, van der Waals, hydrophobic and electrostatic interactions simultaneously governed the process.

Rekharsky and Inoue[111] reviewed the complexation of cyclodextrins and stated that the interactions involved in the inclusion complexation of aromatic guests with CDs could not be simply put down to a hydrophobic effect. They established that complexation could be accounted for, through dipole-dipole interactions. In saying that, Tabushi and his group[140] questioned the role of hydrogen bonding in the complexation process and reported that no dramatic changes of binding were observed, when a modified CD, incapable of hydrogen bonding, was compared to an unmodified CD. They concluded that the

involvement of hydrogen bonding was negligible and hydrophobic interactions dominated the process. Zia *et al*.[113] investigated the complexation ability of a negatively charged CD (~7 negative sites) with a number of neutral and charged guest molecules. They accounted for the increase in the binding affinity, for the oppositely charged guest and CD, to be predominantly hydrophobic, due to the additional interaction sites provided by the negatively charged CD. Okimoto and colleagues[141] also clearly observed stronger interactions occurring between a CD and guest with opposite charges.

The understanding of these complexation processes is complicated, however, it is generally found that van der Waals forces and hydrophobic interactions are regarded as the main driving forces for CD complexation, while, electrostatic interactions and hydrogen bonding can be significantly considered in some inclusion complexation studies. Nevertheless, these attractive features of CDs allow them to be used in a wide range of applications including, the food industry[142]. However, the pharmaceutical industry is the most widely researched area in recent times, specifically in drug formulation and DDS.[143]

#### *1.1.3.4 Applications of CDs in DDS*

Due to their biocompatibility and their ability to form inclusion complexes, CDs have been studied for the use in DDS. They have been considered as drug carriers, as CDs have the potential to act as hydrophobic carriers and control the release of a variety of drugs.[118] Many reviews have recently been published, describing the role of CDs in DDS.[112, 118, 144-147] Irie and Uekama[144] reviewed the role of CDs in peptide and protein delivery and summarised that CDs were able to eliminate a number of undesirable properties of drug formulations, as they form inclusion complexes with the desired drugs, which increase the drug delivery through a number of routes of administration. More recently, Li *et al.*[145] examined the recent progress in the preparation of inclusion complexes between CDs and various polymers as supramolecular biomaterials for drug and gene delivery. They demonstrated the promising field in the self assembly

of inclusion complexes between CDs and biodegradable polymers as injectable DDS.

Ferancova and Labuda[148] also reviewed the use of CDs as electrode modifiers. They summarised the many ways CDs can be immobilised onto electrode surfaces. As discussed in an earlier section, Section 1.1.4.2., the incorporation of CDs, as dopants, during the electrochemical polymerisation of CPs was demonstrated to examine the use of these modified electrodes to deliver neutral drugs.[98] Formulating these materials, correlates the attractive features of both the CDs and the CPs. Bidan *et al*.[98] examined the need for a new DDS that was not limited to charged drugs. They produced polymer films in the presence of an anionic CD and successfully delivered neutral compounds using these novel materials.

Also briefly discussed in Section 1.1.4.2, was the reports made by a number of groups on the polymerisation of CPs in the presence of CDs.[100, 101, 149] These groups have reportedly polymerised pyrrole at potentials usually shown to overoxidise the CP film.[59] Due to this, these papers are unreliable in their reports.

### 1.1.4 Drug release: Controlled release of dopamine

DA is a neurotransmitter produced naturally in the brain. It is well documented that a common factor in neurodegenerative diseases such as Parkinson's (PD) and Schizophrenia is a significant lack of the presence of DA in the *substantia nigra* (mid brain).[150-152] In particular, PD is a slowly progressive disorder known to occur due to the damage of the basal ganglia.[150-152] The disease affects movement, muscle control and balance. Studies on the brains of deceased Parkinson sufferers show a substantial loss of dopamine, particularly, in the *substantia nigra*. The function of the substantia nigra is to produce DA and manage the release of essential neurotransmitters that help control movement and coordination. Sufferers usually show symptoms such as tremors, slowness of movement and impaired balance and coordination. Prolonged loss of DA

gives rise to symptoms such as difficulty in walking, talking, or completing other simple tasks.[150-152]

DA belongs to the well known catecholamine family. These molecules are electroactive and therefore their oxidation can be followed using electrochemistry, in particular, electrochemical methods such as cyclic voltammetry and rotational disc voltammetry. The electrochemical mechanism of oxidation is still not fully agreed; with various groups arguing that the mechanism goes through an ECE step rather than a CE step. For example, Hawley *et al*.[153] have reported that the electrochemical oxidation of dopamine in aqueous solution proceeds through two types of steps, electrochemical (E) and chemical (C). The ECE mechanism is presented in Scheme 1.1.

The first step in the oxidation of dopamine (A) involves the loss of both protons and electrons to form the o-dopaminoquinone (B). The oxidised, o-dopaminoquinone undergoes a 1,4-Michael addition, which results in a intramolecular cyclisation reaction which produces leucodopaminochrome (C). This product is easily oxidised through an electrochemical step to form dopaminochrome (D).[153, 154]

Controlled release studies of DA have been previously investigated.[67, 155-158] McRae-Degueurce *et al*.[156] encapsulated DA into a thermoplastic polyester excipient: PLGA. They found that it was possible to deliver significant amounts of DA for prolonged periods of time by injecting the microencapsulated DA directly into the brain. Uludag and colleagues[157] also examined the release of many therapeutic agents, including DA, from microencapsulated mammalian cells. The mammalian cells and tissues were entrapped in polymeric microcapsules containing the desired bioactive agent.

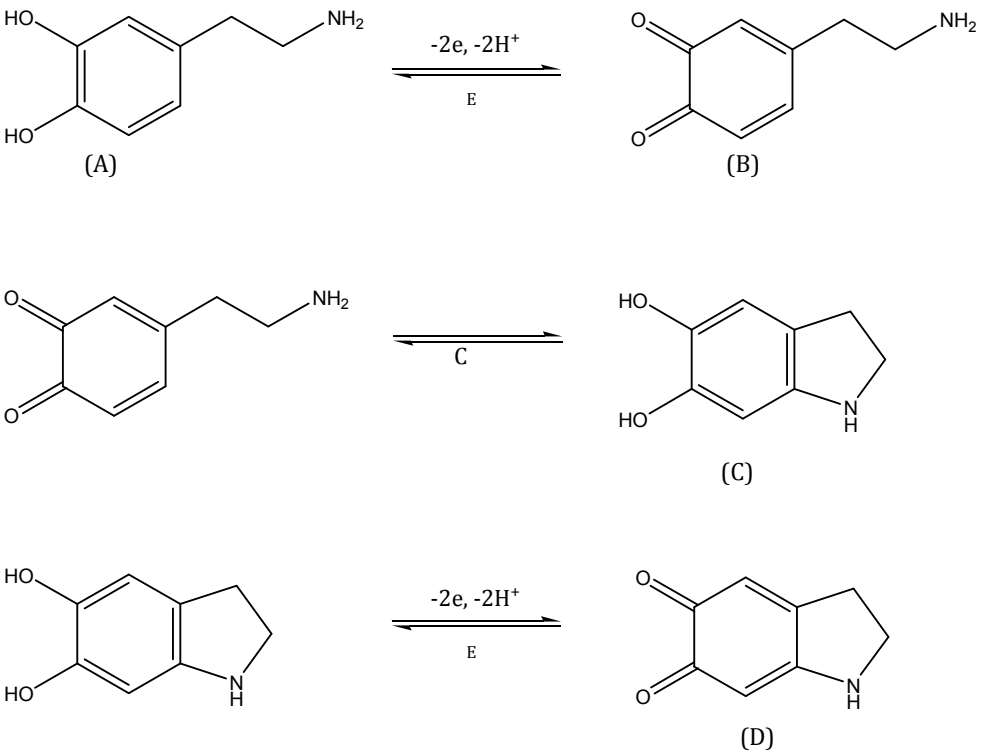


**Scheme 1.1:** The proposed oxidative pathway for dopamine.

In both these cases the release was based on diffusion from the polymeric materials. It is, therefore, difficult to maintain any control over the amount of DA released. Miller[67] and Zhou[158] and co-workers investigated the use of CPs to deliver DA. They introduced the concept of using large immobile dopants, which remain entrapped inside the cavity during polymerisation, to bind and successfully liberate DA from the polymer films.

This is the basis of the work performed in this thesis. As outlined at the start of this chapter, the idea of this research is to develop PPy films for the uptake and release of DA, using a large immobile anionic cyclodextrin. The cyclodextrin, in addition to its large size and immobility, has unique host-guest complexation properties and this offers the prospects of inclusion complexation between the DA and the CD to enhance the drug delivery. If this can be achieved it could potentially serve as a model system in DDS and could be extended to various other cationic drug molecules.

## 1.2 References


1. N. A. Peppas and D. J. A. Ende, *J Appl Polym Sci*, **66**, (1997), 509-513.
2. U. R. Pothakamury and G. V. BarbosaCanovas, *Trends Food Sci Tech*, **6**, (1995), 397-406.
3. B. Singh, D. K. Sharma, and A. Gupta, *J Environ Sci Heal B*, **44**, (2009), 113-122.
4. N. A. Peppas and R. Langer, *Science*, **263**, (1994), 1715-1720.
5. K. E. Uhrich, S. M. Cannizzaro, R. S. Langer, and K. M. Shakesheff, *Chem Rev*, **99**, (1999), 3181-3198.
6. D. L. Wise, Encyclopedic handbook of biomaterials and bioengineering Marcel Dekker, 1995.
7. J. T. Santini, A. C. Richards, R. Scheidt, M. J. Cima, and R. Langer, *Angew Chem Int Edit*, **39**, (2000), 2397-2407.
8. R. Langer, *Mrs Bull*, **31**, (2006), 477-485.
9. L. K. Fung and W. M. Saltzman, *Adv Drug Deliver Rev*, **26**, (1997), 209-230.
10. R. Langer, *Science*, **249**, (1990), 1527-1533.
11. R. Langer, *Nature*, **392**, (1998), 5-10.
12. J. Folkman and D. Long, *JOURNAL OF SURGICAL RESEARCH*, **4**, (1963), 139-142.
13. T. M. Allen and P. R. Cullis, *Science*, **303**, (2004), 1818-1822.
14. J. J. Wang, G. J. Zheng, L. Yang, and W. R. Sun, *Analyst*, **126**, (2001), 438-440.
15. H. Wartlick, K. Michaelis, S. Balthasar, K. Strebhardt, J. Kreuter, and K. Langer, *J Drug Target*, **12**, (2004), 461-471.
16. L. M. Lira and S. I. C. de Torresi, *Electrochem Commun*, **7**, (2005), 717-723.
17. S. Murdan, *J Control Release*, **92**, (2003), 1-17.
18. J. E. Riviere and M. C. Heit, *Pharmaceut Res*, **14**, (1997), 687-697.
19. G. Inzelt, Conducting Polymers, A new era in electrochemistry, Springer, 2008.
20. V. V. Walatka, M. M. Labes, and Perlstei.Jh, *Phys Rev Lett*, **31**, (1973), 1139-1142.
21. H. Shirakawa, E. J. Louis, A. G. Macdiarmid, C. K. Chiang, and A. J. Heeger, *J Chem Soc Chem Comm*, (1977), 578-580.
22. A. J. Heeger, *Angew Chem Int Edit*, **40**, (2001), 2591-2611.
23. A. G. MacDiarmid, *Angew Chem Int Edit*, **40**, (2001), 2581-2590.
24. H. Shirakawa, *Angew Chem Int Edit*, **40**, (2001), 2575-2580.
25. P. Chandrasekhar, Conducting Polymers, Fundamentals and Applications: A practical approach, Kluwer Acandemic Publishers, 1999.
26. A. A. Entezami and B. Massoumi, *Iran Polym J*, **15**, (2006), 13-30.
27. N. K. Guimard, N. Gomez, and C. E. Schmidt, *Prog Polym Sci*, **32**, (2007), 876-921.
28. A. Malinauskas, J. Malinauskiene, and A. Ramanavicius, *Nanotechnology*, **16**, (2005), R51-R62.
29. C. E. Schmidt, V. R. Shastri, J. P. Vacanti, and R. Langer, *P Natl Acad Sci USA*, **94**, (1997), 8948-8953.
30. J. L. Bredas and G. B. Street, *Accounts Chem Res*, **18**, (1985), 309-315.

31. D. L. Wise, Electrical and optical polymer systems, CRC Press, 1998.
32. L. Alcacer, Conducting Polymers: Special Applications (Hardcover), Springer 1986.
33. B. Winther-Jensen, J. Chen, K. West, and G. Wallace, *Polymer*, **46**, (2005), 4664-4669.
34. A. Malinauskas, *Polymer*, **42**, (2001), 3957-3972.
35. R. A. Green, N. H. Lovell, G. G. Wallace, and L. A. Poole-Warren, *Biomaterials*, **29**, (2008), 3393-3399.
36. T. A. Skotheim and J. R. Reynolds, Handbook of conducting polymers: Conjugated polymers, CRC Press, 2007.
37. P. C. Lacaze, J. C. Lacroix, K. C. Ching, and S. Aeiyach, *Actual Chimique*, (2008), 90-91.
38. M. A. Mohamoud, *Plast Eng*, **64**, (2008), 32-+.
39. M. Nikolou and G. G. Malliaras, *Chem Rec*, **8**, (2008), 13-22.
40. E. Smela, *Mrs Bull*, **33**, (2008), 197-204.
41. M. R. Abidian, D. H. Kim, and D. C. Martin, *Adv Mater*, **18**, (2006), 405-409.
42. C. Arbizzani, M. Mastragostino, L. Nevi, and L. Rambelli, *Electrochim Acta*, **52**, (2007), 3274-3279.
43. K. Kontturi, P. Pentti, and G. Sundholm, *J Electroanal Chem*, **453**, (1998), 231-238.
44. Y. L. Li, K. G. Neoh, and E. T. Kang, *J Biomed Mater Res A*, **73A**, (2005), 171-181.
45. J. M. Pernaut and J. R. Reynolds, *J Phys Chem B*, **104**, (2000), 4080-4090.
46. P. Burgmayer and R. W. Murray, *J Am Chem Soc*, **104**, (1982), 6139-6140.
47. A. Dall'Olio, G. Dascola, V. Varacca, and V. Bocchi, *Comptes Rendus de l'Academie des Sciences*, **C267**, (1968), 433-435.
48. A. F. Diaz and J. I. Castillo, *J Chem Soc Chem Comm*, (1980), 397-398.
49. B. Winther-Jensen and N. B. Clark, *React Funct Polym*, **68**, (2008), 742-750.
50. C. K. Baker and J. R. Reynolds, *J Electroanal Chem*, **251**, (1988), 307-322.
51. S. Geetha, C. R. K. Rao, M. Vijayan, and D. C. Trivedi, *Anal Chim Acta*, **568**, (2006), 119-125.
52. Z. X. Wang, C. Roberge, L. H. Dao, Y. Wan, G. X. Shi, M. Rouabhia, R. Guidoin, and Z. Zhang, *J Biomed Mater Res A*, **70A**, (2004), 28-38.
53. Z. Zhang, R. Roy, F. J. Dugre, D. Tessier, and L. H. Dao, *J Biomed Mater Res*, **57**, (2001), 63-71.
54. A. Kotwal and C. E. Schmidt, *Biomaterials*, **22**, (2001), 1055-1064.
55. J. Y. Wong, R. Langer, and D. E. Ingber, *P Natl Acad Sci USA*, **91**, (1994), 3201-3204.
56. B. Garner, A. Georgevich, A. J. Hodgson, L. Liu, and G. G. Wallace, *J Biomed Mater Res*, **44**, (1999), 121-129.
57. X. D. Wang, X. S. Gu, C. W. Yuan, S. J. Chen, P. Y. Zhang, T. Y. Zhang, J. Yao, F. Chen, and G. Chen, *J Biomed Mater Res A*, **68A**, (2004), 411-422.
58. S. Asavapiriyanont, G. K. Chandler, G. A. Gunawardena, and D. Pletcher, *J Electroanal Chem*, **177**, (1984), 229-244.
59. J. Heinze, *Synthetic Met*, **43**, (1991), 2805-2823.
60. G. Inzelt, V. Kertesz, and A. S. Nyback, *J Solid State Electr*, **3**, (1999), 251-257.

61. C. Y. Jin, F. L. Yang, and W. S. Yang, *J Appl Polym Sci*, **101**, (2006), 2518-2522.
62. V. M. Jovanovic, A. Dekanski, G. Vlajnic, and M. S. Jovanvic, *Electroanal*, **9**, (1997), 564-569.
63. S. Sadki, P. Schottland, N. Brodie, and G. Sabouraud, *Chem Soc Rev*, **29**, (2000), 283-293.
64. J. Tamm, A. Alumaa, A. Hallik, U. Johanson, L. Tamm, and T. Tamm, *Russ J Electrochem+*, **38**, (2002), 182-187.
65. M. Pyo and J. R. Reynolds, *Chem Mater*, **8**, (1996), 128-133.
66. M. Hepel and F. Mahdavi, *Microchem J*, **56**, (1997), 54-64.
67. L. L. Miller and Q. X. Zhou, *Macromolecules*, **20**, (1987), 1594-1597.
68. G. A. Husseini and W. G. Pitt, *J Pharm Sci-Us*, **98**, (2009), 795-811.
69. X. L. Xu, X. S. Chen, P. A. Ma, X. R. Wang, and X. B. Jing, *Eur J Pharm Biopharm*, **70**, (2008), 165-170.
70. S. G. Kumbar, L. S. Nair, S. Bhattacharyya, and C. T. Laurencin, *J Nanosci Nanotechno*, **6**, (2006), 2591-2607.
71. L. Feng, S. H. Li, H. J. Li, J. Zhai, Y. L. Song, L. Jiang, and D. B. Zhu, *Angew Chem Int Edit*, **41**, (2002), 1221-+.
72. G. M. Whitesides and B. Grzybowski, *Science*, **295**, (2002), 2418-2421.
73. T. Ondarcuhu and C. Joachim, *Europhys Lett*, **42**, (1998), 215-220.
74. J. Fang, H. T. Niu, T. Lin, and X. G. Wang, *Chinese Sci Bull*, **53**, (2008), 2265-2286.
75. E. R. Kenawy, F. I. Abdel-Hay, M. H. El-Newehy, and G. E. Wnek, *Mat Sci Eng a-Struct*, **459**, (2007), 390-396.
76. Q. J. Xie, S. Kuwabata, and H. Yoneyama, *J Electroanal Chem*, **420**, (1997), 219-225.
77. E. Luong-Van, L. Grondahl, K. N. Chua, K. W. Leong, V. Nurcombe, and S. M. Cool, *Biomaterials*, **27**, (2006), 2042-2050.
78. Z. M. Huang, Y. Z. Zhang, M. Kotaki, and S. Ramakrishna, *Compos Sci Technol*, **63**, (2003), 2223-2253.
79. A. Formhals, Vol. 1975504, 1934.
80. J. Doshi and D. H. Reneker, *J Electrostat*, **35**, (1995), 151-160.
81. D. H. Reneker and I. Chun, *Nanotechnology*, **7**, (1996), 216-223.
82. A. Greiner and J. H. Wendorff, *Angew Chem Int Edit*, **46**, (2007), 5670-5703.
83. D. Li and Y. N. Xia, *Adv Mater*, **16**, (2004), 1151-1170.
84. D. H. Reneker, A. L. Yarin, H. Fong, and S. Koombhongse, *J Appl Phys*, **87**, (2000), 4531-4547.
85. T. Subbiah, G. S. Bhat, R. W. Tock, S. Pararneswaran, and S. S. Ramkumar, *J Appl Polym Sci*, **96**, (2005), 557-569.
86. G. I. Taylor, *Proc. Roy. Soc. Lond.*, **A313**, (1969), 453-475.
87. A. Bernini, O. Spiga, A. Ciutti, M. Scarselli, G. Bottoni, P. Mascagni, and N. Niccolai, *Eur J Pharm Sci*, **22**, (2004), 445-450.
88. H. J. Shin, C. H. Lee, I. H. Cho, Y. J. Kim, Y. J. Lee, I. A. Kim, K. D. Park, N. Yui, and J. W. Shin, *J Biomat Sci-Polym E*, **17**, (2006), 103-119.
89. K. Kim, Y. K. Luu, C. Chang, D. F. Fang, B. S. Hsiao, B. Chu, and M. Hadjiargyrou, *J Control Release*, **98**, (2004), 47-56.
90. R. A. Jain, *Biomaterials*, **21**, (2000), 2475-2490.

91. M. Garinot, V. Fievez, V. Pourcelle, F. Stoffelbach, A. des Rieux, L. Plapied, I. Theate, H. Freichels, C. Jerome, J. Marchand-Brynaert, Y. J. Schneider, and V. Preat, *J Control Release*, **120**, (2007), 195-204.
92. D. Luo, K. Woodrow-Mumford, N. Belcheva, and W. M. Saltzman, *Pharmaceut Res*, **16**, (1999), 1300-1308.
93. X. H. Zong, S. Li, E. Chen, B. Garlick, K. S. Kim, D. F. Fang, J. Chiu, T. Zimmerman, C. Brathwaite, B. S. Hsiao, and B. Chu, *Ann Surg*, **240**, (2004), 910-915.
94. Z. M. Huang, C. L. He, A. Z. Yang, Y. Z. Zhang, X. J. Hang, J. L. Yin, and Q. S. Wu, *J Biomed Mater Res A*, **77A**, (2006), 169-179.
95. E. R. Kenawy, G. L. Bowlin, K. Mansfield, J. Layman, D. G. Simpson, E. H. Sanders, and G. E. Wnek, *J Control Release*, **81**, (2002), 57-64.
96. G. Bidan, B. Ehui, and M. Lapkowski, *J Phys D Appl Phys*, **21**, (1988), 1043-1054.
97. F. R. F. Fan and A. J. Bard, *J Electrochem Soc*, **133**, (1986), 301-304.
98. G. Bidan, C. Lopez, F. Mendesviegas, E. Vieil, and A. Gadelle, *Biosens Bioelectron*, **10**, (1995), 219-229.
99. D. A. Reece, S. F. Ralph, and G. G. Wallace, *J Membrane Sci*, **249**, (2005), 9-20.
100. K. R. Temsamani, O. Ceylan, B. J. Yates, S. Oztemiz, T. P. Gbatu, A. M. Stalcup, H. B. Mark, and W. Kutner, *J Solid State Electr*, **6**, (2002), 494-497.
101. N. Izaoumen, D. Bouchta, H. Zejli, M. El Kaoutit, A. M. Stalcup, and K. R. Temsamani, *Talanta*, **66**, (2005), 111-117.
102. A. Villiers, *C. R Acad. Sci*, **112**, (1891), 536.
103. F. Schardinger, *Wien. Klin. Wochenschr*, **17**, (1904), 207.
104. A. R. Hedges, *Chem Rev*, **98**, (1998), 2035-2044.
105. J. Szejtli, *J Mater Chem*, **7**, (1997), 575-587.
106. W. Saenger, *Angewandte Chemie-International Edition in English*, **19**, (1980), 344-362.
107. D. French, *Method Enzymol*, **3**, (1957), 17-20.
108. H. Dodziuk, Cyclodextrins and Their Complexes, 2006.
109. J. Szejtli, *Chem Rev*, **98**, (1998), 1743-1753.
110. A. Harada and S. Takahashi, *J Chem Soc Chem Comm*, (1984), 645-646.
111. M. V. Rekharsky and Y. Inoue, *Chem Rev*, **98**, (1998), 1875-1917.
112. K. Uekama, F. Hirayama, and T. Irie, *Chem Rev*, **98**, (1998), 2045-2076.
113. V. Zia, R. A. Rajewski, and V. J. Stella, *Pharmaceut Res*, **18**, (2001), 667-673.
114. L. X. Wang, X. G. Li, and Y. L. Yang, *React Funct Polym*, **47**, (2001), 125-139.
115. F. T. A. Chen, G. Shen, and R. A. Evangelista, *J Chromatogr A*, **924**, (2001), 523-532.
116. G. K. E. Scriba, *J Sep Sci*, **31**, (2008), 1991-2011.
117. A. Amini, T. Rundlof, M. B. G. Rydberg, and T. Arvidsson, *J Sep Sci*, **27**, (2004), 1102-1108.
118. F. Hirayama and K. Uekama, *Adv Drug Deliver Rev*, **36**, (1999), 125-141.
119. X. J. Dang, M. Y. Nie, J. Tong, and H. L. Li, *J Electroanal Chem*, **448**, (1998), 61-67.
120. L. Fielding, *Tetrahedron*, **56**, (2000), 6151-6170.

121. P. Job, **9**, (1928), 113-203.
122. J. Mosinger, V. Tomankova, I. Nemcova, and J. Zyka, *Anal Lett*, **34**, (2001), 1979-2004.
123. W. Misiuk and M. Zalewska, *Anal Lett*, **41**, (2008), 543-560.
124. J. B. Chao, H. B. Tong, Y. F. Li, L. W. Zhang, and B. T. Zhang, *Supramol Chem*, **20**, (2008), 461-466.
125. I. Bratu, J. M. Gavira-Vallejo, A. Hernanz, M. Bogdan, and G. Bora, *Biopolymers*, **73**, (2004), 451-456.
126. I. V. Terekhova, R. S. Kumeev, and G. A. Alper, *J Incl Phenom Macro*, **59**, (2007), 301-306.
127. J. R. Cruz, B. A. Becker, K. F. Morris, and C. K. Larive, *Magn Reson Chem*, **46**, (2008), 838-845.
128. H. A. Benesi and J. H. Hildebrand, *J Am Chem Soc*, **71**, (1949), 2703-2707.
129. M. S. Ibrahim, I. S. Shehatta, and A. A. Al-Nayeli, *J Pharmaceut Biomed*, **28**, (2002), 217-225.
130. R. Ramaraj, V. M. Kumar, C. R. Raj, and V. Ganesane, *J Incl Phenom Macro*, **40**, (2001), 99-104.
131. C. Yanez, L. J. Nunez-Vergara, and J. A. Squella, *Electroanal*, **15**, (2003), 1771-1777.
132. G. C. Zhao, J. J. Zhu, J. J. Zhang, and H. Y. Chen, *Anal Chim Acta*, **394**, (1999), 337-344.
133. E. Coutouli-Argyropoulou, A. Kelaidopoulou, C. Sideris, and G. Kokkinidis, *J Electroanal Chem*, **477**, (1999), 130-139.
134. Y. Y. Zhou, C. Liu, H. P. Yu, H. W. Xu, Q. Lu, and L. Wang, *Spectrosc Lett*, **39**, (2006), 409-420.
135. K. A. Connors, *Chem Rev*, **97**, (1997), 1325-1357.
136. L. Liu and Q. X. Guo, *J Incl Phenom Macro*, **42**, (2002), 1-14.
137. W. Saenger and T. Steiner, *Acta Crystallogr A*, **54**, (1998), 798-805.
138. Y. Matsui and A. Okimoto, *B Chem Soc Jpn*, **51**, (1978), 3030-3034.
139. L. X. Song, B. L. Li, R. Jiang, J. G. Ding, and Q. J. Meng, *Chinese Chem Lett*, **8**, (1997), 613-614.
140. I. Tabushi, Y. I. Kiyosuke, T. Sugimoto, and K. Yamamura, *J Am Chem Soc*, **100**, (1978), 916-919.
141. K. Okimoto, R. A. Rajewski, K. Uekama, J. A. Jona, and V. J. Stella, *Pharmaceut Res*, **13**, (1996), 256-264.
142. L. Szente and J. Szejtli, *Trends Food Sci Tech*, **15**, (2004), 137-142.
143. J. Szejtli, *Pure Appl Chem*, **76**, (2004), 1825-1845.
144. T. Irie and K. Uekama, *Adv Drug Deliver Rev*, **36**, (1999), 101-123.
145. J. Li and X. J. Loh, *Adv Drug Deliver Rev*, **60**, (2008), 1000-1017.
146. K. Uekama, *J Incl Phenom Macro*, **44**, (2002), 3-7.
147. K. Uekama, F. Hirayama, and H. Arima, *J Incl Phenom Macro*, **56**, (2006), 3-8.
148. A. Ferancova and J. Labuda, *Fresen J Anal Chem*, **370**, (2001), 1-10.
149. K. R. Temsamani, H. B. Mark, W. Kutner, and A. M. Stalcup, *J Solid State Electr*, **6**, (2002), 391-395.
150. J. A. Kiernan and M. L. Barr, Barr's the Human Nervous System: An Anatomical Viewpoint, Lippincott Williams & Wilkins, 2008.
151. J. Nolte and J. W. Sundsten, The Human Brain: An Introduction to Its Functional Anatomy, Mosby, 1998.

152. R. H. Thompson, The Brain: A Neuroscience Primer, W H Freeman & Co, 1993.
153. M. D. Hawley, S. Tatawawa, S. Piekarsk, and R. N. Adams, *J Am Chem Soc*, **89**, (1967), 447-&.
154. T. Luczak, *Electroanal*, **20**, (2008), 1639-1646.
155. R. Langer, *J Control Release*, **16**, (1991), 53-59.
156. A. Mcraedegueurce, S. Hjorth, D. L. Dillon, D. W. Mason, and T. R. Tice, *Neurosci Lett*, **92**, (1988), 303-309.
157. H. Uludag, J. E. Babensee, T. Roberts, L. Kharlip, V. Horvath, and M. V. Sefton, *J Control Release*, **24**, (1993), 3-11.
158. Q. X. Zhou, L. L. Miller, and J. R. Valentine, *J Electroanal Chem*, **261**, (1989), 147-164.

## 1.1 Introduction

The initial aim of this work was to examine the use of polypyrrole (PPy), a well-known conducting polymer, for the uptake and release of a cationic species, dopamine (DA). DA was chosen as it represents a large family of amine-based drugs. Therefore, if appropriate PPy films could be electrosynthesised and used in the controlled delivery of DA, then the concept could be used more widely in the field of controlled drug delivery.

In Chapter 3, the growth of PPy films in the presence of various dopant anions, including a large anionic cyclodextrin (CD), sulfonated β-cyclodextrin (Sβ-CD) is explored. Although Sβ-CD doped PPy films have been reported in the recent literature, there has been very little work devoted to the characterisation of these films. Accordingly, much of Chapter 3 is devoted to the unique redox properties of the Sβ-CD doped PPy films.

With the growth of the PPy films achieved, Chapter 4, shows the drug release profiles of the protonated DA and reveals that in the case of the polymer films doped with the anionic Sβ-CD, there is a substantial increase in the amount of DA released in comparison to other polymer films. In order to explain the enhanced release profiles, the well-known supramolecular complexation properties of cyclodextrins were considered. However, on searching the literature no reports on the complexation of DA with anionic cyclodextrins were found and consequently this was studied in detail. These findings are presented in Chapter 5, where the host-guest interactions between DA and the anionic Sβ-CD are examined using a variety of techniques, both spectroscopic and electrochemical.

In Chapter 6 the technique of electrospinning is introduced. Details on how it is used to fabricate nanostructured biodegradable polymer films with a high surface area are provided. The approaches used to deposit the Sβ-CD doped PPy films onto the nanostructured biodegradable film are then considered and discussed. It is shown that cyclic voltammetry was the most successful

approach. Moreover, it was possible to control the amount of PPy deposited and to maintain the nanostructured fiber substrate by varying the number of cycles. These high surface area Sβ-CD doped PPy films are promising for the uptake and liberation of DA.

In this introductory chapter, the concept of controlled drug release is firstly introduced. This is then followed with information on conducting polymers, particularly PPy and the current state-of-art in using PPy in drug delivery. The technique of electrospinning is then introduced and linked to DDS. The next section is devoted to cyclodextrins, as it is the Sβ-CD doped PPy films that give the best controlled release properties. Finally, the chapter ends with a short account of the properties of DA and its delivery.

### 1.1.1 Controlled drug release

In the early 1970s, controlled release systems first materialised. Since then, the number and the areas in which a controlled release system is utilised have significantly increased. These systems have been used in areas such as cosmetics[1], food[2], and pesticides[3]. Controlled release systems are focused on obtaining the release of the proposed material, over a certain time without an external influence from any other potential release factor.[4] Polymeric materials have been previously investigated for controlled release as they can be easily manufactured and their composition can be finely tuned.[5] Polymers used in controlled release systems can be natural or synthetic and release can be achieved through the engineering of the polymer substrates, i.e., the degradation of poly($_{D,L}$ – lactide-*co*-glycolide) (PLGA) can be controlled through the polymer composition, higher ratios of PLA lead to a higher degradation rate.[6]

Another important research area under consideration is the development of controlled drug delivery systems (DDS).[7, 8] In 1980, controlled DDS were virtually unknown, yet in 2005, almost 100 million people globally were using some form of polymer based DDS.[8] The aim of a DDS is to supply the drug in its

therapeutically active form to a specific target in the body when the drug is required. In the current administration process there is a critical concentration needed in order to achieve the drug's maximum therapeutic effect. If the concentration goes beyond the maximum level, toxicity problems come into play. Conversely, if the concentration administered is below the minimum level the effect of the drug is not observed. The use of these DDS could potentially eliminate these problems as the release would be of a controlled manner.

Santini *et al.*[7] compared the release profiles of both conventional and controlled methods, as illustrated in Figure 1.1. With conventional methods of drug delivery, outlined in Figure 1.1(A), i.e., oral administration or injections, drug levels rise after initial administration, which could lead to potential toxicity problems, and then decrease until the next dosage, which has consequences on the efficiency of the dosage. The other schematic, Figure 1.1(B), demonstrates the effectiveness of a controlled release system. After dosage, the drug level in the blood remains constant, between the maximum and minimum levels, for a certain period of time.

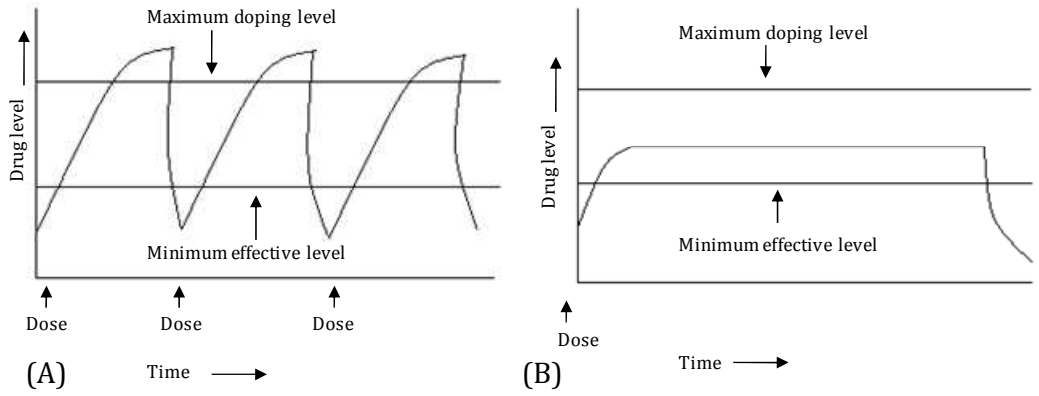


**Figure 1.1:** Drug levels in the blood with (A) conventional drug dosage (B) controlled delivery dosage, taken from Santini *et al.*[7]

In recent years, polymeric materials have been examined and shown to provide an alternate means of delivering drugs. Implanted polymeric pellets or microspheres localise therapy to specific anatomic sites, providing a continuous sustained release of drugs while minimising systemic exposure.[9] Polymers that display a physiochemical response to stimuli have been broadly researched for controlled release systems. Various stimuli include pH, temperature and the application of an electrical field.[10] According to Langer[11], polymeric DDS should i) maintain a constant drug level ii) reduce harmful side effects iii) minimise the amount of drug needed and iv) decrease the amount of doses which will have a pronounced effect on the patient.

The original polymeric controlled DDS was based on a non-biodegradable polymer, silicone rubber, which was designed and tested by Folkman and Long.[12] They loaded a silicone capsule (Silastic*) with a number of different drugs for the treatment of heart block and successfully implanted and monitored their effects over a number of days.

In more recent years there has been considerable interest in the development of new and efficient DDS, particularly with the growth of sophisticated drugs that are based on DNA and proteins.[5, 13] Currently, there are several materials under consideration in drug delivery, for example dendrimers[14], nanoparticles[15] and hydrogels[16]. The most promising opportunities in controlled DDS are in the area of responsive polymeric materials, with the possibility of implantable devices being used to deliver drugs. Murdan[17] exhaustively reviewed the use of hydrogels as 'smart' drug delivery devices. He showed that hydrogels could be engineered for various medicinal treatments depending on the patients needs, for example, pain relief. In the body, drug release can only be accomplished if the drug carrier responds to some class of stimuli, be it chemical, physical or biological. Conversely, an implanted 'smart' drug delivery device should be non-responsive to all other types of stimulus, once inside the body. A way of achieving this form of control is through an electrical stimulus.[17] A number of *in vivo* devices, in the form of iontophoresis, have already been used for this type of controlled release.[17, 18] Murdan presented a case where hydrogels loaded

with a bioactive compound, were implanted at a target site and the drug liberated through the application of an electrical field. In utilising such a system, many advantages including, minimal drug usage and lowering toxicity problems can be achieved. However, a problem arising with the application of an electrical stimuli to polymeric materials like, hydrogels, is that they experience deswelling or bending, which affects the drug release.[17]

To overcome these problems, conducting polymers (CPs) are also receiving much attention in the field of biomedical research, for the application of controlled DDS, due to their light weight, good biocompatibility and ability to function at body temperature. In particular, conducting polymers exhibit a reversible electrochemical response. These reversible oxidation-reduction reactions are attractive for a responsive DDS, as a change in the net charge on a conducting polymer film during its reduction or oxidation requires ions to flow into or out of the film. This, in turn, allows the polymer film to bind and expel ions in response to electrical signals. Controlled release of drugs from polymers offers many advantages over conventional methods including better control of the drug level administered resulting in fewer side effects, local drug delivery, decreased requirements for the total amount of drug and protection of drugs which are rapidly destroyed by the body. However, in order to devise a suitable technology, the polymeric material must be responsive, i.e., it must be capable of altering so that the drug is released in a controlled fashion when needed.

### 1.1.2 Conducting polymers

A polymer is a large molecule made up of smaller repeating units. The name comes from the Greek *poly*, meaning 'many', and *mer*, meaning 'part'. They are built up from simple molecules called *monomers* 'single part'. Polymers are produced through a method known as polymerisation. This polymerisation step can be achieved through chemical or electrochemical methods. Originally polymers with the basic carbon chains were considered only as insulators.[19] The first real interest in conducting polymers can be attributed to Walatka *et al*.[20] in 1973 with the report of highly conducting polysulfur nitride $(SN)_x$. Meanwhile

and towards the late 1970s , MacDiarmid, Shirakawa and Heeger enhanced the discovery of the semi-conducting and metallic properties of the chemically synthesised organic polyacetylene.[21-24] As is well known, the Nobel Prize in Chemistry was awarded to Alan J.Heeger, Alan G. MacDiarmid and Hideki Shirakawa in 2000 for the discovery and development of conducting polymers (CPs).[21-24] In the following years, a wide range of polymeric organic species have been prepared as stable inherent films on inert electrodes via both chemical oxidation and electropolymerisation from aqueous and organic solution.[25]

CPs are organic materials, which generally are comprised simply of C, H and simple heteroatoms such as N and S. Common examples include PPy, polyaniline and polythiophene which are shown in Figure 1.2. These and a number of other conducting polymers have been used in a variety of applications ranging from corrosion protection of materials, sensors to many biomedical applications, such as tissue engineering, nerve cell regeneration and drug delivery.[26-29]

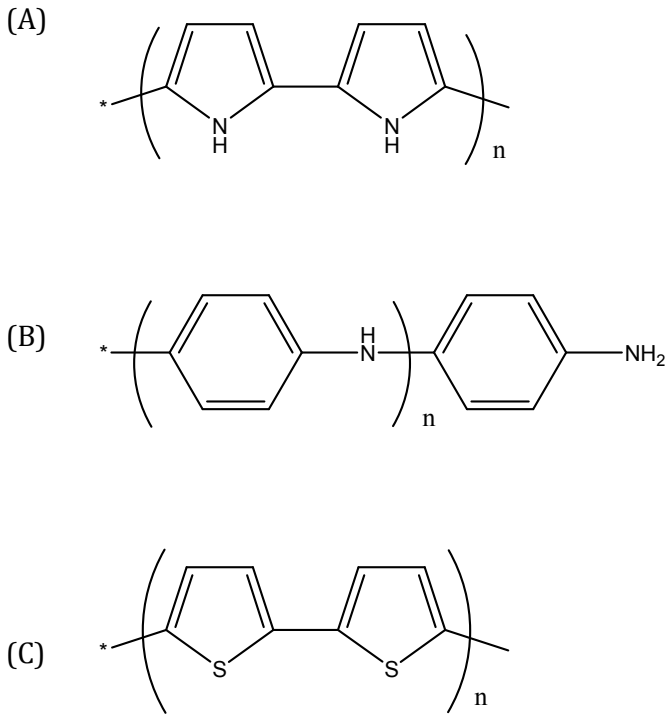


**Figure 1.2:** Chemical structures of (A) polypyrrole (B) polyaniline and (C) polythiophene. All polymers are shown in the dedoped state.

In, general materials are classed depending on their electrical conductivity, κ, where the electrical conductivity of insulators < semiconductors < conductors. Bredas and Street[30] explained this phenomenon in terms of the band gap structure. Figure 1.3 illustrates the difference in each material using the band gap theory. The highest occupied molecular orbital is equivalent to the valence band (VB), while the lowest unoccupied molecular orbital may be equated to the conduction band (CB). The difference between each band is known as the band gap energy ($E_g$) and it is this energy gap that establishes the electrical properties of a material. If $E_g$ > 10 eV, it is difficult to excite electrons into the conduction band and an insulator is formed. If $E_g \sim 1.0$ eV then thermal energy is sufficient to promote the electrons into the conduction band and a semiconductor is formed. If the gap vanishes, with overlap of the valence and conduction band, as shown in Figure 1.3, metallic conduction is observed. For most doped CPs the band gap energy is generally close to 1.0 eV, and consequently, CPs can be classified as semi-conductors.

As pointed out by Bredas and Street[30], the conductivity observed upon doping of the CPs was originally thought to be from the formation of unfilled electronic bands, however this idea was quickly dissipated upon experimental analysis of PPy and polyacetylene and now it is recognised that the conductivity is due to the formation of polarons and bipolarons, which are more energetically favoured.[30, 31]

The π-bonded system of CPs, which comprises of alternating single and double bonds, enabling the delocalisation of electrons along the polymer backbone, is related to the conductivity of the system. The conductivity of these materials arises from a state of relative oxidation or reduction. In these states the polymer either loses (oxidation) or gains (reduction) an electron. Generally, it is said that this process occurs in 1 in every 4 monomer units.[32] In this state the polymer is electronically charged and requires the introduction of counter ions (dopants) to compensate and reform the charge neutrality. The oxidation of the polymer in which an electron is removed from a π-bond, gives rise to a new energy state, which leaves the remaining electron in a non-bonding orbital. This energy level

is higher than the valence band and behaves like a heavily doped semiconductor.[32] The extent of doping can be controlled during the polymerisation of the polymers.

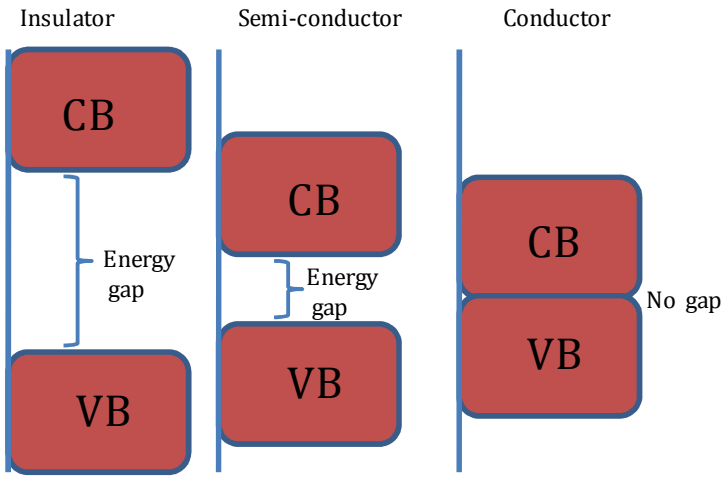


**Figure 1.3:** Schematic of the difference in band gap for Insulators, semi-conductors and metals (conductors).

### *1.1.2.1 Polymerisation methods*

CPs are synthesised through a method known as oxidative polymerisation. This can be generated chemically or electrochemically. Chemical polymerisation involves the use of a chemical oxidant, such as ammonium peroxydisulfate (APS), ferric ions, permanganate, dichromate anions or hydrogen peroxide. The oxidants not only oxidise the monomer but provide dopant anions to neutralise the positive charges formed on the polymer backbone.[33] In the presence of these oxidants, the monomers are oxidised and chemically active cation radicals are formed which further react with the monomer and generate the desired polymer. An advantage of vapour phase chemical polymerisation of CPs is that the polymerisation occurs almost exclusively on the preferred surface and a higher surface area can be attained.[34] Vapour phase chemical polymerisation of

pyrrole leads to further doping after polymerisation and this gives rise to an increase in conductivity.[35]

The electrochemical deposition is a simple and reproducible technique where the dopant is present in the electrolyte during polymerisation. It is generally performed in a conventional three electrode set up, described later in Chapter 2, where current is passed through a solution containing the monomer in the presence of a dopant (electrolyte). The CP is deposited at the positively charged working electrode or anode.[27] Polymerisation is initiated through the oxidation of the monomer which forms a mobile charge carrier known as a polaron (radical cation), that can react with another monomer or polaron to form a bipolaron (radical dication) which leads to the formation of the insoluble polymer chain and deposition of the polymer onto the working electrode.[36]

In his book 'Conducting Polymers' published in 1986, Alcacer commented on the possibility of using CPs to make artificial muscles or perhaps even modification for the brain; little did he realise the extent to which these materials have been extensively researched, over the past 20 years.[32] Since their discovery, the preparation and characterisation of these materials has evolved substantially through the use of electrochemistry. The majority of research is significantly based in this area due to the ease and control of synthesis of these electronically CPs.[19] Reviews on the development of CPs show the various areas to where they can be applied. The applications are ongoing.[37-40] However, in the case of DDS, CPs, in particular PPy, are widely researched for the controlled release of therapeutically active compunds.[41-45] During oxidative polymerisation, a dopant molecule, with an overall anionic charge, is used to compensate for the positive charges originating from the oxidation of the monomer. It is during this process that the concept of drug delivery originated. Burgmayer and Murray[46] observed changes in the ionic permeability of PPy redox membranes using a voltage-controlled electrochemical reaction. This led to further investigations into the application of CPs in DDS.

### *1.1.2.2 Polypyrrole*

#### 1.1.2.2.1 Historical background of polypyrrole

In 1968 Dall'Olio and colleagues prepared black films of an oxypyrrole on platinum by the electrochemical polymerisation of pyrrole from a solution of sulfuric acid.[47] In 1979 Diaz with the help of colleagues modified Dall'Olio's approach and demonstrated that polymerising pyrrole onto platinum in acetonitrile led to a black, adherent film.[48] Elemental analysis showed that the monomer unit was retained in the polymer. PPy in general, was poorly crystalline, and its ideal structure was a planar (α-ά)-bonded chain in which the orientation of the pyrrole molecules alternate.[25]

The monomer unit, pyrrole, is shown in Figure 1.4. PPy is an organic material comprised simply of C, H and a simple N heteroatom, but is highly conducting. It is an inherently conductive polymer due to interchain hopping of electrons. PPy can be synthesised both chemically[49] and electrochemically[48]. The electrochemical synthesis method is a one step synthesis method and allows the simple deposition of polymer films where its surface charge characteristics can easily be modified by changing the dopant anion (A-) that is incorporated into the material during synthesis. In a cell containing an aqueous or non-aqueous solution of the monomer, PPy forms a (semi) conducting film on the working electrode; the film grown is in the oxidised form and can be reduced to the non-conducting insulating form by stepping the potential to more negative values. The potential cycling can be repeated many times between the insulating and (semi) conducting forms without a loss of the electroactivity of the film.[25]

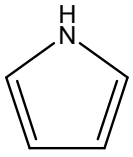


**Figure 1.4:** Schematic illustration of a monomer unit of pyrrole.

PPy in its neutral form is weakly coloured while the oxidised form is a deep blue/black. The switching of the state of the film not only changes its conductivity but it is also accompanied by a marked colour change, termed electrochromism.[36] Materials such as PPy are important in terms of future technological impact as it may be possible to develop them to replace more expensive, often toxic, metallic conductors commonly employed in the electronics industry.[25]

#### 1.1.2.2.2 Polymerisation mechanism of pyrrole

Although there are still various opinions on the mechanistic features of the electropolymerisation of pyrrole, the mechanism proposed by Diaz and his colleagues[48] and later used by Baker and Reynolds is in good agreement with many experimental reports.[50] The mechanism is demonstrated in Figure 1.5.

The initial step is the generation of the radical cation. This cation has different resonance forms, as shown in Figure 1.5. In the next step in the chemical case, the radical cation then attacks another monomer molecule, generating a dimer radical cation. In the electrochemical case, the concentrations of radical cations is much larger than that of neutral monomers in the vicinity of the electrode where reactions are occurring, and radical-radical coupling leads to a radical dication. This coupling between the two pyrrole radicals results in the formation of a bond between the two $\alpha$ positions to give the radical dication, as highlighted in Figure 1.5. This is then followed by the loss of two protons, generating a neutral dimer. This dimer is then oxidised into a radical cation, where the unpaired electron is delocalised over the dimer. The radical dimer then couples with the radical monomer to form a trimer. The polymerisation thus progressing in this fashion to completion.

The controversy in the mechanism of electropolymerisation is not surprising given that many factors, such as the nature of the electrolyte, ionic strength, pH, temperature and potential are important and can influence the mechanism of the reaction.

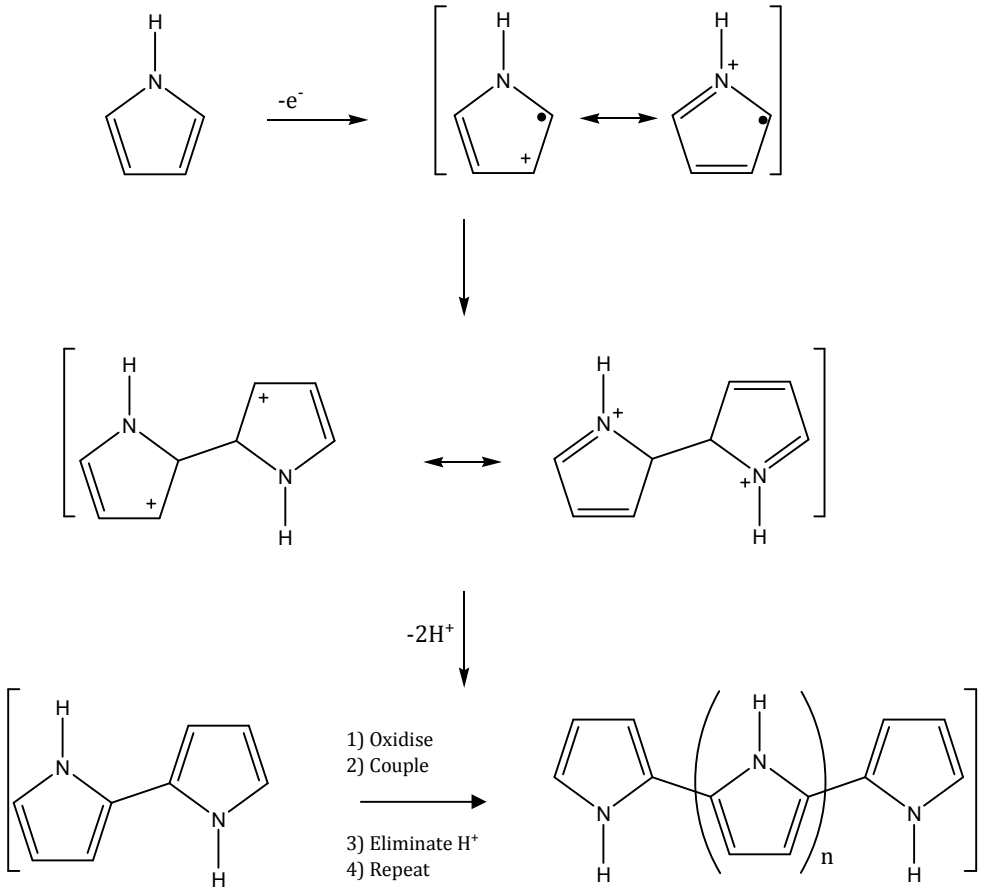


**Figure 1.5:** Mechanism of electrochemical polymerisation of pyrrole.[50]

#### 1.1.2.2.3 Biocompatibility

PPy is one of the most widely researched conductive polymers. The fact that it can form biologically compatible matrices is one of the prominent reasons for the extensive research on the use of PPy in the field of biological applications.[51] Wang *et al.*[52] acknowledged the reality that PPy had showed very good *in vitro* biocompatibility,[29, 53, 54] but they wanted to evaluate further the *in vivo* biocompatibility prospects. They demonstrated that in comparison to no PPy, the presence of PPy/biodegradable composites stimulated no abnormal tissue response and had no affect on the degradation behaviour of the biodegradable materials. In 1994, PPy was one of the first conducting polymers investigated for its effect on mammalian cells.[55] Since then, PPy is known to be

biocompatible, so it can be placed in the body without having adverse effects. It has been shown, in particular, to support cell growth and adhesion of endothelial cells.[29, 55-57] Schmidt *et al*.[29] also demonstrated that PPy was a suitable material for both in vitro nerve cell culture and in vivo implantation. PPy was electrochemically deposited onto ITO-conductive borosilicate glass. Moreover, the application of an external electrical stimulus through the polymer film resulted in enhanced neurite outgrowth. The median neurite length for PC-12 cells grown on PPy film subjected to an electrical stimulus increased nearly two-fold compared with cells grown on PPy without the application of a constant potential. The group also investigated PPy in vivo and their studies showed that PPy promotes little negative tissue and inflammatory response. Due to the good biocompatible factor, studies on the application of an electric field to the PPy have also shown cell compatibility.[29] In some important applications, such as biological sensors and actuators for medical devices it is a very attractive trait and some recent applications show that PPy can enhanced nerve cell regeneration and tissue engineering.[27]

#### 1.1.2.2.4 Electroactivity of polypyrrole

PPy can be easily switched between the neutral, partially oxidised and fully oxidised states, as shown in Figure 1.6. In its neutral state PPy exists as an insulator where the conduction band is empty as all the electrons remain in the valence band. Upon oxidation, an electron is removed from a π-bond (valence band) and a polaron is formed. The separation of the positive charge and the unpaired electron decreases during continual oxidation as the number of polarons increases. This in turn gives rise to the formation of a bipolaron, as depicted in Figure 1.6(C), and the polymer is now in its fully oxidised state.

During oxidation and the generation of positive charge an influx of anions into the polymer matrix is observed in order to maintain charge balance. This can be represented in Equation 1.1, where $PPy^{o}$ refers to the neutral (reduced) polymer, $PPy^{+}$ refers to the oxidised polymer and $A^{-}$ refers to the anionic dopant.

$$PPy^0 + A^- \rightarrow PPy^+A^- + e^- \quad 1.1$$

Typical anionic dopants are chlorides, bromides, iodides, perchlorates, nitrates, sulfates and para-toluene sulfonates.[58-64] The extent of oxidation/reduction is given by the doping level and this is generally expressed as the ratio of dopant anions, $A^-$, incorporated per monomer unit. For example, 1 $A^-$ per 4 monomer units gives a doping level of 0.25 or 25%. The maximum doping level achievable with PPy is 0.33 or 33%, i.e., 1 $A^-$ per 3 pyrrole units. It is important to point out that doping may not always be uniform; there can be islands with high doping levels surrounding by regions with a much lower doping level.

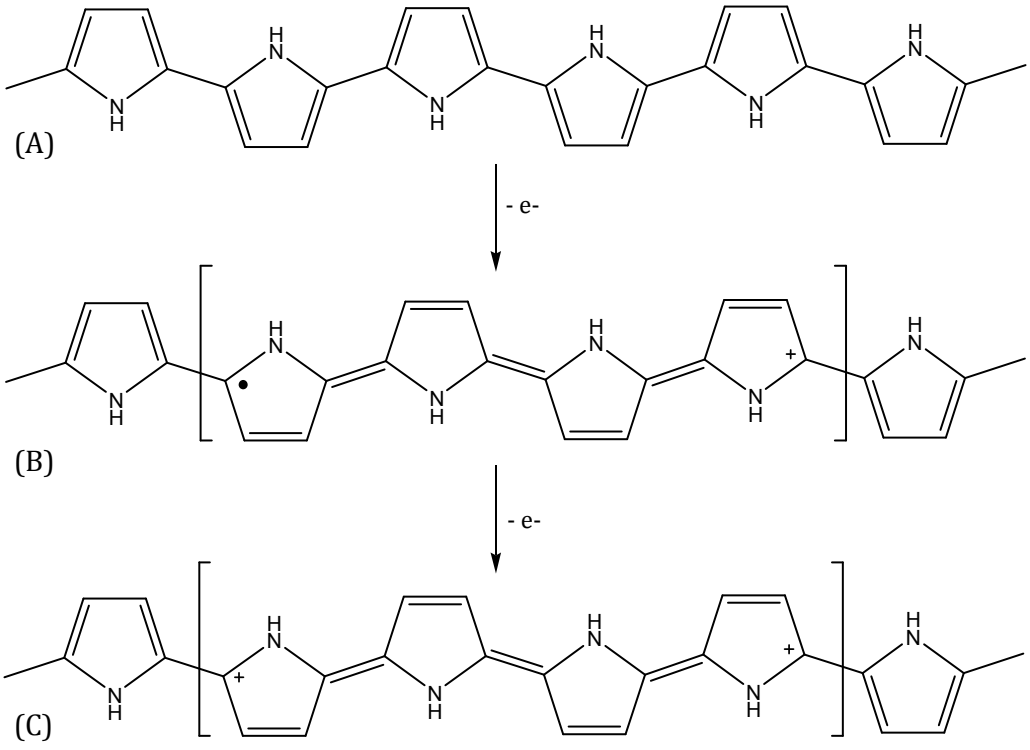


**Figure 1.6:** Electronic structures of (A) neutral PPy, (B) polaron in partially doped PPy and (C) bipolaron in fully doped (oxidised) PPy.[36]

**1.1.2.2.5 Polypyrrole and drug delivery**

The electrochemical switching of PPy films is accompanied by movement of counter or dopant ions in and out of the polymer matrix to maintain the charge neutrality, as shown in Section 1.1.2.3.4. Consequently, PPy films are attractive for the controlled release of drug molecules. The concept of using PPy membranes for the uptake and release of ions was introduced, in the early 1980s, by Burgmayer and Murray[46]. They demonstrated that these polymeric films could be exchanged from their oxidised state to their neutral state. PPy has been seriously considered for drug delivery due to these unique redox properties. PPy gives a responsive material needed in order for the uptake and release of the drug to be controlled; in its oxidised state anions are electrostatically bound to the polymer film. These properties allow the controlled transport of ions. The uptake of these ions can occur in two ways. The first is where the bioactive molecule exists as an anion and is involved in the doping process of the polymeric material during polymerisation, Figure 1.7 (A). Some anions that have been researched include adenosine tri phosphate (ATP)[65], salicylate[26], and dexamethasome[26]. These anions are electrostatically entrapped into the polymer matrix during the growth process upon application of an anodic potential. The anions are consequently liberated during the reduction of the polymer.

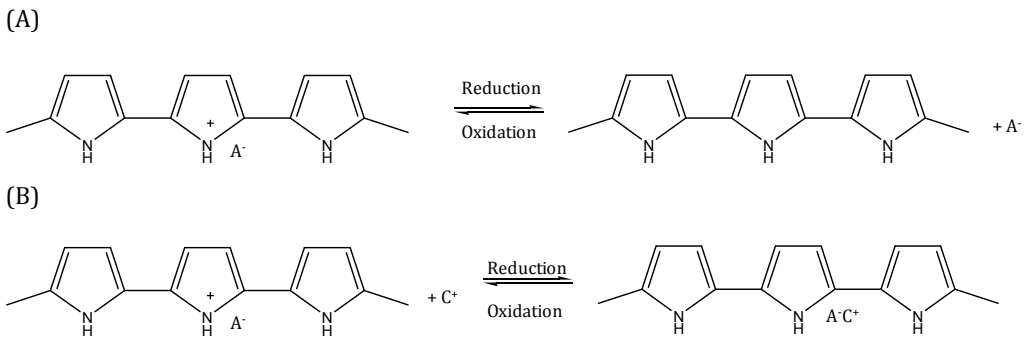


**Figure 1.7:** Interconversion between oxidation and reduction states of PPy (PPy). (A) Anion (A-) incorporation and release which is notably observed in small mobile anions (e.g. Cl-) while, (B) Cation (C+) insertion and liberation from polymer films doped with larger anions (e.g. $DDS^-$) which remain entrapped in the polymer matrix.

In the second case, cations can be incorporated into the system, Figure 1.7 (B), if the properties of the polymer film are modified.[66] This is achieved through the

initial inclusion of a large anion which remains entrapped in the polymer matrix and thus the polymer behaves as a cation exchanger, where, the charge of the polymer system can only be compensated through the uptake of cations. The cations are therefore, taken in during the reduction of the polymer and released upon oxidation. Figure 1.7 demonstrates both these concepts.

Miller and Zhou[67] previously reported the release of dopamine from a poly(*N*-methlypyrrole)/poly(styrenesulfonate) (PNMP/PSS) polymer based on the properties of these redox polymers. Immobilisation of PSS, a large anion, allows the uptake and release of the cation upon appropriate application of a potential. They achieved the release of dopamine using potential control, while more recently, Hepel and Mahdavi[66] demonstrated the controlled release of a cationic species, chloropromazine, from a composite polymer film based on the same principles. They reported the development of a new composite conducting polymer, PPy/melanin, which performed as a cation binder and releaser. The modification of the polymer films, to enable the predominant cationic exchange properties of the CP, is an interesting way of improving the uptake and release of cationic species from these attractive materials.

New ways of improving the controlled release of drugs are continually being sought after. Lately, Abidan *et al*.[41] reported on a method to prepare conducting-polymer nanotubes that can be used for controlled drug release. They introduced a method known as electrospinning to fabricate a nanofibrous mat in which the drug to be delivered had previously been incorporated; followed by electrochemical deposition of PPy films around the drug-loaded, electrospun biodegradable polymers. The drug release was achieved through the electrical stimulation of the PPy nanotubes.

#### 1.1.2.2.6 The application of Nanotechnology in drug delivery

Nanotechnology, although dating back to much earlier times, gained considerable attention in the early 1990s and has been the focus of much research over the last number of years. The introduction of nanotechnology into a controlled DDS has been shown to enhance many physical and chemical properties and overall has been used to increase the surface area of materials. This, in turn, leads to an increase in the amount of drug released from various materials. Many groups have introduced nanotechnology in various forms to improve on the drug delivery of a number of bioactive compounds, including nanoparticles[15], micellar systems[68] and nanofibers[69]. Polymeric nanofibers are gaining substantial interest for various applications including drug delivery[69, 70]. Several techniques have been employed for the production of nanofibers such as template synthesis[71], self assembly[72] and drawing[73]. One technique, in particular that is receiving considerable interest in this field, is electrospinning.[74-77] Electrospinning has been introduced to achieve nanoscale membranes and fibres from various polymeric materials.[78]

**1.1.2.2.7 The application of Electrospinning to drug delivery**

Although electrospinning was first reported by Formhals[79] in 1934 it has only been explored further in recent times.[80, 81] In 1996, Reneker and Chun restored interest in the electrospinning technique by demonstrating the possibility of electrospinning a wide range of organic polymers.[81] Since then the technique of electrospinning has become extremely useful in a variety of applications.[82-85] Electrospinning is a simple and inexpensive means for the formation of nano- to micron polymer fibers.

This technique involves the application of a high electric field between a polymer fluid and a grounded electrode. When the polymer solution is subjected to an external electric field at a critical point the forces overcome the surface tension of the polymer solution to form a droplet with a conical shape, i.e., the Taylor cone.[83, 86] The fluid is drawn into a jet which undergoes a whipping motion. Volatile solvents are used to dissolve the polymer as the subsequent evaporation from the liquid jet results in solid fibers. A more detailed

description of this technique is provided in Chapter 2, Section 2.4.5. In the majority of cases the fibers deposit randomly on the grounded collector. However, many groups have investigated the use of rotating collector plates to produce aligned nanofibers.[87] Figure 1.8 illustrates a typical SEM micrograph of an electrospun fiber mat of PLGA fibers.

This production of nanofibers allows these polymers to be used in a wide variety of applications including, tissue engineering (muscles, skin, cartilage and bones), wound healing and sutures, biosensors and DDS. Shin *et al.*[88] studied the use of PLGA nanofiber scaffold for cartilage reconstruction, while, Kim and colleagues incorporated antibiotics in the fibrous matrix for use in wound dressings.[89] Other groups have also prepared ultrafine polymers via electrospinning for skin regeneration.[74]

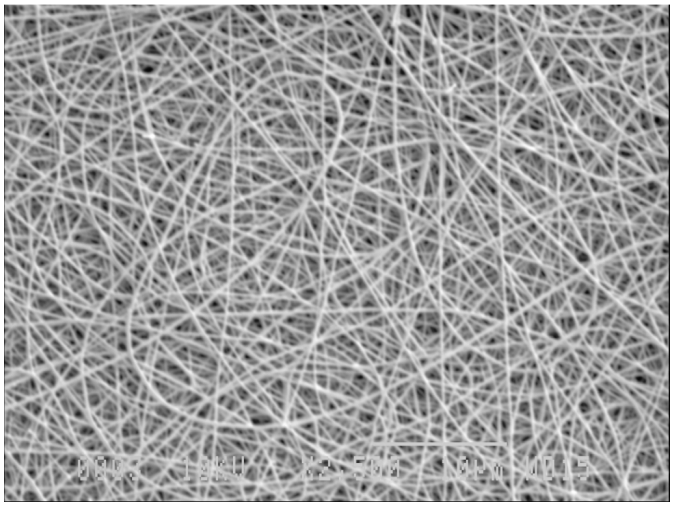

**Figure 1.8:** A typical SEM image of electrospun PLGA nanofibers.

Another attractive feature of using this electrospinning technique is that biodegradable polymeric materials, such as poly(lactic acid) (PLA) and poly($_{D,L}$ – lactide-*co*-glycolide) (PLGA) can be used as a biomedical controlled release system. These biodegradable polymers can be electrospun in the presence of varying amounts of the required medication. They can then be placed in the

body and the drug release achieved through the modification of the polymer matrix's morphology, porosity and composition.[89] These biodegradable polymers have FDA approval for biomedical and drug delivery use.[90-93] In comparison to other delivery forms, the electrospun nanofibers can conveniently incorporate the therapeutic compound during the electrospinning process.[94] Many drugs have been incorporated into PLGA electrospun polymer matrices, in order to achieve delivery of the therapeutic drug, including, tetracycline hydrochloride[95] and mefoxin[89]. In these cases, the drug release was monitored and a burst release was observed and was attributed to the high surface area-to-volume ratio of the electrospun material. This is a disadvantage. In the last few years a small number of groups have deposited electroactive polymers, such as PPy, onto previously electrospun fibers in order to enhance the electrochemical properties[57] of the material. Also, electrospun fibers have been used as a template in order to obtain a high surface area in the hope of achieving a greater uptake and release of drugs.[41]

Another method of improving the DDS of conducting polymers is the use of various dopants during polymerisation of the polymer films. The functionalisation of PPy films with large anionic dopants is not new to this field of research. It has been well reported that the use of large anionic dopants during the electrochemical polymerisation of monomers leads to these bulky negatively charged groups being immobilised within the polymer matrix.[96] In fact, these polymers, with their cationic exchange properties, have been used to incorporate various cationic groups for various applications. For example Fan and Bard in the late 1980s demonstrated the uptake of a positively charge $Ru(NH_3)_6^{3+}$ and methylviologen in PPy/Nafion films.[97]

However, the generation of PPy films in the presence of negatively charged cyclodextrins is a new concept.[98-100] There has been very little work reported on the electropolymerisation of pyrrole in the presence of anionic cyclodextrins. Indeed, much of the current published work is unreliable as very high potentials in the vicinity of 1.8 V vs. SCE were used to form the polymers.[100, 101] It is very well known that these high potentials give rise to the overoxidation of PPy and a

considerable loss in its conductivity.[59] The incorporation of cyclodextrins into conducting polymers provides a unique way of combining the unique host-guest complexation properties of cyclodextrins with the stability, high conductivity and ease of preparation of conducting polymers.

## 1.1.3 Cyclodextrins

### *1.1.3.1 History and structural properties of cyclodextrins*

Cyclodextrins (CD) are macrocyclic oligosaccharides composed of α-D-glucopyranoside units linked by α-(1,4) bonds. They were first discovered by Villiers in 1891[102], while in 1904, Schardinger[103] further developed the cyclic structures hence; CDs are sometimes referred to as Schardinger dextrins. However, it was only in the mid 1970s that the structure and chemical properties of natural cyclodextrins were fully characterised.[104] Cyclodextrins have developed quickly over the past two decades and have become an important branch of host-guest chemistry, specifically due to their ability to be involved in several practical applications.[105] The main interest in cyclodextrins lies in their ability to form inclusion complexes with a variety of compounds. Host-guest chemistry is the study of these inclusion phenomena, where the 'host' molecules are capable of including smaller 'guest' molecules through non-covalent interactions.

CDs are obtained through enzymatic degradation of starch in the presence of a glycosyl transferase, a type of amylase.[106] Many organisms contain glycosyl transferase, however, in general it is obtained from *Bacillus megaterium, Bacillus stereothermophilus and Bacillus macerans.*[106, 107] They are generally made up of glucopyranoside units of $^4C_1$ chair conformation which leads to a truncated cone shape encasing a cavity.[108] Figure 1.9 shows the structures of the most common CD members; α-, β- and γ-CD, which include 6, 7 and 8 repeating glucopyranoside units, respectively. These units orientate themselves in a cyclic manner offering a typical conical or truncated cone structure with a relatively hydrophobic interior and hydrophilic exterior.[109] This structural property gives cyclodextrins good water solubility and the ability to hold appropriately sized

guests, such as amines and ferrocenes[110], through non-covalent interactions such as hydrogen bonding, hydrophobic interactions, and electrostatic interactions.[111] Table 1.1 demonstrates the approximate geometries of the most common CDs.[109]

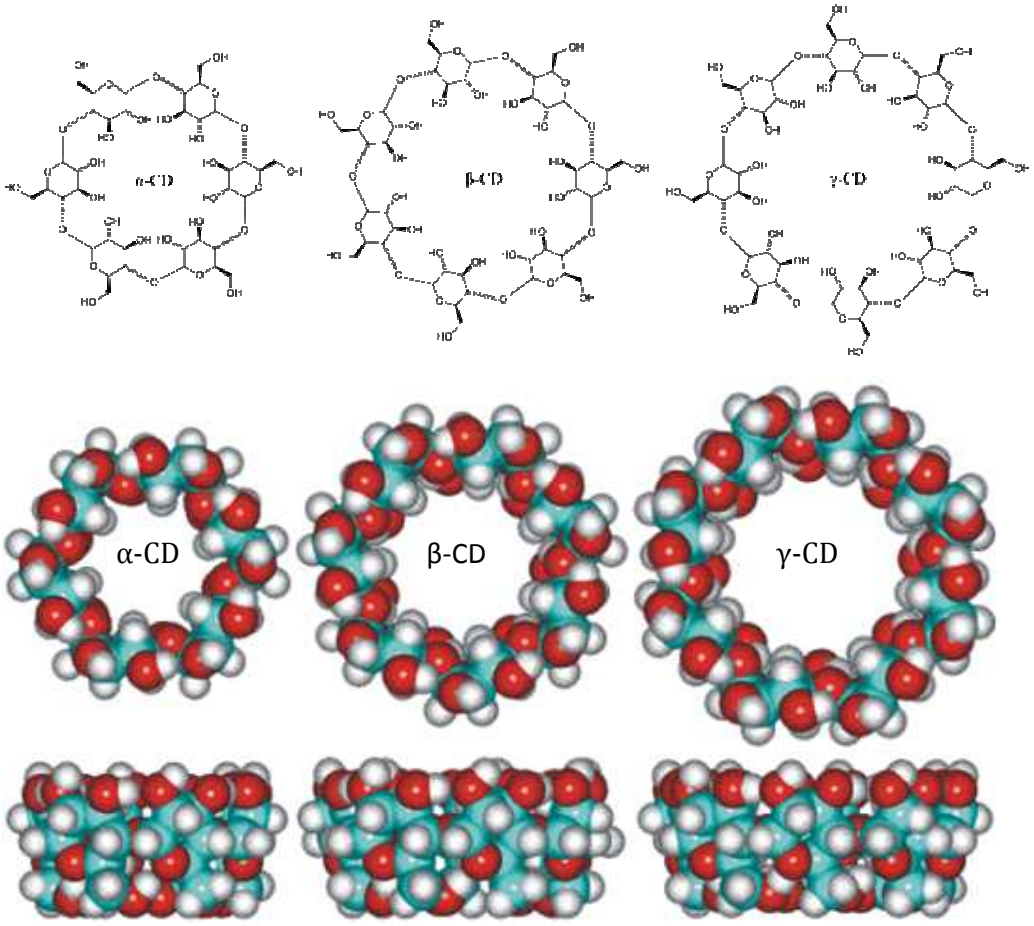


**Figure 1.9:** Structures of α-, β- and γ-cyclodextrin taken from Szjetli.[109]

Due to their exceptional host-guest complexation abilities, CDs have been used in a variety of fields, such as environmental protection through immobilising toxic compounds in their cavities and in the food industry.[104] In fact one of the commercially available applications for CDs is Febreze®, which is an aqueous solution of modified β-cyclodextrins**.** Febreze® is based on the host-guest chemistry of the CDs, with molecules that produce aroma forming inclusion complexes with the modified CDs. In the pharmaceutical industry, CDs are also

used for many applications including, drug delivery to enhance the solubility, stability and bioavailability of drug molecules.[108, 112]

**Table 1.1:** Approximate geometric dimensions of the three common CDs.[106]

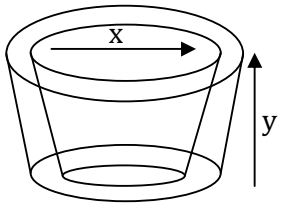


| Cyclodextrin | x / nm | y / nm | Cavity volume / Å$^3$ |
|---|---|---|---|
| **α** | 0.49 | 0.78 | 174 |
| **β** | 0.62 | 0.78 | 262 |
| **γ** | 0.79 | 0.78 | 427 |

Cyclodextrins can also be chemically modified to replace the hydroxyl groups on both the primary and secondary rims of the CDs, with a variety of appropriate alkyl groups (R). It has been reported that this can improve binding affinity.[108] In the research presented here, a negatively charged cyclodextrin with a number of sulfonated groups present on the outer rims was used, sulfonated β-CD (Sβ-CD). Sβ-CD is obtained by substitution of either primary or secondary hydrogen of the hydroxyl group of β-CD with a sulfonate group. Sβ-CD has an average of 7-11 substituents per CD and, therefore, has between 7-11 negative charges associated with it, which are counterbalanced with sodium ions, as illustrated in Figure 1.10.[113] It is reported that β-CD and Sβ-CD have the same ring structure, differing only in the substituent located on the rims of the CD ring.[14] Although Sβ-CD has the same ring structure as other derivativsed CDs the presence of the substituent on the ring contributes to its chiral discrimination properties.[114] A major area in which these sulfonated CDs are being utilised is chromatography, or more specifically capillary electrophoresis, for the enantiomeric separation of acidic and basic compounds. In enantiomeric separation, using neutral CDs, they are not appropriate for neutral racemates as the complex has no electrophoretic mobilities.[115] Therefore, the use of charged

CDs is now been widely researched for the separation of neutral compounds. It has been reported that the use of these sulfonated CDs for the enantiomeric separation of chiral compounds is highly effective as a result of the anionic charges.[116, 117]

A number of groups have also characterised the Sβ-CD.[115, 117] Figure 1.11 illustrates a single glucose unit of an Sβ-CD (comprised of 7 units). On the primary ring there are 7 potential substitution sites corresponding to the C-6 positions, while, on the secondary rim there are 14, represented by the C-2 and C-3 positions. Amini and co-workers[117] reported that substitution of these CDs is predominantly at the C-2 and C-6 positions, while, Chen *et al.*[115] confirmed nearly complete sulfation at the C-6 position of the primary hydroxyl groups and partial sulfation at the C-2 secondary hydroxyl groups. They also reported no substitution at the C-3 positions. From these reports it can be stated that almost the entire primary rim is sulfonated and some of the secondary rim. Due to this phenomenon and the fact that the sulfation brings with it negative charges these CDs are good candidates for the doping of CPs.

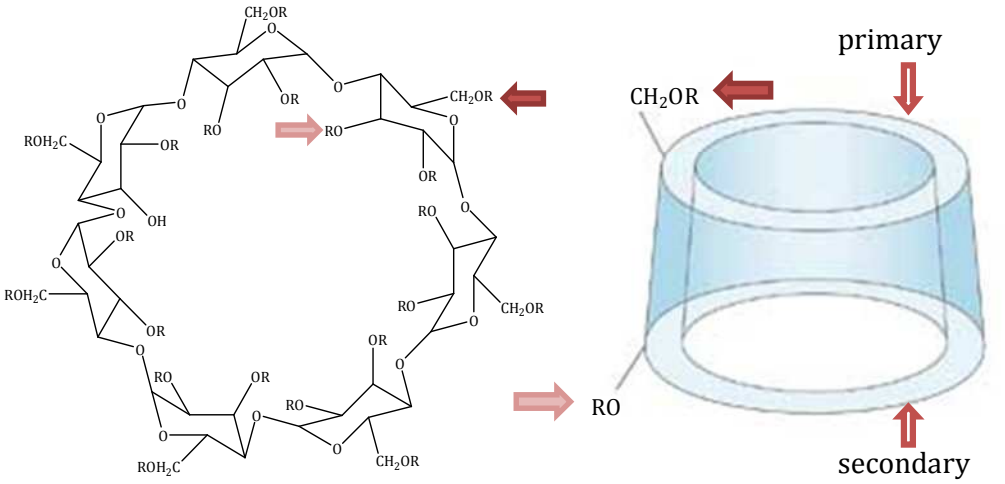


R = $SO_3^-Na^+$ or H ~ 7-11 $SO_3^-Na^+$ groups.

**Figure 1.10:** Structural and schematic representation of sulfonated β-cyclodextrin (Sβ-CD). The arrows point to the primary and secondary rims, respectively.[118]

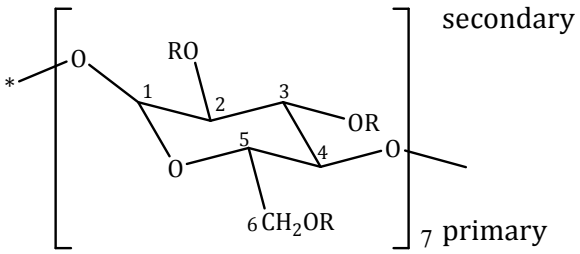


**Figure 1.11:** Chemical structure of Sβ-CD, depicting the numbering carbons.

### *1.1.3.2 Inclusion complexation*

Cyclodextrins (CD) form a group of cyclic oligosaccharides that contain cavities in which guest molecules can be encapsulated.[108, 109] It is well known that the size of the compounds are important and compounds are only capable of including into the cavity of the CD if they are within the dimensions of the CD cavity.[119] In aqueous media, the cavity is filled with water molecules, which becomes displaced by the guest through complexation, as illustrated in Figure 1.12. The guest molecule, xylene, displaces the water molecules and forms an inclusion complex with the CD.

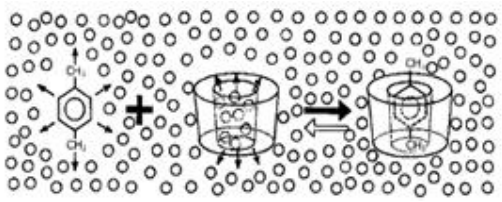

**Figure 1.12:** Schematic representation of xylene forming a complex with a β-cyclodextrin. The small circles represent water molecules taken from Szjetli.[109]

During the formation of an inclusion complex the chemical and the physical properties of the guest molecule change and can be monitored using a number of techniques. Various spectroscopic and electrochemical techniques can be used to confirm complexation, including fluorescence, UV-visible spectroscopy (UV), Nuclear magnetic resonance (NMR) and electrochemical studies. These changes attributed to the complexation can be used to evaluate the apparent

binding or formation constant ($K_f$). However, prior to the determination of the $K_f$ value the stoichiometry of the host-guest complex must be established.[120] This is obtained by the well known continuous variation or Job's method which is described in more detail in Chapter 2, Section 2.6.1.1.[121] Generally, inclusion complexes form a ratio of 1:1, 1:2 and sometimes 2:1 (CD:guest).[122]

NMR is also a useful tool for the study of complexation due to its quantitative information and assuming the guest enters the cavity, NMR, can be also used to locate the protons involved in complexation.[87] Many groups have studied the complexation properties with the neutral β-CD and monitored the changes in the chemical shifts for both the CD, and the guest. However, in the case of the modified CD used in this research, the NMR spectral data are too difficult to differentiate so the chemical shift of the guest is followed.[120, 123-126] Bratu and colleagues[125] studied the chemical shift changes observed when Fenbufen was in the presence of a neutral β-CD. They noticed an up-field shift of the guest protons, some more pronounced than others, and suggested that the complexation was initiated through the benzene moiety of the guest. Cruz *et al*.[127] also used NMR to quantitatively evaluate the binding constant of the complexation of doxepin and a neutral β-CD.

If a guest absorbs light in the UV or visible region then the inclusion phenomenon can be followed and subsequently, evaluated by UV.[106] This technique can be used to confirm complexation and indeed obtain the formation constant associated with the inclusion complex. In the majority of cases the guest that absorbs in the UV-vis region experiences changes in the intensity and the position of the absorption bands in the presence of the CD. These spectral changes can be used to determine the $K_f$ constants. Generally, a Hiedlebrand-Benesi modified equation is used to evaluate the $K_f$ constants.[119, 128, 129] Ramaraj and co-workers[130] monitored the changes attained during the complexation formation of a number of aromatic amines and nitro compounds in the presence of a neutral β-CD. They observed an increase in the intensity of the bands in all cases. Dang *et al*.[119] observed shifts of the absorption bands to longer

wavelengths in the case of 1,4 benzoquinone (BQ) and 9,10 anthraquinone (AQ) in the presence of a neutral β-CD.

Electrochemical techniques can also be performed on the complexation properties of CDs. If the guest is electroactive the peak current and potential can be followed for the free state and compared to the complexed state of the guest in question. Two features are generally observed during these electrochemical observations if an inclusion complex is found. Firstly, a decrease in the peak current can be seen, and, attributed to a decrease in the diffusion of the bulky CD complex as opposed to the more mobile free guest. Secondly, a shift in the peak potential is observed if the complexed species is included in the cavity, as it is harder to oxidise or reduce while located in the cavity. Once again based on these variations a number of equations can be used to verify the formation constant.[129, 131, 132] Coutouli-Argyropoulou and his group[133] reported the effect of complexation on the electrochemical properties of ferrocence derivatives and showed shifts, in both the peak current and peak potential, when higher concentrations of a neutral β-CD were added. Yanez *et al*.[131] showed similar observations for nifedipine (NF) and nicardipine (NC) and estimated apparent formation constants of 135 and 357, respectively.

Complexation studies of DA have been previously demonstrated in the presence of a neutral β-CD by Zhou *et al*.[134] using UV and fluorescence spectroscopy. From the fluorescence technique, utilising a Hiedlebrand-Benesi modified equation, a $K_f$ value of 95.06 was estimated. The degree of the complexation can vary over a wide range due to the stability of the complex, as it depends on a number of factors. In the next section a discussion on the main driving forces, involved in this complexation process are dealt with.

#### *1.1.3.3 Driving forces in the inclusion complexation process*

There are many reviews and books written on the driving forces behind the inclusion complexation abilities of cyclodextrins, not all agree, some refer to the predominantly hydrophobic affects while others state that it is a collection of a

number of weaker interactions (H-bonding, van der Waals, electrostatic interactions).[106, 108, 111, 135, 136] Either way the majority agree that the size of the cavity and shape of the guest are important factors in the complexation process. The most widely studied possible driving forces include

- Hydrogen bonding
- Electrostatic interaction
- Van der Waals
- Hydrophobic effect

Hydrogen bonding is an interaction between an electronegative donor, a hydrogen and an electronegative acceptor.[136] Various groups have demonstrated the importance of hydrogen bonding in the solid state, illustrating crystal structures defining the hydrogen bonding between the guest and the hydroxyls of the CDs.[137] However, during the complexation of the CD and guest, in aqueous solution, the subject is still arguable as few direct measurements of hydrogen bonding have been made, as water molecules can compete with CDs to form hydrogen bonding with guest molecules. However, many groups will still argue over the significance of hydrogen bonding.

Electrostatic interaction occurs when molecules of opposite charges interact. There are three types of electrostatic interactions, ion-ion interaction, ion-dipole interaction and dipole-dipole interaction.[136] Matsui and Okimoto[138] reported that ion-ion interaction is only eligible in the case of modified CDs, where as ion-dipole is considered more favourably due to the fact that CDs are polar molecules however as with hydrogen bonding, in aqueous media, the interaction between the guest and water will also be strong.[136] Therefore, it is the case of dipole-dipole interaction that is mostly considered during complexation.

Van der Waals forces or London dispersion forces are made up of dipole induced dipole contributions or the coordination of the electronic motion in the CD and guest. As CDs are known to have large dipole moments it is logical that

these induction forces are important in complexation. Experimental evidence has shown that the stability of the complex increases with an increase in polarisability. Also, as the polarisability of water is lower than the organic components of the CD cavity, van der Waals forces have an encouraging donation to the stability of the complex due to a stronger interaction of the CD and guest over the water and guest.[136] CDs have also been reported to form stable inclusion complexes in organic solvents like DMF and DMSO confirming the importance of van der Waals forces.[139]

The hydrophobic interaction which is entropically favourable, due to the expulsion of water, leads to the aggregation of non-polar solutes in aqueous solution.[136] As reviewed by Connors[135] the 'classical' hydrophobic interaction is said to be 'entropy driven' and a positive entropy and enthalpy is associated for the interaction between two non polar molecules. However, experimental studies in the complexation of CD and guests, show negative enthalpy and entropy changes,[111] which have been suggested to indicate that these interactions are not a dominant force.

Mosinger *et al*.[122] reported that the formation of an inclusion complex is based on the electrostatic, van der Waals and π-π interactions, where, steric affects and Hydrogen bonding are inevitable. Chao and co-workers[124] investigated the formation of an inclusion complex with β-CD and caffeic acid, they reported that the weak forces of hydrogen bonding, van der Waals, hydrophobic and electrostatic interactions simultaneously governed the process.

Rekharsky and Inoue[111] reviewed the complexation of cyclodextrins and stated that the interactions involved in the inclusion complexation of aromatic guests with CDs could not be simply put down to a hydrophobic effect. They established that complexation could be accounted for, through dipole-dipole interactions. In saying that, Tabushi and his group[140] questioned the role of hydrogen bonding in the complexation process and reported that no dramatic changes of binding were observed, when a modified CD, incapable of hydrogen bonding, was compared to an unmodified CD. They concluded that the

involvement of hydrogen bonding was negligible and hydrophobic interactions dominated the process. Zia *et al*.[113] investigated the complexation ability of a negatively charged CD (~7 negative sites) with a number of neutral and charged guest molecules. They accounted for the increase in the binding affinity, for the oppositely charged guest and CD, to be predominantly hydrophobic, due to the additional interaction sites provided by the negatively charged CD. Okimoto and colleagues[141] also clearly observed stronger interactions occurring between a CD and guest with opposite charges.

The understanding of these complexation processes is complicated, however, it is generally found that van der Waals forces and hydrophobic interactions are regarded as the main driving forces for CD complexation, while, electrostatic interactions and hydrogen bonding can be significantly considered in some inclusion complexation studies. Nevertheless, these attractive features of CDs allow them to be used in a wide range of applications including, the food industry[142]. However, the pharmaceutical industry is the most widely researched area in recent times, specifically in drug formulation and DDS.[143]

#### *1.1.3.4 Applications of CDs in DDS*

Due to their biocompatibility and their ability to form inclusion complexes, CDs have been studied for the use in DDS. They have been considered as drug carriers, as CDs have the potential to act as hydrophobic carriers and control the release of a variety of drugs.[118] Many reviews have recently been published, describing the role of CDs in DDS.[112, 118, 144-147] Irie and Uekama[144] reviewed the role of CDs in peptide and protein delivery and summarised that CDs were able to eliminate a number of undesirable properties of drug formulations, as they form inclusion complexes with the desired drugs, which increase the drug delivery through a number of routes of administration. More recently, Li *et al.*[145] examined the recent progress in the preparation of inclusion complexes between CDs and various polymers as supramolecular biomaterials for drug and gene delivery. They demonstrated the promising field in the self assembly

of inclusion complexes between CDs and biodegradable polymers as injectable DDS.

Ferancova and Labuda[148] also reviewed the use of CDs as electrode modifiers. They summarised the many ways CDs can be immobilised onto electrode surfaces. As discussed in an earlier section, Section 1.1.4.2., the incorporation of CDs, as dopants, during the electrochemical polymerisation of CPs was demonstrated to examine the use of these modified electrodes to deliver neutral drugs.[98] Formulating these materials, correlates the attractive features of both the CDs and the CPs. Bidan *et al*.[98] examined the need for a new DDS that was not limited to charged drugs. They produced polymer films in the presence of an anionic CD and successfully delivered neutral compounds using these novel materials.

Also briefly discussed in Section 1.1.4.2, was the reports made by a number of groups on the polymerisation of CPs in the presence of CDs.[100, 101, 149] These groups have reportedly polymerised pyrrole at potentials usually shown to overoxidise the CP film.[59] Due to this, these papers are unreliable in their reports.

### 1.1.4 Drug release: Controlled release of dopamine

DA is a neurotransmitter produced naturally in the brain. It is well documented that a common factor in neurodegenerative diseases such as Parkinson's (PD) and Schizophrenia is a significant lack of the presence of DA in the *substantia nigra* (mid brain).[150-152] In particular, PD is a slowly progressive disorder known to occur due to the damage of the basal ganglia.[150-152] The disease affects movement, muscle control and balance. Studies on the brains of deceased Parkinson sufferers show a substantial loss of dopamine, particularly, in the *substantia nigra*. The function of the substantia nigra is to produce DA and manage the release of essential neurotransmitters that help control movement and coordination. Sufferers usually show symptoms such as tremors, slowness of movement and impaired balance and coordination. Prolonged loss of DA

gives rise to symptoms such as difficulty in walking, talking, or completing other simple tasks.[150-152]

DA belongs to the well known catecholamine family. These molecules are electroactive and therefore their oxidation can be followed using electrochemistry, in particular, electrochemical methods such as cyclic voltammetry and rotational disc voltammetry. The electrochemical mechanism of oxidation is still not fully agreed; with various groups arguing that the mechanism goes through an ECE step rather than a CE step. For example, Hawley *et al*.[153] have reported that the electrochemical oxidation of dopamine in aqueous solution proceeds through two types of steps, electrochemical (E) and chemical (C). The ECE mechanism is presented in Scheme 1.1.

The first step in the oxidation of dopamine (A) involves the loss of both protons and electrons to form the o-dopaminoquinone (B). The oxidised, o-dopaminoquinone undergoes a 1,4-Michael addition, which results in a intramolecular cyclisation reaction which produces leucodopaminochrome (C). This product is easily oxidised through an electrochemical step to form dopaminochrome (D).[153, 154]

Controlled release studies of DA have been previously investigated.[67, 155-158] McRae-Degueurce *et al*.[156] encapsulated DA into a thermoplastic polyester excipient: PLGA. They found that it was possible to deliver significant amounts of DA for prolonged periods of time by injecting the microencapsulated DA directly into the brain. Uludag and colleagues[157] also examined the release of many therapeutic agents, including DA, from microencapsulated mammalian cells. The mammalian cells and tissues were entrapped in polymeric microcapsules containing the desired bioactive agent.

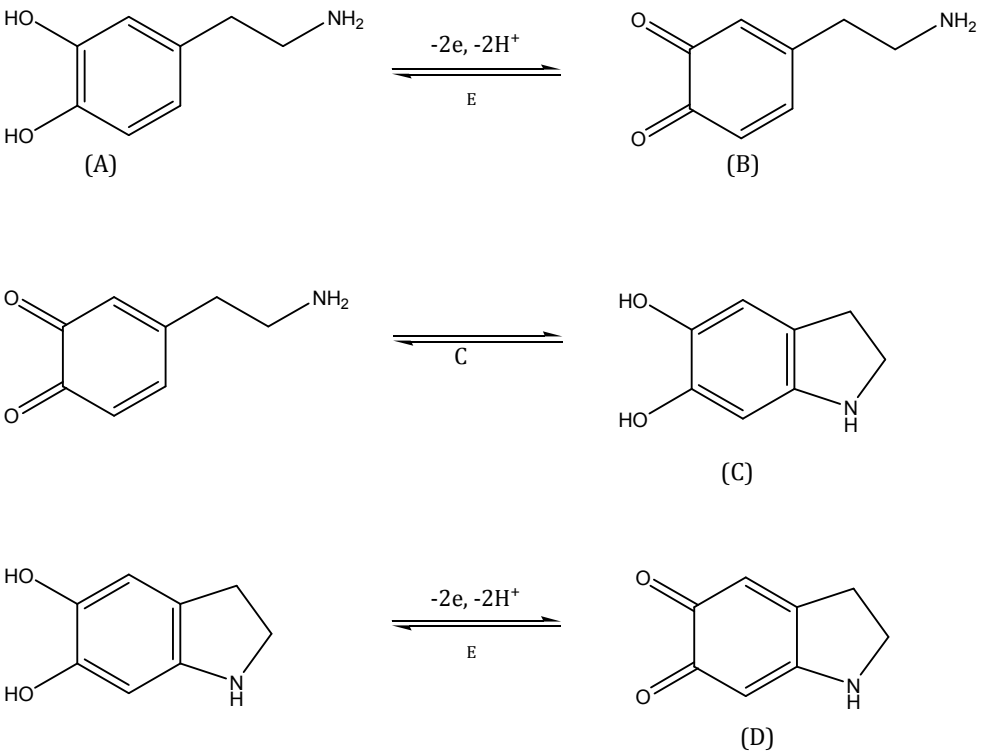


**Scheme 1.1:** The proposed oxidative pathway for dopamine.

In both these cases the release was based on diffusion from the polymeric materials. It is, therefore, difficult to maintain any control over the amount of DA released. Miller[67] and Zhou[158] and co-workers investigated the use of CPs to deliver DA. They introduced the concept of using large immobile dopants, which remain entrapped inside the cavity during polymerisation, to bind and successfully liberate DA from the polymer films.

This is the basis of the work performed in this thesis. As outlined at the start of this chapter, the idea of this research is to develop PPy films for the uptake and release of DA, using a large immobile anionic cyclodextrin. The cyclodextrin, in addition to its large size and immobility, has unique host-guest complexation properties and this offers the prospects of inclusion complexation between the DA and the CD to enhance the drug delivery. If this can be achieved it could potentially serve as a model system in DDS and could be extended to various other cationic drug molecules.

## 1.2 References


1. N. A. Peppas and D. J. A. Ende, *J Appl Polym Sci*, **66**, (1997), 509-513.
2. U. R. Pothakamury and G. V. BarbosaCanovas, *Trends Food Sci Tech*, **6**, (1995), 397-406.
3. B. Singh, D. K. Sharma, and A. Gupta, *J Environ Sci Heal B*, **44**, (2009), 113-122.
4. N. A. Peppas and R. Langer, *Science*, **263**, (1994), 1715-1720.
5. K. E. Uhrich, S. M. Cannizzaro, R. S. Langer, and K. M. Shakesheff, *Chem Rev*, **99**, (1999), 3181-3198.
6. D. L. Wise, Encyclopedic handbook of biomaterials and bioengineering Marcel Dekker, 1995.
7. J. T. Santini, A. C. Richards, R. Scheidt, M. J. Cima, and R. Langer, *Angew Chem Int Edit*, **39**, (2000), 2397-2407.
8. R. Langer, *Mrs Bull*, **31**, (2006), 477-485.
9. L. K. Fung and W. M. Saltzman, *Adv Drug Deliver Rev*, **26**, (1997), 209-230.
10. R. Langer, *Science*, **249**, (1990), 1527-1533.
11. R. Langer, *Nature*, **392**, (1998), 5-10.
12. J. Folkman and D. Long, *JOURNAL OF SURGICAL RESEARCH*, **4**, (1963), 139-142.
13. T. M. Allen and P. R. Cullis, *Science*, **303**, (2004), 1818-1822.
14. J. J. Wang, G. J. Zheng, L. Yang, and W. R. Sun, *Analyst*, **126**, (2001), 438-440.
15. H. Wartlick, K. Michaelis, S. Balthasar, K. Strebhardt, J. Kreuter, and K. Langer, *J Drug Target*, **12**, (2004), 461-471.
16. L. M. Lira and S. I. C. de Torresi, *Electrochem Commun*, **7**, (2005), 717-723.
17. S. Murdan, *J Control Release*, **92**, (2003), 1-17.
18. J. E. Riviere and M. C. Heit, *Pharmaceut Res*, **14**, (1997), 687-697.
19. G. Inzelt, Conducting Polymers, A new era in electrochemistry, Springer, 2008.
20. V. V. Walatka, M. M. Labes, and Perlstei.Jh, *Phys Rev Lett*, **31**, (1973), 1139-1142.
21. H. Shirakawa, E. J. Louis, A. G. Macdiarmid, C. K. Chiang, and A. J. Heeger, *J Chem Soc Chem Comm*, (1977), 578-580.
22. A. J. Heeger, *Angew Chem Int Edit*, **40**, (2001), 2591-2611.
23. A. G. MacDiarmid, *Angew Chem Int Edit*, **40**, (2001), 2581-2590.
24. H. Shirakawa, *Angew Chem Int Edit*, **40**, (2001), 2575-2580.
25. P. Chandrasekhar, Conducting Polymers, Fundamentals and Applications: A practical approach, Kluwer Acandemic Publishers, 1999.
26. A. A. Entezami and B. Massoumi, *Iran Polym J*, **15**, (2006), 13-30.
27. N. K. Guimard, N. Gomez, and C. E. Schmidt, *Prog Polym Sci*, **32**, (2007), 876-921.
28. A. Malinauskas, J. Malinauskiene, and A. Ramanavicius, *Nanotechnology*, **16**, (2005), R51-R62.
29. C. E. Schmidt, V. R. Shastri, J. P. Vacanti, and R. Langer, *P Natl Acad Sci USA*, **94**, (1997), 8948-8953.
30. J. L. Bredas and G. B. Street, *Accounts Chem Res*, **18**, (1985), 309-315.

31. D. L. Wise, Electrical and optical polymer systems, CRC Press, 1998.
32. L. Alcacer, Conducting Polymers: Special Applications (Hardcover), Springer 1986.
33. B. Winther-Jensen, J. Chen, K. West, and G. Wallace, *Polymer*, **46**, (2005), 4664-4669.
34. A. Malinauskas, *Polymer*, **42**, (2001), 3957-3972.
35. R. A. Green, N. H. Lovell, G. G. Wallace, and L. A. Poole-Warren, *Biomaterials*, **29**, (2008), 3393-3399.
36. T. A. Skotheim and J. R. Reynolds, Handbook of conducting polymers: Conjugated polymers, CRC Press, 2007.
37. P. C. Lacaze, J. C. Lacroix, K. C. Ching, and S. Aeiyach, *Actual Chimique*, (2008), 90-91.
38. M. A. Mohamoud, *Plast Eng*, **64**, (2008), 32-+.
39. M. Nikolou and G. G. Malliaras, *Chem Rec*, **8**, (2008), 13-22.
40. E. Smela, *Mrs Bull*, **33**, (2008), 197-204.
41. M. R. Abidian, D. H. Kim, and D. C. Martin, *Adv Mater*, **18**, (2006), 405-409.
42. C. Arbizzani, M. Mastragostino, L. Nevi, and L. Rambelli, *Electrochim Acta*, **52**, (2007), 3274-3279.
43. K. Kontturi, P. Pentti, and G. Sundholm, *J Electroanal Chem*, **453**, (1998), 231-238.
44. Y. L. Li, K. G. Neoh, and E. T. Kang, *J Biomed Mater Res A*, **73A**, (2005), 171-181.
45. J. M. Pernaut and J. R. Reynolds, *J Phys Chem B*, **104**, (2000), 4080-4090.
46. P. Burgmayer and R. W. Murray, *J Am Chem Soc*, **104**, (1982), 6139-6140.
47. A. Dall'Olio, G. Dascola, V. Varacca, and V. Bocchi, *Comptes Rendus de l'Academie des Sciences*, **C267**, (1968), 433-435.
48. A. F. Diaz and J. I. Castillo, *J Chem Soc Chem Comm*, (1980), 397-398.
49. B. Winther-Jensen and N. B. Clark, *React Funct Polym*, **68**, (2008), 742-750.
50. C. K. Baker and J. R. Reynolds, *J Electroanal Chem*, **251**, (1988), 307-322.
51. S. Geetha, C. R. K. Rao, M. Vijayan, and D. C. Trivedi, *Anal Chim Acta*, **568**, (2006), 119-125.
52. Z. X. Wang, C. Roberge, L. H. Dao, Y. Wan, G. X. Shi, M. Rouabhia, R. Guidoin, and Z. Zhang, *J Biomed Mater Res A*, **70A**, (2004), 28-38.
53. Z. Zhang, R. Roy, F. J. Dugre, D. Tessier, and L. H. Dao, *J Biomed Mater Res*, **57**, (2001), 63-71.
54. A. Kotwal and C. E. Schmidt, *Biomaterials*, **22**, (2001), 1055-1064.
55. J. Y. Wong, R. Langer, and D. E. Ingber, *P Natl Acad Sci USA*, **91**, (1994), 3201-3204.
56. B. Garner, A. Georgevich, A. J. Hodgson, L. Liu, and G. G. Wallace, *J Biomed Mater Res*, **44**, (1999), 121-129.
57. X. D. Wang, X. S. Gu, C. W. Yuan, S. J. Chen, P. Y. Zhang, T. Y. Zhang, J. Yao, F. Chen, and G. Chen, *J Biomed Mater Res A*, **68A**, (2004), 411-422.
58. S. Asavapiriyanont, G. K. Chandler, G. A. Gunawardena, and D. Pletcher, *J Electroanal Chem*, **177**, (1984), 229-244.
59. J. Heinze, *Synthetic Met*, **43**, (1991), 2805-2823.
60. G. Inzelt, V. Kertesz, and A. S. Nyback, *J Solid State Electr*, **3**, (1999), 251-257.

61. C. Y. Jin, F. L. Yang, and W. S. Yang, *J Appl Polym Sci*, **101**, (2006), 2518-2522.
62. V. M. Jovanovic, A. Dekanski, G. Vlajnic, and M. S. Jovanvic, *Electroanal*, **9**, (1997), 564-569.
63. S. Sadki, P. Schottland, N. Brodie, and G. Sabouraud, *Chem Soc Rev*, **29**, (2000), 283-293.
64. J. Tamm, A. Alumaa, A. Hallik, U. Johanson, L. Tamm, and T. Tamm, *Russ J Electrochem+*, **38**, (2002), 182-187.
65. M. Pyo and J. R. Reynolds, *Chem Mater*, **8**, (1996), 128-133.
66. M. Hepel and F. Mahdavi, *Microchem J*, **56**, (1997), 54-64.
67. L. L. Miller and Q. X. Zhou, *Macromolecules*, **20**, (1987), 1594-1597.
68. G. A. Husseini and W. G. Pitt, *J Pharm Sci-Us*, **98**, (2009), 795-811.
69. X. L. Xu, X. S. Chen, P. A. Ma, X. R. Wang, and X. B. Jing, *Eur J Pharm Biopharm*, **70**, (2008), 165-170.
70. S. G. Kumbar, L. S. Nair, S. Bhattacharyya, and C. T. Laurencin, *J Nanosci Nanotechno*, **6**, (2006), 2591-2607.
71. L. Feng, S. H. Li, H. J. Li, J. Zhai, Y. L. Song, L. Jiang, and D. B. Zhu, *Angew Chem Int Edit*, **41**, (2002), 1221-+.
72. G. M. Whitesides and B. Grzybowski, *Science*, **295**, (2002), 2418-2421.
73. T. Ondarcuhu and C. Joachim, *Europhys Lett*, **42**, (1998), 215-220.
74. J. Fang, H. T. Niu, T. Lin, and X. G. Wang, *Chinese Sci Bull*, **53**, (2008), 2265-2286.
75. E. R. Kenawy, F. I. Abdel-Hay, M. H. El-Newehy, and G. E. Wnek, *Mat Sci Eng a-Struct*, **459**, (2007), 390-396.
76. Q. J. Xie, S. Kuwabata, and H. Yoneyama, *J Electroanal Chem*, **420**, (1997), 219-225.
77. E. Luong-Van, L. Grondahl, K. N. Chua, K. W. Leong, V. Nurcombe, and S. M. Cool, *Biomaterials*, **27**, (2006), 2042-2050.
78. Z. M. Huang, Y. Z. Zhang, M. Kotaki, and S. Ramakrishna, *Compos Sci Technol*, **63**, (2003), 2223-2253.
79. A. Formhals, Vol. 1975504, 1934.
80. J. Doshi and D. H. Reneker, *J Electrostat*, **35**, (1995), 151-160.
81. D. H. Reneker and I. Chun, *Nanotechnology*, **7**, (1996), 216-223.
82. A. Greiner and J. H. Wendorff, *Angew Chem Int Edit*, **46**, (2007), 5670-5703.
83. D. Li and Y. N. Xia, *Adv Mater*, **16**, (2004), 1151-1170.
84. D. H. Reneker, A. L. Yarin, H. Fong, and S. Koombhongse, *J Appl Phys*, **87**, (2000), 4531-4547.
85. T. Subbiah, G. S. Bhat, R. W. Tock, S. Pararneswaran, and S. S. Ramkumar, *J Appl Polym Sci*, **96**, (2005), 557-569.
86. G. I. Taylor, *Proc. Roy. Soc. Lond.*, **A313**, (1969), 453-475.
87. A. Bernini, O. Spiga, A. Ciutti, M. Scarselli, G. Bottoni, P. Mascagni, and N. Niccolai, *Eur J Pharm Sci*, **22**, (2004), 445-450.
88. H. J. Shin, C. H. Lee, I. H. Cho, Y. J. Kim, Y. J. Lee, I. A. Kim, K. D. Park, N. Yui, and J. W. Shin, *J Biomat Sci-Polym E*, **17**, (2006), 103-119.
89. K. Kim, Y. K. Luu, C. Chang, D. F. Fang, B. S. Hsiao, B. Chu, and M. Hadjiargyrou, *J Control Release*, **98**, (2004), 47-56.
90. R. A. Jain, *Biomaterials*, **21**, (2000), 2475-2490.

91. M. Garinot, V. Fievez, V. Pourcelle, F. Stoffelbach, A. des Rieux, L. Plapied, I. Theate, H. Freichels, C. Jerome, J. Marchand-Brynaert, Y. J. Schneider, and V. Preat, *J Control Release*, **120**, (2007), 195-204.
92. D. Luo, K. Woodrow-Mumford, N. Belcheva, and W. M. Saltzman, *Pharmaceut Res*, **16**, (1999), 1300-1308.
93. X. H. Zong, S. Li, E. Chen, B. Garlick, K. S. Kim, D. F. Fang, J. Chiu, T. Zimmerman, C. Brathwaite, B. S. Hsiao, and B. Chu, *Ann Surg*, **240**, (2004), 910-915.
94. Z. M. Huang, C. L. He, A. Z. Yang, Y. Z. Zhang, X. J. Hang, J. L. Yin, and Q. S. Wu, *J Biomed Mater Res A*, **77A**, (2006), 169-179.
95. E. R. Kenawy, G. L. Bowlin, K. Mansfield, J. Layman, D. G. Simpson, E. H. Sanders, and G. E. Wnek, *J Control Release*, **81**, (2002), 57-64.
96. G. Bidan, B. Ehui, and M. Lapkowski, *J Phys D Appl Phys*, **21**, (1988), 1043-1054.
97. F. R. F. Fan and A. J. Bard, *J Electrochem Soc*, **133**, (1986), 301-304.
98. G. Bidan, C. Lopez, F. Mendesviegas, E. Vieil, and A. Gadelle, *Biosens Bioelectron*, **10**, (1995), 219-229.
99. D. A. Reece, S. F. Ralph, and G. G. Wallace, *J Membrane Sci*, **249**, (2005), 9-20.
100. K. R. Temsamani, O. Ceylan, B. J. Yates, S. Oztemiz, T. P. Gbatu, A. M. Stalcup, H. B. Mark, and W. Kutner, *J Solid State Electr*, **6**, (2002), 494-497.
101. N. Izaoumen, D. Bouchta, H. Zejli, M. El Kaoutit, A. M. Stalcup, and K. R. Temsamani, *Talanta*, **66**, (2005), 111-117.
102. A. Villiers, *C. R Acad. Sci*, **112**, (1891), 536.
103. F. Schardinger, *Wien. Klin. Wochenschr*, **17**, (1904), 207.
104. A. R. Hedges, *Chem Rev*, **98**, (1998), 2035-2044.
105. J. Szejtli, *J Mater Chem*, **7**, (1997), 575-587.
106. W. Saenger, *Angewandte Chemie-International Edition in English*, **19**, (1980), 344-362.
107. D. French, *Method Enzymol*, **3**, (1957), 17-20.
108. H. Dodziuk, Cyclodextrins and Their Complexes, 2006.
109. J. Szejtli, *Chem Rev*, **98**, (1998), 1743-1753.
110. A. Harada and S. Takahashi, *J Chem Soc Chem Comm*, (1984), 645-646.
111. M. V. Rekharsky and Y. Inoue, *Chem Rev*, **98**, (1998), 1875-1917.
112. K. Uekama, F. Hirayama, and T. Irie, *Chem Rev*, **98**, (1998), 2045-2076.
113. V. Zia, R. A. Rajewski, and V. J. Stella, *Pharmaceut Res*, **18**, (2001), 667-673.
114. L. X. Wang, X. G. Li, and Y. L. Yang, *React Funct Polym*, **47**, (2001), 125-139.
115. F. T. A. Chen, G. Shen, and R. A. Evangelista, *J Chromatogr A*, **924**, (2001), 523-532.
116. G. K. E. Scriba, *J Sep Sci*, **31**, (2008), 1991-2011.
117. A. Amini, T. Rundlof, M. B. G. Rydberg, and T. Arvidsson, *J Sep Sci*, **27**, (2004), 1102-1108.
118. F. Hirayama and K. Uekama, *Adv Drug Deliver Rev*, **36**, (1999), 125-141.
119. X. J. Dang, M. Y. Nie, J. Tong, and H. L. Li, *J Electroanal Chem*, **448**, (1998), 61-67.
120. L. Fielding, *Tetrahedron*, **56**, (2000), 6151-6170.

121. P. Job, **9**, (1928), 113-203.
122. J. Mosinger, V. Tomankova, I. Nemcova, and J. Zyka, *Anal Lett*, **34**, (2001), 1979-2004.
123. W. Misiuk and M. Zalewska, *Anal Lett*, **41**, (2008), 543-560.
124. J. B. Chao, H. B. Tong, Y. F. Li, L. W. Zhang, and B. T. Zhang, *Supramol Chem*, **20**, (2008), 461-466.
125. I. Bratu, J. M. Gavira-Vallejo, A. Hernanz, M. Bogdan, and G. Bora, *Biopolymers*, **73**, (2004), 451-456.
126. I. V. Terekhova, R. S. Kumeev, and G. A. Alper, *J Incl Phenom Macro*, **59**, (2007), 301-306.
127. J. R. Cruz, B. A. Becker, K. F. Morris, and C. K. Larive, *Magn Reson Chem*, **46**, (2008), 838-845.
128. H. A. Benesi and J. H. Hildebrand, *J Am Chem Soc*, **71**, (1949), 2703-2707.
129. M. S. Ibrahim, I. S. Shehatta, and A. A. Al-Nayeli, *J Pharmaceut Biomed*, **28**, (2002), 217-225.
130. R. Ramaraj, V. M. Kumar, C. R. Raj, and V. Ganesane, *J Incl Phenom Macro*, **40**, (2001), 99-104.
131. C. Yanez, L. J. Nunez-Vergara, and J. A. Squella, *Electroanal*, **15**, (2003), 1771-1777.
132. G. C. Zhao, J. J. Zhu, J. J. Zhang, and H. Y. Chen, *Anal Chim Acta*, **394**, (1999), 337-344.
133. E. Coutouli-Argyropoulou, A. Kelaidopoulou, C. Sideris, and G. Kokkinidis, *J Electroanal Chem*, **477**, (1999), 130-139.
134. Y. Y. Zhou, C. Liu, H. P. Yu, H. W. Xu, Q. Lu, and L. Wang, *Spectrosc Lett*, **39**, (2006), 409-420.
135. K. A. Connors, *Chem Rev*, **97**, (1997), 1325-1357.
136. L. Liu and Q. X. Guo, *J Incl Phenom Macro*, **42**, (2002), 1-14.
137. W. Saenger and T. Steiner, *Acta Crystallogr A*, **54**, (1998), 798-805.
138. Y. Matsui and A. Okimoto, *B Chem Soc Jpn*, **51**, (1978), 3030-3034.
139. L. X. Song, B. L. Li, R. Jiang, J. G. Ding, and Q. J. Meng, *Chinese Chem Lett*, **8**, (1997), 613-614.
140. I. Tabushi, Y. I. Kiyosuke, T. Sugimoto, and K. Yamamura, *J Am Chem Soc*, **100**, (1978), 916-919.
141. K. Okimoto, R. A. Rajewski, K. Uekama, J. A. Jona, and V. J. Stella, *Pharmaceut Res*, **13**, (1996), 256-264.
142. L. Szente and J. Szejtli, *Trends Food Sci Tech*, **15**, (2004), 137-142.
143. J. Szejtli, *Pure Appl Chem*, **76**, (2004), 1825-1845.
144. T. Irie and K. Uekama, *Adv Drug Deliver Rev*, **36**, (1999), 101-123.
145. J. Li and X. J. Loh, *Adv Drug Deliver Rev*, **60**, (2008), 1000-1017.
146. K. Uekama, *J Incl Phenom Macro*, **44**, (2002), 3-7.
147. K. Uekama, F. Hirayama, and H. Arima, *J Incl Phenom Macro*, **56**, (2006), 3-8.
148. A. Ferancova and J. Labuda, *Fresen J Anal Chem*, **370**, (2001), 1-10.
149. K. R. Temsamani, H. B. Mark, W. Kutner, and A. M. Stalcup, *J Solid State Electr*, **6**, (2002), 391-395.
150. J. A. Kiernan and M. L. Barr, Barr's the Human Nervous System: An Anatomical Viewpoint, Lippincott Williams & Wilkins, 2008.
151. J. Nolte and J. W. Sundsten, The Human Brain: An Introduction to Its Functional Anatomy, Mosby, 1998.

152. R. H. Thompson, The Brain: A Neuroscience Primer, W H Freeman & Co, 1993.
153. M. D. Hawley, S. Tatawawa, S. Piekarsk, and R. N. Adams, *J Am Chem Soc*, **89**, (1967), 447-&.
154. T. Luczak, *Electroanal*, **20**, (2008), 1639-1646.
155. R. Langer, *J Control Release*, **16**, (1991), 53-59.
156. A. Mcraedegueurce, S. Hjorth, D. L. Dillon, D. W. Mason, and T. R. Tice, *Neurosci Lett*, **92**, (1988), 303-309.
157. H. Uludag, J. E. Babensee, T. Roberts, L. Kharlip, V. Horvath, and M. V. Sefton, *J Control Release*, **24**, (1993), 3-11.
158. Q. X. Zhou, L. L. Miller, and J. R. Valentine, *J Electroanal Chem*, **261**, (1989), 147-164.

## 1.1 Introduction

The initial aim of this work was to examine the use of polypyrrole (PPy), a well-known conducting polymer, for the uptake and release of a cationic species, dopamine (DA). DA was chosen as it represents a large family of amine-based drugs. Therefore, if appropriate PPy films could be electrosynthesised and used in the controlled delivery of DA, then the concept could be used more widely in the field of controlled drug delivery.

In Chapter 3, the growth of PPy films in the presence of various dopant anions, including a large anionic cyclodextrin (CD), sulfonated β-cyclodextrin (Sβ-CD) is explored. Although Sβ-CD doped PPy films have been reported in the recent literature, there has been very little work devoted to the characterisation of these films. Accordingly, much of Chapter 3 is devoted to the unique redox properties of the Sβ-CD doped PPy films.

With the growth of the PPy films achieved, Chapter 4, shows the drug release profiles of the protonated DA and reveals that in the case of the polymer films doped with the anionic Sβ-CD, there is a substantial increase in the amount of DA released in comparison to other polymer films. In order to explain the enhanced release profiles, the well-known supramolecular complexation properties of cyclodextrins were considered. However, on searching the literature no reports on the complexation of DA with anionic cyclodextrins were found and consequently this was studied in detail. These findings are presented in Chapter 5, where the host-guest interactions between DA and the anionic Sβ-CD are examined using a variety of techniques, both spectroscopic and electrochemical.

In Chapter 6 the technique of electrospinning is introduced. Details on how it is used to fabricate nanostructured biodegradable polymer films with a high surface area are provided. The approaches used to deposit the Sβ-CD doped PPy films onto the nanostructured biodegradable film are then considered and discussed. It is shown that cyclic voltammetry was the most successful

approach. Moreover, it was possible to control the amount of PPy deposited and to maintain the nanostructured fiber substrate by varying the number of cycles. These high surface area Sβ-CD doped PPy films are promising for the uptake and liberation of DA.

In this introductory chapter, the concept of controlled drug release is firstly introduced. This is then followed with information on conducting polymers, particularly PPy and the current state-of-art in using PPy in drug delivery. The technique of electrospinning is then introduced and linked to DDS. The next section is devoted to cyclodextrins, as it is the Sβ-CD doped PPy films that give the best controlled release properties. Finally, the chapter ends with a short account of the properties of DA and its delivery.

### 1.1.1 Controlled drug release

In the early 1970s, controlled release systems first materialised. Since then, the number and the areas in which a controlled release system is utilised have significantly increased. These systems have been used in areas such as cosmetics[1], food[2], and pesticides[3]. Controlled release systems are focused on obtaining the release of the proposed material, over a certain time without an external influence from any other potential release factor.[4] Polymeric materials have been previously investigated for controlled release as they can be easily manufactured and their composition can be finely tuned.[5] Polymers used in controlled release systems can be natural or synthetic and release can be achieved through the engineering of the polymer substrates, i.e., the degradation of poly($_{D,L}$ – lactide-*co*-glycolide) (PLGA) can be controlled through the polymer composition, higher ratios of PLA lead to a higher degradation rate.[6]

Another important research area under consideration is the development of controlled drug delivery systems (DDS).[7, 8] In 1980, controlled DDS were virtually unknown, yet in 2005, almost 100 million people globally were using some form of polymer based DDS.[8] The aim of a DDS is to supply the drug in its

therapeutically active form to a specific target in the body when the drug is required. In the current administration process there is a critical concentration needed in order to achieve the drug's maximum therapeutic effect. If the concentration goes beyond the maximum level, toxicity problems come into play. Conversely, if the concentration administered is below the minimum level the effect of the drug is not observed. The use of these DDS could potentially eliminate these problems as the release would be of a controlled manner.

Santini *et al.*[7] compared the release profiles of both conventional and controlled methods, as illustrated in Figure 1.1. With conventional methods of drug delivery, outlined in Figure 1.1(A), i.e., oral administration or injections, drug levels rise after initial administration, which could lead to potential toxicity problems, and then decrease until the next dosage, which has consequences on the efficiency of the dosage. The other schematic, Figure 1.1(B), demonstrates the effectiveness of a controlled release system. After dosage, the drug level in the blood remains constant, between the maximum and minimum levels, for a certain period of time.

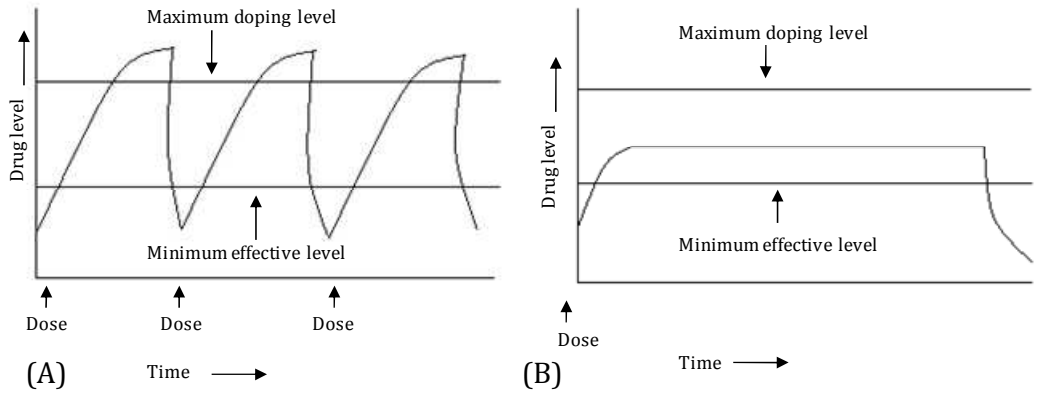


**Figure 1.1:** Drug levels in the blood with (A) conventional drug dosage (B) controlled delivery dosage, taken from Santini *et al.*[7]

In recent years, polymeric materials have been examined and shown to provide an alternate means of delivering drugs. Implanted polymeric pellets or microspheres localise therapy to specific anatomic sites, providing a continuous sustained release of drugs while minimising systemic exposure.[9] Polymers that display a physiochemical response to stimuli have been broadly researched for controlled release systems. Various stimuli include pH, temperature and the application of an electrical field.[10] According to Langer[11], polymeric DDS should i) maintain a constant drug level ii) reduce harmful side effects iii) minimise the amount of drug needed and iv) decrease the amount of doses which will have a pronounced effect on the patient.

The original polymeric controlled DDS was based on a non-biodegradable polymer, silicone rubber, which was designed and tested by Folkman and Long.[12] They loaded a silicone capsule (Silastic*) with a number of different drugs for the treatment of heart block and successfully implanted and monitored their effects over a number of days.

In more recent years there has been considerable interest in the development of new and efficient DDS, particularly with the growth of sophisticated drugs that are based on DNA and proteins.[5, 13] Currently, there are several materials under consideration in drug delivery, for example dendrimers[14], nanoparticles[15] and hydrogels[16]. The most promising opportunities in controlled DDS are in the area of responsive polymeric materials, with the possibility of implantable devices being used to deliver drugs. Murdan[17] exhaustively reviewed the use of hydrogels as 'smart' drug delivery devices. He showed that hydrogels could be engineered for various medicinal treatments depending on the patients needs, for example, pain relief. In the body, drug release can only be accomplished if the drug carrier responds to some class of stimuli, be it chemical, physical or biological. Conversely, an implanted 'smart' drug delivery device should be non-responsive to all other types of stimulus, once inside the body. A way of achieving this form of control is through an electrical stimulus.[17] A number of *in vivo* devices, in the form of iontophoresis, have already been used for this type of controlled release.[17, 18] Murdan presented a case where hydrogels loaded

with a bioactive compound, were implanted at a target site and the drug liberated through the application of an electrical field. In utilising such a system, many advantages including, minimal drug usage and lowering toxicity problems can be achieved. However, a problem arising with the application of an electrical stimuli to polymeric materials like, hydrogels, is that they experience deswelling or bending, which affects the drug release.[17]

To overcome these problems, conducting polymers (CPs) are also receiving much attention in the field of biomedical research, for the application of controlled DDS, due to their light weight, good biocompatibility and ability to function at body temperature. In particular, conducting polymers exhibit a reversible electrochemical response. These reversible oxidation-reduction reactions are attractive for a responsive DDS, as a change in the net charge on a conducting polymer film during its reduction or oxidation requires ions to flow into or out of the film. This, in turn, allows the polymer film to bind and expel ions in response to electrical signals. Controlled release of drugs from polymers offers many advantages over conventional methods including better control of the drug level administered resulting in fewer side effects, local drug delivery, decreased requirements for the total amount of drug and protection of drugs which are rapidly destroyed by the body. However, in order to devise a suitable technology, the polymeric material must be responsive, i.e., it must be capable of altering so that the drug is released in a controlled fashion when needed.

### 1.1.2 Conducting polymers

A polymer is a large molecule made up of smaller repeating units. The name comes from the Greek *poly*, meaning 'many', and *mer*, meaning 'part'. They are built up from simple molecules called *monomers* 'single part'. Polymers are produced through a method known as polymerisation. This polymerisation step can be achieved through chemical or electrochemical methods. Originally polymers with the basic carbon chains were considered only as insulators.[19] The first real interest in conducting polymers can be attributed to Walatka *et al*.[20] in 1973 with the report of highly conducting polysulfur nitride $(SN)_x$. Meanwhile

and towards the late 1970s , MacDiarmid, Shirakawa and Heeger enhanced the discovery of the semi-conducting and metallic properties of the chemically synthesised organic polyacetylene.[21-24] As is well known, the Nobel Prize in Chemistry was awarded to Alan J.Heeger, Alan G. MacDiarmid and Hideki Shirakawa in 2000 for the discovery and development of conducting polymers (CPs).[21-24] In the following years, a wide range of polymeric organic species have been prepared as stable inherent films on inert electrodes via both chemical oxidation and electropolymerisation from aqueous and organic solution.[25]

CPs are organic materials, which generally are comprised simply of C, H and simple heteroatoms such as N and S. Common examples include PPy, polyaniline and polythiophene which are shown in Figure 1.2. These and a number of other conducting polymers have been used in a variety of applications ranging from corrosion protection of materials, sensors to many biomedical applications, such as tissue engineering, nerve cell regeneration and drug delivery.[26-29]

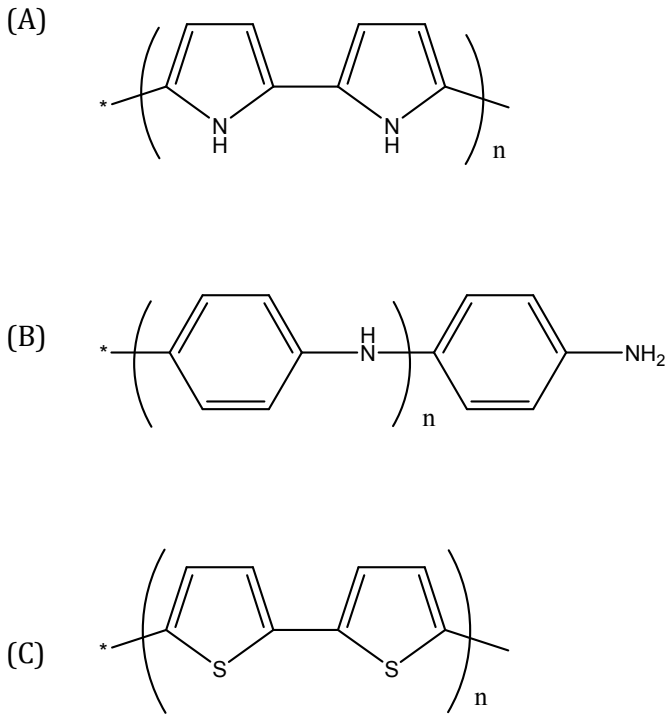


**Figure 1.2:** Chemical structures of (A) polypyrrole (B) polyaniline and (C) polythiophene. All polymers are shown in the dedoped state.

In, general materials are classed depending on their electrical conductivity, κ, where the electrical conductivity of insulators < semiconductors < conductors. Bredas and Street[30] explained this phenomenon in terms of the band gap structure. Figure 1.3 illustrates the difference in each material using the band gap theory. The highest occupied molecular orbital is equivalent to the valence band (VB), while the lowest unoccupied molecular orbital may be equated to the conduction band (CB). The difference between each band is known as the band gap energy ($E_g$) and it is this energy gap that establishes the electrical properties of a material. If $E_g$ > 10 eV, it is difficult to excite electrons into the conduction band and an insulator is formed. If $E_g \sim 1.0$ eV then thermal energy is sufficient to promote the electrons into the conduction band and a semiconductor is formed. If the gap vanishes, with overlap of the valence and conduction band, as shown in Figure 1.3, metallic conduction is observed. For most doped CPs the band gap energy is generally close to 1.0 eV, and consequently, CPs can be classified as semi-conductors.

As pointed out by Bredas and Street[30], the conductivity observed upon doping of the CPs was originally thought to be from the formation of unfilled electronic bands, however this idea was quickly dissipated upon experimental analysis of PPy and polyacetylene and now it is recognised that the conductivity is due to the formation of polarons and bipolarons, which are more energetically favoured.[30, 31]

The π-bonded system of CPs, which comprises of alternating single and double bonds, enabling the delocalisation of electrons along the polymer backbone, is related to the conductivity of the system. The conductivity of these materials arises from a state of relative oxidation or reduction. In these states the polymer either loses (oxidation) or gains (reduction) an electron. Generally, it is said that this process occurs in 1 in every 4 monomer units.[32] In this state the polymer is electronically charged and requires the introduction of counter ions (dopants) to compensate and reform the charge neutrality. The oxidation of the polymer in which an electron is removed from a π-bond, gives rise to a new energy state, which leaves the remaining electron in a non-bonding orbital. This energy level

is higher than the valence band and behaves like a heavily doped semiconductor.[32] The extent of doping can be controlled during the polymerisation of the polymers.

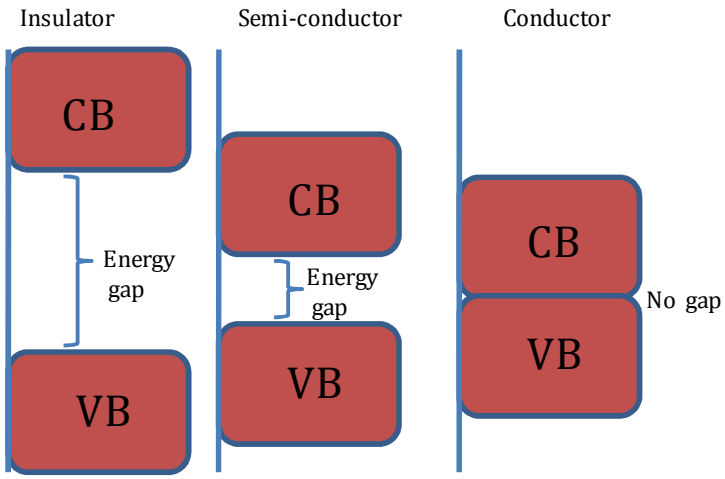


**Figure 1.3:** Schematic of the difference in band gap for Insulators, semi-conductors and metals (conductors).

### *1.1.2.1 Polymerisation methods*

CPs are synthesised through a method known as oxidative polymerisation. This can be generated chemically or electrochemically. Chemical polymerisation involves the use of a chemical oxidant, such as ammonium peroxydisulfate (APS), ferric ions, permanganate, dichromate anions or hydrogen peroxide. The oxidants not only oxidise the monomer but provide dopant anions to neutralise the positive charges formed on the polymer backbone.[33] In the presence of these oxidants, the monomers are oxidised and chemically active cation radicals are formed which further react with the monomer and generate the desired polymer. An advantage of vapour phase chemical polymerisation of CPs is that the polymerisation occurs almost exclusively on the preferred surface and a higher surface area can be attained.[34] Vapour phase chemical polymerisation of

pyrrole leads to further doping after polymerisation and this gives rise to an increase in conductivity.[35]

The electrochemical deposition is a simple and reproducible technique where the dopant is present in the electrolyte during polymerisation. It is generally performed in a conventional three electrode set up, described later in Chapter 2, where current is passed through a solution containing the monomer in the presence of a dopant (electrolyte). The CP is deposited at the positively charged working electrode or anode.[27] Polymerisation is initiated through the oxidation of the monomer which forms a mobile charge carrier known as a polaron (radical cation), that can react with another monomer or polaron to form a bipolaron (radical dication) which leads to the formation of the insoluble polymer chain and deposition of the polymer onto the working electrode.[36]

In his book 'Conducting Polymers' published in 1986, Alcacer commented on the possibility of using CPs to make artificial muscles or perhaps even modification for the brain; little did he realise the extent to which these materials have been extensively researched, over the past 20 years.[32] Since their discovery, the preparation and characterisation of these materials has evolved substantially through the use of electrochemistry. The majority of research is significantly based in this area due to the ease and control of synthesis of these electronically CPs.[19] Reviews on the development of CPs show the various areas to where they can be applied. The applications are ongoing.[37-40] However, in the case of DDS, CPs, in particular PPy, are widely researched for the controlled release of therapeutically active compunds.[41-45] During oxidative polymerisation, a dopant molecule, with an overall anionic charge, is used to compensate for the positive charges originating from the oxidation of the monomer. It is during this process that the concept of drug delivery originated. Burgmayer and Murray[46] observed changes in the ionic permeability of PPy redox membranes using a voltage-controlled electrochemical reaction. This led to further investigations into the application of CPs in DDS.

### *1.1.2.2 Polypyrrole*

#### 1.1.2.2.1 Historical background of polypyrrole

In 1968 Dall'Olio and colleagues prepared black films of an oxypyrrole on platinum by the electrochemical polymerisation of pyrrole from a solution of sulfuric acid.[47] In 1979 Diaz with the help of colleagues modified Dall'Olio's approach and demonstrated that polymerising pyrrole onto platinum in acetonitrile led to a black, adherent film.[48] Elemental analysis showed that the monomer unit was retained in the polymer. PPy in general, was poorly crystalline, and its ideal structure was a planar (α-ά)-bonded chain in which the orientation of the pyrrole molecules alternate.[25]

The monomer unit, pyrrole, is shown in Figure 1.4. PPy is an organic material comprised simply of C, H and a simple N heteroatom, but is highly conducting. It is an inherently conductive polymer due to interchain hopping of electrons. PPy can be synthesised both chemically[49] and electrochemically[48]. The electrochemical synthesis method is a one step synthesis method and allows the simple deposition of polymer films where its surface charge characteristics can easily be modified by changing the dopant anion (A-) that is incorporated into the material during synthesis. In a cell containing an aqueous or non-aqueous solution of the monomer, PPy forms a (semi) conducting film on the working electrode; the film grown is in the oxidised form and can be reduced to the non-conducting insulating form by stepping the potential to more negative values. The potential cycling can be repeated many times between the insulating and (semi) conducting forms without a loss of the electroactivity of the film.[25]

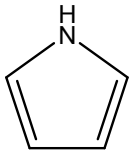


**Figure 1.4:** Schematic illustration of a monomer unit of pyrrole.

PPy in its neutral form is weakly coloured while the oxidised form is a deep blue/black. The switching of the state of the film not only changes its conductivity but it is also accompanied by a marked colour change, termed electrochromism.[36] Materials such as PPy are important in terms of future technological impact as it may be possible to develop them to replace more expensive, often toxic, metallic conductors commonly employed in the electronics industry.[25]

#### 1.1.2.2.2 Polymerisation mechanism of pyrrole

Although there are still various opinions on the mechanistic features of the electropolymerisation of pyrrole, the mechanism proposed by Diaz and his colleagues[48] and later used by Baker and Reynolds is in good agreement with many experimental reports.[50] The mechanism is demonstrated in Figure 1.5.

The initial step is the generation of the radical cation. This cation has different resonance forms, as shown in Figure 1.5. In the next step in the chemical case, the radical cation then attacks another monomer molecule, generating a dimer radical cation. In the electrochemical case, the concentrations of radical cations is much larger than that of neutral monomers in the vicinity of the electrode where reactions are occurring, and radical-radical coupling leads to a radical dication. This coupling between the two pyrrole radicals results in the formation of a bond between the two $\alpha$ positions to give the radical dication, as highlighted in Figure 1.5. This is then followed by the loss of two protons, generating a neutral dimer. This dimer is then oxidised into a radical cation, where the unpaired electron is delocalised over the dimer. The radical dimer then couples with the radical monomer to form a trimer. The polymerisation thus progressing in this fashion to completion.

The controversy in the mechanism of electropolymerisation is not surprising given that many factors, such as the nature of the electrolyte, ionic strength, pH, temperature and potential are important and can influence the mechanism of the reaction.

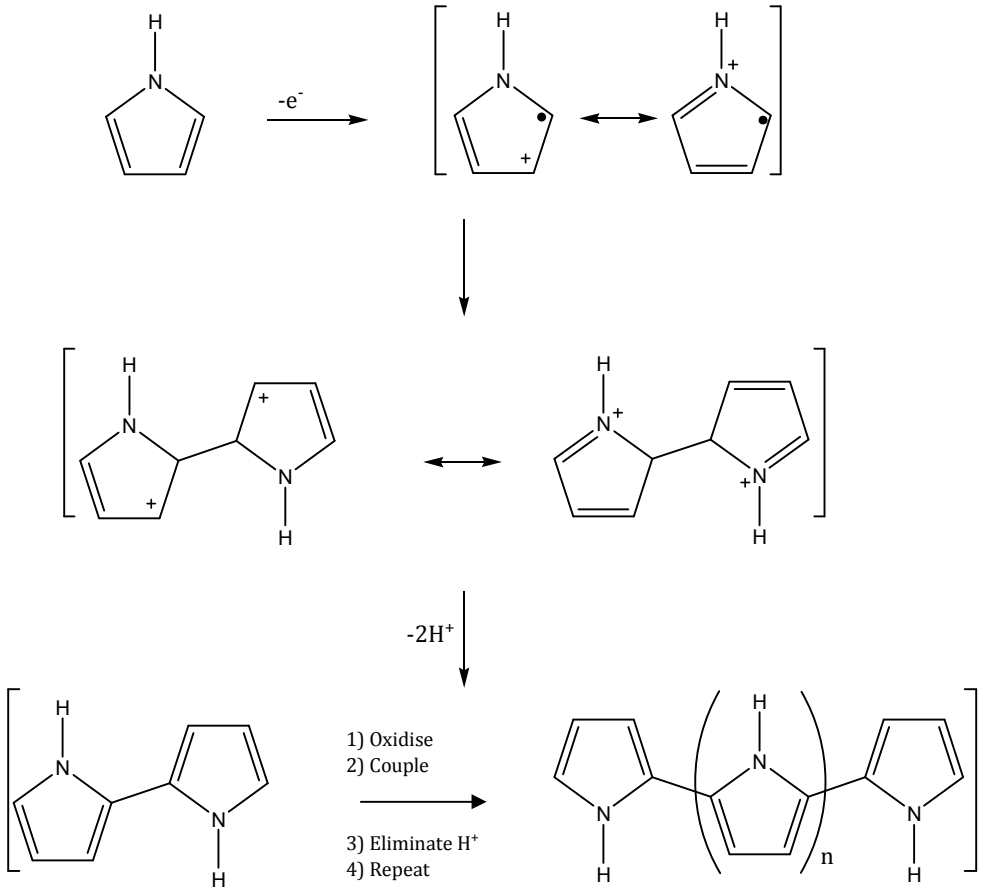


**Figure 1.5:** Mechanism of electrochemical polymerisation of pyrrole.[50]

#### 1.1.2.2.3 Biocompatibility

PPy is one of the most widely researched conductive polymers. The fact that it can form biologically compatible matrices is one of the prominent reasons for the extensive research on the use of PPy in the field of biological applications.[51] Wang *et al.*[52] acknowledged the reality that PPy had showed very good *in vitro* biocompatibility,[29, 53, 54] but they wanted to evaluate further the *in vivo* biocompatibility prospects. They demonstrated that in comparison to no PPy, the presence of PPy/biodegradable composites stimulated no abnormal tissue response and had no affect on the degradation behaviour of the biodegradable materials. In 1994, PPy was one of the first conducting polymers investigated for its effect on mammalian cells.[55] Since then, PPy is known to be

biocompatible, so it can be placed in the body without having adverse effects. It has been shown, in particular, to support cell growth and adhesion of endothelial cells.[29, 55-57] Schmidt *et al*.[29] also demonstrated that PPy was a suitable material for both in vitro nerve cell culture and in vivo implantation. PPy was electrochemically deposited onto ITO-conductive borosilicate glass. Moreover, the application of an external electrical stimulus through the polymer film resulted in enhanced neurite outgrowth. The median neurite length for PC-12 cells grown on PPy film subjected to an electrical stimulus increased nearly two-fold compared with cells grown on PPy without the application of a constant potential. The group also investigated PPy in vivo and their studies showed that PPy promotes little negative tissue and inflammatory response. Due to the good biocompatible factor, studies on the application of an electric field to the PPy have also shown cell compatibility.[29] In some important applications, such as biological sensors and actuators for medical devices it is a very attractive trait and some recent applications show that PPy can enhanced nerve cell regeneration and tissue engineering.[27]

#### 1.1.2.2.4 Electroactivity of polypyrrole

PPy can be easily switched between the neutral, partially oxidised and fully oxidised states, as shown in Figure 1.6. In its neutral state PPy exists as an insulator where the conduction band is empty as all the electrons remain in the valence band. Upon oxidation, an electron is removed from a π-bond (valence band) and a polaron is formed. The separation of the positive charge and the unpaired electron decreases during continual oxidation as the number of polarons increases. This in turn gives rise to the formation of a bipolaron, as depicted in Figure 1.6(C), and the polymer is now in its fully oxidised state.

During oxidation and the generation of positive charge an influx of anions into the polymer matrix is observed in order to maintain charge balance. This can be represented in Equation 1.1, where $PPy^{o}$ refers to the neutral (reduced) polymer, $PPy^{+}$ refers to the oxidised polymer and $A^{-}$ refers to the anionic dopant.

$$PPy^0 + A^- \rightarrow PPy^+A^- + e^- \quad 1.1$$

Typical anionic dopants are chlorides, bromides, iodides, perchlorates, nitrates, sulfates and para-toluene sulfonates.[58-64] The extent of oxidation/reduction is given by the doping level and this is generally expressed as the ratio of dopant anions, $A^-$, incorporated per monomer unit. For example, 1 $A^-$ per 4 monomer units gives a doping level of 0.25 or 25%. The maximum doping level achievable with PPy is 0.33 or 33%, i.e., 1 $A^-$ per 3 pyrrole units. It is important to point out that doping may not always be uniform; there can be islands with high doping levels surrounding by regions with a much lower doping level.

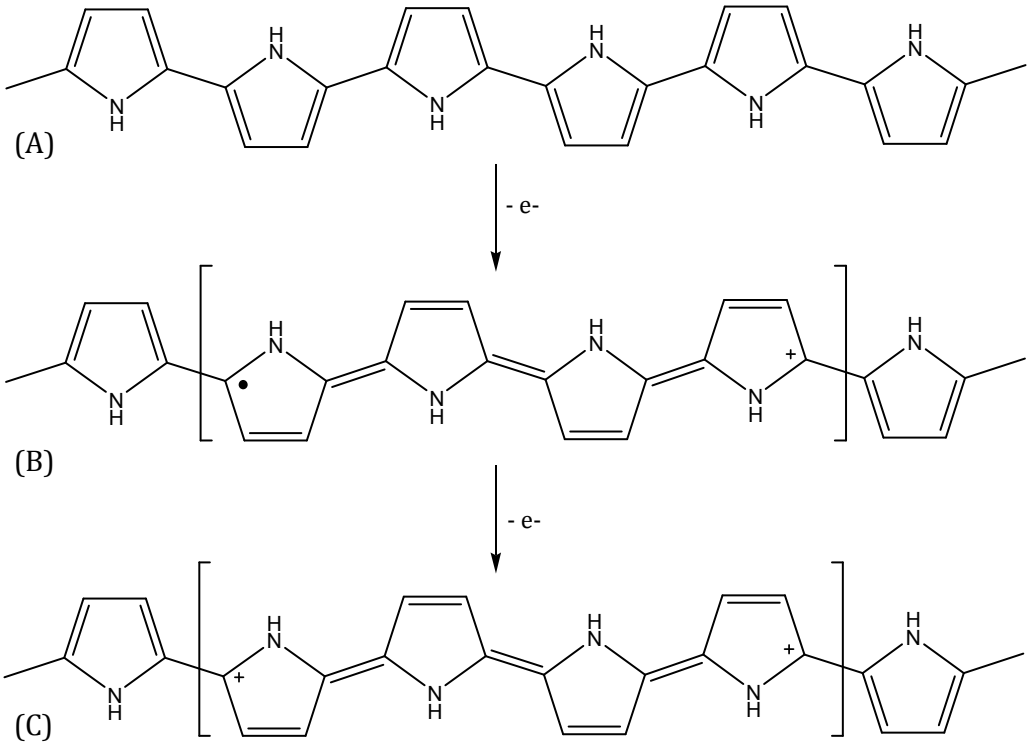


**Figure 1.6:** Electronic structures of (A) neutral PPy, (B) polaron in partially doped PPy and (C) bipolaron in fully doped (oxidised) PPy.[36]

**1.1.2.2.5 Polypyrrole and drug delivery**

The electrochemical switching of PPy films is accompanied by movement of counter or dopant ions in and out of the polymer matrix to maintain the charge neutrality, as shown in Section 1.1.2.3.4. Consequently, PPy films are attractive for the controlled release of drug molecules. The concept of using PPy membranes for the uptake and release of ions was introduced, in the early 1980s, by Burgmayer and Murray[46]. They demonstrated that these polymeric films could be exchanged from their oxidised state to their neutral state. PPy has been seriously considered for drug delivery due to these unique redox properties. PPy gives a responsive material needed in order for the uptake and release of the drug to be controlled; in its oxidised state anions are electrostatically bound to the polymer film. These properties allow the controlled transport of ions. The uptake of these ions can occur in two ways. The first is where the bioactive molecule exists as an anion and is involved in the doping process of the polymeric material during polymerisation, Figure 1.7 (A). Some anions that have been researched include adenosine tri phosphate (ATP)[65], salicylate[26], and dexamethasome[26]. These anions are electrostatically entrapped into the polymer matrix during the growth process upon application of an anodic potential. The anions are consequently liberated during the reduction of the polymer.

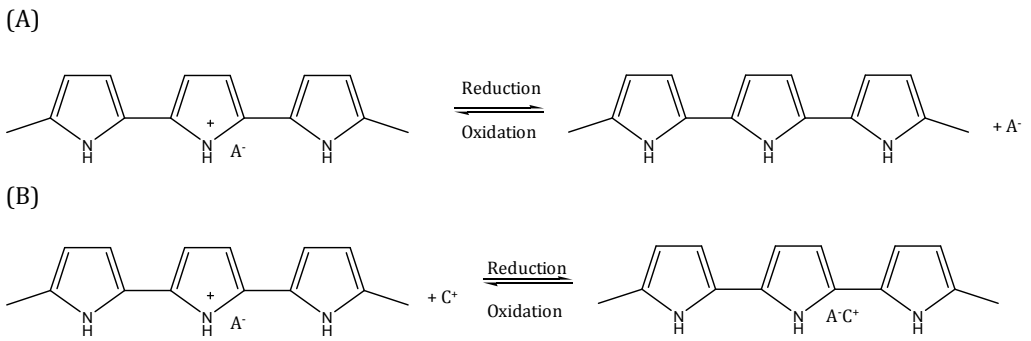


**Figure 1.7:** Interconversion between oxidation and reduction states of PPy (PPy). (A) Anion (A-) incorporation and release which is notably observed in small mobile anions (e.g. Cl-) while, (B) Cation (C+) insertion and liberation from polymer films doped with larger anions (e.g. $DDS^-$) which remain entrapped in the polymer matrix.

In the second case, cations can be incorporated into the system, Figure 1.7 (B), if the properties of the polymer film are modified.[66] This is achieved through the

initial inclusion of a large anion which remains entrapped in the polymer matrix and thus the polymer behaves as a cation exchanger, where, the charge of the polymer system can only be compensated through the uptake of cations. The cations are therefore, taken in during the reduction of the polymer and released upon oxidation. Figure 1.7 demonstrates both these concepts.

Miller and Zhou[67] previously reported the release of dopamine from a poly(*N*-methlypyrrole)/poly(styrenesulfonate) (PNMP/PSS) polymer based on the properties of these redox polymers. Immobilisation of PSS, a large anion, allows the uptake and release of the cation upon appropriate application of a potential. They achieved the release of dopamine using potential control, while more recently, Hepel and Mahdavi[66] demonstrated the controlled release of a cationic species, chloropromazine, from a composite polymer film based on the same principles. They reported the development of a new composite conducting polymer, PPy/melanin, which performed as a cation binder and releaser. The modification of the polymer films, to enable the predominant cationic exchange properties of the CP, is an interesting way of improving the uptake and release of cationic species from these attractive materials.

New ways of improving the controlled release of drugs are continually being sought after. Lately, Abidan *et al*.[41] reported on a method to prepare conducting-polymer nanotubes that can be used for controlled drug release. They introduced a method known as electrospinning to fabricate a nanofibrous mat in which the drug to be delivered had previously been incorporated; followed by electrochemical deposition of PPy films around the drug-loaded, electrospun biodegradable polymers. The drug release was achieved through the electrical stimulation of the PPy nanotubes.

#### 1.1.2.2.6 The application of Nanotechnology in drug delivery

Nanotechnology, although dating back to much earlier times, gained considerable attention in the early 1990s and has been the focus of much research over the last number of years. The introduction of nanotechnology into a controlled DDS has been shown to enhance many physical and chemical properties and overall has been used to increase the surface area of materials. This, in turn, leads to an increase in the amount of drug released from various materials. Many groups have introduced nanotechnology in various forms to improve on the drug delivery of a number of bioactive compounds, including nanoparticles[15], micellar systems[68] and nanofibers[69]. Polymeric nanofibers are gaining substantial interest for various applications including drug delivery[69, 70]. Several techniques have been employed for the production of nanofibers such as template synthesis[71], self assembly[72] and drawing[73]. One technique, in particular that is receiving considerable interest in this field, is electrospinning.[74-77] Electrospinning has been introduced to achieve nanoscale membranes and fibres from various polymeric materials.[78]

**1.1.2.2.7 The application of Electrospinning to drug delivery**

Although electrospinning was first reported by Formhals[79] in 1934 it has only been explored further in recent times.[80, 81] In 1996, Reneker and Chun restored interest in the electrospinning technique by demonstrating the possibility of electrospinning a wide range of organic polymers.[81] Since then the technique of electrospinning has become extremely useful in a variety of applications.[82-85] Electrospinning is a simple and inexpensive means for the formation of nano- to micron polymer fibers.

This technique involves the application of a high electric field between a polymer fluid and a grounded electrode. When the polymer solution is subjected to an external electric field at a critical point the forces overcome the surface tension of the polymer solution to form a droplet with a conical shape, i.e., the Taylor cone.[83, 86] The fluid is drawn into a jet which undergoes a whipping motion. Volatile solvents are used to dissolve the polymer as the subsequent evaporation from the liquid jet results in solid fibers. A more detailed

description of this technique is provided in Chapter 2, Section 2.4.5. In the majority of cases the fibers deposit randomly on the grounded collector. However, many groups have investigated the use of rotating collector plates to produce aligned nanofibers.[87] Figure 1.8 illustrates a typical SEM micrograph of an electrospun fiber mat of PLGA fibers.

This production of nanofibers allows these polymers to be used in a wide variety of applications including, tissue engineering (muscles, skin, cartilage and bones), wound healing and sutures, biosensors and DDS. Shin *et al.*[88] studied the use of PLGA nanofiber scaffold for cartilage reconstruction, while, Kim and colleagues incorporated antibiotics in the fibrous matrix for use in wound dressings.[89] Other groups have also prepared ultrafine polymers via electrospinning for skin regeneration.[74]

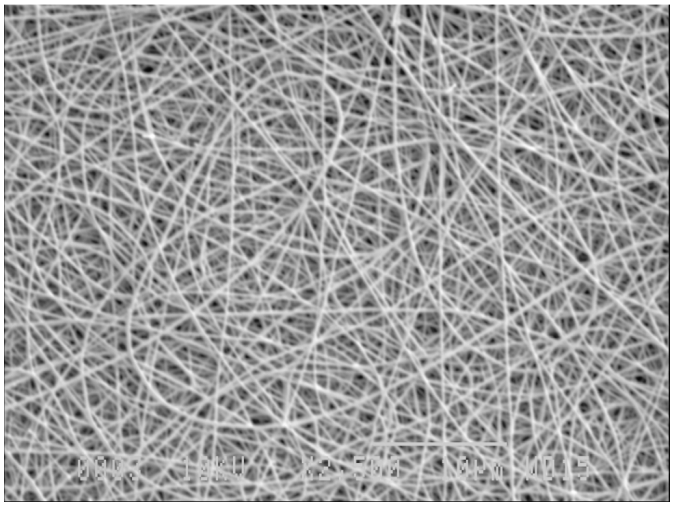

**Figure 1.8:** A typical SEM image of electrospun PLGA nanofibers.

Another attractive feature of using this electrospinning technique is that biodegradable polymeric materials, such as poly(lactic acid) (PLA) and poly($_{D,L}$ – lactide-*co*-glycolide) (PLGA) can be used as a biomedical controlled release system. These biodegradable polymers can be electrospun in the presence of varying amounts of the required medication. They can then be placed in the

body and the drug release achieved through the modification of the polymer matrix's morphology, porosity and composition.[89] These biodegradable polymers have FDA approval for biomedical and drug delivery use.[90-93] In comparison to other delivery forms, the electrospun nanofibers can conveniently incorporate the therapeutic compound during the electrospinning process.[94] Many drugs have been incorporated into PLGA electrospun polymer matrices, in order to achieve delivery of the therapeutic drug, including, tetracycline hydrochloride[95] and mefoxin[89]. In these cases, the drug release was monitored and a burst release was observed and was attributed to the high surface area-to-volume ratio of the electrospun material. This is a disadvantage. In the last few years a small number of groups have deposited electroactive polymers, such as PPy, onto previously electrospun fibers in order to enhance the electrochemical properties[57] of the material. Also, electrospun fibers have been used as a template in order to obtain a high surface area in the hope of achieving a greater uptake and release of drugs.[41]

Another method of improving the DDS of conducting polymers is the use of various dopants during polymerisation of the polymer films. The functionalisation of PPy films with large anionic dopants is not new to this field of research. It has been well reported that the use of large anionic dopants during the electrochemical polymerisation of monomers leads to these bulky negatively charged groups being immobilised within the polymer matrix.[96] In fact, these polymers, with their cationic exchange properties, have been used to incorporate various cationic groups for various applications. For example Fan and Bard in the late 1980s demonstrated the uptake of a positively charge $Ru(NH_3)_6^{3+}$ and methylviologen in PPy/Nafion films.[97]

However, the generation of PPy films in the presence of negatively charged cyclodextrins is a new concept.[98-100] There has been very little work reported on the electropolymerisation of pyrrole in the presence of anionic cyclodextrins. Indeed, much of the current published work is unreliable as very high potentials in the vicinity of 1.8 V vs. SCE were used to form the polymers.[100, 101] It is very well known that these high potentials give rise to the overoxidation of PPy and a

considerable loss in its conductivity.[59] The incorporation of cyclodextrins into conducting polymers provides a unique way of combining the unique host-guest complexation properties of cyclodextrins with the stability, high conductivity and ease of preparation of conducting polymers.

## 1.1.3 Cyclodextrins

### *1.1.3.1 History and structural properties of cyclodextrins*

Cyclodextrins (CD) are macrocyclic oligosaccharides composed of α-D-glucopyranoside units linked by α-(1,4) bonds. They were first discovered by Villiers in 1891[102], while in 1904, Schardinger[103] further developed the cyclic structures hence; CDs are sometimes referred to as Schardinger dextrins. However, it was only in the mid 1970s that the structure and chemical properties of natural cyclodextrins were fully characterised.[104] Cyclodextrins have developed quickly over the past two decades and have become an important branch of host-guest chemistry, specifically due to their ability to be involved in several practical applications.[105] The main interest in cyclodextrins lies in their ability to form inclusion complexes with a variety of compounds. Host-guest chemistry is the study of these inclusion phenomena, where the 'host' molecules are capable of including smaller 'guest' molecules through non-covalent interactions.

CDs are obtained through enzymatic degradation of starch in the presence of a glycosyl transferase, a type of amylase.[106] Many organisms contain glycosyl transferase, however, in general it is obtained from *Bacillus megaterium, Bacillus stereothermophilus and Bacillus macerans.*[106, 107] They are generally made up of glucopyranoside units of $^4C_1$ chair conformation which leads to a truncated cone shape encasing a cavity.[108] Figure 1.9 shows the structures of the most common CD members; α-, β- and γ-CD, which include 6, 7 and 8 repeating glucopyranoside units, respectively. These units orientate themselves in a cyclic manner offering a typical conical or truncated cone structure with a relatively hydrophobic interior and hydrophilic exterior.[109] This structural property gives cyclodextrins good water solubility and the ability to hold appropriately sized

guests, such as amines and ferrocenes[110], through non-covalent interactions such as hydrogen bonding, hydrophobic interactions, and electrostatic interactions.[111] Table 1.1 demonstrates the approximate geometries of the most common CDs.[109]

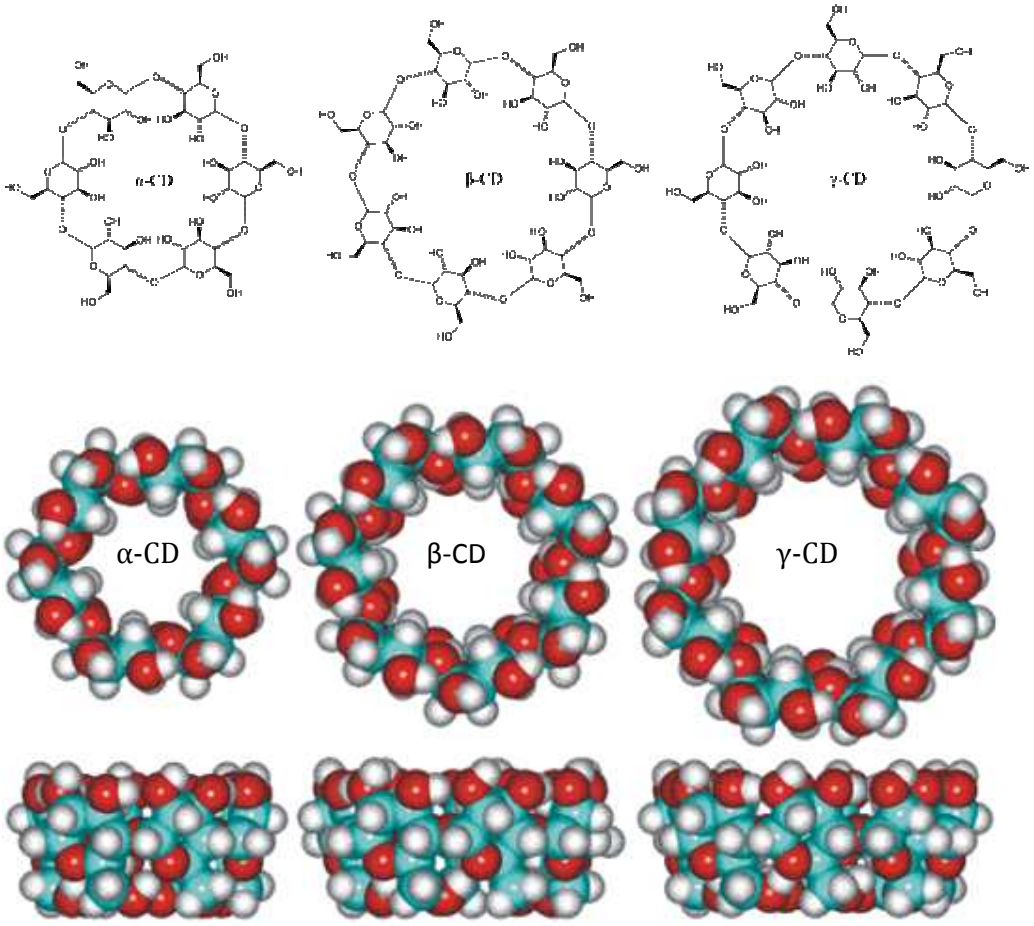


**Figure 1.9:** Structures of α-, β- and γ-cyclodextrin taken from Szjetli.[109]

Due to their exceptional host-guest complexation abilities, CDs have been used in a variety of fields, such as environmental protection through immobilising toxic compounds in their cavities and in the food industry.[104] In fact one of the commercially available applications for CDs is Febreze®, which is an aqueous solution of modified β-cyclodextrins**.** Febreze® is based on the host-guest chemistry of the CDs, with molecules that produce aroma forming inclusion complexes with the modified CDs. In the pharmaceutical industry, CDs are also

used for many applications including, drug delivery to enhance the solubility, stability and bioavailability of drug molecules.[108, 112]

**Table 1.1:** Approximate geometric dimensions of the three common CDs.[106]

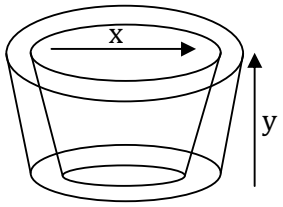


| Cyclodextrin | x / nm | y / nm | Cavity volume / Å$^3$ |
|---|---|---|---|
| **α** | 0.49 | 0.78 | 174 |
| **β** | 0.62 | 0.78 | 262 |
| **γ** | 0.79 | 0.78 | 427 |

Cyclodextrins can also be chemically modified to replace the hydroxyl groups on both the primary and secondary rims of the CDs, with a variety of appropriate alkyl groups (R). It has been reported that this can improve binding affinity.[108] In the research presented here, a negatively charged cyclodextrin with a number of sulfonated groups present on the outer rims was used, sulfonated β-CD (Sβ-CD). Sβ-CD is obtained by substitution of either primary or secondary hydrogen of the hydroxyl group of β-CD with a sulfonate group. Sβ-CD has an average of 7-11 substituents per CD and, therefore, has between 7-11 negative charges associated with it, which are counterbalanced with sodium ions, as illustrated in Figure 1.10.[113] It is reported that β-CD and Sβ-CD have the same ring structure, differing only in the substituent located on the rims of the CD ring.[14] Although Sβ-CD has the same ring structure as other derivativsed CDs the presence of the substituent on the ring contributes to its chiral discrimination properties.[114] A major area in which these sulfonated CDs are being utilised is chromatography, or more specifically capillary electrophoresis, for the enantiomeric separation of acidic and basic compounds. In enantiomeric separation, using neutral CDs, they are not appropriate for neutral racemates as the complex has no electrophoretic mobilities.[115] Therefore, the use of charged

CDs is now been widely researched for the separation of neutral compounds. It has been reported that the use of these sulfonated CDs for the enantiomeric separation of chiral compounds is highly effective as a result of the anionic charges.[116, 117]

A number of groups have also characterised the Sβ-CD.[115, 117] Figure 1.11 illustrates a single glucose unit of an Sβ-CD (comprised of 7 units). On the primary ring there are 7 potential substitution sites corresponding to the C-6 positions, while, on the secondary rim there are 14, represented by the C-2 and C-3 positions. Amini and co-workers[117] reported that substitution of these CDs is predominantly at the C-2 and C-6 positions, while, Chen *et al.*[115] confirmed nearly complete sulfation at the C-6 position of the primary hydroxyl groups and partial sulfation at the C-2 secondary hydroxyl groups. They also reported no substitution at the C-3 positions. From these reports it can be stated that almost the entire primary rim is sulfonated and some of the secondary rim. Due to this phenomenon and the fact that the sulfation brings with it negative charges these CDs are good candidates for the doping of CPs.

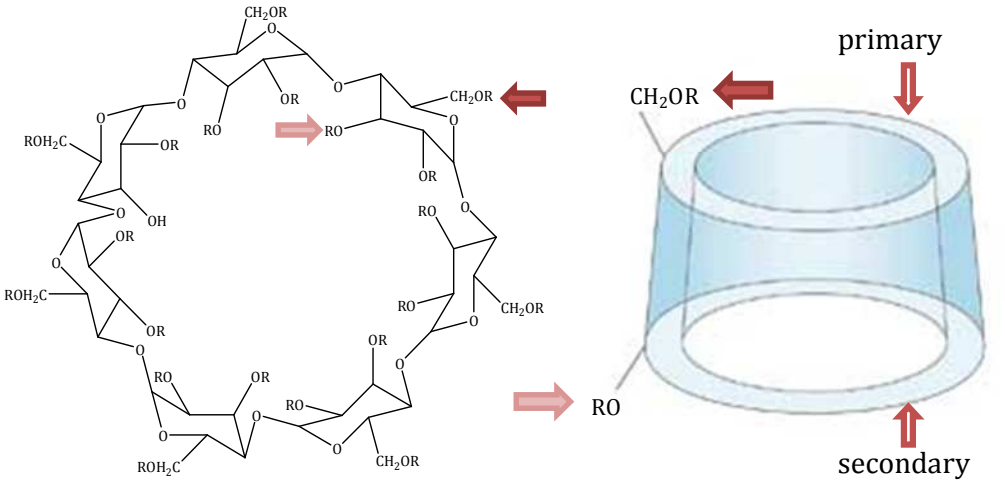


R = $SO_3^-Na^+$ or H ~ 7-11 $SO_3^-Na^+$ groups.

**Figure 1.10:** Structural and schematic representation of sulfonated β-cyclodextrin (Sβ-CD). The arrows point to the primary and secondary rims, respectively.[118]

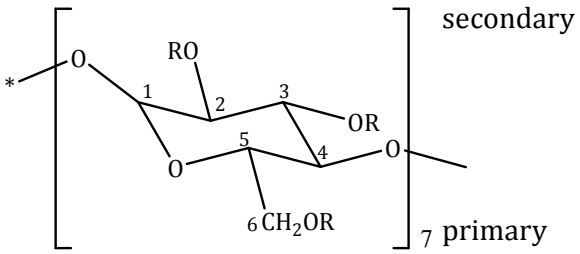


**Figure 1.11:** Chemical structure of Sβ-CD, depicting the numbering carbons.

### *1.1.3.2 Inclusion complexation*

Cyclodextrins (CD) form a group of cyclic oligosaccharides that contain cavities in which guest molecules can be encapsulated.[108, 109] It is well known that the size of the compounds are important and compounds are only capable of including into the cavity of the CD if they are within the dimensions of the CD cavity.[119] In aqueous media, the cavity is filled with water molecules, which becomes displaced by the guest through complexation, as illustrated in Figure 1.12. The guest molecule, xylene, displaces the water molecules and forms an inclusion complex with the CD.

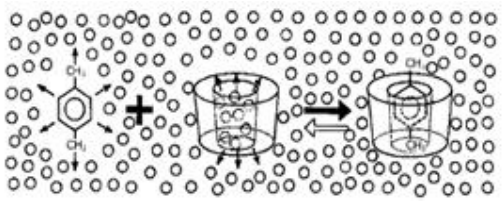

**Figure 1.12:** Schematic representation of xylene forming a complex with a β-cyclodextrin. The small circles represent water molecules taken from Szjetli.[109]

During the formation of an inclusion complex the chemical and the physical properties of the guest molecule change and can be monitored using a number of techniques. Various spectroscopic and electrochemical techniques can be used to confirm complexation, including fluorescence, UV-visible spectroscopy (UV), Nuclear magnetic resonance (NMR) and electrochemical studies. These changes attributed to the complexation can be used to evaluate the apparent

binding or formation constant ($K_f$). However, prior to the determination of the $K_f$ value the stoichiometry of the host-guest complex must be established.[120] This is obtained by the well known continuous variation or Job's method which is described in more detail in Chapter 2, Section 2.6.1.1.[121] Generally, inclusion complexes form a ratio of 1:1, 1:2 and sometimes 2:1 (CD:guest).[122]

NMR is also a useful tool for the study of complexation due to its quantitative information and assuming the guest enters the cavity, NMR, can be also used to locate the protons involved in complexation.[87] Many groups have studied the complexation properties with the neutral β-CD and monitored the changes in the chemical shifts for both the CD, and the guest. However, in the case of the modified CD used in this research, the NMR spectral data are too difficult to differentiate so the chemical shift of the guest is followed.[120, 123-126] Bratu and colleagues[125] studied the chemical shift changes observed when Fenbufen was in the presence of a neutral β-CD. They noticed an up-field shift of the guest protons, some more pronounced than others, and suggested that the complexation was initiated through the benzene moiety of the guest. Cruz *et al*.[127] also used NMR to quantitatively evaluate the binding constant of the complexation of doxepin and a neutral β-CD.

If a guest absorbs light in the UV or visible region then the inclusion phenomenon can be followed and subsequently, evaluated by UV.[106] This technique can be used to confirm complexation and indeed obtain the formation constant associated with the inclusion complex. In the majority of cases the guest that absorbs in the UV-vis region experiences changes in the intensity and the position of the absorption bands in the presence of the CD. These spectral changes can be used to determine the $K_f$ constants. Generally, a Hiedlebrand-Benesi modified equation is used to evaluate the $K_f$ constants.[119, 128, 129] Ramaraj and co-workers[130] monitored the changes attained during the complexation formation of a number of aromatic amines and nitro compounds in the presence of a neutral β-CD. They observed an increase in the intensity of the bands in all cases. Dang *et al*.[119] observed shifts of the absorption bands to longer

wavelengths in the case of 1,4 benzoquinone (BQ) and 9,10 anthraquinone (AQ) in the presence of a neutral β-CD.

Electrochemical techniques can also be performed on the complexation properties of CDs. If the guest is electroactive the peak current and potential can be followed for the free state and compared to the complexed state of the guest in question. Two features are generally observed during these electrochemical observations if an inclusion complex is found. Firstly, a decrease in the peak current can be seen, and, attributed to a decrease in the diffusion of the bulky CD complex as opposed to the more mobile free guest. Secondly, a shift in the peak potential is observed if the complexed species is included in the cavity, as it is harder to oxidise or reduce while located in the cavity. Once again based on these variations a number of equations can be used to verify the formation constant.[129, 131, 132] Coutouli-Argyropoulou and his group[133] reported the effect of complexation on the electrochemical properties of ferrocence derivatives and showed shifts, in both the peak current and peak potential, when higher concentrations of a neutral β-CD were added. Yanez *et al*.[131] showed similar observations for nifedipine (NF) and nicardipine (NC) and estimated apparent formation constants of 135 and 357, respectively.

Complexation studies of DA have been previously demonstrated in the presence of a neutral β-CD by Zhou *et al*.[134] using UV and fluorescence spectroscopy. From the fluorescence technique, utilising a Hiedlebrand-Benesi modified equation, a $K_f$ value of 95.06 was estimated. The degree of the complexation can vary over a wide range due to the stability of the complex, as it depends on a number of factors. In the next section a discussion on the main driving forces, involved in this complexation process are dealt with.

#### *1.1.3.3 Driving forces in the inclusion complexation process*

There are many reviews and books written on the driving forces behind the inclusion complexation abilities of cyclodextrins, not all agree, some refer to the predominantly hydrophobic affects while others state that it is a collection of a

number of weaker interactions (H-bonding, van der Waals, electrostatic interactions).[106, 108, 111, 135, 136] Either way the majority agree that the size of the cavity and shape of the guest are important factors in the complexation process. The most widely studied possible driving forces include

- Hydrogen bonding
- Electrostatic interaction
- Van der Waals
- Hydrophobic effect

Hydrogen bonding is an interaction between an electronegative donor, a hydrogen and an electronegative acceptor.[136] Various groups have demonstrated the importance of hydrogen bonding in the solid state, illustrating crystal structures defining the hydrogen bonding between the guest and the hydroxyls of the CDs.[137] However, during the complexation of the CD and guest, in aqueous solution, the subject is still arguable as few direct measurements of hydrogen bonding have been made, as water molecules can compete with CDs to form hydrogen bonding with guest molecules. However, many groups will still argue over the significance of hydrogen bonding.

Electrostatic interaction occurs when molecules of opposite charges interact. There are three types of electrostatic interactions, ion-ion interaction, ion-dipole interaction and dipole-dipole interaction.[136] Matsui and Okimoto[138] reported that ion-ion interaction is only eligible in the case of modified CDs, where as ion-dipole is considered more favourably due to the fact that CDs are polar molecules however as with hydrogen bonding, in aqueous media, the interaction between the guest and water will also be strong.[136] Therefore, it is the case of dipole-dipole interaction that is mostly considered during complexation.

Van der Waals forces or London dispersion forces are made up of dipole induced dipole contributions or the coordination of the electronic motion in the CD and guest. As CDs are known to have large dipole moments it is logical that

these induction forces are important in complexation. Experimental evidence has shown that the stability of the complex increases with an increase in polarisability. Also, as the polarisability of water is lower than the organic components of the CD cavity, van der Waals forces have an encouraging donation to the stability of the complex due to a stronger interaction of the CD and guest over the water and guest.[136] CDs have also been reported to form stable inclusion complexes in organic solvents like DMF and DMSO confirming the importance of van der Waals forces.[139]

The hydrophobic interaction which is entropically favourable, due to the expulsion of water, leads to the aggregation of non-polar solutes in aqueous solution.[136] As reviewed by Connors[135] the 'classical' hydrophobic interaction is said to be 'entropy driven' and a positive entropy and enthalpy is associated for the interaction between two non polar molecules. However, experimental studies in the complexation of CD and guests, show negative enthalpy and entropy changes,[111] which have been suggested to indicate that these interactions are not a dominant force.

Mosinger *et al*.[122] reported that the formation of an inclusion complex is based on the electrostatic, van der Waals and π-π interactions, where, steric affects and Hydrogen bonding are inevitable. Chao and co-workers[124] investigated the formation of an inclusion complex with β-CD and caffeic acid, they reported that the weak forces of hydrogen bonding, van der Waals, hydrophobic and electrostatic interactions simultaneously governed the process.

Rekharsky and Inoue[111] reviewed the complexation of cyclodextrins and stated that the interactions involved in the inclusion complexation of aromatic guests with CDs could not be simply put down to a hydrophobic effect. They established that complexation could be accounted for, through dipole-dipole interactions. In saying that, Tabushi and his group[140] questioned the role of hydrogen bonding in the complexation process and reported that no dramatic changes of binding were observed, when a modified CD, incapable of hydrogen bonding, was compared to an unmodified CD. They concluded that the

involvement of hydrogen bonding was negligible and hydrophobic interactions dominated the process. Zia *et al*.[113] investigated the complexation ability of a negatively charged CD (~7 negative sites) with a number of neutral and charged guest molecules. They accounted for the increase in the binding affinity, for the oppositely charged guest and CD, to be predominantly hydrophobic, due to the additional interaction sites provided by the negatively charged CD. Okimoto and colleagues[141] also clearly observed stronger interactions occurring between a CD and guest with opposite charges.

The understanding of these complexation processes is complicated, however, it is generally found that van der Waals forces and hydrophobic interactions are regarded as the main driving forces for CD complexation, while, electrostatic interactions and hydrogen bonding can be significantly considered in some inclusion complexation studies. Nevertheless, these attractive features of CDs allow them to be used in a wide range of applications including, the food industry[142]. However, the pharmaceutical industry is the most widely researched area in recent times, specifically in drug formulation and DDS.[143]

#### *1.1.3.4 Applications of CDs in DDS*

Due to their biocompatibility and their ability to form inclusion complexes, CDs have been studied for the use in DDS. They have been considered as drug carriers, as CDs have the potential to act as hydrophobic carriers and control the release of a variety of drugs.[118] Many reviews have recently been published, describing the role of CDs in DDS.[112, 118, 144-147] Irie and Uekama[144] reviewed the role of CDs in peptide and protein delivery and summarised that CDs were able to eliminate a number of undesirable properties of drug formulations, as they form inclusion complexes with the desired drugs, which increase the drug delivery through a number of routes of administration. More recently, Li *et al.*[145] examined the recent progress in the preparation of inclusion complexes between CDs and various polymers as supramolecular biomaterials for drug and gene delivery. They demonstrated the promising field in the self assembly

of inclusion complexes between CDs and biodegradable polymers as injectable DDS.

Ferancova and Labuda[148] also reviewed the use of CDs as electrode modifiers. They summarised the many ways CDs can be immobilised onto electrode surfaces. As discussed in an earlier section, Section 1.1.4.2., the incorporation of CDs, as dopants, during the electrochemical polymerisation of CPs was demonstrated to examine the use of these modified electrodes to deliver neutral drugs.[98] Formulating these materials, correlates the attractive features of both the CDs and the CPs. Bidan *et al*.[98] examined the need for a new DDS that was not limited to charged drugs. They produced polymer films in the presence of an anionic CD and successfully delivered neutral compounds using these novel materials.

Also briefly discussed in Section 1.1.4.2, was the reports made by a number of groups on the polymerisation of CPs in the presence of CDs.[100, 101, 149] These groups have reportedly polymerised pyrrole at potentials usually shown to overoxidise the CP film.[59] Due to this, these papers are unreliable in their reports.

### 1.1.4 Drug release: Controlled release of dopamine

DA is a neurotransmitter produced naturally in the brain. It is well documented that a common factor in neurodegenerative diseases such as Parkinson's (PD) and Schizophrenia is a significant lack of the presence of DA in the *substantia nigra* (mid brain).[150-152] In particular, PD is a slowly progressive disorder known to occur due to the damage of the basal ganglia.[150-152] The disease affects movement, muscle control and balance. Studies on the brains of deceased Parkinson sufferers show a substantial loss of dopamine, particularly, in the *substantia nigra*. The function of the substantia nigra is to produce DA and manage the release of essential neurotransmitters that help control movement and coordination. Sufferers usually show symptoms such as tremors, slowness of movement and impaired balance and coordination. Prolonged loss of DA

gives rise to symptoms such as difficulty in walking, talking, or completing other simple tasks.[150-152]

DA belongs to the well known catecholamine family. These molecules are electroactive and therefore their oxidation can be followed using electrochemistry, in particular, electrochemical methods such as cyclic voltammetry and rotational disc voltammetry. The electrochemical mechanism of oxidation is still not fully agreed; with various groups arguing that the mechanism goes through an ECE step rather than a CE step. For example, Hawley *et al*.[153] have reported that the electrochemical oxidation of dopamine in aqueous solution proceeds through two types of steps, electrochemical (E) and chemical (C). The ECE mechanism is presented in Scheme 1.1.

The first step in the oxidation of dopamine (A) involves the loss of both protons and electrons to form the o-dopaminoquinone (B). The oxidised, o-dopaminoquinone undergoes a 1,4-Michael addition, which results in a intramolecular cyclisation reaction which produces leucodopaminochrome (C). This product is easily oxidised through an electrochemical step to form dopaminochrome (D).[153, 154]

Controlled release studies of DA have been previously investigated.[67, 155-158] McRae-Degueurce *et al*.[156] encapsulated DA into a thermoplastic polyester excipient: PLGA. They found that it was possible to deliver significant amounts of DA for prolonged periods of time by injecting the microencapsulated DA directly into the brain. Uludag and colleagues[157] also examined the release of many therapeutic agents, including DA, from microencapsulated mammalian cells. The mammalian cells and tissues were entrapped in polymeric microcapsules containing the desired bioactive agent.

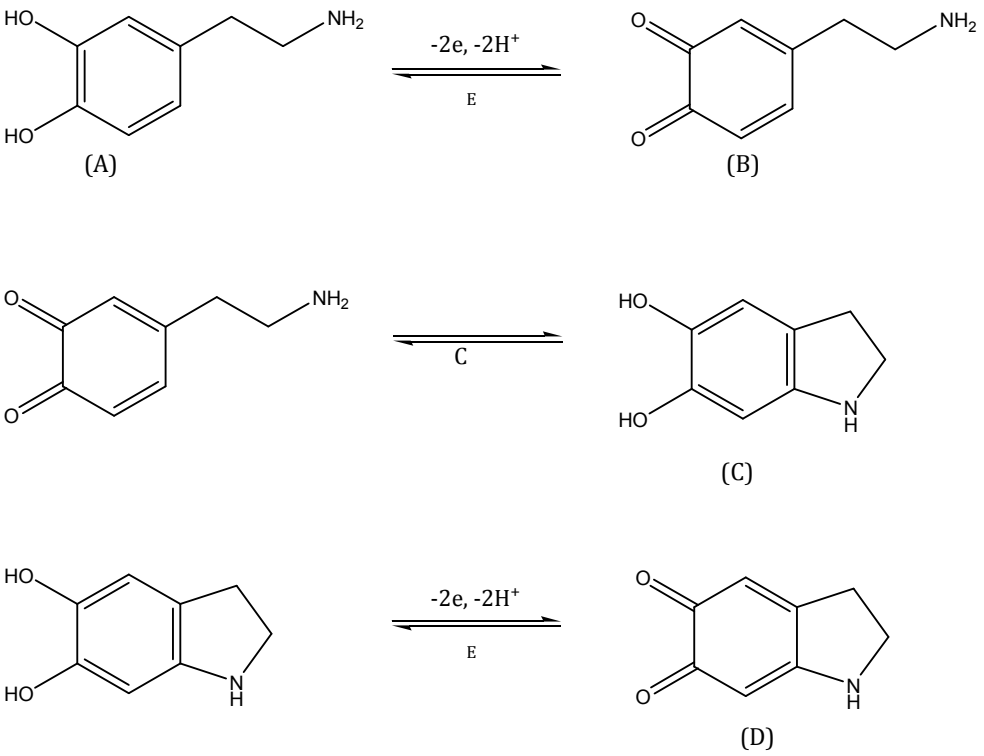


**Scheme 1.1:** The proposed oxidative pathway for dopamine.

In both these cases the release was based on diffusion from the polymeric materials. It is, therefore, difficult to maintain any control over the amount of DA released. Miller[67] and Zhou[158] and co-workers investigated the use of CPs to deliver DA. They introduced the concept of using large immobile dopants, which remain entrapped inside the cavity during polymerisation, to bind and successfully liberate DA from the polymer films.

This is the basis of the work performed in this thesis. As outlined at the start of this chapter, the idea of this research is to develop PPy films for the uptake and release of DA, using a large immobile anionic cyclodextrin. The cyclodextrin, in addition to its large size and immobility, has unique host-guest complexation properties and this offers the prospects of inclusion complexation between the DA and the CD to enhance the drug delivery. If this can be achieved it could potentially serve as a model system in DDS and could be extended to various other cationic drug molecules.

## 1.2 References


1. N. A. Peppas and D. J. A. Ende, *J Appl Polym Sci*, **66**, (1997), 509-513.
2. U. R. Pothakamury and G. V. BarbosaCanovas, *Trends Food Sci Tech*, **6**, (1995), 397-406.
3. B. Singh, D. K. Sharma, and A. Gupta, *J Environ Sci Heal B*, **44**, (2009), 113-122.
4. N. A. Peppas and R. Langer, *Science*, **263**, (1994), 1715-1720.
5. K. E. Uhrich, S. M. Cannizzaro, R. S. Langer, and K. M. Shakesheff, *Chem Rev*, **99**, (1999), 3181-3198.
6. D. L. Wise, Encyclopedic handbook of biomaterials and bioengineering Marcel Dekker, 1995.
7. J. T. Santini, A. C. Richards, R. Scheidt, M. J. Cima, and R. Langer, *Angew Chem Int Edit*, **39**, (2000), 2397-2407.
8. R. Langer, *Mrs Bull*, **31**, (2006), 477-485.
9. L. K. Fung and W. M. Saltzman, *Adv Drug Deliver Rev*, **26**, (1997), 209-230.
10. R. Langer, *Science*, **249**, (1990), 1527-1533.
11. R. Langer, *Nature*, **392**, (1998), 5-10.
12. J. Folkman and D. Long, *JOURNAL OF SURGICAL RESEARCH*, **4**, (1963), 139-142.
13. T. M. Allen and P. R. Cullis, *Science*, **303**, (2004), 1818-1822.
14. J. J. Wang, G. J. Zheng, L. Yang, and W. R. Sun, *Analyst*, **126**, (2001), 438-440.
15. H. Wartlick, K. Michaelis, S. Balthasar, K. Strebhardt, J. Kreuter, and K. Langer, *J Drug Target*, **12**, (2004), 461-471.
16. L. M. Lira and S. I. C. de Torresi, *Electrochem Commun*, **7**, (2005), 717-723.
17. S. Murdan, *J Control Release*, **92**, (2003), 1-17.
18. J. E. Riviere and M. C. Heit, *Pharmaceut Res*, **14**, (1997), 687-697.
19. G. Inzelt, Conducting Polymers, A new era in electrochemistry, Springer, 2008.
20. V. V. Walatka, M. M. Labes, and Perlstei.Jh, *Phys Rev Lett*, **31**, (1973), 1139-1142.
21. H. Shirakawa, E. J. Louis, A. G. Macdiarmid, C. K. Chiang, and A. J. Heeger, *J Chem Soc Chem Comm*, (1977), 578-580.
22. A. J. Heeger, *Angew Chem Int Edit*, **40**, (2001), 2591-2611.
23. A. G. MacDiarmid, *Angew Chem Int Edit*, **40**, (2001), 2581-2590.
24. H. Shirakawa, *Angew Chem Int Edit*, **40**, (2001), 2575-2580.
25. P. Chandrasekhar, Conducting Polymers, Fundamentals and Applications: A practical approach, Kluwer Acandemic Publishers, 1999.
26. A. A. Entezami and B. Massoumi, *Iran Polym J*, **15**, (2006), 13-30.
27. N. K. Guimard, N. Gomez, and C. E. Schmidt, *Prog Polym Sci*, **32**, (2007), 876-921.
28. A. Malinauskas, J. Malinauskiene, and A. Ramanavicius, *Nanotechnology*, **16**, (2005), R51-R62.
29. C. E. Schmidt, V. R. Shastri, J. P. Vacanti, and R. Langer, *P Natl Acad Sci USA*, **94**, (1997), 8948-8953.
30. J. L. Bredas and G. B. Street, *Accounts Chem Res*, **18**, (1985), 309-315.

31. D. L. Wise, Electrical and optical polymer systems, CRC Press, 1998.
32. L. Alcacer, Conducting Polymers: Special Applications (Hardcover), Springer 1986.
33. B. Winther-Jensen, J. Chen, K. West, and G. Wallace, *Polymer*, **46**, (2005), 4664-4669.
34. A. Malinauskas, *Polymer*, **42**, (2001), 3957-3972.
35. R. A. Green, N. H. Lovell, G. G. Wallace, and L. A. Poole-Warren, *Biomaterials*, **29**, (2008), 3393-3399.
36. T. A. Skotheim and J. R. Reynolds, Handbook of conducting polymers: Conjugated polymers, CRC Press, 2007.
37. P. C. Lacaze, J. C. Lacroix, K. C. Ching, and S. Aeiyach, *Actual Chimique*, (2008), 90-91.
38. M. A. Mohamoud, *Plast Eng*, **64**, (2008), 32-+.
39. M. Nikolou and G. G. Malliaras, *Chem Rec*, **8**, (2008), 13-22.
40. E. Smela, *Mrs Bull*, **33**, (2008), 197-204.
41. M. R. Abidian, D. H. Kim, and D. C. Martin, *Adv Mater*, **18**, (2006), 405-409.
42. C. Arbizzani, M. Mastragostino, L. Nevi, and L. Rambelli, *Electrochim Acta*, **52**, (2007), 3274-3279.
43. K. Kontturi, P. Pentti, and G. Sundholm, *J Electroanal Chem*, **453**, (1998), 231-238.
44. Y. L. Li, K. G. Neoh, and E. T. Kang, *J Biomed Mater Res A*, **73A**, (2005), 171-181.
45. J. M. Pernaut and J. R. Reynolds, *J Phys Chem B*, **104**, (2000), 4080-4090.
46. P. Burgmayer and R. W. Murray, *J Am Chem Soc*, **104**, (1982), 6139-6140.
47. A. Dall'Olio, G. Dascola, V. Varacca, and V. Bocchi, *Comptes Rendus de l'Academie des Sciences*, **C267**, (1968), 433-435.
48. A. F. Diaz and J. I. Castillo, *J Chem Soc Chem Comm*, (1980), 397-398.
49. B. Winther-Jensen and N. B. Clark, *React Funct Polym*, **68**, (2008), 742-750.
50. C. K. Baker and J. R. Reynolds, *J Electroanal Chem*, **251**, (1988), 307-322.
51. S. Geetha, C. R. K. Rao, M. Vijayan, and D. C. Trivedi, *Anal Chim Acta*, **568**, (2006), 119-125.
52. Z. X. Wang, C. Roberge, L. H. Dao, Y. Wan, G. X. Shi, M. Rouabhia, R. Guidoin, and Z. Zhang, *J Biomed Mater Res A*, **70A**, (2004), 28-38.
53. Z. Zhang, R. Roy, F. J. Dugre, D. Tessier, and L. H. Dao, *J Biomed Mater Res*, **57**, (2001), 63-71.
54. A. Kotwal and C. E. Schmidt, *Biomaterials*, **22**, (2001), 1055-1064.
55. J. Y. Wong, R. Langer, and D. E. Ingber, *P Natl Acad Sci USA*, **91**, (1994), 3201-3204.
56. B. Garner, A. Georgevich, A. J. Hodgson, L. Liu, and G. G. Wallace, *J Biomed Mater Res*, **44**, (1999), 121-129.
57. X. D. Wang, X. S. Gu, C. W. Yuan, S. J. Chen, P. Y. Zhang, T. Y. Zhang, J. Yao, F. Chen, and G. Chen, *J Biomed Mater Res A*, **68A**, (2004), 411-422.
58. S. Asavapiriyanont, G. K. Chandler, G. A. Gunawardena, and D. Pletcher, *J Electroanal Chem*, **177**, (1984), 229-244.
59. J. Heinze, *Synthetic Met*, **43**, (1991), 2805-2823.
60. G. Inzelt, V. Kertesz, and A. S. Nyback, *J Solid State Electr*, **3**, (1999), 251-257.

61. C. Y. Jin, F. L. Yang, and W. S. Yang, *J Appl Polym Sci*, **101**, (2006), 2518-2522.
62. V. M. Jovanovic, A. Dekanski, G. Vlajnic, and M. S. Jovanvic, *Electroanal*, **9**, (1997), 564-569.
63. S. Sadki, P. Schottland, N. Brodie, and G. Sabouraud, *Chem Soc Rev*, **29**, (2000), 283-293.
64. J. Tamm, A. Alumaa, A. Hallik, U. Johanson, L. Tamm, and T. Tamm, *Russ J Electrochem+*, **38**, (2002), 182-187.
65. M. Pyo and J. R. Reynolds, *Chem Mater*, **8**, (1996), 128-133.
66. M. Hepel and F. Mahdavi, *Microchem J*, **56**, (1997), 54-64.
67. L. L. Miller and Q. X. Zhou, *Macromolecules*, **20**, (1987), 1594-1597.
68. G. A. Husseini and W. G. Pitt, *J Pharm Sci-Us*, **98**, (2009), 795-811.
69. X. L. Xu, X. S. Chen, P. A. Ma, X. R. Wang, and X. B. Jing, *Eur J Pharm Biopharm*, **70**, (2008), 165-170.
70. S. G. Kumbar, L. S. Nair, S. Bhattacharyya, and C. T. Laurencin, *J Nanosci Nanotechno*, **6**, (2006), 2591-2607.
71. L. Feng, S. H. Li, H. J. Li, J. Zhai, Y. L. Song, L. Jiang, and D. B. Zhu, *Angew Chem Int Edit*, **41**, (2002), 1221-+.
72. G. M. Whitesides and B. Grzybowski, *Science*, **295**, (2002), 2418-2421.
73. T. Ondarcuhu and C. Joachim, *Europhys Lett*, **42**, (1998), 215-220.
74. J. Fang, H. T. Niu, T. Lin, and X. G. Wang, *Chinese Sci Bull*, **53**, (2008), 2265-2286.
75. E. R. Kenawy, F. I. Abdel-Hay, M. H. El-Newehy, and G. E. Wnek, *Mat Sci Eng a-Struct*, **459**, (2007), 390-396.
76. Q. J. Xie, S. Kuwabata, and H. Yoneyama, *J Electroanal Chem*, **420**, (1997), 219-225.
77. E. Luong-Van, L. Grondahl, K. N. Chua, K. W. Leong, V. Nurcombe, and S. M. Cool, *Biomaterials*, **27**, (2006), 2042-2050.
78. Z. M. Huang, Y. Z. Zhang, M. Kotaki, and S. Ramakrishna, *Compos Sci Technol*, **63**, (2003), 2223-2253.
79. A. Formhals, Vol. 1975504, 1934.
80. J. Doshi and D. H. Reneker, *J Electrostat*, **35**, (1995), 151-160.
81. D. H. Reneker and I. Chun, *Nanotechnology*, **7**, (1996), 216-223.
82. A. Greiner and J. H. Wendorff, *Angew Chem Int Edit*, **46**, (2007), 5670-5703.
83. D. Li and Y. N. Xia, *Adv Mater*, **16**, (2004), 1151-1170.
84. D. H. Reneker, A. L. Yarin, H. Fong, and S. Koombhongse, *J Appl Phys*, **87**, (2000), 4531-4547.
85. T. Subbiah, G. S. Bhat, R. W. Tock, S. Pararneswaran, and S. S. Ramkumar, *J Appl Polym Sci*, **96**, (2005), 557-569.
86. G. I. Taylor, *Proc. Roy. Soc. Lond.*, **A313**, (1969), 453-475.
87. A. Bernini, O. Spiga, A. Ciutti, M. Scarselli, G. Bottoni, P. Mascagni, and N. Niccolai, *Eur J Pharm Sci*, **22**, (2004), 445-450.
88. H. J. Shin, C. H. Lee, I. H. Cho, Y. J. Kim, Y. J. Lee, I. A. Kim, K. D. Park, N. Yui, and J. W. Shin, *J Biomat Sci-Polym E*, **17**, (2006), 103-119.
89. K. Kim, Y. K. Luu, C. Chang, D. F. Fang, B. S. Hsiao, B. Chu, and M. Hadjiargyrou, *J Control Release*, **98**, (2004), 47-56.
90. R. A. Jain, *Biomaterials*, **21**, (2000), 2475-2490.

91. M. Garinot, V. Fievez, V. Pourcelle, F. Stoffelbach, A. des Rieux, L. Plapied, I. Theate, H. Freichels, C. Jerome, J. Marchand-Brynaert, Y. J. Schneider, and V. Preat, *J Control Release*, **120**, (2007), 195-204.
92. D. Luo, K. Woodrow-Mumford, N. Belcheva, and W. M. Saltzman, *Pharmaceut Res*, **16**, (1999), 1300-1308.
93. X. H. Zong, S. Li, E. Chen, B. Garlick, K. S. Kim, D. F. Fang, J. Chiu, T. Zimmerman, C. Brathwaite, B. S. Hsiao, and B. Chu, *Ann Surg*, **240**, (2004), 910-915.
94. Z. M. Huang, C. L. He, A. Z. Yang, Y. Z. Zhang, X. J. Hang, J. L. Yin, and Q. S. Wu, *J Biomed Mater Res A*, **77A**, (2006), 169-179.
95. E. R. Kenawy, G. L. Bowlin, K. Mansfield, J. Layman, D. G. Simpson, E. H. Sanders, and G. E. Wnek, *J Control Release*, **81**, (2002), 57-64.
96. G. Bidan, B. Ehui, and M. Lapkowski, *J Phys D Appl Phys*, **21**, (1988), 1043-1054.
97. F. R. F. Fan and A. J. Bard, *J Electrochem Soc*, **133**, (1986), 301-304.
98. G. Bidan, C. Lopez, F. Mendesviegas, E. Vieil, and A. Gadelle, *Biosens Bioelectron*, **10**, (1995), 219-229.
99. D. A. Reece, S. F. Ralph, and G. G. Wallace, *J Membrane Sci*, **249**, (2005), 9-20.
100. K. R. Temsamani, O. Ceylan, B. J. Yates, S. Oztemiz, T. P. Gbatu, A. M. Stalcup, H. B. Mark, and W. Kutner, *J Solid State Electr*, **6**, (2002), 494-497.
101. N. Izaoumen, D. Bouchta, H. Zejli, M. El Kaoutit, A. M. Stalcup, and K. R. Temsamani, *Talanta*, **66**, (2005), 111-117.
102. A. Villiers, *C. R Acad. Sci*, **112**, (1891), 536.
103. F. Schardinger, *Wien. Klin. Wochenschr*, **17**, (1904), 207.
104. A. R. Hedges, *Chem Rev*, **98**, (1998), 2035-2044.
105. J. Szejtli, *J Mater Chem*, **7**, (1997), 575-587.
106. W. Saenger, *Angewandte Chemie-International Edition in English*, **19**, (1980), 344-362.
107. D. French, *Method Enzymol*, **3**, (1957), 17-20.
108. H. Dodziuk, Cyclodextrins and Their Complexes, 2006.
109. J. Szejtli, *Chem Rev*, **98**, (1998), 1743-1753.
110. A. Harada and S. Takahashi, *J Chem Soc Chem Comm*, (1984), 645-646.
111. M. V. Rekharsky and Y. Inoue, *Chem Rev*, **98**, (1998), 1875-1917.
112. K. Uekama, F. Hirayama, and T. Irie, *Chem Rev*, **98**, (1998), 2045-2076.
113. V. Zia, R. A. Rajewski, and V. J. Stella, *Pharmaceut Res*, **18**, (2001), 667-673.
114. L. X. Wang, X. G. Li, and Y. L. Yang, *React Funct Polym*, **47**, (2001), 125-139.
115. F. T. A. Chen, G. Shen, and R. A. Evangelista, *J Chromatogr A*, **924**, (2001), 523-532.
116. G. K. E. Scriba, *J Sep Sci*, **31**, (2008), 1991-2011.
117. A. Amini, T. Rundlof, M. B. G. Rydberg, and T. Arvidsson, *J Sep Sci*, **27**, (2004), 1102-1108.
118. F. Hirayama and K. Uekama, *Adv Drug Deliver Rev*, **36**, (1999), 125-141.
119. X. J. Dang, M. Y. Nie, J. Tong, and H. L. Li, *J Electroanal Chem*, **448**, (1998), 61-67.
120. L. Fielding, *Tetrahedron*, **56**, (2000), 6151-6170.

121. P. Job, **9**, (1928), 113-203.
122. J. Mosinger, V. Tomankova, I. Nemcova, and J. Zyka, *Anal Lett*, **34**, (2001), 1979-2004.
123. W. Misiuk and M. Zalewska, *Anal Lett*, **41**, (2008), 543-560.
124. J. B. Chao, H. B. Tong, Y. F. Li, L. W. Zhang, and B. T. Zhang, *Supramol Chem*, **20**, (2008), 461-466.
125. I. Bratu, J. M. Gavira-Vallejo, A. Hernanz, M. Bogdan, and G. Bora, *Biopolymers*, **73**, (2004), 451-456.
126. I. V. Terekhova, R. S. Kumeev, and G. A. Alper, *J Incl Phenom Macro*, **59**, (2007), 301-306.
127. J. R. Cruz, B. A. Becker, K. F. Morris, and C. K. Larive, *Magn Reson Chem*, **46**, (2008), 838-845.
128. H. A. Benesi and J. H. Hildebrand, *J Am Chem Soc*, **71**, (1949), 2703-2707.
129. M. S. Ibrahim, I. S. Shehatta, and A. A. Al-Nayeli, *J Pharmaceut Biomed*, **28**, (2002), 217-225.
130. R. Ramaraj, V. M. Kumar, C. R. Raj, and V. Ganesane, *J Incl Phenom Macro*, **40**, (2001), 99-104.
131. C. Yanez, L. J. Nunez-Vergara, and J. A. Squella, *Electroanal*, **15**, (2003), 1771-1777.
132. G. C. Zhao, J. J. Zhu, J. J. Zhang, and H. Y. Chen, *Anal Chim Acta*, **394**, (1999), 337-344.
133. E. Coutouli-Argyropoulou, A. Kelaidopoulou, C. Sideris, and G. Kokkinidis, *J Electroanal Chem*, **477**, (1999), 130-139.
134. Y. Y. Zhou, C. Liu, H. P. Yu, H. W. Xu, Q. Lu, and L. Wang, *Spectrosc Lett*, **39**, (2006), 409-420.
135. K. A. Connors, *Chem Rev*, **97**, (1997), 1325-1357.
136. L. Liu and Q. X. Guo, *J Incl Phenom Macro*, **42**, (2002), 1-14.
137. W. Saenger and T. Steiner, *Acta Crystallogr A*, **54**, (1998), 798-805.
138. Y. Matsui and A. Okimoto, *B Chem Soc Jpn*, **51**, (1978), 3030-3034.
139. L. X. Song, B. L. Li, R. Jiang, J. G. Ding, and Q. J. Meng, *Chinese Chem Lett*, **8**, (1997), 613-614.
140. I. Tabushi, Y. I. Kiyosuke, T. Sugimoto, and K. Yamamura, *J Am Chem Soc*, **100**, (1978), 916-919.
141. K. Okimoto, R. A. Rajewski, K. Uekama, J. A. Jona, and V. J. Stella, *Pharmaceut Res*, **13**, (1996), 256-264.
142. L. Szente and J. Szejtli, *Trends Food Sci Tech*, **15**, (2004), 137-142.
143. J. Szejtli, *Pure Appl Chem*, **76**, (2004), 1825-1845.
144. T. Irie and K. Uekama, *Adv Drug Deliver Rev*, **36**, (1999), 101-123.
145. J. Li and X. J. Loh, *Adv Drug Deliver Rev*, **60**, (2008), 1000-1017.
146. K. Uekama, *J Incl Phenom Macro*, **44**, (2002), 3-7.
147. K. Uekama, F. Hirayama, and H. Arima, *J Incl Phenom Macro*, **56**, (2006), 3-8.
148. A. Ferancova and J. Labuda, *Fresen J Anal Chem*, **370**, (2001), 1-10.
149. K. R. Temsamani, H. B. Mark, W. Kutner, and A. M. Stalcup, *J Solid State Electr*, **6**, (2002), 391-395.
150. J. A. Kiernan and M. L. Barr, Barr's the Human Nervous System: An Anatomical Viewpoint, Lippincott Williams & Wilkins, 2008.
151. J. Nolte and J. W. Sundsten, The Human Brain: An Introduction to Its Functional Anatomy, Mosby, 1998.

152. R. H. Thompson, The Brain: A Neuroscience Primer, W H Freeman & Co, 1993.
153. M. D. Hawley, S. Tatawawa, S. Piekarsk, and R. N. Adams, *J Am Chem Soc*, **89**, (1967), 447-&.
154. T. Luczak, *Electroanal*, **20**, (2008), 1639-1646.
155. R. Langer, *J Control Release*, **16**, (1991), 53-59.
156. A. Mcraedegueurce, S. Hjorth, D. L. Dillon, D. W. Mason, and T. R. Tice, *Neurosci Lett*, **92**, (1988), 303-309.
157. H. Uludag, J. E. Babensee, T. Roberts, L. Kharlip, V. Horvath, and M. V. Sefton, *J Control Release*, **24**, (1993), 3-11.
158. Q. X. Zhou, L. L. Miller, and J. R. Valentine, *J Electroanal Chem*, **261**, (1989), 147-164.

## 1.1 Introduction

The initial aim of this work was to examine the use of polypyrrole (PPy), a well-known conducting polymer, for the uptake and release of a cationic species, dopamine (DA). DA was chosen as it represents a large family of amine-based drugs. Therefore, if appropriate PPy films could be electrosynthesised and used in the controlled delivery of DA, then the concept could be used more widely in the field of controlled drug delivery.

In Chapter 3, the growth of PPy films in the presence of various dopant anions, including a large anionic cyclodextrin (CD), sulfonated β-cyclodextrin (Sβ-CD) is explored. Although Sβ-CD doped PPy films have been reported in the recent literature, there has been very little work devoted to the characterisation of these films. Accordingly, much of Chapter 3 is devoted to the unique redox properties of the Sβ-CD doped PPy films.

With the growth of the PPy films achieved, Chapter 4, shows the drug release profiles of the protonated DA and reveals that in the case of the polymer films doped with the anionic Sβ-CD, there is a substantial increase in the amount of DA released in comparison to other polymer films. In order to explain the enhanced release profiles, the well-known supramolecular complexation properties of cyclodextrins were considered. However, on searching the literature no reports on the complexation of DA with anionic cyclodextrins were found and consequently this was studied in detail. These findings are presented in Chapter 5, where the host-guest interactions between DA and the anionic Sβ-CD are examined using a variety of techniques, both spectroscopic and electrochemical.

In Chapter 6 the technique of electrospinning is introduced. Details on how it is used to fabricate nanostructured biodegradable polymer films with a high surface area are provided. The approaches used to deposit the Sβ-CD doped PPy films onto the nanostructured biodegradable film are then considered and discussed. It is shown that cyclic voltammetry was the most successful

approach. Moreover, it was possible to control the amount of PPy deposited and to maintain the nanostructured fiber substrate by varying the number of cycles. These high surface area Sβ-CD doped PPy films are promising for the uptake and liberation of DA.

In this introductory chapter, the concept of controlled drug release is firstly introduced. This is then followed with information on conducting polymers, particularly PPy and the current state-of-art in using PPy in drug delivery. The technique of electrospinning is then introduced and linked to DDS. The next section is devoted to cyclodextrins, as it is the Sβ-CD doped PPy films that give the best controlled release properties. Finally, the chapter ends with a short account of the properties of DA and its delivery.

### 1.1.1 Controlled drug release

In the early 1970s, controlled release systems first materialised. Since then, the number and the areas in which a controlled release system is utilised have significantly increased. These systems have been used in areas such as cosmetics[1], food[2], and pesticides[3]. Controlled release systems are focused on obtaining the release of the proposed material, over a certain time without an external influence from any other potential release factor.[4] Polymeric materials have been previously investigated for controlled release as they can be easily manufactured and their composition can be finely tuned.[5] Polymers used in controlled release systems can be natural or synthetic and release can be achieved through the engineering of the polymer substrates, i.e., the degradation of poly($_{D,L}$ – lactide-*co*-glycolide) (PLGA) can be controlled through the polymer composition, higher ratios of PLA lead to a higher degradation rate.[6]

Another important research area under consideration is the development of controlled drug delivery systems (DDS).[7, 8] In 1980, controlled DDS were virtually unknown, yet in 2005, almost 100 million people globally were using some form of polymer based DDS.[8] The aim of a DDS is to supply the drug in its

therapeutically active form to a specific target in the body when the drug is required. In the current administration process there is a critical concentration needed in order to achieve the drug's maximum therapeutic effect. If the concentration goes beyond the maximum level, toxicity problems come into play. Conversely, if the concentration administered is below the minimum level the effect of the drug is not observed. The use of these DDS could potentially eliminate these problems as the release would be of a controlled manner.

Santini *et al.*[7] compared the release profiles of both conventional and controlled methods, as illustrated in Figure 1.1. With conventional methods of drug delivery, outlined in Figure 1.1(A), i.e., oral administration or injections, drug levels rise after initial administration, which could lead to potential toxicity problems, and then decrease until the next dosage, which has consequences on the efficiency of the dosage. The other schematic, Figure 1.1(B), demonstrates the effectiveness of a controlled release system. After dosage, the drug level in the blood remains constant, between the maximum and minimum levels, for a certain period of time.

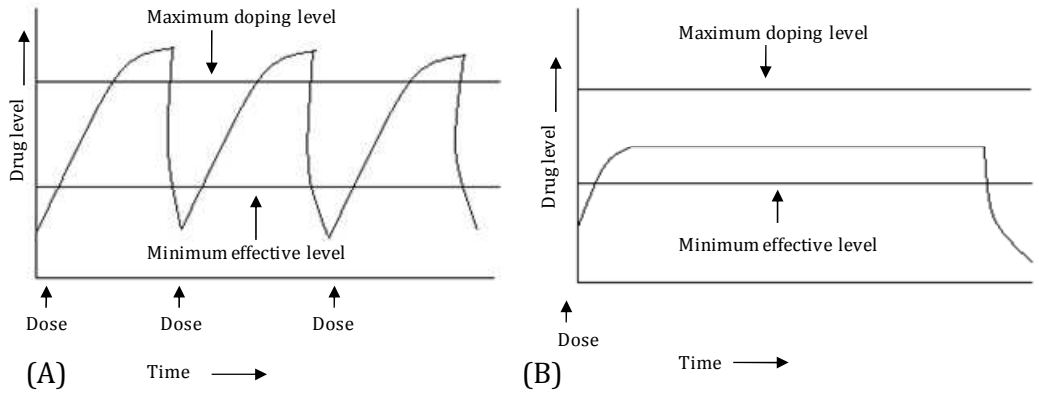


**Figure 1.1:** Drug levels in the blood with (A) conventional drug dosage (B) controlled delivery dosage, taken from Santini *et al.*[7]

In recent years, polymeric materials have been examined and shown to provide an alternate means of delivering drugs. Implanted polymeric pellets or microspheres localise therapy to specific anatomic sites, providing a continuous sustained release of drugs while minimising systemic exposure.[9] Polymers that display a physiochemical response to stimuli have been broadly researched for controlled release systems. Various stimuli include pH, temperature and the application of an electrical field.[10] According to Langer[11], polymeric DDS should i) maintain a constant drug level ii) reduce harmful side effects iii) minimise the amount of drug needed and iv) decrease the amount of doses which will have a pronounced effect on the patient.

The original polymeric controlled DDS was based on a non-biodegradable polymer, silicone rubber, which was designed and tested by Folkman and Long.[12] They loaded a silicone capsule (Silastic*) with a number of different drugs for the treatment of heart block and successfully implanted and monitored their effects over a number of days.

In more recent years there has been considerable interest in the development of new and efficient DDS, particularly with the growth of sophisticated drugs that are based on DNA and proteins.[5, 13] Currently, there are several materials under consideration in drug delivery, for example dendrimers[14], nanoparticles[15] and hydrogels[16]. The most promising opportunities in controlled DDS are in the area of responsive polymeric materials, with the possibility of implantable devices being used to deliver drugs. Murdan[17] exhaustively reviewed the use of hydrogels as 'smart' drug delivery devices. He showed that hydrogels could be engineered for various medicinal treatments depending on the patients needs, for example, pain relief. In the body, drug release can only be accomplished if the drug carrier responds to some class of stimuli, be it chemical, physical or biological. Conversely, an implanted 'smart' drug delivery device should be non-responsive to all other types of stimulus, once inside the body. A way of achieving this form of control is through an electrical stimulus.[17] A number of *in vivo* devices, in the form of iontophoresis, have already been used for this type of controlled release.[17, 18] Murdan presented a case where hydrogels loaded

with a bioactive compound, were implanted at a target site and the drug liberated through the application of an electrical field. In utilising such a system, many advantages including, minimal drug usage and lowering toxicity problems can be achieved. However, a problem arising with the application of an electrical stimuli to polymeric materials like, hydrogels, is that they experience deswelling or bending, which affects the drug release.[17]

To overcome these problems, conducting polymers (CPs) are also receiving much attention in the field of biomedical research, for the application of controlled DDS, due to their light weight, good biocompatibility and ability to function at body temperature. In particular, conducting polymers exhibit a reversible electrochemical response. These reversible oxidation-reduction reactions are attractive for a responsive DDS, as a change in the net charge on a conducting polymer film during its reduction or oxidation requires ions to flow into or out of the film. This, in turn, allows the polymer film to bind and expel ions in response to electrical signals. Controlled release of drugs from polymers offers many advantages over conventional methods including better control of the drug level administered resulting in fewer side effects, local drug delivery, decreased requirements for the total amount of drug and protection of drugs which are rapidly destroyed by the body. However, in order to devise a suitable technology, the polymeric material must be responsive, i.e., it must be capable of altering so that the drug is released in a controlled fashion when needed.

### 1.1.2 Conducting polymers

A polymer is a large molecule made up of smaller repeating units. The name comes from the Greek *poly*, meaning 'many', and *mer*, meaning 'part'. They are built up from simple molecules called *monomers* 'single part'. Polymers are produced through a method known as polymerisation. This polymerisation step can be achieved through chemical or electrochemical methods. Originally polymers with the basic carbon chains were considered only as insulators.[19] The first real interest in conducting polymers can be attributed to Walatka *et al*.[20] in 1973 with the report of highly conducting polysulfur nitride $(SN)_x$. Meanwhile

and towards the late 1970s , MacDiarmid, Shirakawa and Heeger enhanced the discovery of the semi-conducting and metallic properties of the chemically synthesised organic polyacetylene.[21-24] As is well known, the Nobel Prize in Chemistry was awarded to Alan J.Heeger, Alan G. MacDiarmid and Hideki Shirakawa in 2000 for the discovery and development of conducting polymers (CPs).[21-24] In the following years, a wide range of polymeric organic species have been prepared as stable inherent films on inert electrodes via both chemical oxidation and electropolymerisation from aqueous and organic solution.[25]

CPs are organic materials, which generally are comprised simply of C, H and simple heteroatoms such as N and S. Common examples include PPy, polyaniline and polythiophene which are shown in Figure 1.2. These and a number of other conducting polymers have been used in a variety of applications ranging from corrosion protection of materials, sensors to many biomedical applications, such as tissue engineering, nerve cell regeneration and drug delivery.[26-29]

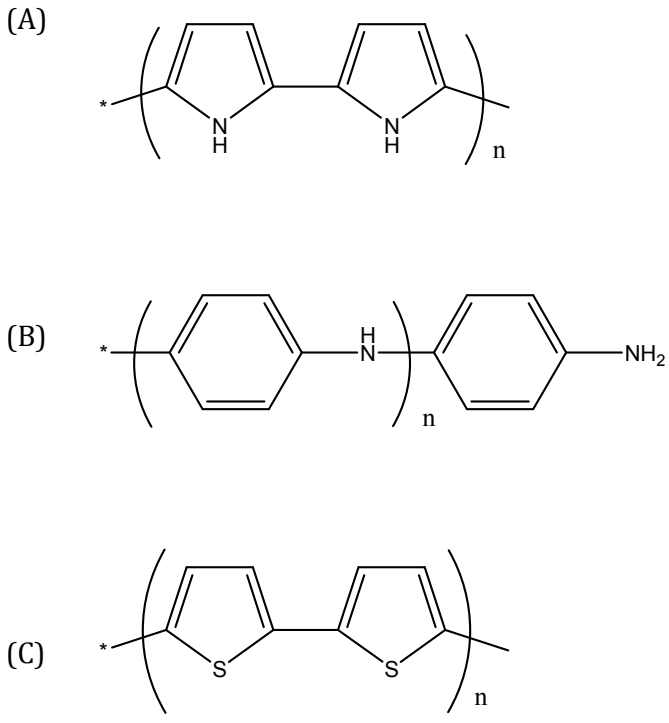


**Figure 1.2:** Chemical structures of (A) polypyrrole (B) polyaniline and (C) polythiophene. All polymers are shown in the dedoped state.

In, general materials are classed depending on their electrical conductivity, κ, where the electrical conductivity of insulators < semiconductors < conductors. Bredas and Street[30] explained this phenomenon in terms of the band gap structure. Figure 1.3 illustrates the difference in each material using the band gap theory. The highest occupied molecular orbital is equivalent to the valence band (VB), while the lowest unoccupied molecular orbital may be equated to the conduction band (CB). The difference between each band is known as the band gap energy ($E_g$) and it is this energy gap that establishes the electrical properties of a material. If $E_g$ > 10 eV, it is difficult to excite electrons into the conduction band and an insulator is formed. If $E_g \sim 1.0$ eV then thermal energy is sufficient to promote the electrons into the conduction band and a semiconductor is formed. If the gap vanishes, with overlap of the valence and conduction band, as shown in Figure 1.3, metallic conduction is observed. For most doped CPs the band gap energy is generally close to 1.0 eV, and consequently, CPs can be classified as semi-conductors.

As pointed out by Bredas and Street[30], the conductivity observed upon doping of the CPs was originally thought to be from the formation of unfilled electronic bands, however this idea was quickly dissipated upon experimental analysis of PPy and polyacetylene and now it is recognised that the conductivity is due to the formation of polarons and bipolarons, which are more energetically favoured.[30, 31]

The π-bonded system of CPs, which comprises of alternating single and double bonds, enabling the delocalisation of electrons along the polymer backbone, is related to the conductivity of the system. The conductivity of these materials arises from a state of relative oxidation or reduction. In these states the polymer either loses (oxidation) or gains (reduction) an electron. Generally, it is said that this process occurs in 1 in every 4 monomer units.[32] In this state the polymer is electronically charged and requires the introduction of counter ions (dopants) to compensate and reform the charge neutrality. The oxidation of the polymer in which an electron is removed from a π-bond, gives rise to a new energy state, which leaves the remaining electron in a non-bonding orbital. This energy level

is higher than the valence band and behaves like a heavily doped semiconductor.[32] The extent of doping can be controlled during the polymerisation of the polymers.

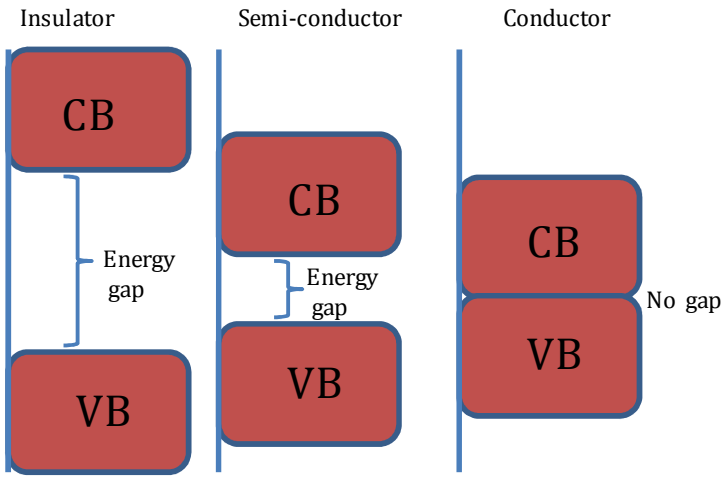


**Figure 1.3:** Schematic of the difference in band gap for Insulators, semi-conductors and metals (conductors).

### *1.1.2.1 Polymerisation methods*

CPs are synthesised through a method known as oxidative polymerisation. This can be generated chemically or electrochemically. Chemical polymerisation involves the use of a chemical oxidant, such as ammonium peroxydisulfate (APS), ferric ions, permanganate, dichromate anions or hydrogen peroxide. The oxidants not only oxidise the monomer but provide dopant anions to neutralise the positive charges formed on the polymer backbone.[33] In the presence of these oxidants, the monomers are oxidised and chemically active cation radicals are formed which further react with the monomer and generate the desired polymer. An advantage of vapour phase chemical polymerisation of CPs is that the polymerisation occurs almost exclusively on the preferred surface and a higher surface area can be attained.[34] Vapour phase chemical polymerisation of

pyrrole leads to further doping after polymerisation and this gives rise to an increase in conductivity.[35]

The electrochemical deposition is a simple and reproducible technique where the dopant is present in the electrolyte during polymerisation. It is generally performed in a conventional three electrode set up, described later in Chapter 2, where current is passed through a solution containing the monomer in the presence of a dopant (electrolyte). The CP is deposited at the positively charged working electrode or anode.[27] Polymerisation is initiated through the oxidation of the monomer which forms a mobile charge carrier known as a polaron (radical cation), that can react with another monomer or polaron to form a bipolaron (radical dication) which leads to the formation of the insoluble polymer chain and deposition of the polymer onto the working electrode.[36]

In his book 'Conducting Polymers' published in 1986, Alcacer commented on the possibility of using CPs to make artificial muscles or perhaps even modification for the brain; little did he realise the extent to which these materials have been extensively researched, over the past 20 years.[32] Since their discovery, the preparation and characterisation of these materials has evolved substantially through the use of electrochemistry. The majority of research is significantly based in this area due to the ease and control of synthesis of these electronically CPs.[19] Reviews on the development of CPs show the various areas to where they can be applied. The applications are ongoing.[37-40] However, in the case of DDS, CPs, in particular PPy, are widely researched for the controlled release of therapeutically active compunds.[41-45] During oxidative polymerisation, a dopant molecule, with an overall anionic charge, is used to compensate for the positive charges originating from the oxidation of the monomer. It is during this process that the concept of drug delivery originated. Burgmayer and Murray[46] observed changes in the ionic permeability of PPy redox membranes using a voltage-controlled electrochemical reaction. This led to further investigations into the application of CPs in DDS.

### *1.1.2.2 Polypyrrole*

#### 1.1.2.2.1 Historical background of polypyrrole

In 1968 Dall'Olio and colleagues prepared black films of an oxypyrrole on platinum by the electrochemical polymerisation of pyrrole from a solution of sulfuric acid.[47] In 1979 Diaz with the help of colleagues modified Dall'Olio's approach and demonstrated that polymerising pyrrole onto platinum in acetonitrile led to a black, adherent film.[48] Elemental analysis showed that the monomer unit was retained in the polymer. PPy in general, was poorly crystalline, and its ideal structure was a planar (α-ά)-bonded chain in which the orientation of the pyrrole molecules alternate.[25]

The monomer unit, pyrrole, is shown in Figure 1.4. PPy is an organic material comprised simply of C, H and a simple N heteroatom, but is highly conducting. It is an inherently conductive polymer due to interchain hopping of electrons. PPy can be synthesised both chemically[49] and electrochemically[48]. The electrochemical synthesis method is a one step synthesis method and allows the simple deposition of polymer films where its surface charge characteristics can easily be modified by changing the dopant anion (A-) that is incorporated into the material during synthesis. In a cell containing an aqueous or non-aqueous solution of the monomer, PPy forms a (semi) conducting film on the working electrode; the film grown is in the oxidised form and can be reduced to the non-conducting insulating form by stepping the potential to more negative values. The potential cycling can be repeated many times between the insulating and (semi) conducting forms without a loss of the electroactivity of the film.[25]

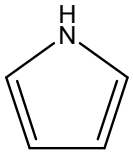


**Figure 1.4:** Schematic illustration of a monomer unit of pyrrole.

PPy in its neutral form is weakly coloured while the oxidised form is a deep blue/black. The switching of the state of the film not only changes its conductivity but it is also accompanied by a marked colour change, termed electrochromism.[36] Materials such as PPy are important in terms of future technological impact as it may be possible to develop them to replace more expensive, often toxic, metallic conductors commonly employed in the electronics industry.[25]

#### 1.1.2.2.2 Polymerisation mechanism of pyrrole

Although there are still various opinions on the mechanistic features of the electropolymerisation of pyrrole, the mechanism proposed by Diaz and his colleagues[48] and later used by Baker and Reynolds is in good agreement with many experimental reports.[50] The mechanism is demonstrated in Figure 1.5.

The initial step is the generation of the radical cation. This cation has different resonance forms, as shown in Figure 1.5. In the next step in the chemical case, the radical cation then attacks another monomer molecule, generating a dimer radical cation. In the electrochemical case, the concentrations of radical cations is much larger than that of neutral monomers in the vicinity of the electrode where reactions are occurring, and radical-radical coupling leads to a radical dication. This coupling between the two pyrrole radicals results in the formation of a bond between the two $\alpha$ positions to give the radical dication, as highlighted in Figure 1.5. This is then followed by the loss of two protons, generating a neutral dimer. This dimer is then oxidised into a radical cation, where the unpaired electron is delocalised over the dimer. The radical dimer then couples with the radical monomer to form a trimer. The polymerisation thus progressing in this fashion to completion.

The controversy in the mechanism of electropolymerisation is not surprising given that many factors, such as the nature of the electrolyte, ionic strength, pH, temperature and potential are important and can influence the mechanism of the reaction.

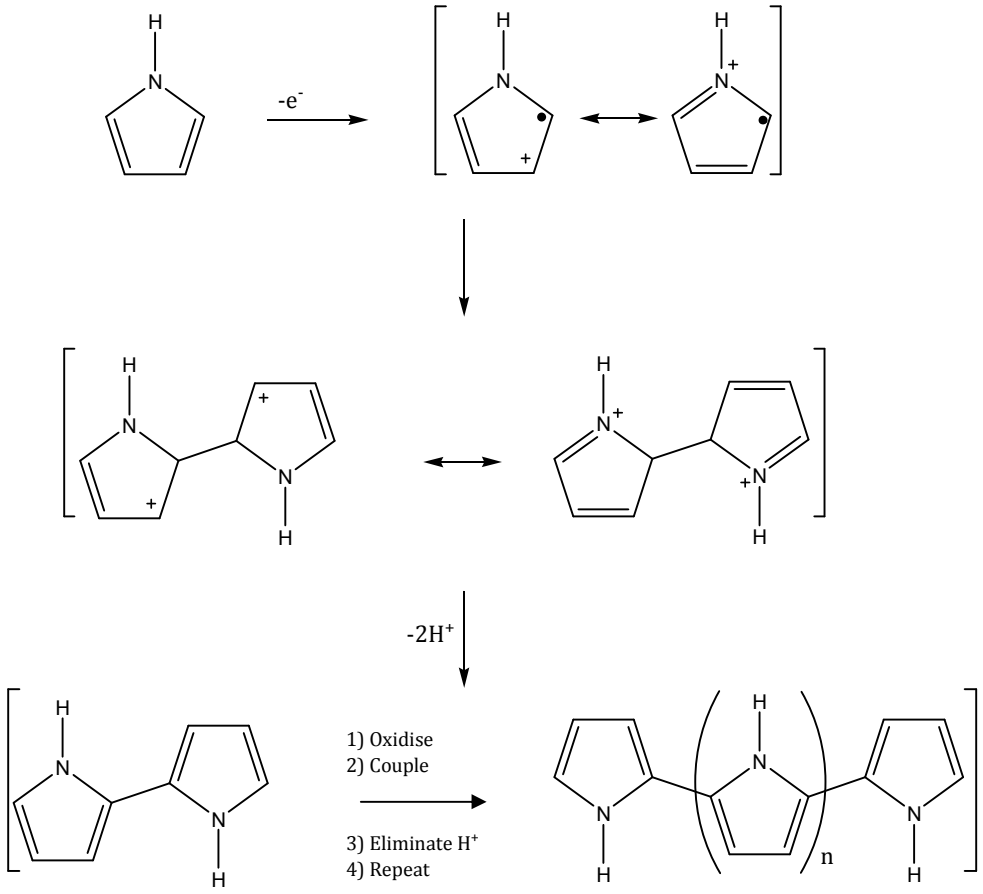


**Figure 1.5:** Mechanism of electrochemical polymerisation of pyrrole.[50]

#### 1.1.2.2.3 Biocompatibility

PPy is one of the most widely researched conductive polymers. The fact that it can form biologically compatible matrices is one of the prominent reasons for the extensive research on the use of PPy in the field of biological applications.[51] Wang *et al.*[52] acknowledged the reality that PPy had showed very good *in vitro* biocompatibility,[29, 53, 54] but they wanted to evaluate further the *in vivo* biocompatibility prospects. They demonstrated that in comparison to no PPy, the presence of PPy/biodegradable composites stimulated no abnormal tissue response and had no affect on the degradation behaviour of the biodegradable materials. In 1994, PPy was one of the first conducting polymers investigated for its effect on mammalian cells.[55] Since then, PPy is known to be

biocompatible, so it can be placed in the body without having adverse effects. It has been shown, in particular, to support cell growth and adhesion of endothelial cells.[29, 55-57] Schmidt *et al*.[29] also demonstrated that PPy was a suitable material for both in vitro nerve cell culture and in vivo implantation. PPy was electrochemically deposited onto ITO-conductive borosilicate glass. Moreover, the application of an external electrical stimulus through the polymer film resulted in enhanced neurite outgrowth. The median neurite length for PC-12 cells grown on PPy film subjected to an electrical stimulus increased nearly two-fold compared with cells grown on PPy without the application of a constant potential. The group also investigated PPy in vivo and their studies showed that PPy promotes little negative tissue and inflammatory response. Due to the good biocompatible factor, studies on the application of an electric field to the PPy have also shown cell compatibility.[29] In some important applications, such as biological sensors and actuators for medical devices it is a very attractive trait and some recent applications show that PPy can enhanced nerve cell regeneration and tissue engineering.[27]

#### 1.1.2.2.4 Electroactivity of polypyrrole

PPy can be easily switched between the neutral, partially oxidised and fully oxidised states, as shown in Figure 1.6. In its neutral state PPy exists as an insulator where the conduction band is empty as all the electrons remain in the valence band. Upon oxidation, an electron is removed from a π-bond (valence band) and a polaron is formed. The separation of the positive charge and the unpaired electron decreases during continual oxidation as the number of polarons increases. This in turn gives rise to the formation of a bipolaron, as depicted in Figure 1.6(C), and the polymer is now in its fully oxidised state.

During oxidation and the generation of positive charge an influx of anions into the polymer matrix is observed in order to maintain charge balance. This can be represented in Equation 1.1, where $PPy^{o}$ refers to the neutral (reduced) polymer, $PPy^{+}$ refers to the oxidised polymer and $A^{-}$ refers to the anionic dopant.

$$PPy^0 + A^- \rightarrow PPy^+A^- + e^- \quad 1.1$$

Typical anionic dopants are chlorides, bromides, iodides, perchlorates, nitrates, sulfates and para-toluene sulfonates.[58-64] The extent of oxidation/reduction is given by the doping level and this is generally expressed as the ratio of dopant anions, $A^-$, incorporated per monomer unit. For example, 1 $A^-$ per 4 monomer units gives a doping level of 0.25 or 25%. The maximum doping level achievable with PPy is 0.33 or 33%, i.e., 1 $A^-$ per 3 pyrrole units. It is important to point out that doping may not always be uniform; there can be islands with high doping levels surrounding by regions with a much lower doping level.

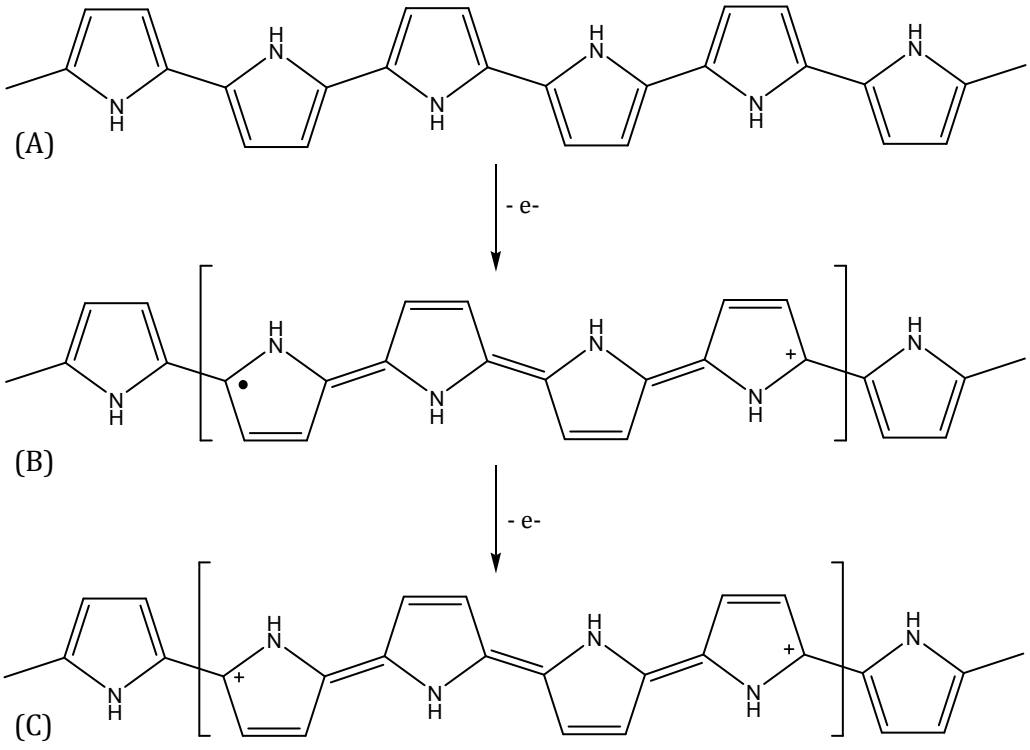


**Figure 1.6:** Electronic structures of (A) neutral PPy, (B) polaron in partially doped PPy and (C) bipolaron in fully doped (oxidised) PPy.[36]

**1.1.2.2.5 Polypyrrole and drug delivery**

The electrochemical switching of PPy films is accompanied by movement of counter or dopant ions in and out of the polymer matrix to maintain the charge neutrality, as shown in Section 1.1.2.3.4. Consequently, PPy films are attractive for the controlled release of drug molecules. The concept of using PPy membranes for the uptake and release of ions was introduced, in the early 1980s, by Burgmayer and Murray[46]. They demonstrated that these polymeric films could be exchanged from their oxidised state to their neutral state. PPy has been seriously considered for drug delivery due to these unique redox properties. PPy gives a responsive material needed in order for the uptake and release of the drug to be controlled; in its oxidised state anions are electrostatically bound to the polymer film. These properties allow the controlled transport of ions. The uptake of these ions can occur in two ways. The first is where the bioactive molecule exists as an anion and is involved in the doping process of the polymeric material during polymerisation, Figure 1.7 (A). Some anions that have been researched include adenosine tri phosphate (ATP)[65], salicylate[26], and dexamethasome[26]. These anions are electrostatically entrapped into the polymer matrix during the growth process upon application of an anodic potential. The anions are consequently liberated during the reduction of the polymer.

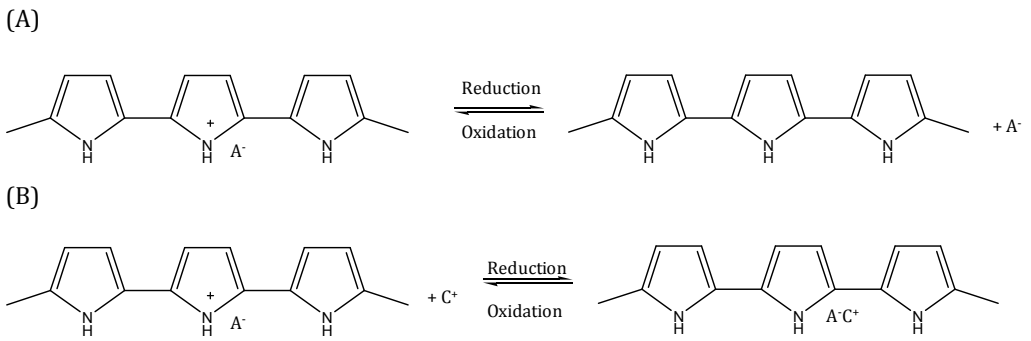


**Figure 1.7:** Interconversion between oxidation and reduction states of PPy (PPy). (A) Anion (A-) incorporation and release which is notably observed in small mobile anions (e.g. Cl-) while, (B) Cation (C+) insertion and liberation from polymer films doped with larger anions (e.g. $DDS^-$) which remain entrapped in the polymer matrix.

In the second case, cations can be incorporated into the system, Figure 1.7 (B), if the properties of the polymer film are modified.[66] This is achieved through the

initial inclusion of a large anion which remains entrapped in the polymer matrix and thus the polymer behaves as a cation exchanger, where, the charge of the polymer system can only be compensated through the uptake of cations. The cations are therefore, taken in during the reduction of the polymer and released upon oxidation. Figure 1.7 demonstrates both these concepts.

Miller and Zhou[67] previously reported the release of dopamine from a poly(*N*-methlypyrrole)/poly(styrenesulfonate) (PNMP/PSS) polymer based on the properties of these redox polymers. Immobilisation of PSS, a large anion, allows the uptake and release of the cation upon appropriate application of a potential. They achieved the release of dopamine using potential control, while more recently, Hepel and Mahdavi[66] demonstrated the controlled release of a cationic species, chloropromazine, from a composite polymer film based on the same principles. They reported the development of a new composite conducting polymer, PPy/melanin, which performed as a cation binder and releaser. The modification of the polymer films, to enable the predominant cationic exchange properties of the CP, is an interesting way of improving the uptake and release of cationic species from these attractive materials.

New ways of improving the controlled release of drugs are continually being sought after. Lately, Abidan *et al*.[41] reported on a method to prepare conducting-polymer nanotubes that can be used for controlled drug release. They introduced a method known as electrospinning to fabricate a nanofibrous mat in which the drug to be delivered had previously been incorporated; followed by electrochemical deposition of PPy films around the drug-loaded, electrospun biodegradable polymers. The drug release was achieved through the electrical stimulation of the PPy nanotubes.

#### 1.1.2.2.6 The application of Nanotechnology in drug delivery

Nanotechnology, although dating back to much earlier times, gained considerable attention in the early 1990s and has been the focus of much research over the last number of years. The introduction of nanotechnology into a controlled DDS has been shown to enhance many physical and chemical properties and overall has been used to increase the surface area of materials. This, in turn, leads to an increase in the amount of drug released from various materials. Many groups have introduced nanotechnology in various forms to improve on the drug delivery of a number of bioactive compounds, including nanoparticles[15], micellar systems[68] and nanofibers[69]. Polymeric nanofibers are gaining substantial interest for various applications including drug delivery[69, 70]. Several techniques have been employed for the production of nanofibers such as template synthesis[71], self assembly[72] and drawing[73]. One technique, in particular that is receiving considerable interest in this field, is electrospinning.[74-77] Electrospinning has been introduced to achieve nanoscale membranes and fibres from various polymeric materials.[78]

**1.1.2.2.7 The application of Electrospinning to drug delivery**

Although electrospinning was first reported by Formhals[79] in 1934 it has only been explored further in recent times.[80, 81] In 1996, Reneker and Chun restored interest in the electrospinning technique by demonstrating the possibility of electrospinning a wide range of organic polymers.[81] Since then the technique of electrospinning has become extremely useful in a variety of applications.[82-85] Electrospinning is a simple and inexpensive means for the formation of nano- to micron polymer fibers.

This technique involves the application of a high electric field between a polymer fluid and a grounded electrode. When the polymer solution is subjected to an external electric field at a critical point the forces overcome the surface tension of the polymer solution to form a droplet with a conical shape, i.e., the Taylor cone.[83, 86] The fluid is drawn into a jet which undergoes a whipping motion. Volatile solvents are used to dissolve the polymer as the subsequent evaporation from the liquid jet results in solid fibers. A more detailed

description of this technique is provided in Chapter 2, Section 2.4.5. In the majority of cases the fibers deposit randomly on the grounded collector. However, many groups have investigated the use of rotating collector plates to produce aligned nanofibers.[87] Figure 1.8 illustrates a typical SEM micrograph of an electrospun fiber mat of PLGA fibers.

This production of nanofibers allows these polymers to be used in a wide variety of applications including, tissue engineering (muscles, skin, cartilage and bones), wound healing and sutures, biosensors and DDS. Shin *et al.*[88] studied the use of PLGA nanofiber scaffold for cartilage reconstruction, while, Kim and colleagues incorporated antibiotics in the fibrous matrix for use in wound dressings.[89] Other groups have also prepared ultrafine polymers via electrospinning for skin regeneration.[74]

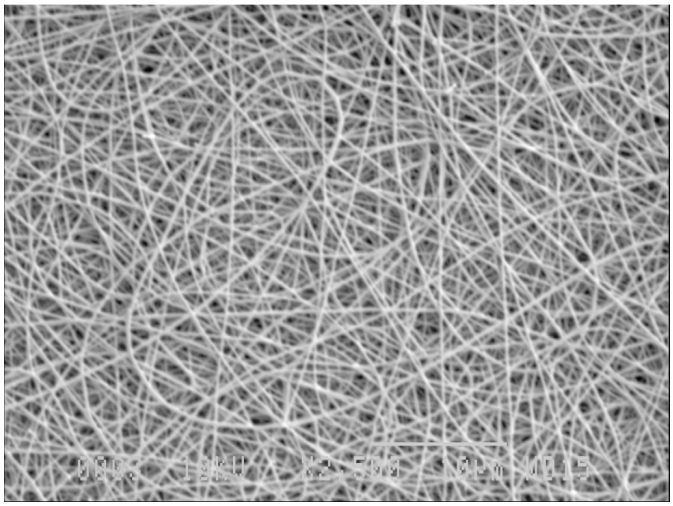

**Figure 1.8:** A typical SEM image of electrospun PLGA nanofibers.

Another attractive feature of using this electrospinning technique is that biodegradable polymeric materials, such as poly(lactic acid) (PLA) and poly($_{D,L}$ – lactide-*co*-glycolide) (PLGA) can be used as a biomedical controlled release system. These biodegradable polymers can be electrospun in the presence of varying amounts of the required medication. They can then be placed in the

body and the drug release achieved through the modification of the polymer matrix's morphology, porosity and composition.[89] These biodegradable polymers have FDA approval for biomedical and drug delivery use.[90-93] In comparison to other delivery forms, the electrospun nanofibers can conveniently incorporate the therapeutic compound during the electrospinning process.[94] Many drugs have been incorporated into PLGA electrospun polymer matrices, in order to achieve delivery of the therapeutic drug, including, tetracycline hydrochloride[95] and mefoxin[89]. In these cases, the drug release was monitored and a burst release was observed and was attributed to the high surface area-to-volume ratio of the electrospun material. This is a disadvantage. In the last few years a small number of groups have deposited electroactive polymers, such as PPy, onto previously electrospun fibers in order to enhance the electrochemical properties[57] of the material. Also, electrospun fibers have been used as a template in order to obtain a high surface area in the hope of achieving a greater uptake and release of drugs.[41]

Another method of improving the DDS of conducting polymers is the use of various dopants during polymerisation of the polymer films. The functionalisation of PPy films with large anionic dopants is not new to this field of research. It has been well reported that the use of large anionic dopants during the electrochemical polymerisation of monomers leads to these bulky negatively charged groups being immobilised within the polymer matrix.[96] In fact, these polymers, with their cationic exchange properties, have been used to incorporate various cationic groups for various applications. For example Fan and Bard in the late 1980s demonstrated the uptake of a positively charge $Ru(NH_3)_6^{3+}$ and methylviologen in PPy/Nafion films.[97]

However, the generation of PPy films in the presence of negatively charged cyclodextrins is a new concept.[98-100] There has been very little work reported on the electropolymerisation of pyrrole in the presence of anionic cyclodextrins. Indeed, much of the current published work is unreliable as very high potentials in the vicinity of 1.8 V vs. SCE were used to form the polymers.[100, 101] It is very well known that these high potentials give rise to the overoxidation of PPy and a

considerable loss in its conductivity.[59] The incorporation of cyclodextrins into conducting polymers provides a unique way of combining the unique host-guest complexation properties of cyclodextrins with the stability, high conductivity and ease of preparation of conducting polymers.

## 1.1.3 Cyclodextrins

### *1.1.3.1 History and structural properties of cyclodextrins*

Cyclodextrins (CD) are macrocyclic oligosaccharides composed of α-D-glucopyranoside units linked by α-(1,4) bonds. They were first discovered by Villiers in 1891[102], while in 1904, Schardinger[103] further developed the cyclic structures hence; CDs are sometimes referred to as Schardinger dextrins. However, it was only in the mid 1970s that the structure and chemical properties of natural cyclodextrins were fully characterised.[104] Cyclodextrins have developed quickly over the past two decades and have become an important branch of host-guest chemistry, specifically due to their ability to be involved in several practical applications.[105] The main interest in cyclodextrins lies in their ability to form inclusion complexes with a variety of compounds. Host-guest chemistry is the study of these inclusion phenomena, where the 'host' molecules are capable of including smaller 'guest' molecules through non-covalent interactions.

CDs are obtained through enzymatic degradation of starch in the presence of a glycosyl transferase, a type of amylase.[106] Many organisms contain glycosyl transferase, however, in general it is obtained from *Bacillus megaterium, Bacillus stereothermophilus and Bacillus macerans.*[106, 107] They are generally made up of glucopyranoside units of $^4C_1$ chair conformation which leads to a truncated cone shape encasing a cavity.[108] Figure 1.9 shows the structures of the most common CD members; α-, β- and γ-CD, which include 6, 7 and 8 repeating glucopyranoside units, respectively. These units orientate themselves in a cyclic manner offering a typical conical or truncated cone structure with a relatively hydrophobic interior and hydrophilic exterior.[109] This structural property gives cyclodextrins good water solubility and the ability to hold appropriately sized

guests, such as amines and ferrocenes[110], through non-covalent interactions such as hydrogen bonding, hydrophobic interactions, and electrostatic interactions.[111] Table 1.1 demonstrates the approximate geometries of the most common CDs.[109]

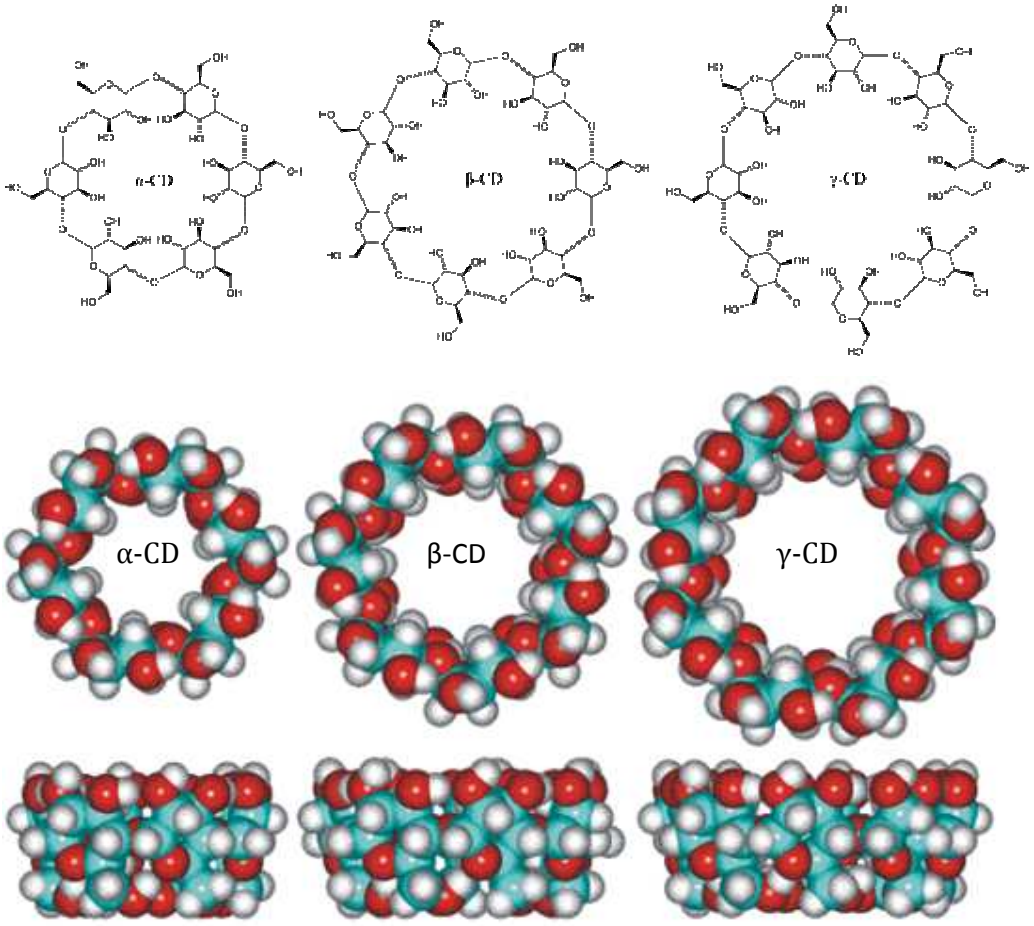


**Figure 1.9:** Structures of α-, β- and γ-cyclodextrin taken from Szjetli.[109]

Due to their exceptional host-guest complexation abilities, CDs have been used in a variety of fields, such as environmental protection through immobilising toxic compounds in their cavities and in the food industry.[104] In fact one of the commercially available applications for CDs is Febreze®, which is an aqueous solution of modified β-cyclodextrins**.** Febreze® is based on the host-guest chemistry of the CDs, with molecules that produce aroma forming inclusion complexes with the modified CDs. In the pharmaceutical industry, CDs are also

used for many applications including, drug delivery to enhance the solubility, stability and bioavailability of drug molecules.[108, 112]

**Table 1.1:** Approximate geometric dimensions of the three common CDs.[106]

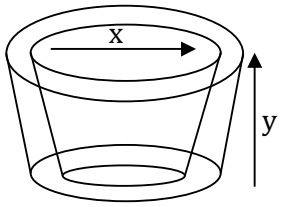


| Cyclodextrin | x / nm | y / nm | Cavity volume / Å$^3$ |
|---|---|---|---|
| **α** | 0.49 | 0.78 | 174 |
| **β** | 0.62 | 0.78 | 262 |
| **γ** | 0.79 | 0.78 | 427 |

Cyclodextrins can also be chemically modified to replace the hydroxyl groups on both the primary and secondary rims of the CDs, with a variety of appropriate alkyl groups (R). It has been reported that this can improve binding affinity.[108] In the research presented here, a negatively charged cyclodextrin with a number of sulfonated groups present on the outer rims was used, sulfonated β-CD (Sβ-CD). Sβ-CD is obtained by substitution of either primary or secondary hydrogen of the hydroxyl group of β-CD with a sulfonate group. Sβ-CD has an average of 7-11 substituents per CD and, therefore, has between 7-11 negative charges associated with it, which are counterbalanced with sodium ions, as illustrated in Figure 1.10.[113] It is reported that β-CD and Sβ-CD have the same ring structure, differing only in the substituent located on the rims of the CD ring.[14] Although Sβ-CD has the same ring structure as other derivativsed CDs the presence of the substituent on the ring contributes to its chiral discrimination properties.[114] A major area in which these sulfonated CDs are being utilised is chromatography, or more specifically capillary electrophoresis, for the enantiomeric separation of acidic and basic compounds. In enantiomeric separation, using neutral CDs, they are not appropriate for neutral racemates as the complex has no electrophoretic mobilities.[115] Therefore, the use of charged

CDs is now been widely researched for the separation of neutral compounds. It has been reported that the use of these sulfonated CDs for the enantiomeric separation of chiral compounds is highly effective as a result of the anionic charges.[116, 117]

A number of groups have also characterised the Sβ-CD.[115, 117] Figure 1.11 illustrates a single glucose unit of an Sβ-CD (comprised of 7 units). On the primary ring there are 7 potential substitution sites corresponding to the C-6 positions, while, on the secondary rim there are 14, represented by the C-2 and C-3 positions. Amini and co-workers[117] reported that substitution of these CDs is predominantly at the C-2 and C-6 positions, while, Chen *et al.*[115] confirmed nearly complete sulfation at the C-6 position of the primary hydroxyl groups and partial sulfation at the C-2 secondary hydroxyl groups. They also reported no substitution at the C-3 positions. From these reports it can be stated that almost the entire primary rim is sulfonated and some of the secondary rim. Due to this phenomenon and the fact that the sulfation brings with it negative charges these CDs are good candidates for the doping of CPs.

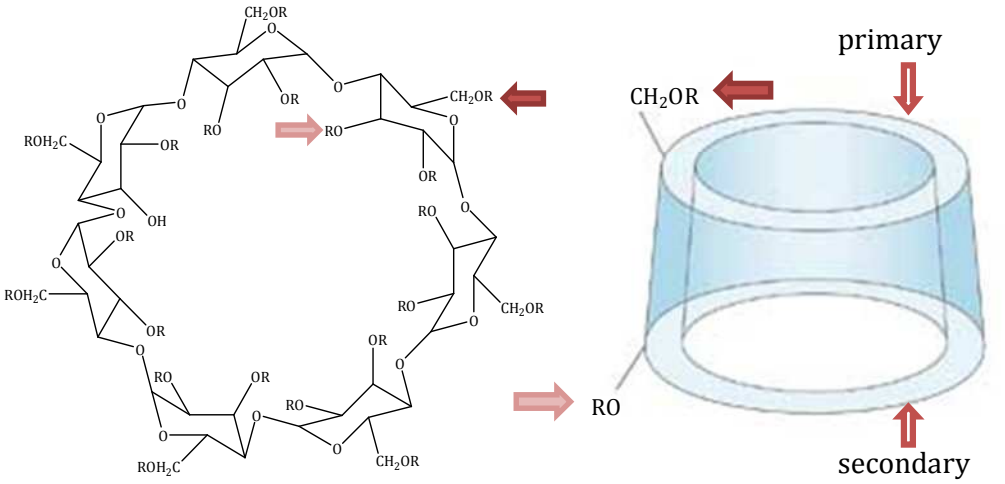


R = $SO_3^-Na^+$ or H ~ 7-11 $SO_3^-Na^+$ groups.

**Figure 1.10:** Structural and schematic representation of sulfonated β-cyclodextrin (Sβ-CD). The arrows point to the primary and secondary rims, respectively.[118]

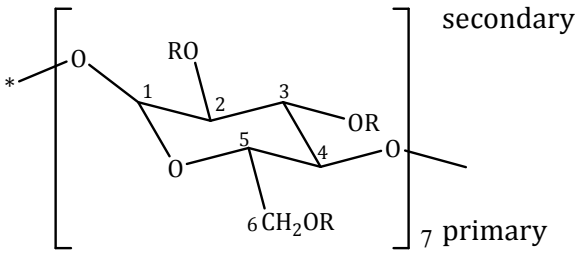


**Figure 1.11:** Chemical structure of Sβ-CD, depicting the numbering carbons.

### *1.1.3.2 Inclusion complexation*

Cyclodextrins (CD) form a group of cyclic oligosaccharides that contain cavities in which guest molecules can be encapsulated.[108, 109] It is well known that the size of the compounds are important and compounds are only capable of including into the cavity of the CD if they are within the dimensions of the CD cavity.[119] In aqueous media, the cavity is filled with water molecules, which becomes displaced by the guest through complexation, as illustrated in Figure 1.12. The guest molecule, xylene, displaces the water molecules and forms an inclusion complex with the CD.

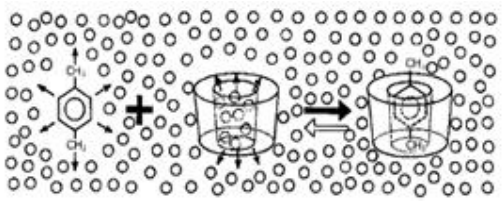

**Figure 1.12:** Schematic representation of xylene forming a complex with a β-cyclodextrin. The small circles represent water molecules taken from Szjetli.[109]

During the formation of an inclusion complex the chemical and the physical properties of the guest molecule change and can be monitored using a number of techniques. Various spectroscopic and electrochemical techniques can be used to confirm complexation, including fluorescence, UV-visible spectroscopy (UV), Nuclear magnetic resonance (NMR) and electrochemical studies. These changes attributed to the complexation can be used to evaluate the apparent

binding or formation constant ($K_f$). However, prior to the determination of the $K_f$ value the stoichiometry of the host-guest complex must be established.[120] This is obtained by the well known continuous variation or Job's method which is described in more detail in Chapter 2, Section 2.6.1.1.[121] Generally, inclusion complexes form a ratio of 1:1, 1:2 and sometimes 2:1 (CD:guest).[122]

NMR is also a useful tool for the study of complexation due to its quantitative information and assuming the guest enters the cavity, NMR, can be also used to locate the protons involved in complexation.[87] Many groups have studied the complexation properties with the neutral β-CD and monitored the changes in the chemical shifts for both the CD, and the guest. However, in the case of the modified CD used in this research, the NMR spectral data are too difficult to differentiate so the chemical shift of the guest is followed.[120, 123-126] Bratu and colleagues[125] studied the chemical shift changes observed when Fenbufen was in the presence of a neutral β-CD. They noticed an up-field shift of the guest protons, some more pronounced than others, and suggested that the complexation was initiated through the benzene moiety of the guest. Cruz *et al*.[127] also used NMR to quantitatively evaluate the binding constant of the complexation of doxepin and a neutral β-CD.

If a guest absorbs light in the UV or visible region then the inclusion phenomenon can be followed and subsequently, evaluated by UV.[106] This technique can be used to confirm complexation and indeed obtain the formation constant associated with the inclusion complex. In the majority of cases the guest that absorbs in the UV-vis region experiences changes in the intensity and the position of the absorption bands in the presence of the CD. These spectral changes can be used to determine the $K_f$ constants. Generally, a Hiedlebrand-Benesi modified equation is used to evaluate the $K_f$ constants.[119, 128, 129] Ramaraj and co-workers[130] monitored the changes attained during the complexation formation of a number of aromatic amines and nitro compounds in the presence of a neutral β-CD. They observed an increase in the intensity of the bands in all cases. Dang *et al*.[119] observed shifts of the absorption bands to longer

wavelengths in the case of 1,4 benzoquinone (BQ) and 9,10 anthraquinone (AQ) in the presence of a neutral β-CD.

Electrochemical techniques can also be performed on the complexation properties of CDs. If the guest is electroactive the peak current and potential can be followed for the free state and compared to the complexed state of the guest in question. Two features are generally observed during these electrochemical observations if an inclusion complex is found. Firstly, a decrease in the peak current can be seen, and, attributed to a decrease in the diffusion of the bulky CD complex as opposed to the more mobile free guest. Secondly, a shift in the peak potential is observed if the complexed species is included in the cavity, as it is harder to oxidise or reduce while located in the cavity. Once again based on these variations a number of equations can be used to verify the formation constant.[129, 131, 132] Coutouli-Argyropoulou and his group[133] reported the effect of complexation on the electrochemical properties of ferrocence derivatives and showed shifts, in both the peak current and peak potential, when higher concentrations of a neutral β-CD were added. Yanez *et al*.[131] showed similar observations for nifedipine (NF) and nicardipine (NC) and estimated apparent formation constants of 135 and 357, respectively.

Complexation studies of DA have been previously demonstrated in the presence of a neutral β-CD by Zhou *et al*.[134] using UV and fluorescence spectroscopy. From the fluorescence technique, utilising a Hiedlebrand-Benesi modified equation, a $K_f$ value of 95.06 was estimated. The degree of the complexation can vary over a wide range due to the stability of the complex, as it depends on a number of factors. In the next section a discussion on the main driving forces, involved in this complexation process are dealt with.

#### *1.1.3.3 Driving forces in the inclusion complexation process*

There are many reviews and books written on the driving forces behind the inclusion complexation abilities of cyclodextrins, not all agree, some refer to the predominantly hydrophobic affects while others state that it is a collection of a

number of weaker interactions (H-bonding, van der Waals, electrostatic interactions).[106, 108, 111, 135, 136] Either way the majority agree that the size of the cavity and shape of the guest are important factors in the complexation process. The most widely studied possible driving forces include

- Hydrogen bonding
- Electrostatic interaction
- Van der Waals
- Hydrophobic effect

Hydrogen bonding is an interaction between an electronegative donor, a hydrogen and an electronegative acceptor.[136] Various groups have demonstrated the importance of hydrogen bonding in the solid state, illustrating crystal structures defining the hydrogen bonding between the guest and the hydroxyls of the CDs.[137] However, during the complexation of the CD and guest, in aqueous solution, the subject is still arguable as few direct measurements of hydrogen bonding have been made, as water molecules can compete with CDs to form hydrogen bonding with guest molecules. However, many groups will still argue over the significance of hydrogen bonding.

Electrostatic interaction occurs when molecules of opposite charges interact. There are three types of electrostatic interactions, ion-ion interaction, ion-dipole interaction and dipole-dipole interaction.[136] Matsui and Okimoto[138] reported that ion-ion interaction is only eligible in the case of modified CDs, where as ion-dipole is considered more favourably due to the fact that CDs are polar molecules however as with hydrogen bonding, in aqueous media, the interaction between the guest and water will also be strong.[136] Therefore, it is the case of dipole-dipole interaction that is mostly considered during complexation.

Van der Waals forces or London dispersion forces are made up of dipole induced dipole contributions or the coordination of the electronic motion in the CD and guest. As CDs are known to have large dipole moments it is logical that

these induction forces are important in complexation. Experimental evidence has shown that the stability of the complex increases with an increase in polarisability. Also, as the polarisability of water is lower than the organic components of the CD cavity, van der Waals forces have an encouraging donation to the stability of the complex due to a stronger interaction of the CD and guest over the water and guest.[136] CDs have also been reported to form stable inclusion complexes in organic solvents like DMF and DMSO confirming the importance of van der Waals forces.[139]

The hydrophobic interaction which is entropically favourable, due to the expulsion of water, leads to the aggregation of non-polar solutes in aqueous solution.[136] As reviewed by Connors[135] the 'classical' hydrophobic interaction is said to be 'entropy driven' and a positive entropy and enthalpy is associated for the interaction between two non polar molecules. However, experimental studies in the complexation of CD and guests, show negative enthalpy and entropy changes,[111] which have been suggested to indicate that these interactions are not a dominant force.

Mosinger *et al*.[122] reported that the formation of an inclusion complex is based on the electrostatic, van der Waals and π-π interactions, where, steric affects and Hydrogen bonding are inevitable. Chao and co-workers[124] investigated the formation of an inclusion complex with β-CD and caffeic acid, they reported that the weak forces of hydrogen bonding, van der Waals, hydrophobic and electrostatic interactions simultaneously governed the process.

Rekharsky and Inoue[111] reviewed the complexation of cyclodextrins and stated that the interactions involved in the inclusion complexation of aromatic guests with CDs could not be simply put down to a hydrophobic effect. They established that complexation could be accounted for, through dipole-dipole interactions. In saying that, Tabushi and his group[140] questioned the role of hydrogen bonding in the complexation process and reported that no dramatic changes of binding were observed, when a modified CD, incapable of hydrogen bonding, was compared to an unmodified CD. They concluded that the

involvement of hydrogen bonding was negligible and hydrophobic interactions dominated the process. Zia *et al*.[113] investigated the complexation ability of a negatively charged CD (~7 negative sites) with a number of neutral and charged guest molecules. They accounted for the increase in the binding affinity, for the oppositely charged guest and CD, to be predominantly hydrophobic, due to the additional interaction sites provided by the negatively charged CD. Okimoto and colleagues[141] also clearly observed stronger interactions occurring between a CD and guest with opposite charges.

The understanding of these complexation processes is complicated, however, it is generally found that van der Waals forces and hydrophobic interactions are regarded as the main driving forces for CD complexation, while, electrostatic interactions and hydrogen bonding can be significantly considered in some inclusion complexation studies. Nevertheless, these attractive features of CDs allow them to be used in a wide range of applications including, the food industry[142]. However, the pharmaceutical industry is the most widely researched area in recent times, specifically in drug formulation and DDS.[143]

#### *1.1.3.4 Applications of CDs in DDS*

Due to their biocompatibility and their ability to form inclusion complexes, CDs have been studied for the use in DDS. They have been considered as drug carriers, as CDs have the potential to act as hydrophobic carriers and control the release of a variety of drugs.[118] Many reviews have recently been published, describing the role of CDs in DDS.[112, 118, 144-147] Irie and Uekama[144] reviewed the role of CDs in peptide and protein delivery and summarised that CDs were able to eliminate a number of undesirable properties of drug formulations, as they form inclusion complexes with the desired drugs, which increase the drug delivery through a number of routes of administration. More recently, Li *et al.*[145] examined the recent progress in the preparation of inclusion complexes between CDs and various polymers as supramolecular biomaterials for drug and gene delivery. They demonstrated the promising field in the self assembly

of inclusion complexes between CDs and biodegradable polymers as injectable DDS.

Ferancova and Labuda[148] also reviewed the use of CDs as electrode modifiers. They summarised the many ways CDs can be immobilised onto electrode surfaces. As discussed in an earlier section, Section 1.1.4.2., the incorporation of CDs, as dopants, during the electrochemical polymerisation of CPs was demonstrated to examine the use of these modified electrodes to deliver neutral drugs.[98] Formulating these materials, correlates the attractive features of both the CDs and the CPs. Bidan *et al*.[98] examined the need for a new DDS that was not limited to charged drugs. They produced polymer films in the presence of an anionic CD and successfully delivered neutral compounds using these novel materials.

Also briefly discussed in Section 1.1.4.2, was the reports made by a number of groups on the polymerisation of CPs in the presence of CDs.[100, 101, 149] These groups have reportedly polymerised pyrrole at potentials usually shown to overoxidise the CP film.[59] Due to this, these papers are unreliable in their reports.

### 1.1.4 Drug release: Controlled release of dopamine

DA is a neurotransmitter produced naturally in the brain. It is well documented that a common factor in neurodegenerative diseases such as Parkinson's (PD) and Schizophrenia is a significant lack of the presence of DA in the *substantia nigra* (mid brain).[150-152] In particular, PD is a slowly progressive disorder known to occur due to the damage of the basal ganglia.[150-152] The disease affects movement, muscle control and balance. Studies on the brains of deceased Parkinson sufferers show a substantial loss of dopamine, particularly, in the *substantia nigra*. The function of the substantia nigra is to produce DA and manage the release of essential neurotransmitters that help control movement and coordination. Sufferers usually show symptoms such as tremors, slowness of movement and impaired balance and coordination. Prolonged loss of DA

gives rise to symptoms such as difficulty in walking, talking, or completing other simple tasks.[150-152]

DA belongs to the well known catecholamine family. These molecules are electroactive and therefore their oxidation can be followed using electrochemistry, in particular, electrochemical methods such as cyclic voltammetry and rotational disc voltammetry. The electrochemical mechanism of oxidation is still not fully agreed; with various groups arguing that the mechanism goes through an ECE step rather than a CE step. For example, Hawley *et al*.[153] have reported that the electrochemical oxidation of dopamine in aqueous solution proceeds through two types of steps, electrochemical (E) and chemical (C). The ECE mechanism is presented in Scheme 1.1.

The first step in the oxidation of dopamine (A) involves the loss of both protons and electrons to form the o-dopaminoquinone (B). The oxidised, o-dopaminoquinone undergoes a 1,4-Michael addition, which results in a intramolecular cyclisation reaction which produces leucodopaminochrome (C). This product is easily oxidised through an electrochemical step to form dopaminochrome (D).[153, 154]

Controlled release studies of DA have been previously investigated.[67, 155-158] McRae-Degueurce *et al*.[156] encapsulated DA into a thermoplastic polyester excipient: PLGA. They found that it was possible to deliver significant amounts of DA for prolonged periods of time by injecting the microencapsulated DA directly into the brain. Uludag and colleagues[157] also examined the release of many therapeutic agents, including DA, from microencapsulated mammalian cells. The mammalian cells and tissues were entrapped in polymeric microcapsules containing the desired bioactive agent.

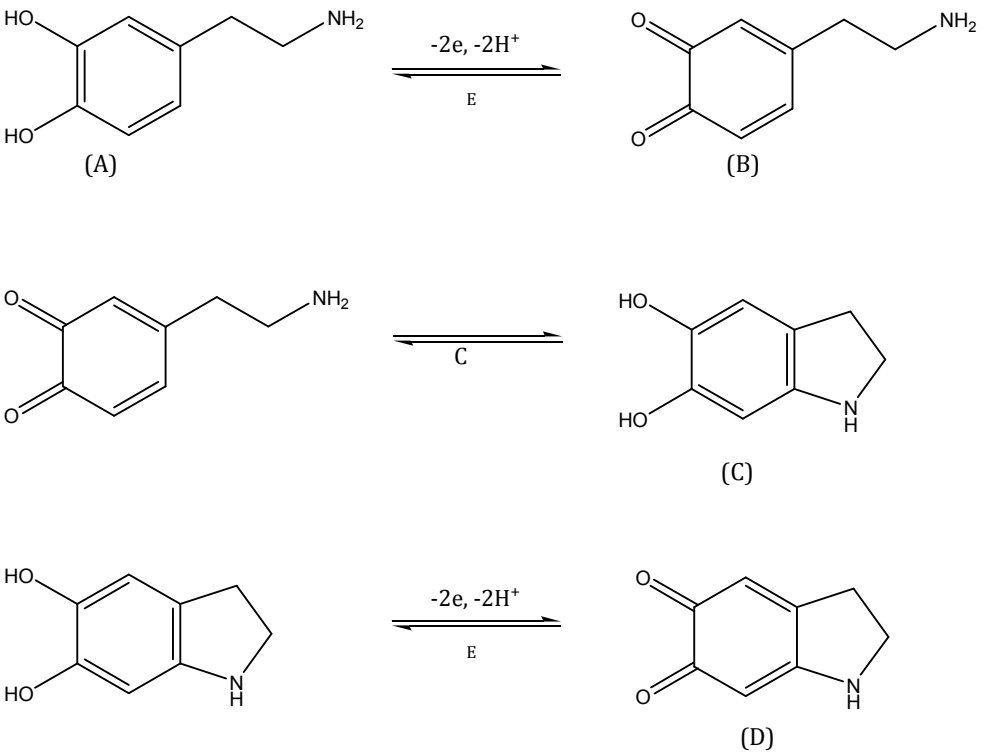


**Scheme 1.1:** The proposed oxidative pathway for dopamine.

In both these cases the release was based on diffusion from the polymeric materials. It is, therefore, difficult to maintain any control over the amount of DA released. Miller[67] and Zhou[158] and co-workers investigated the use of CPs to deliver DA. They introduced the concept of using large immobile dopants, which remain entrapped inside the cavity during polymerisation, to bind and successfully liberate DA from the polymer films.

This is the basis of the work performed in this thesis. As outlined at the start of this chapter, the idea of this research is to develop PPy films for the uptake and release of DA, using a large immobile anionic cyclodextrin. The cyclodextrin, in addition to its large size and immobility, has unique host-guest complexation properties and this offers the prospects of inclusion complexation between the DA and the CD to enhance the drug delivery. If this can be achieved it could potentially serve as a model system in DDS and could be extended to various other cationic drug molecules.

## 1.2 References


1. N. A. Peppas and D. J. A. Ende, *J Appl Polym Sci*, **66**, (1997), 509-513.
2. U. R. Pothakamury and G. V. BarbosaCanovas, *Trends Food Sci Tech*, **6**, (1995), 397-406.
3. B. Singh, D. K. Sharma, and A. Gupta, *J Environ Sci Heal B*, **44**, (2009), 113-122.
4. N. A. Peppas and R. Langer, *Science*, **263**, (1994), 1715-1720.
5. K. E. Uhrich, S. M. Cannizzaro, R. S. Langer, and K. M. Shakesheff, *Chem Rev*, **99**, (1999), 3181-3198.
6. D. L. Wise, Encyclopedic handbook of biomaterials and bioengineering Marcel Dekker, 1995.
7. J. T. Santini, A. C. Richards, R. Scheidt, M. J. Cima, and R. Langer, *Angew Chem Int Edit*, **39**, (2000), 2397-2407.
8. R. Langer, *Mrs Bull*, **31**, (2006), 477-485.
9. L. K. Fung and W. M. Saltzman, *Adv Drug Deliver Rev*, **26**, (1997), 209-230.
10. R. Langer, *Science*, **249**, (1990), 1527-1533.
11. R. Langer, *Nature*, **392**, (1998), 5-10.
12. J. Folkman and D. Long, *JOURNAL OF SURGICAL RESEARCH*, **4**, (1963), 139-142.
13. T. M. Allen and P. R. Cullis, *Science*, **303**, (2004), 1818-1822.
14. J. J. Wang, G. J. Zheng, L. Yang, and W. R. Sun, *Analyst*, **126**, (2001), 438-440.
15. H. Wartlick, K. Michaelis, S. Balthasar, K. Strebhardt, J. Kreuter, and K. Langer, *J Drug Target*, **12**, (2004), 461-471.
16. L. M. Lira and S. I. C. de Torresi, *Electrochem Commun*, **7**, (2005), 717-723.
17. S. Murdan, *J Control Release*, **92**, (2003), 1-17.
18. J. E. Riviere and M. C. Heit, *Pharmaceut Res*, **14**, (1997), 687-697.
19. G. Inzelt, Conducting Polymers, A new era in electrochemistry, Springer, 2008.
20. V. V. Walatka, M. M. Labes, and Perlstei.Jh, *Phys Rev Lett*, **31**, (1973), 1139-1142.
21. H. Shirakawa, E. J. Louis, A. G. Macdiarmid, C. K. Chiang, and A. J. Heeger, *J Chem Soc Chem Comm*, (1977), 578-580.
22. A. J. Heeger, *Angew Chem Int Edit*, **40**, (2001), 2591-2611.
23. A. G. MacDiarmid, *Angew Chem Int Edit*, **40**, (2001), 2581-2590.
24. H. Shirakawa, *Angew Chem Int Edit*, **40**, (2001), 2575-2580.
25. P. Chandrasekhar, Conducting Polymers, Fundamentals and Applications: A practical approach, Kluwer Acandemic Publishers, 1999.
26. A. A. Entezami and B. Massoumi, *Iran Polym J*, **15**, (2006), 13-30.
27. N. K. Guimard, N. Gomez, and C. E. Schmidt, *Prog Polym Sci*, **32**, (2007), 876-921.
28. A. Malinauskas, J. Malinauskiene, and A. Ramanavicius, *Nanotechnology*, **16**, (2005), R51-R62.
29. C. E. Schmidt, V. R. Shastri, J. P. Vacanti, and R. Langer, *P Natl Acad Sci USA*, **94**, (1997), 8948-8953.
30. J. L. Bredas and G. B. Street, *Accounts Chem Res*, **18**, (1985), 309-315.

31. D. L. Wise, Electrical and optical polymer systems, CRC Press, 1998.
32. L. Alcacer, Conducting Polymers: Special Applications (Hardcover), Springer 1986.
33. B. Winther-Jensen, J. Chen, K. West, and G. Wallace, *Polymer*, **46**, (2005), 4664-4669.
34. A. Malinauskas, *Polymer*, **42**, (2001), 3957-3972.
35. R. A. Green, N. H. Lovell, G. G. Wallace, and L. A. Poole-Warren, *Biomaterials*, **29**, (2008), 3393-3399.
36. T. A. Skotheim and J. R. Reynolds, Handbook of conducting polymers: Conjugated polymers, CRC Press, 2007.
37. P. C. Lacaze, J. C. Lacroix, K. C. Ching, and S. Aeiyach, *Actual Chimique*, (2008), 90-91.
38. M. A. Mohamoud, *Plast Eng*, **64**, (2008), 32-+.
39. M. Nikolou and G. G. Malliaras, *Chem Rec*, **8**, (2008), 13-22.
40. E. Smela, *Mrs Bull*, **33**, (2008), 197-204.
41. M. R. Abidian, D. H. Kim, and D. C. Martin, *Adv Mater*, **18**, (2006), 405-409.
42. C. Arbizzani, M. Mastragostino, L. Nevi, and L. Rambelli, *Electrochim Acta*, **52**, (2007), 3274-3279.
43. K. Kontturi, P. Pentti, and G. Sundholm, *J Electroanal Chem*, **453**, (1998), 231-238.
44. Y. L. Li, K. G. Neoh, and E. T. Kang, *J Biomed Mater Res A*, **73A**, (2005), 171-181.
45. J. M. Pernaut and J. R. Reynolds, *J Phys Chem B*, **104**, (2000), 4080-4090.
46. P. Burgmayer and R. W. Murray, *J Am Chem Soc*, **104**, (1982), 6139-6140.
47. A. Dall'Olio, G. Dascola, V. Varacca, and V. Bocchi, *Comptes Rendus de l'Academie des Sciences*, **C267**, (1968), 433-435.
48. A. F. Diaz and J. I. Castillo, *J Chem Soc Chem Comm*, (1980), 397-398.
49. B. Winther-Jensen and N. B. Clark, *React Funct Polym*, **68**, (2008), 742-750.
50. C. K. Baker and J. R. Reynolds, *J Electroanal Chem*, **251**, (1988), 307-322.
51. S. Geetha, C. R. K. Rao, M. Vijayan, and D. C. Trivedi, *Anal Chim Acta*, **568**, (2006), 119-125.
52. Z. X. Wang, C. Roberge, L. H. Dao, Y. Wan, G. X. Shi, M. Rouabhia, R. Guidoin, and Z. Zhang, *J Biomed Mater Res A*, **70A**, (2004), 28-38.
53. Z. Zhang, R. Roy, F. J. Dugre, D. Tessier, and L. H. Dao, *J Biomed Mater Res*, **57**, (2001), 63-71.
54. A. Kotwal and C. E. Schmidt, *Biomaterials*, **22**, (2001), 1055-1064.
55. J. Y. Wong, R. Langer, and D. E. Ingber, *P Natl Acad Sci USA*, **91**, (1994), 3201-3204.
56. B. Garner, A. Georgevich, A. J. Hodgson, L. Liu, and G. G. Wallace, *J Biomed Mater Res*, **44**, (1999), 121-129.
57. X. D. Wang, X. S. Gu, C. W. Yuan, S. J. Chen, P. Y. Zhang, T. Y. Zhang, J. Yao, F. Chen, and G. Chen, *J Biomed Mater Res A*, **68A**, (2004), 411-422.
58. S. Asavapiriyanont, G. K. Chandler, G. A. Gunawardena, and D. Pletcher, *J Electroanal Chem*, **177**, (1984), 229-244.
59. J. Heinze, *Synthetic Met*, **43**, (1991), 2805-2823.
60. G. Inzelt, V. Kertesz, and A. S. Nyback, *J Solid State Electr*, **3**, (1999), 251-257.

61. C. Y. Jin, F. L. Yang, and W. S. Yang, *J Appl Polym Sci*, **101**, (2006), 2518-2522.
62. V. M. Jovanovic, A. Dekanski, G. Vlajnic, and M. S. Jovanvic, *Electroanal*, **9**, (1997), 564-569.
63. S. Sadki, P. Schottland, N. Brodie, and G. Sabouraud, *Chem Soc Rev*, **29**, (2000), 283-293.
64. J. Tamm, A. Alumaa, A. Hallik, U. Johanson, L. Tamm, and T. Tamm, *Russ J Electrochem+*, **38**, (2002), 182-187.
65. M. Pyo and J. R. Reynolds, *Chem Mater*, **8**, (1996), 128-133.
66. M. Hepel and F. Mahdavi, *Microchem J*, **56**, (1997), 54-64.
67. L. L. Miller and Q. X. Zhou, *Macromolecules*, **20**, (1987), 1594-1597.
68. G. A. Husseini and W. G. Pitt, *J Pharm Sci-Us*, **98**, (2009), 795-811.
69. X. L. Xu, X. S. Chen, P. A. Ma, X. R. Wang, and X. B. Jing, *Eur J Pharm Biopharm*, **70**, (2008), 165-170.
70. S. G. Kumbar, L. S. Nair, S. Bhattacharyya, and C. T. Laurencin, *J Nanosci Nanotechno*, **6**, (2006), 2591-2607.
71. L. Feng, S. H. Li, H. J. Li, J. Zhai, Y. L. Song, L. Jiang, and D. B. Zhu, *Angew Chem Int Edit*, **41**, (2002), 1221-+.
72. G. M. Whitesides and B. Grzybowski, *Science*, **295**, (2002), 2418-2421.
73. T. Ondarcuhu and C. Joachim, *Europhys Lett*, **42**, (1998), 215-220.
74. J. Fang, H. T. Niu, T. Lin, and X. G. Wang, *Chinese Sci Bull*, **53**, (2008), 2265-2286.
75. E. R. Kenawy, F. I. Abdel-Hay, M. H. El-Newehy, and G. E. Wnek, *Mat Sci Eng a-Struct*, **459**, (2007), 390-396.
76. Q. J. Xie, S. Kuwabata, and H. Yoneyama, *J Electroanal Chem*, **420**, (1997), 219-225.
77. E. Luong-Van, L. Grondahl, K. N. Chua, K. W. Leong, V. Nurcombe, and S. M. Cool, *Biomaterials*, **27**, (2006), 2042-2050.
78. Z. M. Huang, Y. Z. Zhang, M. Kotaki, and S. Ramakrishna, *Compos Sci Technol*, **63**, (2003), 2223-2253.
79. A. Formhals, Vol. 1975504, 1934.
80. J. Doshi and D. H. Reneker, *J Electrostat*, **35**, (1995), 151-160.
81. D. H. Reneker and I. Chun, *Nanotechnology*, **7**, (1996), 216-223.
82. A. Greiner and J. H. Wendorff, *Angew Chem Int Edit*, **46**, (2007), 5670-5703.
83. D. Li and Y. N. Xia, *Adv Mater*, **16**, (2004), 1151-1170.
84. D. H. Reneker, A. L. Yarin, H. Fong, and S. Koombhongse, *J Appl Phys*, **87**, (2000), 4531-4547.
85. T. Subbiah, G. S. Bhat, R. W. Tock, S. Pararneswaran, and S. S. Ramkumar, *J Appl Polym Sci*, **96**, (2005), 557-569.
86. G. I. Taylor, *Proc. Roy. Soc. Lond.*, **A313**, (1969), 453-475.
87. A. Bernini, O. Spiga, A. Ciutti, M. Scarselli, G. Bottoni, P. Mascagni, and N. Niccolai, *Eur J Pharm Sci*, **22**, (2004), 445-450.
88. H. J. Shin, C. H. Lee, I. H. Cho, Y. J. Kim, Y. J. Lee, I. A. Kim, K. D. Park, N. Yui, and J. W. Shin, *J Biomat Sci-Polym E*, **17**, (2006), 103-119.
89. K. Kim, Y. K. Luu, C. Chang, D. F. Fang, B. S. Hsiao, B. Chu, and M. Hadjiargyrou, *J Control Release*, **98**, (2004), 47-56.
90. R. A. Jain, *Biomaterials*, **21**, (2000), 2475-2490.

91. M. Garinot, V. Fievez, V. Pourcelle, F. Stoffelbach, A. des Rieux, L. Plapied, I. Theate, H. Freichels, C. Jerome, J. Marchand-Brynaert, Y. J. Schneider, and V. Preat, *J Control Release*, **120**, (2007), 195-204.
92. D. Luo, K. Woodrow-Mumford, N. Belcheva, and W. M. Saltzman, *Pharmaceut Res*, **16**, (1999), 1300-1308.
93. X. H. Zong, S. Li, E. Chen, B. Garlick, K. S. Kim, D. F. Fang, J. Chiu, T. Zimmerman, C. Brathwaite, B. S. Hsiao, and B. Chu, *Ann Surg*, **240**, (2004), 910-915.
94. Z. M. Huang, C. L. He, A. Z. Yang, Y. Z. Zhang, X. J. Hang, J. L. Yin, and Q. S. Wu, *J Biomed Mater Res A*, **77A**, (2006), 169-179.
95. E. R. Kenawy, G. L. Bowlin, K. Mansfield, J. Layman, D. G. Simpson, E. H. Sanders, and G. E. Wnek, *J Control Release*, **81**, (2002), 57-64.
96. G. Bidan, B. Ehui, and M. Lapkowski, *J Phys D Appl Phys*, **21**, (1988), 1043-1054.
97. F. R. F. Fan and A. J. Bard, *J Electrochem Soc*, **133**, (1986), 301-304.
98. G. Bidan, C. Lopez, F. Mendesviegas, E. Vieil, and A. Gadelle, *Biosens Bioelectron*, **10**, (1995), 219-229.
99. D. A. Reece, S. F. Ralph, and G. G. Wallace, *J Membrane Sci*, **249**, (2005), 9-20.
100. K. R. Temsamani, O. Ceylan, B. J. Yates, S. Oztemiz, T. P. Gbatu, A. M. Stalcup, H. B. Mark, and W. Kutner, *J Solid State Electr*, **6**, (2002), 494-497.
101. N. Izaoumen, D. Bouchta, H. Zejli, M. El Kaoutit, A. M. Stalcup, and K. R. Temsamani, *Talanta*, **66**, (2005), 111-117.
102. A. Villiers, *C. R Acad. Sci*, **112**, (1891), 536.
103. F. Schardinger, *Wien. Klin. Wochenschr*, **17**, (1904), 207.
104. A. R. Hedges, *Chem Rev*, **98**, (1998), 2035-2044.
105. J. Szejtli, *J Mater Chem*, **7**, (1997), 575-587.
106. W. Saenger, *Angewandte Chemie-International Edition in English*, **19**, (1980), 344-362.
107. D. French, *Method Enzymol*, **3**, (1957), 17-20.
108. H. Dodziuk, Cyclodextrins and Their Complexes, 2006.
109. J. Szejtli, *Chem Rev*, **98**, (1998), 1743-1753.
110. A. Harada and S. Takahashi, *J Chem Soc Chem Comm*, (1984), 645-646.
111. M. V. Rekharsky and Y. Inoue, *Chem Rev*, **98**, (1998), 1875-1917.
112. K. Uekama, F. Hirayama, and T. Irie, *Chem Rev*, **98**, (1998), 2045-2076.
113. V. Zia, R. A. Rajewski, and V. J. Stella, *Pharmaceut Res*, **18**, (2001), 667-673.
114. L. X. Wang, X. G. Li, and Y. L. Yang, *React Funct Polym*, **47**, (2001), 125-139.
115. F. T. A. Chen, G. Shen, and R. A. Evangelista, *J Chromatogr A*, **924**, (2001), 523-532.
116. G. K. E. Scriba, *J Sep Sci*, **31**, (2008), 1991-2011.
117. A. Amini, T. Rundlof, M. B. G. Rydberg, and T. Arvidsson, *J Sep Sci*, **27**, (2004), 1102-1108.
118. F. Hirayama and K. Uekama, *Adv Drug Deliver Rev*, **36**, (1999), 125-141.
119. X. J. Dang, M. Y. Nie, J. Tong, and H. L. Li, *J Electroanal Chem*, **448**, (1998), 61-67.
120. L. Fielding, *Tetrahedron*, **56**, (2000), 6151-6170.

121. P. Job, **9**, (1928), 113-203.
122. J. Mosinger, V. Tomankova, I. Nemcova, and J. Zyka, *Anal Lett*, **34**, (2001), 1979-2004.
123. W. Misiuk and M. Zalewska, *Anal Lett*, **41**, (2008), 543-560.
124. J. B. Chao, H. B. Tong, Y. F. Li, L. W. Zhang, and B. T. Zhang, *Supramol Chem*, **20**, (2008), 461-466.
125. I. Bratu, J. M. Gavira-Vallejo, A. Hernanz, M. Bogdan, and G. Bora, *Biopolymers*, **73**, (2004), 451-456.
126. I. V. Terekhova, R. S. Kumeev, and G. A. Alper, *J Incl Phenom Macro*, **59**, (2007), 301-306.
127. J. R. Cruz, B. A. Becker, K. F. Morris, and C. K. Larive, *Magn Reson Chem*, **46**, (2008), 838-845.
128. H. A. Benesi and J. H. Hildebrand, *J Am Chem Soc*, **71**, (1949), 2703-2707.
129. M. S. Ibrahim, I. S. Shehatta, and A. A. Al-Nayeli, *J Pharmaceut Biomed*, **28**, (2002), 217-225.
130. R. Ramaraj, V. M. Kumar, C. R. Raj, and V. Ganesane, *J Incl Phenom Macro*, **40**, (2001), 99-104.
131. C. Yanez, L. J. Nunez-Vergara, and J. A. Squella, *Electroanal*, **15**, (2003), 1771-1777.
132. G. C. Zhao, J. J. Zhu, J. J. Zhang, and H. Y. Chen, *Anal Chim Acta*, **394**, (1999), 337-344.
133. E. Coutouli-Argyropoulou, A. Kelaidopoulou, C. Sideris, and G. Kokkinidis, *J Electroanal Chem*, **477**, (1999), 130-139.
134. Y. Y. Zhou, C. Liu, H. P. Yu, H. W. Xu, Q. Lu, and L. Wang, *Spectrosc Lett*, **39**, (2006), 409-420.
135. K. A. Connors, *Chem Rev*, **97**, (1997), 1325-1357.
136. L. Liu and Q. X. Guo, *J Incl Phenom Macro*, **42**, (2002), 1-14.
137. W. Saenger and T. Steiner, *Acta Crystallogr A*, **54**, (1998), 798-805.
138. Y. Matsui and A. Okimoto, *B Chem Soc Jpn*, **51**, (1978), 3030-3034.
139. L. X. Song, B. L. Li, R. Jiang, J. G. Ding, and Q. J. Meng, *Chinese Chem Lett*, **8**, (1997), 613-614.
140. I. Tabushi, Y. I. Kiyosuke, T. Sugimoto, and K. Yamamura, *J Am Chem Soc*, **100**, (1978), 916-919.
141. K. Okimoto, R. A. Rajewski, K. Uekama, J. A. Jona, and V. J. Stella, *Pharmaceut Res*, **13**, (1996), 256-264.
142. L. Szente and J. Szejtli, *Trends Food Sci Tech*, **15**, (2004), 137-142.
143. J. Szejtli, *Pure Appl Chem*, **76**, (2004), 1825-1845.
144. T. Irie and K. Uekama, *Adv Drug Deliver Rev*, **36**, (1999), 101-123.
145. J. Li and X. J. Loh, *Adv Drug Deliver Rev*, **60**, (2008), 1000-1017.
146. K. Uekama, *J Incl Phenom Macro*, **44**, (2002), 3-7.
147. K. Uekama, F. Hirayama, and H. Arima, *J Incl Phenom Macro*, **56**, (2006), 3-8.
148. A. Ferancova and J. Labuda, *Fresen J Anal Chem*, **370**, (2001), 1-10.
149. K. R. Temsamani, H. B. Mark, W. Kutner, and A. M. Stalcup, *J Solid State Electr*, **6**, (2002), 391-395.
150. J. A. Kiernan and M. L. Barr, Barr's the Human Nervous System: An Anatomical Viewpoint, Lippincott Williams & Wilkins, 2008.
151. J. Nolte and J. W. Sundsten, The Human Brain: An Introduction to Its Functional Anatomy, Mosby, 1998.

152. R. H. Thompson, The Brain: A Neuroscience Primer, W H Freeman & Co, 1993.
153. M. D. Hawley, S. Tatawawa, S. Piekarsk, and R. N. Adams, *J Am Chem Soc*, **89**, (1967), 447-&.
154. T. Luczak, *Electroanal*, **20**, (2008), 1639-1646.
155. R. Langer, *J Control Release*, **16**, (1991), 53-59.
156. A. Mcraedegueurce, S. Hjorth, D. L. Dillon, D. W. Mason, and T. R. Tice, *Neurosci Lett*, **92**, (1988), 303-309.
157. H. Uludag, J. E. Babensee, T. Roberts, L. Kharlip, V. Horvath, and M. V. Sefton, *J Control Release*, **24**, (1993), 3-11.
158. Q. X. Zhou, L. L. Miller, and J. R. Valentine, *J Electroanal Chem*, **261**, (1989), 147-164.

## 1.1 Introduction

The initial aim of this work was to examine the use of polypyrrole (PPy), a well-known conducting polymer, for the uptake and release of a cationic species, dopamine (DA). DA was chosen as it represents a large family of amine-based drugs. Therefore, if appropriate PPy films could be electrosynthesised and used in the controlled delivery of DA, then the concept could be used more widely in the field of controlled drug delivery.

In Chapter 3, the growth of PPy films in the presence of various dopant anions, including a large anionic cyclodextrin (CD), sulfonated β-cyclodextrin (Sβ-CD) is explored. Although Sβ-CD doped PPy films have been reported in the recent literature, there has been very little work devoted to the characterisation of these films. Accordingly, much of Chapter 3 is devoted to the unique redox properties of the Sβ-CD doped PPy films.

With the growth of the PPy films achieved, Chapter 4, shows the drug release profiles of the protonated DA and reveals that in the case of the polymer films doped with the anionic Sβ-CD, there is a substantial increase in the amount of DA released in comparison to other polymer films. In order to explain the enhanced release profiles, the well-known supramolecular complexation properties of cyclodextrins were considered. However, on searching the literature no reports on the complexation of DA with anionic cyclodextrins were found and consequently this was studied in detail. These findings are presented in Chapter 5, where the host-guest interactions between DA and the anionic Sβ-CD are examined using a variety of techniques, both spectroscopic and electrochemical.

In Chapter 6 the technique of electrospinning is introduced. Details on how it is used to fabricate nanostructured biodegradable polymer films with a high surface area are provided. The approaches used to deposit the Sβ-CD doped PPy films onto the nanostructured biodegradable film are then considered and discussed. It is shown that cyclic voltammetry was the most successful

approach. Moreover, it was possible to control the amount of PPy deposited and to maintain the nanostructured fiber substrate by varying the number of cycles. These high surface area Sβ-CD doped PPy films are promising for the uptake and liberation of DA.

In this introductory chapter, the concept of controlled drug release is firstly introduced. This is then followed with information on conducting polymers, particularly PPy and the current state-of-art in using PPy in drug delivery. The technique of electrospinning is then introduced and linked to DDS. The next section is devoted to cyclodextrins, as it is the Sβ-CD doped PPy films that give the best controlled release properties. Finally, the chapter ends with a short account of the properties of DA and its delivery.

### 1.1.1 Controlled drug release

In the early 1970s, controlled release systems first materialised. Since then, the number and the areas in which a controlled release system is utilised have significantly increased. These systems have been used in areas such as cosmetics[1], food[2], and pesticides[3]. Controlled release systems are focused on obtaining the release of the proposed material, over a certain time without an external influence from any other potential release factor.[4] Polymeric materials have been previously investigated for controlled release as they can be easily manufactured and their composition can be finely tuned.[5] Polymers used in controlled release systems can be natural or synthetic and release can be achieved through the engineering of the polymer substrates, i.e., the degradation of poly($_{D,L}$ – lactide-*co*-glycolide) (PLGA) can be controlled through the polymer composition, higher ratios of PLA lead to a higher degradation rate.[6]

Another important research area under consideration is the development of controlled drug delivery systems (DDS).[7, 8] In 1980, controlled DDS were virtually unknown, yet in 2005, almost 100 million people globally were using some form of polymer based DDS.[8] The aim of a DDS is to supply the drug in its

therapeutically active form to a specific target in the body when the drug is required. In the current administration process there is a critical concentration needed in order to achieve the drug's maximum therapeutic effect. If the concentration goes beyond the maximum level, toxicity problems come into play. Conversely, if the concentration administered is below the minimum level the effect of the drug is not observed. The use of these DDS could potentially eliminate these problems as the release would be of a controlled manner.

Santini *et al.*[7] compared the release profiles of both conventional and controlled methods, as illustrated in Figure 1.1. With conventional methods of drug delivery, outlined in Figure 1.1(A), i.e., oral administration or injections, drug levels rise after initial administration, which could lead to potential toxicity problems, and then decrease until the next dosage, which has consequences on the efficiency of the dosage. The other schematic, Figure 1.1(B), demonstrates the effectiveness of a controlled release system. After dosage, the drug level in the blood remains constant, between the maximum and minimum levels, for a certain period of time.

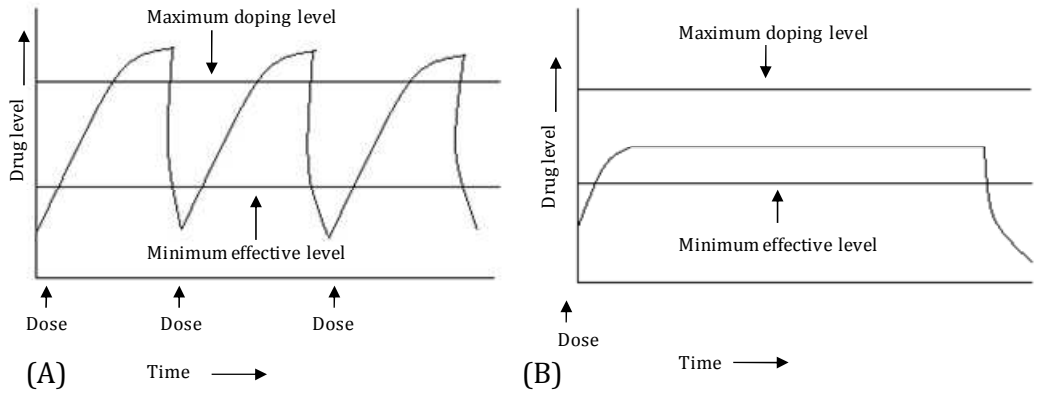


**Figure 1.1:** Drug levels in the blood with (A) conventional drug dosage (B) controlled delivery dosage, taken from Santini *et al.*[7]

In recent years, polymeric materials have been examined and shown to provide an alternate means of delivering drugs. Implanted polymeric pellets or microspheres localise therapy to specific anatomic sites, providing a continuous sustained release of drugs while minimising systemic exposure.[9] Polymers that display a physiochemical response to stimuli have been broadly researched for controlled release systems. Various stimuli include pH, temperature and the application of an electrical field.[10] According to Langer[11], polymeric DDS should i) maintain a constant drug level ii) reduce harmful side effects iii) minimise the amount of drug needed and iv) decrease the amount of doses which will have a pronounced effect on the patient.

The original polymeric controlled DDS was based on a non-biodegradable polymer, silicone rubber, which was designed and tested by Folkman and Long.[12] They loaded a silicone capsule (Silastic*) with a number of different drugs for the treatment of heart block and successfully implanted and monitored their effects over a number of days.

In more recent years there has been considerable interest in the development of new and efficient DDS, particularly with the growth of sophisticated drugs that are based on DNA and proteins.[5, 13] Currently, there are several materials under consideration in drug delivery, for example dendrimers[14], nanoparticles[15] and hydrogels[16]. The most promising opportunities in controlled DDS are in the area of responsive polymeric materials, with the possibility of implantable devices being used to deliver drugs. Murdan[17] exhaustively reviewed the use of hydrogels as 'smart' drug delivery devices. He showed that hydrogels could be engineered for various medicinal treatments depending on the patients needs, for example, pain relief. In the body, drug release can only be accomplished if the drug carrier responds to some class of stimuli, be it chemical, physical or biological. Conversely, an implanted 'smart' drug delivery device should be non-responsive to all other types of stimulus, once inside the body. A way of achieving this form of control is through an electrical stimulus.[17] A number of *in vivo* devices, in the form of iontophoresis, have already been used for this type of controlled release.[17, 18] Murdan presented a case where hydrogels loaded

with a bioactive compound, were implanted at a target site and the drug liberated through the application of an electrical field. In utilising such a system, many advantages including, minimal drug usage and lowering toxicity problems can be achieved. However, a problem arising with the application of an electrical stimuli to polymeric materials like, hydrogels, is that they experience deswelling or bending, which affects the drug release.[17]

To overcome these problems, conducting polymers (CPs) are also receiving much attention in the field of biomedical research, for the application of controlled DDS, due to their light weight, good biocompatibility and ability to function at body temperature. In particular, conducting polymers exhibit a reversible electrochemical response. These reversible oxidation-reduction reactions are attractive for a responsive DDS, as a change in the net charge on a conducting polymer film during its reduction or oxidation requires ions to flow into or out of the film. This, in turn, allows the polymer film to bind and expel ions in response to electrical signals. Controlled release of drugs from polymers offers many advantages over conventional methods including better control of the drug level administered resulting in fewer side effects, local drug delivery, decreased requirements for the total amount of drug and protection of drugs which are rapidly destroyed by the body. However, in order to devise a suitable technology, the polymeric material must be responsive, i.e., it must be capable of altering so that the drug is released in a controlled fashion when needed.

### 1.1.2 Conducting polymers

A polymer is a large molecule made up of smaller repeating units. The name comes from the Greek *poly*, meaning 'many', and *mer*, meaning 'part'. They are built up from simple molecules called *monomers* 'single part'. Polymers are produced through a method known as polymerisation. This polymerisation step can be achieved through chemical or electrochemical methods. Originally polymers with the basic carbon chains were considered only as insulators.[19] The first real interest in conducting polymers can be attributed to Walatka *et al*.[20] in 1973 with the report of highly conducting polysulfur nitride $(SN)_x$. Meanwhile

and towards the late 1970s , MacDiarmid, Shirakawa and Heeger enhanced the discovery of the semi-conducting and metallic properties of the chemically synthesised organic polyacetylene.[21-24] As is well known, the Nobel Prize in Chemistry was awarded to Alan J.Heeger, Alan G. MacDiarmid and Hideki Shirakawa in 2000 for the discovery and development of conducting polymers (CPs).[21-24] In the following years, a wide range of polymeric organic species have been prepared as stable inherent films on inert electrodes via both chemical oxidation and electropolymerisation from aqueous and organic solution.[25]

CPs are organic materials, which generally are comprised simply of C, H and simple heteroatoms such as N and S. Common examples include PPy, polyaniline and polythiophene which are shown in Figure 1.2. These and a number of other conducting polymers have been used in a variety of applications ranging from corrosion protection of materials, sensors to many biomedical applications, such as tissue engineering, nerve cell regeneration and drug delivery.[26-29]

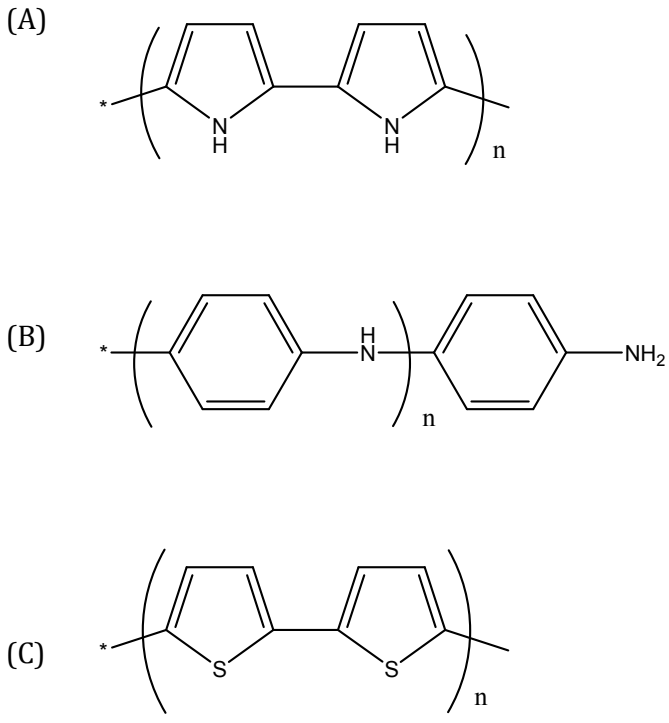


**Figure 1.2:** Chemical structures of (A) polypyrrole (B) polyaniline and (C) polythiophene. All polymers are shown in the dedoped state.

In, general materials are classed depending on their electrical conductivity, κ, where the electrical conductivity of insulators < semiconductors < conductors. Bredas and Street[30] explained this phenomenon in terms of the band gap structure. Figure 1.3 illustrates the difference in each material using the band gap theory. The highest occupied molecular orbital is equivalent to the valence band (VB), while the lowest unoccupied molecular orbital may be equated to the conduction band (CB). The difference between each band is known as the band gap energy ($E_g$) and it is this energy gap that establishes the electrical properties of a material. If $E_g$ > 10 eV, it is difficult to excite electrons into the conduction band and an insulator is formed. If $E_g \sim 1.0$ eV then thermal energy is sufficient to promote the electrons into the conduction band and a semiconductor is formed. If the gap vanishes, with overlap of the valence and conduction band, as shown in Figure 1.3, metallic conduction is observed. For most doped CPs the band gap energy is generally close to 1.0 eV, and consequently, CPs can be classified as semi-conductors.

As pointed out by Bredas and Street[30], the conductivity observed upon doping of the CPs was originally thought to be from the formation of unfilled electronic bands, however this idea was quickly dissipated upon experimental analysis of PPy and polyacetylene and now it is recognised that the conductivity is due to the formation of polarons and bipolarons, which are more energetically favoured.[30, 31]

The π-bonded system of CPs, which comprises of alternating single and double bonds, enabling the delocalisation of electrons along the polymer backbone, is related to the conductivity of the system. The conductivity of these materials arises from a state of relative oxidation or reduction. In these states the polymer either loses (oxidation) or gains (reduction) an electron. Generally, it is said that this process occurs in 1 in every 4 monomer units.[32] In this state the polymer is electronically charged and requires the introduction of counter ions (dopants) to compensate and reform the charge neutrality. The oxidation of the polymer in which an electron is removed from a π-bond, gives rise to a new energy state, which leaves the remaining electron in a non-bonding orbital. This energy level

is higher than the valence band and behaves like a heavily doped semiconductor.[32] The extent of doping can be controlled during the polymerisation of the polymers.

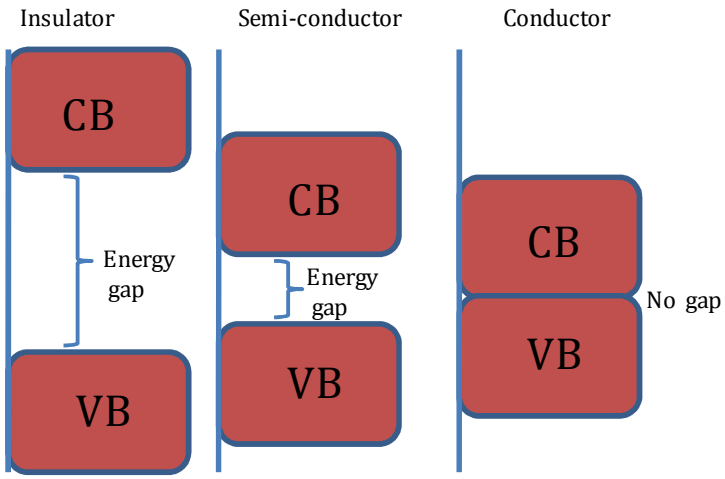


**Figure 1.3:** Schematic of the difference in band gap for Insulators, semi-conductors and metals (conductors).

### *1.1.2.1 Polymerisation methods*

CPs are synthesised through a method known as oxidative polymerisation. This can be generated chemically or electrochemically. Chemical polymerisation involves the use of a chemical oxidant, such as ammonium peroxydisulfate (APS), ferric ions, permanganate, dichromate anions or hydrogen peroxide. The oxidants not only oxidise the monomer but provide dopant anions to neutralise the positive charges formed on the polymer backbone.[33] In the presence of these oxidants, the monomers are oxidised and chemically active cation radicals are formed which further react with the monomer and generate the desired polymer. An advantage of vapour phase chemical polymerisation of CPs is that the polymerisation occurs almost exclusively on the preferred surface and a higher surface area can be attained.[34] Vapour phase chemical polymerisation of

pyrrole leads to further doping after polymerisation and this gives rise to an increase in conductivity.[35]

The electrochemical deposition is a simple and reproducible technique where the dopant is present in the electrolyte during polymerisation. It is generally performed in a conventional three electrode set up, described later in Chapter 2, where current is passed through a solution containing the monomer in the presence of a dopant (electrolyte). The CP is deposited at the positively charged working electrode or anode.[27] Polymerisation is initiated through the oxidation of the monomer which forms a mobile charge carrier known as a polaron (radical cation), that can react with another monomer or polaron to form a bipolaron (radical dication) which leads to the formation of the insoluble polymer chain and deposition of the polymer onto the working electrode.[36]

In his book 'Conducting Polymers' published in 1986, Alcacer commented on the possibility of using CPs to make artificial muscles or perhaps even modification for the brain; little did he realise the extent to which these materials have been extensively researched, over the past 20 years.[32] Since their discovery, the preparation and characterisation of these materials has evolved substantially through the use of electrochemistry. The majority of research is significantly based in this area due to the ease and control of synthesis of these electronically CPs.[19] Reviews on the development of CPs show the various areas to where they can be applied. The applications are ongoing.[37-40] However, in the case of DDS, CPs, in particular PPy, are widely researched for the controlled release of therapeutically active compunds.[41-45] During oxidative polymerisation, a dopant molecule, with an overall anionic charge, is used to compensate for the positive charges originating from the oxidation of the monomer. It is during this process that the concept of drug delivery originated. Burgmayer and Murray[46] observed changes in the ionic permeability of PPy redox membranes using a voltage-controlled electrochemical reaction. This led to further investigations into the application of CPs in DDS.

### *1.1.2.2 Polypyrrole*

#### 1.1.2.2.1 Historical background of polypyrrole

In 1968 Dall'Olio and colleagues prepared black films of an oxypyrrole on platinum by the electrochemical polymerisation of pyrrole from a solution of sulfuric acid.[47] In 1979 Diaz with the help of colleagues modified Dall'Olio's approach and demonstrated that polymerising pyrrole onto platinum in acetonitrile led to a black, adherent film.[48] Elemental analysis showed that the monomer unit was retained in the polymer. PPy in general, was poorly crystalline, and its ideal structure was a planar (α-ά)-bonded chain in which the orientation of the pyrrole molecules alternate.[25]

The monomer unit, pyrrole, is shown in Figure 1.4. PPy is an organic material comprised simply of C, H and a simple N heteroatom, but is highly conducting. It is an inherently conductive polymer due to interchain hopping of electrons. PPy can be synthesised both chemically[49] and electrochemically[48]. The electrochemical synthesis method is a one step synthesis method and allows the simple deposition of polymer films where its surface charge characteristics can easily be modified by changing the dopant anion (A-) that is incorporated into the material during synthesis. In a cell containing an aqueous or non-aqueous solution of the monomer, PPy forms a (semi) conducting film on the working electrode; the film grown is in the oxidised form and can be reduced to the non-conducting insulating form by stepping the potential to more negative values. The potential cycling can be repeated many times between the insulating and (semi) conducting forms without a loss of the electroactivity of the film.[25]

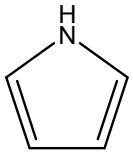


**Figure 1.4:** Schematic illustration of a monomer unit of pyrrole.

PPy in its neutral form is weakly coloured while the oxidised form is a deep blue/black. The switching of the state of the film not only changes its conductivity but it is also accompanied by a marked colour change, termed electrochromism.[36] Materials such as PPy are important in terms of future technological impact as it may be possible to develop them to replace more expensive, often toxic, metallic conductors commonly employed in the electronics industry.[25]

#### 1.1.2.2.2 Polymerisation mechanism of pyrrole

Although there are still various opinions on the mechanistic features of the electropolymerisation of pyrrole, the mechanism proposed by Diaz and his colleagues[48] and later used by Baker and Reynolds is in good agreement with many experimental reports.[50] The mechanism is demonstrated in Figure 1.5.

The initial step is the generation of the radical cation. This cation has different resonance forms, as shown in Figure 1.5. In the next step in the chemical case, the radical cation then attacks another monomer molecule, generating a dimer radical cation. In the electrochemical case, the concentrations of radical cations is much larger than that of neutral monomers in the vicinity of the electrode where reactions are occurring, and radical-radical coupling leads to a radical dication. This coupling between the two pyrrole radicals results in the formation of a bond between the two $\alpha$ positions to give the radical dication, as highlighted in Figure 1.5. This is then followed by the loss of two protons, generating a neutral dimer. This dimer is then oxidised into a radical cation, where the unpaired electron is delocalised over the dimer. The radical dimer then couples with the radical monomer to form a trimer. The polymerisation thus progressing in this fashion to completion.

The controversy in the mechanism of electropolymerisation is not surprising given that many factors, such as the nature of the electrolyte, ionic strength, pH, temperature and potential are important and can influence the mechanism of the reaction.

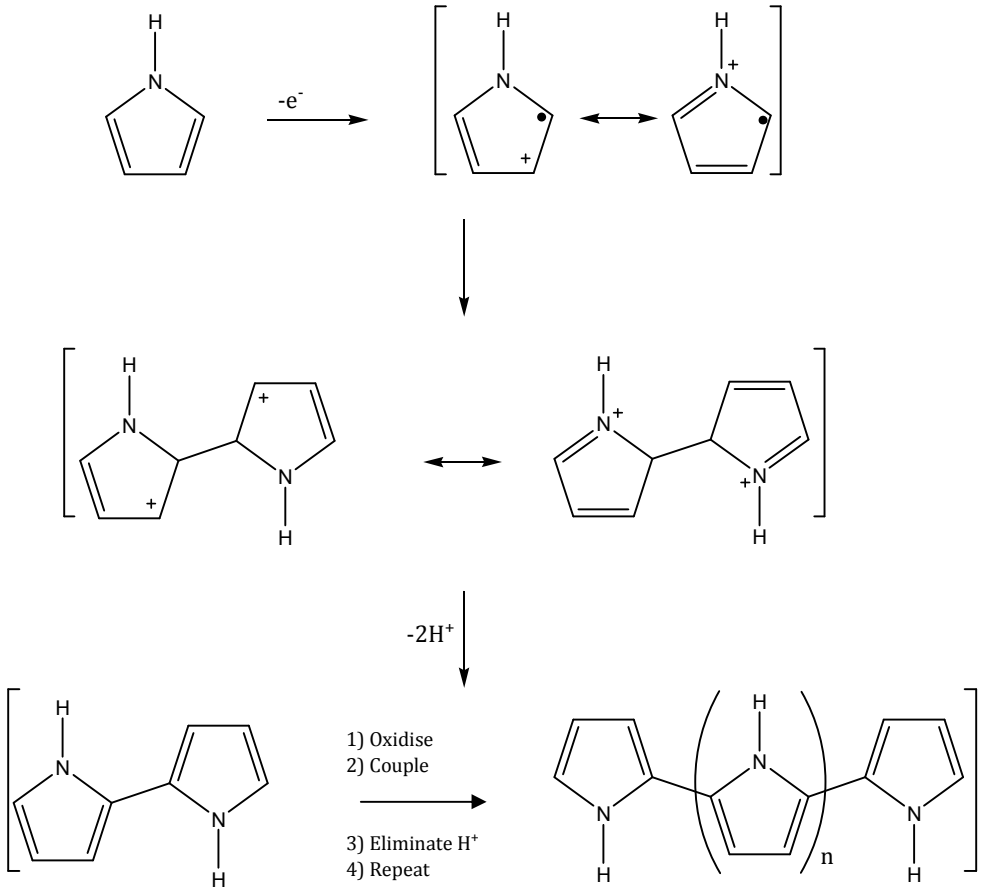


**Figure 1.5:** Mechanism of electrochemical polymerisation of pyrrole.[50]

#### 1.1.2.2.3 Biocompatibility

PPy is one of the most widely researched conductive polymers. The fact that it can form biologically compatible matrices is one of the prominent reasons for the extensive research on the use of PPy in the field of biological applications.[51] Wang *et al.*[52] acknowledged the reality that PPy had showed very good *in vitro* biocompatibility,[29, 53, 54] but they wanted to evaluate further the *in vivo* biocompatibility prospects. They demonstrated that in comparison to no PPy, the presence of PPy/biodegradable composites stimulated no abnormal tissue response and had no affect on the degradation behaviour of the biodegradable materials. In 1994, PPy was one of the first conducting polymers investigated for its effect on mammalian cells.[55] Since then, PPy is known to be

biocompatible, so it can be placed in the body without having adverse effects. It has been shown, in particular, to support cell growth and adhesion of endothelial cells.[29, 55-57] Schmidt *et al*.[29] also demonstrated that PPy was a suitable material for both in vitro nerve cell culture and in vivo implantation. PPy was electrochemically deposited onto ITO-conductive borosilicate glass. Moreover, the application of an external electrical stimulus through the polymer film resulted in enhanced neurite outgrowth. The median neurite length for PC-12 cells grown on PPy film subjected to an electrical stimulus increased nearly two-fold compared with cells grown on PPy without the application of a constant potential. The group also investigated PPy in vivo and their studies showed that PPy promotes little negative tissue and inflammatory response. Due to the good biocompatible factor, studies on the application of an electric field to the PPy have also shown cell compatibility.[29] In some important applications, such as biological sensors and actuators for medical devices it is a very attractive trait and some recent applications show that PPy can enhanced nerve cell regeneration and tissue engineering.[27]

#### 1.1.2.2.4 Electroactivity of polypyrrole

PPy can be easily switched between the neutral, partially oxidised and fully oxidised states, as shown in Figure 1.6. In its neutral state PPy exists as an insulator where the conduction band is empty as all the electrons remain in the valence band. Upon oxidation, an electron is removed from a π-bond (valence band) and a polaron is formed. The separation of the positive charge and the unpaired electron decreases during continual oxidation as the number of polarons increases. This in turn gives rise to the formation of a bipolaron, as depicted in Figure 1.6(C), and the polymer is now in its fully oxidised state.

During oxidation and the generation of positive charge an influx of anions into the polymer matrix is observed in order to maintain charge balance. This can be represented in Equation 1.1, where $PPy^{o}$ refers to the neutral (reduced) polymer, $PPy^{+}$ refers to the oxidised polymer and $A^{-}$ refers to the anionic dopant.

$$PPy^0 + A^- \rightarrow PPy^+A^- + e^- \quad 1.1$$

Typical anionic dopants are chlorides, bromides, iodides, perchlorates, nitrates, sulfates and para-toluene sulfonates.[58-64] The extent of oxidation/reduction is given by the doping level and this is generally expressed as the ratio of dopant anions, $A^-$, incorporated per monomer unit. For example, 1 $A^-$ per 4 monomer units gives a doping level of 0.25 or 25%. The maximum doping level achievable with PPy is 0.33 or 33%, i.e., 1 $A^-$ per 3 pyrrole units. It is important to point out that doping may not always be uniform; there can be islands with high doping levels surrounding by regions with a much lower doping level.

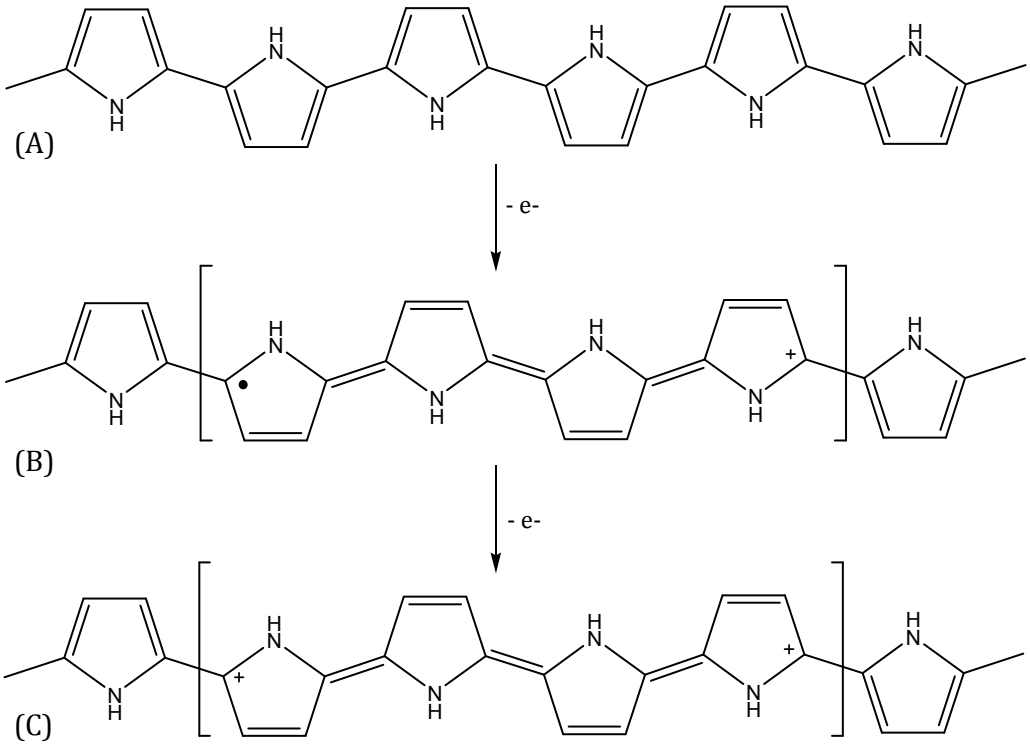


**Figure 1.6:** Electronic structures of (A) neutral PPy, (B) polaron in partially doped PPy and (C) bipolaron in fully doped (oxidised) PPy.[36]

**1.1.2.2.5 Polypyrrole and drug delivery**

The electrochemical switching of PPy films is accompanied by movement of counter or dopant ions in and out of the polymer matrix to maintain the charge neutrality, as shown in Section 1.1.2.3.4. Consequently, PPy films are attractive for the controlled release of drug molecules. The concept of using PPy membranes for the uptake and release of ions was introduced, in the early 1980s, by Burgmayer and Murray[46]. They demonstrated that these polymeric films could be exchanged from their oxidised state to their neutral state. PPy has been seriously considered for drug delivery due to these unique redox properties. PPy gives a responsive material needed in order for the uptake and release of the drug to be controlled; in its oxidised state anions are electrostatically bound to the polymer film. These properties allow the controlled transport of ions. The uptake of these ions can occur in two ways. The first is where the bioactive molecule exists as an anion and is involved in the doping process of the polymeric material during polymerisation, Figure 1.7 (A). Some anions that have been researched include adenosine tri phosphate (ATP)[65], salicylate[26], and dexamethasome[26]. These anions are electrostatically entrapped into the polymer matrix during the growth process upon application of an anodic potential. The anions are consequently liberated during the reduction of the polymer.

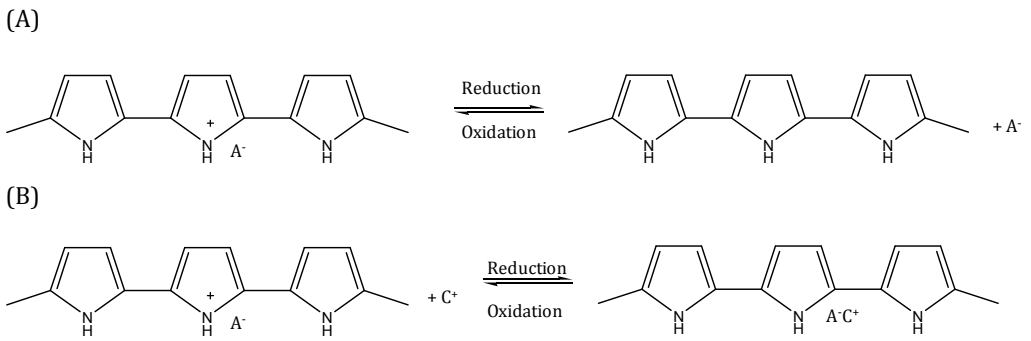


**Figure 1.7:** Interconversion between oxidation and reduction states of PPy (PPy). (A) Anion (A-) incorporation and release which is notably observed in small mobile anions (e.g. Cl-) while, (B) Cation (C+) insertion and liberation from polymer films doped with larger anions (e.g. $DDS^-$) which remain entrapped in the polymer matrix.

In the second case, cations can be incorporated into the system, Figure 1.7 (B), if the properties of the polymer film are modified.[66] This is achieved through the

initial inclusion of a large anion which remains entrapped in the polymer matrix and thus the polymer behaves as a cation exchanger, where, the charge of the polymer system can only be compensated through the uptake of cations. The cations are therefore, taken in during the reduction of the polymer and released upon oxidation. Figure 1.7 demonstrates both these concepts.

Miller and Zhou[67] previously reported the release of dopamine from a poly(*N*-methlypyrrole)/poly(styrenesulfonate) (PNMP/PSS) polymer based on the properties of these redox polymers. Immobilisation of PSS, a large anion, allows the uptake and release of the cation upon appropriate application of a potential. They achieved the release of dopamine using potential control, while more recently, Hepel and Mahdavi[66] demonstrated the controlled release of a cationic species, chloropromazine, from a composite polymer film based on the same principles. They reported the development of a new composite conducting polymer, PPy/melanin, which performed as a cation binder and releaser. The modification of the polymer films, to enable the predominant cationic exchange properties of the CP, is an interesting way of improving the uptake and release of cationic species from these attractive materials.

New ways of improving the controlled release of drugs are continually being sought after. Lately, Abidan *et al*.[41] reported on a method to prepare conducting-polymer nanotubes that can be used for controlled drug release. They introduced a method known as electrospinning to fabricate a nanofibrous mat in which the drug to be delivered had previously been incorporated; followed by electrochemical deposition of PPy films around the drug-loaded, electrospun biodegradable polymers. The drug release was achieved through the electrical stimulation of the PPy nanotubes.

#### 1.1.2.2.6 The application of Nanotechnology in drug delivery

Nanotechnology, although dating back to much earlier times, gained considerable attention in the early 1990s and has been the focus of much research over the last number of years. The introduction of nanotechnology into a controlled DDS has been shown to enhance many physical and chemical properties and overall has been used to increase the surface area of materials. This, in turn, leads to an increase in the amount of drug released from various materials. Many groups have introduced nanotechnology in various forms to improve on the drug delivery of a number of bioactive compounds, including nanoparticles[15], micellar systems[68] and nanofibers[69]. Polymeric nanofibers are gaining substantial interest for various applications including drug delivery[69, 70]. Several techniques have been employed for the production of nanofibers such as template synthesis[71], self assembly[72] and drawing[73]. One technique, in particular that is receiving considerable interest in this field, is electrospinning.[74-77] Electrospinning has been introduced to achieve nanoscale membranes and fibres from various polymeric materials.[78]

**1.1.2.2.7 The application of Electrospinning to drug delivery**

Although electrospinning was first reported by Formhals[79] in 1934 it has only been explored further in recent times.[80, 81] In 1996, Reneker and Chun restored interest in the electrospinning technique by demonstrating the possibility of electrospinning a wide range of organic polymers.[81] Since then the technique of electrospinning has become extremely useful in a variety of applications.[82-85] Electrospinning is a simple and inexpensive means for the formation of nano- to micron polymer fibers.

This technique involves the application of a high electric field between a polymer fluid and a grounded electrode. When the polymer solution is subjected to an external electric field at a critical point the forces overcome the surface tension of the polymer solution to form a droplet with a conical shape, i.e., the Taylor cone.[83, 86] The fluid is drawn into a jet which undergoes a whipping motion. Volatile solvents are used to dissolve the polymer as the subsequent evaporation from the liquid jet results in solid fibers. A more detailed

description of this technique is provided in Chapter 2, Section 2.4.5. In the majority of cases the fibers deposit randomly on the grounded collector. However, many groups have investigated the use of rotating collector plates to produce aligned nanofibers.[87] Figure 1.8 illustrates a typical SEM micrograph of an electrospun fiber mat of PLGA fibers.

This production of nanofibers allows these polymers to be used in a wide variety of applications including, tissue engineering (muscles, skin, cartilage and bones), wound healing and sutures, biosensors and DDS. Shin *et al.*[88] studied the use of PLGA nanofiber scaffold for cartilage reconstruction, while, Kim and colleagues incorporated antibiotics in the fibrous matrix for use in wound dressings.[89] Other groups have also prepared ultrafine polymers via electrospinning for skin regeneration.[74]

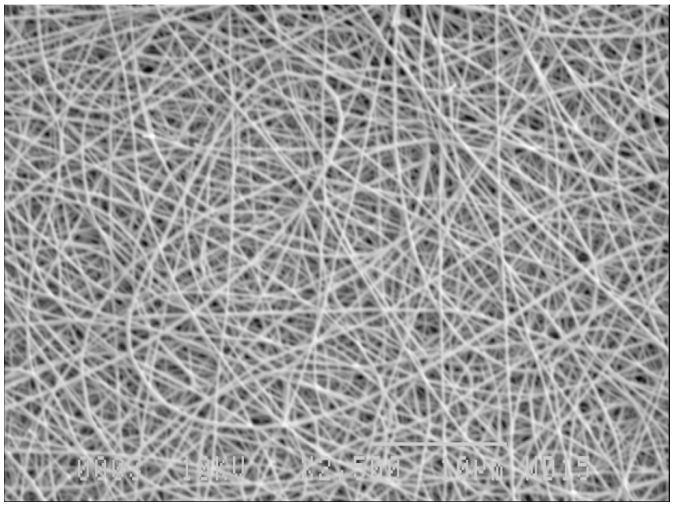

**Figure 1.8:** A typical SEM image of electrospun PLGA nanofibers.

Another attractive feature of using this electrospinning technique is that biodegradable polymeric materials, such as poly(lactic acid) (PLA) and poly($_{D,L}$ – lactide-*co*-glycolide) (PLGA) can be used as a biomedical controlled release system. These biodegradable polymers can be electrospun in the presence of varying amounts of the required medication. They can then be placed in the

body and the drug release achieved through the modification of the polymer matrix's morphology, porosity and composition.[89] These biodegradable polymers have FDA approval for biomedical and drug delivery use.[90-93] In comparison to other delivery forms, the electrospun nanofibers can conveniently incorporate the therapeutic compound during the electrospinning process.[94] Many drugs have been incorporated into PLGA electrospun polymer matrices, in order to achieve delivery of the therapeutic drug, including, tetracycline hydrochloride[95] and mefoxin[89]. In these cases, the drug release was monitored and a burst release was observed and was attributed to the high surface area-to-volume ratio of the electrospun material. This is a disadvantage. In the last few years a small number of groups have deposited electroactive polymers, such as PPy, onto previously electrospun fibers in order to enhance the electrochemical properties[57] of the material. Also, electrospun fibers have been used as a template in order to obtain a high surface area in the hope of achieving a greater uptake and release of drugs.[41]

Another method of improving the DDS of conducting polymers is the use of various dopants during polymerisation of the polymer films. The functionalisation of PPy films with large anionic dopants is not new to this field of research. It has been well reported that the use of large anionic dopants during the electrochemical polymerisation of monomers leads to these bulky negatively charged groups being immobilised within the polymer matrix.[96] In fact, these polymers, with their cationic exchange properties, have been used to incorporate various cationic groups for various applications. For example Fan and Bard in the late 1980s demonstrated the uptake of a positively charge $Ru(NH_3)_6^{3+}$ and methylviologen in PPy/Nafion films.[97]

However, the generation of PPy films in the presence of negatively charged cyclodextrins is a new concept.[98-100] There has been very little work reported on the electropolymerisation of pyrrole in the presence of anionic cyclodextrins. Indeed, much of the current published work is unreliable as very high potentials in the vicinity of 1.8 V vs. SCE were used to form the polymers.[100, 101] It is very well known that these high potentials give rise to the overoxidation of PPy and a

considerable loss in its conductivity.[59] The incorporation of cyclodextrins into conducting polymers provides a unique way of combining the unique host-guest complexation properties of cyclodextrins with the stability, high conductivity and ease of preparation of conducting polymers.

## 1.1.3 Cyclodextrins

### *1.1.3.1 History and structural properties of cyclodextrins*

Cyclodextrins (CD) are macrocyclic oligosaccharides composed of α-D-glucopyranoside units linked by α-(1,4) bonds. They were first discovered by Villiers in 1891[102], while in 1904, Schardinger[103] further developed the cyclic structures hence; CDs are sometimes referred to as Schardinger dextrins. However, it was only in the mid 1970s that the structure and chemical properties of natural cyclodextrins were fully characterised.[104] Cyclodextrins have developed quickly over the past two decades and have become an important branch of host-guest chemistry, specifically due to their ability to be involved in several practical applications.[105] The main interest in cyclodextrins lies in their ability to form inclusion complexes with a variety of compounds. Host-guest chemistry is the study of these inclusion phenomena, where the 'host' molecules are capable of including smaller 'guest' molecules through non-covalent interactions.

CDs are obtained through enzymatic degradation of starch in the presence of a glycosyl transferase, a type of amylase.[106] Many organisms contain glycosyl transferase, however, in general it is obtained from *Bacillus megaterium, Bacillus stereothermophilus and Bacillus macerans.*[106, 107] They are generally made up of glucopyranoside units of $^4C_1$ chair conformation which leads to a truncated cone shape encasing a cavity.[108] Figure 1.9 shows the structures of the most common CD members; α-, β- and γ-CD, which include 6, 7 and 8 repeating glucopyranoside units, respectively. These units orientate themselves in a cyclic manner offering a typical conical or truncated cone structure with a relatively hydrophobic interior and hydrophilic exterior.[109] This structural property gives cyclodextrins good water solubility and the ability to hold appropriately sized

guests, such as amines and ferrocenes[110], through non-covalent interactions such as hydrogen bonding, hydrophobic interactions, and electrostatic interactions.[111] Table 1.1 demonstrates the approximate geometries of the most common CDs.[109]

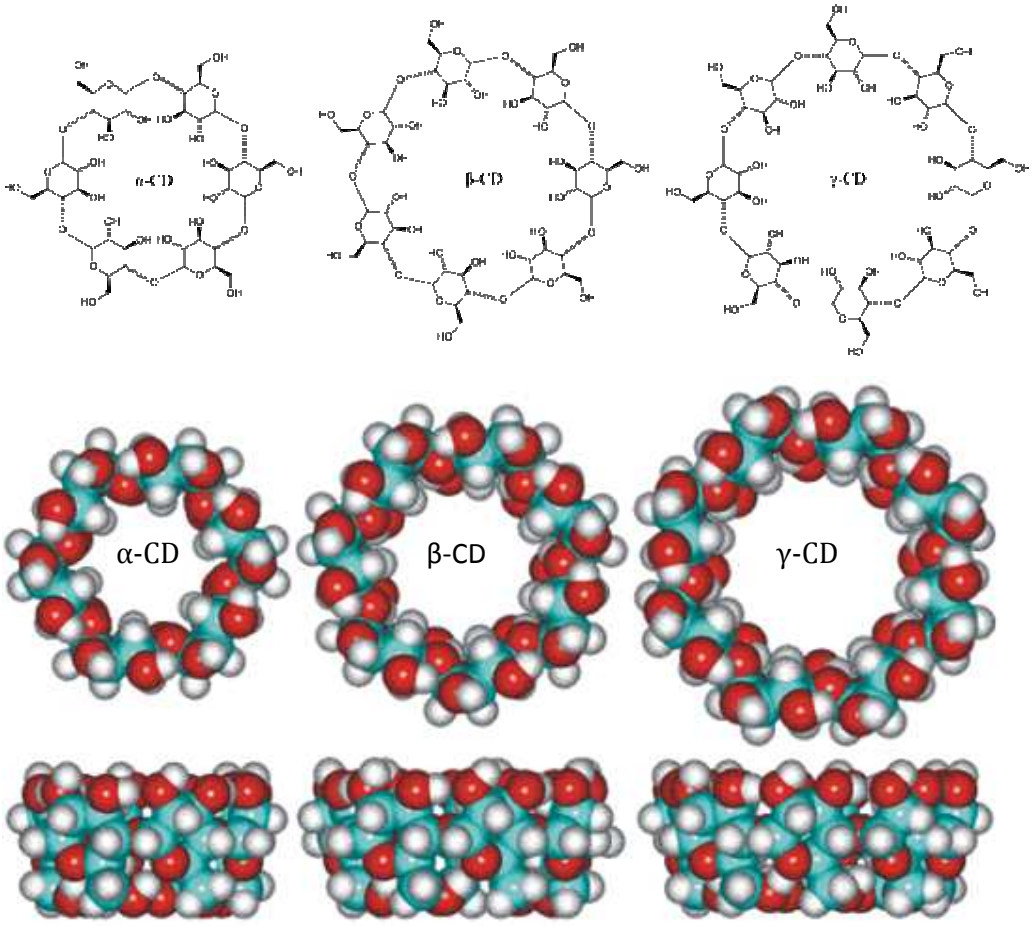


**Figure 1.9:** Structures of α-, β- and γ-cyclodextrin taken from Szjetli.[109]

Due to their exceptional host-guest complexation abilities, CDs have been used in a variety of fields, such as environmental protection through immobilising toxic compounds in their cavities and in the food industry.[104] In fact one of the commercially available applications for CDs is Febreze®, which is an aqueous solution of modified β-cyclodextrins**.** Febreze® is based on the host-guest chemistry of the CDs, with molecules that produce aroma forming inclusion complexes with the modified CDs. In the pharmaceutical industry, CDs are also

used for many applications including, drug delivery to enhance the solubility, stability and bioavailability of drug molecules.[108, 112]

**Table 1.1:** Approximate geometric dimensions of the three common CDs.[106]

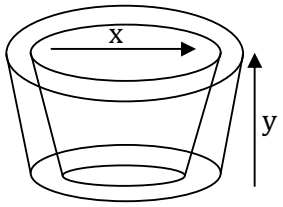


| Cyclodextrin | x / nm | y / nm | Cavity volume / Å$^3$ |
|---|---|---|---|
| **α** | 0.49 | 0.78 | 174 |
| **β** | 0.62 | 0.78 | 262 |
| **γ** | 0.79 | 0.78 | 427 |

Cyclodextrins can also be chemically modified to replace the hydroxyl groups on both the primary and secondary rims of the CDs, with a variety of appropriate alkyl groups (R). It has been reported that this can improve binding affinity.[108] In the research presented here, a negatively charged cyclodextrin with a number of sulfonated groups present on the outer rims was used, sulfonated β-CD (Sβ-CD). Sβ-CD is obtained by substitution of either primary or secondary hydrogen of the hydroxyl group of β-CD with a sulfonate group. Sβ-CD has an average of 7-11 substituents per CD and, therefore, has between 7-11 negative charges associated with it, which are counterbalanced with sodium ions, as illustrated in Figure 1.10.[113] It is reported that β-CD and Sβ-CD have the same ring structure, differing only in the substituent located on the rims of the CD ring.[14] Although Sβ-CD has the same ring structure as other derivativsed CDs the presence of the substituent on the ring contributes to its chiral discrimination properties.[114] A major area in which these sulfonated CDs are being utilised is chromatography, or more specifically capillary electrophoresis, for the enantiomeric separation of acidic and basic compounds. In enantiomeric separation, using neutral CDs, they are not appropriate for neutral racemates as the complex has no electrophoretic mobilities.[115] Therefore, the use of charged

CDs is now been widely researched for the separation of neutral compounds. It has been reported that the use of these sulfonated CDs for the enantiomeric separation of chiral compounds is highly effective as a result of the anionic charges.[116, 117]

A number of groups have also characterised the Sβ-CD.[115, 117] Figure 1.11 illustrates a single glucose unit of an Sβ-CD (comprised of 7 units). On the primary ring there are 7 potential substitution sites corresponding to the C-6 positions, while, on the secondary rim there are 14, represented by the C-2 and C-3 positions. Amini and co-workers[117] reported that substitution of these CDs is predominantly at the C-2 and C-6 positions, while, Chen *et al.*[115] confirmed nearly complete sulfation at the C-6 position of the primary hydroxyl groups and partial sulfation at the C-2 secondary hydroxyl groups. They also reported no substitution at the C-3 positions. From these reports it can be stated that almost the entire primary rim is sulfonated and some of the secondary rim. Due to this phenomenon and the fact that the sulfation brings with it negative charges these CDs are good candidates for the doping of CPs.

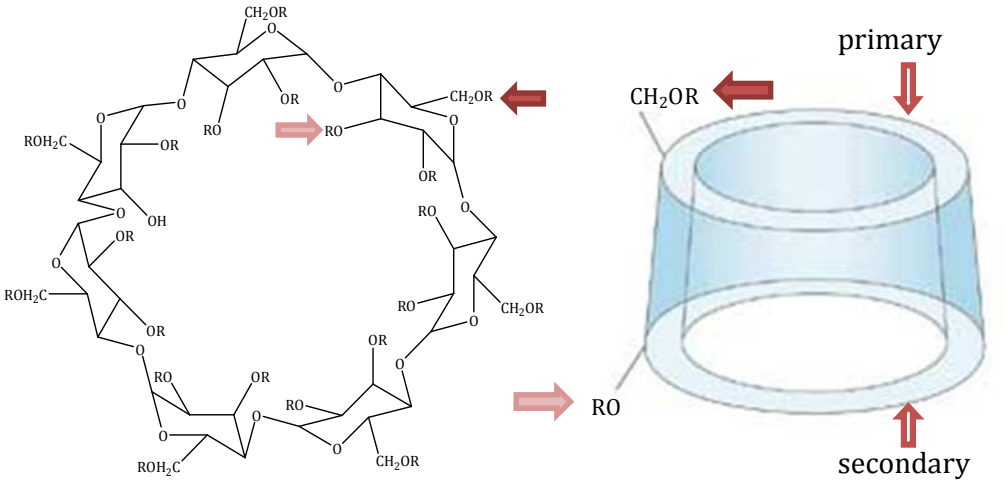


R = $SO_3^-Na^+$ or H ~ 7-11 $SO_3^-Na^+$ groups.

**Figure 1.10:** Structural and schematic representation of sulfonated β-cyclodextrin (Sβ-CD). The arrows point to the primary and secondary rims, respectively.[118]

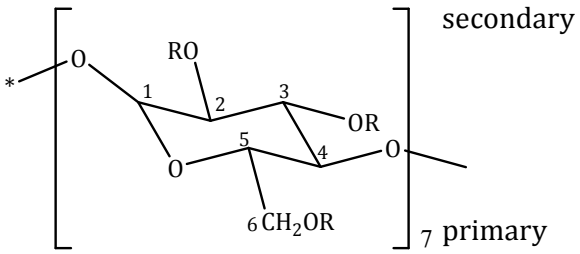


**Figure 1.11:** Chemical structure of Sβ-CD, depicting the numbering carbons.

### *1.1.3.2 Inclusion complexation*

Cyclodextrins (CD) form a group of cyclic oligosaccharides that contain cavities in which guest molecules can be encapsulated.[108, 109] It is well known that the size of the compounds are important and compounds are only capable of including into the cavity of the CD if they are within the dimensions of the CD cavity.[119] In aqueous media, the cavity is filled with water molecules, which becomes displaced by the guest through complexation, as illustrated in Figure 1.12. The guest molecule, xylene, displaces the water molecules and forms an inclusion complex with the CD.

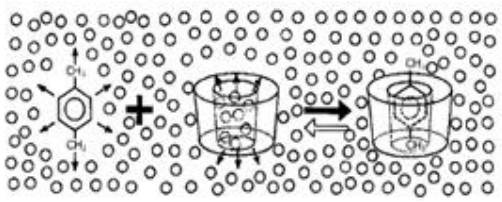

**Figure 1.12:** Schematic representation of xylene forming a complex with a β-cyclodextrin. The small circles represent water molecules taken from Szjetli.[109]

During the formation of an inclusion complex the chemical and the physical properties of the guest molecule change and can be monitored using a number of techniques. Various spectroscopic and electrochemical techniques can be used to confirm complexation, including fluorescence, UV-visible spectroscopy (UV), Nuclear magnetic resonance (NMR) and electrochemical studies. These changes attributed to the complexation can be used to evaluate the apparent

binding or formation constant ($K_f$). However, prior to the determination of the $K_f$ value the stoichiometry of the host-guest complex must be established.[120] This is obtained by the well known continuous variation or Job's method which is described in more detail in Chapter 2, Section 2.6.1.1.[121] Generally, inclusion complexes form a ratio of 1:1, 1:2 and sometimes 2:1 (CD:guest).[122]

NMR is also a useful tool for the study of complexation due to its quantitative information and assuming the guest enters the cavity, NMR, can be also used to locate the protons involved in complexation.[87] Many groups have studied the complexation properties with the neutral β-CD and monitored the changes in the chemical shifts for both the CD, and the guest. However, in the case of the modified CD used in this research, the NMR spectral data are too difficult to differentiate so the chemical shift of the guest is followed.[120, 123-126] Bratu and colleagues[125] studied the chemical shift changes observed when Fenbufen was in the presence of a neutral β-CD. They noticed an up-field shift of the guest protons, some more pronounced than others, and suggested that the complexation was initiated through the benzene moiety of the guest. Cruz *et al*.[127] also used NMR to quantitatively evaluate the binding constant of the complexation of doxepin and a neutral β-CD.

If a guest absorbs light in the UV or visible region then the inclusion phenomenon can be followed and subsequently, evaluated by UV.[106] This technique can be used to confirm complexation and indeed obtain the formation constant associated with the inclusion complex. In the majority of cases the guest that absorbs in the UV-vis region experiences changes in the intensity and the position of the absorption bands in the presence of the CD. These spectral changes can be used to determine the $K_f$ constants. Generally, a Hiedlebrand-Benesi modified equation is used to evaluate the $K_f$ constants.[119, 128, 129] Ramaraj and co-workers[130] monitored the changes attained during the complexation formation of a number of aromatic amines and nitro compounds in the presence of a neutral β-CD. They observed an increase in the intensity of the bands in all cases. Dang *et al*.[119] observed shifts of the absorption bands to longer

wavelengths in the case of 1,4 benzoquinone (BQ) and 9,10 anthraquinone (AQ) in the presence of a neutral β-CD.

Electrochemical techniques can also be performed on the complexation properties of CDs. If the guest is electroactive the peak current and potential can be followed for the free state and compared to the complexed state of the guest in question. Two features are generally observed during these electrochemical observations if an inclusion complex is found. Firstly, a decrease in the peak current can be seen, and, attributed to a decrease in the diffusion of the bulky CD complex as opposed to the more mobile free guest. Secondly, a shift in the peak potential is observed if the complexed species is included in the cavity, as it is harder to oxidise or reduce while located in the cavity. Once again based on these variations a number of equations can be used to verify the formation constant.[129, 131, 132] Coutouli-Argyropoulou and his group[133] reported the effect of complexation on the electrochemical properties of ferrocence derivatives and showed shifts, in both the peak current and peak potential, when higher concentrations of a neutral β-CD were added. Yanez *et al*.[131] showed similar observations for nifedipine (NF) and nicardipine (NC) and estimated apparent formation constants of 135 and 357, respectively.

Complexation studies of DA have been previously demonstrated in the presence of a neutral β-CD by Zhou *et al*.[134] using UV and fluorescence spectroscopy. From the fluorescence technique, utilising a Hiedlebrand-Benesi modified equation, a $K_f$ value of 95.06 was estimated. The degree of the complexation can vary over a wide range due to the stability of the complex, as it depends on a number of factors. In the next section a discussion on the main driving forces, involved in this complexation process are dealt with.

#### *1.1.3.3 Driving forces in the inclusion complexation process*

There are many reviews and books written on the driving forces behind the inclusion complexation abilities of cyclodextrins, not all agree, some refer to the predominantly hydrophobic affects while others state that it is a collection of a

number of weaker interactions (H-bonding, van der Waals, electrostatic interactions).[106, 108, 111, 135, 136] Either way the majority agree that the size of the cavity and shape of the guest are important factors in the complexation process. The most widely studied possible driving forces include

- Hydrogen bonding
- Electrostatic interaction
- Van der Waals
- Hydrophobic effect

Hydrogen bonding is an interaction between an electronegative donor, a hydrogen and an electronegative acceptor.[136] Various groups have demonstrated the importance of hydrogen bonding in the solid state, illustrating crystal structures defining the hydrogen bonding between the guest and the hydroxyls of the CDs.[137] However, during the complexation of the CD and guest, in aqueous solution, the subject is still arguable as few direct measurements of hydrogen bonding have been made, as water molecules can compete with CDs to form hydrogen bonding with guest molecules. However, many groups will still argue over the significance of hydrogen bonding.

Electrostatic interaction occurs when molecules of opposite charges interact. There are three types of electrostatic interactions, ion-ion interaction, ion-dipole interaction and dipole-dipole interaction.[136] Matsui and Okimoto[138] reported that ion-ion interaction is only eligible in the case of modified CDs, where as ion-dipole is considered more favourably due to the fact that CDs are polar molecules however as with hydrogen bonding, in aqueous media, the interaction between the guest and water will also be strong.[136] Therefore, it is the case of dipole-dipole interaction that is mostly considered during complexation.

Van der Waals forces or London dispersion forces are made up of dipole induced dipole contributions or the coordination of the electronic motion in the CD and guest. As CDs are known to have large dipole moments it is logical that

these induction forces are important in complexation. Experimental evidence has shown that the stability of the complex increases with an increase in polarisability. Also, as the polarisability of water is lower than the organic components of the CD cavity, van der Waals forces have an encouraging donation to the stability of the complex due to a stronger interaction of the CD and guest over the water and guest.[136] CDs have also been reported to form stable inclusion complexes in organic solvents like DMF and DMSO confirming the importance of van der Waals forces.[139]

The hydrophobic interaction which is entropically favourable, due to the expulsion of water, leads to the aggregation of non-polar solutes in aqueous solution.[136] As reviewed by Connors[135] the 'classical' hydrophobic interaction is said to be 'entropy driven' and a positive entropy and enthalpy is associated for the interaction between two non polar molecules. However, experimental studies in the complexation of CD and guests, show negative enthalpy and entropy changes,[111] which have been suggested to indicate that these interactions are not a dominant force.

Mosinger *et al*.[122] reported that the formation of an inclusion complex is based on the electrostatic, van der Waals and π-π interactions, where, steric affects and Hydrogen bonding are inevitable. Chao and co-workers[124] investigated the formation of an inclusion complex with β-CD and caffeic acid, they reported that the weak forces of hydrogen bonding, van der Waals, hydrophobic and electrostatic interactions simultaneously governed the process.

Rekharsky and Inoue[111] reviewed the complexation of cyclodextrins and stated that the interactions involved in the inclusion complexation of aromatic guests with CDs could not be simply put down to a hydrophobic effect. They established that complexation could be accounted for, through dipole-dipole interactions. In saying that, Tabushi and his group[140] questioned the role of hydrogen bonding in the complexation process and reported that no dramatic changes of binding were observed, when a modified CD, incapable of hydrogen bonding, was compared to an unmodified CD. They concluded that the

involvement of hydrogen bonding was negligible and hydrophobic interactions dominated the process. Zia *et al*.[113] investigated the complexation ability of a negatively charged CD (~7 negative sites) with a number of neutral and charged guest molecules. They accounted for the increase in the binding affinity, for the oppositely charged guest and CD, to be predominantly hydrophobic, due to the additional interaction sites provided by the negatively charged CD. Okimoto and colleagues[141] also clearly observed stronger interactions occurring between a CD and guest with opposite charges.

The understanding of these complexation processes is complicated, however, it is generally found that van der Waals forces and hydrophobic interactions are regarded as the main driving forces for CD complexation, while, electrostatic interactions and hydrogen bonding can be significantly considered in some inclusion complexation studies. Nevertheless, these attractive features of CDs allow them to be used in a wide range of applications including, the food industry[142]. However, the pharmaceutical industry is the most widely researched area in recent times, specifically in drug formulation and DDS.[143]

#### *1.1.3.4 Applications of CDs in DDS*

Due to their biocompatibility and their ability to form inclusion complexes, CDs have been studied for the use in DDS. They have been considered as drug carriers, as CDs have the potential to act as hydrophobic carriers and control the release of a variety of drugs.[118] Many reviews have recently been published, describing the role of CDs in DDS.[112, 118, 144-147] Irie and Uekama[144] reviewed the role of CDs in peptide and protein delivery and summarised that CDs were able to eliminate a number of undesirable properties of drug formulations, as they form inclusion complexes with the desired drugs, which increase the drug delivery through a number of routes of administration. More recently, Li *et al.*[145] examined the recent progress in the preparation of inclusion complexes between CDs and various polymers as supramolecular biomaterials for drug and gene delivery. They demonstrated the promising field in the self assembly

of inclusion complexes between CDs and biodegradable polymers as injectable DDS.

Ferancova and Labuda[148] also reviewed the use of CDs as electrode modifiers. They summarised the many ways CDs can be immobilised onto electrode surfaces. As discussed in an earlier section, Section 1.1.4.2., the incorporation of CDs, as dopants, during the electrochemical polymerisation of CPs was demonstrated to examine the use of these modified electrodes to deliver neutral drugs.[98] Formulating these materials, correlates the attractive features of both the CDs and the CPs. Bidan *et al*.[98] examined the need for a new DDS that was not limited to charged drugs. They produced polymer films in the presence of an anionic CD and successfully delivered neutral compounds using these novel materials.

Also briefly discussed in Section 1.1.4.2, was the reports made by a number of groups on the polymerisation of CPs in the presence of CDs.[100, 101, 149] These groups have reportedly polymerised pyrrole at potentials usually shown to overoxidise the CP film.[59] Due to this, these papers are unreliable in their reports.

### 1.1.4 Drug release: Controlled release of dopamine

DA is a neurotransmitter produced naturally in the brain. It is well documented that a common factor in neurodegenerative diseases such as Parkinson's (PD) and Schizophrenia is a significant lack of the presence of DA in the *substantia nigra* (mid brain).[150-152] In particular, PD is a slowly progressive disorder known to occur due to the damage of the basal ganglia.[150-152] The disease affects movement, muscle control and balance. Studies on the brains of deceased Parkinson sufferers show a substantial loss of dopamine, particularly, in the *substantia nigra*. The function of the substantia nigra is to produce DA and manage the release of essential neurotransmitters that help control movement and coordination. Sufferers usually show symptoms such as tremors, slowness of movement and impaired balance and coordination. Prolonged loss of DA

gives rise to symptoms such as difficulty in walking, talking, or completing other simple tasks.[150-152]

DA belongs to the well known catecholamine family. These molecules are electroactive and therefore their oxidation can be followed using electrochemistry, in particular, electrochemical methods such as cyclic voltammetry and rotational disc voltammetry. The electrochemical mechanism of oxidation is still not fully agreed; with various groups arguing that the mechanism goes through an ECE step rather than a CE step. For example, Hawley *et al*.[153] have reported that the electrochemical oxidation of dopamine in aqueous solution proceeds through two types of steps, electrochemical (E) and chemical (C). The ECE mechanism is presented in Scheme 1.1.

The first step in the oxidation of dopamine (A) involves the loss of both protons and electrons to form the o-dopaminoquinone (B). The oxidised, o-dopaminoquinone undergoes a 1,4-Michael addition, which results in a intramolecular cyclisation reaction which produces leucodopaminochrome (C). This product is easily oxidised through an electrochemical step to form dopaminochrome (D).[153, 154]

Controlled release studies of DA have been previously investigated.[67, 155-158] McRae-Degueurce *et al*.[156] encapsulated DA into a thermoplastic polyester excipient: PLGA. They found that it was possible to deliver significant amounts of DA for prolonged periods of time by injecting the microencapsulated DA directly into the brain. Uludag and colleagues[157] also examined the release of many therapeutic agents, including DA, from microencapsulated mammalian cells. The mammalian cells and tissues were entrapped in polymeric microcapsules containing the desired bioactive agent.

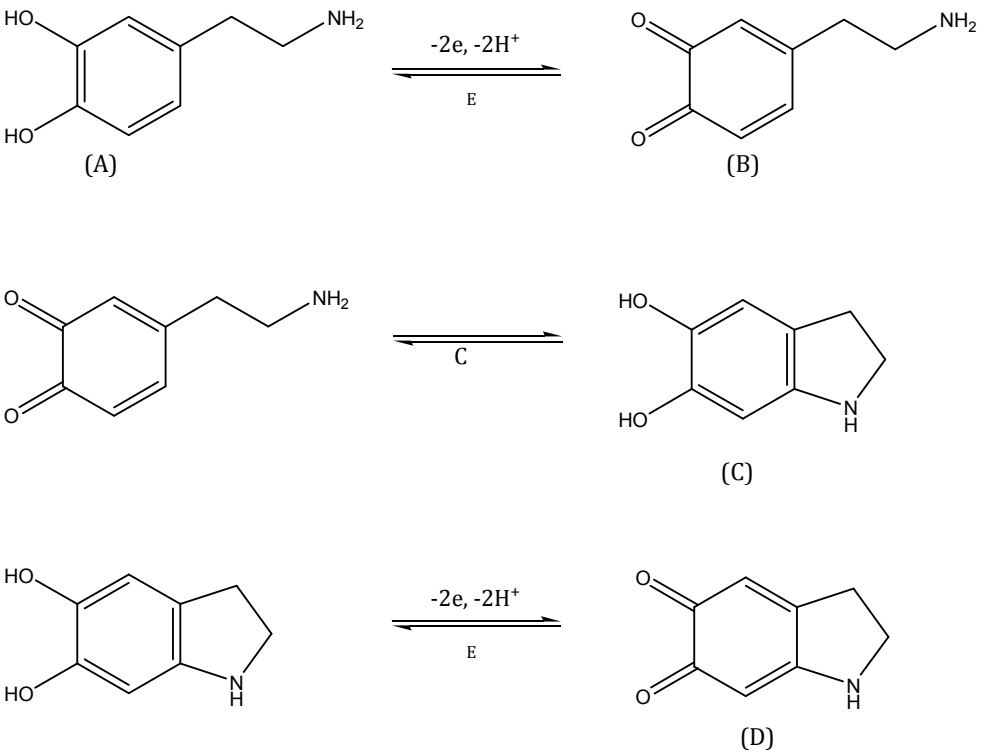


**Scheme 1.1:** The proposed oxidative pathway for dopamine.

In both these cases the release was based on diffusion from the polymeric materials. It is, therefore, difficult to maintain any control over the amount of DA released. Miller[67] and Zhou[158] and co-workers investigated the use of CPs to deliver DA. They introduced the concept of using large immobile dopants, which remain entrapped inside the cavity during polymerisation, to bind and successfully liberate DA from the polymer films.

This is the basis of the work performed in this thesis. As outlined at the start of this chapter, the idea of this research is to develop PPy films for the uptake and release of DA, using a large immobile anionic cyclodextrin. The cyclodextrin, in addition to its large size and immobility, has unique host-guest complexation properties and this offers the prospects of inclusion complexation between the DA and the CD to enhance the drug delivery. If this can be achieved it could potentially serve as a model system in DDS and could be extended to various other cationic drug molecules.

## 1.2 References


1. N. A. Peppas and D. J. A. Ende, *J Appl Polym Sci*, **66**, (1997), 509-513.
2. U. R. Pothakamury and G. V. BarbosaCanovas, *Trends Food Sci Tech*, **6**, (1995), 397-406.
3. B. Singh, D. K. Sharma, and A. Gupta, *J Environ Sci Heal B*, **44**, (2009), 113-122.
4. N. A. Peppas and R. Langer, *Science*, **263**, (1994), 1715-1720.
5. K. E. Uhrich, S. M. Cannizzaro, R. S. Langer, and K. M. Shakesheff, *Chem Rev*, **99**, (1999), 3181-3198.
6. D. L. Wise, Encyclopedic handbook of biomaterials and bioengineering Marcel Dekker, 1995.
7. J. T. Santini, A. C. Richards, R. Scheidt, M. J. Cima, and R. Langer, *Angew Chem Int Edit*, **39**, (2000), 2397-2407.
8. R. Langer, *Mrs Bull*, **31**, (2006), 477-485.
9. L. K. Fung and W. M. Saltzman, *Adv Drug Deliver Rev*, **26**, (1997), 209-230.
10. R. Langer, *Science*, **249**, (1990), 1527-1533.
11. R. Langer, *Nature*, **392**, (1998), 5-10.
12. J. Folkman and D. Long, *JOURNAL OF SURGICAL RESEARCH*, **4**, (1963), 139-142.
13. T. M. Allen and P. R. Cullis, *Science*, **303**, (2004), 1818-1822.
14. J. J. Wang, G. J. Zheng, L. Yang, and W. R. Sun, *Analyst*, **126**, (2001), 438-440.
15. H. Wartlick, K. Michaelis, S. Balthasar, K. Strebhardt, J. Kreuter, and K. Langer, *J Drug Target*, **12**, (2004), 461-471.
16. L. M. Lira and S. I. C. de Torresi, *Electrochem Commun*, **7**, (2005), 717-723.
17. S. Murdan, *J Control Release*, **92**, (2003), 1-17.
18. J. E. Riviere and M. C. Heit, *Pharmaceut Res*, **14**, (1997), 687-697.
19. G. Inzelt, Conducting Polymers, A new era in electrochemistry, Springer, 2008.
20. V. V. Walatka, M. M. Labes, and Perlstei.Jh, *Phys Rev Lett*, **31**, (1973), 1139-1142.
21. H. Shirakawa, E. J. Louis, A. G. Macdiarmid, C. K. Chiang, and A. J. Heeger, *J Chem Soc Chem Comm*, (1977), 578-580.
22. A. J. Heeger, *Angew Chem Int Edit*, **40**, (2001), 2591-2611.
23. A. G. MacDiarmid, *Angew Chem Int Edit*, **40**, (2001), 2581-2590.
24. H. Shirakawa, *Angew Chem Int Edit*, **40**, (2001), 2575-2580.
25. P. Chandrasekhar, Conducting Polymers, Fundamentals and Applications: A practical approach, Kluwer Acandemic Publishers, 1999.
26. A. A. Entezami and B. Massoumi, *Iran Polym J*, **15**, (2006), 13-30.
27. N. K. Guimard, N. Gomez, and C. E. Schmidt, *Prog Polym Sci*, **32**, (2007), 876-921.
28. A. Malinauskas, J. Malinauskiene, and A. Ramanavicius, *Nanotechnology*, **16**, (2005), R51-R62.
29. C. E. Schmidt, V. R. Shastri, J. P. Vacanti, and R. Langer, *P Natl Acad Sci USA*, **94**, (1997), 8948-8953.
30. J. L. Bredas and G. B. Street, *Accounts Chem Res*, **18**, (1985), 309-315.

31. D. L. Wise, Electrical and optical polymer systems, CRC Press, 1998.
32. L. Alcacer, Conducting Polymers: Special Applications (Hardcover), Springer 1986.
33. B. Winther-Jensen, J. Chen, K. West, and G. Wallace, *Polymer*, **46**, (2005), 4664-4669.
34. A. Malinauskas, *Polymer*, **42**, (2001), 3957-3972.
35. R. A. Green, N. H. Lovell, G. G. Wallace, and L. A. Poole-Warren, *Biomaterials*, **29**, (2008), 3393-3399.
36. T. A. Skotheim and J. R. Reynolds, Handbook of conducting polymers: Conjugated polymers, CRC Press, 2007.
37. P. C. Lacaze, J. C. Lacroix, K. C. Ching, and S. Aeiyach, *Actual Chimique*, (2008), 90-91.
38. M. A. Mohamoud, *Plast Eng*, **64**, (2008), 32-+.
39. M. Nikolou and G. G. Malliaras, *Chem Rec*, **8**, (2008), 13-22.
40. E. Smela, *Mrs Bull*, **33**, (2008), 197-204.
41. M. R. Abidian, D. H. Kim, and D. C. Martin, *Adv Mater*, **18**, (2006), 405-409.
42. C. Arbizzani, M. Mastragostino, L. Nevi, and L. Rambelli, *Electrochim Acta*, **52**, (2007), 3274-3279.
43. K. Kontturi, P. Pentti, and G. Sundholm, *J Electroanal Chem*, **453**, (1998), 231-238.
44. Y. L. Li, K. G. Neoh, and E. T. Kang, *J Biomed Mater Res A*, **73A**, (2005), 171-181.
45. J. M. Pernaut and J. R. Reynolds, *J Phys Chem B*, **104**, (2000), 4080-4090.
46. P. Burgmayer and R. W. Murray, *J Am Chem Soc*, **104**, (1982), 6139-6140.
47. A. Dall'Olio, G. Dascola, V. Varacca, and V. Bocchi, *Comptes Rendus de l'Academie des Sciences*, **C267**, (1968), 433-435.
48. A. F. Diaz and J. I. Castillo, *J Chem Soc Chem Comm*, (1980), 397-398.
49. B. Winther-Jensen and N. B. Clark, *React Funct Polym*, **68**, (2008), 742-750.
50. C. K. Baker and J. R. Reynolds, *J Electroanal Chem*, **251**, (1988), 307-322.
51. S. Geetha, C. R. K. Rao, M. Vijayan, and D. C. Trivedi, *Anal Chim Acta*, **568**, (2006), 119-125.
52. Z. X. Wang, C. Roberge, L. H. Dao, Y. Wan, G. X. Shi, M. Rouabhia, R. Guidoin, and Z. Zhang, *J Biomed Mater Res A*, **70A**, (2004), 28-38.
53. Z. Zhang, R. Roy, F. J. Dugre, D. Tessier, and L. H. Dao, *J Biomed Mater Res*, **57**, (2001), 63-71.
54. A. Kotwal and C. E. Schmidt, *Biomaterials*, **22**, (2001), 1055-1064.
55. J. Y. Wong, R. Langer, and D. E. Ingber, *P Natl Acad Sci USA*, **91**, (1994), 3201-3204.
56. B. Garner, A. Georgevich, A. J. Hodgson, L. Liu, and G. G. Wallace, *J Biomed Mater Res*, **44**, (1999), 121-129.
57. X. D. Wang, X. S. Gu, C. W. Yuan, S. J. Chen, P. Y. Zhang, T. Y. Zhang, J. Yao, F. Chen, and G. Chen, *J Biomed Mater Res A*, **68A**, (2004), 411-422.
58. S. Asavapiriyanont, G. K. Chandler, G. A. Gunawardena, and D. Pletcher, *J Electroanal Chem*, **177**, (1984), 229-244.
59. J. Heinze, *Synthetic Met*, **43**, (1991), 2805-2823.
60. G. Inzelt, V. Kertesz, and A. S. Nyback, *J Solid State Electr*, **3**, (1999), 251-257.

61. C. Y. Jin, F. L. Yang, and W. S. Yang, *J Appl Polym Sci*, **101**, (2006), 2518-2522.
62. V. M. Jovanovic, A. Dekanski, G. Vlajnic, and M. S. Jovanvic, *Electroanal*, **9**, (1997), 564-569.
63. S. Sadki, P. Schottland, N. Brodie, and G. Sabouraud, *Chem Soc Rev*, **29**, (2000), 283-293.
64. J. Tamm, A. Alumaa, A. Hallik, U. Johanson, L. Tamm, and T. Tamm, *Russ J Electrochem+*, **38**, (2002), 182-187.
65. M. Pyo and J. R. Reynolds, *Chem Mater*, **8**, (1996), 128-133.
66. M. Hepel and F. Mahdavi, *Microchem J*, **56**, (1997), 54-64.
67. L. L. Miller and Q. X. Zhou, *Macromolecules*, **20**, (1987), 1594-1597.
68. G. A. Husseini and W. G. Pitt, *J Pharm Sci-Us*, **98**, (2009), 795-811.
69. X. L. Xu, X. S. Chen, P. A. Ma, X. R. Wang, and X. B. Jing, *Eur J Pharm Biopharm*, **70**, (2008), 165-170.
70. S. G. Kumbar, L. S. Nair, S. Bhattacharyya, and C. T. Laurencin, *J Nanosci Nanotechno*, **6**, (2006), 2591-2607.
71. L. Feng, S. H. Li, H. J. Li, J. Zhai, Y. L. Song, L. Jiang, and D. B. Zhu, *Angew Chem Int Edit*, **41**, (2002), 1221-+.
72. G. M. Whitesides and B. Grzybowski, *Science*, **295**, (2002), 2418-2421.
73. T. Ondarcuhu and C. Joachim, *Europhys Lett*, **42**, (1998), 215-220.
74. J. Fang, H. T. Niu, T. Lin, and X. G. Wang, *Chinese Sci Bull*, **53**, (2008), 2265-2286.
75. E. R. Kenawy, F. I. Abdel-Hay, M. H. El-Newehy, and G. E. Wnek, *Mat Sci Eng a-Struct*, **459**, (2007), 390-396.
76. Q. J. Xie, S. Kuwabata, and H. Yoneyama, *J Electroanal Chem*, **420**, (1997), 219-225.
77. E. Luong-Van, L. Grondahl, K. N. Chua, K. W. Leong, V. Nurcombe, and S. M. Cool, *Biomaterials*, **27**, (2006), 2042-2050.
78. Z. M. Huang, Y. Z. Zhang, M. Kotaki, and S. Ramakrishna, *Compos Sci Technol*, **63**, (2003), 2223-2253.
79. A. Formhals, Vol. 1975504, 1934.
80. J. Doshi and D. H. Reneker, *J Electrostat*, **35**, (1995), 151-160.
81. D. H. Reneker and I. Chun, *Nanotechnology*, **7**, (1996), 216-223.
82. A. Greiner and J. H. Wendorff, *Angew Chem Int Edit*, **46**, (2007), 5670-5703.
83. D. Li and Y. N. Xia, *Adv Mater*, **16**, (2004), 1151-1170.
84. D. H. Reneker, A. L. Yarin, H. Fong, and S. Koombhongse, *J Appl Phys*, **87**, (2000), 4531-4547.
85. T. Subbiah, G. S. Bhat, R. W. Tock, S. Pararneswaran, and S. S. Ramkumar, *J Appl Polym Sci*, **96**, (2005), 557-569.
86. G. I. Taylor, *Proc. Roy. Soc. Lond.*, **A313**, (1969), 453-475.
87. A. Bernini, O. Spiga, A. Ciutti, M. Scarselli, G. Bottoni, P. Mascagni, and N. Niccolai, *Eur J Pharm Sci*, **22**, (2004), 445-450.
88. H. J. Shin, C. H. Lee, I. H. Cho, Y. J. Kim, Y. J. Lee, I. A. Kim, K. D. Park, N. Yui, and J. W. Shin, *J Biomat Sci-Polym E*, **17**, (2006), 103-119.
89. K. Kim, Y. K. Luu, C. Chang, D. F. Fang, B. S. Hsiao, B. Chu, and M. Hadjiargyrou, *J Control Release*, **98**, (2004), 47-56.
90. R. A. Jain, *Biomaterials*, **21**, (2000), 2475-2490.

91. M. Garinot, V. Fievez, V. Pourcelle, F. Stoffelbach, A. des Rieux, L. Plapied, I. Theate, H. Freichels, C. Jerome, J. Marchand-Brynaert, Y. J. Schneider, and V. Preat, *J Control Release*, **120**, (2007), 195-204.
92. D. Luo, K. Woodrow-Mumford, N. Belcheva, and W. M. Saltzman, *Pharmaceut Res*, **16**, (1999), 1300-1308.
93. X. H. Zong, S. Li, E. Chen, B. Garlick, K. S. Kim, D. F. Fang, J. Chiu, T. Zimmerman, C. Brathwaite, B. S. Hsiao, and B. Chu, *Ann Surg*, **240**, (2004), 910-915.
94. Z. M. Huang, C. L. He, A. Z. Yang, Y. Z. Zhang, X. J. Hang, J. L. Yin, and Q. S. Wu, *J Biomed Mater Res A*, **77A**, (2006), 169-179.
95. E. R. Kenawy, G. L. Bowlin, K. Mansfield, J. Layman, D. G. Simpson, E. H. Sanders, and G. E. Wnek, *J Control Release*, **81**, (2002), 57-64.
96. G. Bidan, B. Ehui, and M. Lapkowski, *J Phys D Appl Phys*, **21**, (1988), 1043-1054.
97. F. R. F. Fan and A. J. Bard, *J Electrochem Soc*, **133**, (1986), 301-304.
98. G. Bidan, C. Lopez, F. Mendesviegas, E. Vieil, and A. Gadelle, *Biosens Bioelectron*, **10**, (1995), 219-229.
99. D. A. Reece, S. F. Ralph, and G. G. Wallace, *J Membrane Sci*, **249**, (2005), 9-20.
100. K. R. Temsamani, O. Ceylan, B. J. Yates, S. Oztemiz, T. P. Gbatu, A. M. Stalcup, H. B. Mark, and W. Kutner, *J Solid State Electr*, **6**, (2002), 494-497.
101. N. Izaoumen, D. Bouchta, H. Zejli, M. El Kaoutit, A. M. Stalcup, and K. R. Temsamani, *Talanta*, **66**, (2005), 111-117.
102. A. Villiers, *C. R Acad. Sci*, **112**, (1891), 536.
103. F. Schardinger, *Wien. Klin. Wochenschr*, **17**, (1904), 207.
104. A. R. Hedges, *Chem Rev*, **98**, (1998), 2035-2044.
105. J. Szejtli, *J Mater Chem*, **7**, (1997), 575-587.
106. W. Saenger, *Angewandte Chemie-International Edition in English*, **19**, (1980), 344-362.
107. D. French, *Method Enzymol*, **3**, (1957), 17-20.
108. H. Dodziuk, Cyclodextrins and Their Complexes, 2006.
109. J. Szejtli, *Chem Rev*, **98**, (1998), 1743-1753.
110. A. Harada and S. Takahashi, *J Chem Soc Chem Comm*, (1984), 645-646.
111. M. V. Rekharsky and Y. Inoue, *Chem Rev*, **98**, (1998), 1875-1917.
112. K. Uekama, F. Hirayama, and T. Irie, *Chem Rev*, **98**, (1998), 2045-2076.
113. V. Zia, R. A. Rajewski, and V. J. Stella, *Pharmaceut Res*, **18**, (2001), 667-673.
114. L. X. Wang, X. G. Li, and Y. L. Yang, *React Funct Polym*, **47**, (2001), 125-139.
115. F. T. A. Chen, G. Shen, and R. A. Evangelista, *J Chromatogr A*, **924**, (2001), 523-532.
116. G. K. E. Scriba, *J Sep Sci*, **31**, (2008), 1991-2011.
117. A. Amini, T. Rundlof, M. B. G. Rydberg, and T. Arvidsson, *J Sep Sci*, **27**, (2004), 1102-1108.
118. F. Hirayama and K. Uekama, *Adv Drug Deliver Rev*, **36**, (1999), 125-141.
119. X. J. Dang, M. Y. Nie, J. Tong, and H. L. Li, *J Electroanal Chem*, **448**, (1998), 61-67.
120. L. Fielding, *Tetrahedron*, **56**, (2000), 6151-6170.

121. P. Job, **9**, (1928), 113-203.
122. J. Mosinger, V. Tomankova, I. Nemcova, and J. Zyka, *Anal Lett*, **34**, (2001), 1979-2004.
123. W. Misiuk and M. Zalewska, *Anal Lett*, **41**, (2008), 543-560.
124. J. B. Chao, H. B. Tong, Y. F. Li, L. W. Zhang, and B. T. Zhang, *Supramol Chem*, **20**, (2008), 461-466.
125. I. Bratu, J. M. Gavira-Vallejo, A. Hernanz, M. Bogdan, and G. Bora, *Biopolymers*, **73**, (2004), 451-456.
126. I. V. Terekhova, R. S. Kumeev, and G. A. Alper, *J Incl Phenom Macro*, **59**, (2007), 301-306.
127. J. R. Cruz, B. A. Becker, K. F. Morris, and C. K. Larive, *Magn Reson Chem*, **46**, (2008), 838-845.
128. H. A. Benesi and J. H. Hildebrand, *J Am Chem Soc*, **71**, (1949), 2703-2707.
129. M. S. Ibrahim, I. S. Shehatta, and A. A. Al-Nayeli, *J Pharmaceut Biomed*, **28**, (2002), 217-225.
130. R. Ramaraj, V. M. Kumar, C. R. Raj, and V. Ganesane, *J Incl Phenom Macro*, **40**, (2001), 99-104.
131. C. Yanez, L. J. Nunez-Vergara, and J. A. Squella, *Electroanal*, **15**, (2003), 1771-1777.
132. G. C. Zhao, J. J. Zhu, J. J. Zhang, and H. Y. Chen, *Anal Chim Acta*, **394**, (1999), 337-344.
133. E. Coutouli-Argyropoulou, A. Kelaidopoulou, C. Sideris, and G. Kokkinidis, *J Electroanal Chem*, **477**, (1999), 130-139.
134. Y. Y. Zhou, C. Liu, H. P. Yu, H. W. Xu, Q. Lu, and L. Wang, *Spectrosc Lett*, **39**, (2006), 409-420.
135. K. A. Connors, *Chem Rev*, **97**, (1997), 1325-1357.
136. L. Liu and Q. X. Guo, *J Incl Phenom Macro*, **42**, (2002), 1-14.
137. W. Saenger and T. Steiner, *Acta Crystallogr A*, **54**, (1998), 798-805.
138. Y. Matsui and A. Okimoto, *B Chem Soc Jpn*, **51**, (1978), 3030-3034.
139. L. X. Song, B. L. Li, R. Jiang, J. G. Ding, and Q. J. Meng, *Chinese Chem Lett*, **8**, (1997), 613-614.
140. I. Tabushi, Y. I. Kiyosuke, T. Sugimoto, and K. Yamamura, *J Am Chem Soc*, **100**, (1978), 916-919.
141. K. Okimoto, R. A. Rajewski, K. Uekama, J. A. Jona, and V. J. Stella, *Pharmaceut Res*, **13**, (1996), 256-264.
142. L. Szente and J. Szejtli, *Trends Food Sci Tech*, **15**, (2004), 137-142.
143. J. Szejtli, *Pure Appl Chem*, **76**, (2004), 1825-1845.
144. T. Irie and K. Uekama, *Adv Drug Deliver Rev*, **36**, (1999), 101-123.
145. J. Li and X. J. Loh, *Adv Drug Deliver Rev*, **60**, (2008), 1000-1017.
146. K. Uekama, *J Incl Phenom Macro*, **44**, (2002), 3-7.
147. K. Uekama, F. Hirayama, and H. Arima, *J Incl Phenom Macro*, **56**, (2006), 3-8.
148. A. Ferancova and J. Labuda, *Fresen J Anal Chem*, **370**, (2001), 1-10.
149. K. R. Temsamani, H. B. Mark, W. Kutner, and A. M. Stalcup, *J Solid State Electr*, **6**, (2002), 391-395.
150. J. A. Kiernan and M. L. Barr, Barr's the Human Nervous System: An Anatomical Viewpoint, Lippincott Williams & Wilkins, 2008.
151. J. Nolte and J. W. Sundsten, The Human Brain: An Introduction to Its Functional Anatomy, Mosby, 1998.

152. R. H. Thompson, The Brain: A Neuroscience Primer, W H Freeman & Co, 1993.
153. M. D. Hawley, S. Tatawawa, S. Piekarsk, and R. N. Adams, *J Am Chem Soc*, **89**, (1967), 447-&.
154. T. Luczak, *Electroanal*, **20**, (2008), 1639-1646.
155. R. Langer, *J Control Release*, **16**, (1991), 53-59.
156. A. Mcraedegueurce, S. Hjorth, D. L. Dillon, D. W. Mason, and T. R. Tice, *Neurosci Lett*, **92**, (1988), 303-309.
157. H. Uludag, J. E. Babensee, T. Roberts, L. Kharlip, V. Horvath, and M. V. Sefton, *J Control Release*, **24**, (1993), 3-11.
158. Q. X. Zhou, L. L. Miller, and J. R. Valentine, *J Electroanal Chem*, **261**, (1989), 147-164.

## 2.1 Introduction

The experimental techniques and procedures employed in this study are outlined in this chapter. Firstly, a description of the electrochemical instrumentation and the electrochemical set-up are provided. Then, the techniques used in the preparation of the polymer samples are introduced, however specific details on concentrations or experimental parameters are not provided, as these are given in a separate experimental section in Chapters 3, 4, 5 and 6. General information on the characterisation of the samples is presented in Section 2.5. Again, specific details are not given, rather an overview of how the technique was used to characterise the sample is provided. Finally, a summary of the theories and related equations employed in this work is provided in Section 2.6.

## 2.2 Electrochemical set up

### *2.2.1 Electrochemical apparatus*

Electrochemical experiments such as potentiostatic, galvanostatic, cyclic voltammetry (CV), open-circuit potential and electrochemical quartz crystal microbalance (EQCM) measurements were carried out using one of three potentiostats; a Solartron (Model SI 1285), an eDAQ Potentiostat or a CHi440 instrument (Model EA160). Each system was controlled by a computer and the various software packages used were CorrWare for Windows™, Version 2.1, eDAQ Echem Version 2.0.2 and CHi440 software Version 1.0.0.1, respectively. A schematic of the electrochemical equipment is shown in Figure 2.1. In all cases, experiments were carried out using a conventional three-electrode system, as described in Section 2.2.2.

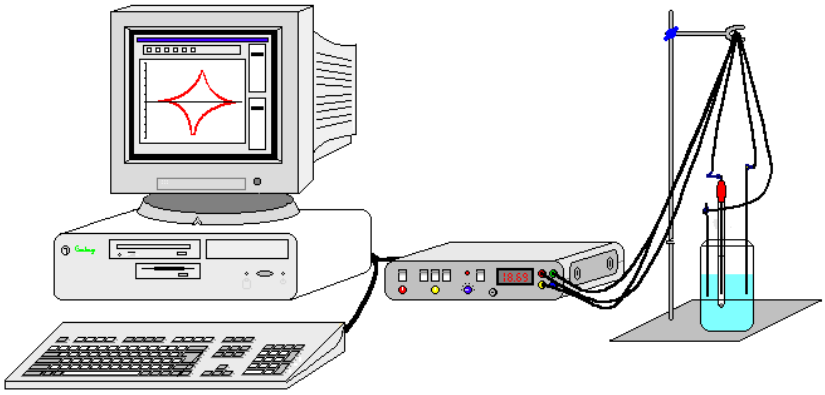

**Figure 2.1:** Experimental set up used to record all electrochemical measurements.

### *2.2.2 The electrochemical cell*

The electrochemical cell shown in Figure 2.2 is a standard three-electrode cell consisting of a working electrode (WE), an auxiliary or counter electrode (CE) and a reference electrode (RE). A standard calomel electrode (SCE) was utilised for the majority of this work, except in the case of the work carried out for the release of dopamine (DA) from the nanofiber substrates where, a silver / silver chloride (Ag/AgCl) electrode (3.0 mol $dm^{-3}$ NaCl filling solution) was used. The working electrode varied from one experiment to the next. For the bulk drug release studies, platinum wire was used. In the nanofiber studies, poly($_{D,L}$ – lactide-*co*-glycolide) PLGA fibers mounted on a gold coated mylar substrate were examined, while in the complexation studies a glassy carbon (GC) electrode was employed. A platinum wire/mesh electrode was used as the auxiliary (counter) electrode. The electrodes were connected to the potentiostat using coloured wires and the experiments and the results were computer controlled, as shown in Figure 2.1.

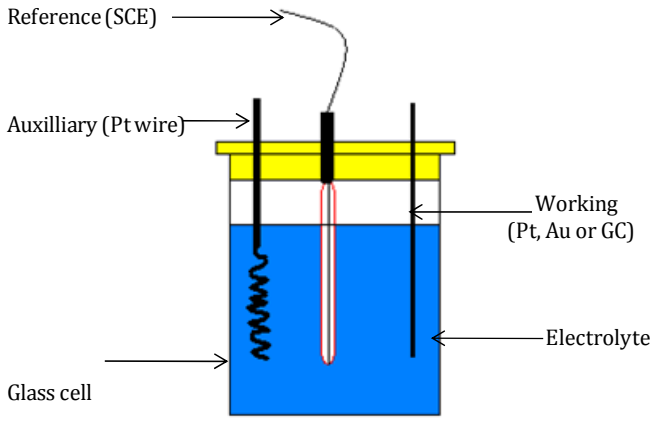


**Figure 2.2:** Diagram of electrode and electrochemical cell.

### *2.2.3 Electrode materials and preparation*

All electrode materials were purchased from Goodfellow Metals and Alfa Aesar. For the most part of the drug release study, platinum wire was used and for the CV techniques a platinum disc encased in Teflon and set in place using epoxy resin was used, a schematic of which is illustrated in Figure 2.3. In both cases the platinum wire and disc comprised of a purity grade of 99.9 % and had a 1 mm and 4 mm diameter, respectively. The platinum wire was polished using 1200 grade paper and rinsed well using distilled water, to generate a clean and smooth surface. The platinum disc electrode was polished using 1 μm diamond polish (Buehler MetaDi Monocrystalline Diamond suspension) on a Buehler micro-cloth and washed with distilled water to ensure a clean surface. The nanofiber study utilised Poly($_{D,L}$ – lactide-*co*-glycolide) (PLGA 50:50) electrospun onto a gold coated mylar substrate.

For the electrochemical complexation studies, a GC rod (4 mm) was utilised. This GC rod was similarly encased into a larger insulating Teflon sheath and set in place using epoxy resin, as observed with the platinum disc electrode. The electrical contact was achieved using a copper wire. A schematic is shown in Figure 2.3. For the GC surface, diameter of 4 mm, the electrode was polished as outlined above for the platinum disc electrode.

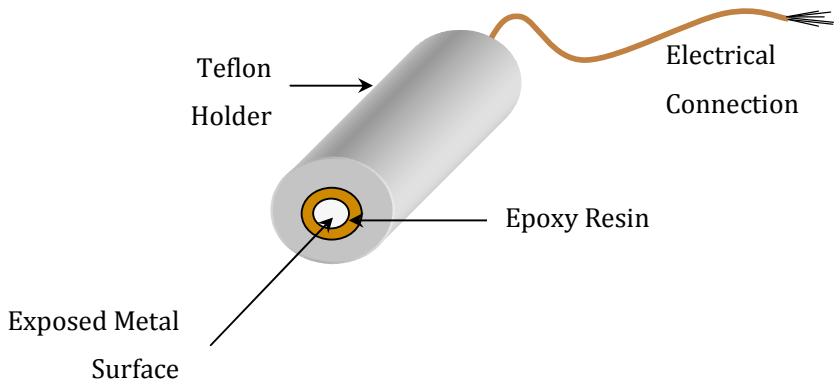


**Figure 2.3:** Schematic diagram of electrode assembly.

## 2.3 Chemicals and purification

For all reagents the highest analytical grade possible was purchased and used as received. With two exceptions, the first was the pyrrole monomer; it was purchased from Aldrich and purified by distillation. It was stored in the dark, in the fridge at low temperatures. Secondly, sulfonated β-cyclodextrin (Sβ-CD) sodium salt was purchased from Aldrich (substitution ca. 7-11 moles per mole of β-CD as reported by Aldrich). The molecular mass of this compound was calculated, assuming an average of 9 substituted sulfonated groups were present. During experimental analysis an impurity was discovered. Nuclear Magnetic Resonance spectroscopy (NMR) (technique described later in more detail in Section 2.5.6) and Mass spectrometry (MS) techniques were employed to determine the nature of the impurity as shown in Figure 2.4 (A) and (B), respectively. The NMR data were obtained using a 300 MHz Bruker instrument, in $D_20$. Figure 2.4 (A) shows the $^1H$ NMR spectra of a sample of Sβ-CD in 0.10 mol $dm^{-3}$ KCl in $D_2O$. In this figure, the highlighted blue region corresponds to the protons of the impurity. The impurity was confirmed to be pyridine. Figure 2.5 shows the chemical structure of pyridine. MS was also performed to determine the impurity present in the Sβ-CD, on an Agilent Technologies 6200 Series Accurate-Mass Time-of-Flight (TOF) LC/MS. MS is a technique used to

measure the weight of a molecule or fragments of it. In this study, the technique involves the ionisation of the sample. Samples were placed in an Agilent 1200 series high powered liquid chromatogram (HPLC) and passed through a gradient mobile phase of acetronitrile/water/formic acid. This process purified and separated the sample. The sample was then delivered to the mass spectrometer, in order to detect the positive ions. The sample was sent through a skimmer, where the neutral ions where removed. Using an Agilent time of flight (TOF) system, the positive ions were then pulsed up the flight tube and with the help of a reflectron, divided and, consequently, monitored by a detector. A spectrum illustrating the abundance of each positive ion as a function of mass/charge (*m/z*) was recorded. Figure 2.4 (B) shows the data recorded for a sample of the Sβ-CD. Pyridine has a molar mass of 79.101 g $mol^{-1}$. However, MS deals with the $(M+H)^+$ peak. In Figure 2.4 (B), the peak highlighted at *m/z* ratio 80.400 is equivalent to a pyridine $(M+H)^+$ peak. Table 2.1 illustrates both the calculated and the measured *m/z* ratio for the pyridine $(M+H)^+$ peak, with a calculated error of ± 0.5 % which is within the % error governed by the RSC.

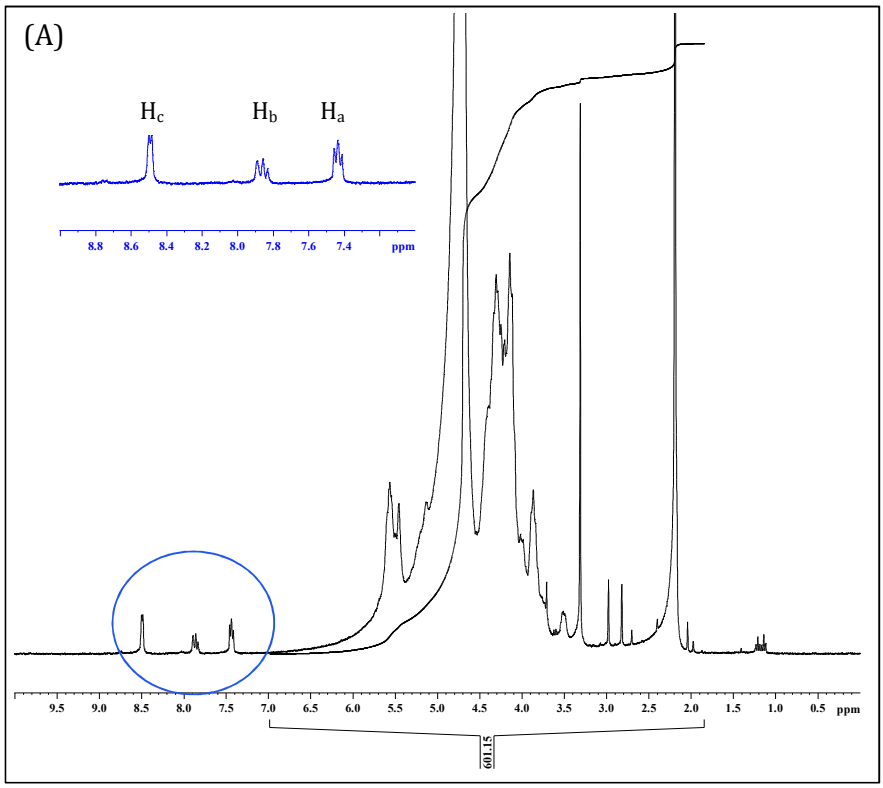

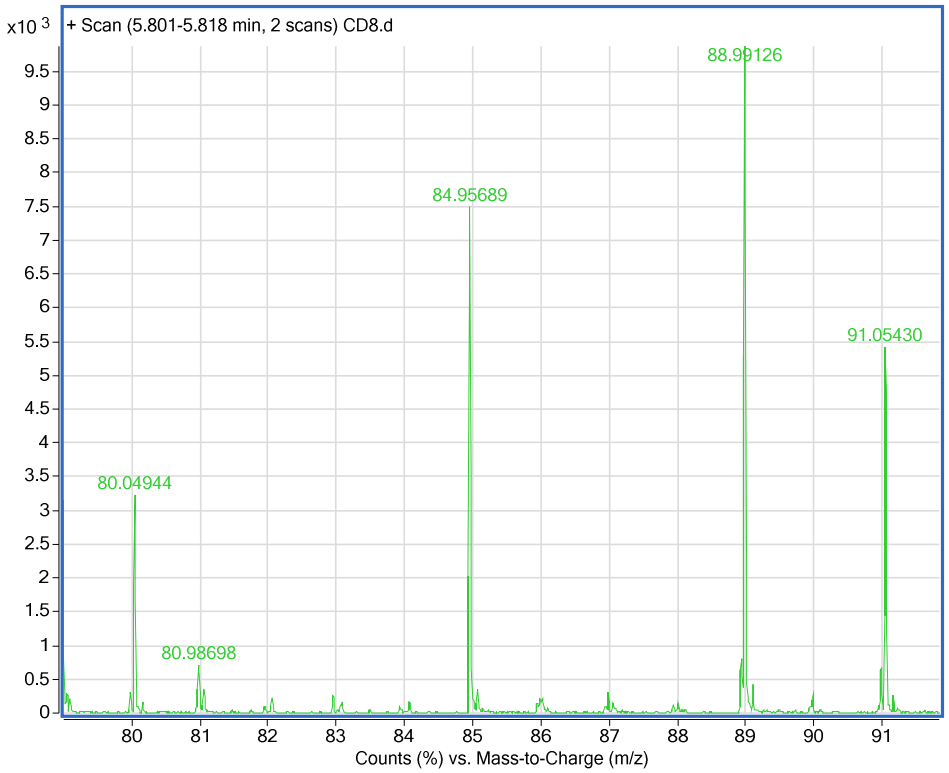


**Figure 2.4:** (A) $^{1}H$ NMR spectra of 1.0 x $10^{-2}$ mol $dm^{-3}$ Sβ-CD in 0.1 mol $dm^{-3}$ KCl in $D_2O$. Highlighted in blue is the presence of the peaks corresponding to pyridine. (B) Mass spectrum of a sample of Sβ-CD.

**Table 2.1:** Table of calculated and measured *m/z* ratios for Sβ-CD sample.

| | Calculated, *m/z* | Measured, *m/z* | % ppm error |
|---|---|---|---|
| $(M+H)^+$ | 80.04948 | 80.04944 | ± 0.5 |

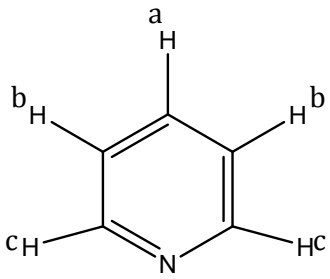


**Figure 2.5:** Structure of pyridine. (300 MHz, $D_2O$): δ 7.45 (1H, *m,* a-H), δ 8.49 (2H, *m*, b-H), δ 7.84 (2H, *m*, c-H).

Methods in purifying the salt were also carried out. A common way of removing pyridine is by dissolving the salt in toluene and rotary evaporating the solvent off. However, Sβ-CD is insoluble in this solvent system and the purification step was unsuccessful. However, the main concern with the impurity was the possible interaction of pyridine with the Sβ-CD and preventing the interaction of the Sβ-CD with the dopamine. To eliminate the possibility of interference a simple CV experiment was performed. Firstly, a 50 mL volume of a 5.0 x $10^{-4}$ mol $dm^{-3}$ DA solution was prepared in a citrate phosphate buffer, pH~3.2. This solution was divided in two sample cells, where 40 μL of pyridine was added to one of the cells. CV was run, using a three electrode set up as described in Section 2.2.2 with a GC as the working electrode, on the DA solution in the absence and presence of pyridine. The potential was swept from -0.250 to 0.800 V vs. SCE at 50 mV $s^{-1}$ for 10 cycles. Figure 2.6 shows the results obtained for the oxidation of DA in the absence and presence of 40 μL (2.0 x $10^{-2}$ mol $dm^{-3}$) of pyridine.

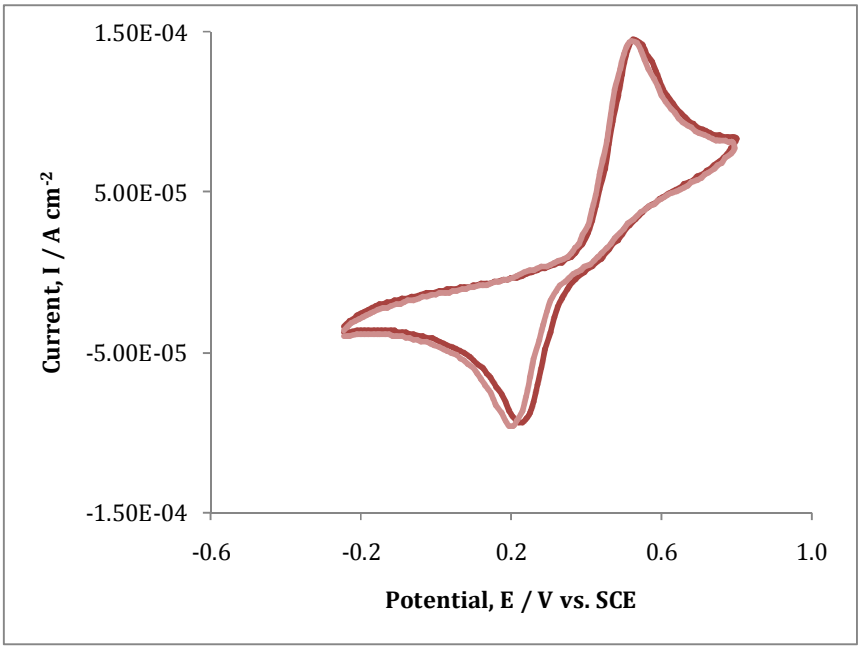


**Figure 2.6:** Cyclic voltammograms recorded in a citrate-phosphate buffer (pH ~ 3.2) at a GC electrode. Data were recorded in a 5.0 x $10^{-4}$ mol $dm^{-3}$ DA solution in the absence and presence of pyridine. The potential was swept from -0.250 to 0.800 V vs. SCE at 50 mV $s^{-1}$.

From the data, identical voltammograms were recorded in the presence and absence of pyridine. It is evident that no interference is observed in the presence of a large excess of pyridine. In light of this, all results shown in the complexation studies are true for the inclusion complexation of DA with Sβ-CD.

## 2.4 Preparation of polymer samples

Using various techniques polypyrrole was electrochemically and chemically deposited on a number of substrates. Here, the techniques employed are briefly summarised. The solution preparation and other more detailed parameters are discussed in the results chapters.

### *2.4.1 Potentiostatic techniques*

These studies were carried out by applying a constant potential to the electrode and then recording the current density as a function of time. This technique was employed to electrochemically deposit polypyrrole on the desired substrate. This involved applying an anodic potential of > 0.500 V vs. SCE to the electrode of interest in the polymer forming electrolyte.

This technique was also used to incorporate and release the drugs by reducing and oxidising the polymer film. In the case of the cationic drugs, i.e., DA, the incorporation was achieved by imposing a potential of –0.900 V vs. SCE for a period of 30 min in a 0.1 mol $dm^{-3}$ DA solution and, an applied potential of 0.100 V vs. SCE for 60 min in a 0.1 mol $dm^{-3}$ $Na_2S0_4$ solution was required for the release.

### *2.4.2 Galvanostatic techniques*

This technique was employed to electrochemically deposit polypyrrole onto the electrospun nanofibers on gold coated mylar. This technique involves the application of a constant current to the electrochemical cell. In the case of polypyrrole growth on the electrospun PLGA nanofibers a constant current of 1

mA $cm^{-2}$ was applied and the potential was recorded as a function of time, or until a suitable charge was passed.

### *2.4.3 Cyclic voltammetry*

This technique was utilised as an alternative technique to electrochemically deposit polypyrrole on particular substrates of interest. Cyclic voltammetry, (CV), involves sweeping the potential applied to the working electrode between two potential limits at a required scan rate, where the change in current is monitored.[1] The resulting cyclic voltammogram is a plot of applied potential as a function of current. The working electrode serves as the surface where the electron transfer of the redox reaction takes place and the electrical current created is known as the faradic current. The CE balances this faradic process with an electron transfer in the opposite direction. (e.g., if oxidation takes place at the WE, reduction takes place at the CE). The redox reaction occurs within the potential range defined by the two chosen potential limits, and the potential at which the reduction or oxidation takes place provides qualitative information about the electroactive species under investigation. The working electrode can act as an electrochemical reductant or oxidant depending on the applied potential to the surface. As the applied potential becomes more negative, the electrode becomes a better reducing agent. Equally, as the applied potential becomes more positive, the electrode becomes a better oxidising agent.

### *2.4.4 Vapour phase polymerisation*

Vapour phase polymerisation (VPP) was another technique employed for the deposition of polypyrrole onto various substrates. This technique is relatively simple and is useful for the deposition of polymers onto insulating substrates. In this case an oxidant, 40% Fe(III)/PTS made up in ethanol, was spin coated onto a desired substrate, flashed off using a heating mantle and placed in a chamber containing the monomer. The oxidant initiates polymerisation of the monomer which is followed by the formation of polypyrrole onto the surface.

### *2.4.5 Electrospinning*

Electrospinning is a technique that was used to form nanostructured fibers onto a substrate which subsequently was used to polymerise pyrrole. In this technique, a strong electric field was employed to convert a polymer solution into solid fibers. The electrospinning apparatus used is shown in Figure 2.7. This consisted of a high voltage power supply (Gamma High Voltage), a digital syringe pump (Kd Scientific Pump) and an electrically grounded collector plate made of galvanised iron mounted on a stand.

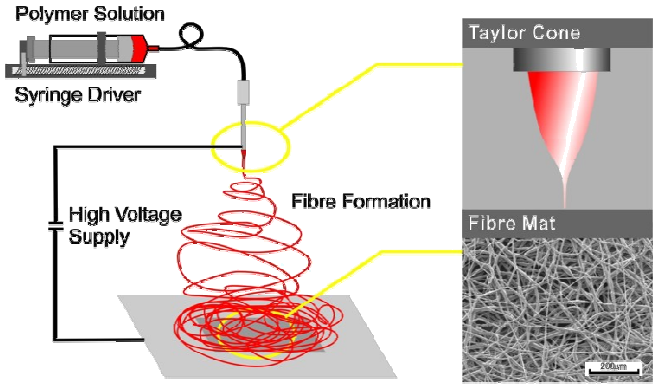


**Figure 2.7:** Schematic diagram of the Electrospinning set-up.

In order to produce the electrospun fibers a high voltage was applied to the needle containing the polymer solution, this induces the formation of a liquid jet. A solid fiber is generated and is continuously stretched due to the electrostatic repulsions between the surface charges and the evaporation of the solvent. Intrinsic properties, such as the type of polymer, concentration (viscosity), elasticity, electrical conductivity, polarity and surface tension of the solvent are all important in the formation of the fibers and are studied as detailed in Chapter 6. Operational properties, such as the strength of the electric field, the distance from the spinneret and collector and the flow rate of the polymer were also taken into consideration. Au coated mylar was used as the conducting substrate. This consists of a plastic sheet with a coating of gold. One side is conducting and the other insulating. It comes in large rolls and is easy to

use, flexible and can be shaped in various sizes to achieve uniform substrates. In the electrospinning process, samples were initially cut into 5 x 5 cm squares and clipped onto a metal template.

## 2.5 Characterisation of samples

Various techniques were used to characterise the polymers, confirm inclusion complexation and evaluate the amount of drug released from the polymer systems.

### *2.5.1 EQCM measurements*

Additional information on the synthesis and electrochemical behaviour of the conducting polymers, as well as the drug release studies was obtained using an Electrochemical Quartz Crystal Microbalance (EQCM) technique. The experiments were performed on a CHI400 EQCM, a schematic of which is shown in Figure 2.8. The equipment consisted of a quartz crystal oscillator, a frequency counter, a fast digital function generator, a high-resolution and high-speed data acquisition circuitry, a potentiostat, a galvanostat and a computer. EQCM measurements calculate the mass change occurring at the electrode surface by monitoring the changes in the resonant frequency ($f_0$) of an oscillating quartz crystal. The frequency is related to the mass through the Sauerbrey equation, Equation 2.1:

$$\Delta f = -\frac{2f_0^2 \Delta M}{A\sqrt{\rho\mu}} \qquad 2.1$$

where $f_0$ is the resonant frequency, $\Delta M$ is the mass change, A is the surface area of the electrode or film, 0.203 $cm^2$, ρ is the density of quartz , 2.648 g $cm^{-3}$, and μ is the shear modulus of quartz, 2.947 x $10^{11}$ g $cm^{-1}$ $s^{-2}$. In this equation the change in frequency ($\Delta f$) is equal to minus the change in mass ($\Delta m$) per unit area ($A$) times a constant. The frequency, therefore, decreases as the mass increases.

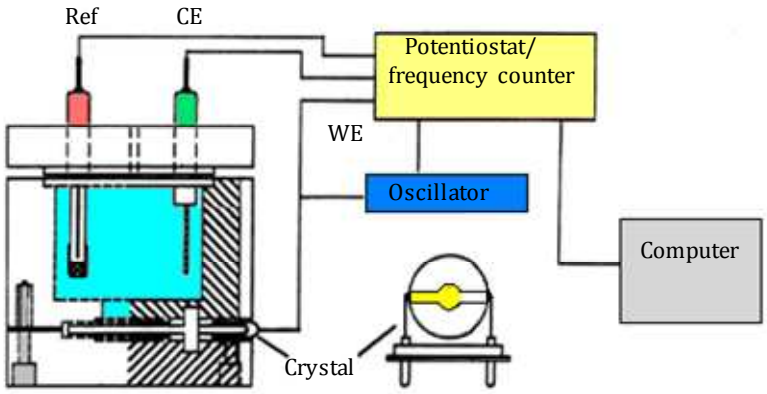


**Figure 2.8**: EQCM set-up.

### *2.5.2 UV-visible spectroscopy*

UV-visible spectroscopy measures the amount of ultraviolet and visible light transmitted or absorbed by a sample placed in the spectrometer. The wavelength at which a chemical absorbs light is a function of its electronic structure and the intensity of the light absorption is related to the amount of the chemical between the light source and the detector, so a UV-visible spectrum can be used to identify some chemical species. Also, it is well suited for the quantitative study of association constants since the measured absorbance values are proportional to the respective concentration by the Beer-Lambert law.[2]

A Varian Cary series spectrophotometer was used for all of the analysis on monitoring the drug release and complexation studies. It comprises a Xenon lamp and has a maximum scan rate of 24 000 nm per minute. This technique was employed to monitor the release of dopamine investigated in the drug delivery studies. Spectra were obtained and analysed to calculate the amount of drug released upon application of a reduction/oxidation or open-circuit potential. In all cases, a quartz crystal cuvette with a diameter of 1 cm was used. The drug concentration was investigated at the wavelength of maximum absorption, $\lambda_{max}$ of the drug. For example, the wavelength at 280 nm was monitored in the release studies of dopamine. To determine the concentration, or the amount of drug released, a calibration curve was firstly obtained. The

amount of drug released can be determined by measuring the absorbance at a particular wavelength and applying the Beer-Lambert law, Equation 2.2.

$$A = \varepsilon bc \qquad 2.2$$

where $A$ is the absorbance, ε is the molar absorbtivity, $b$ is the path length and $c$ is the concentration of the compound in solution. From the linear relationship between concentration and absorbance a slope value can be obtained. When samples from the release of the drug were taken and the absorbance values were recorded, these values were expressed as concentration when used in conjunction with the Beer Lambert law and the slope value. For example, Figure 2.9 shows a calibration curve of DA which has a $\lambda_{max}$ = 280 nm. The equation of this line is:

$$y = 2487.68\ x$$

where y is the absorbance and x is the concentration.

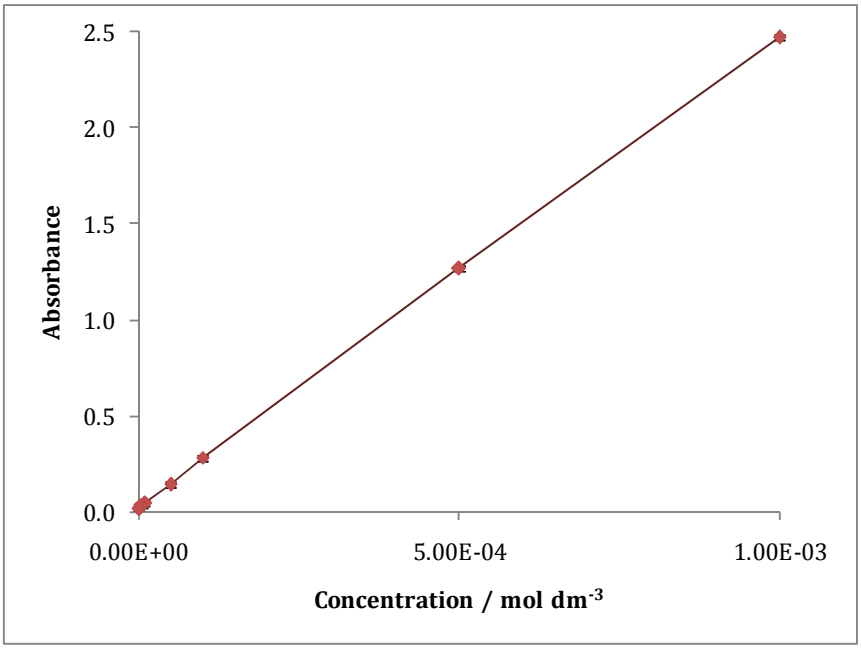


**Figure 2.9:** Calibration curve for dopamine in water. Absorbance as a function of concentration. From the data the slope was obtained.

### *2.5.3 Cyclic voltammetry*

This technique was utilised as an alternative technique to electrochemically deposit polypyrrole on particular substrates of interest. Secondly, it was used as an investigative tool to study the growth and the properties of the polymer.[3] Thirdly, it was used to determine the binding constants for DA and Sβ-CD. The scan rates employed in the specific experiments are illustrated in the figure captions or corresponding text in the results section.

As detailed in Section 2.3.3, the CV experiment involves scanning the potential between two limits at a particular scan rate. It is particularly useful in studying the reversibility of a redox couple. For a simple redox couple, the voltammogram exhibits an oxidation wave, with a peak current, and a corresponding reduction wave, centred at a peak potential.

For a reversible couple, the ratio of the reverse-to-forward peak currents, $i_{pr}/i_{pf}$, is unity, while the separation between the peak potentials is given by Equation 2.3. Also, this peak separation is independent of the scan rate. Thus, the peak separation can be used to determine the number of electrons transferred, *n*, and as a criterion for the Nernstian behaviour:

$$\Delta E_p = E_{pa} - E_{pc} = 59\ mV/n \qquad 2.3$$

In addition, the peak current for a reversible couple is given by the Randles-Sevcik equation:

$$ip = k\ n^{3/2} A\ D^{1/2}\ c\ v^{1/2} \qquad 2.4$$

where the constant, *k*, has a value of 2.69 x $10^5$, $i_p$ is the peak current, *n* is the number of electrons transferred per mole of electroactive species; *A* is the area of the electrode in $cm^2$; *D* is the diffusion coefficient in $cm^2\ s^{-1}$; *c* is the concentration in mol $cm^{-3}$; *v* is the scan rate of the potential in V $s^{-1}$.[4] The $i_p$ is linearly proportional to the concentration, *c*, of the electroactive species and the

square root of the scan rate, $\nu^{1/2}$. Thus if linear plots of $i_p$ *vs.* $\nu^{1/2}$ are obtained the electrode reaction is under diffusion control, which is the mass transport of the electroactive species to the surface of the electrode across a concentration gradient. Using Equation 2.4, the diffusion coefficients were evaluated from the slopes of the corresponding, $i_p$ *vs.* $\nu^{1/2}$ plots.

However, the situation is very different when the redox reaction is slow or when it is coupled with a chemical reaction. For an irreversible process (slow electron exchange), the redox peaks are reduced in size and are separated by a large potential. Totally irreversible systems are characterised by a shift of the peak potential with the scan rate, as detailed in Equation 2.5:

$$E_p = E^0 - (RT/\alpha nF)[0.78 - \ln\left(\frac{k^0}{(D)^{\frac{1}{2}}}\right) + \ln(\frac{\alpha nF\nu}{RT})^{1/2}] \qquad 2.5$$

where $\alpha$ is the transfer coefficient and $n$ is the number of electrons involved in the charge-transfer step. Thus, $E_p$ occurs at potentials higher than $E^0$, with the overpotential related to the rate of the reaction, $k^0$, and α. For quasi-reversible systems (with $10^{-1} > k^0 > 10^{-5}$ cm $s^{-1}$) the peaks exhibit a larger separation in peak potentials compared to the reversible redox system, Equation 2.3.

### *2.5.4 Rotation disc voltammetry*

Rotation Disc Voltammetry, (RDV), was another technique employed in the determination of diffusion coefficients of DA in the absence and presence of Sβ-CD. A schematic of the equipment involved is shown in Figure 2.11. A rotation disc electrode, similar to the electrode shown in Figure 2.3 was used for these studies. The RDV set up consists of an electrode attached to a rotor spindle via a suitable electrical contact. When the circular disc is rotated at a particular rotation speed in solution, fresh reactant is brought to the surface. A well defined flow pattern, shown in Figure 2.11 (B), is obtained where the rotating electrode acts as a 'pump', dragging the solution perpendicular to the electrode

surface which is subsequently thrown out in a radial direction on contact with the electrode surface.[5]

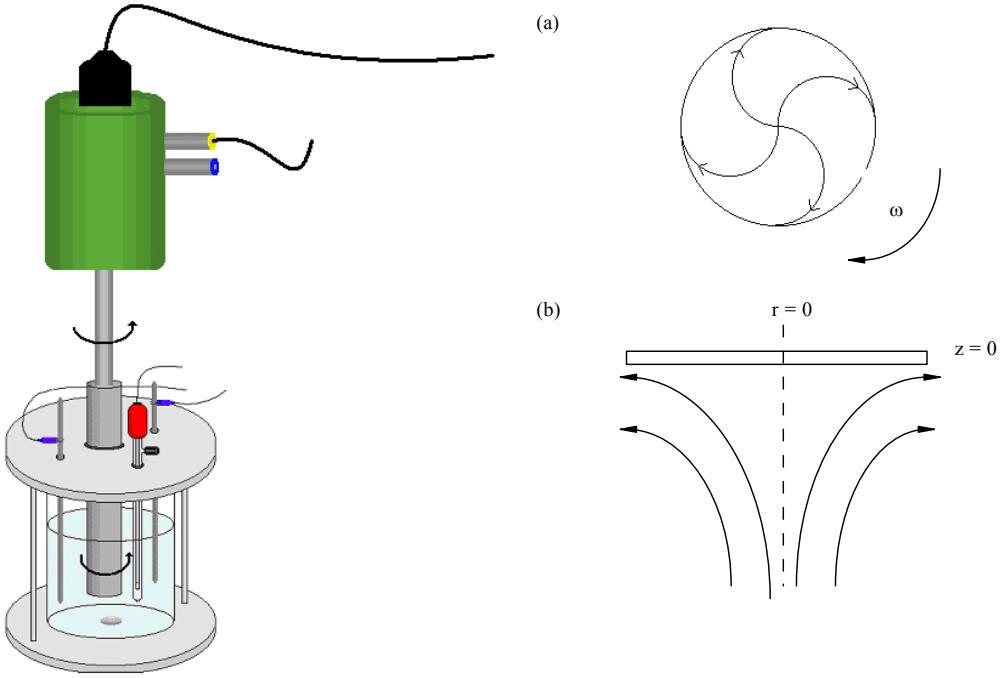


**Figure 2.11:** Schematic diagram of electrode in the RDV set up. The patterns of flow to a rotating disc electrode (A) viewed from below the electrode face and (B) across its surface as viewed from the side.

This technique has an advantage over cyclic voltammetry where the diffusion layer is time dependent. The thickness of the diffusion layer using RDV can be controlled by changing the rotation speed of the electrode. This approach leads to higher currents, greater sensitivity and reproducibility due to the increased transport of electroactive species to the electrode surface. The electrode is rotated at a known frequency, $f$, where the angular velocity, $\omega = 2\pi f/60$. The rotation of the electrode must not be so fast as to cause turbulence in the solution, therefore ensuring laminar flow of the substrate to the electrode surface.[1] Since the current is proportional to the concentration, the observed current should increase with the increase in ω. With this statement, the Levich equation is defined. This equation applies to the total mass-transport-limited

condition at the electrode surface. Using the Levich equation, for an electrochemical process the observed current is limited by diffusion, this current can be related to the rotation speed of the electrode, Equation 2.6.

$$i_L = 0.621nFAD^{2/3}v^{-1/6}c\omega^{1/2} \quad 2.6$$

where,

$$Slope = 0.621nFAD^{2/3}v^{-1/6}c$$

$i_L$ is the limiting current, $n$ is the number of electrons transferred, $F$ is Faraday's constant (96485.3415 C $mol^{-1}$), $A$ is the surface area, $D$ is the diffusion coefficient, $cm^2\ s^{-1}$, ν is the kinematic viscosity, $c$ is the concentration and ω is the rotational speed in rad $s^{-1}$.

In this thesis, the Levich equation was used to determine $D_f$ and $D_c$, which are the diffusion coefficients of DA obtained in the absence and presence of an excess of Sβ-CD, respectively. In this case, the limiting current was recorded as a function of the rotation rate for a solution of DA in the absence and presence of Sβ-CD. The limiting current is directly proportional to the square root of the rotation speed. The subsequent Levich plot, $i_L$ *vs.* $\omega^{1/2}$, should return a straight line through the origin whose slope can be used to estimate the diffusion coefficient. The diffusion coefficient, $D$ can be obtained from the slopes if the parameters $n$ and $c$ are known.

The Koutecky-Levich equation was also applied to the RDE data to evaluate the apparent rate constant, $k_{DA}$, for the oxidation of DA, in the presence and absence of Sβ-CD. The Koutecky-Levich equation is a modification of the Levich equation and is generally used if the Levich plot, $i_L$ *vs.* $\omega^{1/2}$, deviates from linearity due to a kinetic limitation in the electron transfer reaction.[1] In this instance the Koutecky-Levich plot, $1/i_L$ vs. $1/\omega^{1/2}$, was used to estimate the rate constants of the DA oxidation. The Koutecky-Levich equation is given by Equation 2.7:

$$\frac{1}{i_L} = \frac{1}{i_K} + \frac{1}{i_{lev}} = \frac{1}{nFAk_{DA}c} + \frac{1.61}{nFAv^{-1/6}D^{2/3}\omega^{1/2}c} \quad 2.7$$

In this analysis, $i_L$ represents the measured limiting current, $i_K$ is the current of the electron transfer between the DA and the electrode and $i_{lev}$ is the Levich current, which corresponds to the mass transfer of DA in the solution. The $i_K$ is not influenced by the rotation rate, as expressed in Equation 2.8:

$$i_k = nFAk_{DA}c \quad 2.8$$

where $n$ is the number of electrons transferred, $F$ is Faraday's constant (96485.3415 C mol$^{-1}$), $A$ is the surface area, $k_{DA}$ is the reaction rate constant, and $c$ is the concentration.

A plot of $1/i_L$ against $1/\omega^{1/2}$ should be linear. The rate constant, $k_{DA,}$ for DA in the absence and presence of Sβ-CD can be obtained from the intercept of the Koutecky-Levich plot, $1/i_L$ vs. $1/\omega^{1/2}$.

### *2.5.5 Nuclear magnetic resonance*

Proton ($^1$H) Nuclear Magnetic Resonance (NMR) is widely used for the determination of the structure of organic compounds. For the purpose of these studies it is the most effective structural tool for investigating the interaction between a cyclodextrin and a guest.[6]

$^1$H NMR is relative quantitative; the number of hydrogen nuclei can be measured by integrating the area under the peak. It also reveals the connectivity of the structure due to the coupling of the protons, and more importantly, for this research, the chemical shifts give a reliable indication of the local chemistry. Radio waves are used to study the energy level differences of $^1$H nuclei. Hydrogen nuclei have a nuclear spin of a half and so have two energy levels: they can be aligned either with or against the applied magnetic field. The

chemical shift provides much information and is a measure of the shielding of the nucleus by the electrons around it.[7] In these studies, $^1$H NMR was used to confirm the stoichiometry, the binding constant and the geometric factors involved in the complexation between DA and Sβ-CD. A change in the chemical shift of DA in the presence and absence of Sβ-CD allowed for the evaluation of the binding constants. $^1$H-NMR experiments were performed on a Bruker 300 MHz NMR spectrometer at 293 K in $D_20$. $^1$H NMR peak protons were reported in ppm relative to internal reference.

### *2.5.6 Optical and scanning electron microscopy*

Optical and Scanning Electron Microscopy (SEM) allows the observation and characterisation of samples on a micrometer (μm) to a nanometer (nm) scale. Optical images were preformed on a Leica DMEP DFC-280 and an Olympus BX51M system using Leica application suite and Olympus DP Version 3.2, software, respectively. The majority of SEM images were obtained from a Joel 840 SEM, while, the Energy dispersive X-ray Analysis (EDAX) and SEM analysis were performed on a Hitachi FE-Scanning Electron Microscope. The image processing and analysis to study the formation of fibers and the morphology of the polymers as a function of the various parameters applied were performed using both techniques.

For the analysis of the growth and morphology of polypyrrole, images were obtained on various substrates, including platinum, gold, and Au coated mylar. For the electrospinning studies, samples were electrospun using various parameters and images were taken using both techniques. In the case of SEM, Au coated mylar was used as the substrate which was gold sputter coated prior to analysis using an Emitech K550x Gold Sputter Coater. Optical images were taken on glass slides, and Au coated mylar samples.

### *2.5.7 Solution properties*

Solution properties such as pH and ionic conductivity, were determined using an Orion model 720A pH meter and a Jenway 4510 conductivity meter, respectively. The equipment was calibrated each time prior to experimental analysis using buffered solutions, pH 7.0 and 4.0 obtained from Fluka, and 0.1 mol $dm^{-3}$ KCl from Sigma. Where necessary, the pH and conductivity of the solutions were adjusted by adding HCl / $H_2SO_4$ or NaOH.

## 2.6 Theory of experimental techniques and equations used

In order to understand various processes occurring many theories and related equations were used. The following is an overview of the theories where the background is also provided.

### 2.6.1 Complexation studies

In order to evaluate complexation between DA and Sβ-CD the formation constant was determined using four techniques: UV, CV, RDV and NMR. Also, the Job's method was employed to distinguish the stoichiometric value of the complex. The related theory behind each of the equations used is described in this section.

#### *2.6.1.1 Job's method*

Before any structural or associative measures are performed on a host-guest interaction, it is important to determine the stoichiometry of the complex. A common way to confirm this stoichiometric value is well known as the continuous variation or Job's method.[8-10] This method is an experimental mixing technique widely used in the determination of stoichiometric ratios of each constituent involved. This method can be applied to various analytical techniques, such as Fluorescence[11], UV-visible spectroscopy[12] and $^1$H NMR[13, 14]. In each method, the Job's plot is based on the spectral change observed either for the guest or the host.

This method involves the preparation of a series of solutions where the sum of the guest [G] and host [H] concentrations is kept constant while changing the mole fraction. This is achieved by mixing different volumes of the two components, G and H, such that the overall volume remains the same along the series. Experimentally, some property (such as chemical shifts in the NMR or absorbance values in UV) whose value changes when the guest and host form a complex, is measured in each solution.[2]

The data for the Job's plot is generated by taking the product of the mole fraction with the change of the property from that of an equal concentration of free guest. This product is then plotted as a function of the mole fraction. The stoichiometry is determined from the x-coordinate at a maximum value of the Job's curve.

#### *2.6.1.2 Formation constants*

In aqueous solutions, cyclodextrins and guest molecules are well known to form inclusion complexes.[2, 15-19] An equilibrium is established between these species and is expressed as the complex formation, stability, equilibrium or binding constant, $K_f$. The formation constant for the inclusion complex has to be evaluated for the quantitative analysis.[20] In complexation studies, a simple way of determining the formation constant for a 1:1 complex is based on the following equilibrium:

$$G + H \rightleftharpoons C \qquad 2.9$$

with G representing the guest, H the host and C the complex. From here, the formation constant can be defined as:

$$K_f = \frac{[C]}{[G][H]} \qquad 2.10$$

where [G] and [H] are the equilibrium concentration of the guest and host, respectively. The encapsulation of a guest inside a CD cavity leads to alterations

in the chemical and physical properties of the guest. In this instance it is feasible to calculate the formation constant by monitoring these changes. Depending on the experiment being performed, a certain property is monitored. For example, in UV-visible spectroscopy the absorbance change is monitored. In all of the following cases these methods are known as approximation methods, as each method includes one or more approximation. In all cases of evaluating the formation constant the concentration of the guest was held constant and the host concentration was varied. The two main approximations for these evaluations are (i) the host is in excess of the guest and (ii) the stoichiometric value is 1:1, for the G:H inclusion complex.

**2.6.1.2.1 UV-visible studies**

UV-visible spectroscopy is considered to be well suited for the quantitative study of the formation constant due to the measured absorbance being proportional to the concentrations because of the Beer-Lambert law.[2] There are limitations but in cases where the absorbance of the guest increases upon complexation, a suitably modified Hiedelbrand-Benesi equation[21] can be used to estimate the formation constant. In this study the modified Hiedelbrand-Benesi, Equation 2.11, reported by Dang and co-workers[17] and Ibrahim *et al.*[22] was used.

$$\frac{A_0}{A - A_0} = \frac{\varepsilon_G}{\varepsilon_{H-G} - \varepsilon_G} + \frac{\varepsilon_G}{\varepsilon_{H-G} - \varepsilon_G} \times \frac{1}{K_f[CD]} \qquad 2.11$$

$A_0$ and $A$ are the absorbencies of the free guest and the complex, respectively, $\varepsilon_G$ and $\varepsilon_{H\text{-}G}$ are the absorption coefficients of the guest and the complex, respectively. The formation constant expressed in Equation 2.11 implies that a Hiedelbrand-Benesi plot of $A_0/A_0\text{-}A$ versus 1/[CD] should give a straight line, and from the slope and the intercept of the straight line plots, the $K_f$ values can be obtained.

#### 2.6.1.2.2 Electrochemical studies

The formation of an inclusion complex between a redox-active guest and cyclodextrin can be followed using electrochemical approaches such as CV and RDV. The peak current and peak potential of the redox-active guest is measured in the absence and presence of a large excess of CD. As the CD is large and bulky the included guest will diffuse more slowly than the free guest giving rise to a reduction in the peak current. Likewise, a higher applied potential is required to oxidise the included guest. These electrochemical changes attributed to the complexation of a guest in the presence of cyclodextrins are well discussed in the literature.[17, 23, 24] The formation constant for the inclusion complex can be calculated using changes in the peak current data by using Equation 2.12, expressed as follows:[22, 25, 26]

$$\frac{1}{[S\beta - CD]} = K_f \frac{(1 - A)}{(1 - {}^{i}/_{i_0})} - K_f \qquad 2.12$$

Here, [Sβ-CD] is the concentration of sulfonated β-CD, $i_0$ and $i$ are the peak currents without and with CD. $A$ is a proportional constant. This equation is valid when the concentration of the CD is in large excess of the guest and a 1:1 relationship is obtained for the complex.

In order to follow the changes in the oxidation potential of the guest as it is included in the cavity the RDV technique was used. For the RDV data, the equation originally proposed by Galus[27] and used by Coutouli-Argyropoulou *et al.*[16] and Ibrahim *et al.*[22] was used, Equation 2.13. As mentioned in Section 2.5.3, the limiting currents obtained using the RDV scale linearly with the square root of the rotation frequency. The diffusion coefficient can be determined by means of the Levich equation. The half-wave potentials can also be evaluated from the RDV data. With these values, the formation constant can be evaluated using the following equation:

$$\left(\frac{F}{RT}\right)\left\{(E_{\frac{1}{2}})_{app} - (E_{\frac{1}{2}})_f\right\} = \ln(1 + K[S\beta - CD]) + \ln(D_c / D_f)^{1/2} \qquad 2.13$$

Here, $F$ is Faraday's constant (96485.3415 C mol$^{-1}$), $R$ is the gas constant and $T$ is temperature in K, $(E_{1/2})_{app}$ and $(E_{1/2})_f$ are the half-wave potentials of the electroactive guest obtained in the presence and absence of the Sβ-CD, respectively, while $D_f$ and $D_c$ are the diffusion coefficients of the guest obtained in the absence and in the presence of a large excess of Sβ-CD. Again this equation is only valid when the concentration of the CD is in excess of the guest and a 1:1 relationship is obtained for the stoichiometry of the complex.

**2.6.1.2.3 NMR studies**

As previously said NMR is a sensitive technique for monitoring the interactions between molecules. With this said, it is a good method for understanding the complexation in solution. NMR spectra of the Sβ-CD were too complicated to analyse due to the large number of functional groups and the low average molecular symmetry.[2] In this case the property monitored for the host guest complexation was the chemical shift of the signals due to the guest. A NMR titration experiment can be performed to obtain structural and binding information on the complex. A spectrum of the free host and the free guest is measured, along with a number of solutions made up where the guest is held at a constant concentration and the host is varied. Upon complexation, the electronic environments of host and guest change, by monitoring the chemical shift of the guest, the structural conformation of the complex can be understood and the formation constant evaluated. The stability constant is determined under fast exchange; the rate of complexation is usually faster than the NMR time scale.[2, 28] The formation constant is evaluated using a non-linear least square analysis obtained with the following relationships, described in Equation 2.14.[28]

$$\delta = \delta_h - \frac{\Delta\delta}{2}\left(b - \sqrt{b^2 - 4R}\right) \qquad 2.14$$

where

$$b = 1 + R + \frac{1}{(K[CD])}$$

Here, δ is the observed chemical shift and $\delta_h$ is the chemical shift observed in the presence of Sβ-CD. $R$ is the mole fraction. A plot of Δδ as a function of the concentration ratio of Sβ-CD is obtained for each proton. In this analysis, it is assumed that δ and $\delta_h$ are independent of concentration and temperature. This non-linear least squares data treatment of the NMR titration is widely applicable and is acceptable if a 1:1 stoichiometric value for the host and guest is obtained.

## 2.7 References


1. F. R. F. Fan and A. J. Bard, *J Electrochem Soc*, **133**, (1986), 301-304.
2. H. Dodzuik, Cyclodextrins and Their Complexes, Wiley-VCH, 2006.
3. A. F. Diaz, J. I. Castillo, J. A. Logan, and W. Y. Lee, *J Electroanal Chem*, **129**, (1981), 115-132.
4. S. E. group, Instrumental methods in electrochemistry, 1985.
5. R. Greef, R. Peat, L. M. Peter, D. Pletcher, and J. Robinson, Instrumental methods in electrochemistry, Ellis Horwood Ltd, 1985.
6. M. Garinot, V. Fievez, V. Pourcelle, F. Stoffelbach, A. des Rieux, L. Plapied, I. Theate, H. Freichels, C. Jerome, J. Marchand-Brynaert, Y. J. Schneider, and V. Preat, *J Control Release*, **120**, (2007), 195-204.
7. J. Clayden, N. Greeves, S. Warren, and P. Wothers, Organic Chemistry, 2001.
8. S. Gibaud, S. Ben Zirar, P. Mutzenhardt, I. Fries, and A. Astier, *Int J Pharm*, **306**, (2005), 107-121.
9. P. Job, **9**, (1928), 113-203.
10. D. Landy, F. Tetart, E. Truant, P. Blach, S. Fourmentin, and G. Surpateanu, *J Incl Phenom Macro*, **57**, (2007), 409-413.
11. Y. Y. Zhou, C. Liu, H. P. Yu, H. W. Xu, Q. Lu, and L. Wang, *Spectrosc Lett*, **39**, (2006), 409-420.
12. I. V. Terekhova, R. S. Kumeev, and G. A. Alper, *J Incl Phenom Macro*, **59**, (2007), 301-306.
13. L. Fielding, *Tetrahedron*, **56**, (2000), 6151-6170.
14. V. M. S. Gil and N. C. Oliveira, *Journal of Chemical Education*, **67**, (1990), 473-478.
15. K. Connors, Binding Constants, A wiley interscience, 1987.
16. E. Coutouli-Argyropoulou, A. Kelaidopoulou, C. Sideris, and G. Kokkinidis, *J Electroanal Chem*, **477**, (1999), 130-139.
17. X. J. Dang, M. Y. Nie, J. Tong, and H. L. Li, *J Electroanal Chem*, **448**, (1998), 61-67.

18. P. Fini, M. Castagnolo, L. Catucci, P. Cosma, and A. Agostiano, *Thermochim Acta*, **418**, (2004), 33-38.
19. R. Ramaraj, V. M. Kumar, C. R. Raj, and V. Ganesane, *J Incl Phenom Macro*, **40**, (2001), 99-104.
20. K. Hirose, *J Incl Phenom Macro*, **39**, (2001), 193-209.
21. H. A. Benesi and J. H. Hildebrand, *J Am Chem Soc*, **71**, (1949), 2703-2707.
22. M. S. Ibrahim, I. S. Shehatta, and A. A. Al-Nayeli, *J Pharmaceut Biomed*, **28**, (2002), 217-225.
23. Z. N. Gao, X. L. Wen, and H. L. Li, *Pol J Chem*, **76**, (2002), 1001-1007.
24. T. Matsue, D. H. Evans, T. Osa, and N. Kobayashi, *J. Am. Chem. Soc.*, **107**, (1985), 3411-3417.
25. C. Yanez, L. J. Nunez-Vergara, and J. A. Squella, *Electroanal*, **15**, (2003), 1771-1777.
26. G. C. Zhao, J. J. Zhu, J. J. Zhang, and H. Y. Chen, *Anal Chim Acta*, **394**, (1999), 337-344.
27. Z. Galus, (1976), 363.
28. R. S. Macomber, *Journal of Chemical Education* **69**, (1992), 375-378.

## 3.1 Introduction

In the very early stages of polymer chemistry all carbon-based polymers were regarded as insulators.[1] However, the discovery of the conducting polymer opened up many doors for the new age of polymer technology. Since their discovery in the 1970's the preparation and characterisation of these materials has evolved substantially through the use of electrochemistry.

Polypyrrole (PPy), a conducting polymer has been extensively researched for several applications, as discussed previously in Chapter 1. However, for the purpose of this research it is in the area of drug delivery that PPy finds its most attractive application.[2-6] It is also well documented that chemically modified electrodes using cyclodextrins (CDs) offer a wide range of possibilities in the field of electrochemistry.[7] CDs, as previously described in Chapter 1, are macrocyclic oligosaccharides built of α-D-glucopyranoside units linked by α-(1,4) bonds. In this case the use of negatively charged CDs was investigated for the potential growth of the polymers and subsequent uptake and release of some pharmaceutically important compounds. However, there is little literature published on the electrochemical deposition of conducting polymers in the presence of the cyclodextrin used in this research, sulfonated β-cyclodextrin, (Sβ-CD).

The present studies concentrate on the deposition of PPy in the presence of these charged CDs. The Sβ-CD is only soluble in aqueous media and as PPy is one of the few conducting polymers that can be prepared in aqueous solutions, it was the most promising polymer to work with. It is reported that PPy films can vary in their characteristics depending on the parameters applied during electrochemical polymerisation including dopant anion and thickness.[8] In this chapter a preliminary investigation into the growth of the polymer films in the presence of various dopants specifically, in the presence of Sβ-CD, was investigated. Sβ-CD is a large anionic cyclodextrin with approximately 7-11 anionic groups positioned around its cavity.

This chapter discusses the deposition of PPy in the presence of Sβ-CD which was achieved by a simple one-step electrochemical synthesis using both constant potential and cyclic voltammetry (CV) techniques. The film characterisation and consequently the redox properties of the polymer films were also analysed using CV. Electrochemical quartz crystal microgravimetry (EQCM) measurements were also obtained for the PPy/Sβ-CD films, to obtain information on its ion exchange properties.

## 3.2 Experimental

### 3.2.1 Materials

#### *3.2.1.1 Reagents*

Pyrrole monomer (98 %) was obtained from Aldrich and was purified by distillation prior to experimental procedures. It was stored in the dark in the fridge. Unless otherwise stated, 0.20 mol $dm^{-3}$ (0.35 ml in 25 ml supporting electrolyte) of pyrrole was dissolved in the electrolyte solution for all electrochemical deposition experiments. Analytical reagents, sodium sulfate ($Na_2SO_4$), sulfonated β-cyclodextrin (Sβ-CD) sodium salt (substitution ca. 7-11 moles per mole of β-CD as reported by Aldrich), sodium chloride (NaCl) and *para*-toluene-sulfonic (PTS) acid were purchased from Aldrich and used as received. Distilled water was used in all solution preparations.

#### *3.2.1.2 Electrodes and Instruments*

For the bulk experiments electrochemical deposition of PPy and analysis of the samples was carried out using a Solartron Model SI 1285 potentiostat. All measurements were made at room temperature. A platinum wire (99 %, 1 mm in diameter) electrode where the exposed surface area was recorded separately for every experiment was used for the deposition of PPy. A SCE and a platinum wire CE were also used in the electrode set up. For the CV experiments a platinum disc electrode encased in a Teflon holder, previously described in Chapter 2, Figure 2.3 was used with an exposed surface area of 0.1256 $cm^2$. In

both cases, the wire and the disc electrode were polished using a 1 μm diamond polish and Buehler micro-cloth and rinsed well with distilled water to ensure a smooth surface finish, as outlined in Chapter 2.

For the mass change analyses, electrochemical quartz crystal microgravimetry (EQCM) measurements were performed with a CHI440 instrument. The polymers were deposited onto polished Au quartz crystal electrodes (Cambria Scientific) with an exposed surface area of 0.203 $cm^2$. The electrochemical cell consisted of a specially made Teflon holder in which the crystal was placed between two o-rings (CHI125), a picture of which is shown in Figure 3.1. The set up was completed using a platinum wire counter and a 3.0 mol $dm^{-3}$ Ag/AgCl reference electrode.

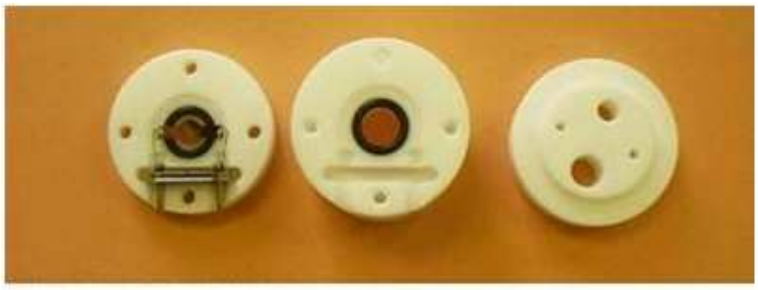

**Figure 3.1:** Picture of the Teflon holder including the o-rings where the crystal is placed during EQCM.

The conductivity measurements were carried out using a Jenway 4510 conductivity meter, while optical images were carried out of an Olympus BX51M system using Leica application suite and Olympus DP Version 3.2 and the EDAX and SEM were performed on a Hitachi FE-Scanning Electron Microscope.

## 3.2.2 Procedures

### *3.2.2.1 Polymer film preparation*

The synthesis of PPy was carried out using an electro-synthesis method, which deposited the polymer film at the working electrode. Polymers were prepared

in various electrolyte solutions containing 0.20 mol $dm^{-3}$ pyrrole, unless otherwise stated. A summary of the various electrolytes used in the electrochemical deposition of PPy are given in Table 3.1. PPy was grown in a conventional three-electrode cell where a saturated calomel reference electrode (SCE) and a platinum wire counter electrode were used. A platinum wire (99 %, 1 mm in diameter) electrode was used as the working electrode in the majority of cases. For the imaging analysis flat platinum or glassy carbon disc electrodes (SA = 0.1256 $cm^2$) were utilised. For the CV characterisation the polymers were deposited onto Pt disc electrodes encased in Teflon (SA = 0.1256 $cm^2$).

**Table 3.1:** Summary of the electrolytes used for the deposition of PPy.

| Electrolyte | Concentration / mol $dm^{-3}$ |
|---|---|
| Sodium sulfate, $Na_2SO_4$ | 0.10, 0.05, 0.01 |
| Sodium chloride, NaCl | 0.10, 0.05, 0.01 |
| *para*-toluene-sulfonic acid, PTS | 0.10, 0.05, 0.01 |
| Sulfonated β-cyclodextrin, Sβ-CD | 0.10, 0.05, 0.01 |

To investigate if Sβ-CD was a suitable electrolyte to polymerise pyrrole, conductivity measurements on a series of Sβ-CD concentrations were obtained. A 2.0 x $10^{-2}$ mol $dm^{-3}$ Sβ-CD solution was prepared in deionised water from which a series of solutions were generated by serial dilution to 2.0 x $10^{-5}$ mol $dm^{-3}$. The conductivity of each solution was measured and corrected for the conductivity of deionised water, at 25 $^0$C. PPy/Sβ-CD films were subsequently grown potentiostatically by applying a constant potential in the range of 0.600 to 1.000 V vs. SCE, for a desired time or until a certain charge was passed. The growth solution was an aqueous pyrrole/Sβ-CD mixture with 0.20 mol $dm^{-3}$ pyrrole and 0.01 mol $dm^{-3}$ Sβ-CD, unless otherwise stated. In this way Sβ-CD sodium salt is the only electrolyte present and so was incorporated into the growing PPy film as the charge balancing counter anion. Conductivity measurements were also performed on the supporting electrolytes used during the electrochemical polymerisation of pyrrole.

The various techniques employed included constant potential (V), and cyclic voltammetry (CV). For CV growth the potential was swept from 0.000 to 0.800 V vs. SCE at a scan rate of 50 mV $s^{-1}$, where the cycle number was varied. For constant potential experiments, a potential in the range of 0.600 to 1.000 V vs. SCE was applied until a sufficient charge was passed.

### *3.2.2.2 Film characterisation*

After electrochemical deposition, the PPy films were characterised using CV. A three electrode cell was used for all CV experiments. A platinum disc electrode, encased in Teflon, was used as the working electrode, a SCE and platinum wire was used as the reference and counter electrodes, respectively. The redox properties of the PPy films were monitored by cycling in a potential window of -0.900 to 0.900 V vs. SCE, in a monomer solution containing 0.20 mol $dm^{-2}$ pyrrole and the supporting electrolytes shown in Table 3.1, or in a monomer free electrolyte.

For the optical images, polymers were synthesised onto an Au disc electrode from an aqueous solution of 0.10 mol $dm^{-3}$ $Na_2SO_4$ or a 0.01 mol $dm^{-3}$ Sβ-CD solution, in the presence of 0.20 mol $dm^{-3}$ pyrrole at 0.900 V until a charge of 0.3, 1.0 or 3.0 C $cm^{-2}$ were passed. For the SEM and EDAX measurements, PPy/Sβ-CD polymers were electrochemically deposited from an aqueous solution of 0.20 mol $dm^{-3}$ pyrrole and 0.01 mol $dm^{-3}$ Sβ-CD, onto flat Pt disc electrodes at 0.900 V vs. SCE to a charge of 3.0 C $cm^{-2}$, unless otherwise stated. Samples were sputtered coated with gold prior to analysis.

### *3.2.2.3 Electrochemical quartz crystal microgravimetry*

In the case of the EQCM measurements, PPy films were electrochemically deposited onto gold quartz crystal electrodes with an active surface area (SA) of 0.2033 $cm^2$, at an oxidation potential of 0.700 V vs. SCE from a solution of 0.20 mol $dm^{-3}$ pyrrole and 0.10 mol $dm^{-3}$ $Na_2SO_4$ or 0.01 mol $dm^{-3}$ Sβ-CD, respectively. All solutions were prepared using distilled water. A Pt wire was

used as a counter electrode while a 3.0 mol $dm^{-3}$ Ag/AgCl electrode was used as the reference.

The EQCM electrodes were placed in between two O-rings of the commercially designed Teflon holder, as shown in Figure 3.1. This setup was then connected to the external oscillator box which measured the frequency change. Unless otherwise stated, the charge passed during polymer formation was 1.50 x $10^{-2}$ C $cm^{-2}$. For the EQCM measurements during CV experiments, films electrodeposited using Sβ-CD as the dopant were placed in a 0.10 mol $dm^{-3}$ $Na_2SO_4$ solution and cycled between -0.900 and 0.600 V vs. SCE at scan rates of 50 and 5 mV $s^{-1}$. The frequency shift, caused by changes in the mass during the electrochemical experiments, was measured using a frequency counter and related to mass using the Sauerbrey equation, Equation 2.1, Section 2.5.1.

## 3.3 Results and Discussion

### 3.3.1 Polymer synthesis

It is well known that during electrochemical polymerisation of pyrrole (Py), positively charged chains of the polymer are created. In order to maintain charge neutrality anionic counter ions, or dopants, are taken up into the polymer film. The electropolymerisation of pyrrole can be represented by the simple scheme, depicted in Figures 3.2 and 3.3, where A- represents the counter ion.

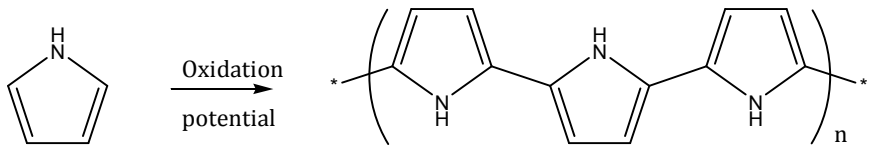


Pyrrole PPy

**Figure 3.2:** Schematic representation of the electrochemical polymerisation of pyrrole to form PPy, with the polymer presented in the reduced state.

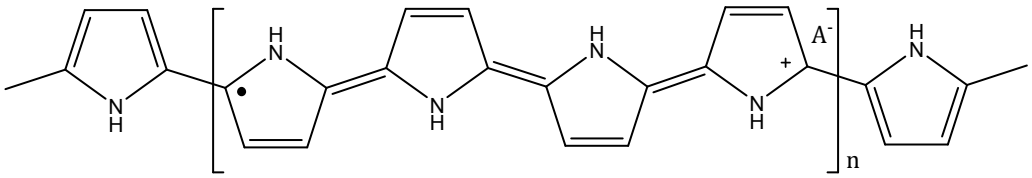


**Figure 3.3:** Structure of partially doped PPy, $A^-$ represents the dopant anion.

The PPy oxidation level is reported to be between 0.20 and 0.33 per monomer unit depending on the nature of the dopant anion. This means that for every 3 to 4 monomer subunits a counter ion is needed to maintain charge neutrality, as indicated in Figure 3.3.[9] Commonly, small mobile anions, such as chlorides, are used as dopants for the electrochemical deposition of PPy. When large anions are used, such as polystyrene sulfonate (PSS)[10] or Nafion[11], these bulky anions remain entrapped in the polymer film and are not involved in the redox reaction. This is also the case for the anionic dopant used in these studies, Sβ-CD.

It is also important to point out the reason for choosing the β-CD over the α-CD or indeed the γ-CD. As mentioned in Chapter 1, the most common commercially available cyclodextrins are the α-CD, β-CD and the γ-CD which differ in the number of glucose units present, 6, 7 or 8, respectively. The cavity size depends on the number of glucose units, with the β-CD cavity being the most acceptable size for including compounds for drug delivery, whereas the α-CD is known to be insufficent in size for many drugs[12], while the γ-CD is very expensive. It should also be highlighted that to the best of our knowledge there has been very little research shown on the electrochemical synthesis of PPy/Sβ-CD films and from the literature that was reviewed the polymerisation of the polymer films was continually deposited in the presence of an additional supporting electrolyte, lithium perchlorate ($LiClO_4$).[13] However, it must be pointed out that the work presented by Temsamani and colleagues[13] shows the electrochemical synthesis of the polymers at extreme oxidation potentials cycled up as high as 1.800 V vs. SCE. At these potentials, the PPy films are well known to over-

oxidise.[9] The over-oxidation of the PPy film is an irreversible process and leads to the degradation of the film which in turn leads to the loss of the redox activity, the conductivity and hence the electroactivity of the polymer.[14, 15] For Temsamani and co-workers, these high potentials can only lead to increased porosity of the polymer film and, therefore, a higher affinity for the electrochemical activity of the electrode surface to be observed. In analysing their data presented in the papers, the CV plots illustrate redox activity more than likely attributed to the gold oxide forming from the gold substrate used during electrochemical deposition.

An important factor in both the physical properties and the morphology of PPy films is the nature of the doping anion. It is documented that in general ~30 % of the weight of the polymer corresponds to the dopant.[16] The dopant anion can be organic or inorganic. Some prime examples vary from the extensively used chloride anion to pharmaceutically important compounds, such as adenosine 5'-triphosphate (ATP)[17, 18] and dexamethasone[6]. They can also vary in size from *para*-toluene sulfonic acid (PTS)[19, 20] to dodecylbenzenesulfonate (DBS)[14], the size of the dopant can control the structure and porosity of the polymer.[16] Kassim *et al.*[21] reported that the stability and mechanical properties of PPy films were enhanced in the presence of large anionic dopants over smaller ones. It is reported that PPy/$SO_4$ films differ from PPy films doped with large entrapped dopants.[22]

For the formation of the PPy films used in this study, two methods were employed; the first, CV, was used to determine the oxidation potential of the monomer in the presence of Sβ-CD and other dopants, for comparative purposes. The second method was constant potential polymerisation, which involved the application of a constant potential to the electrode in the presence of the monomer solution and supporting electrolyte.

### *3.3.1.1 Investigations on the growth of PPy in various dopant electrolytes*

To acknowledge that Sβ-CD is a suitable electrolyte for the polymerisation of pyrrole, conductivity measurements of Sβ-CD in varying concentrations were obtained. In the case of Sβ-CD the conductivity increases linearly with increasing concentration as shown in Figure 3.4, this is evidence of the presence of a strong electrolyte.[23] A good linear correlation value of 0.997 was obtained for these data. Figure 3.5 shows the molar conductivity as a function of the square root of the Sβ-CD concentration. Although a linear plot was not obtained between the molar conductivity and the square root of concentration to satisfy the relationship, $\Lambda = \Lambda^o - b\sqrt{c}$, which is characteristic of a strong electrolyte, the molar conductivity is high. Moreover, a near-linear relationship is observed as the limiting molar conductivity is approached, as opposed to the exponential relationship which is typical of weak electrolytes. This is a further indication for a strong electrolyte. Therefore, it can be concluded that Sβ-CD is an appropriate electrolyte to dope the polymer and no other supporting electrolyte is necessary.

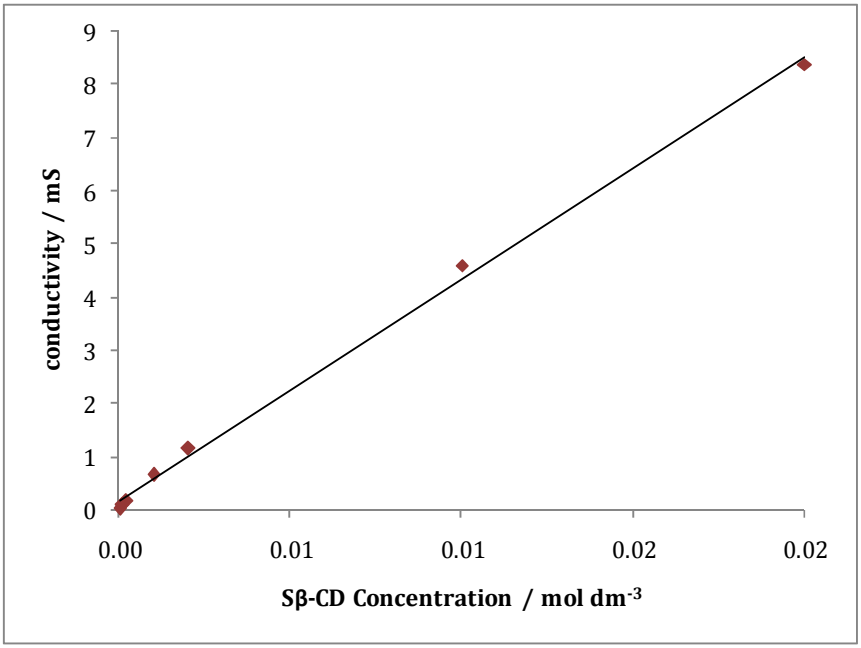


**Figure 3.4:** Conductivity of Sβ-CD measured at 25 $^0$C as a function of concentration.

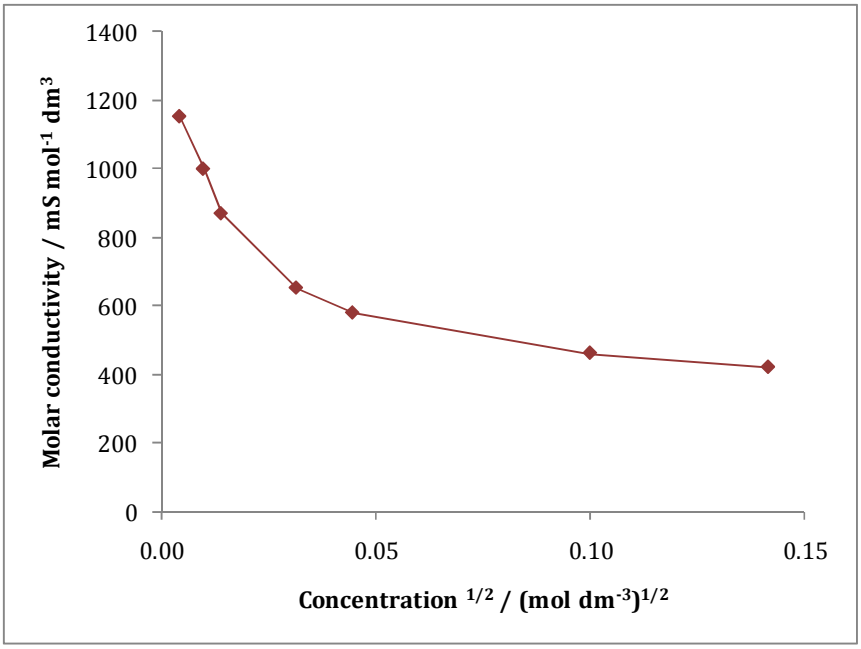


**Figure 3.5:** Molar conductivity of Sβ-CD as a function of the square root of concentration.

Figure 3.6 shows representative CV data for the electropolymerisation of pyrrole in NaCl, $Na_2SO_4$, PTS and Sβ-CD electrolytes. An oxidation wave corresponding to electron transfer and oxidation of the monomer is seen for all dopant anions. It is clearly evident that the oxidation potential of the monomer varies with the nature of the dopant. For example, the oxidation of pyrrole occurs at 0.530, 0.584, 0.589 and 0.595 V vs. SCE for the Sβ-CD, PTS, $Na_2SO_4$ and NaCl systems, respectively, indicating easier oxidation of the monomer in the Sβ-CD electrolyte. Furthermore, the rate of oxidation, as evidenced from the slope of the current-potential curve between 0.600 and 0.900 V vs. SCE, varies considerably with the nature of the dopants. The rate of oxidation is observed as: Sβ-CD > PTS > $Na_2SO_4$ > NaCl. Indeed, the rate of oxidation is 0.098 A $V^{-1}$ for the Sβ-CD system compared to 0.023 A $V^{-1}$ for the chloride system, a significant 4-fold increase in the presence of the Sβ-CD anions. Again, this clearly indicates a higher rate of oxidation of the pyrrole monomer in the Sβ-CD electrolyte. According to the mobility of the anions this is an unusual result, as the mobility

of the anions would follow the opposite trend, i.e., NaCl > $Na_2SO_4$ >PTS > Sβ-CD. Furthermore, the Sβ-CD will have a much lower mobility than the other anions due to its large size.

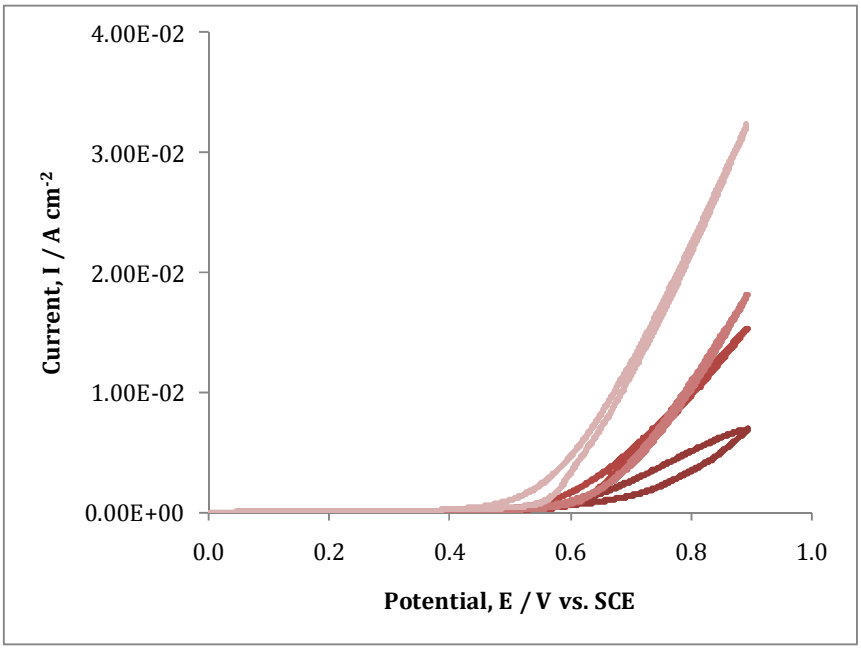


**Figure 3.6:** Cyclic voltammograms, first cycle, for the polymerisation of pyrrole in the presence of 0.20 mol $dm^{-3}$ pyrrole and 0.05 mol $dm^{-3}$ concentrations of various dopants. NaCl $Na_2SO_4$ PTS and Sβ-CD . The potential was swept from 0.000 to 0.900 V vs. SCE at a 50 mV $s^{-1}$.

Although the electrolytes are maintained at equal concentrations, the conductivity and ionic strength of the solutions will vary. The ionic strength of each solution was computed using Equation 3.1, where $c_A$ is the molar concentration of ion, A, and $z_A$ is the charge number of that ion, and the sum is taken over all ions in the solution.

$$I_c = \frac{1}{2}\Sigma c_A z_A^2 \qquad 3.1$$

These parameters are provided in Table 3.2. The high anionic charge on the Sβ-CD, approximately 7-11 anionic sites, provides the solution with a high ionic strength and a higher conductivity which certainly will have some role to play in the higher rates of oxidation of the monomer and higher rates of electropolymerisation.

**Table 3.2:** Conductivity measurements and ionic strength for each supporting electrolyte.

| **Dopant / 0.05 mol dm$^{-3}$** | **Conductivity/ mS** | **Ionic strength / mol dm$^{-3}$** |
|---|---|---|
| Sβ-CD | 21.40 | 2.25 |
| PTS | 16.89 | 0.05 |
| $Na_2SO_4$ | 8.65 | 0.15 |
| NaCl | 2.82 | 0.05 |

Figure 3.7 illustrates the CV data obtained for the deposition of PPy films in the presence of Sβ-CD and in the presence of a 10-fold increase in the concentration of chloride (0.5 mol dm$^{-3}$). Now, these two electrolytes have similar conductivities. In comparing these two voltammograms, there is very little difference between the traces. The oxidation of the monomer and subsequent currents reached are in close agreement. This verifies that conductivity is a major influence in the polymerisation of these polymers and accounts for the apparently higher rates observed with the Sβ-CD, Figure 3.6.

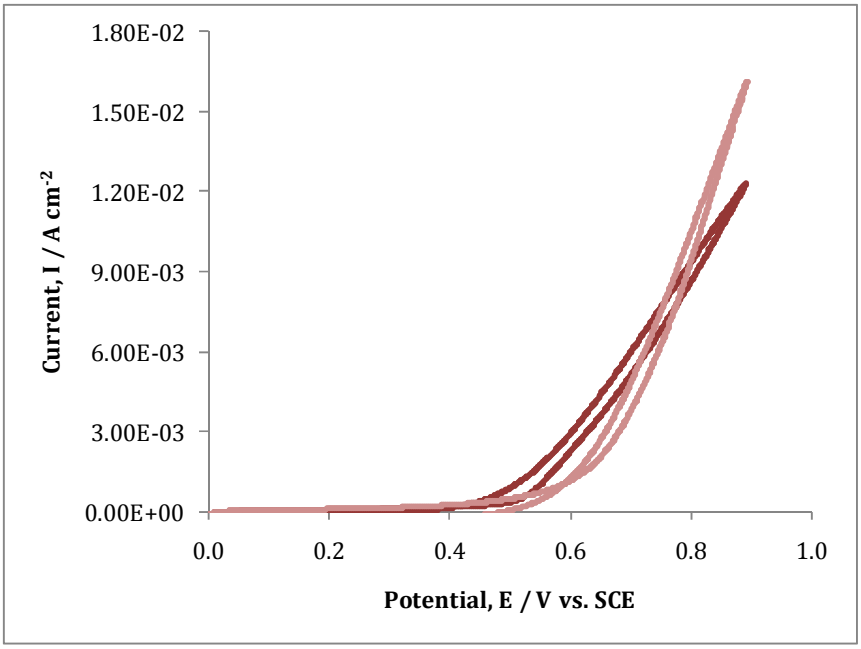


**Figure 3.7:** Cyclic voltammograms for the deposition of PPy, onto a Pt disk electrode in the presence of 0.20 mol $dm^{-3}$ pyrrole and ♦0.01 mol $dm^{-3}$ Sβ-CD and ♦0.10 mol $dm^{-3}$ NaCl. The potential was swept from 0.000 to 0.900 V vs. SCE.

It is has been reported that a shift of the anodic potential in the positive direction, during the electrochemical polymerisation of pyrrole in the presence of a neutral β-cyclodextrin, is due to the formation of an inclusion complex between the monomer and the CD. For example, Arjomandi and Holze observed an increase in the oxidation potential of pyrrole in the presence of a neutral β-CD in $LiClO_4$.[24] This was not observed in this work, as is clearly deduced from Figures 3.6 and 3.7, where there is no evidence of any anodic potential shift in the oxidation potential of pyrrole. However, this possibility was further investigated using NMR. Figure 3.8 shows the NMR spectra obtained for a sample of pyrrole monomer in the absence and presence of an excess of Sβ-CD. It has been well documented that if an inclusion complex is formed, a change in the chemical shift is observed.[25] In the case presented here, no alteration in the chemical shift was observed, suggesting no complexation. Clearly, complexation does not occur between the Sβ-CD and the pyrrole monomer.

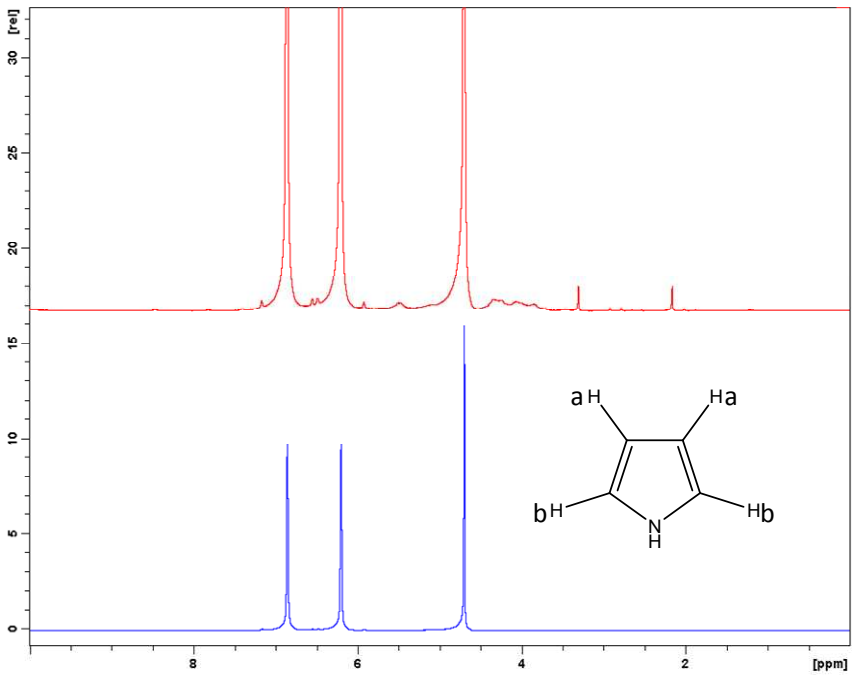


**Figure 3.8:** NMR spectra of ♦Py monomer ♦Py monomer with a 4-fold excess of Sβ-CD in $D_20$. (300 MHz, $D_2O$): δ 6.78 (2H, *d*, a-H), δ 6.23 (2H, *d,* b-H).

In order to gain more information on the growth of PPy in the presence of Sβ-CD, additional experiments were performed to probe the influence of the concentration of the Sβ-CD and the monomer on the rate of electropolymerisation.

Figure 3.9 shows the CV data obtained for the electropolymerisation and simultaneous redox activities of the polymer film doped in the presence of 0.01 mol $dm^{-3}$ Sβ-CD. There is a clear change in the voltammograms as the cycle number increases, with an increase in the peak current, corresponding to the oxidation of the polymer, at ~ -0.2 V vs. SCE and an increase in the reduction peak, observed at ~ -0.6 V vs. SCE. This is consistent with the deposition of high amounts of conducting PPy.

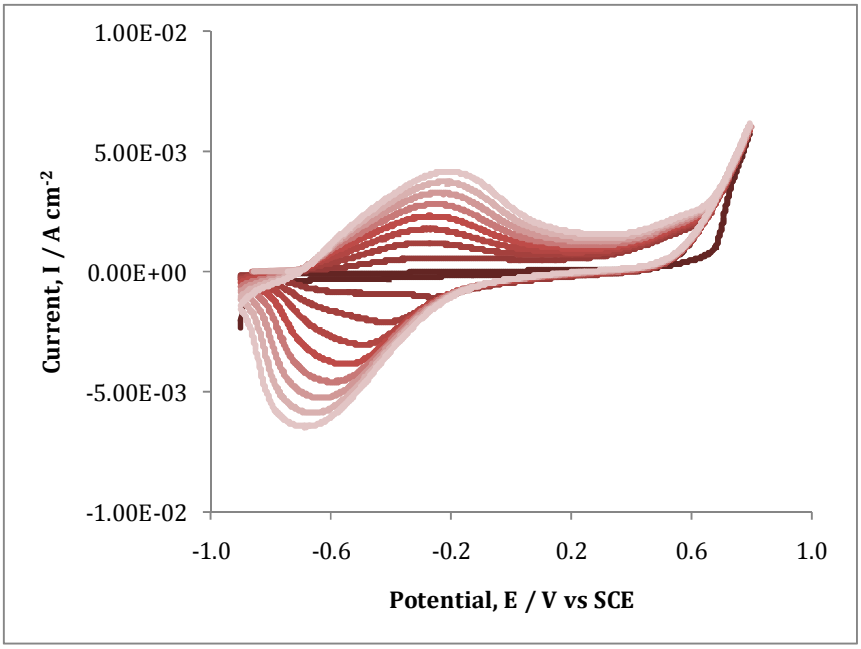


**Figure 3.9:** CV of PPy/ Sβ-CD in the presence of 0.05 mol $dm^{-3}$ pyrrole and 0.01 mol $dm^{-3}$ Sβ-CD

Figure 3.10 shows the current, measured at a potential of ~-0.2 V vs. SCE taken from the cyclic voltammograms depicted in Figure 3.9, plotted as a function of cycle number. The polymers were deposited onto platinum in the presence of increasing concentrations of Sβ-CD. It is clear that as the concentration of Sβ-CD is increased, the rate of oxidation of the monomer and the rate of polymer growth increase. Also, the current continues to increase with cycle number. The continued increase in current indicates that the deposited PPy is indeed conducting, even after 40 cycles of high rates of polymer growth.

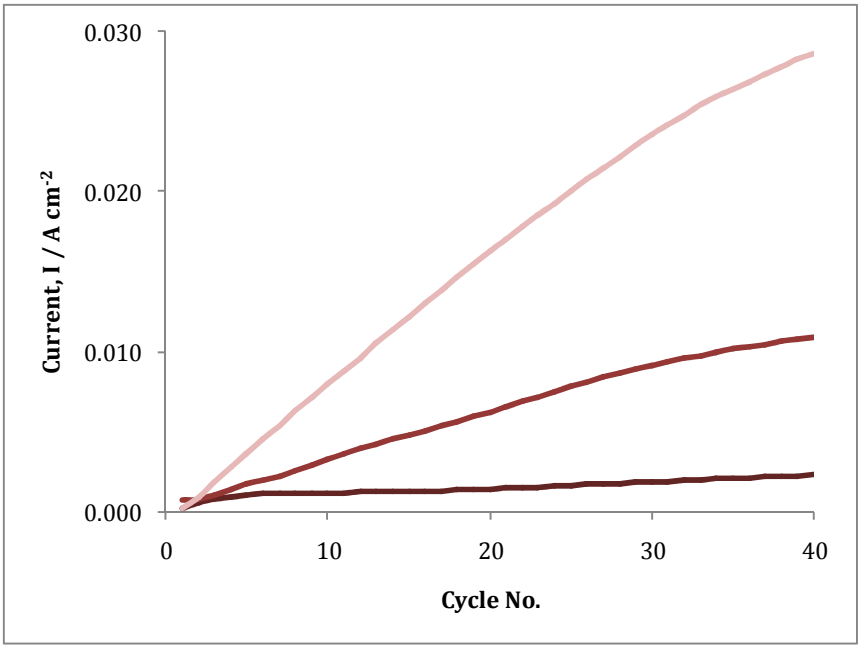


**Figure 3.10:** Current as a function of cycle number for the growth of PPy on a Pt disc electrode, in the presence of 0.20 mol $dm^{-3}$ pyrrole and varying concentration of Sβ-CD, 0.01 0.05 and 0.10 mol $dm^{-3}$. The voltammograms were recorded from -0.900 to 0.800 V vs. SCE at a 50 mV $s^{-1}$.

More detailed information on the rate of deposition of the polymer can be obtained by using the charge in the voltammograms where oxidation of the monomer is not contributing to the current. Figure 3.11 shows the integrated anodic charge of the oxidation peak shown in Figure 3.9, as a function of cycle number for varying concentrations of the monomer (Py) in the presence of a constant concentration of the Sβ-CD. In this case, the computed charge is dominated by the oxidation of the deposited polymer, and it can be taken as a measure of the amount of polymer deposited. It is clear from this figure that the amount of PPy deposited increases at a faster rate in the presence of higher concentrations of the monomer. The rate of growth, which can be measured from the slopes of the linear charge-time plots (charge-cycle number) were calculated as 1.63, 1.89, 1.91, and 2.13 C $cm^{-2}$ $s^{-1}$ for monomer concentrations of 0.05, 0.10, 0.15 and 0.20 mol $dm^{-3}$, respectively. These findings are in good agreement with literature reports where the monomer concentration is

important in the kinetics of polymer growth. Indeed, Kim *et al.*[26] reported similar observations for the polymerisation of pyrrole in the presence of a large anion tetrabutylammonium perchlorate (TBAP).

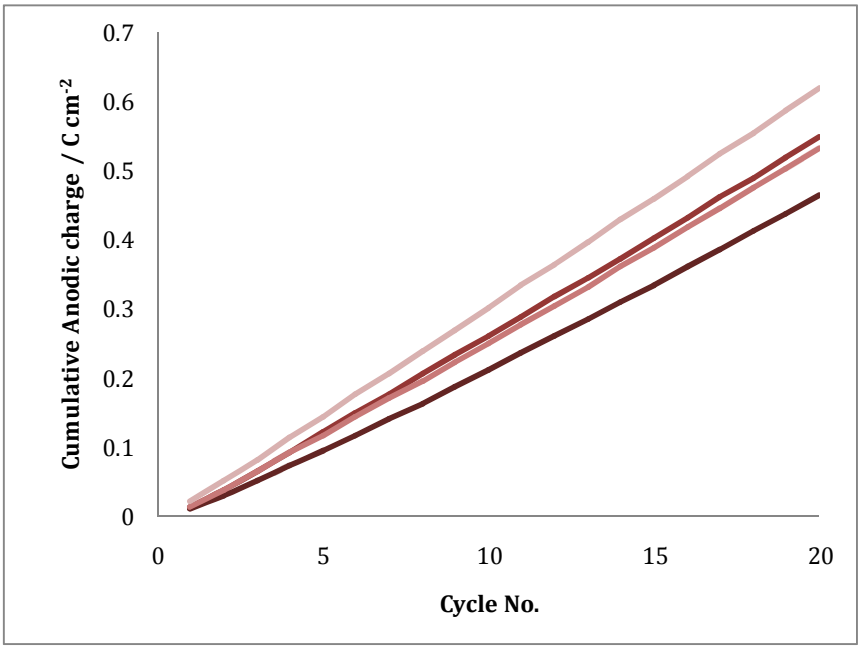


**Figure 3.11:** Accumulative anodic charge for the oxidation of the pyrrole monomer during electrochemical polymerisation in various pyrrole concentrations. The Sβ-CD concentration was held at 0.01 mol $dm^{-3}$ and the pyrrole concentration was 0.20 0.15 0.10 and 0.05 mol $dm^{-3}$. The potential was swept from -0.900 V to 0.800 V vs. SCE at 50 mV $s^{-1}$.

A similar analysis showing the influence of the concentration of the Sβ-CD is provided in Figure 3.12, where the charge integrated under the oxidation peak is plotted as a function of cycle number. Again, linear plots are obtained and the influence of the dopant anion can be seen by a comparison of the slopes of these plots. At the higher Sβ-CD concentration of 0.10 mol $dm^{-3}$, the rate of growth is given as 8.74 C $cm^{-2}$ $s^{-1}$ compared to the value of 2.13 C $cm^{-2}$ $s^{-1}$ for the lower Sβ-CD concentration, 0.01 mol $dm^{-3}$. This highlights the significant role of the Sβ-CD anion in the deposition of PPy and is in good agreement with results obtained with smaller dopant anions, such as nitrates. [27]

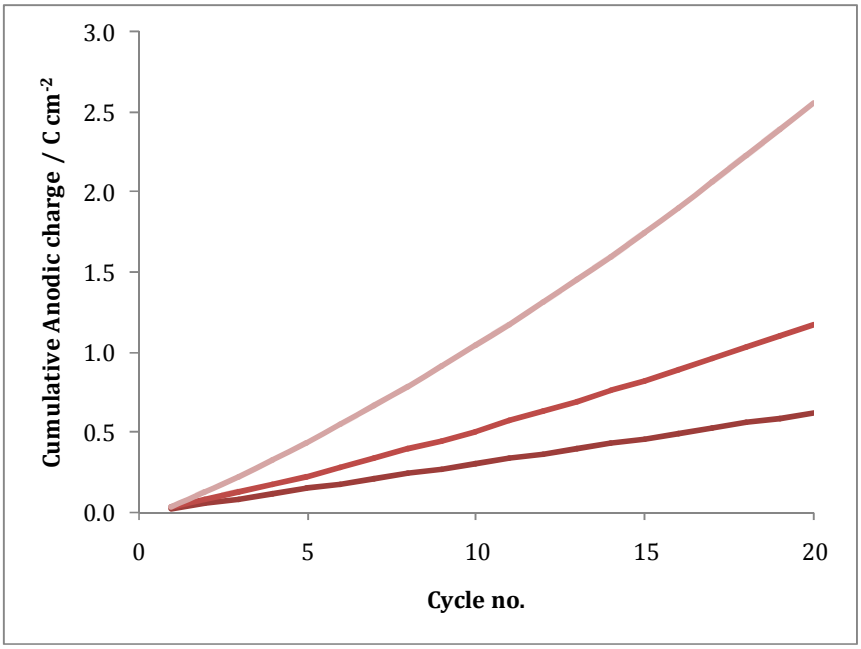


**Figure 3.12:** Accumulative anodic charge for the oxidation of the pyrrole monomer during electrochemical polymerisation in various Sβ-CD concentrations. The pyrrole concentration was held at 0.20 mol $dm^{-3}$ and the Sβ-CD concentration was varied from 0.01 0.05 and 0.10 mol $dm^{-3}$. The potential was swept from -0.900 V to 0.800 V vs. SCE at 50 mV $s^{-1}$.

### *3.3.1.2 Polymer synthesis using constant potential*

Baker and Reynolds[10] have comprehensively discussed the mechanism behind the polymerisation of pyrrole during electrochemical oxidation at a constant potential, as previously discussed in Chapter 1. They report that the current-time transients obtained during the polymerisation of pyrrole occur in three stages. The first stage described by Baker and Reynolds was the current spike whose decay is dependent on potential and is said to represent the electrode surface coverage with a monolayer thick polymer film. The second stage involves the rise in current lasting for a number of seconds and the third stage is represented by the continued current flow for the remainder of the electrochemical deposition.

The three stages described by Baker and Reynolds were observed during the potentiostatic deposition of the PPy films in the presence of 0.01 mol $dm^{-3}$ Sβ-CD. Figure 3.13 shows a typical current-time plot for the potentiostatic growth of PPy films onto a platinum electrode in the presence of 0.01 mol $dm^{-3}$ Sβ-CD. The electrochemical deposition shown in this figure was achieved at 0.700 V vs. SCE. It is evident from this figure that the initial current spikes, which is associated with the nucleation process of the electrosynthesis of PPy, and this is followed by a rise in current until a plateau is reached. Many papers have also reported current-time plots for the electrochemical polymerisation of pyrrole showing this behaviour.[28, 29] This typical result is in agreement with various other reports where the polymer film deposition onto the electrode surface is achieved through a mechanism generally accepted for the cathodic synthesis of a metal onto a particular substrate.[29]

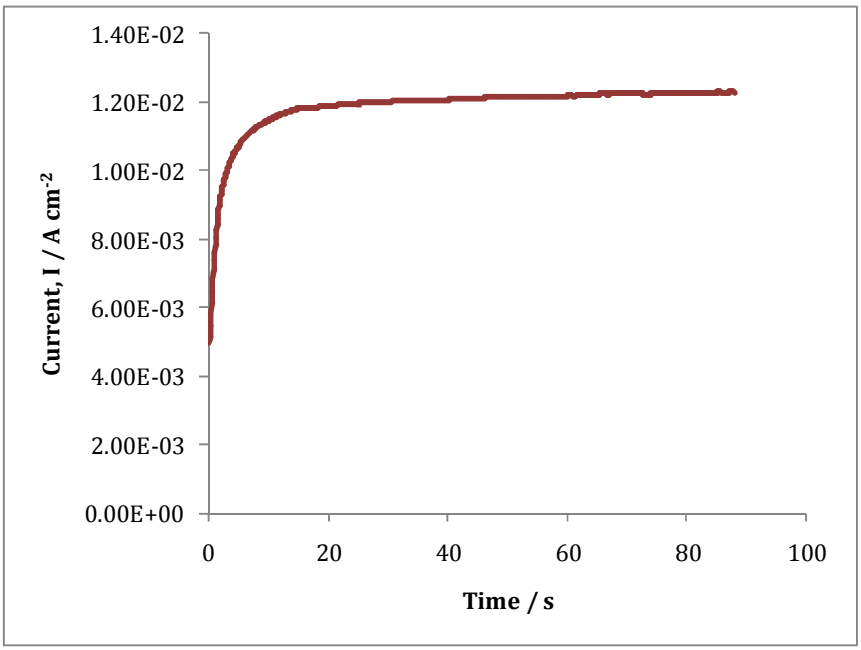


**Figure 3.13:** Current-time plot for the potentiostatic growth of PPy at 0.900 V vs. SCE to a charge of 1.0 C $cm^{-2}$. Polymers were electrochemically deposited onto Pt wire in the presence of 0.2 mol $dm^{-3}$ Py and 0.01 mol $dm^{-3}$ Sβ-CD.

Figure 3.14 shows the current as a function of time for the polymerisation of 0.20 mol $dm^{-3}$ pyrrole in the presence of 0.01 mol $dm^{-3}$ Sβ-CD at various oxidation potentials. It can be seen from this figure that the magnitude of the current increases as the deposition potential is made more positive. These observations are in agreement with the results recorded by Asavapiriyanont *et al.*[28] for the potential deposition of PPy in the presence of aqueous $KNO_3$ solutions and demonstrate that the shape of the current-time transients correspond to immediate nucleation with three-dimensional growth. Reece *et al.*[30] also commented on the increase in current observed as a result of increasing potential during the growth of PPy films, on platinum, in the presence of both α and β sulfonated cyclodextrins.

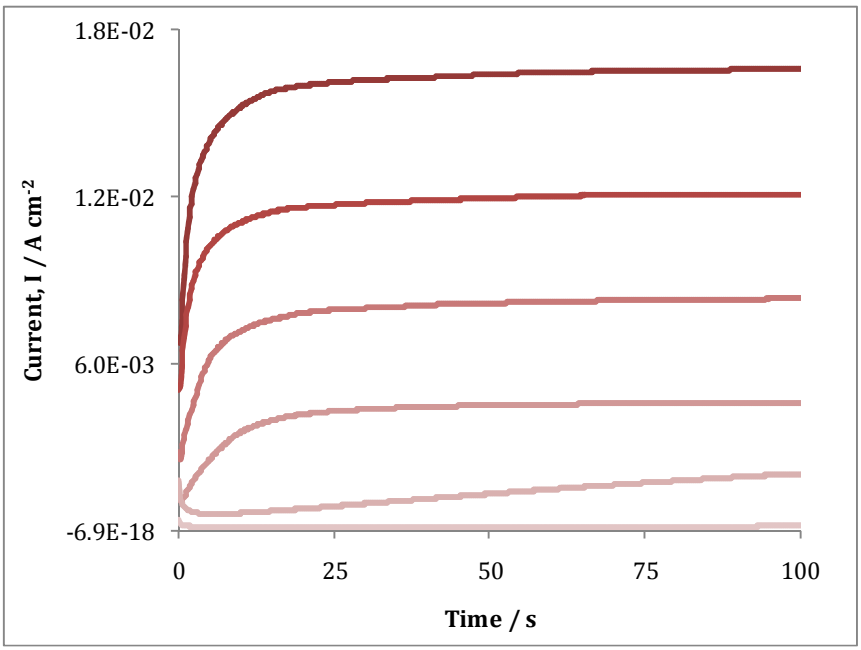


**Figure 3.14:** Current as a function of time for the potentiostatic growth of PPy at various potentials to a charge of 1.00 C $cm^{-2}$. Polymers were electrochemically deposited onto Pt wire in the presence of 0.20 mol $dm^{-3}$ Py and 0.01 mol $dm^{-3}$ Sβ-CD.

1.0 V, 0.9 V, 0.8 V, 0.7 V, 0.6 V and 0.5 V vs. SCE.

Figure 3.15 illustrates the steady-state current as a function of potential for the data shown in Figure 3.14. The slope of the current-potential trace for the lower potentials was recorded at 0.019 A $cm^{-2}$ $V^{-1}$ and 0.039 A $cm^{-2}$ $V^{-1}$ in the case of the higher potentials. Therefore, the rate of the reaction approximately doubles as the potential increases from 0.500 V to 0.700 V vs. SCE.

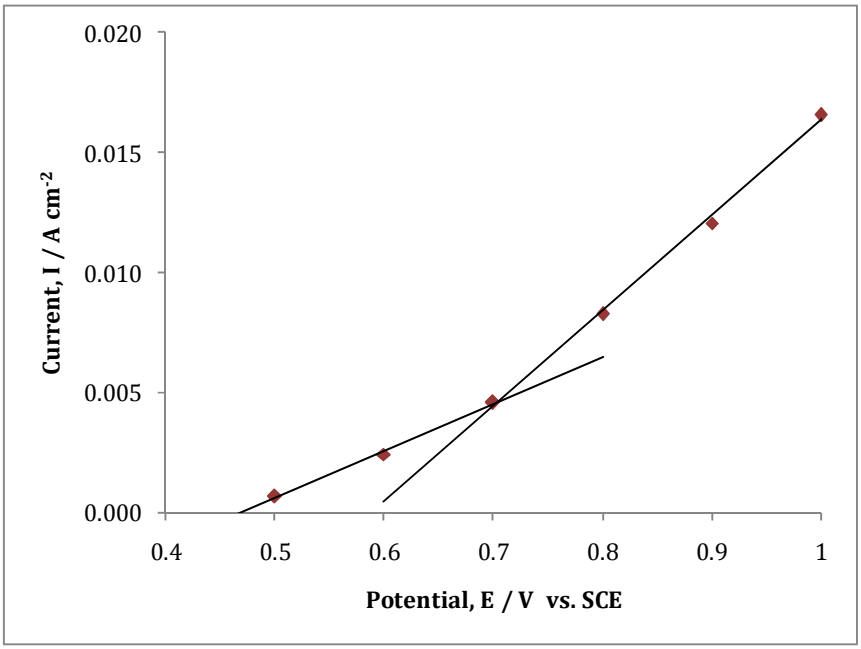


**Figure 3.15:** Current as a function of potential applied during the electropolymerisation of pyrrole. Polymers were electrochemically deposited onto Pt wire in the presence of 0.20 mol $dm^{-3}$ Py and 0.01 mol $dm^{-3}$ Sβ-CD.

## 3.3.2 Film characterisation

### *3.3.2.1 Probing the redox properties using CV*

Cyclic voltammetry is a technique widely used for the characterisation of the electroactivity of conducting polymers.[9] Redox properties of PPy films are associated with the exchange of ions, be they anionic, cationic, or both. These exchange properties are significantly dependent on the dopant used during polymerisation.[14] The redox properties of a number of polymer films doped with various counter ions were investigated using CV. It is well demonstrated in

the literature that in the presence of large anionic dopants that are immobilised into the polymer films the first electrochemical reduction is due to the uptake of cations to compensate for the anions present from the bulky entrapped dopant in the polymer film. This is very different to the anion exchange properties of the classical polymer doped with small, mobile anions.[31]

Figure 3.16 shows the CV data for the polymerisation of pyrrole and the subsequent redox activity of the film, in the presence of 0.20 mol $dm^{-3}$ pyrrole and 0.01 mol $dm^{-3}$ of Sβ-CD. The oxidation peak observed at ~ 0.5 V represents the oxidation of the monomer. These PPy/Sβ-CD films only take up and release cations, which is due to the large bulky nature and immobility of the anionic cyclodextrin. The well defined broad reduction and oxidation peaks, which are highlighted in this figure, can be attributed to the uptake and release of $Na^+$ cations.

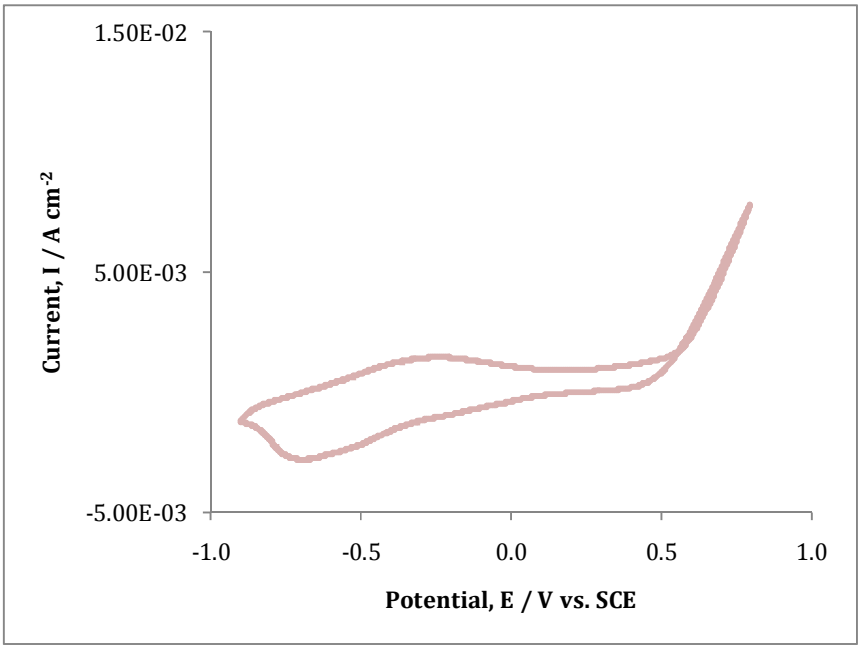


**Figure 3.16:** CV voltammogram, 20th cycle, at 50 mV $s^{-1}$ recorded for PPy/Sβ-CD electrodes in 0.20 mol $dm^{-3}$ pyrrole in the presence of 0.01 mol $dm^{-3}$ Sβ-CD. Highlighted is the oxidation/reduction of the PPy film.

As reported in the literature, the properties of the dopant anions, such as size, charge and mobility, are very important in distinguishing the characteristics of the conducting polymer.[22, 32] Figure 3.17 shows the CV data obtained for the electropolymerisation and simultaneous redox activities of the polymer film doped in the presence of various dopants at a concentration of 0.10 mol $dm^{-3}$. It is obvious from these data that the redox activities of the PPy/Sβ-CD are far more superior and well-defined compared to the PPy/Cl and PPy/$SO_4$ films. It has been well documented that the redox peaks corresponding to the chloride and sulfate dopants can be hard to distinguish and appear broad and give ill-shaped cyclic voltammograms.[22]

On the other hand, well defined redox peaks are visible with the PPy/Sβ-CD film, as evident in Figures 3.16 and 3.17. Interestingly, the reduction peak is sharper than the corresponding oxidation peak, indicating a considerable variation in the kinetics of the two processes. The broad oxidation peak indicates a slow conversion of the polymer from the reduced to oxidised state, while the sharper reduction peak indicates a faster rate of reduction. This is somewhat unusual as during oxidation of the polymer, the layer next to the electrode surface is oxidised first giving a conducting layer which facilitates oxidation of the adjacent layers until the conducting zone reaches the solution. Conversely, on reduction of the polymer, the layer adjacent to the electrode is reduced first to give an insulating interface, making the overall reduction process more difficult and slower. The sharper reduction wave is a clear indication that the incorporation of $Na^+$ during the reduction of the polymer is a relatively fast process, $PPy^{n+}S\beta\text{-}CD^{n-} + ne^- \rightarrow PPy^{o}S\beta\text{-}CD^{n-}(nNa^+)$, whereas the oxidation of the polymer is much slower due to a slow release of $Na^+$, or alternatively the slow incorporation of anions, to balance the charge.

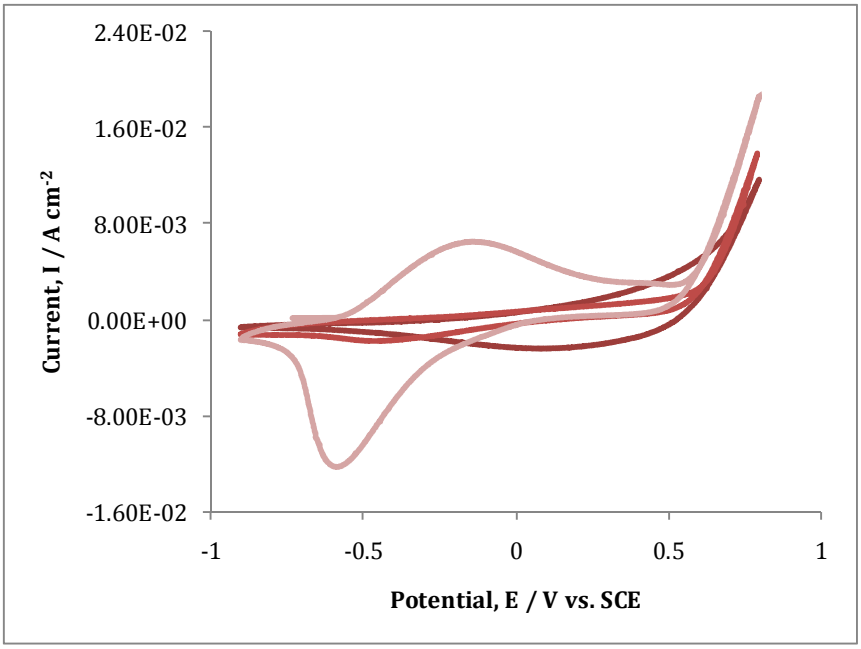


**Figure 3.17:** CV voltammograms of PPy films in the monomer solution containing the pyrrole monomer, 0.20 mol $dm^{-3}$, in the presence of 0.10 mol $dm^{-3}$ NaCl $Na_2SO_4$ and $Na_n$Sβ-CD. This analysis was obtained from cycle 20. The potential was swept from -0.900 to 0.800 V vs. SCE at a scan rate of 50 mV $s^{-1}$.

### *3.3.2.3 Probing the redox properties using EQCM measurements*

Ion transport is the key phenomenon in the application of PPy for a drug delivery system. In order to comprehend the ion flow during the switching of the polymer and measure the mass changes involved during the electrochemical reactions at the solution-electrode interface, EQCM measurements were performed. This technique is one of the most common techniques used to follow the charging and discharging reactions that take place in conducting polymer films.[10, 33]

Two different types of polymer systems were considered. The first is where a PPy film is doped with relatively small mobile anions, $SO_4^{2-}$. The application of a positive potential generates an oxidised polymer film (creating positive charges on the PPy); this allows the incorporation and subsequent transfer of anions in order to maintain charge neutrality. Contrary to this, upon application of a

reduction potential, the PPy film becomes reduced and electrons flow into the film to neutralise the positive charges, expelling the anions from the polymer matrix. This type of polymer system is well known as an anion exchanger. However, in the case of large anionic dopants and the case discussed here, where the PPy film is doped with a bulky anionic dopant which remains immobilised in the polymer matrix, anions are not exchanged. Instead, cations are taken up during reduction of the polymer film in order to maintain charge neutrality, and hence these polymers acquire the term cation exchanger.

Firstly, the growth of two separate polymer systems was investigated using EQCM. Figure 3.18 shows the plots of the change in mass of the oscillating quartz crystal as a function of the charge passed during the electrochemical synthesis of PPy/Sβ-CD and PPy/$SO_4$ films. According to Syritski *et al.*[34] who reported the EQCM measurements for various PPy films, the good linearity observed in both cases can be attributed to linear and homogenous film growth on the EQCM gold electrode.

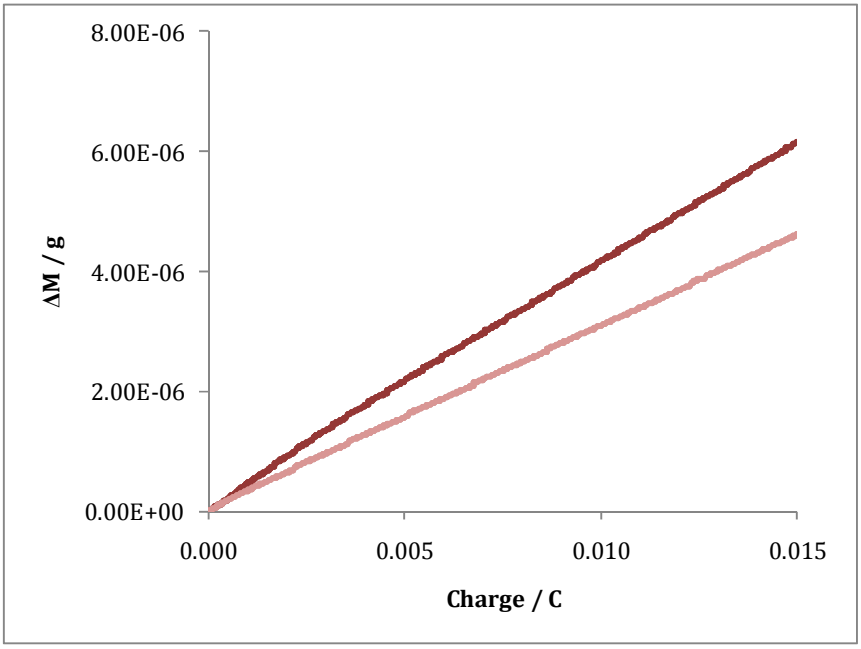


**Figure 3.18:** Mass as a function of charge passed for polymers electrochemically synthesised at a constant potential of 0.700 V vs. Ag/AgCl on gold EQCM electrodes in the presence of ♦ 0.10 mol $dm^{-3}$ $Na_2S0_4$ and ♦ 0.01 mol $dm^{-3}$ Sβ-CD.

It is well known from the Sauerbrey equation, Equation 2.1, that a decrease in the resonating frequency is indicative of an increase in the mass of the electrode. Figure 3.19 shows the overall mass as a function of time for the growth of these two different polymers; the Sβ-CD-doped polymer was polymerised in the presence of 0.01 mol $dm^{-3}$ Sβ-CD and the other in the presence of 0.10 mol $dm^{-3}$ $Na_2SO_4$. In both cases the PPy films were electrochemically deposited at a potential of 0.700 V vs. Ag/AgCl to a final charge of 1.50 x $10^{-2}$ C $cm^{-2}$. It is interesting to note from Figure 3.19, in the case of the Sβ-CD film that there is an induction time observed for approximately 7 s before the mass begins to increase, this is not seen with the sulfate system. This characteristic feature is probably due to the time that is needed for the large and bulky Sβ-CD anions to diffuse to the surface. However, it is clearly evident that once the induction time has elapsed, the growth rate increases significantly.

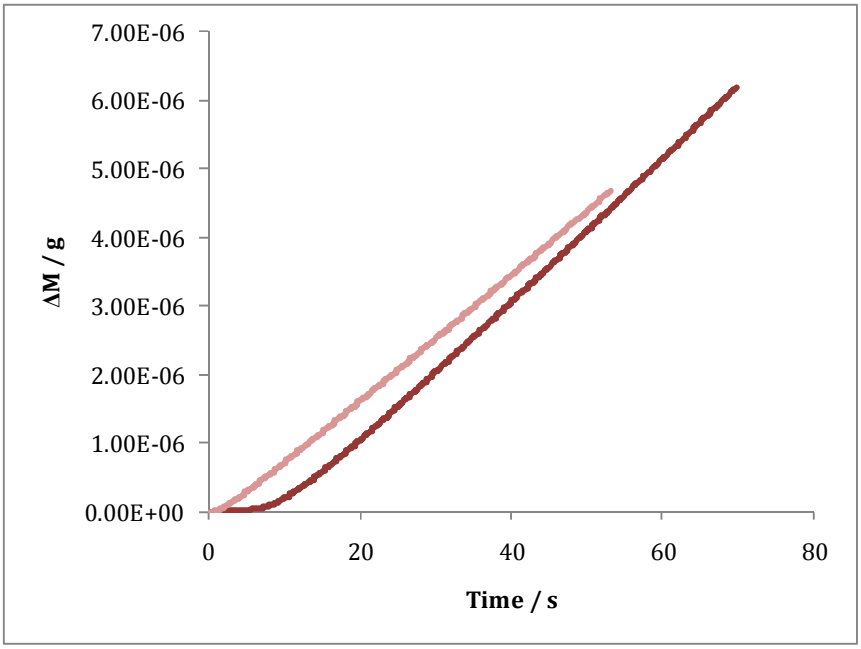


**Figure 3.19:** Mass as a function of time for polymers electrochemically synthesised at 0.700 V vs. Ag/AgCl on EQCM in the presence of ♦ 0.10 mol $dm^{-3}$ $Na_2SO_4$ and ♦0.01 mol $dm^{-3}$ Sβ-CD until a charge of 1.50 x $10^{-2}$ C was passed.

EQCM measurements in conjunction with the CV technique were also carried out to study the mass change involved during the polarisation of the PPy/Sβ-CD films at different scan rates. This study was performed to understand the ion uptake and release capabilities of the polymer system. The films were firstly synthesised then washed with distilled water prior to being subjected to a monomer free 0.10 mol $dm^{-3}$ $Na_2SO_4$ solution. The current, as well as the mass change, was recorded simultaneously while the samples were swept from a potential close to the original polymerisation potential, 0.600 V vs. Ag/AgCl, to a reduction potential, -0.900 V vs. Ag/AgCl, at a scan rate of 5 and 50 mV $s^{-1}$.

As described by Syritski *et al*.[34] there are two types of behaviour for the reduction/oxidation of a PPy film, which is dependent on the dopant. Equation 3.2, proposed by Syritski *et al*.[34] illustrates the anticipated behaviour during reduction and oxidation of a polymer film doped with a large immobile dopant which remains entrapped into the polymer film, as in the case of the PPy/Sβ-CD film. After oxidative polymerisation of the monomer and subsequent doping to form the polymer film the cations are incorporated during the reduction process in order to compensate the negative charges (3.2 a). Accordingly, upon application of an oxidation potential the compensation of charge can be achieved by both cation expulsion and anion incorporation from the supporting electrolyte (3.2 b).

(a) 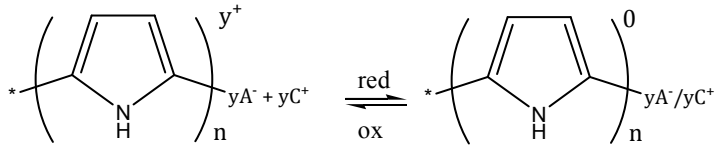


(b) 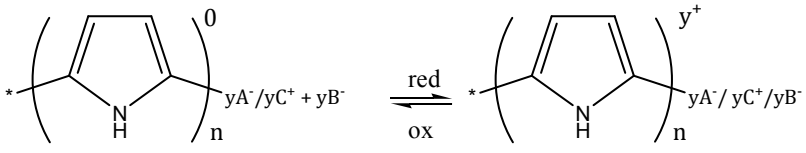


3.2

The expected results for these films, synthesised with the large immobilised anionic dopant, is for the film to behave as a cation exchanger. Figure 3.20 shows the CV data for a PPy/Sβ-CD film cycled in 0.10 mol $dm^{-3}$ $Na_2SO_4$, scanned at 50 mV $s^{-1}$. Again, as observed in Figures 3.16 and 3.17, a sharp reduction wave is seen, while the corresponding oxidation wave is much broader. However, in this figure, it is interesting to note that the first cycle is somewhat different from the subsequent cycles, due to the large influx of cations on the first reductive sweep.

Tamm *et al.*[22] discussed the voltammograms of PPy films doped with DBS and demonstrated similar results to those observed in Figure 3.20. They showed that the first cycle was not very reversible and that the subsequent cycles were considerably different to the first. They attributed this to the 'break in' phenomena. The 'break in' phenomena is the number of cycles needed to reach a steady state and can vary due to the scan rate, temperature and nature of supporting electrolyte.

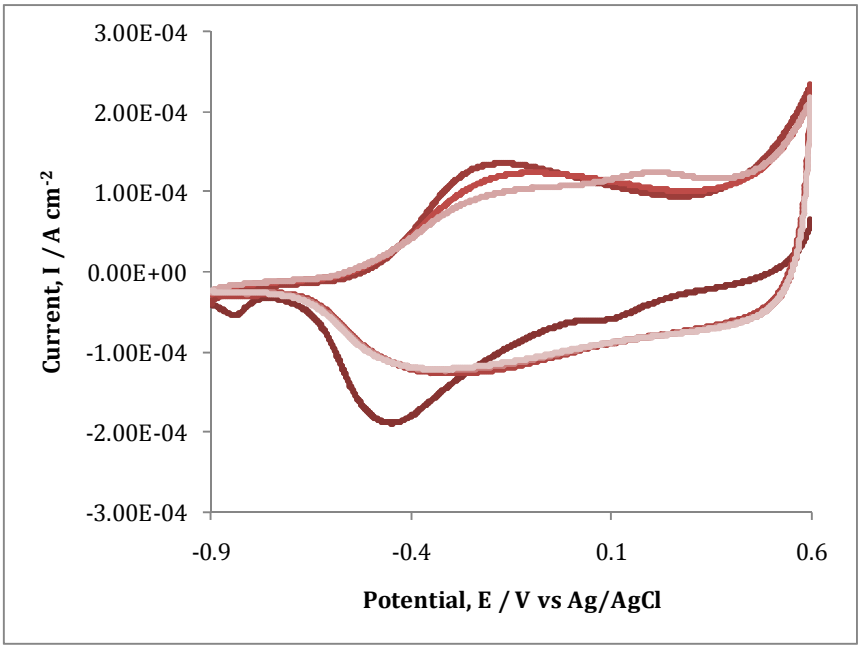


**Figure 3.20:** CV data for a PPy/Sβ-CD film cycled in a 0.10 mol $dm^{-3}$ $Na_2SO_4$ aqueous solution. The potential was swept from 0.600 to -0.900 V vs. Ag/AgCl at 50 mV $s^{-1}$.

In the case of DBS, and indeed the Sβ-CD, the nature of these anions in the polymer matrix allows them to become immobilised into the polymer film, which in turn requires only cations to achieve electroneutrality. The influx of the cations upon reduction of the polymer film in effect changes the structure of the polymer film and thus increases the mobility of ions in the film. Therefore, the changes observed between the first and the following cycles is believed to be due to this large initial cation uptake.[22] Khalkhali *et al.*[14] observed similar results when characterising PPy films electrochemically deposited in the presence of the large anionic dopant, DBS. They also attributed the oxidation and reduction of polymers synthesised in the presence of large immobilised dopants, to the movement of cations.

Figure 3.21 shows the first cycle for both the cyclic voltammogram recorded at 50 mV $s^{-1}$ and the corresponding mass change involved during the cycling, in a monomer free 0.10 mol $dm^{-3}$ $Na_2SO_4$ solution. The polymer was previously synthesised potentiostatically at 0.700 V vs. Ag/AgCl in the presence of 0.01 mol $dm^{-3}$ Sβ-CD. The polymer was then cycled from 0.600 V vs. Ag/AgCl in the cathodic direction. It is evident from the mass change data that during the reduction scan an increase in the mass occurs, corresponding to the uptake of cations. This increase in mass is observed at ~0.1 V vs. Ag/AgCl and continues to increase, reaching a maximum rate, at potentials close to the reduction peak observed in the voltammogram. On the reverse cycle, the mass slowly decreases corresponding to the release of the cations. This corresponds to the behaviour of a cation exchanger. Assuming the mass change was predominantly due to the uptake of cations, the mass increase was ~ 5.8 x $10^{-8}$ moles of $Na^+$. On closer inspection of Figure 3.21, it can be seen that the rate of the mass increase (forward cycle) is considerably higher than the rate of the mass loss (reverse cycle), again highlighting the fact that the reduction process is faster than the oxidation process. It is also noticeable from Figure 3.21, that a small mass increase occurs between 0.1 and 0.6 V vs. Ag/AgCl on the reverse scan. This is probably related to the uptake of sulfate anions from the supporting electrolyte, as outlined in Equation 3.2, or the intake of solvent water molecules.

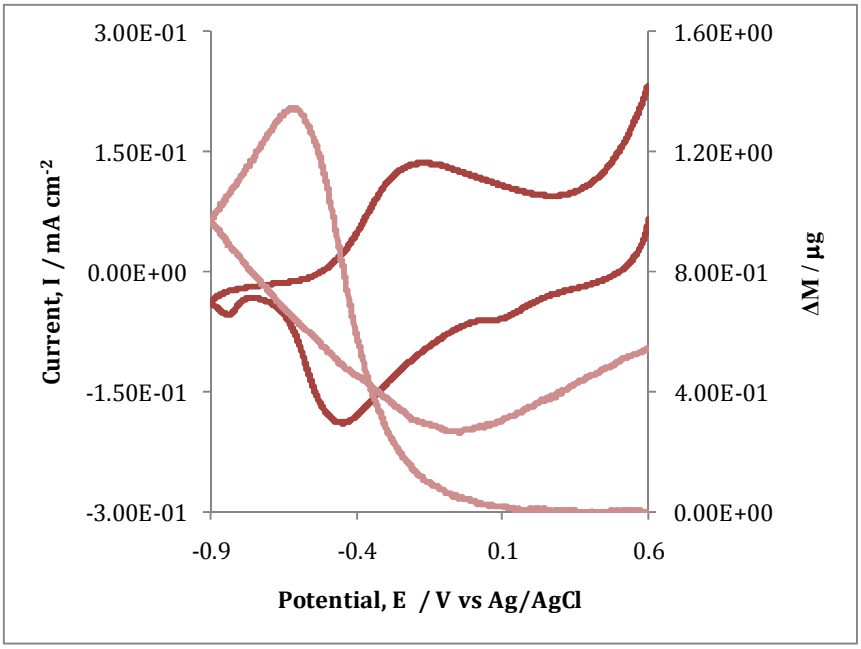


**Figure 3.21:** CV data for the current (♦) and the mass change (♦) as a function of potential obtained for a PPy/Sβ-CD film cycled in a 0.10 mol $dm^{-3}$ $Na_2SO_4$ aqueous solution. The potential was swept from 0.600 to -0.900 V vs. Ag/AgCl at a scan rate of 50 mV $s^{-1}$.

As discussed previously, typical doping levels reported for PPy are in the ratio of 1:3 to 1:4 dopant:pyrrole.[35] Previously, Reece, Ralph and Wallace using microanalytical data, suggested that the doping level of the PPy films doped with either the α or the β sulfonated CD, had a doping ratio of 1:4.5 slightly lower than the more commonly reported doping levels.[30] Several groups have used EQCM data to quantify polymer systems and to give an approximate calculation of the doping level.[34] In the results presented here, EQCM measurements along with Equation 3.3 a derivation of Faraday's law, was used to estimate the doping levels. In these equations, $M$ is the total mass of the deposited polymer, $Q$ is the charge reached, $M_m$ is the mass of the monomer, $M_{dop}$ is the mass of the dopant, $x$ is the doping level and $F$ is Faraday's constant, 95484.56 C $mol^{-1}$.

$$M = \frac{Q(M_m)}{(2+x)F} + \frac{Q(M_{dop})x}{(2+x)F} \quad 3.3$$

$$\frac{M}{Q} = \frac{(M_m) + (M_{dop})x}{(2+x)F} \quad 3.4$$

Figure 3.22 demonstrates the experimental and theoretical results obtained for the growth of a PPy film doped with a small mobile chloride anion (0.10 mol $dm^{-3}$ NaCl); slope values of 0.0032 g $C^{-1}$ and 0.0035 g $C^{-1}$ were extrapolated, respectively. In analysing the initial growth, highlighted in Figure 3.22, there was very good correlation between the experimental and the theoretical data. However, as the film thickness (charge) increased a deviation from the theoretical slope was observed. In evaluating these data using Equation 3.4, it was assumed that the maximum doping level of 0.33 was achieved. The slight deviation from the theoretical slope obtained was possibly due to the maximum doping level not being reached. Another reason for the lower experimental mass per unit charge is the formation of dimers or oligomers, which in turn consume the current and, consequently, the charge, but are not involved in the deposition of the polymer to give the corresponding mass increase.

A good agreement between the theoretical and experimental mass was obtained in Figure 3.22, similar data were collected for the Sβ-CD-doped polymer and used in an attempt to estimate the doping level of the Sβ-CD. As discussed earlier, the Sβ-CD is a cyclodextrin with 7-11 substituted anions present on the outer rims. Unlike the chloride model, which has only one anion involved in the doping process, the cyclodextrin is a complex molecule with a minimum of 7 and a maximum of 11 anions possibly involved in the doping process.

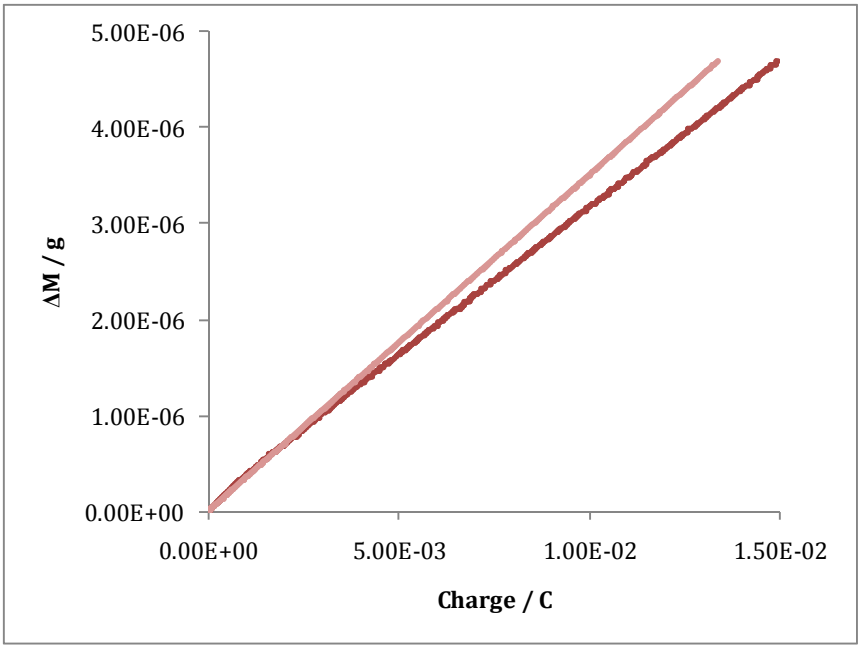


**Figure 3.22:** Mass as a function of charge for the growth on a PPy/Cl film in the presence of 0.20 mol $dm^{-3}$ pyrrole and 0.10 mol $dm^{-3}$ NaCl. Polymers were deposited at 0.700 V vs. Ag/AgCl until a charge of 1.5 x $10^{-2}$ C $cm^{-2}$ was reached. ♦Theoretical and ♦experimental data.

In using Equation 3.4 to estimate the doping level for the PPy/Sβ-CD system, two hypotheses were necessary. In case 1, it was assumed that the maximum doping level of 0.33 was attained and that each sulfonated group participated in the doping process. Figure 3.23 shows the EQCM measurements, mass as a function of charge, obtained for the growth of a PPy/Sβ-CD polymer at 0.700 V vs. Ag/AgCl. The experimental and theoretical analysis, where the number of anions present on the CD and participating in the doping process was varied, are evaluated. In the case of the theoretical (Thl) trace, the estimated molar mass of the Sβ-CD, 2053.43 g, was used and each Sβ-CD provided only one anionic charge in the doping. It is obvious from these data displayed in Figure 3.23 that there is a very large deviation from the theoretical and experimental slopes, 0.0033 g $C^{-1}$ to 0.00041 g $C^{-1}$, respectively. This clearly indicates that each Sβ-CD provides more than one sulfonated anion to dope the polymer. Equation 3.4 was then used to estimate the mass charge relationship assuming that each Sβ-CD provided from 1 to 11 anions in the doping process. These

theoretical plots are provided in Figure 3.23 and show increasing agreement between the theoretical and experimental data as each Sβ-CD provides a higher number of anions in the doping process. However, it is very clear from this plot that there is still a significant gap between the theoretical and experimental profiles assuming that each Sβ-CD provides 11 sulfonate groups to dope the polymer. Obviously, the doping level is considerably lower than 0.33, as is commonly obtained with other dopants.

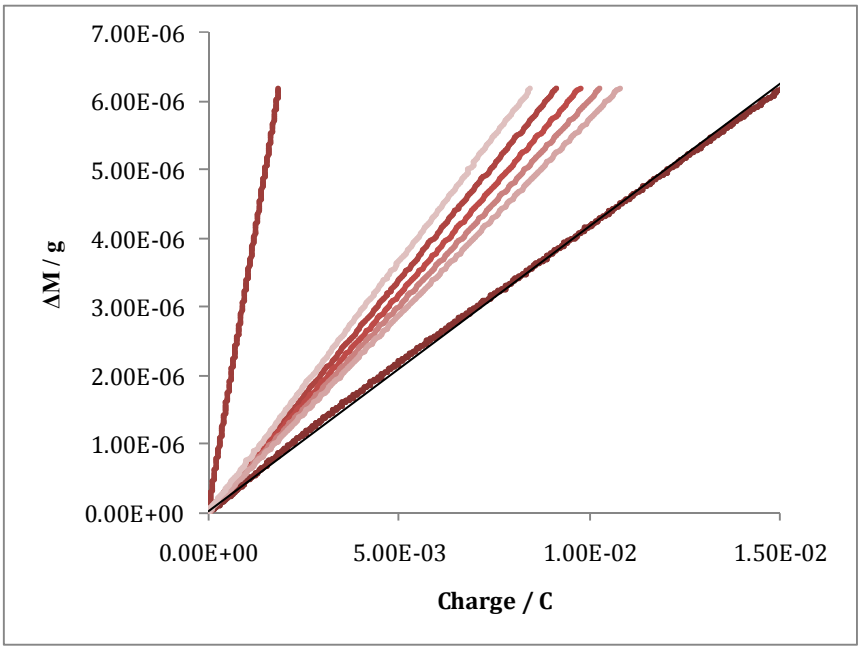


**Figure 3.23:** Mass as a function of charge for the growth on a PPy/Sβ-CD film in the presence of 0.20 mol $dm^{-3}$ pyrrole and 0.01 mol $dm^{-3}$ Sβ-CD. Polymers were deposited at 0.700 V vs. Ag/AgCl until a charge of 1.5 x $10^{-2}$ C $cm^{-2}$ was reached. ♦Theoretical and ♦experimental data.

In the second case, the assumption that 9 sulfonated groups were involved in the doping process was made and using Equation 3.2, the charge was calculated for a number of possible doping levels. Figure 3.24 illustrates the data obtained for each doping level. The theoretical (Thl) analysis is for the maximum doping level of 0.33, for an Sβ-CD with 9 sulfonated groups where all are involved in the doping process. In comparison to the data obtained in Figure 3.23, the slopes

are now in closer proximity, as the doping level decreases. A summary of the analysis in Figure 3.24 is given in Table 3.3. Using these data the doping level was estimated to be 0.083.

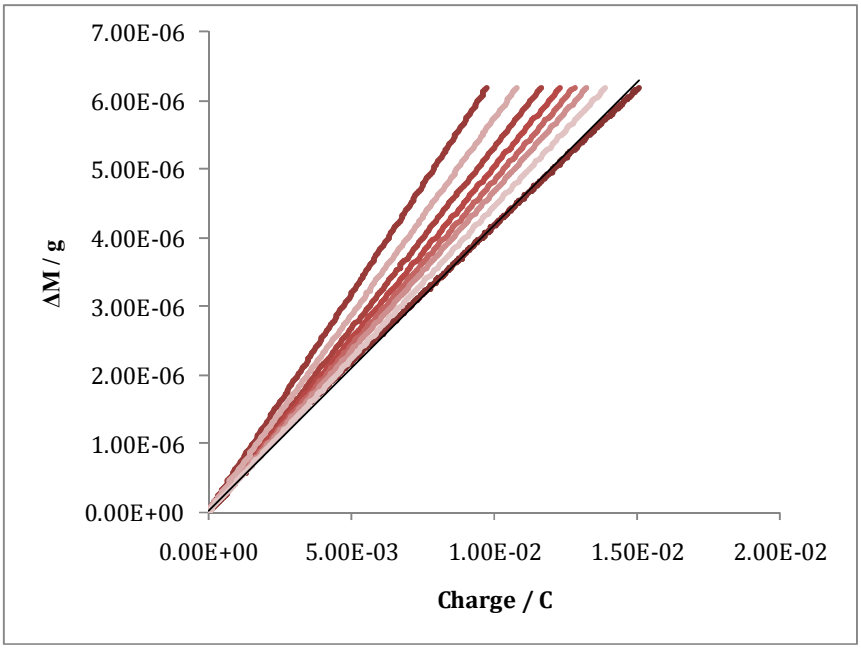


**Figure 3.24:** Mass as a function of charge for the growth on a PPy/Sβ-CD film in the presence of 0.20 mol $dm^{-3}$ pyrrole and 0.01 mol $dm^{-3}$ Sβ-CD. Polymers were deposited at 0.700 V vs. Ag/AgCl until a charge of 1.5 x $10^{-2}$ C $cm^{-2}$ was reached. ♦Theoretical (assuming 9 sulfonated groups) and ♦experimental data.

To summarise on these hypotheses, it was demonstrated that the maximum doping level, 0.33, with PPy films is not evident in the presence of the Sβ-CD. Due to the complexity of the Sβ-CD molecule, and the uncertainties in the amount of substituted groups, which is directly related to the number of anionic sulfonated groups present, it is difficult to define the level of doping. Although, Reece *et al.*[30] approximated a value of 1:4.5 (Sβ-CD:Py) and also stated the difficulties in evaluating the doping level due to the unknown degree of sulfation of the CD, our approximations point in the direction of a much lower doping level of 1:12. However, based on the assumption that all sulfonated groups are

involved in the compensation of the charge, it is highly unlikely that the doping level is >0.10. At these levels it would mean that for approximately every 10 Py units 1 Sβ-CD would compensate for the charge. However, if all the sulfonated groups on the Sβ-CD were involved in charge balance this would not only place strain on the cyclodextrin but also on the polymer. Therefore, it is highly probable that some free sulfonated groups are present within the polymer.

Clearly, the doping level is very different with these large polyanionic dopants. The doping level of 0.33, commonly found with small dopants, was not evident with the Sβ-CD. Although the true doping level could not be obtained, the doping levels estimated between 0.08 and 0.10 seem reasonable given the large size of the Sβ-CD dopant.

**Table 3.3:** Evaluated slopes for the varying doping levels, assuming 9 anions are present on the Sβ-CD.

| Doping level | Doping ratio (Py:Sβ-CD) | Slope /g $C^{-1}$ |
|---|---|---|
| Experimental | Experimental | 0.00042 |
| 0.334 | 3:1 | 0.00063 |
| 0.250 | 4:1 | 0.00057 |
| 0.200 | 5:1 | 0.00053 |
| 0.167 | 6:1 | 0.00050 |
| 0.143 | 7:1 | 0.00048 |
| 0.125 | 8:1 | 0.00047 |
| 0.100 | 10:1 | 0.00044 |
| 0.083 | 12:1 | 0.00042 |

Next, an examination into the ion and solvent flux observed during cycling of the PPy/Sβ-CD was made using the EQCM data. Hillman *et al.*[36, 37] examined the ion and solvent flux data as a function of potential for a poly(3,4-ethylenedioxythiophene) PEDOT system. The simultaneous CV data and the EQCM measurements recorded were used to analyse the fluxes. Hillman and co-

workers proposed the following equations for the flux of the anion, however in this case the equations are denoted for the cations, as the PPy/Sβ-CD film is a cation exchanger, Figure 3.21. Various approximations were used in these equations, including the films are permselective, the total mass change at any stage of the redox process is the sum of the contributions from cation and solvent transfers, $\Delta m_A$ and $\Delta m_S$, respectively. Here, the time differentials are denoted by a prime.

The mass contributions are related by Equation 3.5 where the total mass is given by the sum of the mass of the cations and solvent.

$$m'_T = m'_C + m'_S \tag{3.5}$$

Using the electroneutrality conditions and Faraday's law, the ion flux, $j_C$, which express the individual species contributions, is given by Equation 3.6,

$$j_C = \frac{m'_C}{M_C} = \frac{i}{z_C F} \tag{3.6}$$

where $M_C$ and $z_C$ are the molar mass and charge number of the cation, respectively. The total mass flux, $j_T$ is then denoted as,

$$j_T = \frac{m'_T}{M_C} \tag{3.7}$$

Therefore, by comparing both $j_C$ and $j_T$, information on the solvent transfer can be obtained. The solvent flux is defined by Equation 3.8, where $M_S$ is the solvent molar mass.

$$j_S = \frac{m'_S}{M_S} \tag{3.8}$$

Combining these equations gives the expression in Equation 3.9.

$$j_s = \frac{\left(m'_T - \frac{iM_C}{z_C F}\right)}{M_S} \qquad 3.9$$

The data previously shown in Figure 3.20 were used to calculate the individual cation and solvent fluxes using Equations 3.5 to 3.9. It was shown earlier, Figure 3.21, that this polymer acts as a cation exchanger. Therefore, contrary to Hillman, who evaluated the recorded data for the flux of the anion, these proposed equations were used for the analysis of the transport of the cation. Figure 3.25 demonstrates the flux of cations as a function of the potential applied during cycling in a 0.10 mol $dm^{-3}$ $Na_2SO_4$ solution. From this figure an increase in the number of cations is evident as the potential is reduced; with a maximum flux occurring at ~-0.4 vs. Ag/AgCl, which corresponds to the cathodic peak previously observed for a PPy/Sβ-CD film, shown in Figure 3.20.

In Figure 3.26 a comparison of the cation and solvent flux observed during the cycling of the PPy/Sβ-CD film is made. On comparing the flux of cation and solvent transport, it is clear that there is a higher flux of solvent. Also in comparing this graph and evaluating the moles of water and cations, approximately twice as much solvent is taken up by the polymer in comparison to the cation uptake. This evidence points to a large uptake of water into the polymer system. These studies also show that the reduced film is in the most solvated state. This is consistent with the simultaneous uptake of cations and water molecules on reduction of the film. Each cation is encased by a solvated cage and it is not surprising that both the cations and water molecules are incorporated simultaneously.

Figure 3.27 shows the overall mass change involved during the solvent uptake. Upon reduction, there is an almost linear increase in the mass of the solvent taken into the polymer. On the reverse scan, there is a loss of the solvent, but this is a non-linear relationship, with the rate of loss being greater from -0.700 to -0.400 V vs. Ag/AgCl. More solvent is incorporated again from 0.000 to 0.300 V vs. Ag/AgCl.

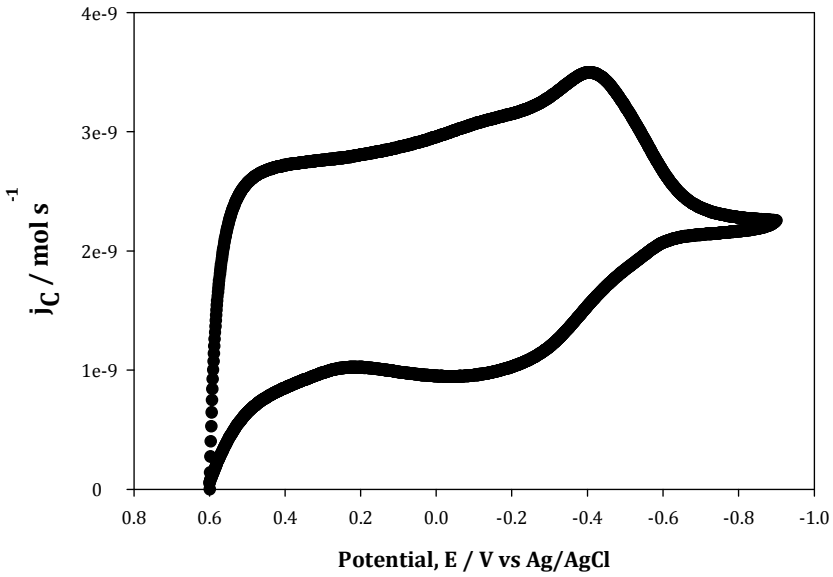


**Figure 3.25:** Flux of the cationic species as a function of the potential. The potential was swept from 0.600 V to -0.900 V vs. Ag/AgCl at a scan rate of 50 mV $s^{-1}$.

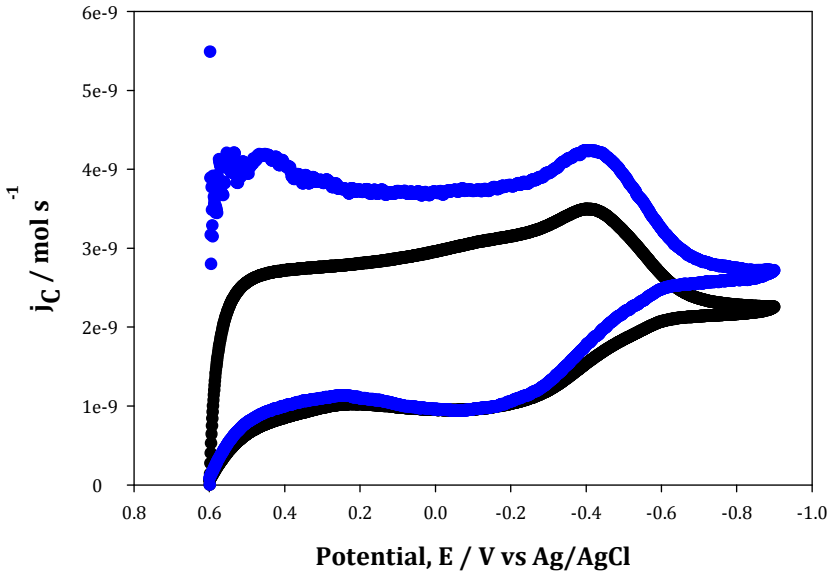


**Figure 3.26:** Fluxes for the ♦ cation and ♦ solvent as a function of potential on cycling PPy/Sβ-CD films in 0.10 mol $dm^{-3}$ $Na_2SO_4$ at 50 mV $s^{-1}$.

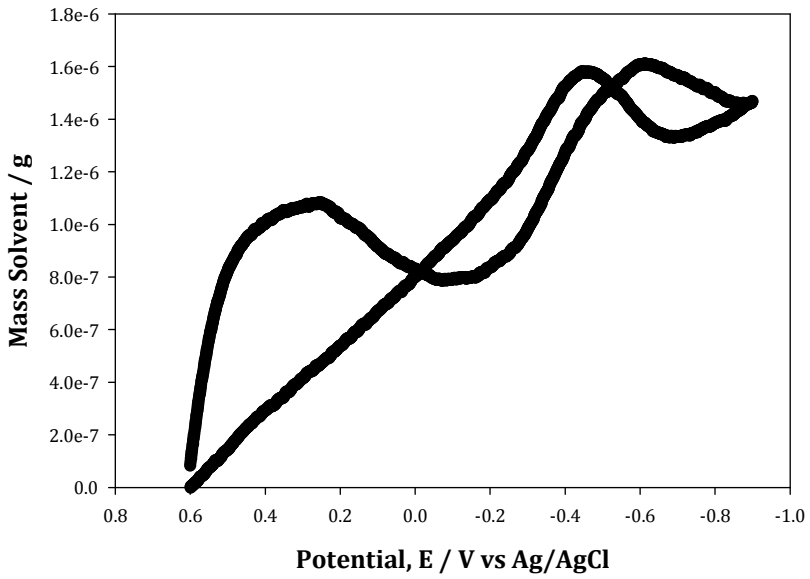


**Figure 3.27:** Solvent mass as a function of potential on cycling PPy/Sβ-CD films in 0.10 mol $dm^{-3}$ $Na_2SO_4$ at 50 mV $s^{-1}$.

Using this analysis, proposed by Hillman *et al*.[36, 37] it is evident that the polymer incorporates a substantial amount of water during reduction. This has been reported in the literature.[22] In addition to the solvent influx with cations, it is likely that a considerable amount of water will remain in the cavity of the Sβ-CD.

## 3.3.3 Analysis of the PPy/Sβ-CD films

### *3.3.3.1 SEM and optical images*

Optical imaging techniques were performed on various polymers. PPy films were firstly synthesised, washed thoroughly with distilled water, dried and images recorded. The PPy films were polymerised in the presence of an aqueous sodium sulfate solution and an aqueous Sβ-CD solution. The optical images of both PPy films are shown in Figure 3.28. The typical cauliflower, globular morphology is evident in both cases.

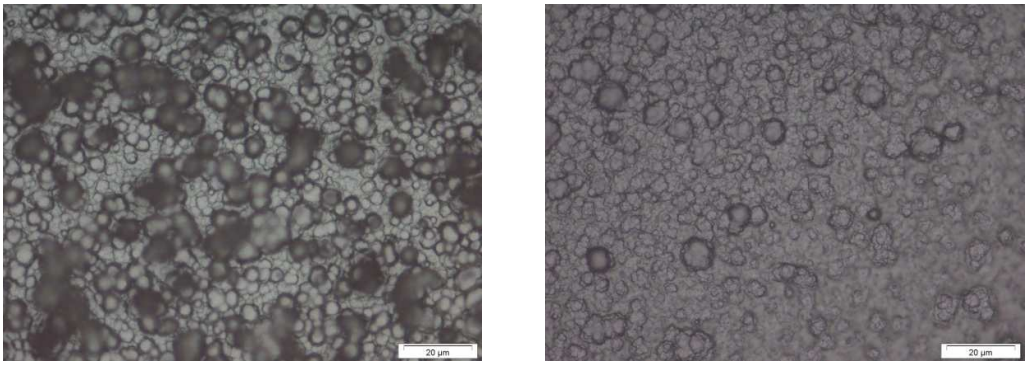


**Figure 3.28:** Optical images of (A) PPy-$SO_4$ and (B) PPy/Sβ-CD on Au. Polymers were electrochemically deposited from aqueous solutions of 0.10 mol dm-3 $Na_2SO_4$ and 0.01 mol $dm^{-3}$ Sβ-CD, in the presence of 0.20 mol $dm^{-3}$ pyrrole, at 0.900 V vs. SCE to a charge of 3.0 C $cm^{-2}$.

In general, PPy films present a *cauliflower*-like morphology constituted by micro-spherical grains. It has been reported that this *cauliflower* structure is related to the dopant intercalation difficulty in the disordered polymeric chain.[38, 39] It is also well documented that PPy films observe a cauliflower like morphology.[30, 40] Figure 3.29 shows an SEM image of a PPy/Sβ-CD film potentiostatically grown at 0.900 V vs. SCE to a charge of 3.0 C $cm^{-2}$ on a Pt disc, with the corresponding EDAX data shown in Figure 3.31. Interestingly, in the case of the Sβ-CD doped polymer, although the typical cauliflower morphology is clear, it behaves in a more organised manner as apparent from Figure 3.29. The polymer growth seems to lay itself in almost evenly distributed rows, as highlighted in Figure 3.29. Other groups who have investigated the morphology of PPy films in the presence of cyclodextrins have also observed a different oriented, organisational mode in comparison to 'typical' PPy films.[13, 41, 42]

Izaoumen *et al.*[41] also reported this type of polymer arrangement for a PPy film electrochemically synthesised in the presence of a neutral β-cyclodextrin and $LiClO_4$ supporting electrolyte solution. In their case the polymers were synthesised using CV. Figure 3.30 illustrates the SEM image obtained for their polymer film, the organisational feature is evident. Temsamani and co

workers[13] also demonstrated similar SEM images for the PPy/Sβ-CD polymers grown in the presence of $LiClO_4$ supporting electrolyte.

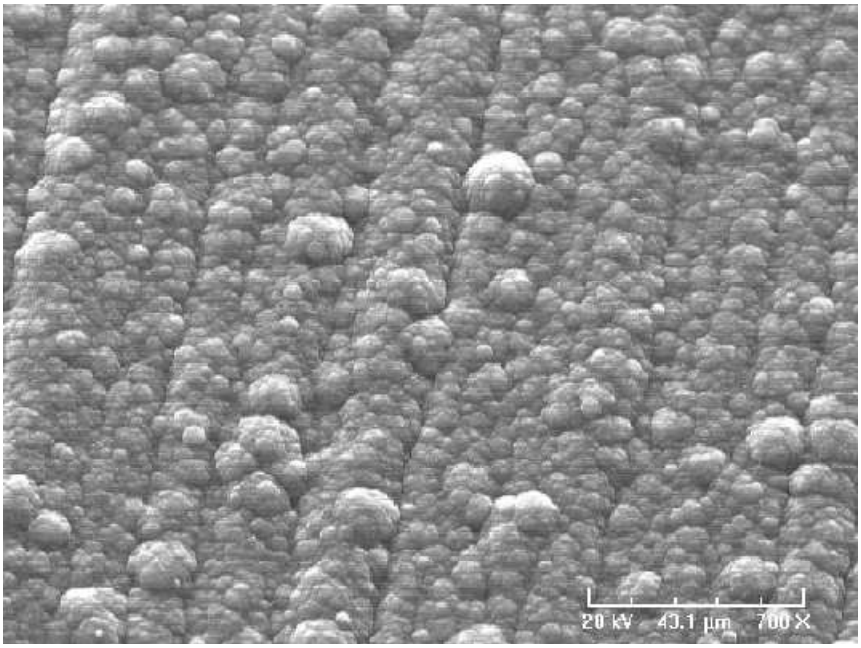


**Figure 3.29:** SEM micrographs of a PPy/Sβ-CD film electrochemical deposited onto a platinum disc electrode at a potential of 0.900 V to a charge of 3.0 C $cm^{-2}$.

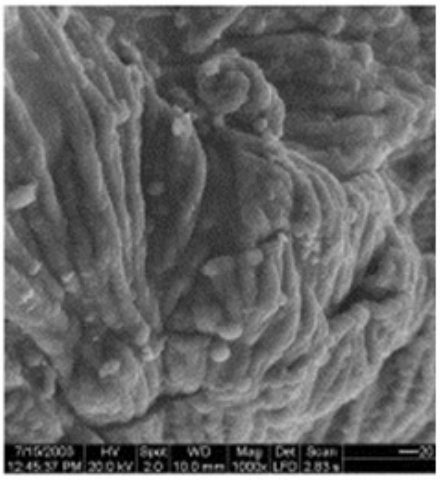

**Figure 3.30:** SEM image of PPy/β-CD film obtained by CV growth (35 cycles) from a PPy/β-CD/$LiClO_4$ solution taken from Izaoumen *et al.* [41]

### *3.3.3.2 EDAX*

To confirm the incorporation of Sβ-CD into the polymer film EDAX measurements were performed, where PPy films were electrochemically deposited in the presence of 0.01 mol $dm^{-3}$ Sβ-CD onto flat platinum disc electrodes. Figure 3.31 shows the data obtained when a polymer was synthesised at a potential of 0.900 V vs. SCE until a charge of 3.0 C $cm^{-2}$ was passed. As is evident from the figure, EDAX analysis of the doped PPy film revealed the presence of sulfur which can only correspond to the incorporation of the Sβ-CD anions during electrochemical synthesis, as no other supporting electrolyte was used.

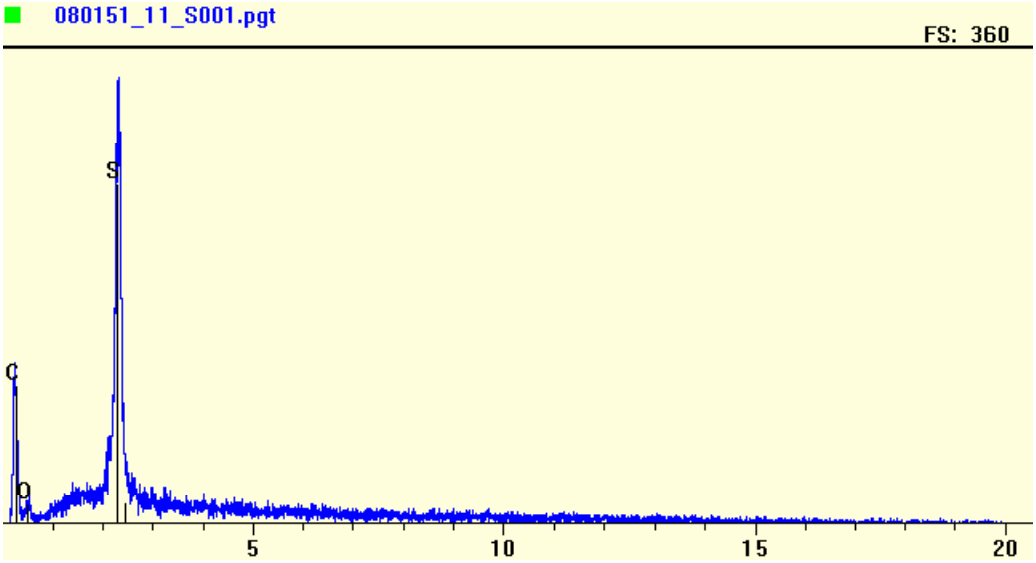


**Figure 3.31:** EDAX spectra of a PPy/Sβ-CD a sample. Polymerisaed electrochemically at 0.900 V vs. SCE to a charge of 3 C $cm^{-2}$ onto a Pt disc.

In the following chapter a study on the incorporation and release of a cationic drug, dopamine, using PPy films syntheised electrochemically in the presence of $Na_2SO_4$ or Sβ-CD are investigated.

## 3.4 Summary of results

The synthesis and characterisation of PPy films through the use of electrochemistry was investigated in this chapter. Sβ-CD was established to be a suitable electrolyte, through conductivity measurements, for the electrochemical polymerisation of pyrrole. CV data recorded for the polymerisation of the pyrrole monomer in the presence of a number of dopants, including Sβ-CD, showed interesting results. These studies demonstrated that the Sβ-CD facilitated the oxidation of the monomer at lower anodic potentials in comparison to the smaller, more mobile dopants, such as the chloride anion. Also, the rate of electropolymerisation was much higher. However, it was verified that the major influence in the rate of electropolymerisation was the conductivity of the solution. The Sβ-CD has a 10 fold higher conductivity in comparison to an equimolar concentration of NaCl. Analysis of the CV data observed an increase in the current as the polymerisation step progressed, indicating that the polymer film retained its conductivity even at high rates of deposition.

PPy/Sβ-CD films were also electrochemically deposited using a potentiostatic method. The current-time transients demonstrated the typical behaviour observed for the deposition of PPy films, corresponding to the nucleation of the polymer. The rate of the reaction was also investigated and was shown to increase by a factor of two as higher anodic potentials were applied during synthesis.

The redox properties of the polymer films were examined using CV. In the case of the PPy/Sβ-CD films, the redox activity of the films was clearly observed in contrast to other polymer films doped with smaller anions. EQCM measurements also demonstrated the redox properties of the polymer films where an increase in mass was observed during the reduction of the polymer films, signifying cationic exchange properties. EQCM measurements were also recorded during the potentiostatic growth of the PPy/Sβ-CD films and showed a delayed rate of reaction at the initial polymerisation step. However, once this

induction time was overcome, the rate of polymer growth increased substantially.

An evaluation into the doping level of the PPy/Sβ-CD films was initiated through an equation derived from Faraday's law. Preliminary results verify that the doping level is not 0.33, which is generally observed for the doping of PPy films in the presence of chloride anions. However, a doping level of 0.083 was estimated assuming 9 of the sulfonated groups on the cyclodextrin ring were all involved in the doping process. The participation of 9 sulfonated groups in the doping process is high and is unlikely as it would cause a substantial strain not only for the CD but for the overall composition of the polymers.

Finally, it was shown that this PPy/Sβ-CD system has cationic exchange properties. An investigation into the cation and solvent fluxes was initiated through an analysis proposed by Hillman. It showed that a large amount of the mass change achieved during the potential cycling of the polymer film in a 0.10 mol $dm^{-3}$ $Na_2SO_4$ solution, was attributed to the uptake of water.

EDAX and SEM analysis also confirmed the presence of the Sβ-CD in the polymer matrix and the morphology of the polymer.

Temsamani and co-workers also suggested that these PPy/Sβ-CD films could be potentially useful for the extraction of cations due to the enhanced electrostatic effects from the sulfate moieties and also due to the fact that cyclodextrins are well known to form supramolecular inclusion formation complexes with various guest molecules.[13] This property leads to the study of PPy/Sβ-CD films for the uptake and release of a cationic species. With this in mind, the use of these biocompatible films for an implantable drug delivery release system was investigated using dopamine as a model cationic drug. These findings are presented in Chapter 4.

## 3.5 References


1. G. Inzelt, Conducting Polymers, A new era in electrochemistry, Springer, 2008.
2. B. Garner, A. Georgevich, A. J. Hodgson, L. Liu, and G. G. Wallace, *J Biomed Mater Res*, **44**, (1999), 121-129.
3. Y. L. Li, K. G. Neoh, and E. T. Kang, *J Biomed Mater Res A*, **73A**, (2005), 171-181.
4. J. S. Moreno, S. Panero, and B. Scrosati, *Electrochim Acta*, **53**, (2008), 2154-2160.
5. C. E. Schmidt, V. R. Shastri, J. P. Vacanti, and R. Langer, *P Natl Acad Sci USA*, **94**, (1997), 8948-8953.
6. R. Wadhwa, C. F. Lagenaur, and X. T. Cui, *J Control Release*, **110**, (2006), 531-541.
7. A. Ferancova and J. Labuda, *Fresen J Anal Chem*, **370**, (2001), 1-10.
8. J. M. Fonner, L. Forciniti, H. Nguyen, J. D. Byrne, Y. F. Kou, J. Syeda-Nawaz, and C. E. Schmidt, *Biomed Mater*, **3**, (2008), 1-25.
9. J. Heinze, *Synthetic Met*, **43**, (1991), 2805-2823.
10. C. K. Baker and J. R. Reynolds, *J Electroanal Chem*, **251**, (1988), 307-322.
11. Q. J. Xie, S. Kuwabata, and H. Yoneyama, *J Electroanal Chem*, **420**, (1997), 219-225.
12. R. Challa, A. Ahuja, J. Ali, and R. K. Khar, *Aaps Pharmscitech*, **6**, (2005), 329-357.
13. K. R. Temsamani, O. Ceylan, B. J. Yates, S. Oztemiz, T. P. Gbatu, A. M. Stalcup, H. B. Mark, and W. Kutner, *J Solid State Electr*, **6**, (2002), 494-497.
14. R. A. Khalkhali, *Russ J Electrochem+*, **41**, (2005), 950-955.
15. J. N. Barisci, T. W. Lewis, G. M. Spinks, C. O. Too, and G. G. Wallace, *J Intel Mat Syst Str*, **9**, (1998), 723-731.
16. S. Sadki, P. Schottland, N. Brodie, and G. Sabouraud, *Chem Soc Rev*, **29**, (2000), 283-293.
17. J. M. Pernaut and J. R. Reynolds, *J Phys Chem B*, **104**, (2000), 4080-4090.
18. M. Pyo and J. R. Reynolds, *Chem Mater*, **8**, (1996), 128-133.
19. C. Y. Jin, F. L. Yang, and W. S. Yang, *J Appl Polym Sci*, **101**, (2006), 2518-2522.
20. A. Mirmohseni, W. E. Price, and G. G. Wallace, *Synthetic Met*, **84**, (1997), 823-824.
21. A. Kassim, F. J. Davis, and G. R. Mitchell, *Synthetic Met*, **62**, (1994), 41-47.
22. J. Tamm, A. Alumaa, A. Hallik, U. Johanson, L. Tamm, and T. Tamm, *Russ J Electrochem+*, **38**, (2002), 182-187.
23. D. B. Hibbert, Introduction to electrochemistry, The MacMillan Press LTD, 1993.
24. J. Arjomandi and R. Holze, *J Solid State Electr*, **11**, (2007), 1093-1100.
25. I. V. Terekhova, R. S. Kumeev, and G. A. Alper, *J Incl Phenom Macro*, **59**, (2007), 301-306.
26. B. S. Kim, W. H. Kim, S. N. Hoier, and S. M. Park, *Synthetic Met*, **69**, (1995), 455-458.
27. Y. F. Li and J. Yang, *J Appl Polym Sci*, **65**, (1997), 2739-2744.

28. S. Asavapiriyanont, G. K. Chandler, G. A. Gunawardena, and D. Pletcher, *J Electroanal Chem*, **177**, (1984), 229-244.
29. E. De Giglio, M. R. Guascito, L. Sabbatini, and G. Zambonin, *Biomaterials*, **22**, (2001), 2609-2616.
30. D. A. Reece, S. F. Ralph, and G. G. Wallace, *J Membrane Sci*, **249**, (2005), 9-20.
31. G. Bidan, B. Ehui, and M. Lapkowski, *J Phys D Appl Phys*, **21**, (1988), 1043-1054.
32. T. A. Skotheim, R. L. Elsenbaumer, and J. R. Reynolds, Handbook of conducting polymers, CRC Press, 1998.
33. G. Inzelt, V. Kertesz, and A. S. Nyback, *J Solid State Electr*, **3**, (1999), 251-257.
34. V. Syritski, A. Opik, and O. Forsen, *Electrochim Acta*, **48**, (2003), 1409-1417.
35. G. G. Wallace, G. M. Spinks, L. A. P. Kane-Maguire, and P. R. Teasdale, Conductive Electroactive Polymers: Intelligent Materials Systems, CRC Press, 2003.
36. A. R. Hillman, S. J. Daisley, and S. Bruckenstein, *Electrochem Commun*, **9**, (2007), 1316-1322.
37. A. R. Hillman, S. J. Daisley, and S. Bruckenstein, *Electrochim Acta*, **53**, (2008), 3763-3771.
38. M. Bazzaoui, L. Martins, E. A. Bazzaoui, and J. I. Martins, *Electrochim Acta*, **47**, (2002), 2953-2962.
39. A. S. Liu and M. A. S. Oliveira, *J Brazil Chem Soc*, **18**, (2007), 143-152.
40. A. C. Partridge, C. Milestone, C. O. Too, and G. G. Wallace, *J Membrane Sci*, **132**, (1997), 245-253.
41. N. Izaoumen, D. Bouchta, H. Zejli, M. El Kaoutit, A. M. Stalcup, and K. R. Temsamani, *Talanta*, **66**, (2005), 111-117.
42. K. R. Temsamani, H. B. Mark, W. Kutner, and A. M. Stalcup, *J Solid State Electr*, **6**, (2002), 391-395.

## 4.1 Introduction

An area that is of increased interest is the controlled delivery of drug molecules that have a direct therapeutic affect on living tissues and cells. Many people suffering from diseases, such as diabetes, go through everyday life having to endure the painful process of daily injections in order to keep their particular disease under control. Therefore, advances in the use of implantable medical devices to control the release of bioactive molecules are of huge interest. In this chapter, an examination into the controlled release of dopamine (DA), a neurotransmitter, is investigated. For conditions such as Parkinson's disease, there is no known cure. As presented in Chapter 1, Parkinson's disease affects the levels of DA found in the *substantia nigra*. Logically, due to the discovery of low levels of DA, the first thought would be to administer a sufferer a quantity of dopamine; however, it is well reported that dopamine is too large to cross the blood brain barrier, and so alternative routes must be investigated.[1-3]

Conducting polymers have been considered for use as a membrane for controlled drug delivery due to their distinctive properties which see the electrochemical switching of the polymer take place under various applied potentials.[4-9] This redox switching from the oxidised or doped state (conductive) to the reduced or neutral state (non-conducting) of the polymer, requires the uptake and release of ions to maintain charge neutrality.[10, 11] Burgmayer and Murray[12] showed that the ionic resistance of a polypyrrole film could be controlled by changing the applied potential, and therefore the oxidation state of the polymer, using electrochemical means.

In this research and chapter, polypyrrole (PPy) was the conducting polymer investigated for its role as a drug delivery system (DDS). There are many attractive reasons for choosing these conducting polymers. Firstly, PPy films are biocompatible.[9, 13-16] Secondly, PPy films are responsive materials and can be stimulated electrochemically to uptake and release ions. With this movement of ions, various groups have already investigated the prospect of using a number of anions to dope the polymer during electrochemical polymerisation, and upon

application of a reduction potential achieve the release of the anion. During electrochemical polymerisation, anionic species are incorporated into the polymer film to compensate the positive charge of the oxidised polypyrrole. Upon appropriate application of a potential, these anionic species can be released. In this way various anionic dopants, including possible pharmaceutical drugs, such as adenosine 5'-triphosphate (ATP)[11], Heparin[17] and Dexamethasone[18] (Dex) can be released upon electrical stimulation.

This research, however, investigates the role of a modified PPy electrode in the controlled drug delivery of a cationic species at physiological pH, DA. Equally, with the immobilisation of large anionic dopants which remain entrapped in the film, cations can potentially be incorporated and released upon application of appropriate reduction and oxidation potentials, respectively. The presence of the large anionic dopant could potentially allow the uptake and release of cations, such as DA, during appropriate electrochemical stimulation.

This chapter gives an insight into the potential use of PPy films as a DDS, particularly for the delivery of DA. Various parameters were investigated, including a study on the potential applied during growth of the polymer, the thickness of the polymer film, the potentials employed during incorporation and release of the DA, pH of DA solution, as well as, concentration and variations in the nature of the anionic dopant. A variety of dopants were used, varying from simple mobile anions to an anionic cyclodextrin.

## 4.2 Experimental

### 4.2.1 Materials

#### *4.2.1.1 Reagents*

Pyrrole monomer (98 %) was obtained from Aldrich and was purified by distillation prior to use. It was stored in the dark in the freezer at -4 $^0$C. Unless otherwise stated, 0.20 mol dm$^{-3}$ (0.35 ml in 25 ml supporting electrolyte) pyrrole was dissolved in the electrolyte solution for the electrochemical deposition experiments. Analytical reagents, sodium sulfate ($Na_2SO_4$), dopamine

hydrochloride salt (DA), sulfonated β-cyclodextrin (Sβ-CD) sodium salt, sodium chloride (NaCl) and para-toluene-sulfonic acid (PTS) were purchased from Aldrich and used as received. In the case of altering the pH, a 0.1 mol $dm^{-3}$ $H_2SO_4$ or a 0.1 mol $dm^{-3}$ NaOH solution was used to adjust the pH, accordingly.

#### *4.2.1.2 Electrodes and Instruments*

Electrochemical deposition of polypyrrole and analysis of the samples was carried out using a Solartron Model SI 1285 potentiostat. All measurements were made at room temperature. A platinum wire (99 %, 1 mm in diameter) electrode, where the exposed surface area was recorded separately for every experiment, was used for the deposition of polypyrrole and the successive uptake and release of DA. A saturated calomel reference electrode (SCE) and a platinum wire counter electrode (CE) were also used in the cell set up.

Electrochemical quartz crystal microgravimetry (EQCM) measurements were carried out using a CHI440 instrument. The polymers were deposited onto polished Au quartz crystal electrodes (Cambria Scientific) with an exposed surface area of 0.203 $cm^2$. The electrochemical cell consisted of a specially made Teflon holder in which the crystal was placed between two o-rings, a schematic of which is shown previously in Chapter 3, Figure 3.1. The set up was completed using a platinum wire counter electrode and a 3.0 mol $dm^{-3}$ Ag|AgCl reference electrode. UV studies on the release of the DA were carried out on a Varian Instruments Cary 50 Conc UV-visible spectrophotometer using a 1 cm path length quartz crystal cuvette.

### 4.2.2 Procedures

#### *4.2.2.1 Polymer film preparation*

PPy film fabrication was carried out using an electro-synthesis method, which deposited the polymer film at the working electrode (platinum wire). Polymers were prepared in various electrolyte solutions containing 0.20 mol $dm^{-3}$ pyrrole. A summary of the various electrolytes used in the electrochemical deposition of

polypyrrole are given in Table 4.1. In all cases, distilled water was used to prepare the solutions. Electropolymerisation of the pyrrole monomer was achieved using a constant potential. The potentials applied for the deposition ranged from 0.500 to 1.000 V vs. SCE, and were applied until a certain constant charge was passed, to ensure uniform film thickness.

**Table 4.1:** Electrolytes investigated in the deposition of polypyrrole.

| Electrolyte | Concentration / mol $dm^{-3}$ |
|---|---|
| Sodium sulfate, $Na_2SO_4$ | 0.10 |
| Sodium chloride, NaCl | 0.10 |
| para-toluene-sulfonic acid, PTS | 0.10 |
| Sulfonated β-cyclodextrin, Sβ-CD | 0.01 |

#### *4.2.2.2 Incorporation of drug*

After polymerisation, the prepared polymer films were gently washed with distilled water and immersed in a 0.10 mol $dm^{-3}$ DA solution, prepared in a supporting electrolyte of 0.10 mol $dm^{-3}$ $Na_2SO_4$. In general, the DA incorporation step involved the application of a reduction potential of -0.900 V vs. SCE, for 30 min. The polymer was then washed with distilled water and transferred to a fresh 0.10 mol $dm^{-3}$ $Na_2SO_4$ solution and held at a reduction potential of -0.900 V vs. SCE for 10 min in order to liberate any excess DA present on the surface of the polymer.

#### *4.2.2.3 Release of drug*

UV-visible spectroscopy was used to monitor the rate of release of the drug molecule, DA. To determine the concentration of the drug released for each experiment, a calibration curve was first prepared using DA concentrations ranging from $1.0 \times 10^{-3}$ to $1.0 \times 10^{-6}$ mol $dm^{-3}$. The absorbance values measured during the drug release experiment were then converted to DA concentration using the calibration curve. A typical calibration curve is shown in Figure 2.9, Chapter 2.

For the PPy/$SO_4$ system, the drug loaded polymers were transferred to a quartz crystal cuvette with 3 mL of 0.10 mol $dm^{-3}$ $Na_2SO_4$ and then inserted in the UV spectrophotometer. Counter and reference electrodes, Pt and Ag wire, respectively, were placed in the cuvette, avoiding the path of the light beam. An oxidation potential of 0.100 V was applied for 60 min in order to release the drug. The samples were analysed over a spectral range of 500 to 200 nm every 30 s over the period of 60 min. However, it proved difficult to eliminate slow release effects and a new method of analysing the amount of DA released from the PPy/Sβ-CD polymers was used. In this case, the electrochemical set up was transferred to 25 mL of 0.10 mol $dm^{-3}$ $Na_2SO_4$ solution in a glass cell. To facilitate the mixing of the released drug with the release medium, the solution was agitated with a stirring bead. An oxidation potential of 0.100 V vs. SCE, unless otherwise stated, was applied for 60 min. To monitor release, 3.0 mL aliquots were sampled from the medium and ran in the UV spectrophotometer over a spectral range of 500 to 200 nm every 10 min over the period of 60 min, unless otherwise stated. After each sampling, the 3.0 mL aliquots were returned, so as not to distort the volume.

#### *4.2.2.4 Influence of varying parameters for the PPy/$SO_4$ system*

##### 4.2.2.4.1 Influence of varying the growth potential and charge

The influence of the nature of the polypyrrole film was firstly examined. In these experiments, polymers were electrochemically deposited onto a platinum wire in the presence of 0.20 mol $dm^{-3}$ pyrrole and 0.10 mol $dm^{-3}$ $Na_2SO_4$ at different electropolymerisation potentials. The oxidation potentials were varied from 0.500 to 0.900 V vs. SCE, while maintaining a constant charge of 5.0 C $cm^{-2}$. The thickness of the polymers, where the charges consumed were varied from 1.0 to 10.0 C $cm^{-2}$, was also examined. The incorporation and release of DA was then carried out as described in Sections 4.2.2.2 and 4.2.2.3, respectively.

#### 4.2.2.4.2 Influence of varying the incorporation step

In this study, the polypyrrole films were electrochemically deposited in the presence of 0.20 mol $dm^{-3}$ pyrrole and 0.10 mol $dm^{-3}$ $Na_2SO_4$, at 0.600 V to a charge of 5.0 C $cm^{-2}$. They were then washed with distilled water and placed in a 0.10 mol $dm^{-3}$ DA solution made up in 0.10 mol $dm^{-3}$ $Na_2SO_4$. The DA was incorporated into the polymer by immersing the electrochemical set up into the DA solution and applying various reduction potentials, in the range of -1.000 to -0.400 V vs. SCE, for 30 min. The release of the DA was achieved as explained in Section 4.2.2.3.

The pH of the DA solution during the incorporation period was also studied to see if this parameter had any influence on the uptake and subsequent release of the DA. In this instance, the pH was adjusted using 0.10 mol $dm^{-3}$ $H_2SO_4$ or NaOH to give a final pH in the range of 1.1 to 6.9. Again, the incorporation and release steps were carried out as detailed in Sections 4.2.2.2 and 4.2.2.3, respectively.

#### 4.2.2.4.3 Influence of varying the release step

As described in Section 4.2.2.3, the release of DA was achieved through the application of an anodic potential. In examining this process for the PPy/$SO_4$ system, polymers were electrochemically deposited onto platinum wire, in the presence of 0.20 mol $dm^{-3}$ pyrrole and 0.10 mol $dm^{-3}$ $Na_2SO_4$, at 0.600 V vs. SCE to a charge of 1.0 C $cm^{-2}$. DA was incorporated as detailed in Section 4.2.2.2 and the release achieved through varying the potential from 0.100 to 0.300 V vs. SCE.

#### 4.2.2.4.4 Influence of the nature of the dopant anion

The final parameter varied in this section was the influence of the electrolyte solution in which the polymer was grown. In these experiments, polymers were electrochemically synthesised under a constant potential of 0.600 V vs. SCE to a charge of 5.0 C $cm^{-2}$ in the presence of 0.20 mol $dm^{-3}$ pyrrole and various dopant anions, Table 4.1. The uptake and release of DA was performed as outlined in Sections 4.2.2.2 and 4.2.2.3, respectively.

### *4.2.2.5 Influence of varying parameters for the PPy/Sβ-CD system*

Information on the characterisation of the redox properties of the PPy/Sβ-CD system was performed using cyclic voltammetry (CV). For the CV data, the polymers were deposited onto a platinum disc electrode using a constant potential of 0.700 V vs. SCE to a charge of 0.6 C $cm^{-2}$ in the presence of 0.20 mol $dm^{-3}$ pyrrole and 0.01 mol $dm^{-3}$ Sβ-CD. The polymer film, after careful washing, was then cycled through a potential window of 0.600 to -0.900 V at 50 mV $s^{-1}$ for 10 cycles.

#### 4.2.2.5.1 Influence of varying the growth potential and charge

In this set of experiments, polymers were electrochemically deposited onto a platinum wire in the presence of 0.20 mol $dm^{-3}$ pyrrole and 0.01 mol $dm^{-3}$ Sβ-CD dissolved in water. The oxidation potentials employed for this deposition step were varied from 0.500 to 1.000 V vs. SCE, until a charge of 2.0 C $cm^{-2}$ was passed. The thickness of the polymers, where the charges consumed were varied from 1.0 to 10.0 C $cm^{-2}$, was also examined, in this case a constant potential of 0.900 V vs. SCE was applied to achieve electrochemical growth. The incorporation and release of DA was then carried out as described in Sections 4.2.2.2 and 4.2.2.3, respectively.

An investigation into the influence of a supporting electrolyte during polymer growth was also carried out. In this section, polymer films were synthesised at 0.900 V vs. SCE to a charge of 1.0 C $cm^{-2}$, in the presence of 0.20 mol $dm^{-3}$ pyrrole, where 0.01 mol $dm^{-3}$ Sβ-CD was prepared in 0.10 mol $dm^{-3}$ $Na_2SO_4$. Incorporation and release of DA was achieved, as previously outlined in Section 4.2.2.2 and 4.2.2.3, respectively.

#### 4.2.2.5.2 Investigations into the oxidation of DA at thicker PPy/Sβ-CD films

Oxidation of DA was observed on release from the thicker Sβ-CD-doped polypyrrole films. In order to gain an understanding of how the DA was oxidised, various experiments were performed, focussing on both the

incorporation and release steps, with the aim of identifying the point where oxidation of DA occurred.

An electrochemical cell, in a quartz crystal cuvette, was set up in the UV spectrophotometer. In the cell, 0.5 mL of pyrrole was added to a 1.5 x $10^{-4}$ mol $dm^{-3}$ DA solution in water, where a constant potential of 0.200 V vs. SCE was applied for 10 min. A UV spectrum was taken before and after the potential was applied to determine if the DA was oxidised during the applied potential step.

CV experiments were also carried out. Polymers were synthesised in the presence of 0.20 mol $dm^{-3}$ pyrrole and 0.01 mol $dm^{-3}$ Sβ-CD in water at 0.900 V vs. SCE to 1.0 C $cm^{-2}$. Cyclic voltammograms were recorded in 0.10 mol $dm^{-3}$ DA solution in 0.10 mol $dm^{-3}$ $Na_2SO_4$ solution, at a scan rate of 50 mV $s^{-1}$, for both a bare and the modified platinum electrode (SA = 0.479 $cm^2$).

$KNO_3$ salt bridges were prepared using the method outlined by Shakhashiri.[19] The growth of the polymers was achieved, as described in Section 4.2.2.5.1, where the potential applied was 0.900 V vs. SCE and the polymers were grown to a thickness corresponding to a charge of 10.0 C $cm^{-2}$. The incorporation and release steps were carried out as described in Sections 4.2.2.2 and 4.2.2.3, respectively, however the counter electrode was separated from the DA solution, in order to prevent the possible oxidation of DA at the counter electrode.

#### 4.2.2.5.3 Influence of varying the incorporation step

In this step, all polymers were synthesised onto a platinum wire in the presence of 0.20 mol $dm^{-3}$ pyrrole and 0.01 mol $dm^{-3}$ Sβ-CD in water, where a 0.900 V vs. SCE potential was applied until 2.0 C $cm^{-2}$ of a charge was passed, unless otherwise stated. DA was incorporated by transferring the set up to a 0.10 mol $dm^{-3}$ DA solution and applying various reduction potentials, ranging from -0.900 to -0.400 V vs. SCE, for 30 min. In addition, the reduction period was varied by

changing the amount of time the polymers were subjected to a potential of -0.900 V vs. SCE.

In all cases, the DA solution used for the incorporation stage was made up in the presence of a supporting electrolyte, 0.10 mol $dm^{-3}$ $Na_2SO_4$. An examination into the presence of this supporting electrolyte was performed where its concentration was varied from 0.0 to 0.10 mol $dm^{-3}$ $Na_2SO_4$. Polymers were prepared, DA was incorporated and released, as summarised previously.

#### 4.2.2.5.4 Influence of varying the release step

In examining this process for the PPy/Sβ-CD system, the polymers were electrochemically deposited onto the platinum wire, in the presence of 0.20 mol $dm^{-3}$ pyrrole and 0.01 mol $dm^{-3}$ Sβ-CD, polarised at 0.900 V vs. SCE to a charge of 3.0 C $cm^{-2}$, unless otherwise stated. DA was incorporated, as outlined in Section 4.2.2.2, and the release was achieved by applying a potential from -0.300 to 0.300 V vs. SCE. The amount of time allowed for the release was also varied from 30 to 720 min.

### *4.2.2.6 EQCM measurements*

EQCM data were recorded for the uptake and release of DA in the PPy/Sβ-CD system. In the case of all the EQCM measurements, polypyrrole films were electrochemically deposited onto gold quartz crystal electrodes with an active surface area (SA) of 0.203 $cm^2$, at an oxidation potential of 0.700 V vs. SCE from a solution of 0.20 mol $dm^{-3}$ pyrrole and 0.01 mol $dm^{-3}$ Sβ-CD, until a charge of either 1.5 x $10^{-2}$ C or 3.6 x $10^{-2}$ C was passed. All solutions were prepared using distilled water. A Pt wire was used as a counter electrode, while a 3.0 mol $dm^{-3}$ Ag/AgCl electrode was used for the reference electrode. Once the polymers were prepared they were washed well with distilled water and immersed in a 0.10 mol $dm^{-3}$ DA solution prepared in distilled water.

The DA was incorporated by applying a reduction potential of -0.900 V vs. SCE for either 100 or 600 s. The electrodes were again washed with distilled water

and transferred to a 0.10 mol $dm^{-3}$ $Na_2SO_4$ solution where the release of the DA was achieved by applying 0.100 V vs. SCE for either 100 or 600 s.

This technique, in conjunction with chronoamperometry, was also used to monitor the release of the DA during the switching of the potential. As outlined above the polymers were electrochemically deposited at an oxidation potential of 0.700 V vs. SCE from a solution of 0.20 mol $dm^{-3}$ pyrrole and 0.01 mol $dm^{-3}$ Sβ-CD until a charge of 1.5 x $10^{-2}$ C was passed. The polymers were then washed and immersed in a 0.10 mol $dm^{-3}$ DA solution prepared in a 0.10 mol $dm^{-3}$ $Na_2SO_4$ supporting electrolyte and the potential was pulsed from -0.900 to 0.100 V vs. SCE every 100 s.

As described previously in Section 2.5.1, the frequency shift, caused by changes in the mass during the electrochemical experiments, was measured using a frequency counter. The resonant frequency shift, $\Delta f$, relates to the mass change, $\Delta M$, in accordance with the Sauerbrey equation, Equation 4.1:

$$\Delta f = -\frac{2f_0^2 \Delta M}{A\sqrt{\rho\mu}} \qquad 4.1$$

where $f_0$ is the resonant frequency, $\Delta M$ is the mass change, $A$ is the surface area of the electrode or film, $\rho$ is the density of quartz , 2.648 g $cm^{-3}$, and $\mu$ is the shear modules of quartz, 2.947 x $10^{11}$ g $cm^{-1}$ $s^{-2}$. Only thin polymer films were used, and accordingly, the Sauerbrey equation is valid giving a very good estimate of the mass changes accompanying the release of DA.

## 4.3 Results and Discussion

### 4.3.1 Dopamine, a cationic model drug

The objectives of any drug delivery system (DDS) are to incorporate a drug into a drug carrier and to deliver these drugs into the body in a controlled manner, at the target site, at a required time and at a particular concentration. The

current methods of drug delivery exhibit specific problems that scientists are attempting to address. For example, the potencies and therapeutic properties of many drugs are limited, or otherwise reduced, because of the partial degradation that occurs before they reach a desired target in the body. Time-release medications, upon intake, deliver treatment continuously. However, this can be a disadvantage as the drug can become unresponsive to the symptoms.

Therefore, the goal of any DDS is to deploy drugs intact to specifically targeted areas which can be controlled by means of either a physiological or chemical trigger. Materials already under consideration are dendrimers[20], liposomes[21], and hydrogels[22]. Release mechanisms vary from diffusion, swelling and degradation of the DDS. Although these concepts of release are good, they are not very efficient as there is no way of controlling the amount of drug released. For example, in the case of diffusion, which is a slow process, there is no control of delivery or concentration to the site. The same can be said for the swelling and degradation processes. Accordingly, the challenge is to provide an ideal system which responds to a biological environment, i.e., deliver the drug when it is needed and switch off the delivery when it is no longer required. Several other experimental drug delivery systems show exciting signs of promise, including those composed of electroactive polymers. In this chapter results are presented and discussed on electroactive PPy films for the controlled delivery of a well-known neurotransmitter, dopamine, DA.

Dopamine, Figure 4.1, in an aqueous media pH~6, exists as a cationic species. As described in Chapter 1, dopamine is a neurotransmitter and is of considerable interest due to its use in the treatment of Parkinson's disease. To deliver this cationic species, the PPy films were doped with a number of large anions, with particular focus on the use of the large anionic and immobile dopant, sulfonated β-cyclodextrin (Sβ-CD).

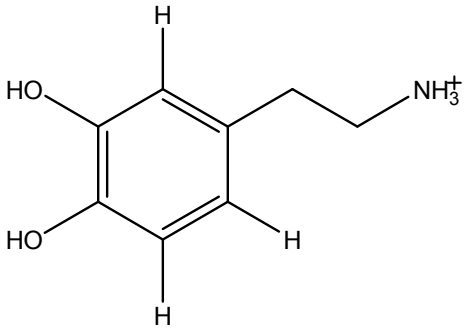


**Figure 4.1:** Structure of DA in its protonated state.

Many authors have investigated the uptake and release of pharmaceutically important compounds from conducting polymer films and have monitored the release using various techniques, including cyclic voltammetry (CV)[23], high powered liquid chromatography (HPLC)[24], radio labelling[15] in addition to the most common of all, and the technique employed in these studies, UV-visible spectroscopy (UV)[25-27]. As DA absorbs in the UV region, this technique was employed. Figure 4.2 shows the absorbance as a function of wavelength for a 1.0 x $10^{-4}$ mol $dm^{-3}$ DA solution in water. The DA compound absorbs between 260 and 300 nm, with a $\lambda_{max}$ of 280 nm.

However, DA is light and oxygen sensitive. As previously shown in Chapter 1, catecholamine compounds can undergo both electrochemical and chemical oxidation.[28, 29] The oxidation of the catecholamine group has been documented to show changes in the UV spectral data, with the quinone showing a $\lambda_{max}$ of 310 nm.[28, 30] Therefore, an investigation into the time frame allowed for experiments to be carried out on the DA solutions, under normal conditions, were considered. Figure 4.3 shows the UV data obtained for a 1.0 x $10^{-4}$ mol $dm^{-3}$ DA solution monitored over 240 min with exposure to air and light. From this figure, the oxidation of DA is clearly observed from the increase in the absorbance at 310 nm. After 120 min, oxidation of DA was evident, while considerable oxidation is seen after 240 min. During the oxidation of DA a band at ~ 310 nm progressively increases in intensity until it overlaps the band observed at 280 nm, along with a band forming at ~ 470 nm and is characteristic of the chrome form of the oxidation product of the DA.[30] This

oxidation limited the potentials that could be applied to release DA, Sections 4.3.3.3 and 4.3.4.3, and its exposure to air and light, during the release steps.

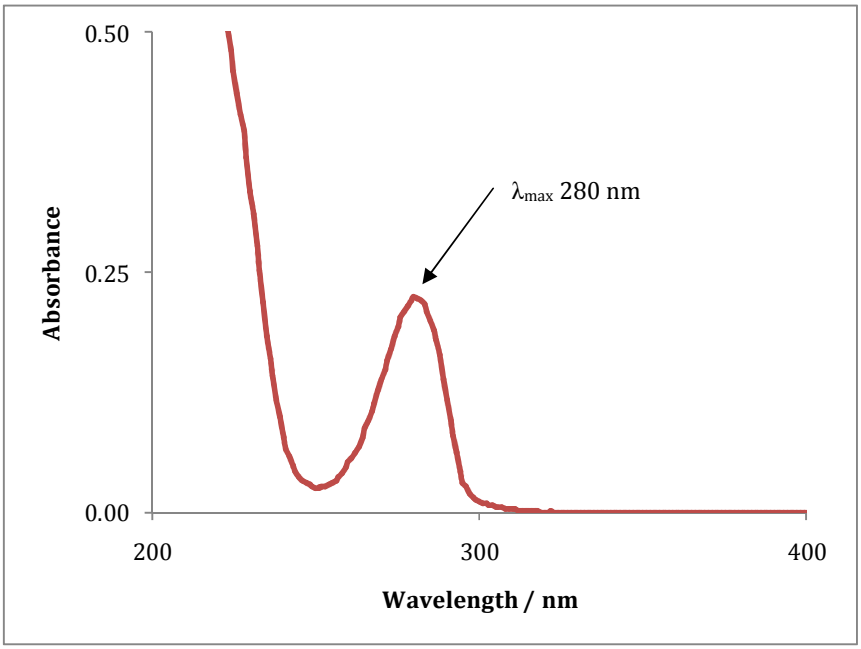


**Figure 4.2:** UV spectrum of 1.0 x $10^{-4}$ mol $dm^{-3}$ DA in water.

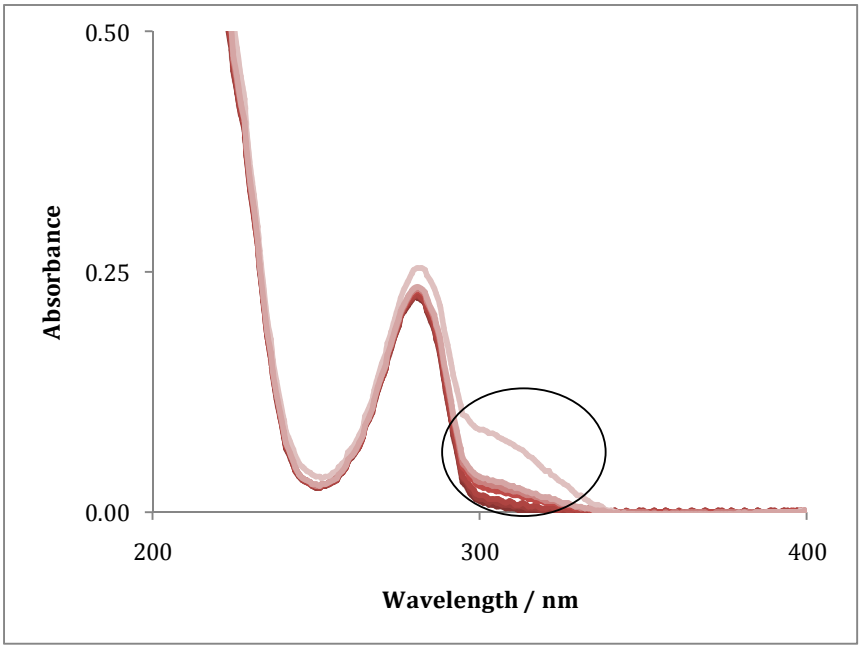


**Figure 4.3:** Absorbance plotted as a function of wavelength for 1 x $10^{-4}$ mol $dm^{-3}$ DA in water over time. Absorbance spectra recorded after ♦ 60 ♦ 120 ♦ 180 and ♦ 240 min. Highlighted region indicates oxidation.

### 4.3.2 Polymer preparation

In the 1980's, research into the use of PPy films for the uptake and release of biochemical molecules was suggested and proved by Burgmayer and Murray[12], and Miller *et al*.[23] A decade later the research on these materials was focused on finding new composite films to uptake and release many different types of drugs.[31] Recent studies have investigated the use of PPy for the uptake and release of more complex compounds, including proteins.[15] It is well known that PPy films have the capabilities to incorporate and release chemical substances be it dyes[32], anionic drugs[5, 11, 18, 26] cationic species[23] and proteins[15]. In all cases the release of the substances can be achieved using electrochemical stimulation.

As discussed in Chapter 3, electrochemical deposition of the pyrrole monomer occurs during the oxidation of the monomer and the incorporation of anions or dopants to maintain charge neutrality. It has been well reported that anionic species such as ATP[11] and salicylate[5] can be simultaneously incorporated or doped during electrochemical polymerisation of the pyrrole. This is due to the fact that during the oxidation of the monomer cations (polarons and bipolarons) are produced along the polymer backbone and the inclusion of anions to compensate these charges involves the uptake of these anionic species. However, although it was attempted (results are not shown), DA is a cationic species and cannot act as a dopant during the polymerisation of pyrrole. Accordingly, in order to investigate the uptake and release of this cationic species, polymers were firstly electrochemically deposited onto the working electrode in the presence of various anions. After polymerisation, the polymers are in their fully oxidised state and when reduced in the presence of the cationic species in solution, some of these cations will be incorporated within the polymer matrix. They can be subsequently released upon application of an appropriate oxidation potential. Scheme 4.1 illustrates the mechanism and concept behind the binding and release of the cationic DA.

The first system discussed here is the PPy/$SO_4$ system; all experimental details are provided in Section 4.2.2.4. Different parameters were varied to optimise the uptake and release of DA.

$$PPy^{+}A^{-} + e^{-} + DA^{+} \rightarrow PPy^{0}A^{-}DA^{+}$$ Reduction

$$PPy^{0}A^{-}DA^{+} - e^{-} \rightarrow PPy^{+}A^{-} + DA^{+}$$ Oxidation

**Scheme 4.1:** Processes involved during reduction and oxidation of the PPy film in the presence of the cationic DA, where $A^-$ represents an immobile dopant anion.

### 4.3.3 Influence of varying parameters for PPy/$SO_4$ system

As previously mentioned, PPy has the ability to bind and release ions, due to its redox properties. During polymerisation of the monomer, where the polymer was doped with $SO_4^{2-}$ or $HSO_4^-$ anions, the black polymer films were deposited onto the platinum wire. Figure 4.4 shows typical current-time transients recorded for the growth of a PPy/$SO_4$ film in an aqueous solution. Two separate growth curves are presented which indicate a reasonably good reproducibility from experiment to experiment and is characteristic of the results obtained throughout these studies. These distinctive growth transients have been discussed in Chapter 3, Section 3.3.1. In this case, the polymer backbone is oxidised and anions, $A^-$, are needed to compensate for the charge and consequently are incorporated into the polymer matrix, as demonstrated in Scheme 4.2.

$$Py + MA \rightleftharpoons PPy^{+}A^{-}$$

**Scheme 4.2**: Doping of PPy with anions, $A^-$, during electropolymerisation in a solution of MA.

Following the electrochemical synthesis, the polymer films were then washed with copious amounts of distilled water and transferred to the cationic DA solution, where a reduction potential was applied. Figure 4.5 shows a typical current-time transient for the reduction of the polymer film in the presence of the cationic DA solution with a supporting sulfate electrolyte at -0.900 V vs. SCE.

There is an initial rapid decrease in the reduction current, which is followed by a slower rate of reduction until most of the PPy film is reduced.

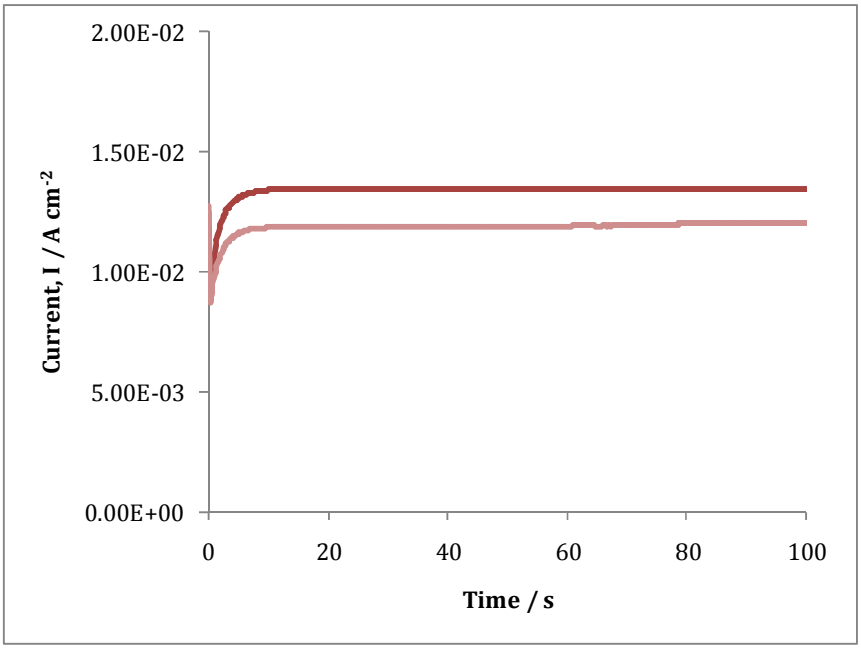


**Figure 4.4:** Current as a function of time for the electro-oxidation of pyrrole in the presence of 0.10 mol $dm^{-3}$ $Na_2S0_4$ at 0.750 V vs. SCE.

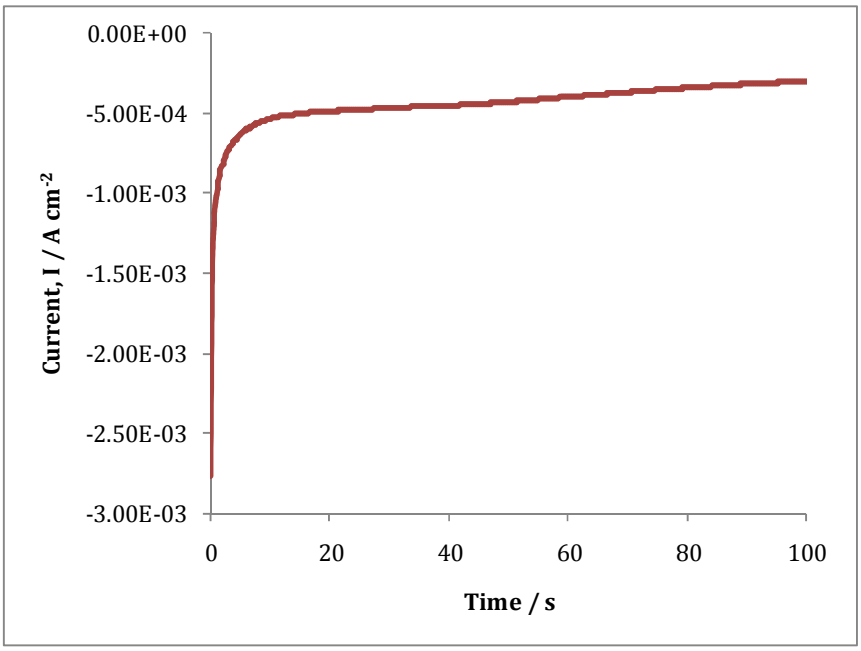


**Figure 4.5:** Current as a function of time for the reduction of $PPy/SO_4$ film in a solution of 0.10 mol $dm^{-3}$ DA in 0.10 mol $dm^{-3}$ $Na_2S0_4$ at -0.900 V vs. SCE.

Subsequently, after reduction of the polymer films in the DA solution, the films were washed with 0.10 mol $dm^{-3}$ $Na_2SO_4$, and transferred to a cuvette placed in the UV spectrophotometer, where an oxidation potential was applied to stimulate the release of DA. Upon application of an anodic potential, the polymer film was re-oxidised and therefore any cations incorporated during the reduction step, should be released to maintain the charge neutrality, Scheme 4.1. Figure 4.6 shows a representative current-time transient recorded when an oxidation potential of 0.200 V vs. SCE was applied to the PPy film.

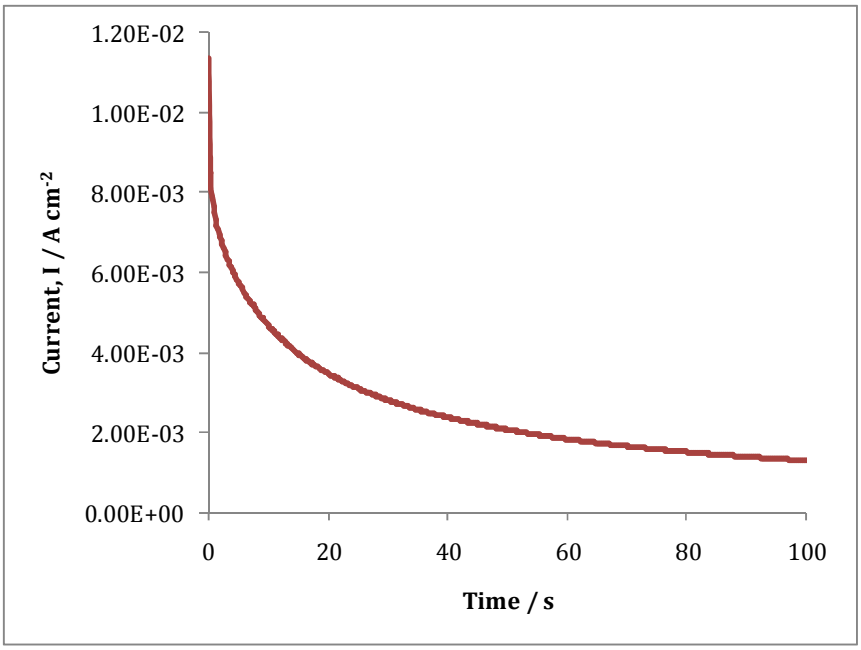


**Figure 4.6:** Current as a function of time for the oxidation of the $PPy/SO_4$ film loaded with DA to achieve the release of DA into 0.10 mol $dm^{-3}$ $Na_2SO_4$ at 0.200 V vs. SCE.

As detailed in Section 4.2, UV-visible spectroscopy was used to monitor the release of the DA as a function of time. As discussed earlier, Section 4.3.1, DA has a strong absorbance peak in the UV region at a $\lambda_{max}$ of 280 nm. Figure 4.7 illustrates the spectral data obtained for the release of DA, from a $PPy/SO_4$ polymer film synthesised at 0.750 V vs. SCE to 1.0 C $cm^{-2}$, where the incorporation of DA was achieved by applying a reduction potential of -0.900 V vs. SCE for 30 min and where the release was accomplished through the

application of an oxidation potential of 0.200 V vs. SCE. Release of DA was monitored over a 60 min period. Using the DA calibration curve, as detailed in Section 2.5.2, Figure 2.9, the amount of DA released was computed as a function of time. It is clear from Figure 4.7, that DA is indeed released from the PPy/$SO_4$ film and that the absorbance continues to increase with increasing time.

Accordingly, as the DA was successfully incorporated and released, a number of parameters were varied in order to optimise the release of the DA from the prepared PPy/$SO_4$ films. This included studies on the polymer thickness, the incorporation potential, the pH of the incorporating DA solution, the release potential and the dopant used during the electrochemical polymerisation of pyrrole.

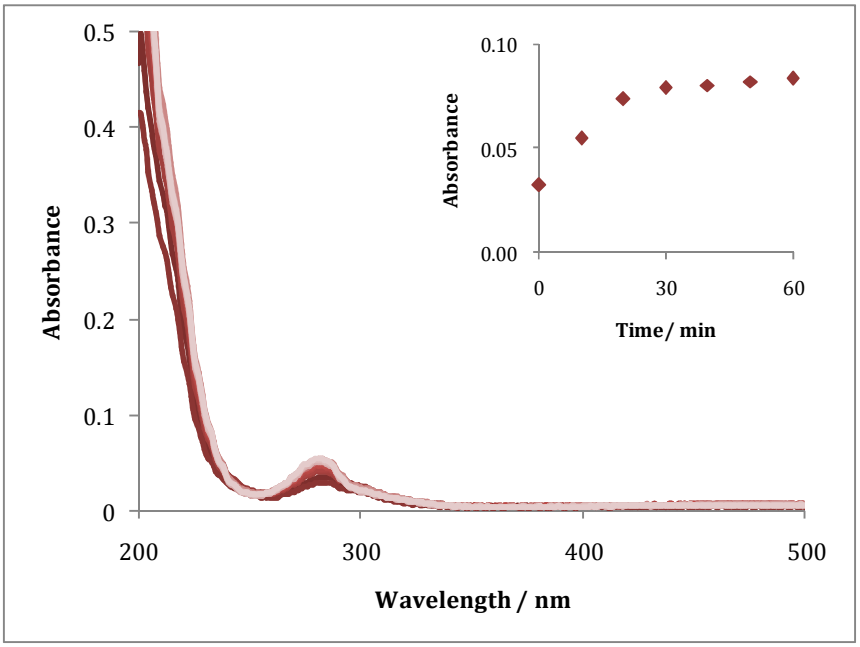


**Figure 4.7:** Absorbance as a function of wavelength for the release of the DA upon the application of an oxidation potential of 0.200 V vs. SCE to a PPy/$SO_4$ film where DA was incorporated upon reduction of the film in 0.10 mol $dm^{-3}$ DA/0.10 mol $dm^{-3}$ $Na_2SO_4$ at -0.900 V vs. SCE. Release medium was 0.10 mol $dm^{-3}$ $Na_2S0_4$. Data were recorded for 60 min. Inset shows the release as a function of time.

#### *4.3.3.1 Influence of varying the growth potential and charge of PPy/$SO_4$ film*

The first parameter examined was the anodic potential applied during the deposition of the polypyrrole film from the sulfate solution. As previously mentioned, the pyrrole monomer oxidises to form a polymer chain which incorporates anions to neutralise the charge. In applying a number of oxidation potentials to the polypyrrole film, the physical and mechanical properties of the film can change. In this set of experiments, the polymers were synthesised in the presence of 0.20 mol $dm^{-3}$ pyrrole and 0.10 mol $dm^{-3}$ $Na_2S0_4$, until a charge of 5.0 C $cm^{-2}$ was reached. The DA was incorporated and the procedures outlined in Section 4.2.2.4.1 were then used to achieve the release of the DA. Figure 4.8 shows the amount of DA released after 60 min, upon application of an oxidation potential, 0.100 V vs SCE, to the PPy/$S0_4$/DA loaded film. It is clear from this figure that there is no significant change in the amount of DA released from the films grown at different potentials in the range between 0.500 and 0.900 V vs. SCE. The maximum amount of DA released is 50 nmol $cm^{-2}$ and this occurs at a growth potential of 0.75 V vs. SCE.

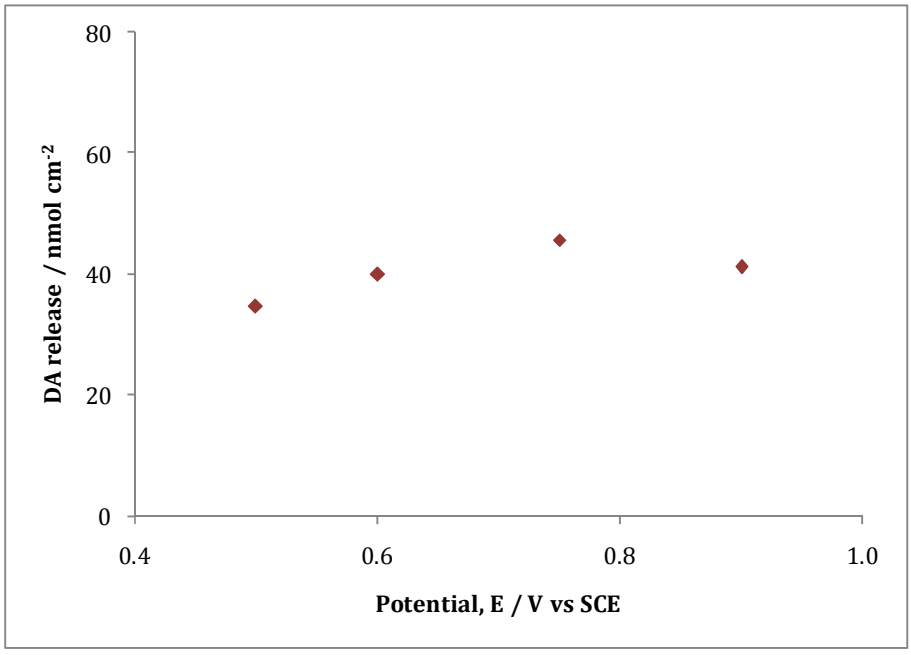


**Figure 4.8:** DA released as a function of the potential applied during electrochemical polymerisation of PPy/$SO_4$ films grown to a charge of 5.0 C $cm^{-2}$. DA was incorporated at -0.900 V vs. SCE and released at 0.100 V vs. SCE.

The thickness of the polymer films was also considered. The polymer films were electrochemically deposited to three different charges which were deposited at a constant potential of 0.600 V vs. SCE. The release of DA was achieved as described in Section 4.2.2.2. Figure 4.9 demonstrates the release of DA as a function of the charge reached during electrochemical deposition. It is evident from this figure that as the charge increases, which is proportional to the thickness of the film, the amount of DA released over 60 min increases considerably, reaching 200 nmol $cm^{-2}$ for polymers grown to a charge of 10.0 C $cm^{-2}$.

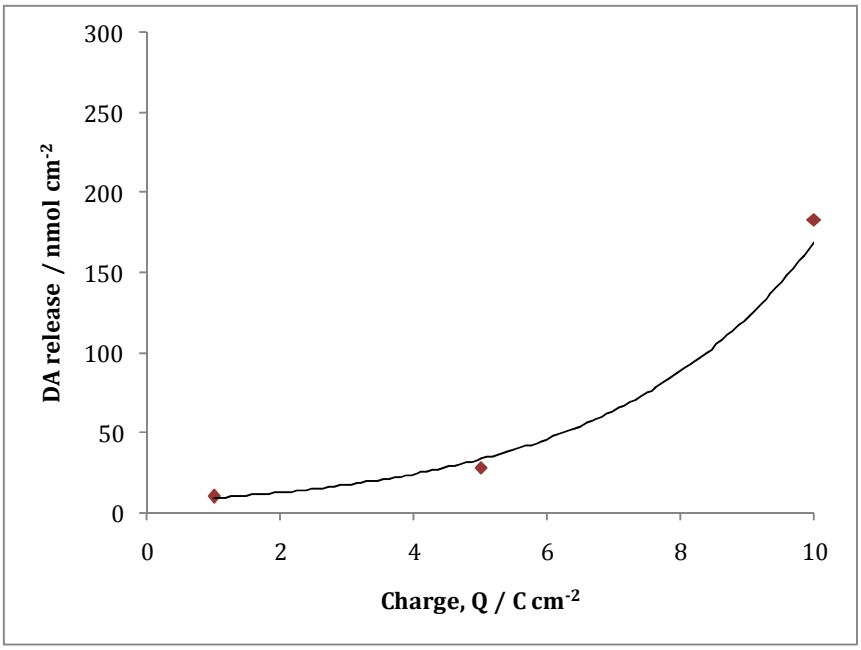


**Figure 4.9:** DA released as a function of the charge passed during the polymerisation of pyrrole at an oxidation potential of 0.600 V vs. SCE in 0.1 mol $dm^{-3}$ $Na_2SO_4$. DA was incorporated at -0.900 V vs. SCE and released at 0.100 V vs. SCE for 60 min.

### *4.3.3.2 Influence of varying the incorporation step*

Next, a series of experiments was carried out to optimise the incorporation of DA into the polypyrrole films. Both the potential used to reduce the polymer, i.e., the incorporation potential and the pH of the DA solution were varied.

#### 4.3.3.2.1 Influence of varying the incorporation potential

The incorporation potential was varied from -0.400 to -1.000 V vs. SCE. This step is an important one as it determines the amount of DA incorporated into the polymer film. Figure 4.10 shows the amount of DA released after oxidation of the PPy film, as described in Section 4.2.2.4.2, where the DA was incorporated at various reduction potentials. It is clear that as the incorporation potential is reduced to lower reduction potentials, greater amounts of DA are bound and on subsequent oxidation, the polymer film shows an increased release of DA.

Figure 4.11 shows some of the corresponding current-time transients for these data. It is evident from this figure that the lower reduction potentials give rise to more efficient reduction of the polymer film, which in turn enables the ingress of the cationic DA. There is a three-fold increase in the amount of DA released on varying the reduction potential from -0.400 to -1.000 V vs. SCE, which indicates that not alone is DA incorporated, but the sulfate anions are not ejected on reduction. If these anions are lost, then the reduced polymer, $PPy^{o}$, will not bind the cationic DA.

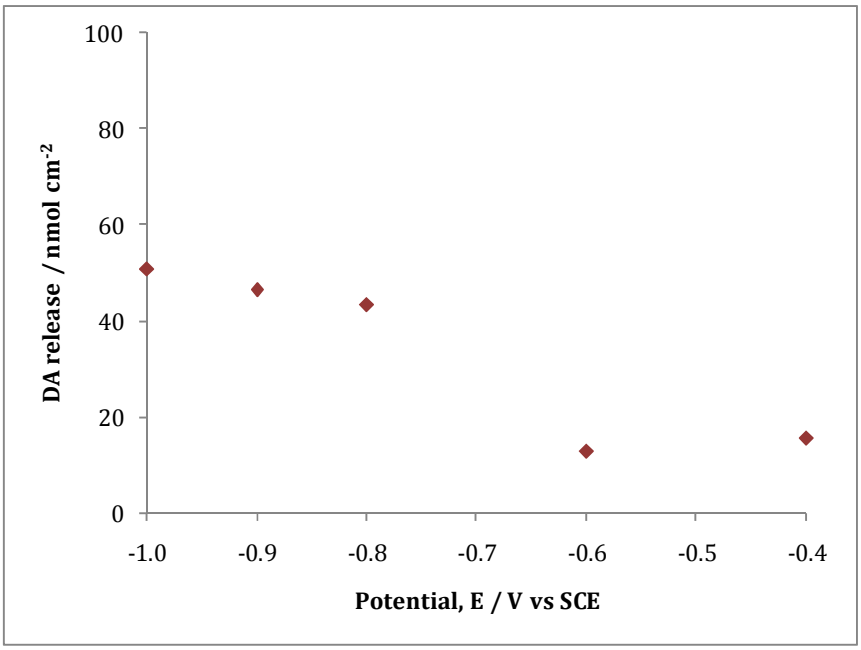


**Figure 4.10:** DA released as a function of the potential applied to the polymer films during the reduction or incorporation step.

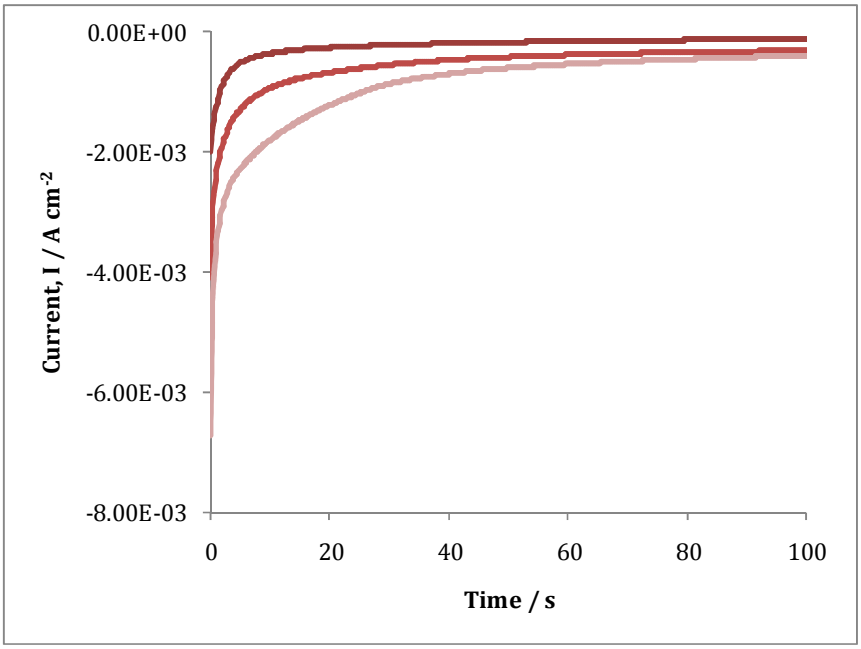


**Figure 4.11:** Current-time transients recorded for the reduction of the polypyrrole film in the DA solution. ♦ -0.200 V vs. SCE ♦-0.600 V vs. SCE ♦-1.000 V vs. SCE.

#### 4.3.3.2.2 Influence of varying the pH of the incorporating DA solution

DA exists as a protonated species in aqueous media. Consequently, the influence of the pH of the incorporating DA solution was investigated. Figure 4.12 shows the DA released after 60 min from polymers which were synthesised as described in Section 4.2.2.4.2, but the pH of the DA solution was varied during the DA-incorporation step. From this figure it is evident that a change in the pH of the DA incorporation solution has no significant effect on the amount of DA incorporated or released from the polypyrrole films.

This result is consistent with the fact that the amount of DA in its protonated form is reasonably constant over this pH range. The ratio of DA in the neutral and protonated states can be obtained by considering the Henderson Hasselbalch equation, Equation 4.2, and using $HA^+$ to represent the protonated DA and A to indicate the neutral form ($HA^+ \rightleftharpoons H^+ + A$). This relationship can be

arranged to give Equation 4.3, providing the ratio of the neutral to the protonated DA, in terms of the pH and p*K*a value of DA, which is 8.92.

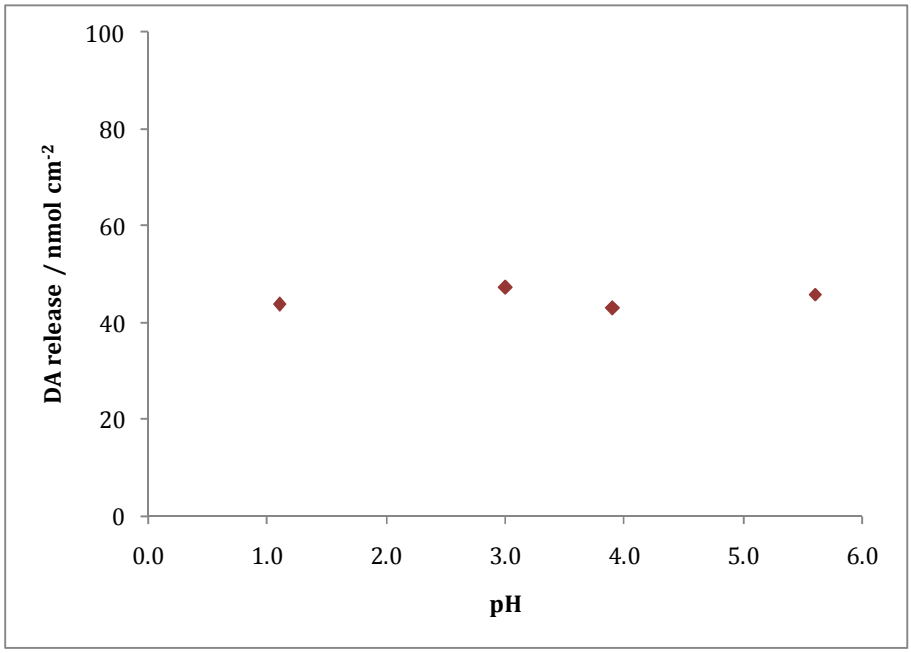


**Figure 4.12:** DA released, nmol $cm^{-2}$, from the $PPy/SO_4$ films as a function of the pH of the DA incorporation solution, 0.10 mol $dm^{-3}$ DA and 0.10 mol $dm^{-3}$ $Na_2SO_4$.

——— 4.2

——— 4.3

Using Equations 4.2 and 4.3, the ratio of protonated DA to the neutral DA can be computed and it remains essentially constant at 99.9% between the pH values from 1.0 to 6.0. Therefore, it is not surprising that the amount of DA released remains essentially constant between pH values of 1.0 and 6.0, Figure 4.12.

### *4.3.3.3 Influence of varying the release step*

#### 4.3.3.3.1 Influence of varying the release potential

In the final step of optimising the parameters for the delivery of DA from the PPy/$SO_4$ system, the release process was investigated. This step involves the application of an anodic potential in order to re-oxidise the polymer film which, in turn, releases the cations from the polymer matrix. Once again, the polymers were electrochemically synthesised as outlined in Section 4.2.2.4.3, and the DA was incorporated using a potential of -0.900 V vs. SCE for 30 min. The release of the DA was then achieved by varying the oxidation potential. Figure 4.13 shows the UV spectral data obtained when various potentials were applied to the prepared polymers. It is apparent from these data that there is a considerable variation in the UV absorbance. This is due to the oxidation of the DA molecule as previously described. The DA is converted to the quinone form with applied potentials greater than 0.200 V vs. SCE. Therefore, the oxidation potential was limited to values $\leq$ 0.100 V vs. SCE to ensure that DA was released in its pure un-oxidised form.

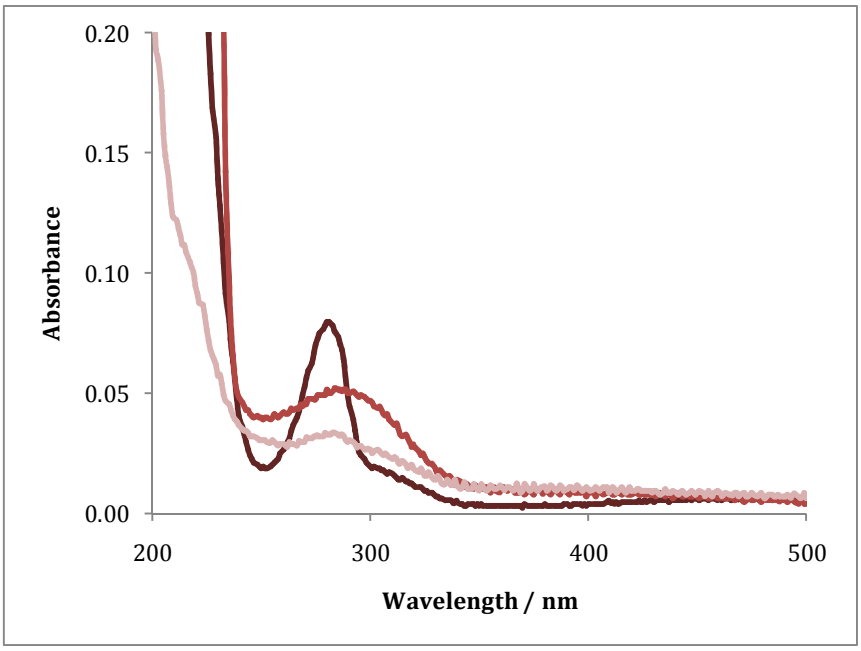


**Figure 4.13:** UV spectra of DA release from polymers grown to 1.0 C $cm^{-2}$ from 0.20 mol $dm^{-3}$ pyrrole and 0.10 mol $dm^{-3}$ $Na_2SO_4$ at 0.600 V vs. SCE. Release of the DA was achieved by applying ♦ 0.100 ♦ 0.200 ♦ 0.300 V vs. SCE for 60 min.

#### *4.3.3.4 Influence of varying electrolyte*

It has been reported that the use of different dopants can change the structure and porosity of polypyrrole.[33] With this in mind, the dopant anion was varied to investigate its influence for the uptake and release of DA. Polymers were prepared using the experimental procedures outlined in Section 4.2.2.4.3, where the only variation was the dopant anion. The incorporation of the DA was accomplished by applying a reduction potential of -0.900 V vs. SCE in the presence of 0.10 mol $dm^{-3}$ DA. Subsequent release of the DA, which was monitored using UV-visible spectroscopy, is shown in Figure 4.14 for each dopant. It should be pointed out that the concentration of Sβ-CD was 10 times lower than the concentration of the other dopant anions. Figure 4.15 shows representative UV absorption peaks centred at 280 nm for the DA release from each polymer composite after 60 min. It is clear that the release of DA from the PPy/Sβ-CD system is significantly improved in comparison to the DA released from the other PPy films. There is no, or negligible release, of DA from the PPy/Cl system. This is probably connected with the fact that the chloride anion is a mobile dopant and as the oxidised polypyrrole film is reduced in the DA solution, the chloride anions are expelled, with little or no uptake of the cationic DA. The larger PTS and Sβ-CD are immobile and reduction of the polypyrrole is accompanied by the ingress of the cationic DA.

Table 4.2 expresses the amount of DA released in nmol $cm^{-2}$ as a function of the dopant anion used during the electrochemical synthesis. This reiterates that the amount of DA released is far superior from the PPy/Sβ-CD films when compared to the other films investigated. It is also important to point out that there is an increase in the stability of the DA released, Figure 4.15. Due to this significant improvement, the PPy/Sβ-CD system was explored in greater detail, the results of which are presented in Section 4.3.4.

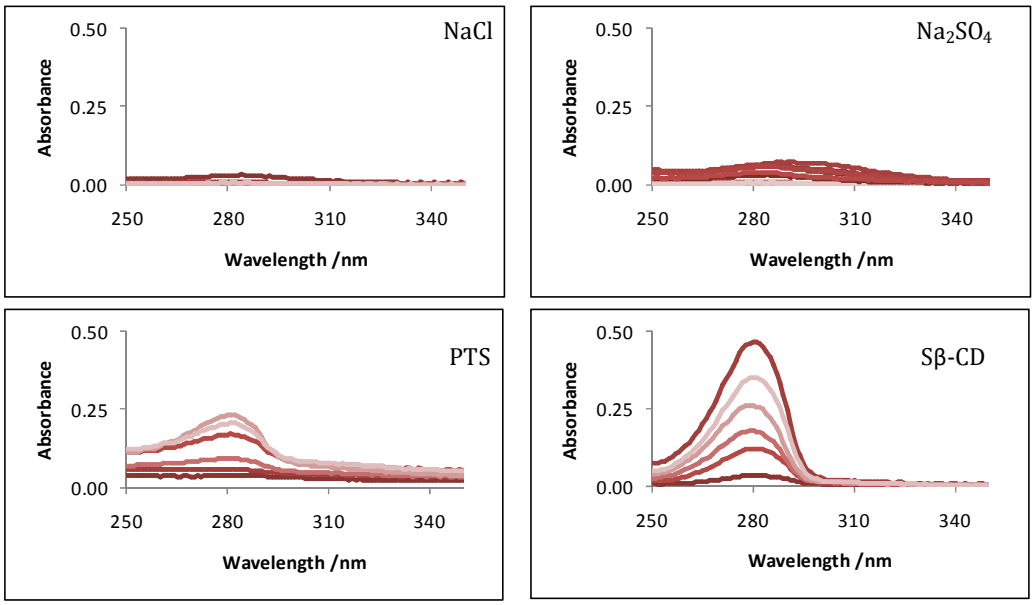


**Figure 4.14:** UV data for the release of DA at 0.100 V vs. SCE from polymers prepared with the various anionic dopants shown in the plots.

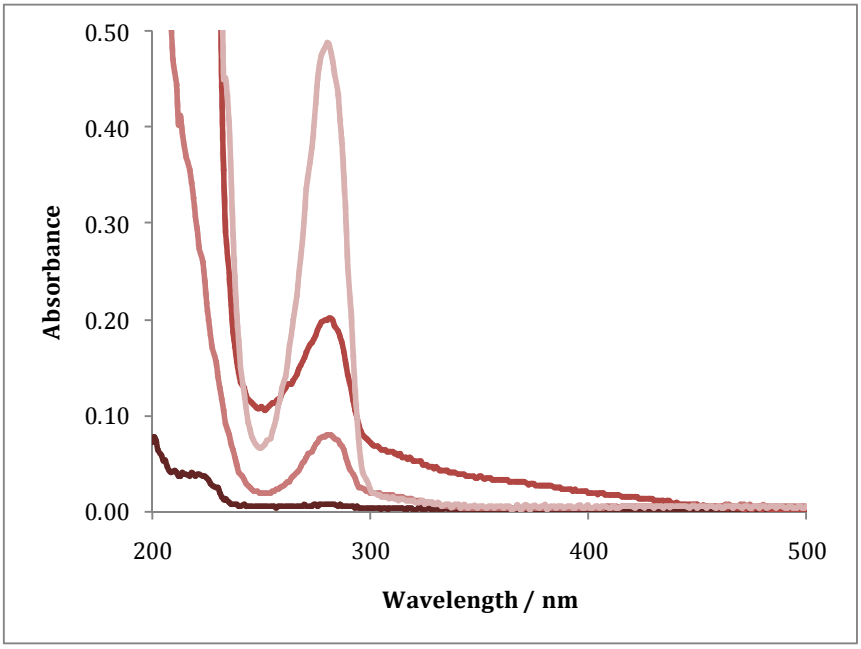


**Figure 4.15:** UV data for the release of DA at 0.100 V vs. SCE after 60 min from polymers prepared with the various anionic dopants: ♦ NaCl ♦ $Na_2SO_4$ ♦ PTS ♦ Sβ-CD.

**Table 4.2:** DA released after 60 min from the various polymer films doped with different anions.

| Dopant | DA release / nmol $cm^{-2}$ |
|---|---|
| NaCl | 5 |
| $Na_2SO_4$ | 60 |
| PTS | 165 |
| Sβ-CD | 404 |

### 4.3.4 Influence of varying parameters for PPy/Sβ-CD system

Due to the substantial increase in the amount of DA released when the polymer was doped with the large immobile anionic Sβ-CD dopant, this novel material for the uptake and subsequent release of DA was further investigated. Bidan *et al*.[34] reported that during the electrochemical polymerisation of pyrrole in the presence of Sβ-CD anions, due to their size and immobility, they remain entrapped within the polymer matrix and as a consequence require the uptake of cations to compensate for the charge. Figure 4.16 shows a typical voltammogram of the redox properties of a PPy/Sβ-CD film. The nature of the ionic species exchanged during the cycling is evident. In the first segment of cycle 1, as the potential is cycled from an initial potential of 0.500 V vs. SCE to more negative values, there is a pronounced cathodic peak at -0.556 V vs. SCE, which corresponds to the incorporation of the cationic species. Accordingly, the corresponding anodic peak at -0.322 V vs. SCE represents to the point where both cations and anions are expelled and inserted, respectively. It is also evident that this behavior, although slightly suppressed, is observed for the successive cycles, indicating that the ionic exchange is potential dependent, reversible and stable. Bidan and co-workers[34] also reported similar observations of the PPy/Sβ-CD films cycled in the presence of 0.50 mol $dm^{-3}$ $LiCI0_4$ aqueous solutions.

Therefore, when a reduction potential is applied to the PPy/Sβ-CD film, cations from the solution flow into the film to maintain the charge neutrality. Upon application of an oxidation potential, the process is reversed and the expulsion of the cations is observed. This behaviour has thus widened the use of these films for the application of drug delivery devices. An examination into the various stages of the synthesis and uptake and release was hence performed and these results are now presented.

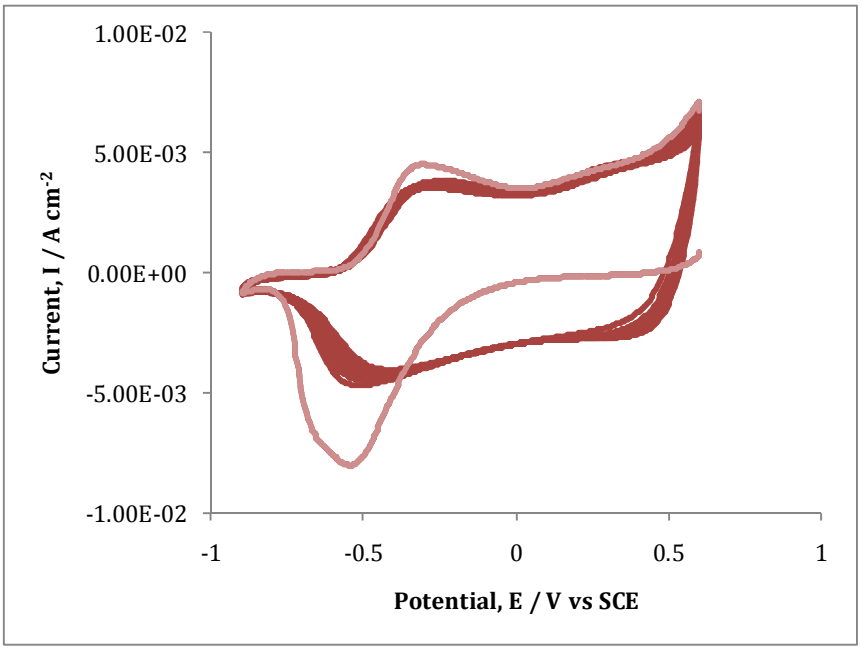


**Figure 4.16:** CV data recorded in 0.10 mol $dm^{-3}$ $Na_2SO_4$ at 50 mV $s^{-1}$ for a PPy/Sβ-CD film synthesised at 0.700 V vs. SCE from an aqueous solution containing 0.20 mol $dm^{-3}$ pyrrole and 0.01 mol $dm^{-3}$ Sβ-CD to a charge of 0.6 C $cm^{-2}$. ♦ Cycle 1 ♦ Cycles 2 – 10.

### *4.3.4.1 Influence of varying the PPy film growth conditions*

#### 4.3.4.1.1 Influence of varying potential applied upon growth of the polymer

The first parameter studied for the uptake and release of DA from these PPy/Sβ-CD films was the potential applied during the growth of the polymer films. The current-time transients recorded were previously shown in Chapter 3, Figure

3.11. This figure showed that as the anodic potential was increased during the potentiostatic growth, the currents increased, indicating a higher rate of electropolymerisation at the higher applied potentials. Figure 4.17 illustrates the maximum amount of DA released, from these PPy/Sβ-CD films synthesised, as a function of the deposition potential.

There were two observations taken from this figure. The first is that the polymers synthesised at 1.000 V vs. SCE appear to observe a lower amount of DA released after 60 min, in comparison to the other PPy/Sβ-CD films. This is possibly due to the fact that at this high formation potential, the resistance of the films is high, as it is well known that polypyrrole films are easily over-oxidised with potentials higher than 0.800 V vs. SCE. This high resistivity can lead to the loss of activity of the film and, therefore, a decrease in its conductivity.[35] In turn, the amount of DA incorporated is suppressed.

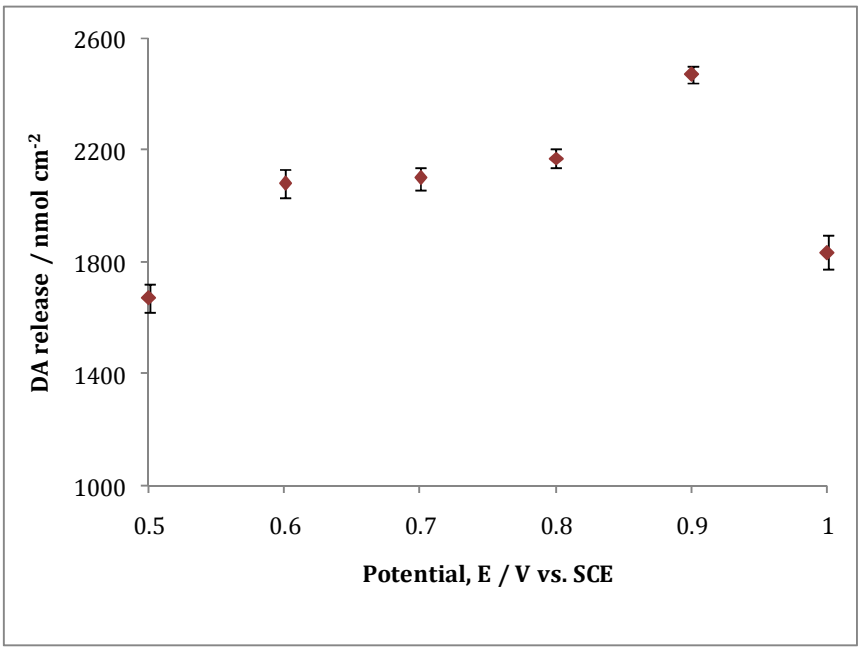


**Figure 4.17:** DA release from the PPy/Sβ-CD films electrochemically deposited onto platinum wire at various potentials. Polymers were synthesised using 0.20 mol $dm^{-3}$ pyrrole and 0.01 mol $dm^{-3}$ Sβ-CD to a charge of 2.0 C $cm^{-2}$.

The second observation is that polymers electropolymerised at 0.500 V vs. SCE also lead to a decreased amount of DA released. It is known that as the potential, applied during electropolymerisation, is increased it changes the physical and mechanical properties of the polymer structure; an increase in the porosity of the polymer is observed. Therefore, at this lower deposition potential the polymer matrix is not as porous as the polymers deposited at higher anodic potentials and, in turn, this gives rise to a decrease in the number of DA cations incorporated within the polymer composite. Furthermore, the doping levels are known to increase with increasing formation potential.[36] At a formation potential of 0.500 V vs. SCE, lower levels of the sulfonated β-CD are incorporated as a dopant within the polymer matrix. Since it is the immobile Sβ-CD dopant that gives rise to the ingress and incorporation of DA during the reduction of the polymer, a decrease in its concentration will lead to a reduction in the amount of DA incorporated and bound in the polymer.

As 0.900 V vs. SCE yields the greatest DA release over a 60 min period, this potential was used to synthesise the polymers for the investigation of the influence of the polymer thickness and most subsequent experiments.

#### 4.3.4.1.2 Influence of varying polymer thickness

In varying the thickness of the polymer films, as long as the constant potential applied allows for the further oxidation of the monomer, the only limitation in how thick a film can be grown is the availability of the pyrrole monomer.[35] For this study, polymers were potentiostatically synthesised onto platinum wire from 0.2 mol $dm^{-3}$ pyrrole where the thickness of the PPy films deposited at the working electrode was varied by holding the potential constant and changing the growth time. In these cases the potential was held at 0.900 V vs. SCE. The DA was incorporated, washed and released as described, in Section 4.2.2.5.1.

Figure 4.18 shows the charge plotted as a function of time for the growth plots of the various PPy/Sβ-CD films used in this study. It can be seen that higher charges are measured with increasing polymerisation times, increasing in a

linear manner at a rate of 0.089 ± 0.001 C $cm^{-2}$ $s^{-1}$. In addition, there is very good reproducibility from experiment to experiment. Figure 4.19 shows the total amount of DA released after 60 min as a function of the charge to which the polymer films were synthesised. The figure shows a linear relationship between the DA released and the electropolymerisation charge. As observed with the PPy/$SO_4$ films, it is the thickness of the PPy/Sβ-CD films which has the greatest effect on the amount of DA released.

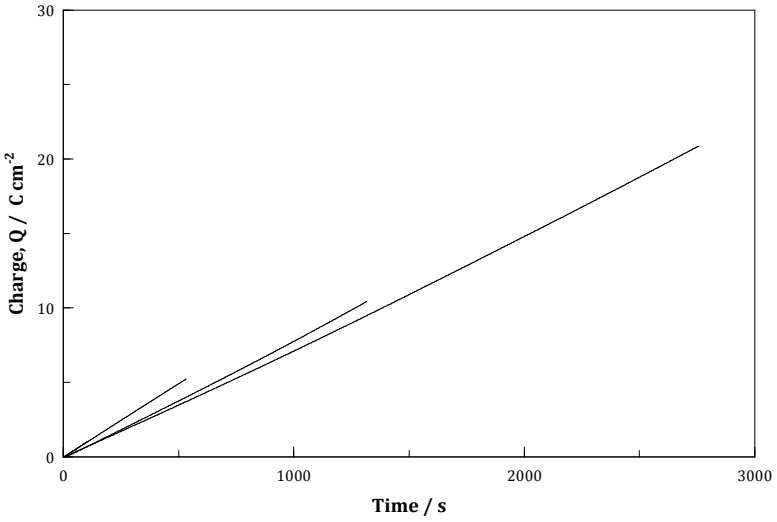


**Figure 4.18** Charge as a function of time for the potentiostatic growth of PPy films from 0.20 mol $dm^{-3}$ pyrrole and 0.01 mol $dm^{-3}$ Sβ-CD where a potential of 0.900 V vs. SCE was applied.

The amount of charge consumed as a function of their corresponding DA release, upon reduction and oxidation, of films grown to various thickness is shown in Figure 4.20 and 4.21, respectively. The final release amounts show a linear relationship with the charge consumed during both potential applications. Zhou *et al.*[37] obtained similar findings for a polymer system investigating the release of dimethyldopamine ($1H^+$) from a poly(N-methylpyrrole)/poly(styrenesulfonate) ($PMP^+PSS^-$) film. They attributed these results to the fact that the release of the $1H^+$ was instigated electrochemically by the redox process.

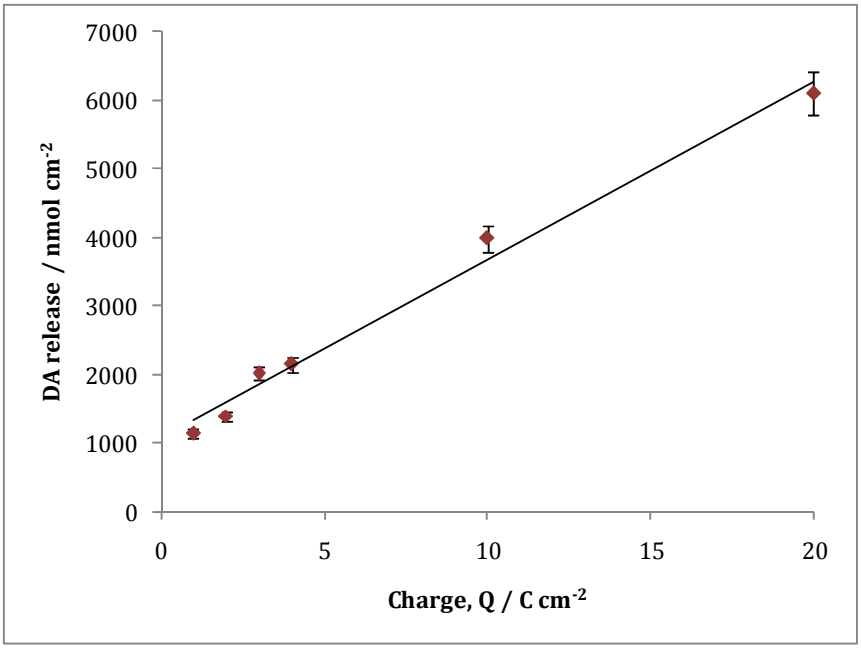


**Figure 4.19:** DA release from the polymers potentiostatically grown at 0.900 V vs. SCE to various charges in the presence of 0.20 mol $dm^{-3}$ pyrrole and 0.01 mol $dm^{-3}$ Sβ-CD where DA was incorporated and released upon application of -0.900 and 0.100 V vs. SCE, respectively.

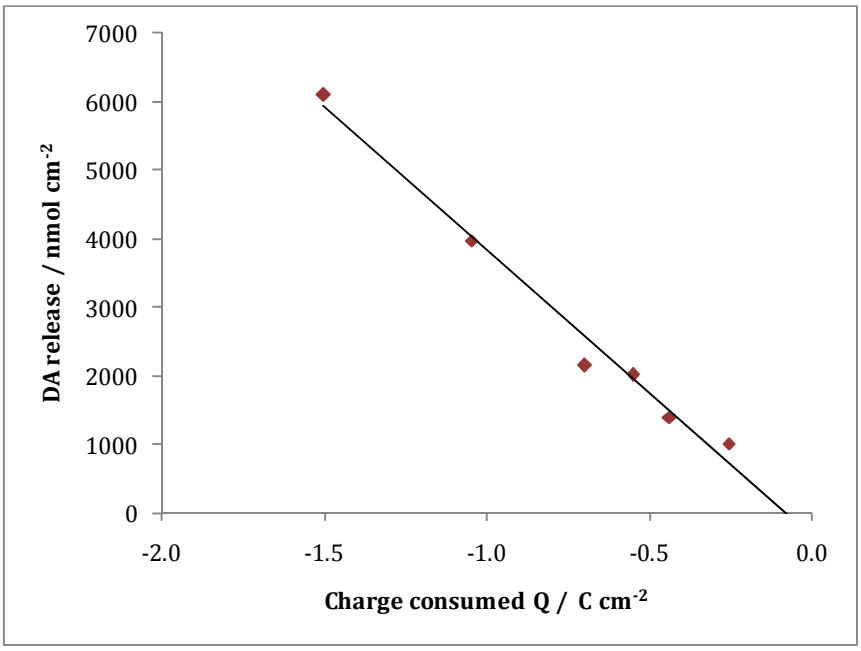


**Figure 4.20:** DA release as a function of the charge consumed during the incorporation of DA where polymers were potentiostatically grown at 0.900 V vs. SCE to various charges in the presence of 0.20 mol $dm^{-3}$ pyrrole and 0.01 mol $dm^{-3}$ Sβ-CD. DA was released upon application of -0.900 V vs. SCE for 30 min.

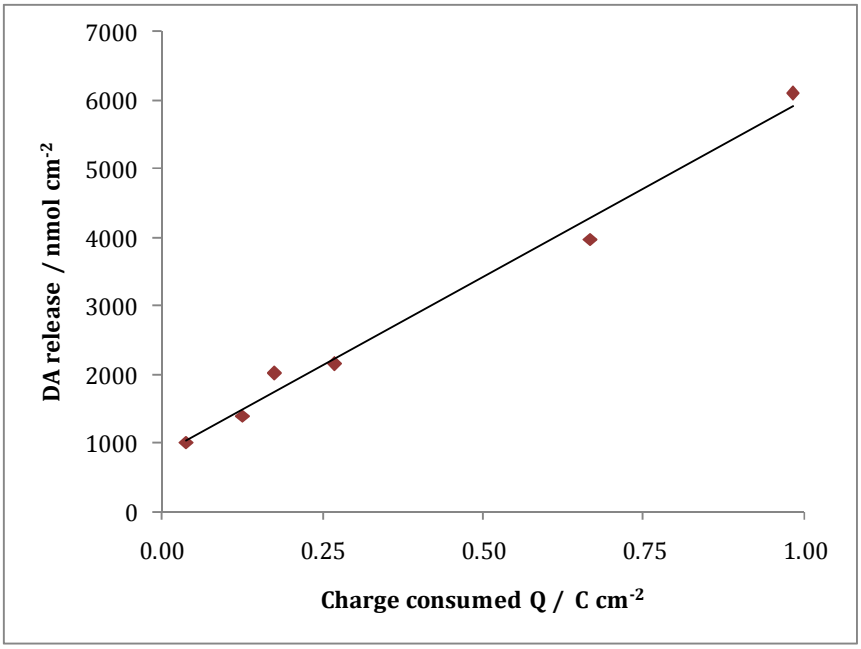


**Figure 4.21:** DA release as a function of the charge consumed during the release of DA where polymers were potentiostatically grown at 0.900 V vs. SCE to various charges in the presence of 0.20 mol $dm^{-3}$ pyrrole and 0.01 mol $dm^{-3}$ Sβ-CD. DA was released upon application of 0.100 V vs. SCE for 60 min.

However, an unusual observation was made with the thicker polymer films; a shift in the absorption peak of DA from 280 nm to about 298 nm was identified with polymers which were potentiostatically grown to charges ≥ 4.0 C $cm^{-2}$. This peak shift is reported to be due to the presence of the oxidised species of DA, as discussed previously in Section 4.3.1.[28]

To understand this phenomenon several additional experiments were performed. The first possibility that was considered, and subsequently ruled out, was an interaction between the pyrrole monomer and the DA. During polymerisation of thick polymer films some monomer may remain entrapped within the matrix which could then potentially come into contact with the incorporated DA. Accordingly, a mixture of both the pyrrole monomer and the DA dissolved in water, were placed in an electrochemical cell in the UV spectrophotometer, and an anodic potential of 0.200 V vs. SCE was applied to the system for 10 min. Figure 4.22 shows the UV data obtained. It is clear from

these data that there is no shift between the spectra taken before and after the application of the anodic potential.

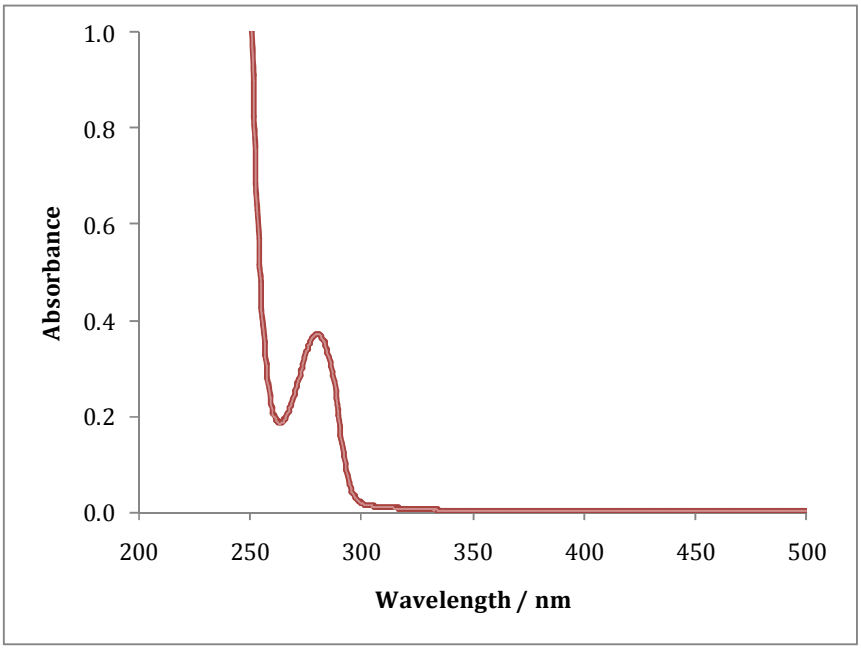


**Figure 4.22:** UV data obtained for a mixture of pyrrole and DA obtained ♦ before and ♦ after an application of an anodic potential of 0.200 V vs. SCE for 10 min.

It was then thought that the solutions contained too much oxygen and so, nitrogen gas was bubbled through all solutions; during the growth of the PPy/Sβ-CD films as well as the incorporation and release of the DA, (results not shown). The absorption peak shift was still evident, and so DA oxidation by dissolved oxygen was ruled out.

Consequently, hydrogen evolution was considered. During electrochemical reactions at a bare platinum working electrode, hydrogen evolution is evident at potentials closely related to the reduction potentials applied during the incorporation of the DA. If the rate of hydrogen evolution was high at the electrode surface during incorporation of the DA cation, it is possible that a local alkaline region may be created at the electrode surface. A local alkaline region in contact with the DA during incorporation could subsequently oxidise the DA upon uptake. However, Figure 4.23 shows CV data of a bare platinum electrode

and a modified PPy/Sβ-CD electrode cycled in 0.10 mol $dm^{-3}$ DA from -1.000 to 0.650 V vs. SCE at a scan rate of 50 mV $s^{-1}$. It is apparent from this figure that the hydrogen evolution occurring at the higher reduction potentials is considerably suppressed in the presence of the modified polymer. This result also rules out the involvement of the hydrogen evolution reaction in this event.

Another reason thought to be causing this event was the oxidation of the DA at the counter electrode. In the electrochemical cell the counter electrode (CE) allows current to flow through the analyte solution without passing current into or out of the reference electrode. Thus IR drop and electrode polarisation are eliminated.[38] However, if a reaction takes place at the CE, the species produced can easily diffuse throughout the electrochemical cell. It has been shown previously in Section 4.3.1, that DA oxidises at potentials > 0.200 V. Therefore, if the DA was being oxidised at the CE, coupled with the fact that the WE and CE are in close proximity to each other, the oxidised DA species may be incorporated into the film and consequently released.

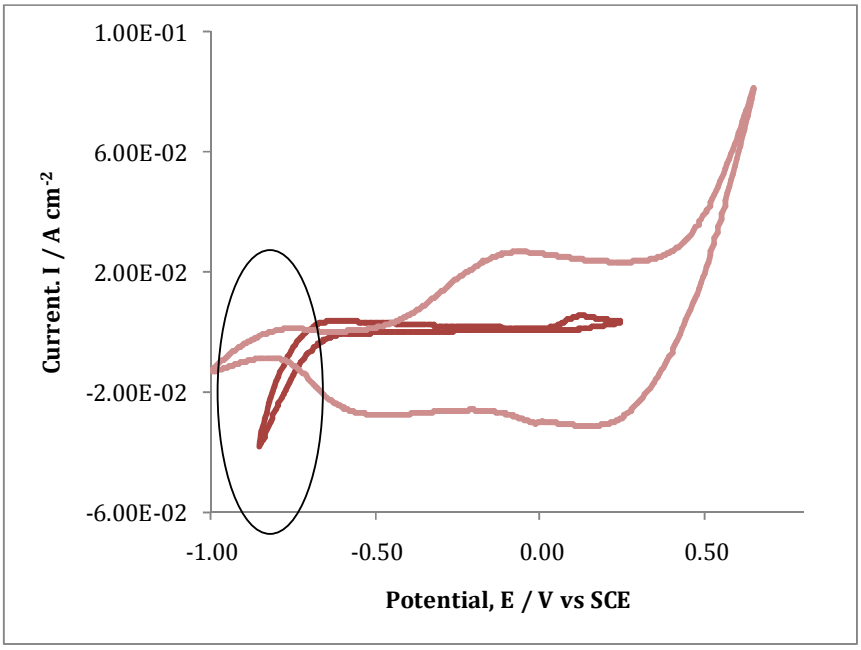


**Figure 4.23:** CV data recorded in 0.10 mol $dm^{-3}$ DA in the supporting electrolyte, 0.10 mol $dm^{-3}$ $Na_2SO_4$, at ♦ bare platinum ♦ PPy/Sβ-CD film. Scan rate was 50 mV $s^{-1}$. Highlighted is the region where hydrogen evolution readily occurs.

In general, a common way of eliminating the possibility of contaminating the electrochemical cell with the product of the chemical reactions taking place at the CE is the introduction of a salt bridge. A salt bridge allows for the flow of ions between two solutions while preventing mixing.[38] Therefore, a $KNO_3$ salt bridge was prepared in U-tubes, as outlined in Section 4.2.2.5.2, where, the CE was separated from the electrochemical cell. A schematic of which is illustrated in Figure 4.24.

Using this set up the incorporation and release of DA at the thicker PPy/Sβ-CD films was investigated. PPy/Sβ-CD films were synthesised at 0.900 V vs. SCE to a charge of 10.0 C $cm^{-2}$, where the DA was incorporated and released as normal using the set up shown in Figure 4.24. Figure 4.25 illustrates the absorbance as a function of wavelength for the release of DA at 0.100 V vs. SCE for 60 min. However, as is evident from Figure 4.25, the DA is still being released in its oxidised state.

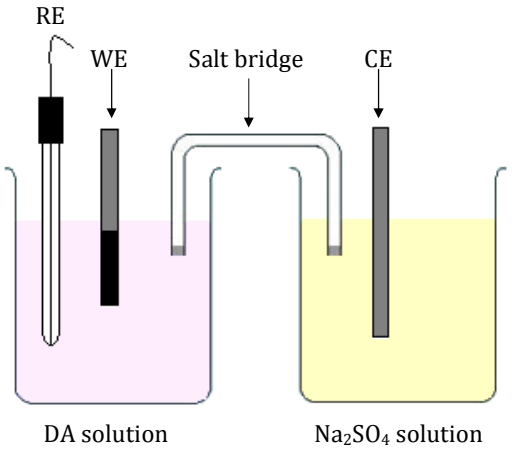


**Figure 4.24:** A schematic of the electrochemical set up using the salt bridge.

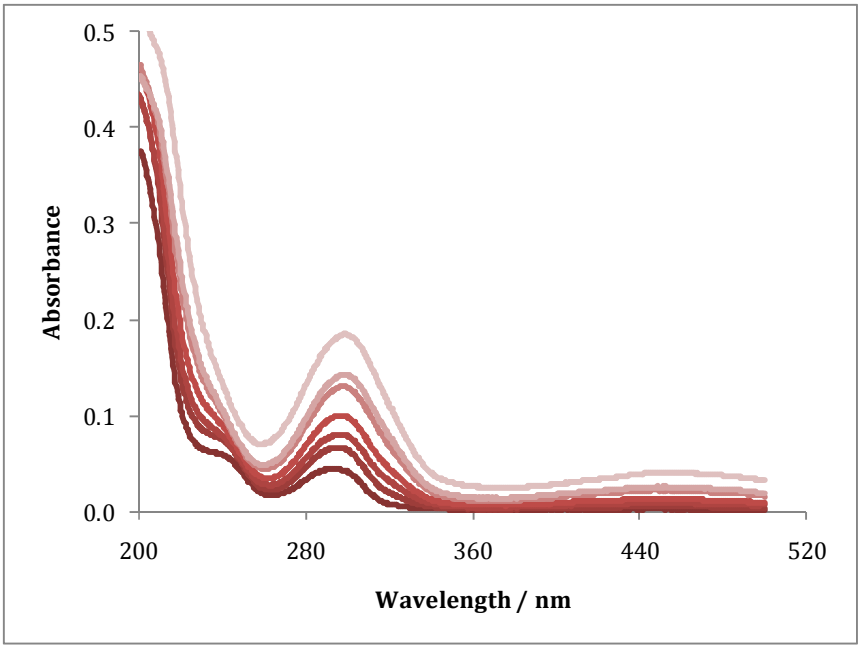


**Figure 4.25:** Absorbance as a function of wavelength for the release of DA, from a PPy/Sβ-CD film synthesised electrochemically onto a platinum wire at 0.900 V vs. SCE to 10.0 C $cm^{-2}$, where the DA was incorporated at -0.900 V vs. SCE and subsequently released at 0.100 V vs. SCE for 60 min using the salt bridge set up, shown in Figure 4.22.

The final suggestion for this phenomenon, and the one that appears to fit, is the possibility of localised capacitance. Capacitance, which is a build up of charge, can occur in areas where conjugation is not ideal and the current flow is suppressed. During the release of DA, from the polymer matrix, an anodic potential of 0.100 V vs. SCE is generally applied. A capacitive charge build up, due to the application of these potentials, can be present where the DA is bound. At a certain point, the capacitance charge can overcome the resistance of the conducting medium. This can lead to a build up of a greater amount of potential at capacitive regions, than that applied to the polymer system. DA can potentially (i) donate two electrons and (ii) act as a conducting medium, due to the presence of the protonated amine group. However, instead of acting like a normal ion which would carry the current, the DA may get oxidised. This event is not seen in thin polymer films because electrolyte ions can penetrate the

polymer layer easily and conjugation is not restricted, so a capacitive charge build up does not occur.

Although this problem has not been pinpointed, it can be overcome through limiting the polymer growth to $< 4.0$ C $cm^{-2}$. With this thickness limitation, the next step investigated in the optimisation of this drug delivery system was the incorporation step of the DA.

#### 4.3.4.1.3 Uptake and release of DA from PPy/Sβ-CD films synthesised in the presence of a supporting electrolyte

As already stated, there has been very little research reported in using Sβ-CD as a dopant for the polymerisation of pyrrole. In the experiments reported here, the electropolymerisation of pyrrole is carried out in the presence of Sβ-CD only. Therefore, it can be confirmed that it is the only anion doping the polymer film. Similar to this research, Bidan *et al*.[34] and Reece *et al*.[39] are the only groups found that carried out the same type of electropolymerisation in the presence, only, of the Sβ-CD anion. However, the other literature surveyed demonstrated the electropolymerisation of pyrrole in the presence of Sβ-CD and another supporting electrolyte.[40] These authors state that the large immobile anion is preferentially used to dope the polymer over the small mobile anion. Accordingly, this lead to a number of experiments being performed where the polymers were electrochemically deposited in the presence of a mixture of Sβ-CD and a supporting electrolyte, $Na_2SO_4$, and hence investigated for their uptake and release of DA.

Figure 4.26 shows the release of DA, from two different PPy films, as a function of time. Both polymers were electrochemically deposited at 0.900 V vs. SCE until a charge of 1.0 C $cm^{-2}$ was reached. In the first instance, the polymer was polymerised in the presence of Sβ-CD with 0.10 mol $dm^{-3}$ $Na_2SO_4$ supporting electrolyte, where as in the second case, the polymer was deposited, as normal, without any supporting electrolyte. In both systems the DA was incorporated and released as detailed in Section 4.2.2.5.1.

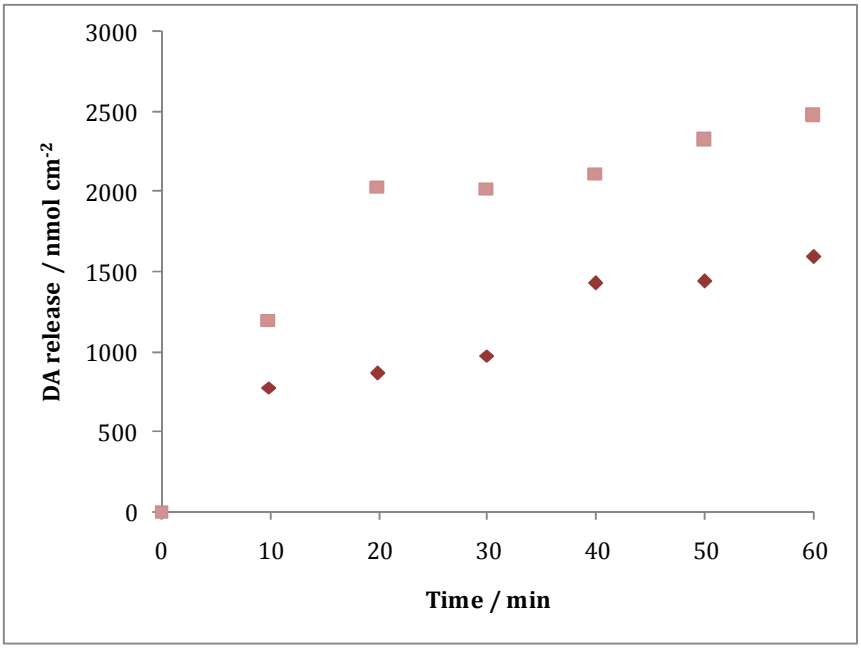


**Figure 4.26:** DA release as a function of time. Polymer films were synthesised in the presence of 0.20 mol $dm^{-3}$ pyrrole and 0.01 Sβ-CD (i) ♦ in 0.10 mol $dm^{-3}$ $Na_2SO_4$ and (ii) ■ in water.

It is evident that there is more DA released from the polymer synthesised without the $Na_2SO_4$ supporting electrolyte. However, in comparison to the amount released from a PPy/$SO_4$ polymer film, under the same conditions, there is a significant difference. For a PPy/$SO_4$ polymer film the DA released over a period of 60 min is ~ 100 nmol $cm^{-2}$, compared to ~ 1700 nmol $cm^{-2}$ from the combined PPy/$SO_4$, Sβ-CD system. If it were the case that the more mobile anion was doping the polymer then ideally similar results should be observed with the PPy/$SO_4$ and PPy/$SO_4$, Sβ-CD systems. However, this is not the case as the amount of DA released has increased more than 10 fold. This would suggest that the large immobile anionic cyclodextrin is indeed preferentially doping the polymer film over the smaller anion; there is only a small reduction in the amount of DA released when the mixed dopant system is used.

### *4.3.4.2 Influence of varying the incorporation step*

#### 4.3.4.2.1 Influence of varying the incorporation potential

The influence of the application of the reduction potential applied was investigated. We observe, from the EQCM data shown in Chapter 3, Figure 3.18, as well as the CV data shown in Figure 4.16, that the redox properties of the PPy/Sβ-CD films show a cathodic peak at ~ - 0.5 V. It is at this stage that the cations are taken up into the film. Figure 4.27 shows a typical current-time transient for the reduction of a PPy/Sβ-CD film in the presence of 0.10 mol $dm^{-3}$ DA in a supporting electrolyte of 0.10 mol $dm^{-3}$ $Na_2SO_4$. The current decays over the 200 s period, as the polypyrrole film is converted from the oxidised to the reduced state.

Figure 4.28 shows the amount of DA released as a function of the potential applied during the incorporation step. The PPy/Sβ-CD films were prepared as outlined in Section 4.2.2.5.2, where the DA was incorporated at various applied reduction potentials and subsequently released upon application of an anodic potential of 0.100 V vs. SCE for 60 min.

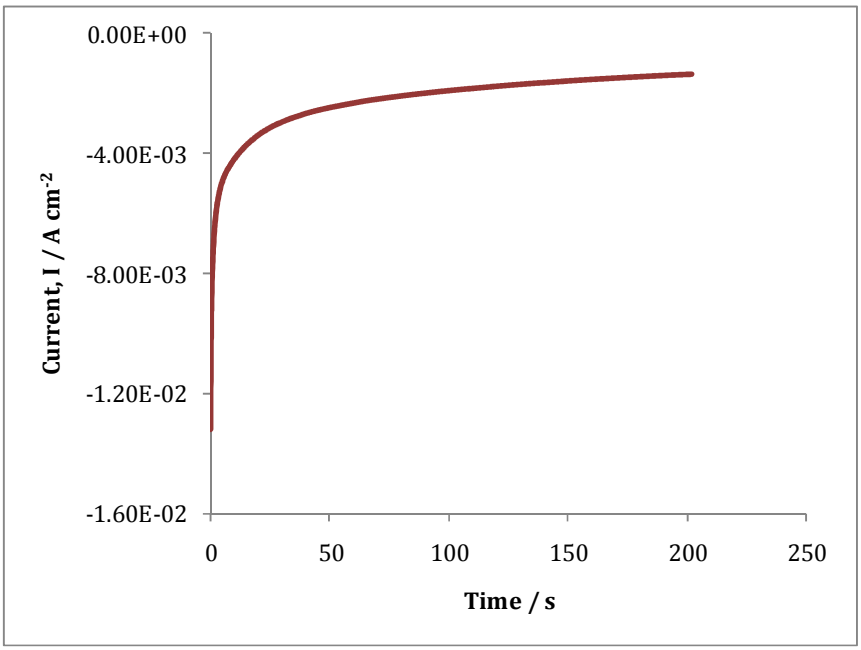


**Figure 4.27:** Current as a function of time for the reduction of the PPy/Sβ-CD film at -0.800 V vs. SCE in the DA solution.

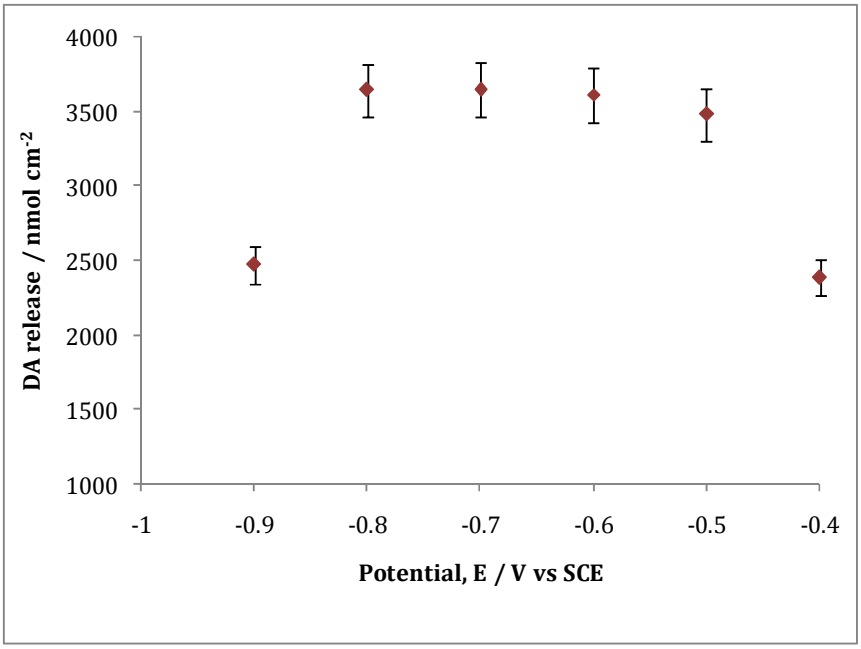


**Figure 4.28:** DA release as a function of the potential applied during the incorporation of DA. Films were grown at 0.900 V vs. SCE to 2.0 C $cm^{-2}$ in the presence of 0.20 mol $dm^{-3}$ pyrrole and 0.01 mol $dm^{-3}$ Sβ-CD, where DA was released upon application of 0.100 V vs. SCE for 60 min.

It is clear from this figure that at potentials more anodic than -0.500 V vs. SCE less DA is taken up into the film. It is also evident that there is little difference observed when the DA is incorporated at potentials in the range of -0.600 to -0.800 V vs. SCE. These findings are in good agreement with the redox properties of the PPy/Sβ-CD films, where the polymer is reduced at -0.556 V vs. SCE, Figure 4.16. However, at a potential of -0.900 V vs. SCE there is less DA released which correlates to less DA incorporated. This may be connected with the competing reduction of hydrogen ions at this potential.

Another experiment examined was the possibility of the uptake of DA through diffusion, where no potential was applied. The prepared polymers were immersed in a 1.0 x $10^{-3}$ mol $dm^{-3}$ DA solution and left standing over night. In order to eliminate the possibility of the DA oxidising during this experiment, a lower concentration was used, and the solutions were degassed with nitrogen gas and left with a blanket of $N_2$ overnight. After the set up was left to stand

overnight, the polymer was washed with distilled water and placed in a fresh, 0.10 mol $dm^{-3}$ $Na_2SO_4$ solution and monitored for release without applying a potential for 60 min. After this, an oxidation potential of 0.100 V vs. SCE was applied to investigate the release at an applied potential over a 120 min period. Figure 4.29 shows the DA concentration, expressed as absorbance, released over the total period of 180 min. From this figure the first observation is that DA was incorporated, while being immersed in a DA solution over night, without the application of a reduction potential. It also shows the DA is released slowly without the application of an oxidation potential. And finally, it demonstrates that there is a considerable rise, as highlighted on the figure at the 60 min time interval, in the amount released upon application of an oxidation potential. However, these absorbance values are low and correspond to DA levels of 200 nmol $cm^{-2}$. In summary, reduction of the polymer is required for the ingress of high amounts of DA and an oxidation potential is essential for the efficient release of the DA.

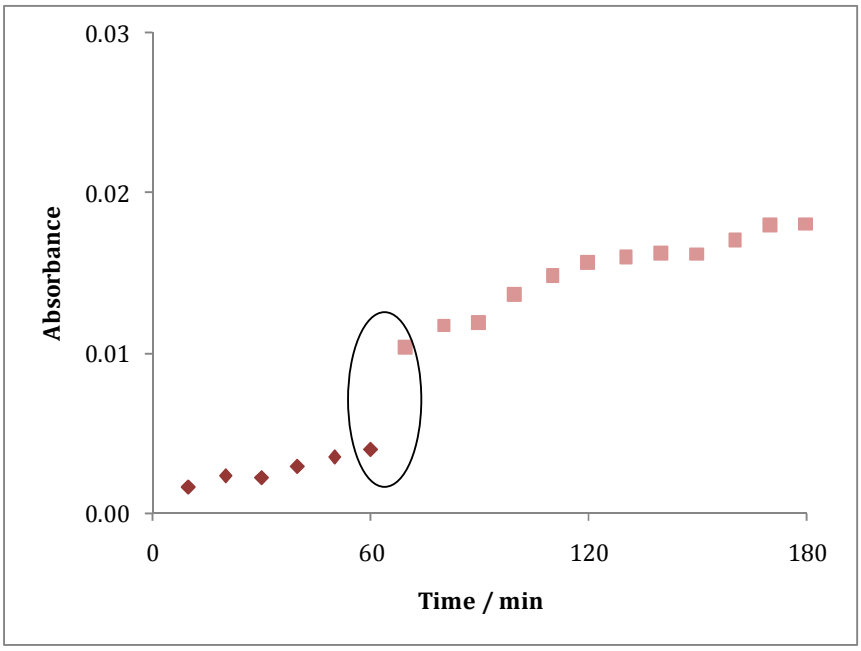


**Figure 4.29:** Absorbance at 280 nm as a function of time, where a PPy/Sβ-CD was electrodeposited onto the platinum wire at 0.900 V vs. SCE to 1.0 C $cm^{-2}$. DA was incorporated under open-circuit conditions for 12 hrs. DA release ♦ 1st 60 min under open-circuit conditions, ▪ a further 180 min at 0.100 V vs. SCE.

#### 4.3.4.2.2 Influence of varying incorporating time

Throughout the incorporation step a reduction potential is applied in order to uptake the DA cations into the polymer film. As shown in Figure 4.27, reduction of the polymer is not instantaneous, but takes place relatively slowly over time. In this section the period of this reduction step, or incorporation step, was varied. PPy films were deposited onto a platinum wire using the Sβ-CD as the dopant. The DA was then incorporated upon application of a reduction potential of -0.900 V vs. SCE for a varying amount of time. After the incorporation step, the polymers were subjected to the release step by applying an oxidation potential of 0.100 V vs. SCE for 60 min. Figure 4.30 shows the results obtained, the DA release is expressed in nmol $cm^{-2}$ and is shown as a function of the reduction or incorporation period. It is clear from this figure that the amount of DA liberated from the polymer films, increases with an increase in the timescale for the incorporation step, particularly during the first 30 min.

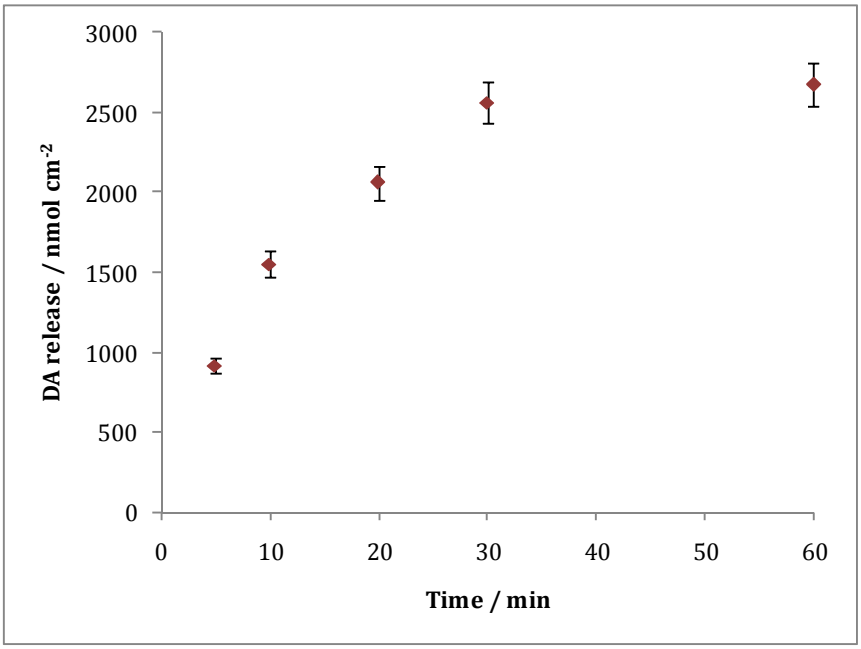


**Figure 4.30:** DA release as a function of the DA incorporation period at -0.900 V vs. SCE for PPy/Sβ-CD films that were grown at 0.900 V vs. SCE to 3.0 C $cm^{-2}$, where DA was released upon application of 0.100 V vs. SCE for 60 min.

#### 4.3.4.2.3 Influence of varying supporting electrolyte concentration

One issue that might arise during this incorporation step, in the presence of a supporting electrolyte, is competition between the cations. In order to determine the level of competition between DA and $Na^+$, the supporting electrolyte concentration was varied. Polymers were synthesised at 0.900 V vs. SCE to 3.0 C $cm^{-2}$, then reduced in a 0.10 mol $dm^{-3}$ DA solution in the presence of varying concentrations of $Na_2SO_4$. The incorporation of DA was achieved at -0.900 V vs. SCE for 30 min. Consequently, DA was released from the polymer film through an oxidation step, by applying an anodic potential of 0.100 V vs. SCE for 60 min. Figure 4.31 shows the amount of DA released as a function of the supporting electrolyte concentration. Although a substantial amount of DA is released when the DA is incorporated from water, indicating competition at low $Na^+$ concentrations, more efficient release is achieved in the presence of 0.1 mol $dm^{-3}$ $Na_2SO_4$. This can be explained in terms of the more efficient reduction of the polymer in the more conducting electrolyte solution.

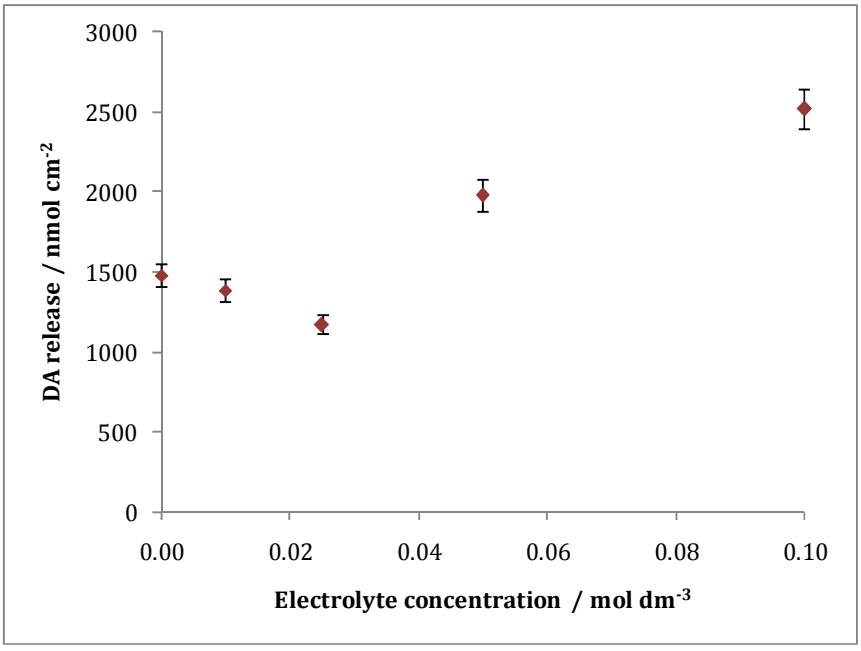


**Figure 4.31:** DA release as a function of the $Na_2SO_4$ electrolyte concentration used in the DA incorporation step from 0.10 mol $dm^{-3}$ DA for PPy/Sβ-CD films grown at 0.900 V vs. SCE to 3.0 C $cm^{-2}$, where DA was released upon application of 0.100 V vs. SCE for 60 min.

### *4.3.4.3 Influence of varying the release step*

#### 4.3.4.3.1 Influence of the release potential

Finally, the release step was examined for its influence on the delivery of DA. As discussed earlier in Section 4.3.1, DA oxidises under anodic conditions. Miller *et al*.[23] also suggested limiting the applied release, or anodic potential, of PPy films for the release of DA to $\leq$ 0.600 V. To investigate the influence of the release potentials applied in this PPy/Sβ-CD system, polymers were prepared electrochemically, as outlined in Section 4.2.2.5.3, and the DA was incorporated during the reduction of the polymer films at a potential of -0.900 V vs. SCE for 30 min. Figure 4.32 shows the UV spectra of the DA released after various oxidation potentials were applied to the film, in order to release the drug. From these data it is apparent that potentials > 0.200 V vs. SCE are not suitable for this release system, as there was clear evidence of the oxidation product of DA being formed, particularly at 0.300 V vs. SCE. This result is in agreement with the results previously shown in Section 4.3.3.3 for the release of DA from the PPy/$SO_4$ system. It can be understood that, at these anodic potentials, the DA is being oxidised and so the potential must be limited to $\leq$ 0.100 V vs. SCE to achieve release of the pure DA species.

As shown in Figure 4.16, oxidation of the PPy/Sβ-CD films occurs in the vicinity of -0.300 V vs. SCE. As this correlates with the release of the cations, the release potentials were varied from $\geq$ -0.300 V vs. SCE to 0.100 V vs. SCE to achieve the release of the DA from the PPy/Sβ-CD system. The PPy/Sβ-CD films were electrochemically deposited at 0.900 V vs. SCE to 3.0 C $cm^{-2}$, and then reduced in 0.10 mol $dm^{-3}$ DA solution in the presence of 0.10 mol $dm^{-3}$ $Na_2SO_4$ at -0.900 V vs. SCE for 30 min. DA was released from the polymer film through the application of an oxidation step, which was varied from -0.300 to 0.100 V vs. SCE for 60 min. Figure 4.33 shows the amount of DA released as a function of the release potential applied. From this figure it can be seen that there is no significant change in the amount of DA released upon application of the various release potentials. However, there is a gradual increase in the amount released as the potential is increased, from -0.100 to 0.100 V vs. SCE.

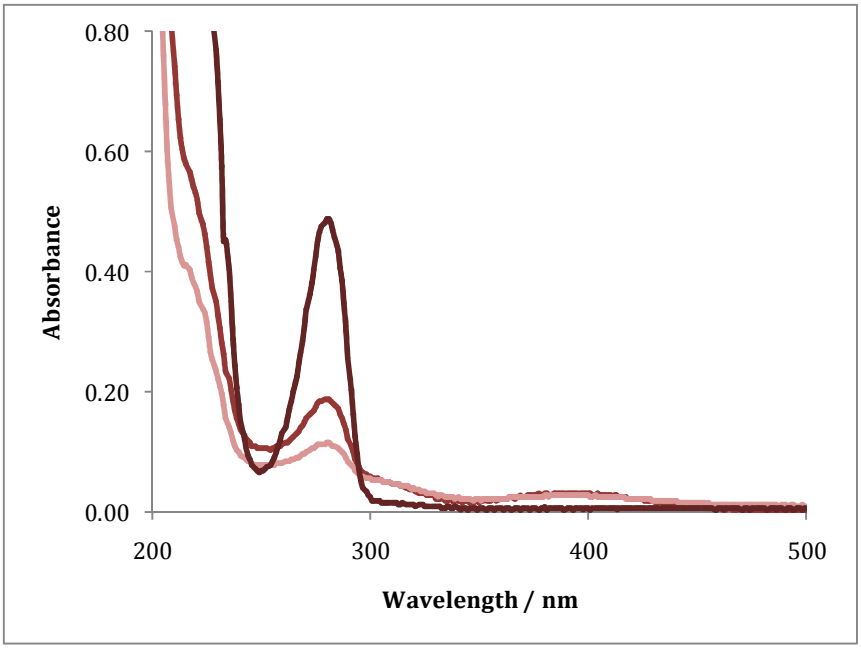


**Figure 4.32:** UV spectra of DA release from polymers grown to 2.0 C $cm^{-2}$ from 0.20 mol $dm^{-3}$ Py and 0.01 mol $dm^{-3}$ Sβ-CD at 0.600 V vs. SCE. Release of the DA was achieved by applying ♦0.100 ♦0.200 ♦0.300 V vs. SCE for 60 min.

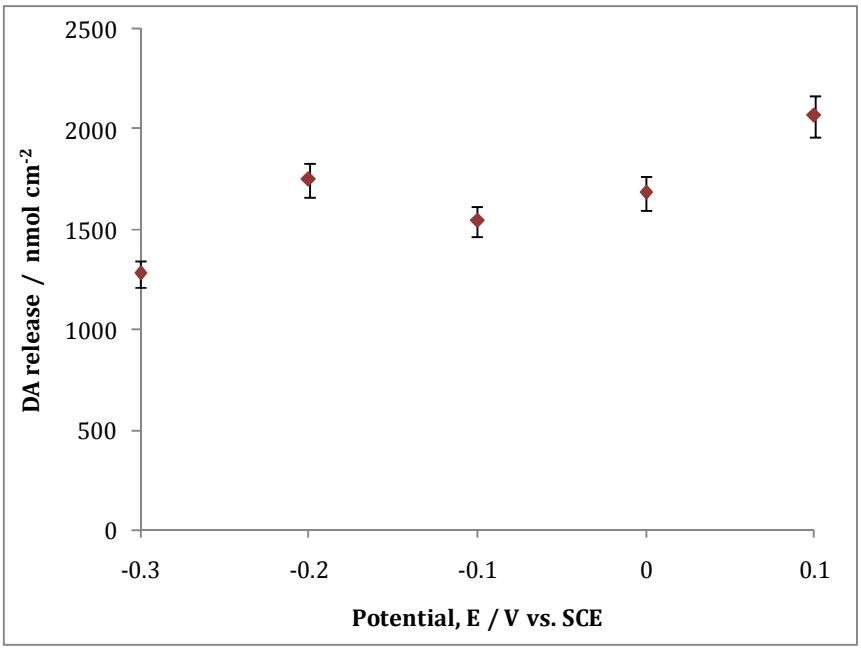


**Figure 4.33:** DA release as a function of the potential applied during release for polymers that were grown at 0.900 V vs. SCE to 3.0 C $cm^{-2}$, DA was incorporated at -0.900 V vs. SCE for 30 min in a 0.10 mol $dm^{-3}$ DA and 0.10 mol $dm^{-3}$ $Na_2SO_4$ solution.

#### 4.3.4.3.2 Kinetics of the release process

Finally, the release of the DA was examined as a function of time. It must be pointed out however, that DA is light and air sensitive and so, there were limitations to investigating longer time periods. The films were grown at a constant potential and DA was incorporated and released as described in Section 4.2.2.5.3. The amount of DA released was monitored as a function of time where the polymers were subjected to the 0.100 V vs. SCE release potential. Figure 4.34 displays the release of DA from a number of polymers as a function of time. Evidently from this figure it can be seen that more DA is released when polymers are monitored over longer release times.

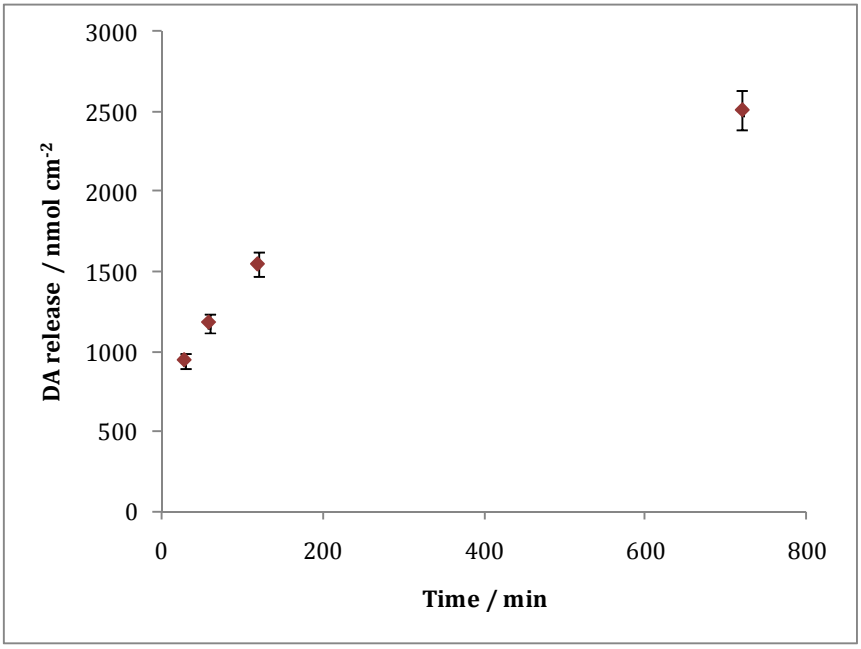


**Figure 4.34:** DA release as a function of the release time at 0.100 V vs. SCE. Polymers were grown at 0.900 V vs. SCE to 3.0 C $cm^{-2}$, DA was incorporated at -0.900 V vs. SCE for 30 min in a 0.10 mol $dm^{-3}$ DA and 0.1 mol $dm^{-3}$ $Na_2SO_4$ solution.

Figure 4.35 shows the release of DA as a function of time over a period of 120 min. Monitoring this more closely, it was observed that there was a higher rate of release during the early release times, giving a rate of release of 39.53 nmol

$cm^{-2}$ $min^{-1}$, compared to the lower rate of release at longer release times, 1.63 nmol $cm^{-2}$ $min^{-1}$.

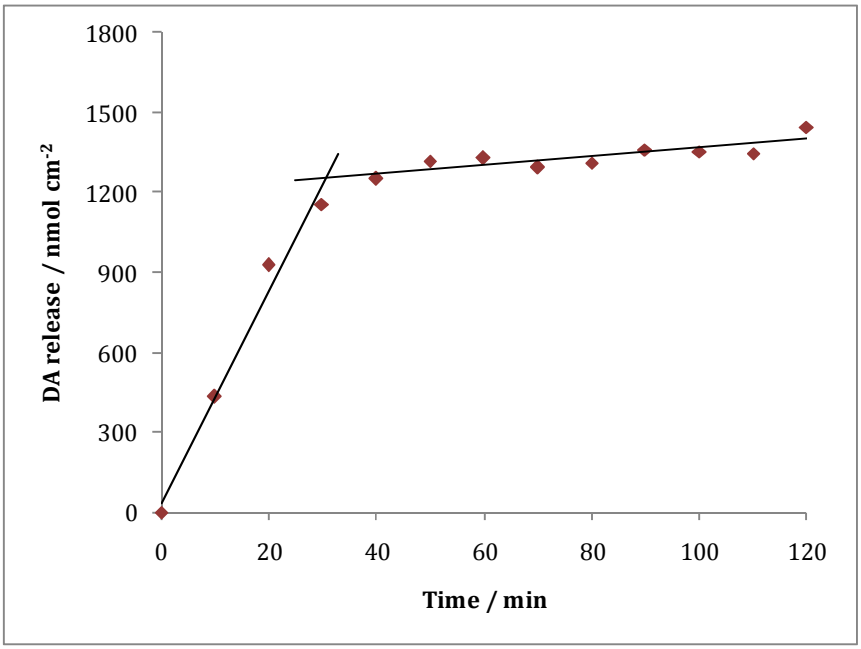


**Figure 4.35:** DA release as a function of time at 0.100 V vs. SCE. The polymer was grown at 0.900 V vs. SCE to 3.0 C $cm^{-2}$, DA was incorporated at -0.900 V vs. SCE for 30 min in a 0.10 mol $dm^{-3}$ DA and 0.1 mol $dm^{-3}$ $Na_2SO_4$ solution.

#### 4.3.4.3.3 Electrochemical stimulation

The most attractive feature regarding the use of conducting films for the uptake and release of a number of compounds is the manner in which the polymers can be stimulated using an applied potential, i.e. electrochemical stimulation. Indeed, many groups have investigated the use of electrochemical potentials to release different types of anionic and cationic species from various composite polymer films.[6, 10, 13, 26, 31, 34, 41, 42]

As shown in Figure 4.33, DA is released over a wide potential window and in order to explore this release in more detail, the release stimulated on the application of an oxidation potential was compared to the release observed in the absence of electrochemical stimulation. Polymers were grown and DA was

incorporated as outlined in Section 4.2.2.5.3. The release of DA was then investigated where a potential of 0.100 V vs. SCE was applied and compared to the release of DA from the polymer film under open-circuit conditions (OCP). Figure 4.36 compares the release of DA with electrochemical stimulation at 0.100 V vs. SCE and under OCP conditions. It is obvious that the amount of DA released, when a potential of 0.100 V vs. SCE is applied, is considerably higher; almost 80 % of an increase compared to the data obtained under OCP conditions. Also, it is evident that the rate of release during the first 30 min has significantly increased with the application of the electrical stimulus. This is due to the fact that the polymer film at OCP conditions is in a reduced state after the incorporation of the DA at -0.900 V vs. SCE. The film therefore would need some chemical or electrochemical oxidant in order to oxidise the film and allow for the liberation of the DA. Figure 4.37 is a typical potential-time transient, for the measurement of OCP conditions, of a PPy/Sβ-CD film during release of DA. It can be seen from this figure that in the time frame, where the DA release is monitored, the polymer remains in a reduced state.

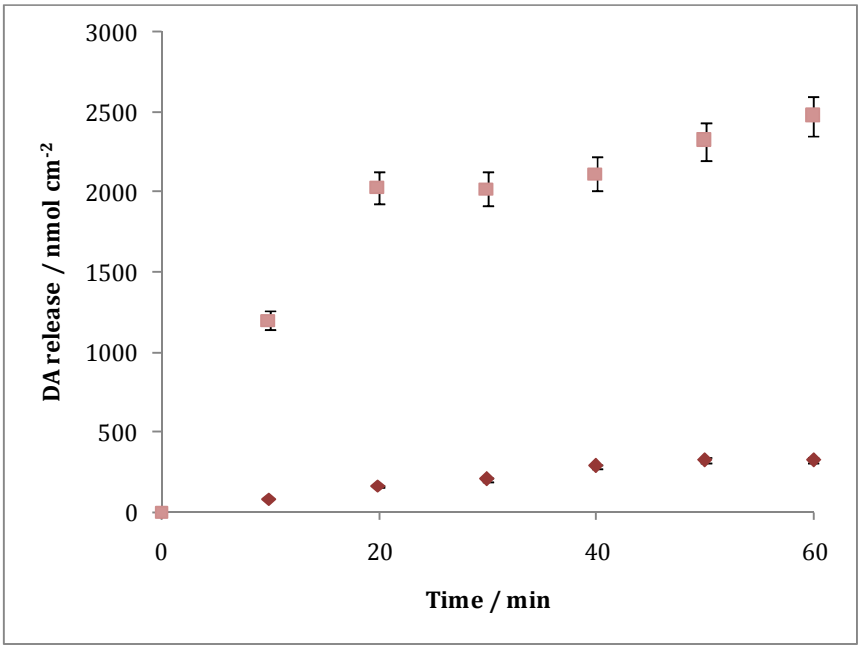


**Figure 4.36:** DA release as a function of time for polymers stimulated at ▪ 0.100 V vs. SCE and ♦ under open-circuit conditions. Polymers were grown at 0.900 V vs. SCE to 3.0 C $cm^{-2}$. DA was incorporated at -0.900 V vs. SCE for 30 min in 0.10 mol $dm^{-3}$ DA and 0.10 mol $dm^{-3}$ $Na_2SO_4$ solution.

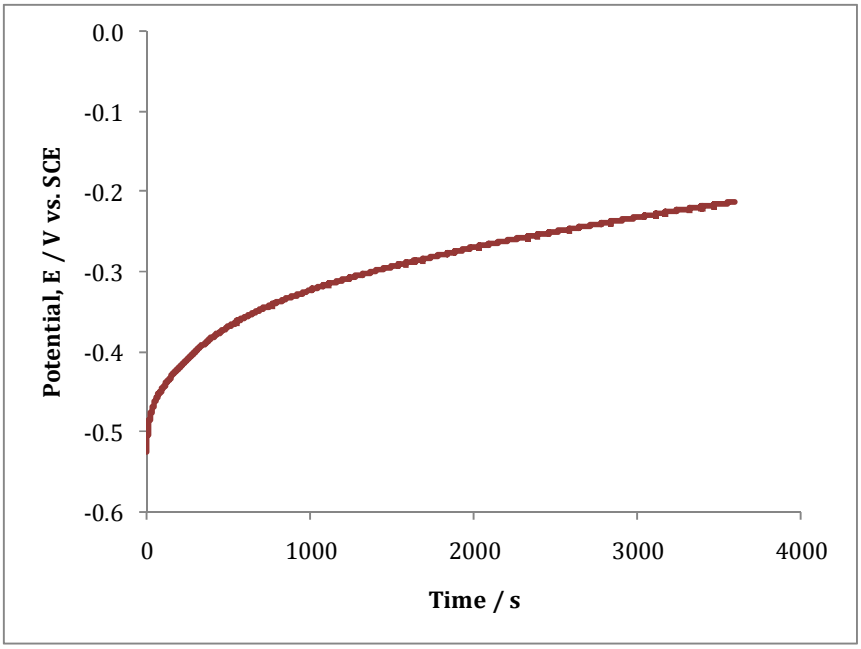


**Figure 4.37:** OCP conditions monitored over 60 min, of a PPy/Sβ-CD film where growth was obtained at 0.900 V vs. SCE to 3.0 C $cm^{-2}$ and DA was incorporated at -0.900 V vs. SCE for 30 min in 0.10 mol $dm^{-3}$ DA and 0.10 mol $dm^{-3}$ $Na_2SO_4$ solution. OCP was monitored in a 0.10 mol $dm^{-3}$ $Na_2SO_4$ solution for 60 min.

Zhou and colleagues[37] commented on the affect of the OCP conditions during the release of dimethlydopamine from PMP/PSS films. They also reported that the application of a constant or pulse potential was required, in comparison to OCP.

Many other groups have shown the release of various compounds using electrical stimulation. Kontturi *et al*.[31] demonstrated the release of salicylate from PPy films, up to 130 nmol $cm^{-2}$, while Zinger and Miller[43] confirmed the release of glutamate from PPy films to be ~ 27 nmol $cm^{-2}$, with respect to a 5 μm thick PPy film. Pyo and Reynolds[27] showed ATP release from PPy films in the region of 65 nmol $cm^{-2}$ from films 0.5 μm thick. In comparing these amounts with some of the results presented here for the PPy/Sβ-CD system, where DA levels in the region of 2500 nmol $cm^{-2}$ were released, it is clear that the PPy/Sβ-CD system is more superior to the other PPy system reported to date.

To the best of our knowledge the only other paper reporting the release of DA, using PPy films, was published by Miller and Zhou[23] in 1987. They used CV to monitor the release of DA and determined the DA released from the PPy films, grown galvanostatically to a charge of 0.6 C, to be 110 nmol $cm^{-2}$. In comparing this value to the values obtained where PPy/Sβ-CD films were synthesised to 1.0 C $cm^{-2}$ system, this result is 20 times smaller than the typical release of DA, shown in these studies.

## 4.3.5 EQCM

### *4.3.5.1 EQCM measurements for the incorporation of DA*

Due to the little knowledge previously reported about these PPy/Sβ-CD films, preliminary results show that these films are exceptionally good in taking up and releasing cations. Temsamani and co-workers[40] show the uptake and release of $K^+$ and $Na^+$ ions from PPy/Sβ-CD films synthesised in the presence of a supporting electrolyte, ($LiClO_4$). They demonstrated that the uptake of the $K^+$ and $Na^+$ ions was achieved during an open-circuit potential, through a slow release controlled ion exchange, and also under potential control at a reduction potential of -0.500 V. They also reported almost 100 % release of the cations upon application of an oxidation potential of 1.400 V. However, as discussed in Chapter 3, their application of high oxidation potentials applied during electrochemical deposition of the PPy films creates over-oxidation of the polymers and therefore, uncertainties over their findings. Despite this, Bidan *et al*.[44] who successfully synthesised PPy films in aqueous solutions of Sβ-CD also proved the release of a neutral drug, N-methylphenothiazine (NMP) upon application of a suitable potential, reinforcing the point made in this chapter that the application of appropriate potentials to the PPy/Sβ-CD films considerably increases the rate of uptake and release of cations.

EQCM measurements were used to show the uptake and release of DA using both PPy/$SO_4$ and PPy/Sβ-CD films. In Chapter 3, Figure 3.19, EQCM data were examined during cycling of the PPy/Sβ-CD film in a supporting electrolyte. A

mass increase was observed for the uptake of sodium cations upon application of a reduction potential, reaching a maximum value at -0.600 V vs. SCE. These results observed exemplified the region that was to be concentrated on for the uptake of the DA cations.

Figure 4.38 shows the EQCM data obtained for the uptake of DA from a 0.10 mol $dm^{-3}$ DA solution on applying -0.900 V vs. SCE to a $PPy/SO_4$ film. The polymers were previously prepared from a 0.20 mol $dm^{-3}$ Py and 0.10 mol $dm^{-3}$ $Na_2SO_4$ solution at 0.700 V vs. SCE until a charge of 1.5 x $10^{-2}$ C $cm^2$ was passed. It is evident from this plot that the simultaneous frequency decrease and mass increase is due to the uptake of DA cations into the reduced polymer film in order to neutralise the charge.

Figure 4.39 shows similar EQCM data obtained for the uptake of DA from a 0.10 mol $dm^{-3}$ DA solution on applying -0.900 V vs. SCE to the PPy/Sβ-CD film. The polymers were previously prepared from a 0.20 mol $dm^{-3}$ Py and 0.01 mol $dm^{-3}$ Sβ-CD solution at 0.700 V vs. SCE until a charge of 1.5 x $10^{-2}$ C $cm^{-2}$ was passed. Again, there is a clear decrease in the frequency and an increase in the mass due to the uptake of DA cations into the reduced polymer film. In comparing both figures, Figure 4.35 and 4.36, it shows that the cations are incorporated into the PPy/Sβ-CD polymer films at a faster rate than the $PPy/SO_4$ system.

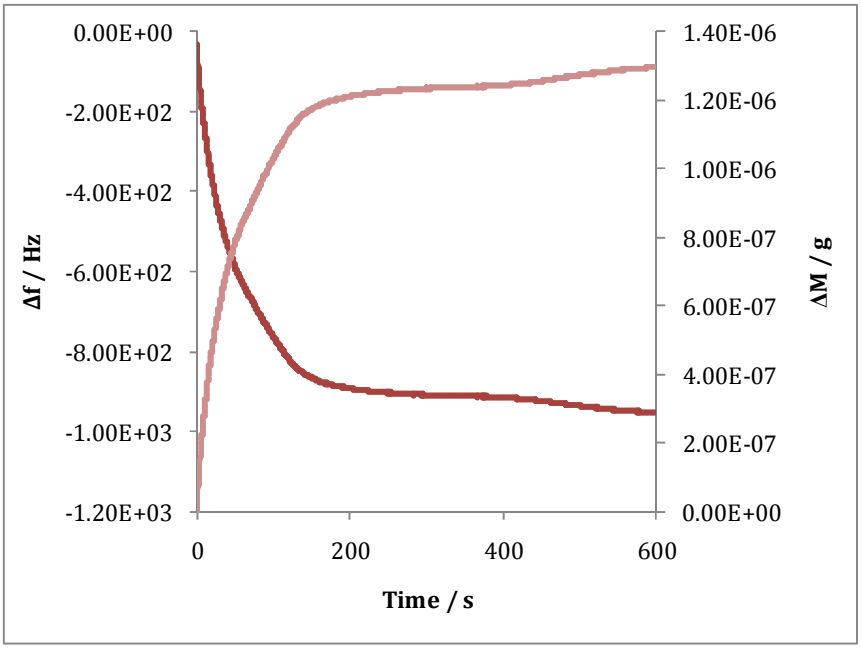


**Figure 4.38:** Frequency(♦) and mass change (♦) as a function of time on reduction of a PPy/$SO_4$ film at -0.900 V vs. SCE, the film was prepared from 0.20 mol $dm^{-3}$ Py and 0.10 mol $dm^{-3}$ $Na_2SO_4$ at 0.700 V vs. SCE, to 1.5 x $10^{-2}$ C $cm^{-2}$.

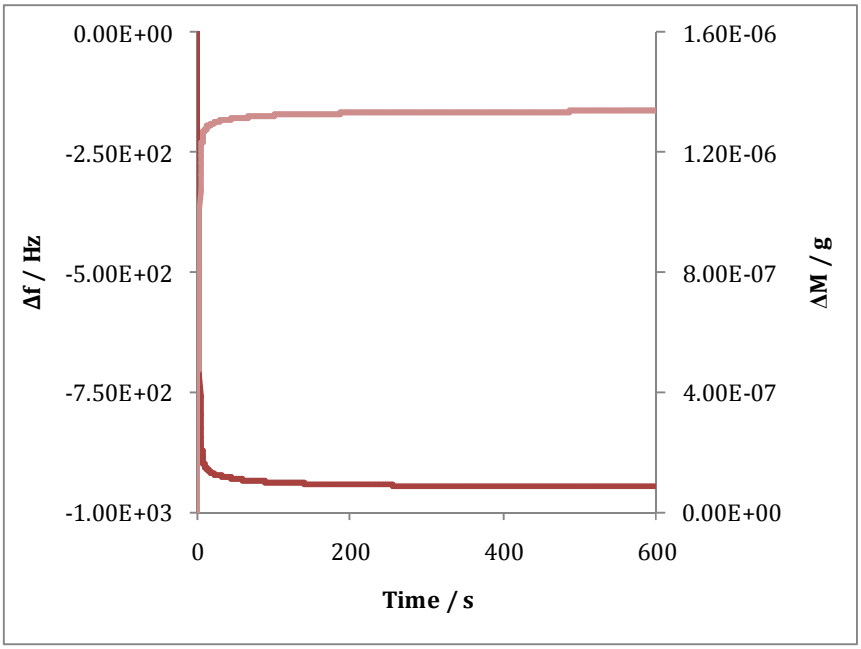


**Figure 4.39:** Frequency(♦) and mass change (♦) as a function of time on reduction of a PPy/ Sβ-CD film at -0.900 V vs. SCE, the film was prepared from 0.20 mol $dm^{-3}$ Py and 0.10 mol $dm^{-3}$ Sβ-CD at 0.700 V vs. SCE, to 1.5 x $10^{-2}$ C $cm^{-2}$.

### *4.3.5.2 EQCM data for the release of DA*

Release of DA was also monitored using the EQCM technique. The mass changes attributed to the change in frequency were measured during the application of 0.100 V vs. SCE to a polymer prepared using Sβ-CD as the dopant, where the DA was incorporated at a potential of -0.900 V vs. SCE. Figure 4.40 shows the frequency and corresponding mass changes for the release of DA as a function of time from a PPy/Sβ-CD film previously prepared and consequently loaded with the DA cations. The mass decreases rapidly during the first 20 s and then reaches a near constant mass after about 100 s. This is consistent with the loss of DA from the film.

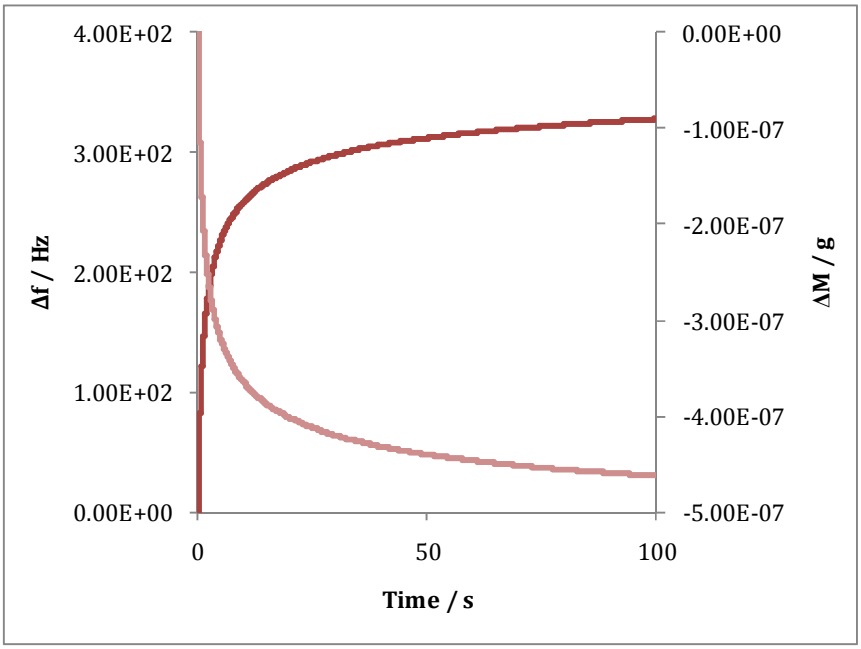


**Figure 4.40:** Frequency(♦) and mass change (♦) as a function of time obtained on the application of 0.100 V vs. SCE to the PPy/Sβ-CD film loaded with DA. Film was prepared from a 0.20 mol $dm^{-3}$ Py and 0.01 mol $dm^{-3}$ Sβ-CD aqueous solution at 0.700 V vs. SCE until a charge of 3.6 x $10^{-2}$ C $cm^{-2}$ was passed.

The EQCM measurements were also utilised to quantify the amount of DA released from these thin polymer films. Figure 4.41 shows the mass changes measured when a PPy/Sβ-CD film was firstly polarised to promote the intake of

DA and then subsequently polarised to release DA. The comparison between the uptake and release is illustrated in this figure. These data were recorded for a thin polymer film, where the incorporation and the release were attained over a period of 100 s. In examining the data, where the polymers were prepared as outlined in Section 4.2.2.6, the uptake and release was monitored for either 100 (shown in Figure 4.41) or 600 s. The % amount of DA released over 100 s for polymers grown to a charge of 1.5 x $10^{-2}$ and 3.6 x $10^{-2}$ C, was on average 10.97 % and 17.57 %, respectively, of the initial amount incorporated. However, relating these thin polymers to the larger polymers used in the bulk system is not straightforward, as the thinner polymers are more compact and less porous and this could affect the % of DA released.

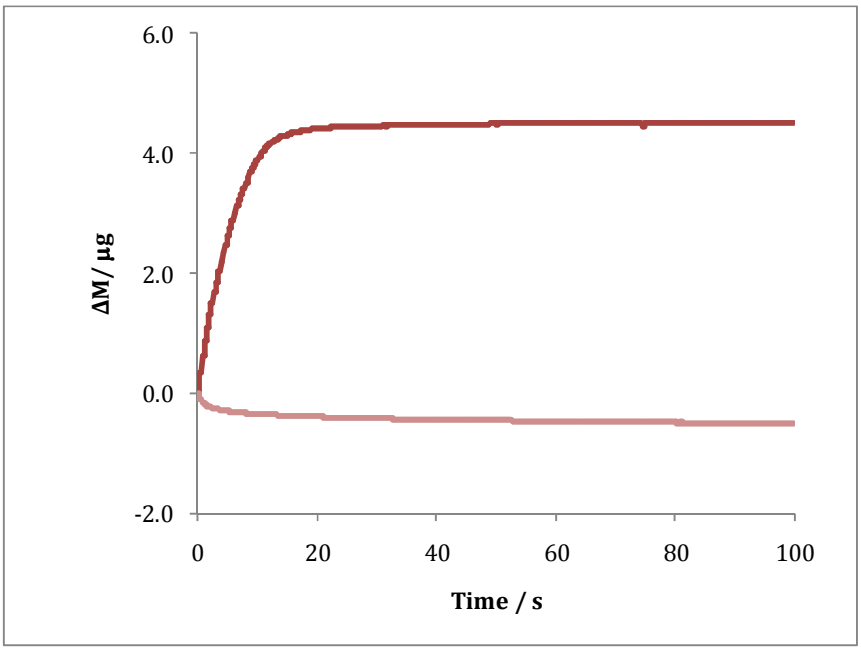


**Figure 4.41:** Mass change as a function of time for the uptake(♦) and release (♦) of DA, obtained for a PPy/Sβ-CD film prepared from a 0.20 mol $dm^{-3}$ Py and 0.01 mol $dm^{-3}$ Sβ-CD aqueous solution at 0.700 V vs. SCE until a charge of 3.6 x $10^{-2}$ C $cm^{-2}$ was passed. Constant potentials of -0.900 V vs. SCE and 0.100 V vs. SCE were applied to incorporate and release the DA, respectively.

The switching of the polymer between its reduced and oxidised state during the uptake and release of DA was also examined using EQCM. Figure 4.42 shows the frequency data as a function of time recorded for the first 1200 s at a polymer prepared at 0.700 V vs. SCE in the presence of 0.01 mol $dm^{-3}$ Sβ-CD and 0.20 mol $dm^{-3}$ pyrrole which was subsequently, immersed in a 0.10 mol $dm^{-3}$ DA aqueous solution and switched from -0.900 to 0.100 V vs. SCE every 100 s. The first 100 s period corresponds to the intake of DA, while the second 100 s period gives the release of DA. On application of the release potential, there is a clear gradual increase in the frequency, corresponding to a gradual decrease in mass and loss of the DA. This is seen with all the release steps.

The mass changes involved during the oxidation processes were also recorded as a function of time and are shown in Figure 4.43. It is clear that the overall mass of the polymer increases with time. From the inset, the difference between the start and finish of each 100 s, oxidative process, was plotted as a function of time and it can be seen that the mass decreases slightly over time as the DA was released. This is due to the observation made earlier; that only ~ 11 % of the DA was released during the subsequent oxidation step. Therefore, throughout this experiment, stepping the potential from one state to the next results in an overall mass increase as only ~ 11 % of the DA originally incorporated is released.

Hepel and Mahdavi[25] also carried out similar experiments to examine the uptake and release of chlorpromazine (CPZ) from a PPy/melanin composite films. They also observed an overall increase in the mass of the polymer and verified faster uptake than release of the drug, stepping the potential from -0.800 to 0.200 V vs. SCE every 2 min.

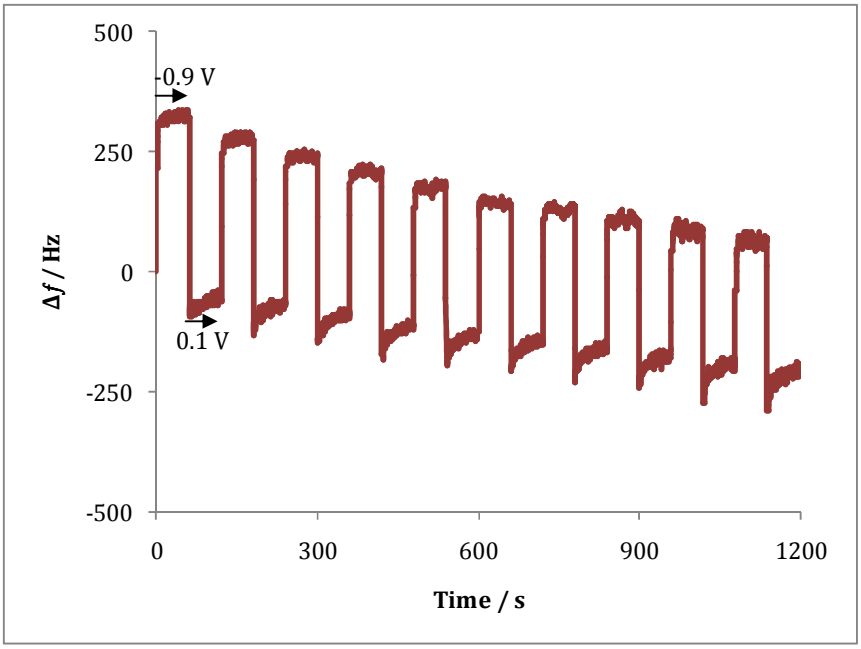


**Figure 4.42:** Frequency change as a function of time recorded upon pulsed potential steps from -0.900 V vs. SCE to 0.100 V vs. SCE in a solution of 0.10 mol $dm^{-3}$ DA, in a supporting 0.10 mol $dm^{-3}$ $Na_2SO_4$ electrolyte solution, at a PPy/Sβ-CD film electrodeposited onto an EQCM gold electrode.

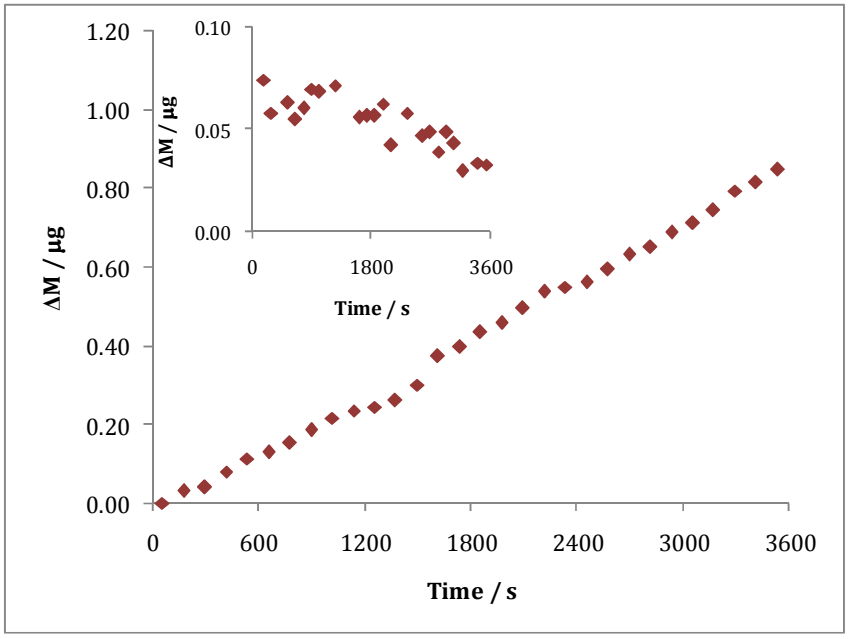


**Figure 4.43:** Mass changes as a function of time recorded upon pulsed potential steps from -0.900 V vs. SCE to 0.100 V vs. SCE in a solution of 0.10 mol $dm^{-3}$ DA solution in a supporting 0.10 mol $dm^{-3}$ $Na_2SO_4$ electrolyte solution, at a PPy/Sβ-CD film electrodeposited onto an EQCM gold electrode.

### 4.3.6 Comparing PPy/$SO_4$ to PPy/Sβ-CD

In comparing the PPy/$SO_4$ and PPy/Sβ-CD films for the uptake and release of DA, it can be concluded that there is a considerable difference between both systems. Clearly, the PPy/Sβ-CD films are capable of binding more DA and are more efficient in the release of DA, giving better release profiles. These results can only be attributed to the presence of the Sβ-CD anion, which is immobile and permanently incorporated within the polypyrrole backbone. However, as shown in Figure 4.14, other large dopants, such as PTS, are considerably poorer than the Sβ-CD system in the uptake and release of DA. The cyclodextrin family is well known to form inclusion complexes and this unique property of the Sβ-CD dopant may be a factor in the significant increase in the uptake and subsequent release of DA. An investigation into the complexation of DA was therefore performed using a variety of techniques. These results are presented and discussed in Chapter 5.

## 4.4 Summary of results

The use of the electroactive PPy film for the binding and delivery of the DA cations was investigated in this chapter. Varying the dopant anion upon polymerisation of the pyrrole monomer and subsequently using these composite films for the uptake and release of DA lead to some interesting results. The DA was successfully released from all the polymer systems. However, DA release profiles obtained for the PPy/Sβ-CD system were considerably higher than the release obtained from the other polymer systems.

It was confirmed that the application of anodic potentials higher than 0.100 V vs. SCE, to the electrochemical system, resulted in the oxidation of DA. It was also observed that polymers synthesised to a charge $\geq$ 4.0 C $cm^{-2}$ resulted in the oxidation of the DA. Many reasons were suggested, the majority of which were ruled out. However, this unusual effect could be eliminated by synthesising thinner polymer films. It was also shown that the application of an appropriate potential to release the drug is an important parameter, with both the rate of release and the amount released increasing with higher release potentials. In

comparison to the release of DA under applied potentials, OCP showed a slow release with very little DA liberated, as the polymer does not reach its oxidising potentials over the time monitored.

The results obtained for the PPy/Sβ-CD system were intriguing and so lead to an investigation into why this large anion might possibly increase the release of DA in comparison to a polymer doped with other anions. A common characteristic of the cyclodextrin family is the fact that they can form inclusion complexes in solution with a variety of organic and inorganic compounds. In the following chapter, Chapter 5, an exhaustive investigation into the inclusion properties of Sβ-CD in the presence of DA will be examined. This inclusion complexation between the cyclodextrin and DA could be a potential benefit in the delivery of DA, giving a distinct increase in the uptake and release, in comparison to other anionic dopants.

The world of Nanotechnology is also coming alive at present and the idea of increasing the surface area of polymer films in order to increase the amount of drug incorporated and released is a promising field for these biomedical applications. With this said an investigation into increasing the surface area of the PPy/Sβ-CD polymer films and subsequent uptake and release properties of these polymers was carried out. These results are described in Chapter 6.

Although these polymer composite films were only shown here to deliver DA, this can be regarded as a model cationic species, and so this model system leads the way for various other biomolecules and drugs to be delivered in this fashion. The ability to control the release through electrical stimulation provides more flexibility than other release systems that rely on polymer degradation for delivery.

## 4.5 References


1. J. A. Kiernan and M. L. Barr, Barr's the Human Nervous System: An Anatomical Viewpoint, Lippincott Williams & Wilkins, 2008.
2. J. Nolte and J. W. Sundsten, The Human Brain: An Introduction to Its Functional Anatomy, Mosby, 1998.
3. R. H. Thompson, The Brain: A Neuroscience Primer, W H Freeman & Co, 1993.
4. L. M. Lira and S. I. C. de Torresi, *Sensor Actuat B-Chem*, **130**, (2008), 638-644.
5. B. Massoumi and A. Entezami, *Eur Polym J*, **37**, (2001), 1015-1020.
6. J. M. Pernaut and J. R. Reynolds, *J Phys Chem B*, **104**, (2000), 4080-4090.
7. M. Pyo, G. Maeder, R. T. Kennedy, and J. R. Reynolds, *J Electroanal Chem*, **368**, (1994), 329-332.
8. J. R. Reynolds and P. J. Kinlen, *Abstr Pap Am Chem S*, **217**, (1999), U565-U565.
9. C. E. Schmidt, V. R. Shastri, J. P. Vacanti, and R. Langer, *P Natl Acad Sci USA*, **94**, (1997), 8948-8953.
10. B. Massoumi and A. A. Entezami, *Polym Int*, **51**, (2002), 555-560.
11. M. Pyo and J. R. Reynolds, *Chem Mater*, **8**, (1996), 128-133.
12. P. Burgmayer and R. W. Murray, *J Am Chem Soc*, **104**, (1982), 6139-6140.
13. M. R. Abidian, D. H. Kim, and D. C. Martin, *Adv Mater*, **18**, (2006), 405-409.
14. D. H. Kim, S. M. Richardson-Burns, J. L. Hendricks, C. Sequera, and D. C. Martin, *Adv Funct Mater*, **17**, (2007), 79-86.
15. B. C. Thompson, S. E. Moulton, J. Ding, R. Richardson, A. Cameron, S. O'Leary, G. G. Wallace, and G. M. Clark, *J Control Release*, **116**, (2006), 285-294.
16. X. D. Wang, X. S. Gu, C. W. Yuan, S. J. Chen, P. Y. Zhang, T. Y. Zhang, J. Yao, F. Chen, and G. Chen, *J Biomed Mater Res A*, **68A**, (2004), 411-422.
17. B. Garner, A. Georgevich, A. J. Hodgson, L. Liu, and G. G. Wallace, *J Biomed Mater Res*, **44**, (1999), 121-129.
18. R. Wadhwa, C. F. Lagenaur, and X. T. Cui, *J Control Release*, **110**, (2006), 531-541.
19. B. Z. Shakhashiri, Chemical Demonstration: A handbook for Teachers of Chemistry, University of Wisconsin Press, 1992.
20. H. Yang and W. Y. J. Kao, *J Biomat Sci-Polym E*, **17**, (2006), 3-19.
21. J. Huwyler, D. F. Wu, and W. M. Pardridge, *P Natl Acad Sci USA*, **93**, (1996), 14164-14169.
22. B. Jeong, Y. H. Bae, D. S. Lee, and S. W. Kim, *Nature*, **388**, (1997), 860-862.
23. L. L. Miller and Q. X. Zhou, *Macromolecules*, **20**, (1987), 1594-1597.

24. R. Okner, M. Oron, N. Tal, A. Nyska, N. Kumar, D. Mandler, and A. J. Domb, *J Biomed Mater Res A*, **88A**, (2009), 427-436.
25. M. Hepel and F. Mahdavi, *Microchem J*, **56**, (1997), 54-64.
26. B. Massoumi and A. Entezami, *J Bioact Compat Pol*, **17**, (2002), 51-62.
27. M. Pyo and J. R. Reynolds, *Synthetic Met*, **71**, (1995), 2233-2236.
28. S. M. Chen and K. T. Peng, *J Electroanal Chem*, **547**, (2003), 179-189.
29. M. D. Hawley, S. Tatawawa, S. Piekarsk, and R. N. Adams, *J Am Chem Soc*, **89**, (1967), 447-&.
30. W. J. Barreto, S. Ponzoni, and P. Sassi, *Spectrochim Acta A*, **55**, (1999), 65-72.
31. K. Kontturi, P. Pentti, and G. Sundholm, *J Electroanal Chem*, **453**, (1998), 231-238.
32. B. Winther-Jensen and N. B. Clark, *React Funct Polym*, **68**, (2008), 742-750.
33. S. Sadki, P. Schottland, N. Brodie, and G. Sabouraud, *Chem Soc Rev*, **29**, (2000), 283-293.
34. G. Bidan, C. Lopez, F. Mendesviegas, E. Vieil, and A. Gadelle, *Biosens Bioelectron*, **10**, (1995), 219-229.
35. S. Asavapiriyanont, G. K. Chandler, G. A. Gunawardena, and D. Pletcher, *J Electroanal Chem*, **177**, (1984), 229-244.
36. K. Aoki and Y. Tezuka, *J Electroanal Chem*, **267**, (1989), 55-66.
37. Q. X. Zhou, L. L. Miller, and J. R. Valentine, *J Electroanal Chem*, **261**, (1989), 147-164.
38. A. E. Kaifer, Supramolecular Electrochemistry, Wiley-VCH, , 1999.
39. D. A. Reece, S. F. Ralph, and G. G. Wallace, *J Membrane Sci*, **249**, (2005), 9-20.
40. K. R. Temsamani, O. Ceylan, B. J. Yates, S. Oztemiz, T. P. Gbatu, A. M. Stalcup, H. B. Mark, and W. Kutner, *J Solid State Electr*, **6**, (2002), 494-497.
41. J. N. Barisci, T. W. Lewis, G. M. Spinks, C. O. Too, and G. G. Wallace, *J Intel Mat Syst Str*, **9**, (1998), 723-731.
42. S. Geetha, C. R. K. Rao, M. Vijayan, and D. C. Trivedi, *Anal Chim Acta*, **568**, (2006), 119-125.
43. B. Zinger and L. L. Miller, *J Am Chem Soc*, **106**, (1984), 6861-6863.
44. G. Bidan, A. Gadelle, R. Teoule, and E. Vieil, *Sensor Mater*, **8**, (1996), 179-184.

## 5.1 Introduction

From the results obtained in Chapter 4 it was interesting to note that the release of dopamine (DA) increased significantly when sulfonated β-cyclodextrin (Sβ-CD) was used as the dopant for the polymer system. As described in Chapter 1, cyclodextrin (CD) molecules are commonly known as 'hosts'. The presence of an internal cavity allows guest molecules, which can be inorganic, organic or ionic, to enter the cavity and form non-covalent host-guest inclusion complexes.[1] It is this key property that we investigate in this chapter, with the view to establishing the reasons why the polymer doped with the sulfonated β-CD gives the best release profile for DA.

The effects of cyclodextrin encapsulation on the electrochemical and chemical properties of guest molecules have been widely investigated, as discussed in Chapter 1.[2-7] When forming inclusion complexes the host and guest redox properties can change, and this allows us to study the host-guest interactions spectroscopically and electrochemically. Inclusion complexation depends on many factors, including the size of the CD cavity. As described in Chapter 1, α, β, and γ CD cavities have different diameters and, therefore, the size of the guest molecule is equally important.[8]

In this chapter, results are presented and discussed on the inclusion of a DA guest molecule within sulfonated β-cyclodextrin host in aqueous solution. The complexation was investigated using UV, CV, RDV and $^1$H NMR. The binding stoichiometry was determined by a continuous variation method or Job's method using CV, UV and $^1$H NMR and these methods were also used to evaluate the stability constant, $K_f$, of the DA-Sβ-CD complex.

The inclusion of DA with a neutral β-cyclodextrin has been reported by Zhou *et al.*[4] with a stability constant, $K_f$, of 95.06. However, to the best of our knowledge there are no published data on the interaction of DA and Sβ-CD and their host-guest complexation. In this chapter reports are made on the interactions of DA

with Sβ-CD, along with some of the factors that influence the complexation, including a comparison of the inclusion abilities of sulfonated α-cyclodextrin (Sα-CD). In addition, a study on the factors that influence complexation including cavity size, pH and supporting electrolyte was carried out.

## 5.2 Experimental

### 5.2.1 Materials

#### *5.2.1.1 Reagents*

Dopamine hydrochloric salt, sulfonated β-cyclodextrin, sodium salt and sulfonated α-cyclodextrin sodium salt were purchased from Sigma, and $D_2O$ (> 99.92 % isotopic purity) was purchased from Apollo Scientific. All other reagents were of analytical grade either from Sigma-Aldrich or Riedel de–Haen and were used as received. Distilled water was used throughout the study. In the majority of electrochemical and spectroscopy experiments, a citrate-phosphate buffer was utilised for pH ranges 3-6. In the case of pH~1, 0.1 mol $dm^{-3}$ $H_2SO_4$ was used. In the NMR titrations and Job's measurements, 0.1 mol $dm^{-3}$ KCl was used to buffer the ionic strength, since the Sβ-CD is highly charged.

#### *5.2.1.2 Electrodes and Instruments*

CV and RDV measurements were carried out using a Solartron Model SI 1285 potentiostat. All measurements were made at room temperature. Gold, platinum and glassy carbon (GC) flat disc electrodes were prepared, as detailed in Section 2.2.3, and used to investigate the electrochemical studies of the complexation. Details on the instruments used in the UV and $^1$H-NMR studies are provided in Section 2.5.2 and 2.5.6, respectively.

#### *5.2.1.3 Buffer solutions*

A citrate-phosphate buffer was used in all measurements, except for the studies at pH values of 1.0. Table 5.1 shows the volumes used to obtain the required pH

for the citrate-phosphate buffers in 100 mL volumes. In the case of the acidic electrolytes, at pH values close to 1.0, a 0.1 mol $dm^{-3}$ $H_2SO_4$ solution was used.

**Table 5.1:** Volumes of stock solution required to obtain pH values for 100 mL of the citrate-phosphate buffers.

| Desired pH | $H_2SO_4$ / 0.1 mol $dm^{-3}$ (mL) | $Na_2HPO_4$ / 0.2 mol $dm^{-3}$ (mL) | $C_6H_8O_7$ / 0.1 mol $dm^{-3}$ (mL) |
|---|---|---|---|
| 1 | 100 | - | - |
| 3 | - | 20.5 | 79.5 |
| 4 | - | 37.0 | 63.0 |
| 5 | - | 49.3 | 50.7 |
| 6 | - | 62.1 | 37.9 |

## 5.2.2 Procedures

### *5.2.2.1 Determination of the stoichiometry of Sβ-CD and DA*

The stoichiometry of the Sβ-CD and DA complex was determined by using the well known Job's plot or continuous variation method.[9] This method was employed for both UV and CV techniques. For the UV data two stock solutions of 1.0 x $10^{-4}$ mol $dm^{-3}$ DA and 1.0 x $10^{-4}$ mol $dm^{-3}$ Sβ-CD in water were prepared. A series of solutions were prepared in which the sum of the number of moles, of DA and Sβ-CD, was kept constant, but the relative amount of the two was systematically varied, according to Table 5.2. The UV absorption spectrum of each solution was obtained, using distilled water as a reference. For the CV data, two stock solutions of 1.0 x $10^{-2}$ mol $dm^{-3}$ DA and 1.0 x $10^{-2}$ mol $dm^{-3}$ Sβ-CD in citrate-phosphate buffer at pH 5.0 were prepared. Different volumes of the two stock solutions were combined, keeping the final volume constant at 10.0 mL, shown in Table 5.3. For the CV studies, a GC electrode was used as the working electrode, while a SCE and a platinum wire served as the reference and the counter electrodes, respectively. The CVs were recorded in the -0.250 to 0.800 V vs. SCE interval by applying a potential scan rate of 50 mV $s^{-1}$.

**Table 5.2:** The solution composition for the UV Job's plot measurements (total volume is 3.0 mL).

| Solution | 1 x $10^{-4}$ mol $dm^{-3}$ Sβ-CD (mL) | 1 x $10^{-4}$ mol $dm^{-3}$ DA (mL) | [DA]/([DA]+[Sβ-CD]) Mole fraction |
|---|---|---|---|
| 1 | 3.0 | 0.0 | 0.0 |
| 2 | 2.7 | 0.3 | 0.1 |
| 3 | 2.4 | 0.6 | 0.2 |
| 4 | 2.1 | 0.9 | 0.3 |
| 5 | 1.8 | 1.2 | 0.4 |
| 6 | 1.5 | 1.5 | 0.5 |
| 7 | 1.2 | 1.8 | 0.6 |
| 8 | 0.9 | 2.1 | 0.7 |
| 9 | 0.6 | 2.4 | 0.8 |
| 10 | 0.3 | 2.7 | 0.9 |
| 11 | 0.0 | 3.0 | 1.0 |

**Table 5.3.**The solution composition for the CV Job's plot measurements (total volume is 10.0 mL).

| Solution | 1 x $10^{-2}$ mol $dm^{-3}$ Sβ-CD (mL) | 1 x $10^{-2}$ mol $dm^{-3}$ DA (mL) | [DA]/([DA]+[Sβ-CD]) Mole fraction |
|---|---|---|---|
| 1 | 10.0 | 0.0 | 0.0 |
| 2 | 9.0 | 1.0 | 0.1 |
| 3 | 8.0 | 2.0 | 0.2 |
| 4 | 7.0 | 3.0 | 0.3 |
| 5 | 6.0 | 4.0 | 0.4 |
| 6 | 5.0 | 5.0 | 0.5 |
| 7 | 4.0 | 6.0 | 0.6 |
| 8 | 3.0 | 7.0 | 0.7 |
| 9 | 2.0 | 8.0 | 0.8 |
| 10 | 1.0 | 9.0 | 0.9 |
| 11 | 0.0 | 10.0 | 1.0 |

### *5.2.2.2 Determination of the stability constant of Sβ-CD and DA*

Both spectroscopic and electrochemical methods were used to determine the stability constant of the DA-Sβ-CD complex. For the UV method the DA guest was kept at a constant concentration of 5.00 x $10^{-4}$ mol $dm^{-3}$ in a citrate-phosphate buffer (pH of 6.0), while the concentration of the Sβ-CD host was varied over the range of 5.65 x $10^{-4}$ to 2.00 x $10^{-2}$ mol $dm^{-3}$. The UV absorption spectrum of each sample was obtained and the data were analysed at 280 nm ($\lambda_{max}$ of DA). The Sβ-CD does absorb slightly at 280 nm. Accordingly, all measurements made at 280 nm, to follow the DA inclusion events were corrected by subtracting the corresponding Sβ-CD solution absorbance at 280 nm. The $K_f$ value was determined for the complex based on the absorbance changes of the different DA/Sβ-CD mixtures.

For the CV method the DA guest was kept at a constant concentration of 5.00 x $10^{-4}$ mol $dm^{-3}$ in a citrate-phosphate buffer (pH of 6.0), while the concentration of the Sβ-CD host was varied over the range of 3.12 x $10^{-4}$ to 2.00 x $10^{-2}$ mol $dm^{-3}$. The cyclic voltammograms were recorded using a GC working electrode in the potential range of -0.500 to 0.800 V vs. SCE at a potential scan rate of 50 mV $s^{-1}$. CVs were also recorded where the scan rate was varied between 50, 100, 150, 200, 300, 400 and 500 mV $s^{-1}$.

RDV data were recorded using the same electrochemical set-up as CV, except a GC rotating disc electrode was used. For the RDV method, the DA guest was kept at a constant concentration of 5.00 x $10^{-4}$ mol $dm^{-3}$ in a citrate-phosphate buffer (pH of 6.0), while the concentration of the Sβ-CD host was varied over the range of 6.25 x $10^{-4}$ to 2.00 x $10^{-2}$ mol $dm^{-3}$. The rotations were varied from 50 to 700 rpm.

### *5.2.2.3 NMR analysis*

To obtain a stoichiometric value for the complex, the Job's method was applied to chemical shift data collected by NMR. The mole fraction of DA was varied

from 0.0 to 1.0 in increments of 0.1. Each DA/Sβ-CD solution was prepared from a 1.0 x $10^{-2}$ mol $dm^{-3}$ DA or Sβ-CD stock solution in the presence of 0.1 mol $dm^{-3}$ KCl/$D_20$ in order to maintain a constant pH and ionic strength. The volume of each stock solution used to give the required mole fraction values are shown in Table 5.4.

Verification of the formation of an inclusion complex was achieved by adding varying amounts of Sβ-CD to 0.5 mL volumes of a 5.00 x $10^{-4}$ mol $dm^{-3}$ DA stock solution made up in 0.1 mol $dm^{-3}$ KCl/$D_20$, such that samples with final Sβ-CD concentrations ranging from 1.00 x $10^{-4}$ to 2.50 x $10^{-3}$ mol $dm^{-3}$ were produced. The samples were allowed to equilibrate for 60 min before acquiring their $^1$H NMR spectrum. Due to the complexity of the Sβ-CD spectra the aromatic spectral region of the DA was used to monitor chemical shift variations. The $K_f$ value for host-guest complexation was determined using a non-linear curve fitting programme. Finally, this information was used to analyse and obtain information on the geometry of the complex.

**Table 5.4:** The volumes of stock solutions used for the NMR Job's plot measurements. Total volume is 0.5 mL in 0.1 mol $dm^{-3}$ KCl /$D_20$.

| Solution | 1 x $10^{-2}$ mol $dm^{-3}$ Sβ-CD (mL) | 1 x $10^{-2}$ mol $dm^{-3}$ DA (mL) | [DA]/([DA]+[Sβ-CD]) |
|---|---|---|---|
| 1 | 0.50 | 0.00 | 0.0 |
| 2 | 0.45 | 0.05 | 0.1 |
| 3 | 0.40 | 0.10 | 0.2 |
| 4 | 0.35 | 0.15 | 0.3 |
| 5 | 0.30 | 0.20 | 0.4 |
| 6 | 0.25 | 0.25 | 0.5 |
| 7 | 0.20 | 0.30 | 0.6 |
| 8 | 0.15 | 0.35 | 0.7 |
| 9 | 0.10 | 0.40 | 0.8 |
| 10 | 0.05 | 0.45 | 0.9 |
| 11 | 0.00 | 0.50 | 1.0 |

### *5.2.2.4 Varying the pH*

The binding constants between DA and Sβ-CD were determined as a function of pH. Firstly, acid-base titrations were employed in order to investigate if the change in pH affected the ionisation of the sulfonated groups on the Sβ-CD. Stock solutions of 0.02 mol $dm^{-3}$ NaOH in the absence and presence of 5.00 x $10^{-3}$ mol $dm^{-3}$ Sβ-CD were prepared and the pH was varied by adding a dilute solution of $H_2SO_4$. The conductivity and pH were recorded simultaneously using a Jenway 4510 conductivity meter and an Orion model 720A pH meter, respectively.

In the pH studies, citrate-phosphate buffers were used to achieve pH values between 3.0 and 6.0, while 0.1 mol $dm^{-3}$ $H_2SO_4$ was used to further reduce the pH value to 1.4. The DA concentrations were held constant at 5.00 x $10^{-4}$ mol $dm^{-3}$ and the absorption spectra of DA ($\lambda_{max}$ =280 nm) in the absence and presence of Sβ-CD concentrations, which were varied in the range of 5.65 x $10^{-4}$ to 2.00 x $10^{-2}$ mol $dm^{-3}$, were recorded. Accordingly, all measurements made at 280 nm, to follow the DA absorption, were corrected by subtracting the corresponding Sβ-CD solution absorbance at 280 nm.

CV experiments were also performed at pH values of 1.36, 3.20, 4.01, 5.01 and 6.06. Again, the solutions were prepared using a citrate-phosphate buffer for pH values in the region of 3.20 to 6.06, while $H_2SO_4$ was used for solutions of pH 1.36. Data were obtained for DA, 5.00 x $10^{-4}$ mol $dm^{-3}$, in the absence and presence of varying concentrations of Sβ-CD, ranging from 2.00 x $10^{-2}$ to 3.12 x $10^{-4}$ mol $dm^{-3}$ for each pH. The CVs were recorded as detailed in Section 5.2.2.1.

### *5.2.2.5 Varying the electrolyte*

Supporting electrolytes sodium chloride, calcium chloride, ammonium chloride, potassium chloride, sodium sulfate, sodium citrate and disodium hydrogen phosphate were obtained from Aldrich and used without further purification. 0.2 mol $dm^{-3}$ stock solutions of the various electrolytes were prepared (Table

5.5). HCl, $H_2SO_4$, $NaH_2PO_4$ and $[C(OH)(CH_2CO_2)_2(CO_2)]$ were used to adjust the pH to ~ 5. CV data were first obtained for a 5.00 x $10^{-4}$ mol $dm^{-3}$ DA solution in the presence of the electrolyte and subsequently for a 5.00 x $10^{-4}$ mol $dm^{-3}$ DA/2.00 x $10^{-2}$ mol $dm^{-3}$ Sβ-CD solution. The CVs were recorded using the procedure outlined in Section 5.2.2.1.

**Table 5.5:** Electrolytes used to investigate the presence of a supporting electrolyte in Sβ-CD complexation.

| **Electrolyte / 0.2 mol $dm^{-3}$** | **pH** |
|---|---|
| NaCl | 5.09 |
| KCl | 4.99 |
| $CaCl_2$ | 4.93 |
| $NH_4Cl$ | 5.10 |
| $Na_2SO_4$ | 4.96 |
| $Na_2HPO_4$ | 4.98 |
| $[C(OH)(CH_2CO_2)_2(CO_2)]$ | 5.03 |

### *5.2.2.6 Varying the size of the cavity*

The Sα-CD was obtained from Aldrich and used without further purification. DA was kept at a constant concentration of 5.00 x $10^{-4}$ mol $dm^{-3}$ in a citrate-phosphate buffer (pH of 5.0), while the Sα-CD was maintained in excess. The Sα-CD concentrations which were prepared in a citrate-phosphate buffer, were varied from 2.00 x $10^{-2}$ mol $dm^{-3}$ to 3.12 x $10^{-4}$ mol $dm^{-3}$. CV measurements were employed as detailed in Section 5.2.2.1.

#### *5.2.2.7 Complexation studies of levodopa and tyrosine with Sβ-CD*

The stoichiometry of the complexes formed between levodopa (L-dopa) and Sβ-CD and between tyrosine (Tyr) and Sβ-CD were determined by applying the Job's method to UV absorption spectra of mixtures of Sβ-CD and either L-dopa or Tyr. Two stock solutions of 1.0 x $10^{-4}$ mol $dm^{-3}$ for L-dopa and Tyr were prepared in 0.1 mol $dm^{-3}$ $H_2SO_4$ and 1.0 x $10^{-4}$ mol $dm^{-3}$ Sβ-CD. A series of solutions was prepared, in which the sums of the number of moles of L-dopa or Tyr and Sβ-CD were kept constant, but the relative amount of either guest molecule was systematically varied, as given in Table 5.2 for DA. In each case, 0.1 mol $dm^{-3}$ $H_2SO_4$ was used as a reference.

The stability constant for the L-dopa and Sβ-CD complexation was determined using UV-visible spectroscopy. L-dopa was kept at a constant concentration of 5.00 x $10^{-4}$ mol $dm^{-3}$ in a citrate-phosphate buffer (pH of 2.3), while the Sβ-CD was maintained in excess and varied from 2.00 x $10^{-2}$ mol $dm^{-3}$ to 1.25 x $10^{-3}$ mol $dm^{-3}$. Absorption spectra of all samples were obtained and the data were analysed at 280 nm ($\lambda_{max}$ of L-dopa). The contribution of Sβ-CD at 280 nm was eliminated by the use of an Sβ-CD concentration calibration curve generated at 280 nm.

CV was used to determine Tyr-Sβ-CD complexation at pH values of 2.44 and 12.1. Experiments were carried out at these pH values in order to eliminate the presence of Tyr zwitterions. CV was employed as detailed in Section 5.2.2.1.

### 5.2.3 Evaluation of the stability constants

The theory behind each of the equations presented below is described in Chapter 2. The assumptions and values for each parameter are also shown in Chapter 2. Here, a short synopsis of the equations used to evaluate the stability constant for each of the techniques studied is provided. The $K_f$ value for the inclusion complex was calculated from the absorption spectra data using the modified Heildebrand Benesi, Equation 5.1.[7, 10, 11]

$$\frac{A_0}{A - A_0} = \frac{\varepsilon_G}{\varepsilon_{H-G} - \varepsilon_G} + \frac{\varepsilon_G}{\varepsilon_{H-G} - \varepsilon_G} \times \frac{1}{K_f[S\beta - CD]} \quad 5.1$$

The $K_f$ value for the inclusion complex was calculated from the CV data using Equation 5.2,[10, 12, 13], while the RDV data were analysed using Equation 5.3. The Levich equation, Equation 5.4, was used to determine $D_c$ and $D_f$:

$$\frac{1}{[S\beta - CD]} = K_f \frac{(1 - A)}{(1 - {}^{i}/_{i_0})} - K_f \quad 5.2$$

$$\left(\frac{F}{RT}\right)\left\{(E_{\frac{1}{2}})_{app} - (E_{\frac{1}{2}})_f\right\} = \ln(1 + K[S\beta - CD]) + \ln(D_c / D_f)^{1/2} \quad 5.3$$

$$i_L = 0.621nFD^{2/3}v^{-1/6}c\omega^{1/2} \quad 5.4$$

The Koutecky-Levich equation was applied to evaluate the apparent rate constant, $k_{DA}$, for the oxidation of DA in the presence and absence of Sβ-CD:

$$\frac{1}{i_L} = \frac{1}{i_K} + \frac{1}{i_{lev}} = \frac{1}{nFAk_{DA}c} + \frac{1.61}{nFAv^{-1/6}D^{2/3}\omega^{1/2}c} \quad 5.5$$

where $i_K$ is given by the expression in Equation 5.6.

$$i_K = nFAkc \quad 5.6$$

The NMR spectra were analysed using Equation 5.7. The $K_f$ value was evaluated from a non-linear analysis using the relationships in Equation 5.7[14]

$$\delta = \delta_h - \frac{\Delta\delta}{2}\left(b - \sqrt{b^2 - 4R}\right) \quad 5.7$$

where

$$b = 1 + R + \frac{1}{(K[S\beta - CD])}$$

## 5.3 Results and Discussion

### 5.3.1 Determination of the stoichiometry of Sβ-CD and DA

#### *5.3.1.1 UV data*

The UV spectra of 1.0 x $10^{-4}$ mol $dm^{-3}$ solutions of DA and Sβ-CD are overlaid in Figure 5.1. The band centred at approximately 280 nm results from the absorption of DA, while that centred at approximately 256 nm is from Sβ-CD. Figure 5.1 reveals an approximate 4 times greater extinction coefficient for DA compared to Sβ-CD. Although Sβ-CD exhibits a minimal absorption at 280 nm, spectral intensity at 280 nm from a DA/ Sβ-CD mixture would be expected to result overwhelmingly from DA absorption. In the interest of accuracy, however, all measurements made at 280 nm for DA/ Sβ-CD solutions were corrected by subtracting the corresponding absorption resulting from Sβ-CD.

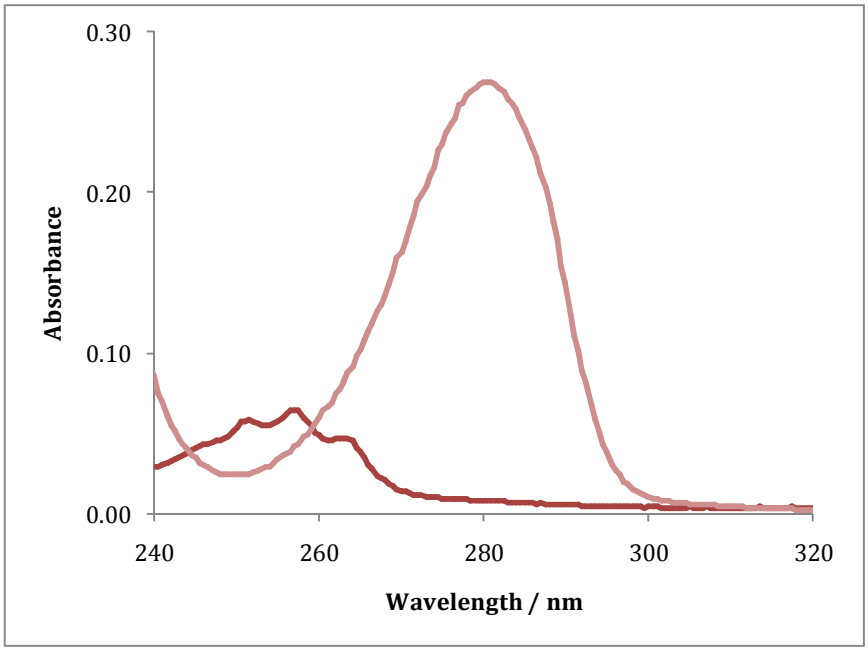


**Figure 5.1:** UV spectra of ♦ 1.0 x $10^{-4}$ mol $dm^{-3}$ DA, $\lambda_{max}$ = 280 nm and ♦ 1.0 x $10^{-4}$ mol $dm^{-3}$ Sβ-CD, $\lambda_{max}$ = 256 nm.

Absorption spectra of DA/Sβ-CD of varying mole fractions are overlaid in Figure 5.2, whereby the DA band intensity increases with increasing DA mole fraction. For example, the absorbance at 280 nm was 0.04 for a DA mole fraction of 0.1, while the absorbance increased to 0.19 when the mole fraction of DA was 0.7.

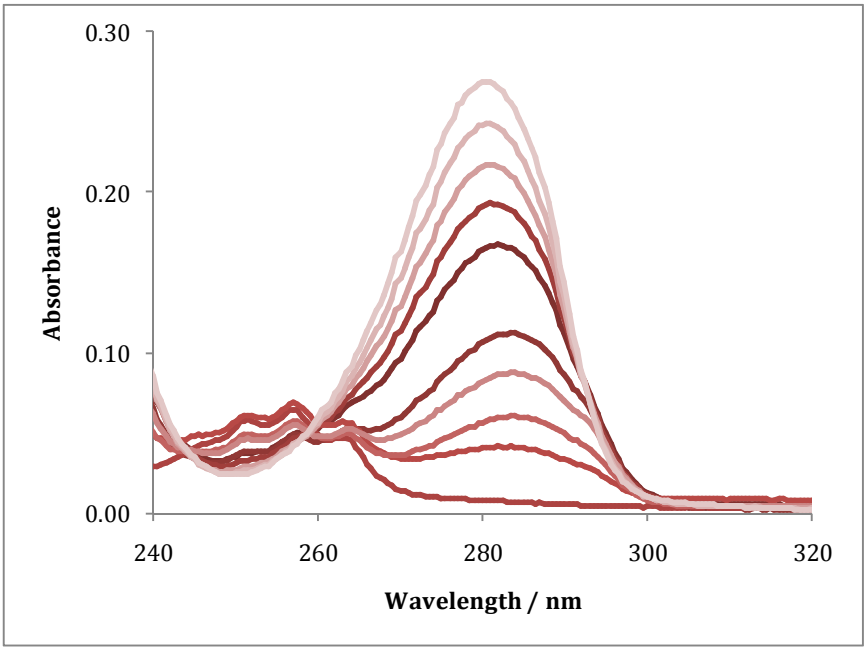


**Figure 5.2:** UV spectra for the Job's plot titration curve with Sβ-CD and DA. From low to high absorbance values, the value of [DA]/([DA]+[ Sβ-CD]) increases from 0.0 to 1.0, in increments of 0.1.

For the UV analysis the Job's plot was generated from the change of the absorbance at a wavelength of 280 nm relative to that of an equal concentration of free DA using the equation:

$$\Delta A = A_0 - A \qquad 5.8$$

where $A_0$ and $A$ are the absorbance values for DA in the absence and presence of Sβ-CD, respectively. These $\Delta A$ values were then multiplied by the corresponding mole fraction and the product was plotted as a function of the DA mole fraction. Figure 5.3 shows the Job's plot of the UV absorbance change at 280 nm of the complex when varying the DA mole fraction of the DA/Sβ-CD solutions. The maximum absorbance value was achieved at the 0.5 mole fraction and this is evidence that there exists a 1:1 DA:Sβ-CD complex stoichiometry.

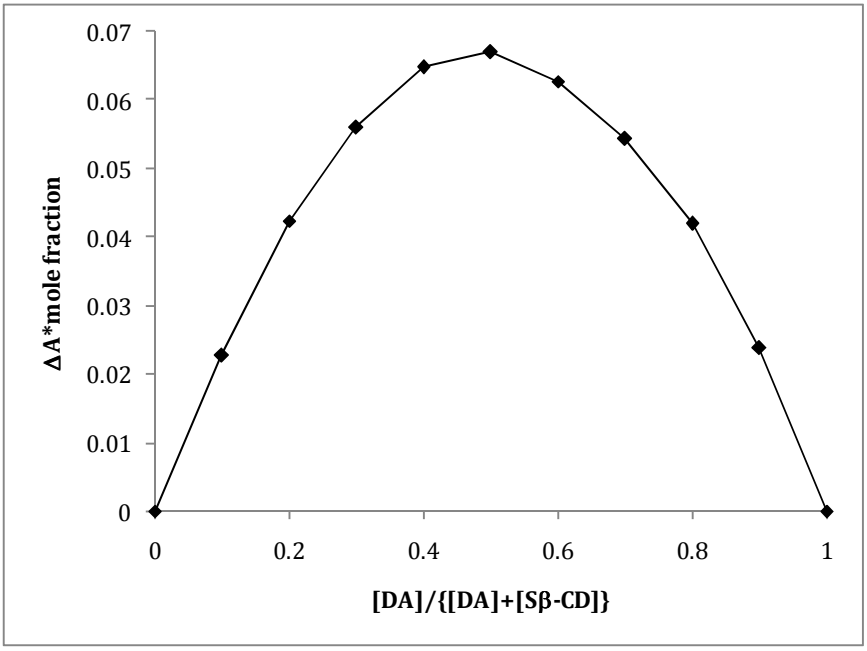


**Figure 5.3:** Job's plot curve of UV absorbance change (280 nm) of DA upon the addition of Sβ-CD, indicating the formation of 1:1 host-guest complex.

### *5.3.1.2 CV data*

Cyclic voltammetry is a technique commonly employed to investigate the interactions between the host and guest molecules or ions; as long as either the host or guest is electroactive.[15, 16] DA is electroactive and its electrochemical behaviour has been previously investigated.[17, 18] There is much debate over the exact steps in the electrochemical oxidation of DA. Wen *et al.*[18] suggest it to be

an ECC process, where two consecutive one electron transfer reactions occur, as shown in Scheme 5.1. The successive two electron transfer from protonated DA **1** generates the DA ortho-quinone **2**. However, Chen and co-workers[17] state that it is a direct two-electron transfer process of DA to DA ortho-quinone. For the purpose of these CV experiments, DA (p*K*a = 8.92)[19] was taken to exhibit a *quasi* reversible two electron redox process.

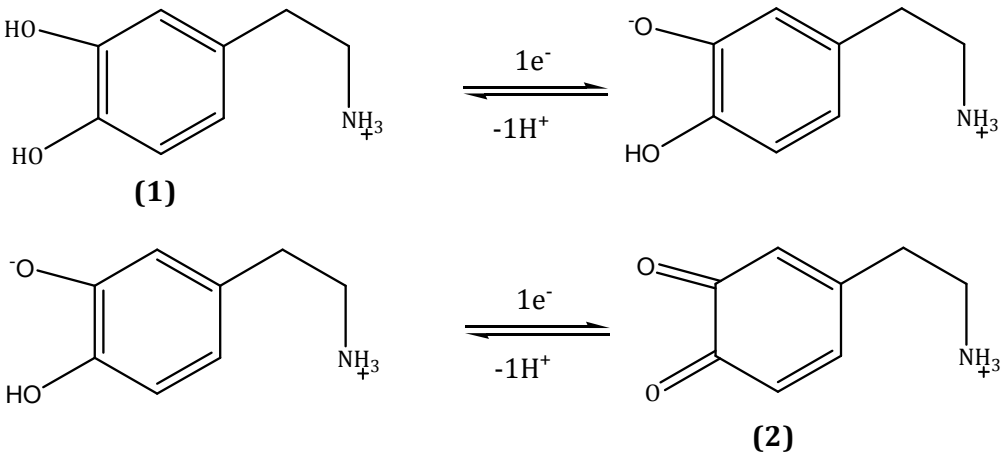


**Scheme 5.1:** Oxidation reaction of DA.

Figure 5.4 shows cyclic voltammograms of 1.0 x $10^{-2}$ mol $dm^{-3}$ Sβ-CD (A) and 1.0 x $10^{-4}$ mol $dm^{-3}$ DA (B) at each electrode surface. The GC flat disc electrode was chosen for the electrochemical studies of the complexation analysis; not only did it show no electroactivity in the presence of 1.0 x $10^{-2}$ mol $dm^{-3}$ Sβ-CD in citrate-phosphate buffer, as shown in Figure 5.4(A), but it also gave the best defined peak for the oxidation of a 1.0 x $10^{-4}$ mol $dm^{-3}$ DA solution, as evident from Figure 5.4(B).

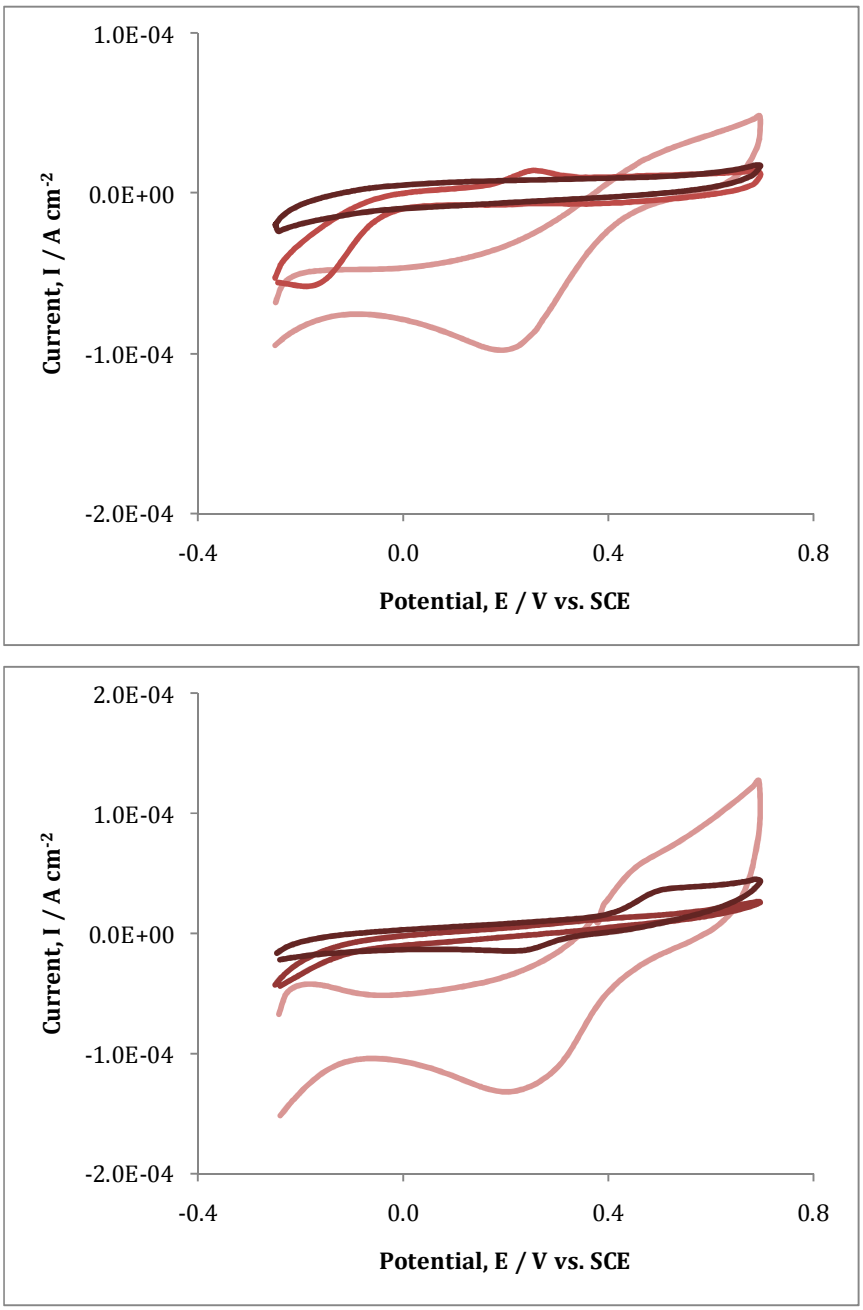


**Figure 5.4:** The cyclic voltammograms recorded in a citrate-phosphate buffer (pH = 3.17) at various electrode surfaces; GC gold and platinum. The potential was swept from -0.250 to 0.700 V vs. SCE at 50 mV $s^{-1}$. A) Data recorded in 1.0 x $10^{-2}$ mol $dm^{-3}$ Sβ-CD and B) data recorded in 1.0 x $10^{-4}$ mol $dm^{-3}$ DA.

The electrochemical properties of DA solution of 5.0 x $10^{-4}$ mol $dm^{-3}$ in aqueous citrate-phosphate buffer solutions (pH of 5.0) are shown in Figure 5.5. This typical voltammogram in the potential range of -0.250 to 0.800 V vs. SCE, at a GC electrode shows a well defined pair of redox peaks for DA. An anodic peak, $E_{pa}$, appears at 0.323 V vs. SCE, which corresponds to the oxidation of the protonated DA to the ortho-quinone. Upon reversal of the potential, a cathodic peak, $E_{pc}$, at 0.193 V vs. SCE is observed and is associated with the reduction of ortho-quinone back to DA.

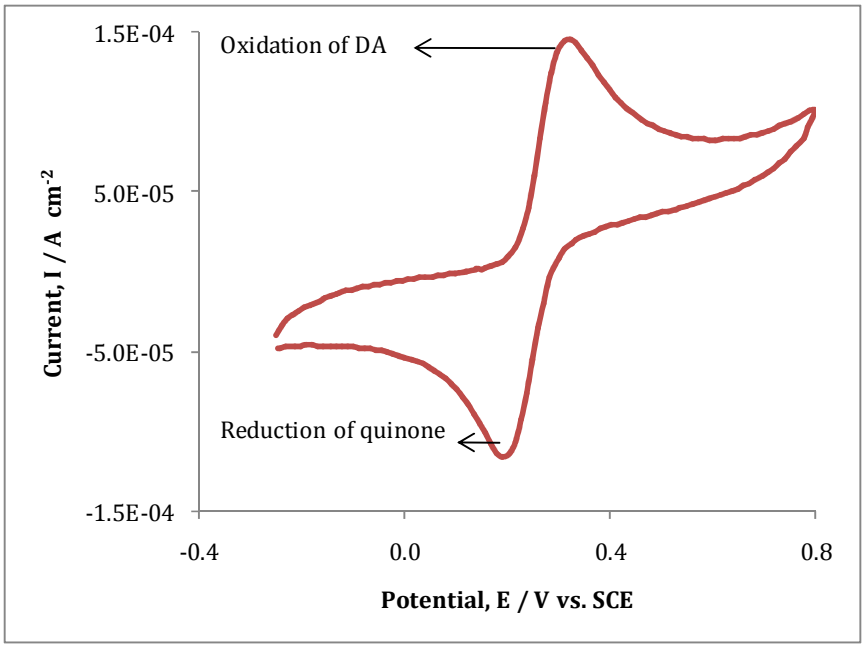


**Figure 5.5:** Cyclic voltammogram of DA (5.0 x $10^{-4}$ mol $dm^{-3}$) on GC in citrate phosphate buffer pH=5.0. Scan rate 50 mV $s^{-1}$.

Figure 5.6 shows cyclic voltammograms of DA at different potential scan rates, ($v$). The peak currents for both the anodic and cathodic reactions are directly proportional to the scan rate and vary linearly with the square root of scan rate, as seen in Figure 5.7 which plots the peak current, $i_p$, as a function of the square root of the scan rate, $v^{1/2}$. $R^2$ values of 0.999 and 0.995 for the anodic and

cathodic peak currents, respectively, were achieved. Figure 5.7 shows that the reaction is diffusion-controlled. Consequently, an electrochemical approach is ideal for probing the complexation between DA and the Sβ-CD. Furthermore, the Sβ-CD is not electroactive and only the electrochemistry of the DA is observed in this electrochemical approach. Bersier *et al.*[20] stated that in these voltammetric methods the transport of the electroactive species should be diffusion controlled. With this confirmed, the electrochemical approach was used to study the complexation of DA with the Sβ-CD.

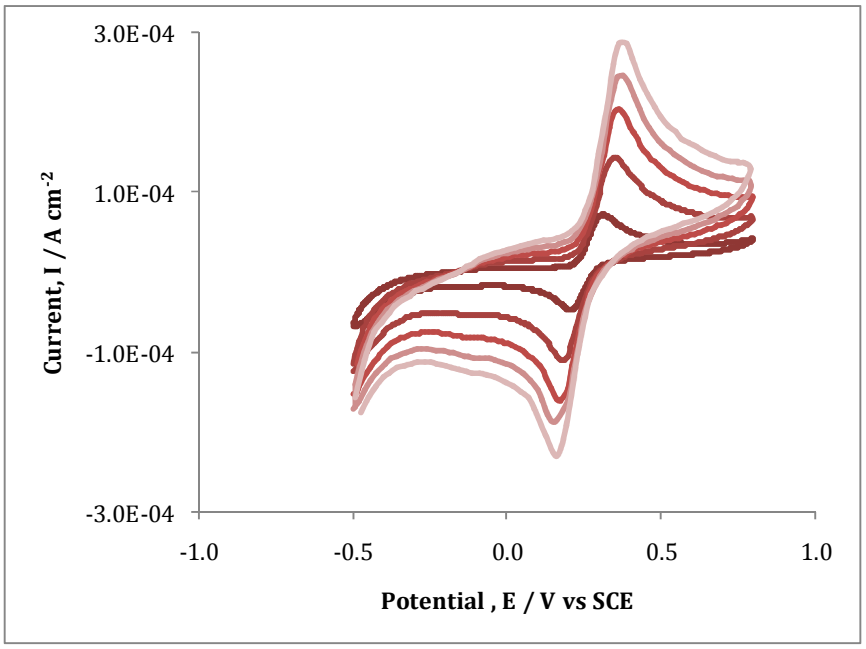


**Figure 5.6:** Cyclic voltammograms of DA (5.0 x $10^{-4}$ mol $dm^{-3}$) on GC in citrate phosphate buffer pH=5.0. Scan rate $v$/mV $s^{-1}$: (1) 50; (2) 100; (3) 150; (4) 200; (5) 300. Currents vary in the order (1) < (2) < (3) < (4) < (5).

Figure 5.8 shows the cyclic voltammograms of DA in the presence of Sβ-CD. From Figure 5.8 it can be seen that the peak current increases with increasing DA mole fraction. For example, the peak current for 0.1 mole fraction was 1.11 x $10^{-4}$ A $cm^{-2}$, in comparison to 1.29 x $10^{-3}$ A $cm^{-2}$ for the mole fraction value of 1.0.

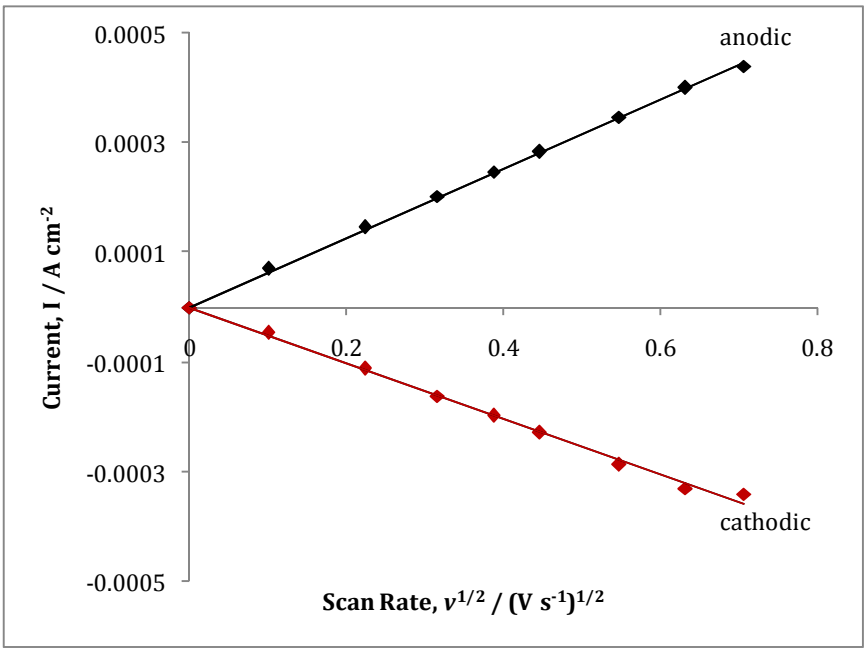


**Figure 5.7:** The plot of $i_p$ versus $\nu^{1/2}$ of DA (5.0 x $10^{-4}$ mol $dm^{-3}$) on GC in citrate phosphate buffer pH=5.0.

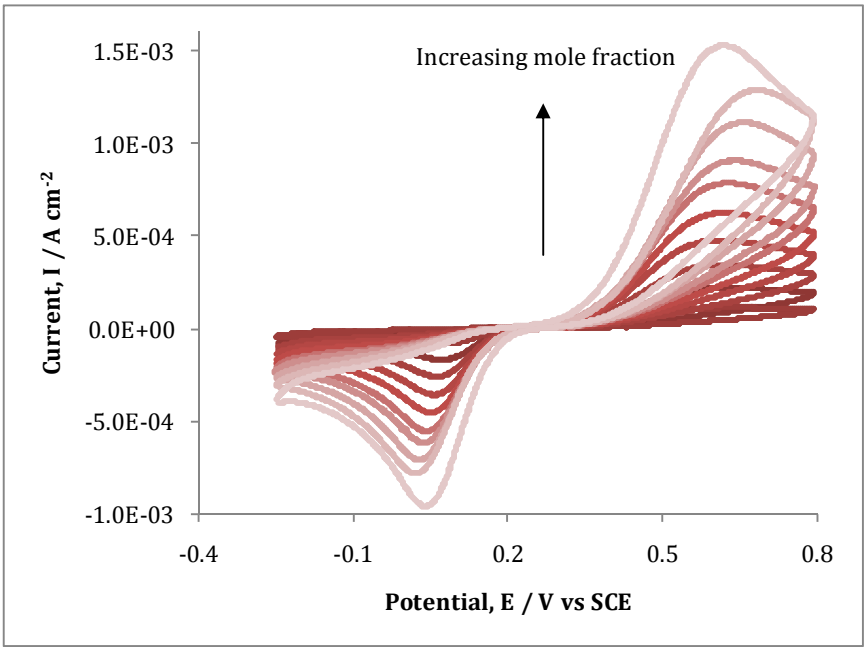


**Figure 5.8:** Cyclic voltammograms used to construct the Job's plot titration curve of Sβ-CD and DA in a citrate-phosphate buffer, pH = 5.0. From bottom to top, the DA mole fraction increases from 0.0 to 1.0, in increments of 0.1.

To generate the Job's plot from the CV analysis the continuous variation method was used to follow the changes in the peak current of DA using the equation

$$\Delta i_p = i_{p0} - i_{px} \quad 5.9$$

where $i_{p0}$ and $i_{px}$ are the peak currents of DA in the absence and presence of Sβ-CD, respectively. These $\Delta i_p$ values were then multiplied by the corresponding mole fraction ($\Delta i_p$ x mole fraction) and the product was plotted as a function of the mole fraction ([DA]/([DA]+[Sβ-CD])).

Figure 5.9 shows a Job's plot generated from the data presented in Figure 5.8. The Job's plot reaches a maximum value at 0.50 mole fraction, confirming the formation of a 1:1 DA/Sβ-CD complex. This is in excellent agreement with the spectroscopy measurements, Figure 5.3.

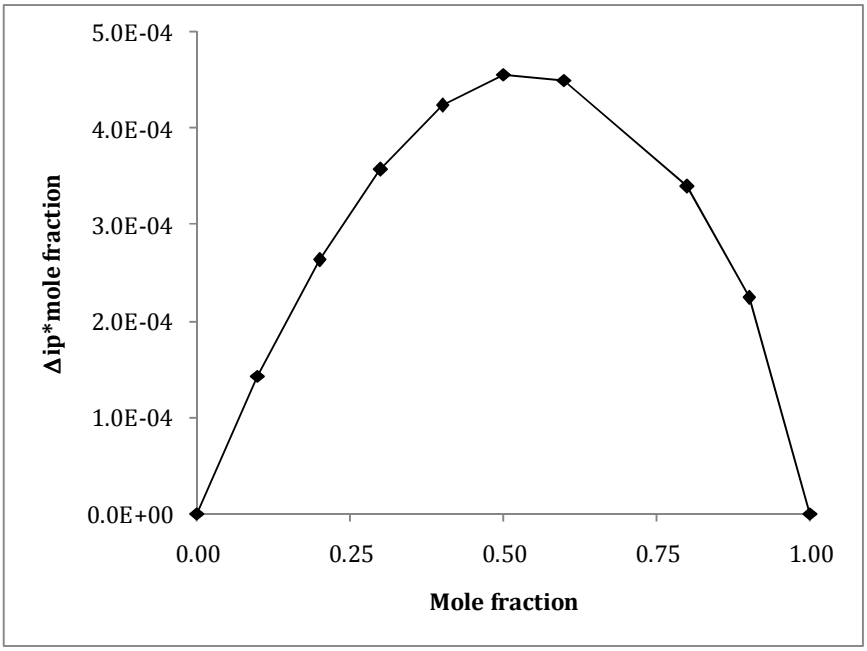


**Figure 5.9:** Job's plot curve of a change in peak current of DA upon the addition of Sβ-CD, as a function of the mole fraction of DA, indicating the formation of 1:1 host-guest complex.

## 5.3.2 DA-Sβ-CD complex stability constant

### *5.3.2.1 Determination of $K_f$ by UV*

The absorption spectra of DA ($\lambda_{max}$ =280 nm) in the absence and presence of varying concentrations of Sβ-CD are overlaid in Figure 5.10. From Figure 5.10 it can be seen that increasing the concentrations of Sβ-CD gives rise to an overall decrease in band intensity at 280 nm, or a hypochromic effect. This hypochromic effect is shown in Figure 5.11, which plots the absorbance value against the concentration of Sβ-CD present in the sample solution. Additional to this hypochromic effect, a shift in the wavelengths of the absorption bands was observed. This red shift of the DA spectral band to longer wavelengths, or bathochromic effect, has been reported previously and is due to an influence of substitution or to a change in environment. [21, 22] In our case there is a change in the environment due to complex formation, giving rise to the observed red shift. Both hypochromic and bathochromic effects were clearly present in all DA-Sβ-CD complex UV spectra as greater amounts of Sβ-CD were added. Similar bathochromic effects to that seen here were reported by Taraszewska *et al.*[23] for flutamide and Zhang and co-workers for cresyl blue in the complexation studies with β-cyclodextrin.[22] Ramaraj and co-workers also reported an overall increase in the intensity of the absorption band for the inclusion studies of various aromatic amines and nitro-compounds with β-cyclodextrin.[24] The changes in the absorption spectrum of DA upon addition of Sβ-CD are consistent with the formation of an inclusion complex between DA and Sβ-CD.

Figure 5.11 shows the change in the absorbance at 280 nm with increasing Sβ-CD concentration. The absorbance becomes smaller at higher concentrations of Sβ-CD, suggesting that the DA is completely included within the cavity when an excess of the Sβ-CD is present in solution. A similar observation was made by Yanez *et al.*[12] for the complexation of Nicardipine (NC) with β-CD.

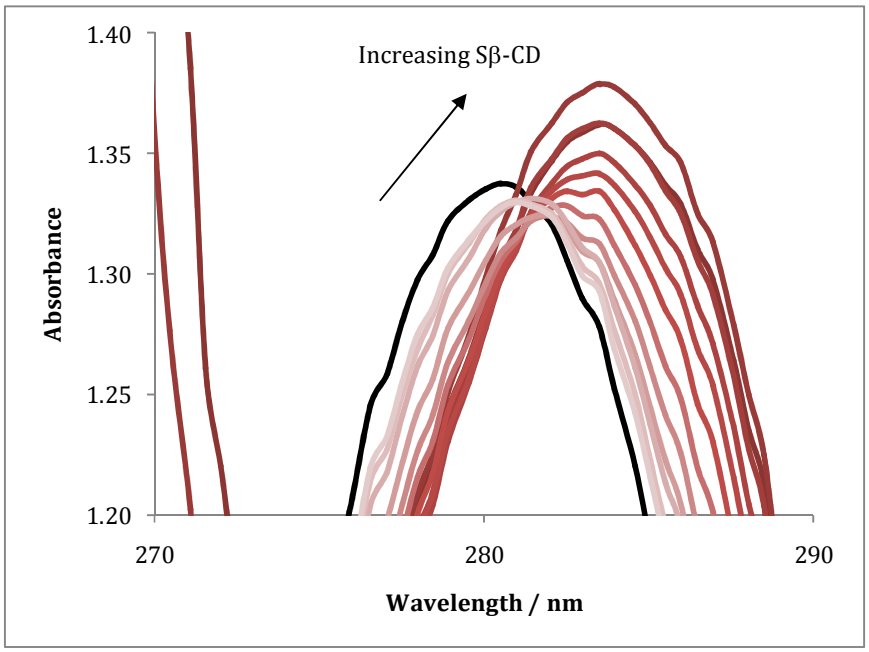


**Figure 5.10:** UV spectra of DA (5.00 x $10^{-4}$ mol $dm^{-3}$) in the absence (black trace) and presence of varying amounts of Sβ-CD in a citrate–phosphate buffer, pH=6.0 (red traces) (Sβ-CD concentrations were varied from 5.65 x $10^{-4}$ to 2.00 x $10^{-2}$ mol $dm^{-3}$).

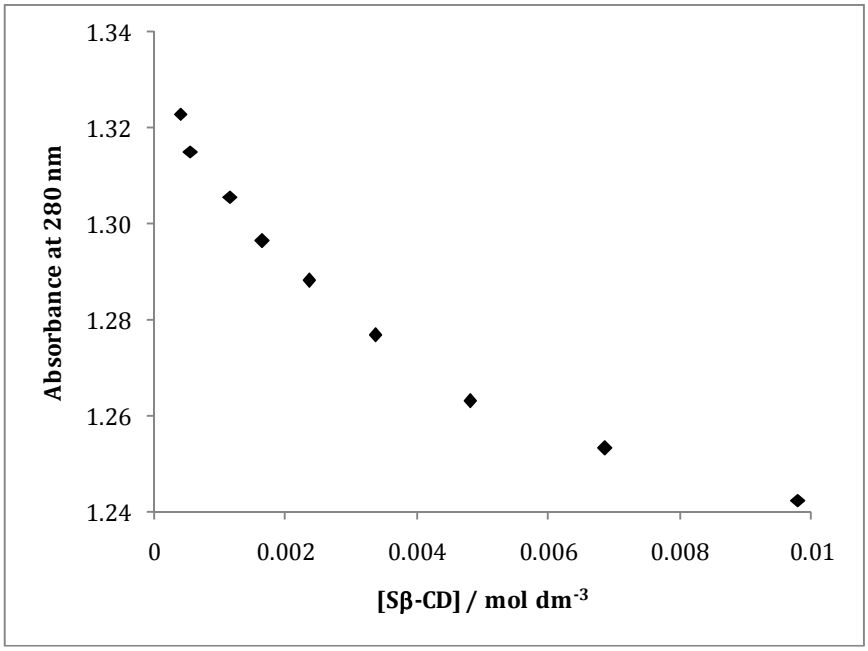


**Figure 5.11:** UV data of DA (5.0 x $10^{-4}$ mol $dm^{-3}$) at its $\lambda_{max}$ = 280 nm as a function of increasing amounts of Sβ-CD in a citrate–phosphate buffer, pH=6.0.

In calculating the value of $K_f$, Equation 5.1 assumes that a 1:1 inclusion complex is formed between DA and Sβ-CD (Section 5.3.1), and that an excess of Sβ-CD is present. Figure 5.12 shows a Heildebrand-Benesi plot constructed using Figure 5.10, showing a linear relationship with a correlation coefficient of 0.997. This linear relationship is further support for a 1:1 complex stoichiometry.[4]

From the intercept and slope of Figure 5.12, a $K_f$ value of 336.92 ± 24.83 was computed using Equation 5.1. This is considerably higher than the value reported for the inclusion complex between DA and neutral β-CD.[7]

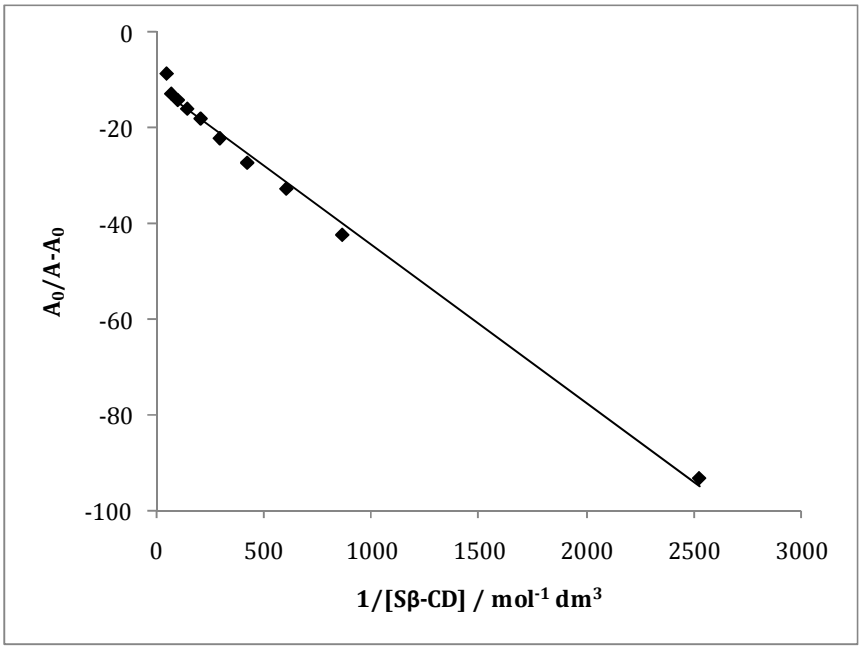


**Figure 5.12:** Plot of ($A_0/A_0$-A) as a function of (1/[Sβ-CD]) for the evaluation of the stability constant, ($K_f$), for DA inclusion within Sβ-CD.

### *5.3.2.2 Determination of $K_f$ by CV*

The inclusion phenomenon was also investigated using electrochemical methods. The CV and RDV techniques were chosen for their sensitivity and because they allow data to be retrieved at low concentrations of the

electroactive species.[6, 10] Section 5.3.1.2 reveals that DA is electroactive, quasi-reversible and under diffusion control.

Figure 5.13 shows the cyclic voltammograms obtained for DA at a pH of 6.0 in the absence and presence of 2.00 x $10^{-2}$ mol $dm^{-3}$ Sβ-CD. It is clear from this figure that the addition of Sβ-CD decreases the peak current and shifts the oxidation peak potential in the positive direction.

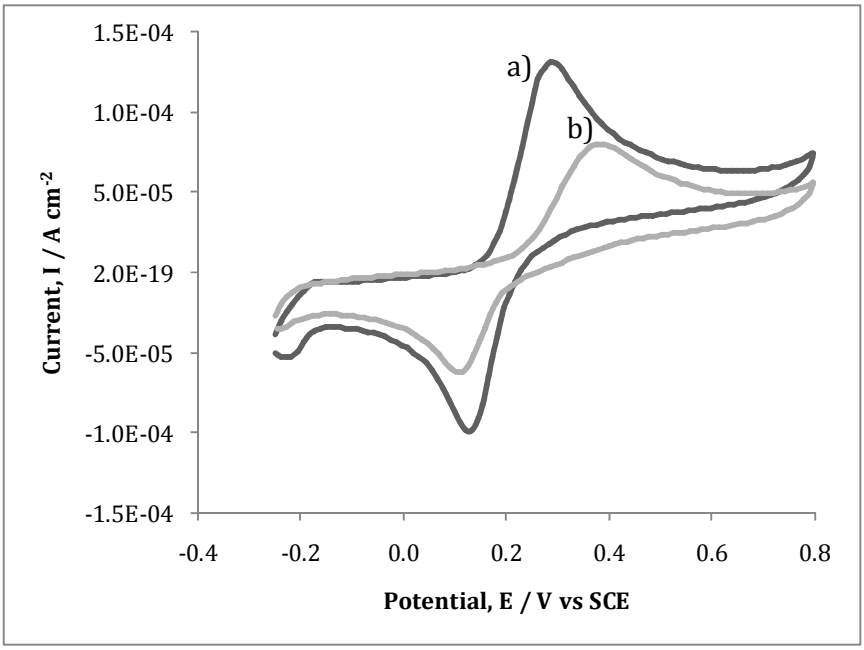


**Figure 5.13:** Cyclic voltammograms of DA (5.0 x $10^{-4}$ mol $dm^{-3}$) a) in the absence and b) in the presence of 2.0 x $10^{-2}$ mol $dm^{-3}$ Sβ-CD at pH=6.0 citrate-phosphate buffer. The potential was swept from -0.250 to 0.800 V vs. SCE at 50 mV $s^{-1}$.

The influence of the Sβ-CD can be seen more evidently in the cyclic voltammograms of DA in Figure 5.14, recorded with increasing concentrations of Sβ-CD ranging from 3.12 x $10^{-4}$ to 2.00 x $10^{-2}$ mol $dm^{-3}$. Although the voltammograms recorded in the presence of the Sβ-CD have similar characteristics to that recorded in a pure DA solution, there is a significant

difference in the oxidation of DA. The inset of Figure 5.14 shows a plot of the peak potential, $E_p$, for the oxidation of DA as a function of Sβ-CD concentration and reveals a gradual increase in the peak potential with increasing concentration of Sβ-CD. This indicates that DA is more difficult to oxidise in the presence of Sβ-CD and is consistent with the formation of an inclusion complex. Figure 5.14 also shows a decrease in the peak current, with increasing concentration of Sβ-CD, which is attributable to the change in the diffusion coefficient of DA. A lower diffusion coefficient is expected when a guest is included within the bulky cyclodextrin cavity, as has been shown in several other works with a variety of electroactive guests.[16, 25, 26]

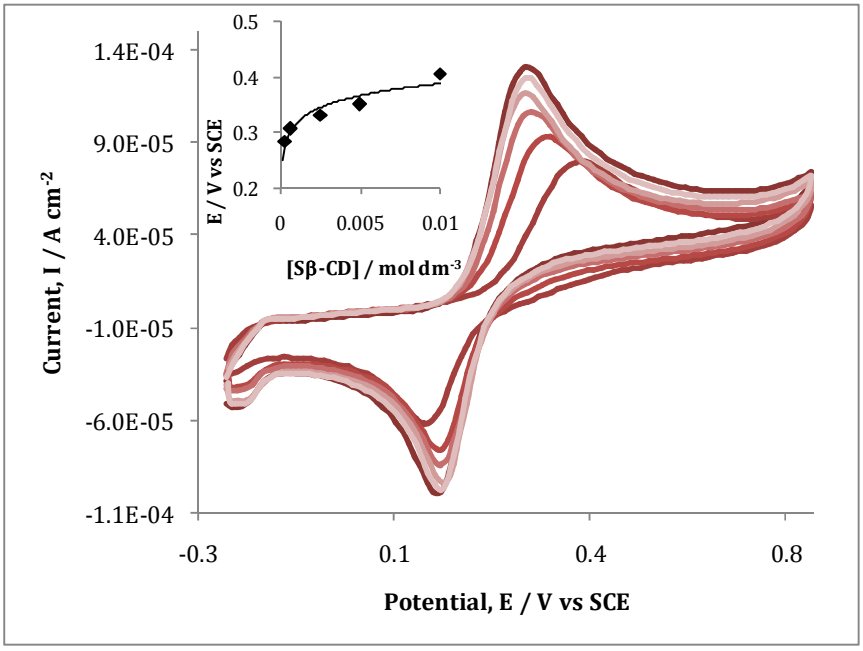


**Figure 5.14:** Cyclic voltammograms of 5.0 x $10^{-4}$ mol $dm^{-3}$ DA in a citrate-phosphate buffer, pH=6.0, at a GC electrode in the absence and in the presence of increasing concentrations of Sβ-CD. The potential is swept from -0.250 to 0.800 V vs. SCE at 50 mV $s^{-1}$ for 10 cycles. Inset shows the anodic peak potential as a function of [Sβ-CD].

Similar changes in the peak currents and potentials observed here are well represented within the literature and are indicative of inclusion complex

formation.[6, 25, 27] Dang *et al.*[7, 25] reported similar results for the complexation of benzoquinone and anthraquinone with β-CD. This trend was also observed by Li and co-workers in the investigation into the interactions of Basic Brown G with β-CD.[3] While, Gao *et al.*[26] investigated the inclusion complexation of another catecholamine, adrenaline (AD), and found that a similar increase in the shift of the oxidation potential was observed. They reported that it was due to the AD being more strongly bound to the hydrophobic cavity than of it's reduced state.

Figure 5.15 plots the peak potentials for the cathodic peak resulting from the reduction of quinone and it is interesting to note that there is no significant change in the peak potentials. This would suggest that the quinone is not included in the cavity. From this it seems likely that once the DA becomes oxidised it is expelled from the cavity.

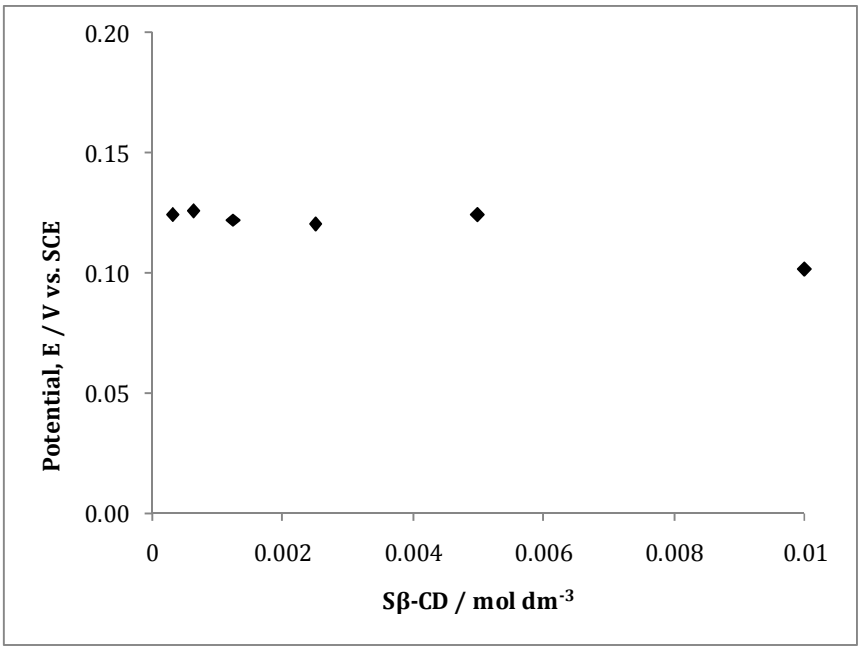


**Figure 5.15:** The cathodic peak potential plotted as a function of [Sβ-CD] in a 5.0 x $10^{-4}$ mol $dm^{-3}$ solution of DA in a citrate-phosphate buffer, pH=6.0, at a GC electrode in the presence of increasing concentrations of Sβ-CD.

Figure 5.16 shows the peak current for the oxidation of 5.00 x $10^{-4}$ mol $dm^{-3}$ DA and the corresponding reduction of the quinone as a function of the square root of the scan rate, in the absence and presence of 2.00 x $10^{-2}$ mol $dm^{-3}$ Sβ-CD. These plots have a good linear relationship with correlation coefficients of 0.999 and 0.998 for DA in the absence and presence of Sβ-CD, respectively, for the anodic peak. The diffusion coefficients were evaluated from the slopes of these plots using the Randles-Sevcik equation, Equation 5.10,

$$Ip = k\, n^{3/2} A\, D^{1/2}\, c\, v^{1/2} \qquad 5.10$$

where $k$ has a value of 2.69 x $10^5$, $I_p$ is the peak current density, $c$ is the concentration of DA in mol $cm^{-3}$ and $v$ is the scan rate of the potential in V $s^{-1}$. [28] $I_p$ is linearly proportional to the bulk concentration, $c$, of the electroactive species and the square root of the scan rate, $v^{1/2}$.

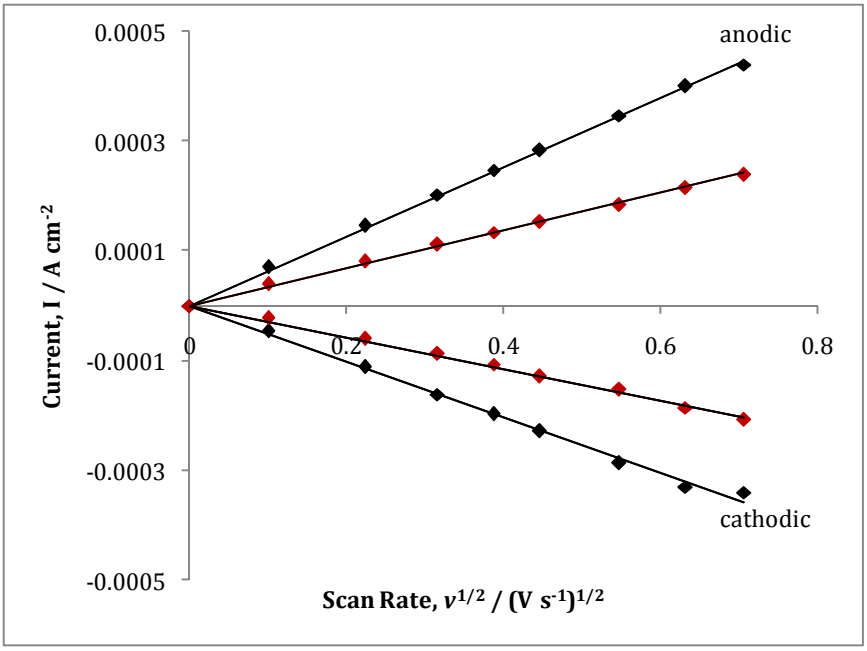


**Figure 5.16:** The plot of $I_p$ versus $v^{1/2}$ (cyclic voltammograms) on a GC disc electrode in citrate-phosphate buffer, pH=5, for 5.0 x $10^{-4}$ mol $dm^{-3}$ DA in the absence ♦ and presence ♦ of 2.0 x $10^{-2}$ mol $dm^{-3}$ Sβ-CD.

Table 5.6 gives a summary of the diffusion coefficients obtained for DA alone and in the presence of a large excess of Sβ-CD. From these linear relationships in Figure 5.16 it can be seen that the diffusion coefficient of DA in the presence of the Sβ-CD decreases. It is known that β-CD could cause an increase in the viscosity of the solution and, therefore, a decrease in the diffusion coefficient. However, according to the literature no change in β-CD viscosity was detected over the concentration range 0.00 to 1.00 x $10^{-2}$ mol $dm^{-3}$.[16, 25, 26] Therefore, with respect to that of free DA, this decrease can be attributed to the DA inside the cavity and the formation of an inclusion complex. The sulfonated CD is very large compared to DA and this will influence the diffusion of DA when DA is confined within the cavity of the CD.

**Table 5.6:** The diffusion coefficients obtained for the oxidation of DA in the absence and presence of Sβ-CD using the Randles-Sevcik equation.

| | **Slope / A $cm^2$ $V^{-1/2}s^{1/2}$** | **Diffusion coefficient / $cm^2$ $s^{-1}$** |
|---|---|---|
| **DA** | 6.32 x $10^{-4}$ | 2.76 x $10^{-6}$ |
| **Sβ-CD+DA** | 3.41 x $10^{-4}$ | 8.05 x $10^{-7}$ |

Figure 5.17 shows a plot of the experimental data, 1/[Sβ-CD] vs. $1/(1-i/i_0)$ which gives a linear relationship with a correlation coefficient of 0.999. According to Equation 5.2 such linear plots not only confirm the existence of a 1:1 complex,[29] but can also be used to calculate the stability constant. Accordingly, the $K_f$ value was calculated as 255.88 ± 7.97. Again, this is in good agreement with the value obtained from UV analysis, Section 5.3.2.1.

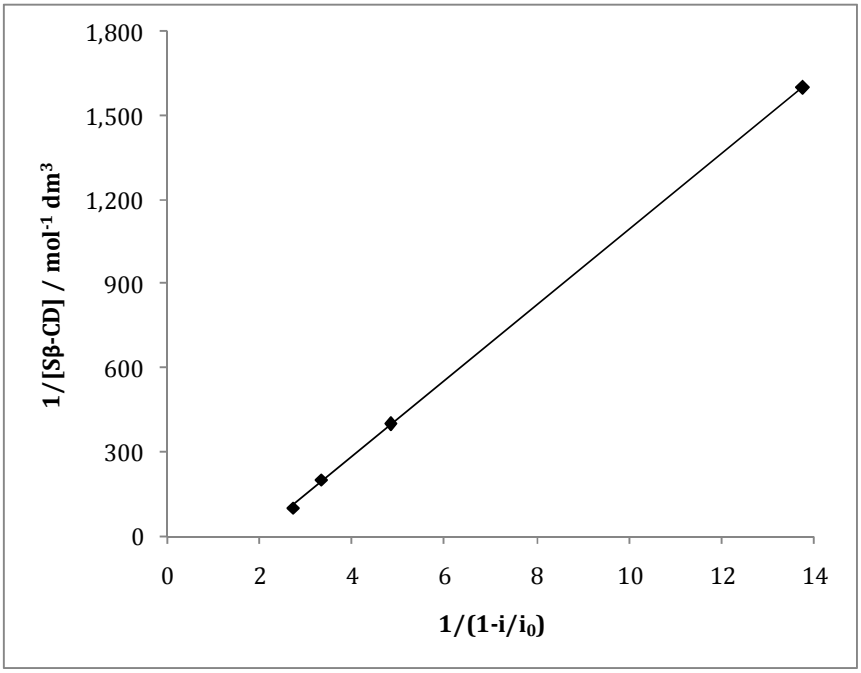


**Figure 5.17:** Plot of 1/[Sβ-CD] as a function of 1/(1-$i/i_0$) for the evaluation of the stability constant, ($K_f$), for DA in citrate phosphate buffer, pH=6.0.

### *5.3.2.3 Determination of $K_f$ by RDV*

It has been suggested that as the peak potential shifts to more positive potentials, due to an increase in the presence of cyclodextrins, the shift can be used to determine the $K_f$ of the complex.[16] To undertake these experiments an excess of Sβ-CD is needed and the experiments should be performed at slow scan rates. RDV is thought to be more suited for these studies because it provides enhanced conditions for a reversible charge-transfer.[6]

Figure 5.18 shows the RDV voltammograms for DA ($5.00 \times 10^{-4}$ mol dm$^{-3}$) as a function of the rotation speed. The data obtained at the GC rotating disc electrode show that the limiting current ($i_L$) of DA increases with increasing rotation frequencies. There is a clear linear relationship between the limiting current and the square root of the rotation speed, as shown by the inset of Figure 5.18, indicating that the system follows the Levich equation (Equation 5.5). It also indicates that the limiting current is mass transport controlled.

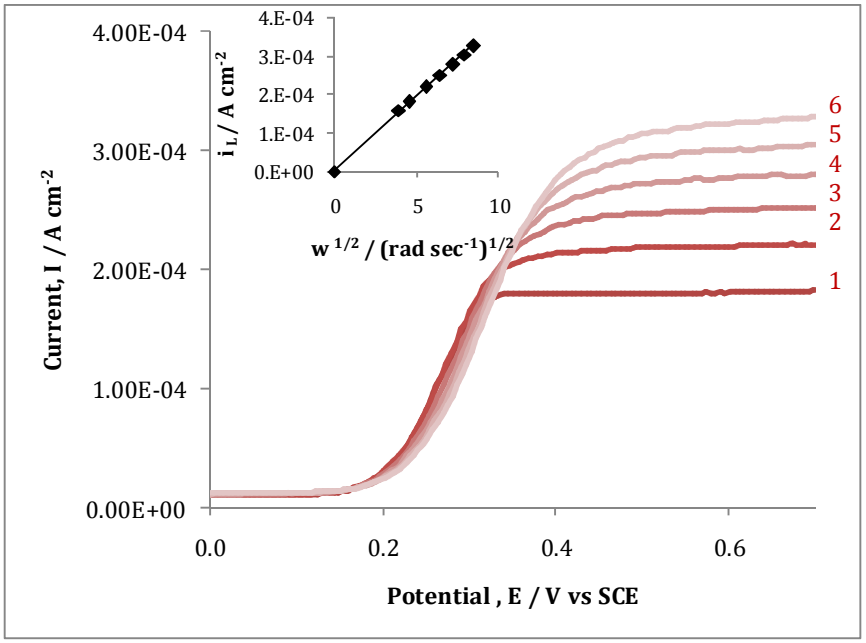


**Figure 5.18:** RDV voltammograms of DA (5.0 x $10^{-4}$ mol $dm^{-3}$) on a GC disc electrode in a citrate-phosphate buffer pH=6.0. Rotation frequency, rpm: (1) 200; (2) 300; (3) 400; (4) 500; (5) 600; (6) 700. The inset shows a plot of $i_L$ versus $\omega^{1/2}$.

Figure 5.19 shows the effect of Sβ–CD concentration on the RDV voltammograms of DA. As the Sβ-CD concentration is increased the half-wave potentials ($E_{1/2}$) for DA oxidation continue to shift to more positive potentials, as shown in the inset of Figure 5.19. Additional experiments were carried out where the limiting current for the oxidation of DA was measured as a function of the rotation speed both alone and in the presence of varying concentrations of Sβ-CD.

Levich plots, where the limiting current is plotted as a function of the square root of the rotation speed are shown in Figure 4.20. Good linear relationships are observed with correlation coefficients exceeding 0.986, indicating that the system is indeed under diffusion control.

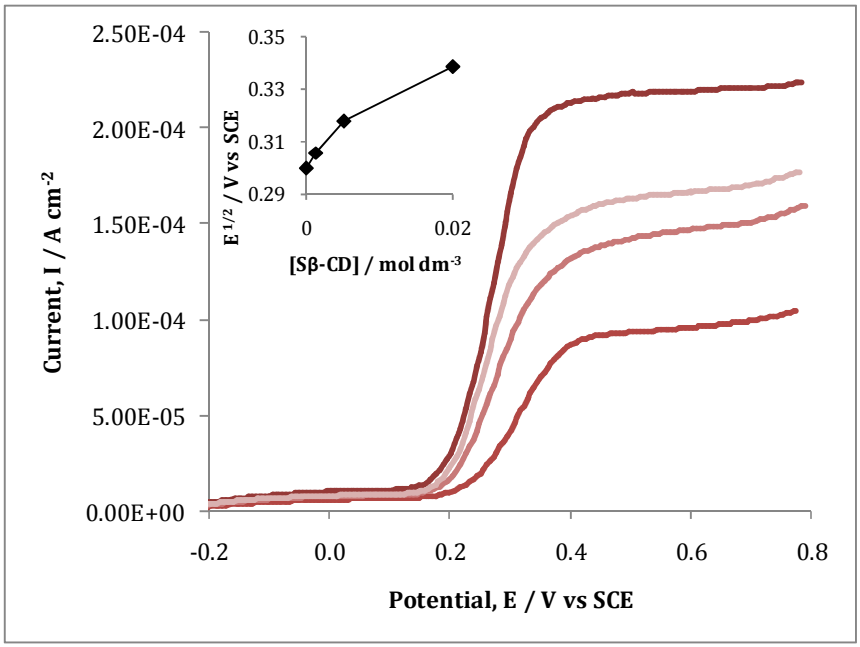


**Figure 5.19:** Effect of Sβ-CD concentration on the rotating-disc voltammograms of DA (5 x $10^{-4}$ mol $dm^{-3}$) on a GC disc electrode in citrate-phosphate buffer (pH=6.0). [Sβ-CD]/ mol $dm^{-3}$: (1) 0.000; (2) 0.005; (3) 0.010; (4) 0.020. Rotation frequency 500 rpm ($\nu$ = 50 mV $s^{-1}$). The inset shows a plot of $E_{1/2}$ versus [Sβ-CD].

The slopes of the Levich plots for free DA and for DA in the presence of 0.02 mol $dm^{-3}$ Sβ-CD were used with Equation 5.5, to evaluate the diffusion coefficients, $D_f$ and $D_c$. A decrease in the diffusion coefficient was found with increasing concentration of Sβ-CD, as is evident from the inset in Figure 5.20. A $D_f$ value of 5.11 x $10^{-6}$ $cm^2$ $s^{-1}$ was found for free DA, while the diffusion coefficient of the complexed species, $D_c$, was evaluated as 2.44 x $10^{-6}$ $cm^2$ $s^{-1}$. Again, this is attributed to the formation of a DA-Sβ-CD inclusion complex, which has a slower diffusion rate due to the large size of the cyclodextrin. These values are in general agreement with the diffusion coefficients calculated using CV (Table 5.6). However, the RDV diffusion coefficient values are considered to be more accurate because of the elimination of mass transport related kinetic restrictions. A $D_c/D_f$ value of 0.47 was obtained and this is in very good agreement with ratios found in the literature for the complexation of ferrocenes with CDs.[6, 16]

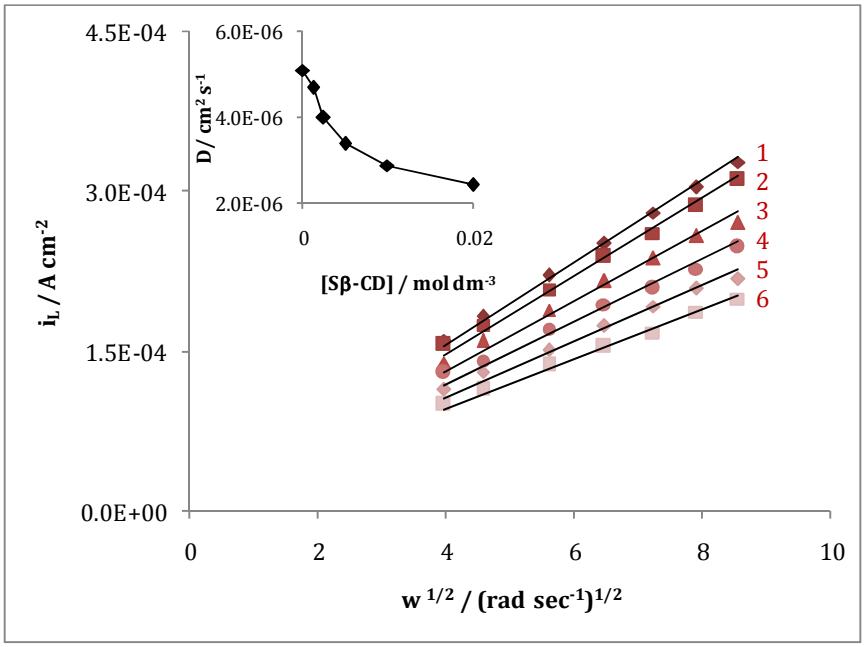


**Figure 5.20:** Plot of $i_L$ versus $\omega^{1/2}$ at rotating-disc voltammograms of DA (5.0 x $10^{-4}$ mol $dm^{-3}$) on a GC disc electrode in citrate-phosphate buffer, (pH=6), in the presence of varying amounts of [Sβ-CD] / mol $dm^{-3}$. 1) 0.00 2) 1.25 x $10^{-3}$ 3) 2.50 x $10^{-3}$ 4) 5.00 x $10^{-3}$ 5) 1.00 x $10^{-2}$ and 6) 2.00 x $10^{-2}$. The inset shows a plot of the diffusion coefficients as a function of increasing Sβ-CD concentrations.

Using Equation 5.3 and the $D_c/D_f$ value of 0.47, the $K_f$ value for the DA-Sβ-CD inclusion complex was calculated as 331.28 ± 5.85. Equation 5.3 is valid when the concentration of the cyclodextrin is larger than the total concentration of the guest. The kinematic viscosity of the system was taken to be 0.92 x $10^{-6}$ $m^2$ $s^{-1}$.[30] The diffusion coefficient evaluated for DA is in close agreement with values reported in the literature in the range of 1.9 x $10^{-6}$ to 6.3 x $10^{-6}$ $cm^2$ $s^{-1}$.[31-33] Also, both the CV and RDV methods in computing the diffusion coefficient are in good accordance with each other.

Additionally, from these data the Koutecky-Levich equation (Equation 5.6) was used to calculate the heterogeneous charge transfer rate constant, *k*, for DA in the absence and presence of the varying concentrations of Sβ-CD. Figure 5.21

shows the Koutecky-Levich plots ($i_L^{-1}$ vs. $\omega^{-1/2}$) for DA alone and in the presence of varying concentration of Sβ-CD. For each Sβ-CD concentration a linear Koutecky-Levich relationship was observed and from the y-intercept of each plot the *k* values were obtained and are presented in Table 5.7. From the inset in Figure 5.21 it is evident that the rate constant for the oxidation of DA decreased as the concentration of Sβ-CD increased. This decrease in rate constant can be attributed to the formation of an inclusion complex. It is reasonable to expect that the rate of the electron-transfer reaction will be higher when the DA is free in solution, compared to when it is complexed within the cavity of the CD species. Using Marcus theory[34], this can be explained in terms of the reorganisation energy. In the semi-classical Marcus theory, the rate of electron transfer is given by the equation

$$k = \frac{2\pi}{h} \frac{H_{DA}^2}{\sqrt{4\pi\lambda RT}} e^{\frac{(\Delta G^0 + \lambda)^2}{4\lambda RT}} \qquad 5.11$$

where $H_{DA}$ is the electronic coupling matrix element, $\Delta G^o$ is the Gibbs energy change and λ is the re-organisation energy, which is the energy associated with relaxing the geometry of the system after the electron-transfer step. This reorganisation energy is likely to be higher when the DA is confined within the cavity of the Sβ-CD, leading to a lower rate constant, in accordance with Equation 5.11.

Typical rate constants for the oxidation of DA in the literature are in the range of 1.3 x $10^{-2}$ cm $s^{-1}$ to 3.88 x $10^{-3}$ cm $s^{-1}$ on different materials and the higher values are in good agreement with the values obtained in Table 5.7.[33, 35-37]

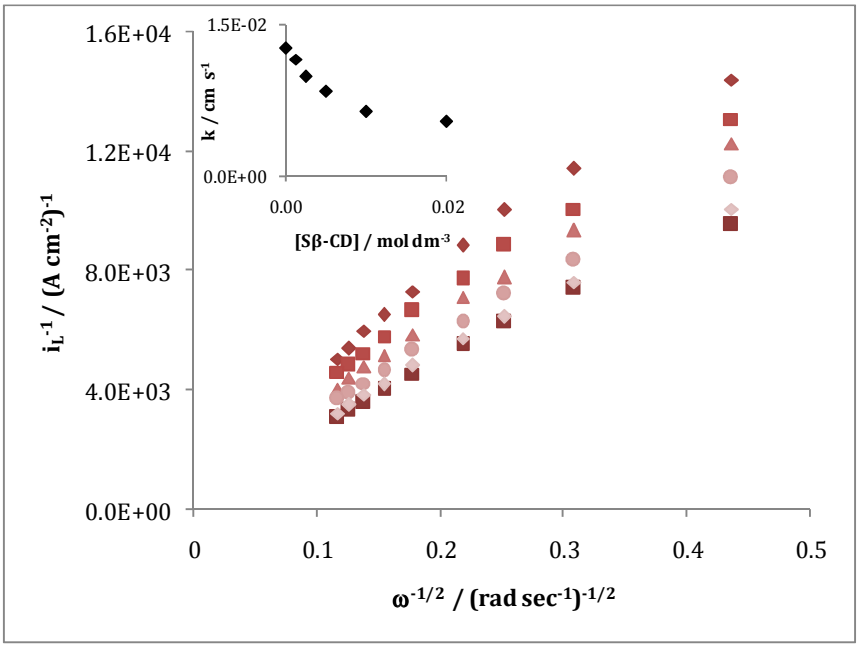


**Figure 5.21:** Koutecky-Levich plots for DA in the absence and presence of varying concentrations of [Sβ-CD] / mol dm$^{-3}$. 1) 0.00 2) 1.25 x 10$^{-3}$ 3) 2.50 x 10$^{-3}$ 4) 5.00 x 10$^{-3}$ 5) 1.00 x 10$^{-2}$ and 6) 2.00 x 10$^{-2}$. Experiments were carried out in a citrate-phosphate buffer (pH=6.0). Current was read at +0.700 V. The inset shows the rate constant as a function of increasing Sβ-CD concentrations.

Table 5.8 shows the stability constants obtained using the three techniques discussed here. In all cases the data were obtained in a citrate-phosphate aqueous buffer with a pH of 6.0. From Table 5.8 the stability constants are in close agreement, validating both the different methods and the stability constants obtained. In comparing these values with the values obtained with the neutral β-cyclodextrin ($K_f$ = 95.06)[4] we can confirm that the presence of the sulfonated groups on the cyclodextrin aids complexation. This could be due to the fact that one of the main driving forces in complexation is electrostatic interactions[38] and as the DA in solution is protonated there is a strong electrostatic interaction between the protonated N atom on the DA and the negatively charged sulfonated groups on the CD. This in turn allows the aromatic moiety of the DA to enter the cavity.[38]

**Table 5.7:** The effect of the concentration of Sβ-CD on the rate constant, *k*, evaluated using the Koutecky-Levich equation.

| [Sβ-CD] / mol $dm^{-3}$ | rate constant, k / cm $s^{-1}$ | $R^2$ |
|---|---|---|
| 0.00 | $1.26 \times 10^{-2}$ | 0.992 |
| $1.25 \times 10^{-3}$ | $1.11 \times 10^{-2}$ | 0.996 |
| $2.50 \times 10^{-3}$ | $9.79 \times 10^{-3}$ | 0.997 |
| $5.00 \times 10^{-3}$ | $8.39 \times 10^{-3}$ | 0.997 |
| $1.00 \times 10^{-2}$ | $6.31 \times 10^{-3}$ | 0.993 |
| $2.00 \times 10^{-2}$ | $5.37 \times 10^{-3}$ | 0.986 |

**Table 5.8:** The stability constants obtained from UV, CV and RDV.

| Formation constants of DA and Sβ-CD pH~6.0 | | |
|---|---|---|
| $K_f$ by UV spectra | $K_f$ by CV | $K_f$ by RDV |
| 336.92 ± 24.83 | 255.88 ± 7.97 | 331.28 ± 5.85 |

These results are consistent with the formation of an inclusion complex, according to the equilibrium,

$$\text{Guest} + \text{CD} \rightleftharpoons \text{Guest-CD}$$

where the Guest-CD represents the inclusion complex of DA with Sβ-CD.

In the next section NMR is used to investigate the structural relationship between DA and Sβ-CD and a proposed structure for the inclusion complex is presented and discussed.

### 5.3.3 Analysis of the DA-Sβ-CD complex by NMR

NMR spectroscopy is a sensitive technique for monitoring the interactions between molecules and it has been widely used to study complexes between CDs and a variety of guests to give structural information on a range of complexes.[39, 40] In this study, chemical shifts generated from complexation were used to estimate the apparent complexation constants and confirm a 1:1 DA:Sβ–CD complex stoichiometry.

#### *5.3.3.1 Determination of the DA-Sβ-CD complex molecular structure by NMR*

NMR is a very appropriate tool for the structural analysis of the complexation mechanism by comparison of the DA spectra in the absence and presence of Sβ–CD. In general, cyclodextrins have an overall cylindrical truncated cone shape, which has a predominantly hydrophobic internal cavity due to the presence of the lone pairs of glycosidic oxygen atoms.[41] This cavity is open at both ends, which have different diameters, and these ends are referred to as the primary and secondary ends due to the presence of the primary and secondary hydroxyl groups.[8] Generally, in the NMR process of determining the geometric factor between the host and guest, the host protons H3 and H5 are monitored because they face the internal cavity and are located near the secondary and primary ends, respectively. They can, therefore, be used to explore the internal cavity of cyclodextrins for the presence of a guest molecule and identify the nature of its interaction.[40] Unfortunately, in the case of Sβ-CD, the NMR spectra are too complicated (the Sβ-CD sample is a structure of substituted CDs, with the degrees of substitution varying between 7 and 11) to follow the chemical shifts of these protons and so analysis of the guest protons was necessary.

Figure 5.22 shows the chemical structure of DA; it has five types of hydrogen: a-H, b-H, c-H, d-H and e-H. The protons designated as a-H, b-H and c-H correspond to the aromatic protons, while the protons d-H and e-H correspond to the methylene (-$CH_2$-) group protons.

Figure 5.23 shows a $^{1}H$ NMR spectra of 5 x $10^{-3}$ mol $dm^{-3}$ DA in 0.1 mol $dm^{-3}$ KCl in $D_2O$. In this figure, the two proton regions are highlighted. The red region corresponds to the aromatic protons a-H, b-H and c-H and the blue region corresponds to the d-H and e-H 2-$CH_2$ group protons, as illustrated in Figure 5.22.

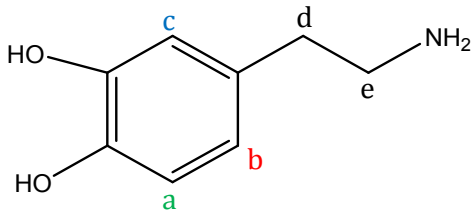


**Figure 5.22:** Chemical structure of DA. The protons are designated with letters.

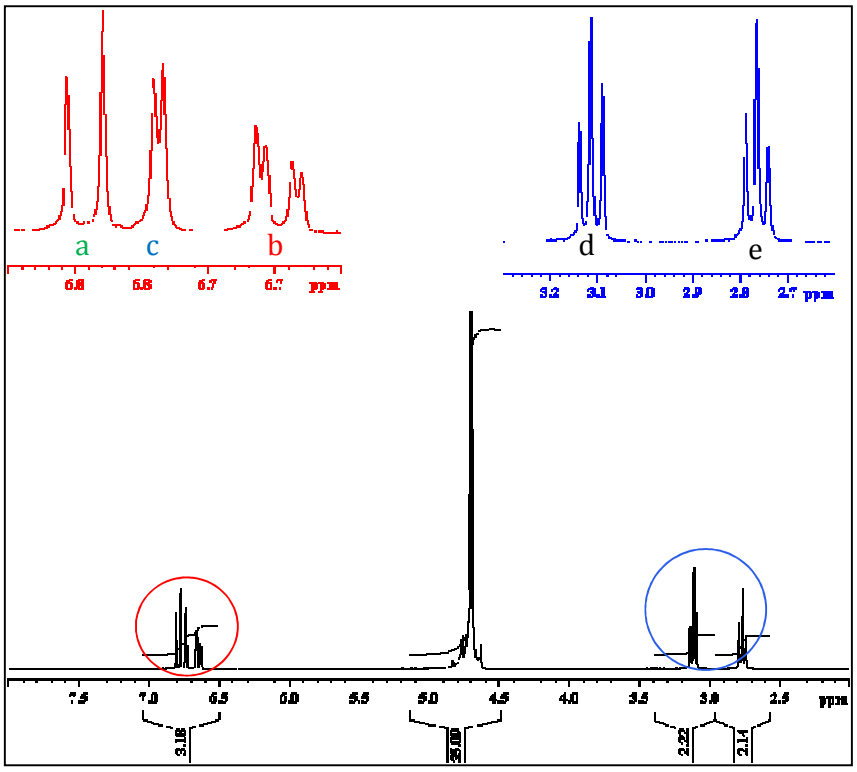


**Figure 5.23:** $^{1}H$ NMR spectra of 5 x $10^{-3}$ mol $dm^{-3}$ DA in 0.1 mol $dm^{-3}$ KCl in $D_2O$. DA $^{1}H$ NMR (300 MHz, $D_2O$): δ 6.79 (1H, *d*, *J*=8.1, a-H), 6.64 (1H, *dd*, *J*=1.3, 8.0, b-H), 6.74 (1H, *d*, J=2.1, c-H), 3.11 (2H, *t*, *J*=7.2, d-H), 2.76 (2H, *t*, *J*=7.2, e-H).

The main interest of the NMR technique is that a change in the chemical shift indicates complexation. As Sβ-CD does not interfere with the aromatic region (Figure 5.24) it was easy to monitor the chemical shift change in DA. This information can be used to approximate which moiety of the molecule was included and, hence, the structural identity of the complex. In Figure 5.24 the aromatic region of the $^{1}H$ NMR spectra of 2.0 x $10^{-2}$ mol $dm^{-3}$ Sβ–CD, 5.0 x $10^{-3}$ mol $dm^{-3}$ DA and a mixture of DA-Sβ–CD are shown. In Figure 5.22 the coloured letters represent each aromatic proton; these colours are shown in Figure 5.24 to illustrate the shift of each individual proton in the presence of Sβ-CD.

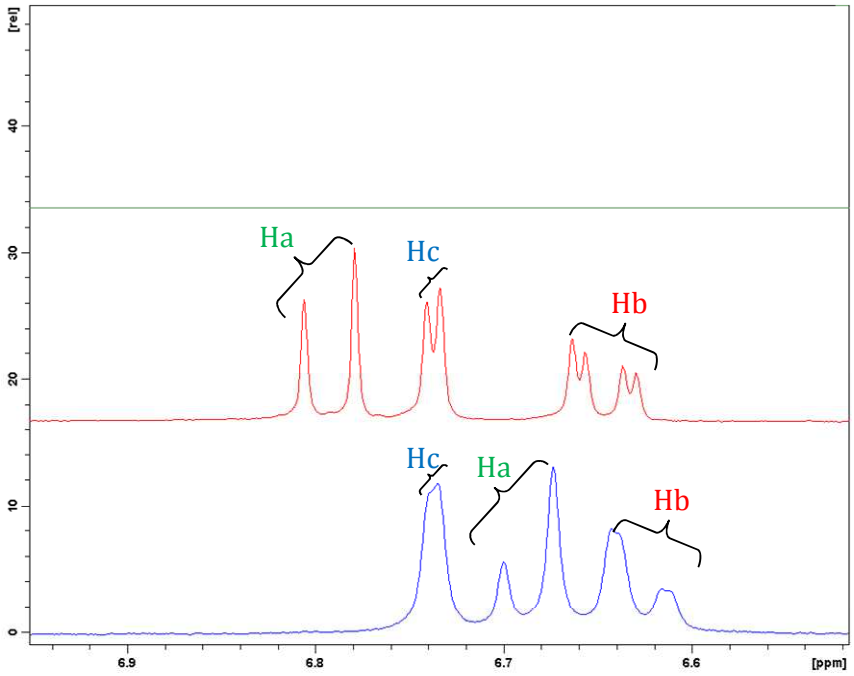


**Figure 5.24:** $^{1}H$ NMR spectra of the aromatic region, Sβ-CD (green), DA (red), and DA in the presence Sβ-CD (blue) in buffered $D_2O$ solutions. The corresponding protons are colour coded to differentiate the chemical shift.

Comparing the $^{1}H$ NMR spectra of DA in the absence and presence of Sβ-CD the protons implied in the inclusion process can be located. It is evident from Figure 5.24 that the chemical shift of the a-H proton of DA is significant. Also evident

from Figure 5.24 is that the b-H proton also experiences a moderate shift, while the c-H proton's chemical shift is only slightly affected, suggesting that it remains outside the CD cavity. It should be noted that all these chemical shifts are in the same upfield direction. A summary of the changes observed for the protons of DA in the presence and absence of Sβ-CD is given in Table 5.9.

**Table 5.9:** $^{1}$H NMR chemical shifts (ppm) of DA in the absence and presence of Sβ-CD.

| DA | δ without Sβ-CD | δ with Sβ-CD | Δδ |
|---|---|---|---|
| **Ha** | 6.7932 | 6.6873 | -0.1058 |
| **Hb** | 6.6472 | 6.6299 | -0.0173 |

The significant upfield or low frequency shift of the aromatic protons indicates a shielding effect, which is possibly due to the increase in the electron density inside the cavity from the non-bonding electron pairs of the glycosidic oxygen bridges.[8] This is further evidence that the aromatic ring is penetrating the cavity. The complex illustrated in Figure 5.25 is consistent with the findings presented in Table 5.9.

The region of the aromatic ring that enters the Sβ-CD cavity can be deduced from the observed chemical shift in Figure 5.24 and this process is illustrated in Figure 5.25. Bratu *et al.*[42] observed shifts of a similar nature for Fenbufen (FEN) in the presence of neutral β-CD. They observed that the methylene groups of the FEN remained outside the cavity and the FEN molecule entered from the larger side or the secondary opening of the β-CD ring. Also Chao and co-workers[43] demonstrated with NMR that the aromatic ring of caffeic acid, a molecule with similarities to DA, lay inside the β-CD cavity while the more polar groups remained outside.

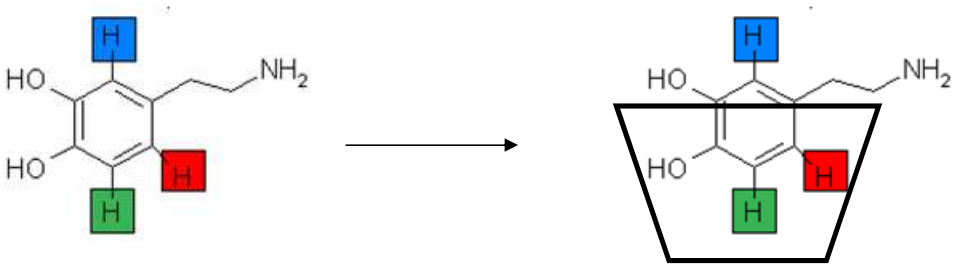


**Figure 5.25:** A proposed structural representation deduced from the NMR data. The aromatic protons are differentiated with a colour code: a-H, b-H, c-H.

### *5.3.3.2 Determination of complex stoichiometry by NMR*

NMR is also often used to determine the stoichiometry of the complex by the well known continuous variation method (Job's method), in which stoichiometry can be determined by the position of highest point.[9, 44, 45] Most current stoichiometric ratios between β-CD and guest molecules reported in the literature are 1:1, 1:2 and 2:1. [7, 40, 43] As shown previously in Section 5.3.1, a stoichiometric value of 1:1 for the Sβ-CD and DA complex was determined using both spectrophotometric and electrochemical procedures.

The NMR spectra of each solution, given in Table 5.4, were recorded and Figure 5.26 shows a comparison plot of all 11 samples. The experimentally observed parameter in this case is the chemical shift of the aromatic protons of the DA, where an upfield shift of proton a-H and b-H was observed. For example, the chemical shift for a-H was 6.87 ppm when the mole fraction of DA was 1.0 and it changed to 6.74 ppm for a DA mole fraction of 0.1.

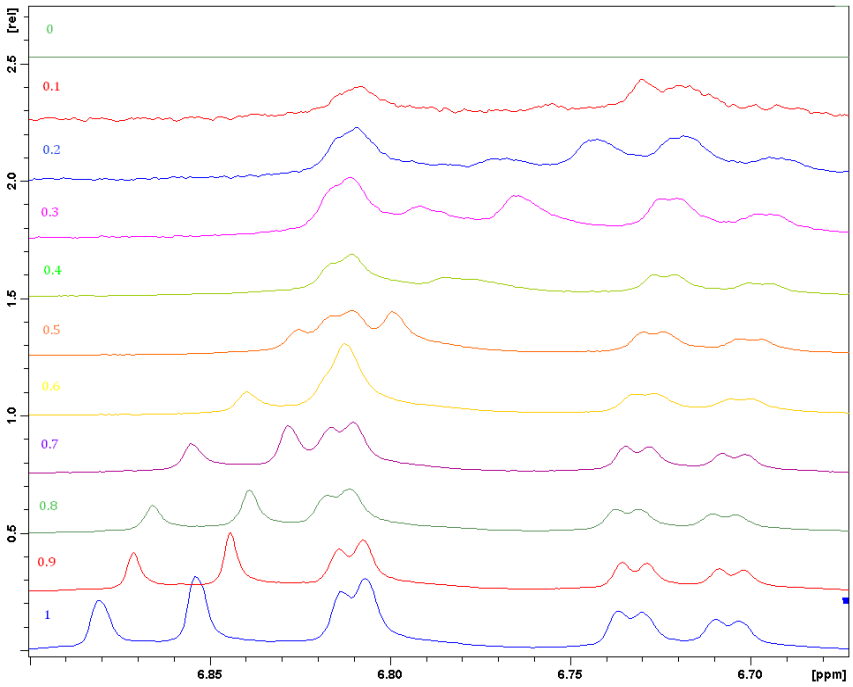


**Figure 5.26:** $^{1}H$ NMR spectra (aromatic region) in 0.1 mol $dm^{-3}$ $KCl/D_2O$. This is the spectra obtained for the Job's method where the mole fraction was varied from 0.0 to 1.0, as shown on the diagram.

To generate the Job's plot and establish the stoichiometry of the complex, the continuous variation method was used to follow the changes in chemical shifts of the DA aromatic protons a-H and b-H that showed the most distinct variations. The Job's plot was created by evaluating the change of the chemical shift, Δδ, from that of an equal concentration of DA using the equation:

$$\Delta\delta = \delta_0 - \delta_c \qquad 5.12$$

where $\delta_0$ and $\delta_c$ are the chemical shift values for DA in the absence and presence of Sβ-CD, respectively. These Δδ values were then multiplied by the corresponding mole fraction (Δδ x mole fraction) and the product was plotted as a function of the mole fraction ([DA]/([DA]+[Sβ-CD])).

The results for the a-H proton are shown in Figure 5.27. The maximum value of the Job's plot for the a-H proton (Figure 5.27) occurs at a DA mole fraction of 0.5. A similar Job's plot to that of Figure 5.27 resulted from the chemical shift changes of the b-H proton (data not shown) with a maximum at 0.5 DA mole fraction. Taken together this is strong evidence for a 1:1 complex stoichiometry.

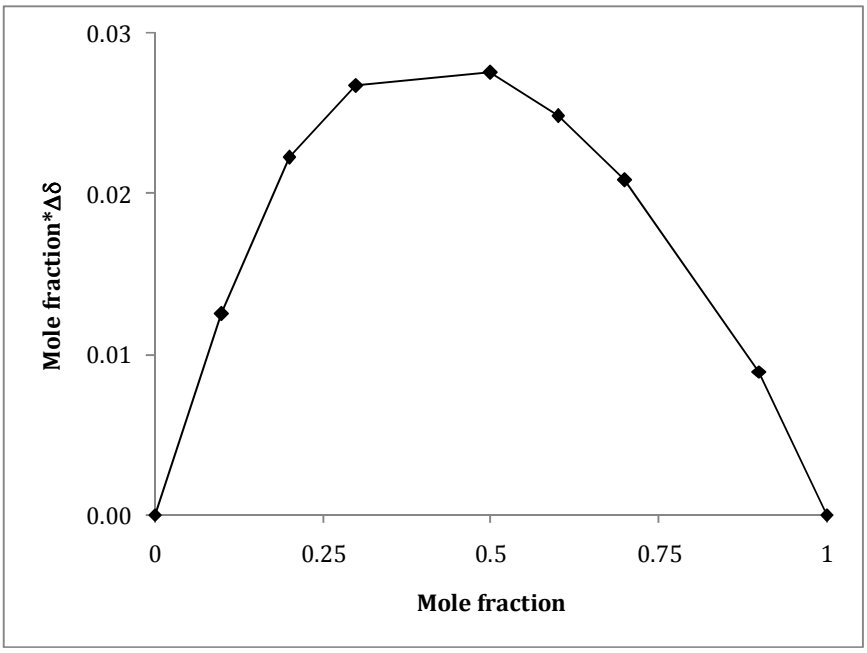


**Figure 5.27:** The Job's plot for the determination of the stoichiometry of the a-H proton of the DA.

### *5.3.3.3 Determination of the $K_f$ value by NMR*

A NMR titration experiment was performed to obtain host-guest binding information on the DA/ Sβ-CD system. The spectrum of the DA in a deuterated solvent was first measured, small aliquots of Sβ-CD were then added and the spectrum was recorded. In all these experiments, the concentration of the DA, guest, was kept constant and the concentration of Sβ-CD, host, was varied. During the complexation procedure of DA with Sβ-CD a change in the chemical shift was observed, as shown in Figure 5.28. This figure shows a typical upfield shift of the aromatic protons of DA in the presence of Sβ-CD.

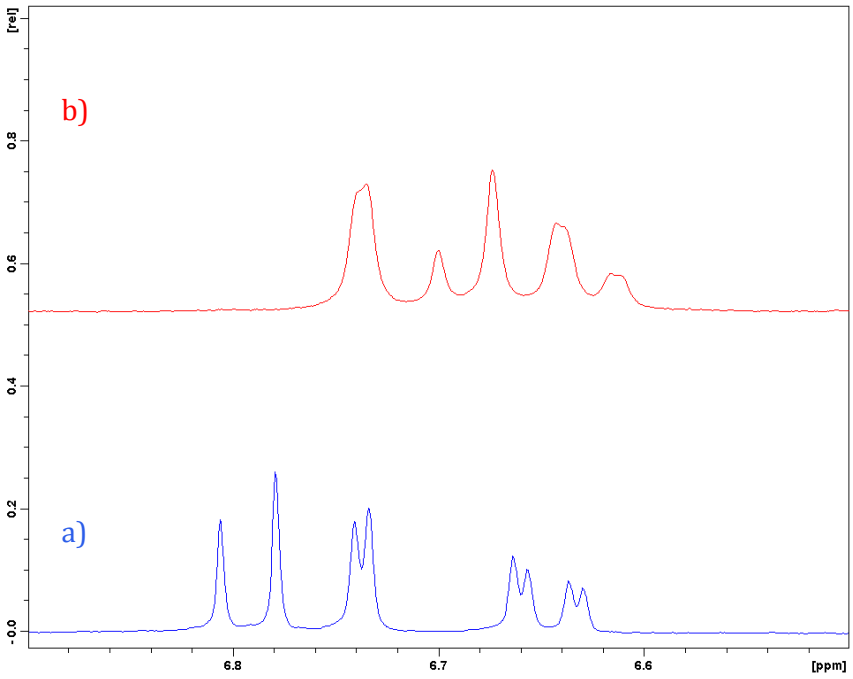


**Figure 5.28:** $^{1}$H NMR spectra (aromatic region) in 0.1 mol dm$^{-3}$ KCl/$D_2O$ of a) DA b) DA in the presence of Sβ-CD.

Figure 5.29 plots the $\Delta\delta$ of the a-H, b-H and c-H protons of DA as a function of the Sβ-CD molar ratio using a non-linear curve fitting method (Chapter 2), and from this the evaluation of the $K_f$ value for each proton was determined using Equation 5.7 and these constants are presented in Table 5.10. There is very good agreement between the $K_f$ values evaluated for both a-H and b-H protons, while the constant evaluated using c-H is somewhat lower. This is probably connected to the small variations in the chemical shifts observed for the c-H proton.

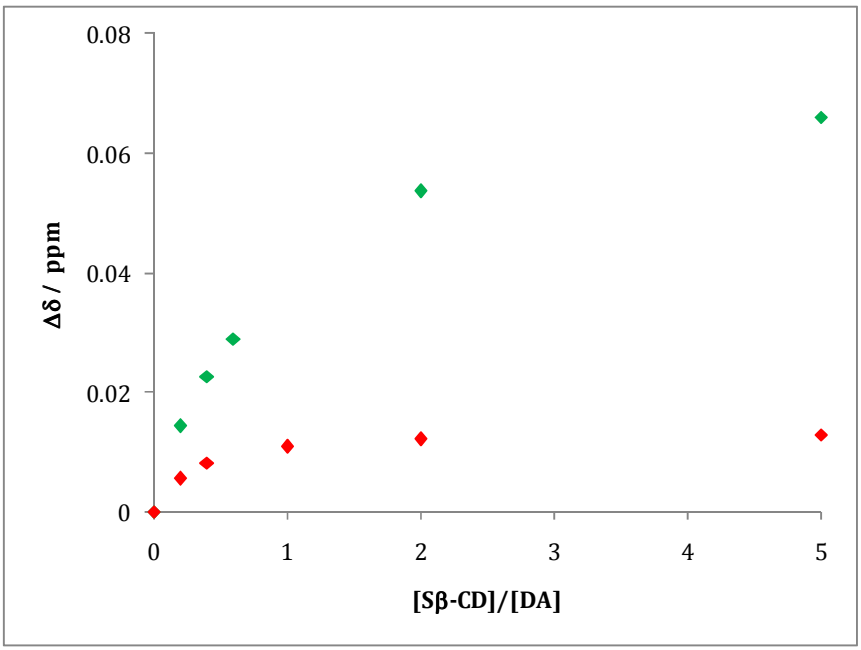


**Figure 5.29:** Difference in the observed chemical shift in the absence and presence of Sβ-CD for each of the DA aromatic protons. ♦a-H ♦b-H.

**Table 5.10:** Stability constants, $K_f$, of DA-Sβ-CD complex evaluated using the non-linear curve data for the NMR technique.

| Proton | Stability constant, $K_f$ |
|---|---|
| **Ha** | 384.48 |
| **Hb** | 394.39 |

Table 5.11 gives the results obtained for the stability constant of DA in the presence of Sβ-CD using the techniques outlined in this chapter. The NMR data for DA are thus in good agreement with UV, CV and RDV results and confirm inclusion of the aromatic ring of DA within the cavity of the Sβ-CD molecule.

**Table 5.11:** Stability constants, $K_f$, of DA-Sβ-CD complex evaluated using UV, CV, RDV and NMR.

| Formation constants of DA and Sβ-CD pH~6 | | | |
|---|---|---|---|
| $K_f$ by UV spectra | $K_f$ by CV | $K_f$ by RDV | $K_f$ by NMR |
| 336.92 ± 24.83 | 255.88 ± 7.97 | 331.28 ± 5.85 | 384.48 ± 164.81 |

## 5.3.4 Factors that influence DA-Sβ-CD Complexation

In addition to the geometry of the inclusion complex, the driving forces leading to the complexation are also of importance. The interactions between charged cyclodextrins and guest molecules are still very much absent in the literature.[46] For this reason it is difficult to establish what specific interactions are involved in complexation, with charged cyclodextrins. Nevertheless, some potential factors involved are discussed in this section, including electrostatic interaction, the influence of supporting electrolyte and cavity size of the host.

### *5.3.4.1 Influence of pH*

In terms of electrostatic interaction, three types are of most importance, i.e. ion-ion interaction, ion-dipole interaction, and dipole-dipole interaction.[47] The aim of this study was to alter the charge on the DA molecule, by varying the pH of the solution between a pH of 1.4 and 6.0 and then to determine the influence of the charge of DA (level of protonation) on the magnitude of the complexation constant. Unfortunately, higher pH values could not be employed, as it was too difficult to prevent the oxidation of DA, which is well known to be unstable in the presence of oxygen at higher pH values.[35-37]

In addition to the charged DA guest, the sulfonate groups on the Sβ-CD are also ionised. Although sulfonated groups tend to be fully ionised (sulfonic acids are considered strong acids, with dissociation constants of about $10^{-2}$) [48] an experiment was designed to establish if significant changes in pH would alter

the charge on the Sβ-CD. This involved an acid-base titration which served to give rise to variations in the pH of the solution, while simultaneous measurements on the conductivity of the solution gave an indication of the number of charged species. Figure 5.30 shows the conductivity as a function of pH for the Sβ-CD initially dissolved in a NaOH solution (to give a pH of approximately 12.0). The conductivity is also plotted for an equivalent concentration of NaOH, but in the absence of the Sβ-CD. The conductivity of the Sβ-CD containing NaOH solution is much higher than the pure NaOH solution, which clearly shows that the Sβ-CD is contributing to the conductivity measured. Indeed, the conductivity of the Sβ-CD is high, similar to that of a 0.020 mol $dm^{-3}$ NaOH solution, indicating a very high degree of dissociation of the sulfonated groups. By comparing the difference between the conductivity of the NaOH and the NaOH solution containing the Sβ-CD, it is clear that the Sβ-CD contributes a near constant conductivity to the solution, over the entire pH range from 3.0 to about 11.0, confirming that the extent of dissociation is not affected by the pH of the solution.

In order to study the complexation between DA and the Sβ-CD as a function of pH, both UV and CV methods were employed. For the spectrophotometric data the measurements were performed at three pH values, pH 6.0, 3.0 and 1.4. As discussed previously in Section 5.3.2.1, increasing the concentrations of Sβ-CD gave rise to a shift in the $\lambda_{max}$ from 280 to 283 nm. An overall increase in the intensity was observed as an excess of Sβ-CD, was added but a decrease in absorbance intensity at 280 nm was observed. Based on the variation in the absorbance at $\lambda_{max}$ = 280 nm, the formation constant ($K_f$) of the inclusion complex was evaluated using the Heildebrand-Benesi relationship, Equation 5.1. The formation constant was determined for the complex based on the absorbance changes, ΔA. ΔA values were computed using Equation 5.10 and then $A_0/\Delta A$ was plotted as a function of 1/[Sβ-CD], as demonstrated in Figure 5.31. The plot shows a good linear relationship for all of the experimental data. Correlation coefficients of 0.997, 0.997and 0.992 were obtained for pH values of 6.0, 3.0 and 1.4, respectively.

The formation constants were determined from the slope and the intercept of the straight line plots, in Figure 5.31 in association with Equation 5.1. The formation constants evaluated for each pH studied are correlated in Table 5.12. From these data the formation constants show little variation at different pH values. It is noted that the constants of the DA-Sβ-CD complex are somewhat stronger in acidic media, than in more neutral media in the citrate-phosphate buffer system.

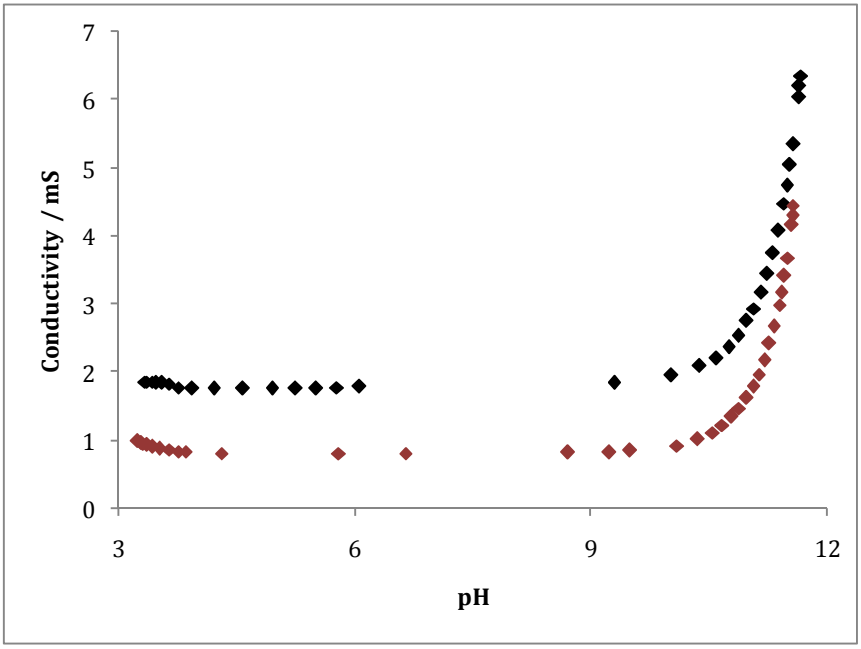


**Figure 5.30:** Conductivity as a function of pH for a solution of 0.020 mol $dm^{-3}$ NaOH in the absence ♦ and presence ♦ of 0.005 mol $dm^{-3}$ Sβ-CD.

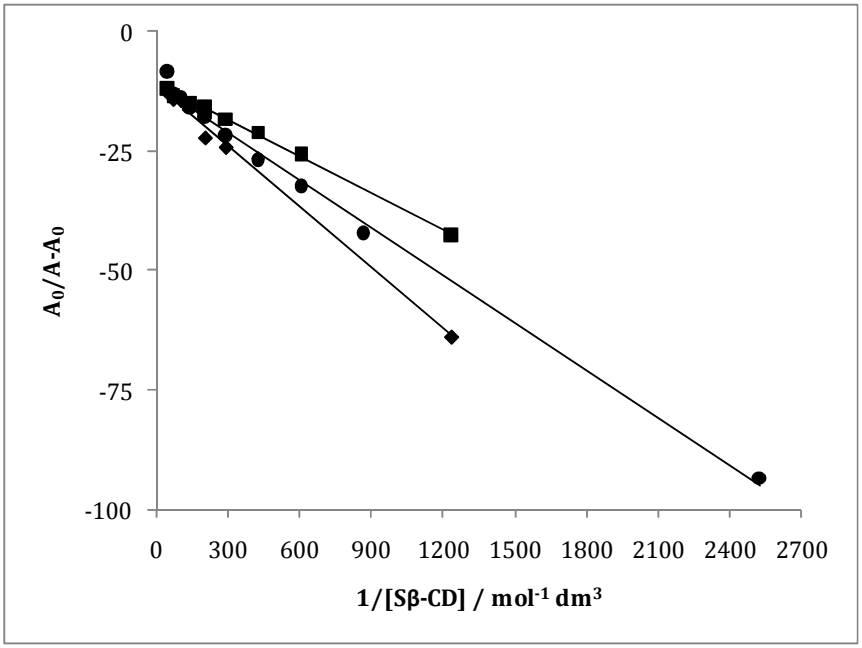


**Figure 5.31:** Linear relationship of $A_0/A\text{-}A_0$ as a function of 1/[Sβ-CD] for 5.0 x $10^{-4}$ mol $dm^{-3}$ DA in the presence of varying concentrations of Sβ-CD at the following pH values, ♦pH=1.4 in $H_2SO_4$ and ■pH=3.0 •pH=6.0 in citrate phosphate buffers.

**Table 5.12:** Stability constants for the inclusion complex formed at the various pH values obtained from UV spectroscopy.

| pH | Stability Constant, $K_f$ | $R^2$ |
|---|---|---|
| 1.4 | 261.87 ± 28.61 | 0.992 |
| 3.0 | 452.68 ± 12.45 | 0.997 |
| 6.0 | 336.93 ± 24.82 | 0.993 |

The ratio of DA in the neutral and protonated states can be obtained by considering the Henderson Hasselbalch equation given below and using $HA^+$ to represent the protonated DA and A to indicate the neutral form ($HA^+ \rightleftharpoons H^+ + A$).

$$pH = pK_a + log\frac{[A]}{[HA^+]}$$

This relationship can be arranged to give Equation 5.13, providing the ratio of the neutral to the protonated DA in terms of the pH and p*K*a value of DA, which is 8.9.

$$10^{pH-pKa} = \frac{[A]}{[HA^+]} \qquad 5.13$$

Using this relationship, the ratio of protonated DA to the neutral DA can be computed as 3 x $10^7$, 7 x $10^5$ and 7 x $10^3$ at pH values of 1.4, 3.0 and 6.0, respectively, indicating a slightly higher proportion of neutral DA molecules at pH 6.0 compared to pH 3.0, which may be connected to the increase in the $K_f$ value as the pH is varied from 6.0 to 3.0, Table 5.12.

The pH study was also investigated using CV. It is well documented that the peak potential, $E_p$, is dependent on pH and decreases with increasing pH.[17, 49, 50] Figure 5.32 shows a plot of the oxidation peak, $E_p$, of DA as a function of pH. Both citrate-phosphate buffer solutions for the range of pH 2.0 - 7.0 and $H_2SO_4$ for lower pH solutions were used to prepare the solutions. These results show that the DA is becoming harder to oxidise at lower pH values. This pH dependence indicates that protons are directly involved in the rate-determining step for the oxidation of DA. The equation relating peak potential with pH, over the pH range 3.1 to 7.0, is $E_p$ = 0.536 – 0.037 pH. The slope value of 37 mV is consistent with the overall reaction being a two-electron and two proton process.

Complexation studies using CV were performed at various pH values using solutions of 5.00 x $10^{-4}$ mol $dm^{-3}$ DA in the presence of increasing amounts of Sβ-CD. The change in the peak oxidation potential of DA as a function of the pH for DA in the absence and presence of a large excess of Sβ-CD, 2.00 x $10^{-2}$ mol $dm^{-3}$, was obtained and is expressed in Figure 5.33. From these results it is seen that the potential difference between DA and DA in the presence of Sβ-CD increases as the pH increases. There is a significant difference between pH values close to 1.4 and those in the range 3.0 to 6.0. However, this may be due to the presence of different anions in the two solutions. As detailed in Section

5.2.1.3 sulfate anions are used in the preparation of the solutions at a pH of 1.4, while the citrate/phosphate anions are present at pH values between 3.0 and 6.0. This will be discussed later in Section 5.3.4.2.

Using Equation 5.2, the stability constants, $K_f$ were evaluated as a function of pH and are shown in Table 5.13 and plotted in Figure 5.34. There is a significant increase in the $K_f$ value as the pH is increased from 1.4 to 3.0. This is consistent with the small shift in the peak potential observed at a pH of 1.4, compared to that obtained at a pH of 3.0, Figure 5.33. These data are also in good agreement with the spectroscopic measurements, Table 5.12, and show a decrease in the magnitude of $K_f$ as the pH is increased from 3.20 to 6.06.

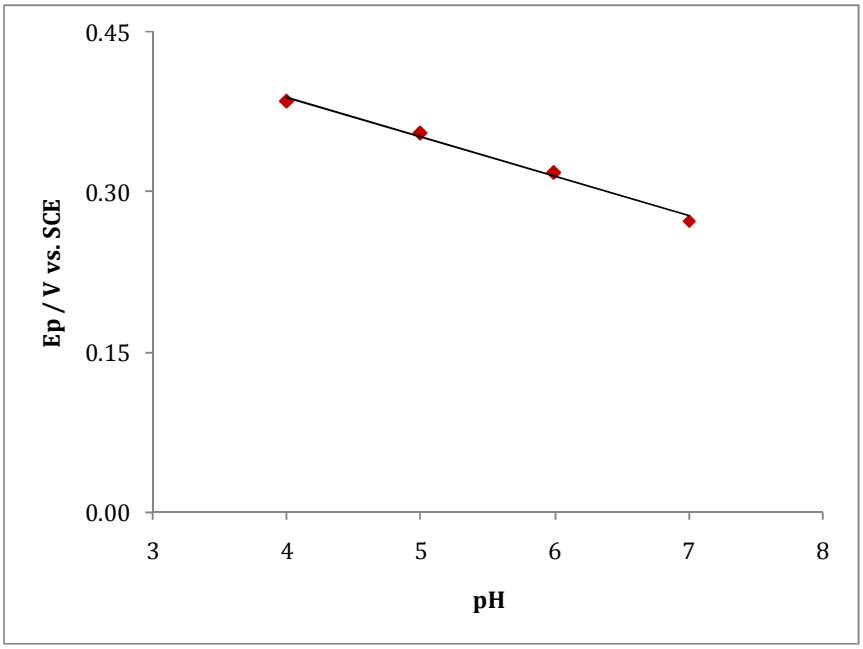


**Figure 5.32:** The peak oxidation potential of 5.00 x $10^{-4}$ mol $dm^{-3}$ DA as a function of pH. Potential was swept from -0.250 to 0.800 V vs. SCE at 50 mV $s^{-1}$.

Nevertheless, there is less agreement between the potential shifts observed in Figure 5.33 and the computed $K_f$ values shown in Table 5.12 and Figure 5.34 at higher pH values. There is a small increase in the $\Delta E_p$ values with increasing pH from 3.0 to 6.0 in Figure 5.33, However there is a decrease in the magnitude of

$K_f$ as the solution is brought to higher pH values, as shown in Table 5.13. This may be connected to the manner in which the stability constants were calculated; only the peak currents and Equation 5.2 was used to calculate the $K_f$ value.

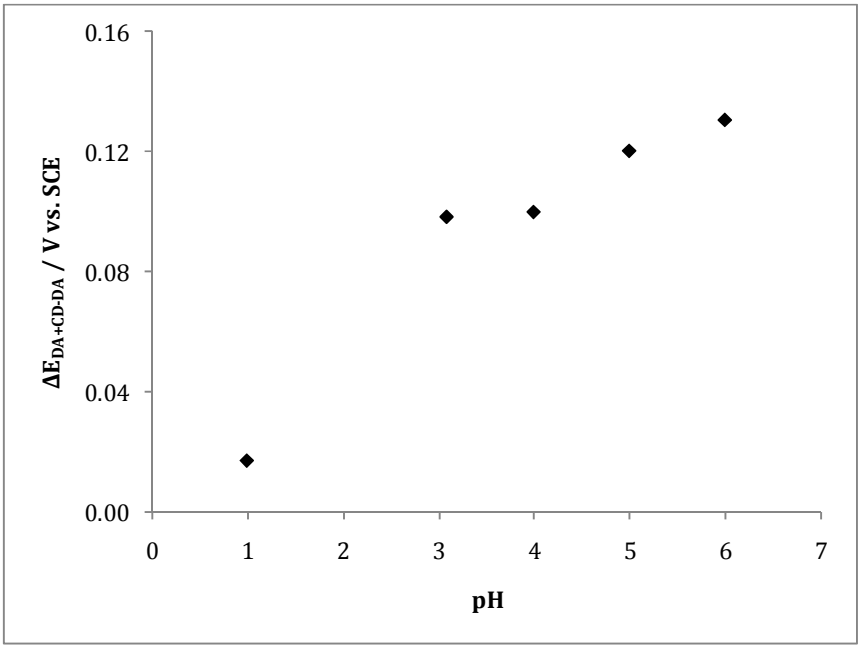


**Figure 5.33:** The change in the oxidation peak potential, $\Delta E_p$ of 5.00 x $10^{-4}$ mol $dm^{-3}$ DA in the absence and presence of 2.0 x $10^{-2}$ mol $dm^{-3}$ Sβ-CD as a function of pH. Potential was swept from -0.250 to 0.800 V vs. SCE at 50 mV $s^{-1}$.

**Table 5.13:** Stability constants for the inclusion complex formed at the various pH values. Data were obtained from CV measurements.

| pH | Stability constant, $K_f$ |
|---|---|
| 1.36 | 372.62 ± 32.52 |
| 3.20 | 673.84 ± 12.64 |
| 4.01 | 489.99 ± 140.50 |
| 5.01 | 238.57 ± 278.47 |
| 6.06 | 255.88 ± 7.97 |

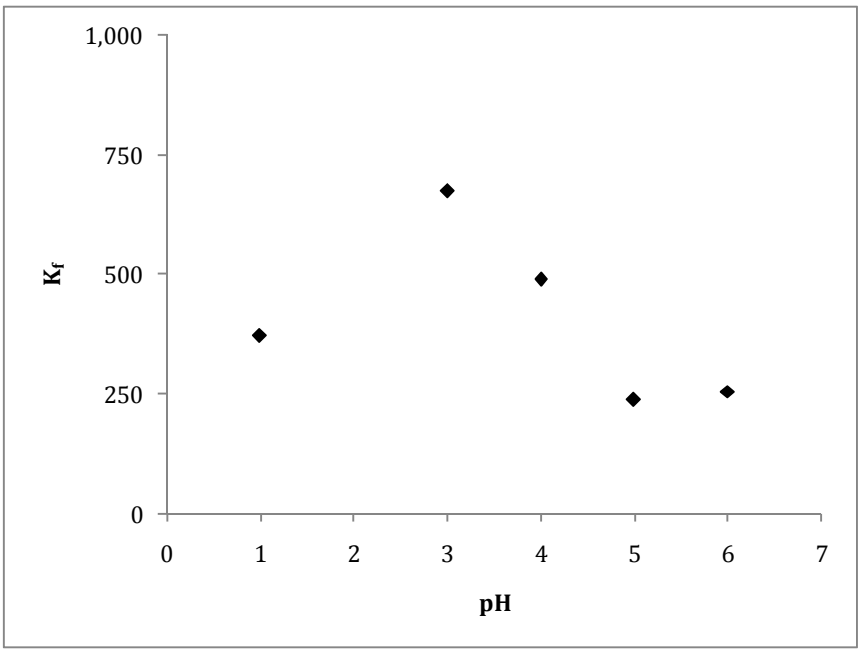


**Figure 5.34:** Stability constants obtained for the DA-Sβ-CD complex using 5.00 x $10^{-4}$ mol $dm^{-3}$ DA in the presence of varying concentrations of Sβ-CD as a function of pH.

These findings are in good agreement with other investigations which have been carried out with charged guests. For example, Li *et al.*[51] suggest that the relief of conformational strain and electrostatic forces are the main driving forces for complexation. Rajewski and co-workers[52, 53] investigated the role of charge by comparing the binding of neutral and charged cyclodextrins with neutral and charged guests. They found that in the case of complexing with neutral species that the negatively charged sulfobutyl ether β-CD had a higher binding affinity than neutral β-CD. In the case of a protonated species, papaverine, the binding constant was evaluated in the presence of the neutral β-CD and the negatively charged β-CD and values of 10 and 570 were obtained, respectively. They found the presence of charge on the cyclodextrin gave a further site of interaction for the guest molecule in comparison to the neutral cyclodextrin. However, they also stated that the complexation of the negatively charged CD, sulfobutyl ether β-CD, with the positively charged species is highly dependent on the solution electrolyte concentration which is important in the

charge interactions of the complex. Indeed, this is consistent with the variations observed between the sulfate and the citrate/phosphate systems described here. It appears from the stability constants that the citrate/phosphate species promote the formation of the inclusion complex.

These results are also in very good agreement with Zia *et al.*[52] who stated that as the positive charge is increased it has an encouraging effect on the binding constants. Wenz *et al.*[46] also stated that the orientation of the guest inside the cavity is influenced by interactions with functional groups on the cyclodextrin. In view of Wenz's statement it could be said that because of the presence of the positive and negative charges the interaction between the two components could have some affect on the geometrical factors of the complex. As shown in Section 5.3.3, the aromatic ring of the DA was inside the cavity while the protonated amine group was predicted to remain outside the cavity. This orientation may differ slightly once the pH ranges from 1.4 to 6.0, but it is likely that the polar amine group will remain outside the cavity and bind electrostatically with the anionic sulfonated groups.

### *5.3.4.2 Influence of counter ions*

Although the variation of the stability constant with pH, Table 5.13, is in agreement with charge considerations, there is a significant difference between the stability constants at pH 1.4 and 3.0, which cannot be explained fully in terms of charge. The fraction of DA molecules in the neutral state at pH 1.4 and 3.0 can be estimated using the analysis presented in Equations 5.14 to 5.16. The degree of dissociation, α, can be represented in accordance with Equation 5.14.

$$\begin{array}{ccccc} HA^+ & \rightleftharpoons & A & + & H^+ \\ (1-\alpha) & \rightleftharpoons & \alpha & + & \alpha \end{array} \qquad 5.14$$

Accordingly, α can be expressed in terms of both the pH and p*K*a values, as shown in Equations 5.15 to 5.17, and finally the % ionisation can be expressed in terms of Equation 5.18.

$$\frac{\alpha}{1-\alpha} = \frac{[A]}{[HA^+]} = 10^{pH-pKa} \quad 5.15$$

$$\frac{1}{\alpha} - \frac{\alpha}{\alpha} = 10^{pKa-pH} \quad 5.16$$

$$\alpha = \frac{1}{1+10^{pKa-pH}} \quad 5.17$$

$$\%\ ionised = \frac{100}{1+10^{pKa-pH}} \quad 5.18$$

Using this analysis, the % of non-ionised, protonated DA molecules is close to 100% both at pH 1.4 and 3.0. As the supporting electrolyte is different in the pH 1.4 and 3.0 studies, this may point to an influence of the counter ions. Accordingly, experiments were carried out to establish if the sulfate and citrate anions had any role to play in the complexation of DA with the Sβ-CD. In addition, the influence of cations was investigated by using chloride salts of sodium, ammonium, potassium and calcium. The ammonium cation was selected as the $NH_4^+$ can be related to the protonated DA and may compete with the electrostatic interactions between protonated DA and the sulfonated groups on the Sβ-CD.

The presence of a supporting electrolyte in solution could alter the interaction between the host and guest. A change in the activity coefficient of ions could influence the equilibrium constants and therefore the ability to generate an inclusion complex.[15] In solution, ions can vary the dielectric constant and the water activity; in the case of charged molecules like DA, ions can also be directly involved in the formation of non-covalent bindings.[54]

CV experiments of 5.00 x $10^{-4}$ mol $dm^{-3}$ DA were carried out in the absence and presence of 2.00 x $10^{-2}$ mol $dm^{-3}$ Sβ-CD in each supporting electrolyte. The pH

was maintained in the range of 4.96 to 5.10. Regarding the influence of the cations, the anion was kept constant; only chloride salts were used. Figure 5.35 shows the CV data obtained for the oxidation of DA in each supporting electrolyte; 0.20 mol $dm^{-3}$ solutions of NaCl, KCl, $CaCl_2$ and $NH_4Cl$. In the case of these supporting electrolytes upon the addition of an excess of Sβ-CD a substantial shift in the peak current of the DA oxidation was noticed. A summary of the peak current and the peak potential ratios obtained for DA in the absence and presence of Sβ-CD are specified in Table 5.14. As can be seen no significant difference was observed. This clearly shows that the cations, $Na^+$, $K^+$, $Ca^{2+}$ and $NH_4^+$ exert no influence on the complexation between DA and the Sβ-CD.

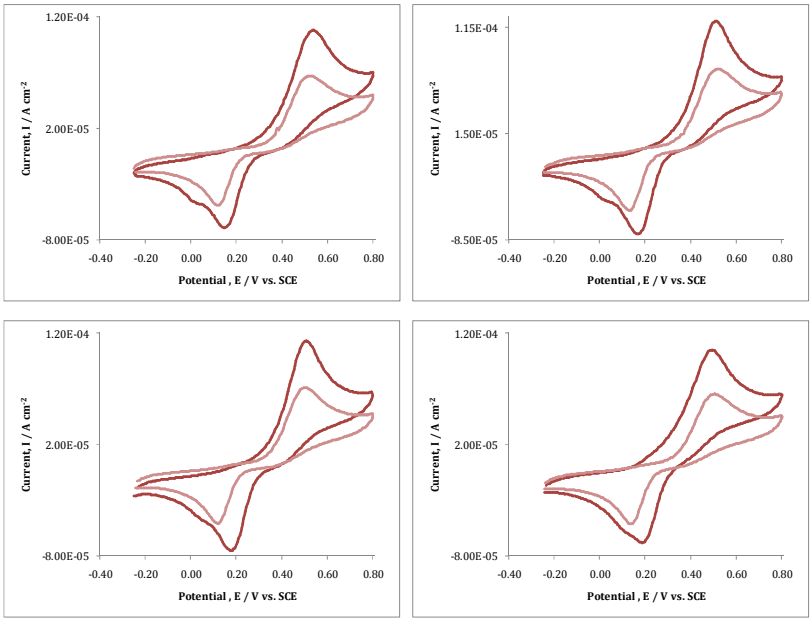


**Figure 5.35:** Cyclic voltammograms of 5.00 x $10^{-4}$ mol $dm^{-3}$ DA in the ♦absence and ♦presence of 0.02 mol dm-3 of Sβ-CD and 0.20 mol $dm^{-3}$ supporting electrolyte. A. NaCl. B. KCl C. $CaCl_2$. D. $NH_4Cl$. Potential was swept -0.250 to 0.800 V vs. SCE at 50 mV $s^{-1}$ using a GC electrode.

**Table 5.14:** A summary of the data obtained for the CV in 5.00 x $10^{-4}$ mol $dm^{-3}$ DA in the absence and presence of 2.00 x $10^{-2}$ mol $dm^{-3}$ Sβ-CD with each supporting electrolyte.

| **Cation 0.20 mol $dm^{-3}$** | **$i_p$ (DA)/ $i_p$ (DA+Sβ-CD)** | **$E_p$ (DA)/ $E_p$(DA+Sβ-CD)** |
|---|---|---|
| NaCl | 1.610 | 1.023 |
| KCl | 1.591 | 0.995 |
| $CaCl_2$ | 1.593 | 1.012 |
| $NH_4Cl$ | 1.611 | 0.968 |

However, it is well known that the composition of the electrolyte can influence the manner in which an electroactive species is oxidised or reduced. For example, Wang *et al.*[55] in investigating the effect of supporting electrolytes found that in one particular buffer, the reduction peak of the molecule being detected showed a more clear and sensitive peak. As the data obtained with the citrate/phosphate buffer and the sulfate electrolyte cannot be explained in terms of pH alone, additional experiments were carried out in an attempt to obtain information on the role of the anions.

CV experiments were carried in a similar manner as described above to investigate the influence of the anions. The supporting electrolytes were sodium chloride, sodium sulfate and citrate-phosphate buffer. The data obtained are summarised in Table 5.15. It can be clearly seen that there is a significant change in the peak current ratios as well as the peak potential ratios. This clearly shows that the anions do have a significant influence on the degree of complexation between DA and the Sβ-CD.

**Table 5.15:** A summary of the data obtained for the CV of 5.00 x $10^{-4}$ mol $dm^{-3}$ DA in the absence and presence of 2.00 x $10^{-2}$ mol $dm^{-3}$ Sβ-CD with each supporting electrolyte.

| **Anion 0.2 mol $dm^{-3}$** | **$i_p$ (DA)/ $i_p$ (DA+Sβ-CD)** | **$E_p$ (DA)/ $E_p$ (DA+Sβ-CD)** |
|---|---|---|
| NaCl | 1.610 | 1.023 |
| $Na_2SO_4$ | 1.773 | 0.834 |
| Citrate phosphate | 1.915 | 0.747 |

Firstly, it was thought that the ionic strength may have a major influence on the complexation. The ionic strength of each solution was computed using Equation 5.19, where $c_A$ is the molar concentration of ion A (mol $dm^{-3}$), $z_A$ is the charge number of that ion, and the sum is taken over all ions in the solution.

$$I_c = \frac{1}{2}\Sigma c_A z_A^2 \qquad 5.19$$

It was found that the ionic strength varied in the order: citrate/phosphate > $Na_2SO_4$ > NaCl. So in order to investigate if it was indeed ionic strength that influenced the degree of complexation, NaCl solutions were prepared at various ionic strengths to match the corresponding ionic strength of the other anions and the CV experiments were repeated. These data are summarised in Table 5.16. While ionic strength is clearly important in electrochemistry, it can be seen that ionic strength has no influence on the complexation of DA in the presence of Sβ-CD when the ionic strength is varied between 0.2 and 0.9 mol $dm^{-3}$.

The only other explanation for this phenomenon is that the anion has an influence. Therefore, additional CV experiments with the sodium chloride, sodium sulfate and the two components of the citrate phosphate buffer, sodium citrate and sodium phosphate, individually prepared at a concentration of 0.2 mol $dm^{-3}$ solution, were completed. In each case the oxidation of DA, at a

concentration of 5.00 x $10^{-4}$ mol $dm^{-3}$, was followed in the absence and presence of 2.00 x $10^{-2}$ mol $dm^{-3}$ Sβ-CD.

**Table 5.16:** A summary of the data obtained for the CV of 5.00 x $10^{-4}$ mol $dm^{-3}$ DA in the absence and presence of 2.00 x $10^{-2}$ mol $dm^{-3}$ Sβ-CD in NaCl where the ionic strength was varied.

| **NaCl Ionic strength/ mol $dm^{-3}$** | **$i_p$ (DA)/ $i_p$ (DA+Sβ-CD)** | **$E_p$ (DA)/ $E_p$ (DA+Sβ-CD)** |
|---|---|---|
| **0.2** | 1.61 | 1.02 |
| **0.3** | 1.56 | 1.05 |
| **0.9** | 1.48 | 1.06 |

After analysing the CV data of DA it was observed that in the absence of Sβ-CD the anion contributing to each supporting electrolyte had an influence on the oxidation potential of DA. Figure 5.36 shows the redox peak potential of 5.00 x $10^{-4}$ mol $dm^{-3}$ DA in 0.20 mol $dm^{-3}$ of each supporting electrolyte, at the bare GC electrode. This figure indicates that the electrochemical oxidation of DA was more strongly suppressed when NaCl was used as a supporting electrolyte than in the case where sodium phosphate, sulfate or citrate were used. The peak oxidation potential shifted to higher potentials in the following order: NaCl > $Na_2SO_4$ > $Na_2H(C_3H_5O(COO)_3)$ > $Na_2HPO_4$. These results are shown in Table 5.17, and indicate that the presence of the larger anionic groups in the phosphate and citrate media promote the electrochemical oxidation of DA.

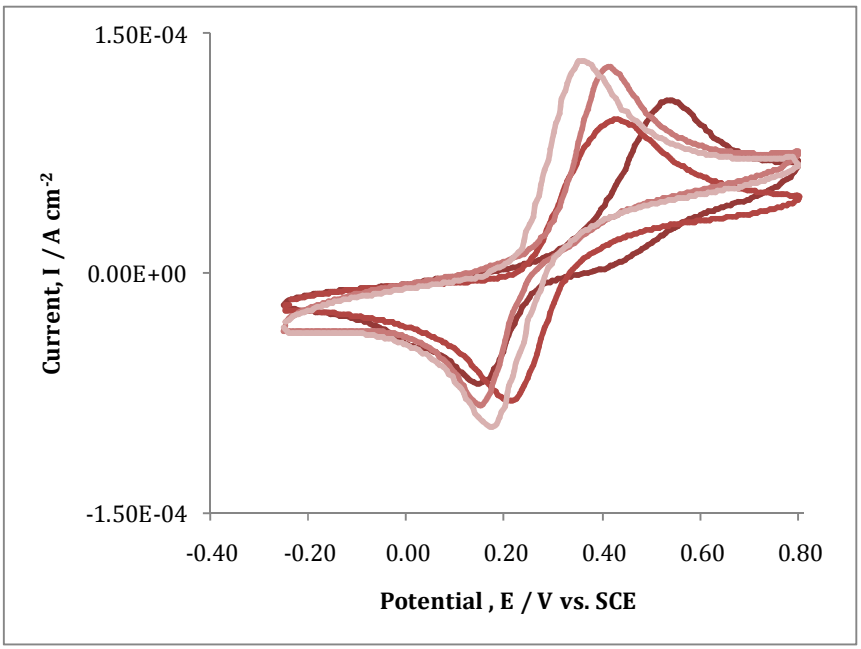


**Figure 5.36:** Cyclic voltammograms of 5.00 x $10^{-4}$ mol $dm^{-3}$ DA in 0.20 mol $dm^{-3}$ NaCl $Na_2SO_4$ $Na_2H(C_3H_5O(COO)_3)$ $Na_2HPO_4$. Potential was swept -0.250 to 0.800 V vs. SCE at 50 mV $s^{-1}$ using a GC electrode.

These observations can be explained in terms of the size and polarisability of the anions. The small chloride anions have a stronger electrostatic binding with the protonated DA, making it more difficult to oxidise the DA molecule. The larger more diffuse anions, where the negative charge can be delocalised, have a lower attraction for the protonated DA, enabling the oxidation of DA at a slightly lower potential. This analysis can also be used to explain the more efficient formation of the inclusion complex in the citrate/phosphate media, as evident from Figure 5.34. The equilibrium between the free DA and the DA included within the cavity of the Sβ-CD, is shown below.

$$DA + S\beta\text{-}CD \rightleftharpoons DA\text{-}S\beta\text{-}CD$$

It is well known from the literature that the main driving force for complex formation (and a shift in the equilibrium to favour the complex), is the

displacement of water molecules from the cavity by more hydrophobic guest molecules, assuming that there is a fit between the size of the guest and the cavity of the cyclodextrin[1, 46, 56, 57]. The energetically favourable interactions are the displacement of the polar water molecules from the hydrophobic cavity. Once outside the cavity, the displaced water forms hydrogen bonds with the neighbouring water molecules. On the other hand, the repulsive interactions between the guest and the aqueous environment are reduced as the guest enters the cavity. Accordingly, in the presence of the chloride and sulfate ($SO_4^{2-}$ and $HSO_4^-$) anions, the DA is stabilised in the solution and the equilibrium lies to the left in favour of the un-complexed species. In contrast, the larger citrate/phosphate species have a lower stabilisation effect on the protonated DA and it is now the formation of the complex that is more energetically favoured. This in turn leads to slightly higher stability constants in the phosphate/citrate buffer compared to that obtained with the sulfate anions as the supporting electrolyte.

**Table 5.17:** A summary of the data obtained for the CV of 5.00 x $10^{-4}$ mol $dm^{-3}$ DA only in the presence of each supporting electrolyte.

| **Anion / 0.2 mol $dm^{-3}$** | **$i_p$ DA / A $cm^{-2}$** | **$E_p$ DA / V vs. SCE** |
|---|---|---|
| $Na_2HPO_4$ | 1.329 x $10^{-4}$ | 0.368 |
| $[C(OH)(CH_2CO_2)_2(CO_2)]$ | 1.287 x $10^{-4}$ | 0.411 |
| $Na_2SO_4$ | 1.075 x $10^{-4}$ | 0.475 |
| NaCl | 1.086 x $10^{-4}$ | 0.524 |

### *5.3.4.3 Varying the size of the Cavity*

An investigation into the complexation of DA with Sα-CD was also carried out. As previously discussed in Chapter 1, the α-CD has similar complexing properties to the β-CD. One of the major characteristic differences between the two cyclodextrins is the number of glucose rings which affects the diameter of the cavity; the diameter of the α-CD is smaller than the β-CD cavity, as it only contains 6 glucose rings where as the β-CD has 7 rings. Connors *et al.*[1] reported that cavity size was an important parameter in complexation. Therefore, in this study the Sα-CD was selected to explore the influence of the size of the cavity.

Using CV, the complexation between DA and Sα-CD was investigated. The DA concentration was kept constant at 5.00 x $10^{-4}$ mol $dm^{-3}$ and using a citrate phosphate buffer, the pH was maintained at 5.0. The Sα-CD concentrations were varied from 2.00 x $10^{-2}$ mol $dm^{-3}$ to 3.12 x $10^{-4}$ mol $dm^{-3}$. The results obtained are shown in Figure 5.37. There is little evidence of any change in the voltammograms on the addition of the Sα-CD. The anodic peak potentials of DA in the absence and presence of 2.00 x $10^{-2}$ mol $dm^{-3}$ of Sα-CD were 0.441 V vs. SCE and 0.448 V vs. SCE, respectively. Also, peak currents of 8.25 x $10^{-5}$ and 8.52 x $10^{-5}$ A $cm^{-2}$, in the absence and presence of 2.00 x $10^{-2}$ mol $dm^{-3}$ Sα-CD are similar. These results are very different to those presented in Section 5.3.1.2, where a shift in the peak potentials and a decrease in the peak currents were observed when Sβ-CD was added to the DA solution. These shifts were attributed to complexation. The results obtained here in the presence of Sα-CD suggest that no complexation has transpired. If little or no complexation is occurring in the case of the Sα-CD it can only be assumed that this is due to the difference in the diameter of the cavities of the α and β sulfonated CDs.

The approximate diameters of both the neutral α- and β- CD cavities are shown in Figure 5.38.[56, 58, 59] Wang *et al.*[60] have reported that the sulfonated β-cyclodextrin and other derivatised cyclodextrins have the same ring structure, as β-cyclodextrin. The only difference between them is the substituents on the rim of the cyclodextrin ring. Due to this statement we can assume that the

diameters of the cavities with and without the sulfonated groups are approximately the same.

It is also noted that the diameter decreases in width from the secondary hydroxyl rim to the primary rim.[1] In order to investigate if in fact the DA is structurally able to fit inside the α-CD cavity, the diameter of DA was first calculated using a Quantum mechanical calculation using density functional theory (DFT). This method considers the electron density at a point and optimises the geometry from which the diameter can be calculated. Illustrations of both the face and side geometry of DA are shown in Figure 5.39. The total diameter is taken from the O-H group on the aromatic ring to the hydrogen on the nitrogen atom, as illustrated in the figure. A total diameter of 8.95 Å was obtained.

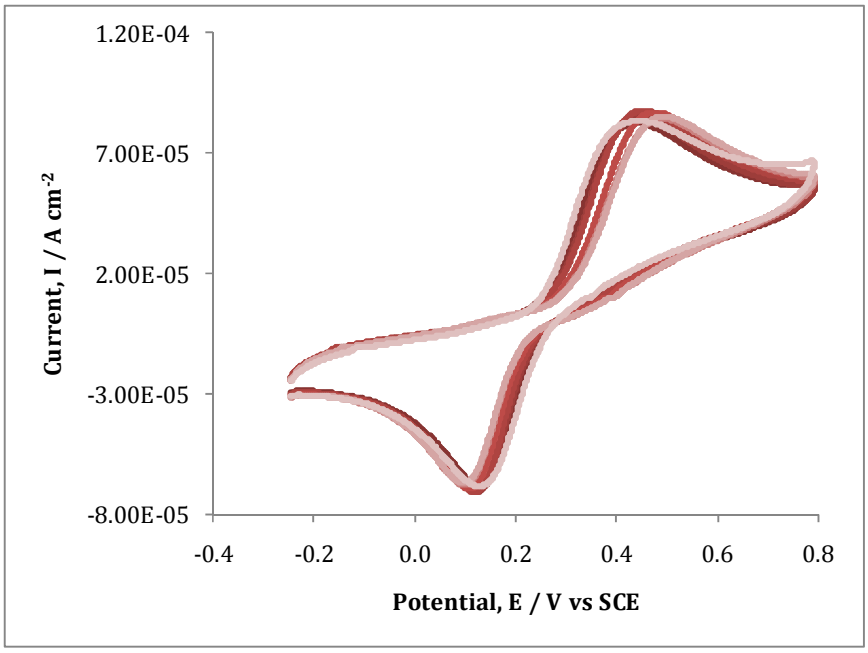


**Figure 5.37:** Cyclic voltammograms of DA (5.00 x $10^{-4}$ mol $dm^{-3}$) in the absence and presence of varying amounts of Sα-CD at pH=5.0 in a citrate-phosphate buffer. The potential was swept from -0.250 to 0.800 V vs. SCE at 50 mV $s^{-1}$.

It is also interesting to note the orientation of the $NH_2$ group in the molecule. The bulk of the molecule is planar except for the amine group which extends out almost perpendicular to the rest of the molecule. This orientation could bare some connotations to the complexation in the CD cavity. From the models shown, the diameter of DA was evaluated to be approximately 9.0 Å. Therefore, it would not be possible for the DA to completely fit inside either cavity; as the diameter of the α and β-CD cavities are 4.9 and 6.2 Å, respectively. The width of the aromatic ring with the hydroxyl groups was calculated to be ~ 6.05 Å, as shown in Figure 5.39.

Based on this analysis it is clear that DA cannot form an inclusion complex with Sα-CD due to the fact that the diameter of the Sα-CD is not sufficiently large for the DA to fit inside the cavity. It is this reason why there is little or no complexation observed in the electrochemical studies between DA and Sα-CD. It has been reported that benzene can fully fit inside the α-CD cavity;[1] however in the case of DA, the presence of the hydroxyl groups and the side chain could be inhibiting complexation due to their size.

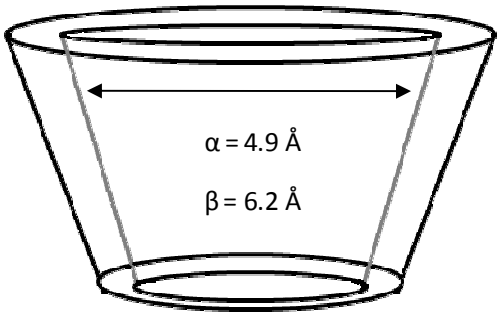


**Figure 5.38:** An illustration of the diameters of the cavity for neutral α and β CDs.

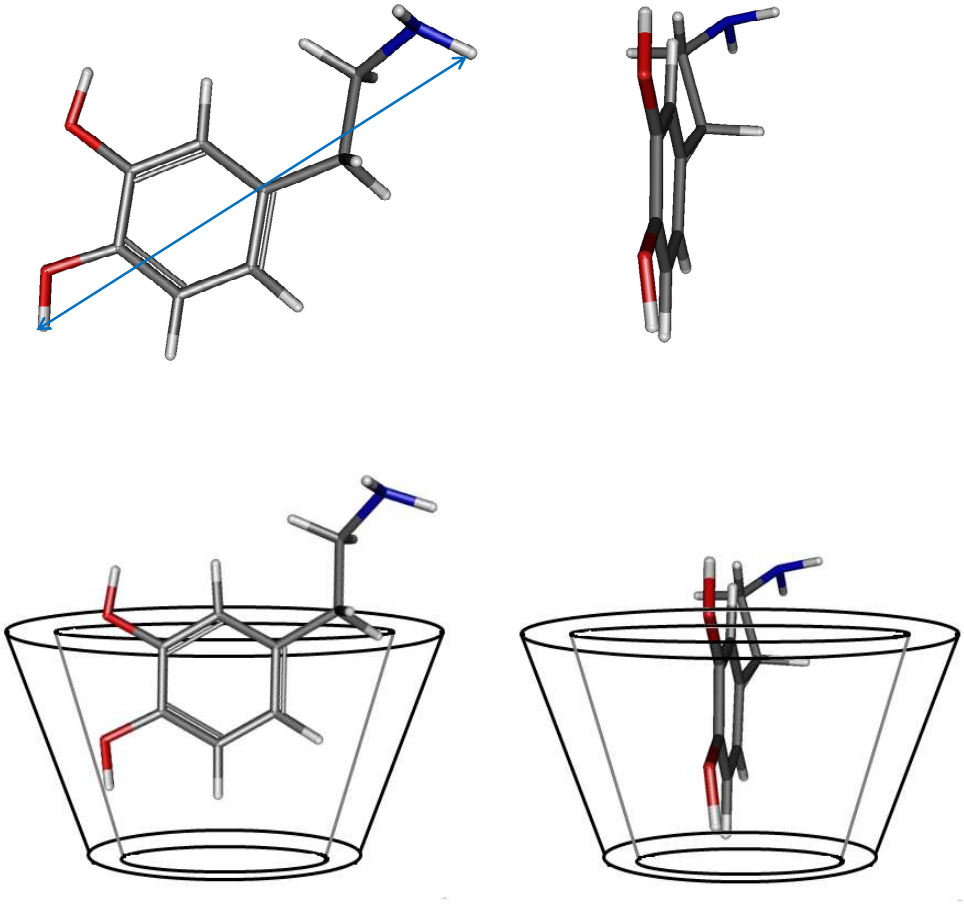

**Figure 5.39:** Illustration of the DA molecule and its orientation using DFT. The intermolecular distances from the furthest points are shown. Also shown is the proposed geometry of DA inside the Sβ-CD cavity.

For the Sβ-CD, the cavity is just the right diameter to fit the aromatic ring only and this consolidates the NMR results presented in Section 5.3.3. This proposed structure can also support the electrostatic interactions discussed in Section 5.3.4.1 where the protonated amine group is interacting with the negatively charged sulfonate groups on the secondary rim of the cyclodextrin. It has been previously reported that the β-CD is more suitable for the complexation of guests than the α-CD due to the size of the cavity. Terekhova *et al.*[61] found that the formation constants for the complexation of aminobenzoic acid (ABA), with α-CD and β-CD differed due to the ABA guest entering the cavities at different depths.

## 5.3.5 Complexation studies of a related structure to DA

### *5.3.5.1 Levodopa*

There are various molecules related to the DA structure. One such molecule is Levodopa (L-dopa or 3,4 dihyroxy-L-phenylalanine). Due to its similarity in structure to DA, as seen in Figure 5.40 its complexation with Sβ-CD was investigated using UV.

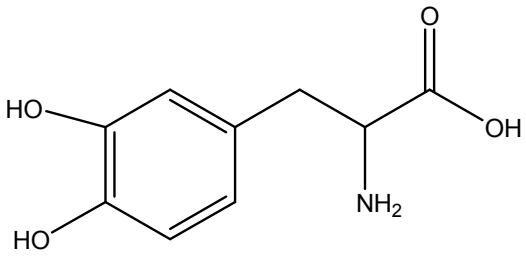


**Figure 5.40:** The chemical structure of Levodopa.

As the pH is changed, the L-dopa characteristics change. An intra-molecular neutralisation reaction leads to a salt-like ion called a zwitterion. At pH < 2.32, the amine group is protonated and the carboxylic group is un-dissociated to generate a positively charged species. At pH > 8.11, the carboxyl group can lose a hydrogen ion to become negatively charged. Figure 5.41 demonstrates this concept, which is characteristic of all amino acids.

p*K*a(COOH) = 2.32 p*K*a($NH_3^+$) = 8.11

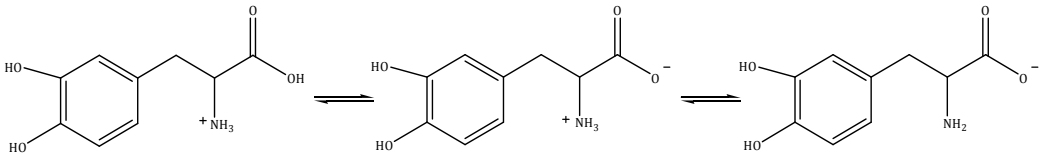

pH < 2.32 2.32 < pH > 8.11 pH > 8.11

Positive charge Negative charge

**Figure 5.41:** Schematic showing the cationic, zwitterionic and anionic forms of levodopa.[62]

It is documented in the literature that L-dopa exists as a zwitterion between pH 2.32 and 8.11.[63] In order to generate the protonated species, pH values less than a pH of 2.32 were used.

Firstly, UV spectra were used to confirm a 1:1 inclusion complex stoichiometry with L-dopa and Sβ-CD. UV spectra of 1.0 x $10^{-4}$ mol $dm^{-3}$ L-dopa and 1.0 x $10^{-4}$ mol $dm^{-3}$ Sβ-CD are shown in Figure 5.42. L-dopa and Sβ-CD have a $\lambda_{max}$ of 280 and 256 nm, respectively. As discussed previously, Section 5.3.1.1, the absorbance from 200 to 260 nm can be attributed to Sβ-CD. Accordingly, all measurements made at 280 nm, to follow the L-dopa inclusion events, were corrected by subtracting the absorbance of the corresponding Sβ-CD solution at 280 nm.

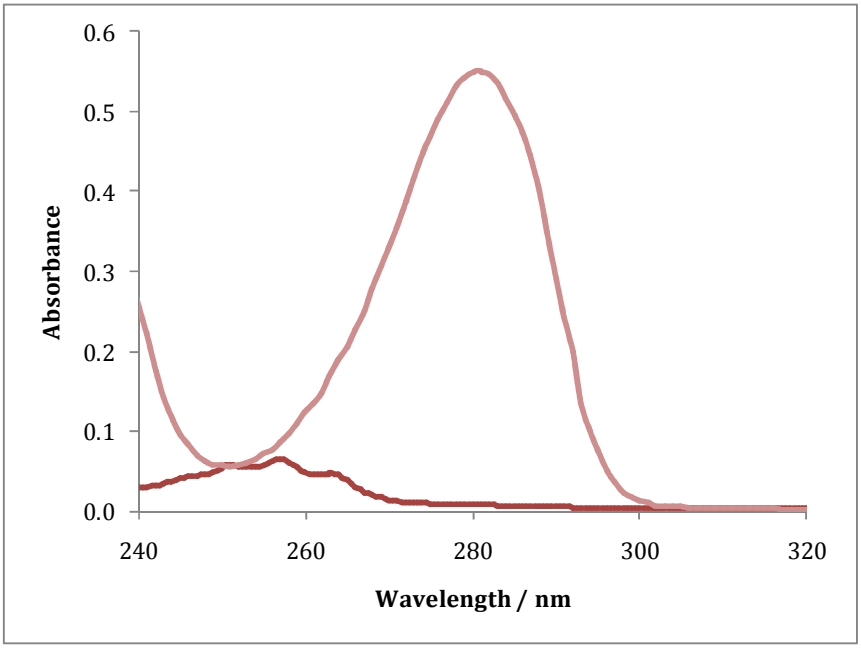


**Figure 5.42:** UV spectra of 1.0 x $10^{-4}$ mol $dm^{-3}$ L-dopa and 1.0 x $10^{-4}$ mol $dm^{-3}$ Sβ-CD.

For this study, the solutions were prepared in a 0.1 mol $dm^{-3}$ $H_2SO_4$ to give a pH of 2.0. Equimolar solutions of 1.0 x $10^{-4}$ mol $dm^{-3}$ sβ-CD and 1.0 x $10^{-4}$ mol $dm^{-3}$ L-dopa were prepared. The UV data were recorded with 11 different solutions, where the mole fraction of L-dopa varied from 0.0 to 1.0, in increments of 0.1. The Job's plot was obtained from the absorbance changes at 280 nm in the mixtures of Sβ-CD and L-dopa. The UV spectrum of each solution was recorded. Typical spectra are shown in Figure 5.43. An increase in complex absorbance was observed on increasing the mole fraction of L-dopa**.** For example, the absorbance at 280 nm was 0.032 for an L-dopa mole fraction of 0.1, while the absorbance increased to 0.255 when the mole fraction of L-dopa was 0.8. To generate the Job's plot shown in Figure 5.44, the change in the absorbance at a wavelength of 280 nm (from that of an equal concentration of free guest) was computed using Equation 5.8.

These ΔA values were then multiplied by the corresponding mole fraction, ΔA x mole fraction, and the product was plotted as a function of the mole fraction ([L-dopa]/([L-dopa]+[Sβ-CD])), as shown in Figure 5.44. The maximum absorbance value was achieved at the 0.5 mole fraction and this proves that these complexes are formed with 1:1, Sβ-CD:L-dopa stoichiometry.

The determination of the formation constant for the complex was computed on the same basis as previously calculated for the DA-Sβ-CD complex, Section 5.3.2.1. Based on the variation in the absorbance at $\lambda_{max}$ = 280 nm of L-dopa in the absence and presence of varying concentrations of Sβ-CD, the formation constant ($K_f$) of the inclusion complex was evaluated using the Heildebrand-Benesi relationship, Equation 5.1.

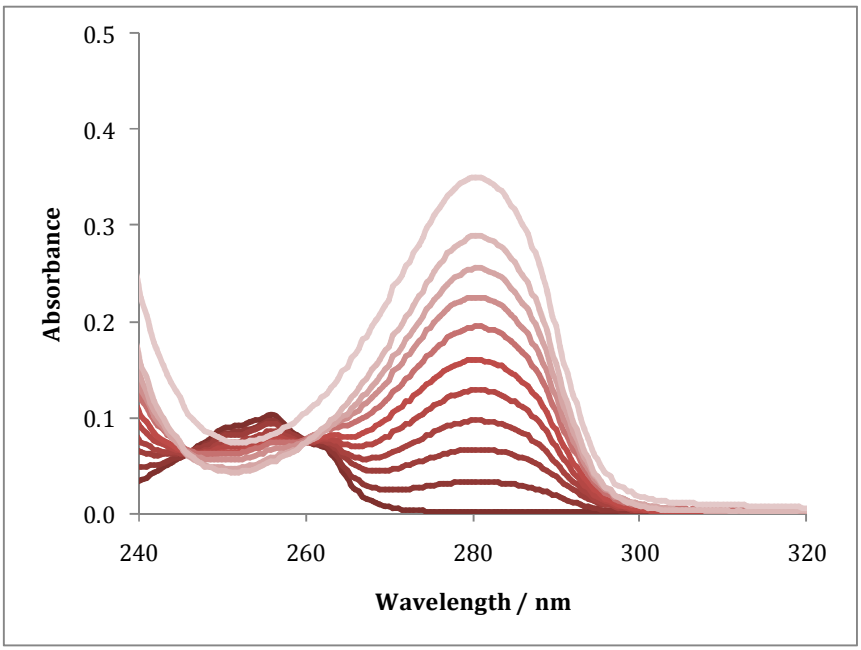


**Figure 5.43:** UV spectra for the Job's plot titration curve with Sβ-CD and L-dopa. From low to high absorbance values, the value of [L-dopa]/([ L-dopa]+[ Sβ-CD]) increases from 0.0 to 1.0, in increments of 0.1.

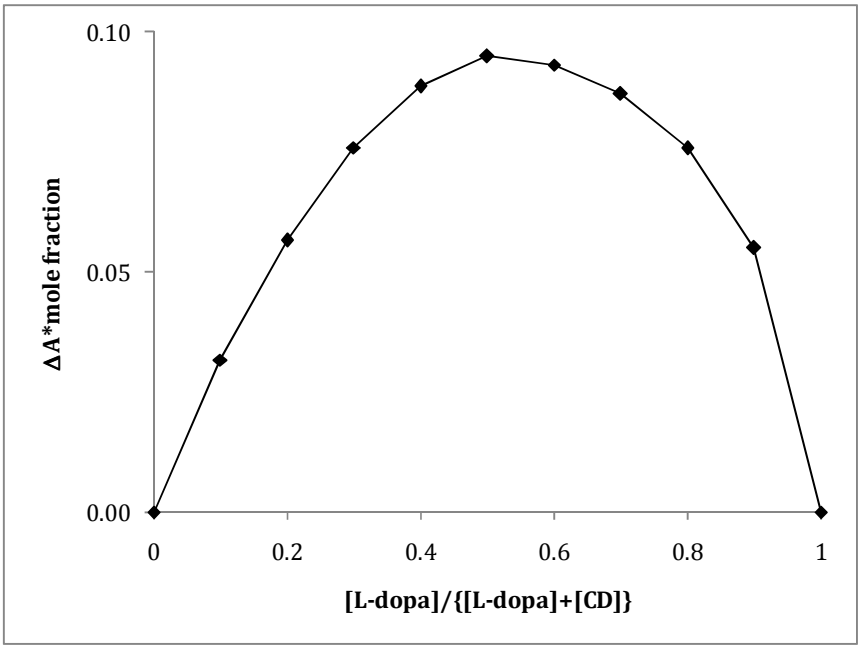


**Figure 5.44:** Job's plot curve of UV absorbance change (280 nm) of L-dopa upon the addition of Sβ-CD, indicating the formation of 1:1 host-guest complex.

A Heildebrand-Benesi plot for the experimental data is demonstrated in Figure 5.45 showing a good linear relationship with a correlation coefficient of 0.984. The linear relationship obtained based on the Hildebrand-Benesi equation, is further support for a 1:1 stoichiometry.[4] According to Equation 5.1, $A_0/(A-A_0)$ vs. 1/[Sβ-CD] plot, the ratio of the intercept to the slope was used to give a formation constant of $K_f$ = 321.02 ± 92.52 in a solution of pH~1. This value is close to that obtained with DA, Tables 5.12 and 5.13. This is not surprising as the structures are related and it is likely that the aromatic ring resides inside the cavity while the protonated amine group is bound electrostatically to the anionic sulfonated groups on the rim of the CD.

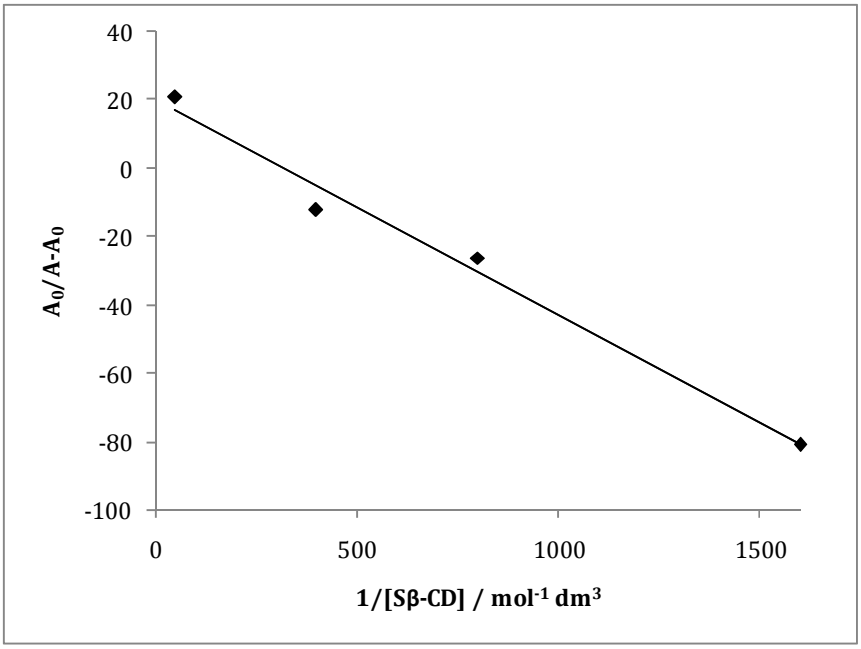


**Figure 5.45:** Plot of ($A_0/A_0$-A) vs. (1/[Sβ-CD]) for the evaluation of the stability constant, ($K_f$), for L-dopa. Experiments were carried out at pH=1.3.

### *5.3.5.2 Tyrosine*

Tyrosine (Tyr) is an amino acid and similarly to L-dopa exists as a zwitterion. Its structure, shown in Figure 5.46, has similarities to DA. Unlike DA and L-dopa, Tyr does not readily oxidise at neutral and alkaline pH values. Figure 5.47 shows its form in the cationic, zwitterionic and anionic form.

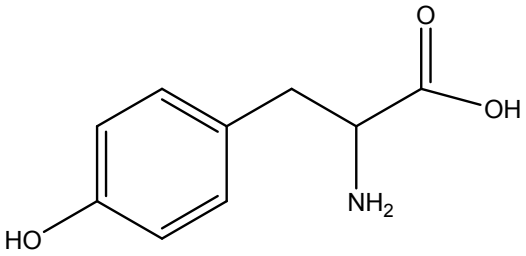


**Figure 5.46:** The chemical structure of tyrosine.

pKa(COOH) = 2.21 pKa($NH_3^+$) = 9.21

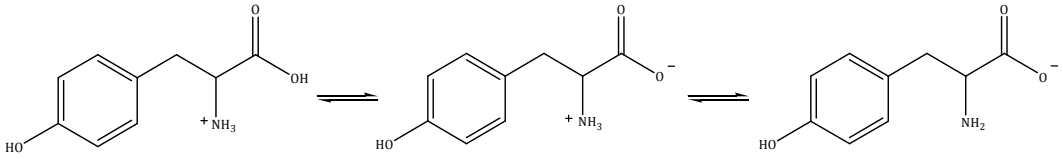

pH < 2.21 2.21 < pH > 9.21 pH > 9.21

Positive charge Negative charge

**Figure 5.47:** Schematic showing the cationic, zwitterionic and anionic forms of Tyrosine.[62]

To investigate the influence of electrostatic interactions, experiments were carried out in both acidic and alkaline pH values out of the range where Tyr can exist as a zwitterion. Similar to DA and L-dopa, Tyr absorbs in the UV region with a $\lambda_{max}$ = 275 nm. This property allowed the Job's method to be applied in order to confirm stoichiometry of the complex. The UV spectrum of each solution was recorded. An increase in complex absorbance was observed on

increasing the mole fraction**.** Figure 5.48 shows the Job's plot obtained from the absorbance changes at 275 nm in the mixtures of Sβ-CD and Tyr. The maximum absorbance value was achieved at the 0.5 mole fraction and confirms that these complexes are formed with 1:1 (Sβ-CD to Tyr) stoichiometry.

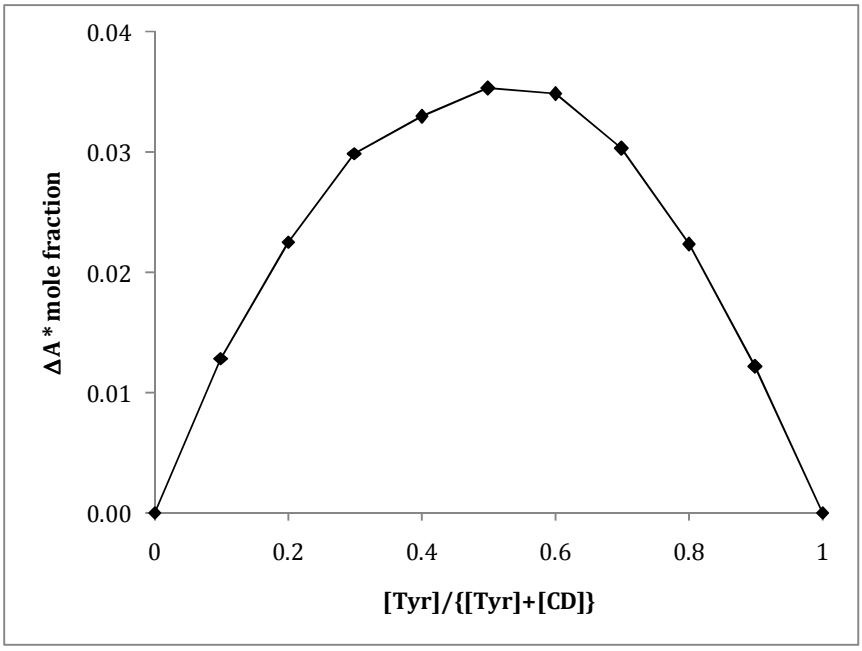


**Figure 5.48:** Job's plot curve of UV absorbance change (275 nm) of tyrosine upon the addition of Sβ-CD, indicating the formation of 1:1 host-guest complex. pH was 1.44.

CV data were obtained at both acidic and alkaline solutions, pH 2.44 and 12.1, respectively. Using Equation 5.18 the amount of Tyr protonated at pH 12.1 is negligible. Figure 5.49 shows the cyclic voltammogram recorded for 5.00 x $10^{-4}$ mol $dm^{-3}$ Tyr in the absence and presence of 2.00 x $10^{-2}$ mol $dm^{-3}$ Sβ-CD at pH 12.1. It is evident from these data that no complexation occurs at this pH as there is no shift in the current or the potential at which the Tyr is oxidised. This can be explained easily in terms of the charge on the Tyr. At pH 12.1, the carboxylate group is dissociated, giving the Tyr a negative charge. It is unlikely that this negatively charge Tyr molecule could approach the negatively charged sulfonated groups and form an inclusion complex.

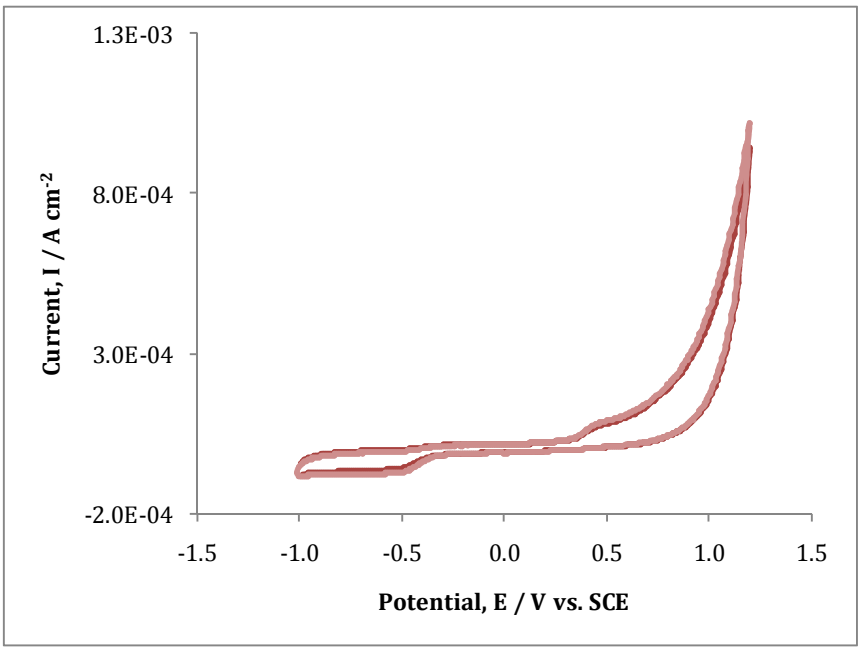


**Figure 5.49:** Cyclic voltammograms of Tyr (5.00 x $10^{-4}$ mol $dm^{-3}$) in the absence ♦ and presence ♦ of 2.00 x $10^{-2}$ mol $dm^{-3}$ Sβ-CD on GC pH=12.1. Scan rate 50 mV $s^{-1}$.

However, as shown in Figure 5.50 there is evidence for the formation of an inclusion complex when the pH is reduced to 2.44. In this figure, there is a substantial shift in the peak current and a slight shift in the peak potential. At this pH, the Tyr is protonated through the amine group and the carboxylate group remains un-dissociated to give a positively charged Tyr species, Figure 5.47. Accordingly, the Tyr is attracted to the negatively charged Sβ-CD and it is likely that the aromatic ring fits inside the cavity while the protonated amine binds with the sulfonated groups on the rim of the CD.

In examining these compounds which have similar structures to DA some insight into the inclusion complexation of DA with the Sβ-CD can be obtained. The stability constant for L-dopa was found to be in good agreement with the binding constant values obtained for DA with Sβ-CD in acidified solutions. However, it is the results obtained with the Tyr that highlight the contribution that electrostatic interactions play in the complexation of DA with Sβ-CD. As it is

impossible to study the electrochemistry of DA at pH values of 12, Tyr was chosen and the experiments with Tyr clearly show that the protonated Tyr species form an inclusion complex, while the anionic Tyr is unable to include inside the cavity of the Sβ-CD.

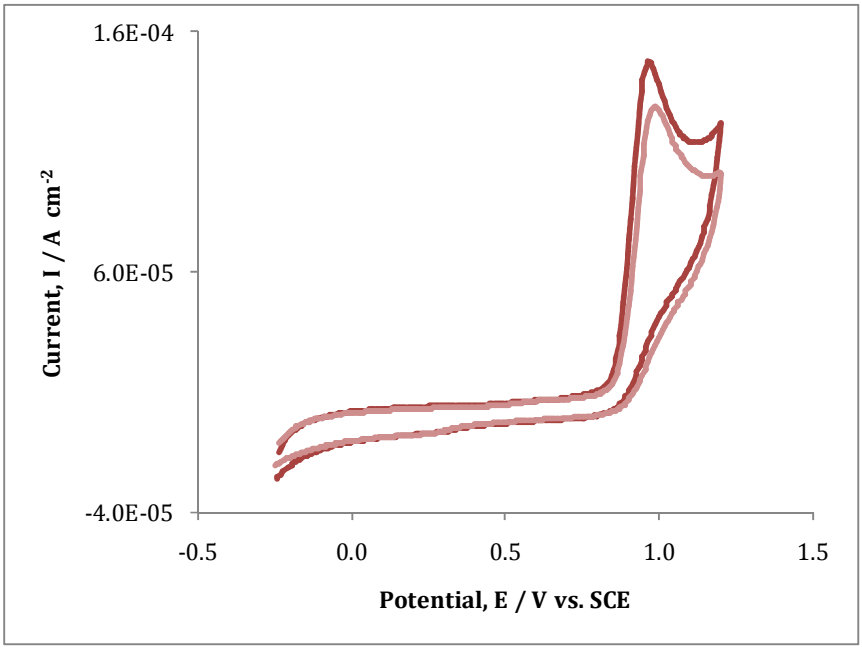


**Figure 5.50:** Cyclic voltammograms of Tyr (5.00 x $10^{-4}$ mol $dm^{-3}$) in the absence ♦ and presence ♦ of 2.00 x $10^{-2}$ mol $dm^{-3}$ Sβ-CD on GC pH=2.44. Scan rate 50 mV $s^{-1}$.

## 5.4 Summary of results

It was demonstrated using spectrophotometric studies that DA can be included in Sβ–CD and, in turn, forms an inclusion complex with a 1:1 stoichiometry. UV spectra showed a shift in the wavelength of the DA in the presence of Sβ–CD confirming a change in the environment of the DA. The Heildebrand-Benesi equation was utilised to evaluate stability constants. The formation of the complex and the stoichiometry of DA and Sβ-CD were further confirmed by electrochemical studies. The DA oxidation potentials shifted to more elevated potentials upon the addition of Sβ-CD, while the potential of the corresponding

reduction wave was not influenced by the presence of the Sβ-CD. This means that DA is bound more strongly to the host in comparison to the quinone form. There was a noticeable change in the peak currents; a decrease as the CD concentration was increased. Again this can be attributed to the formation of an inclusion complex due to the decrease in the diffusion coefficient of DA. Structural information on the inclusion complex was obtained from NMR studies. The NMR experiments confirmed the 1:1 inclusion complex and showed that the aromatic DA ring was included inside the cavity, while the protonated amine was bound through electrostatic interactions to the sulfonated groups on the rim of the CD.

The electrochemical, spectroscopic and structural analysis in determining the formation constants at a pH of 6.0 are in very close agreement, validating our results. Accordingly, any of the methods examined here for the formation of an inclusion complex can be recommended as a reliable option to determining the formation constants of the inclusion complex of Sβ–CD, with a guest.

The role of charge interactions with the negatively charged CD and the cationic DA was investigated using UV and CV by altering the pH. DA at more acidic pH displayed a larger binding affinity to Sβ-CD compared to that at higher pH values. This is probably due to the charge-charge interaction between the negatively charge CD and positively charged guest. In comparing the data obtained in these experiments to data found in the literature for the neutral β-CD, it can be concluded that the negatively charged sulfonate groups on the CD play an important role in the complexation and increase the binding affinities in the case of protonated DA.

The influence of supporting electrolyte was examined and subsequent analysis of CV experiments established that a change in the cation has no influence on the DA-Sβ-CD complexation. However, it was verified using CV that a change in the anion was significant. The influence of the size of the cavity was also considered and after approximate measurements of the diameter of DA using a

DFT method, it was concluded that the DA molecule is too large to fit inside the cavity of the Sα-CD cavity but it is sufficient in size for most of it to fit inside the Sβ-CD cavity. The CV data of DA in the presence of Sα-CD confirmed this analysis.

## 5.5 References


1. K. Connors, Binding Constants, A wiley interscience, 1987.
2. P. Fini, R. Loseto, L. Catucci, P. Cosma, and A. Agostiano, *Bioelectrochemistry*, **70**, (2007), 44-49.
3. Y. Q. Li, Y. J. Guo, X. F. Li, and J. H. Pan, *Dyes Pigments*, **74**, (2007), 67-72.
4. Y. Y. Zhou, C. Liu, H. P. Yu, H. W. Xu, Q. Lu, and L. Wang, *Spectrosc Lett*, **39**, (2006), 409-420.
5. C. R. Raj and R. Ramaraj, *Electrochim Acta*, **44**, (1999), 2685-2691.
6. E. Coutouli-Argyropoulou, A. Kelaidopoulou, C. Sideris, and G. Kokkinidis, *J Electroanal Chem*, **477**, (1999), 130-139.
7. X. J. Dang, M. Y. Nie, J. Tong, and H. L. Li, *J Electroanal Chem*, **448**, (1998), 61-67.
8. J. Szejtli, *Chem Rev*, **98**, (1998), 1743-1753.
9. Job.P, **9**, (1928), 113-203.
10. M. S. Ibrahim, I. S. Shehatta, and A. A. Al-Nayeli, *J Pharmaceut Biomed*, **28**, (2002), 217-225.
11. H. A. Benesi and J. H. Hildebrand, *J Am Chem Soc*, **71**, (1949), 2703-2707.
12. C. Yanez, L. J. Nunez-Vergara, and J. A. Squella, *Electroanal*, **15**, (2003), 1771-1777.
13. G. C. Zhao, J. J. Zhu, J. J. Zhang, and H. Y. Chen, *Anal Chim Acta*, **394**, (1999), 337-344.
14. R. S. Macomber, *Journal of Chemical Education* **69**, (1992), 375-378.
15. M. J. Palys and Z. Stojek, *J Incl Phenom Macro*, **35**, (1999), 3-10.
16. T. Matsue, D. H. Evans, T. Osa, and N. Kobayashi, *J Am Chem Soc*, **107**, (1985), 3411-3417.
17. S. M. Chen and K. T. Peng, *J Electroanal Chem*, **547**, (2003), 179-189.
18. X. L. Wen, Y. H. Jia, and Z. L. Liu, *Talanta*, **50**, (1999), 1027-1033.
19. M. D. Hawley, S. V. Tatawawa, S. Piekarsk, and R. N. Adams, *J Am Chem Soc*, **89**, (1967), 447-&.

20. P. M. Bersier, J. Bersier, and B. Klingert, *Electroanal*, **3**, (1991), 443-455.
21. Y. Liu, B. H. Han, and Y. T. Chen, *J Phys Chem B*, **106**, (2002), 4678-4687.
22. Q. F. Zhang, Z. T. Jiang, Y. X. Guo, and R. Li, *Spectrochim Acta A*, **69**, (2008), 65-70.
23. J. Taraszewska, K. Migut, and M. Kozbial, *J Phys Org Chem*, **16**, (2003), 121-126.
24. R. Ramaraj, V. M. Kumar, C. R. Raj, and V. Ganesane, *J Incl Phenom Macro*, **40**, (2001), 99-104.
25. X. J. Dang, J. Tong, and H. L. Li, *J Inclus Phenom Mol*, **24**, (1996), 275-286.
26. Z. N. Gao, X. L. Wen, and H. L. Li, *Pol J Chem*, **76**, (2002), 1001-1007.
27. P. Fini, F. Longobardi, L. Catucci, P. Cosma, and A. Agostiano, *Bioelectrochemistry*, **63**, (2004), 107-110.
28. S. E. group, Instrumental methods in electrochemistry, 1985.
29. C. Yanez, J. Basualdo, P. Jara-Ulloa, and J. A. Squella, *J Phys Org Chem*, **20**, (2007), 499-505.
30. http://www.engineeringtoolbox.com/water-dynamic-kinematic-viscosity-d_596.html.
31. D. W. M. Arrigan, M. Ghita, and V. Beni, *Chem Commun*, (2004), 732-733.
32. V. S. Vasantha and S. M. Chen, *J Electroanal Chem*, **592**, (2006), 77-87.
33. G. R. Xu, M. L. Xu, H. M. Zhang, S. Kim, and Z. U. Bae, *Bioelectrochemistry*, **72**, (2008), 87-93.
34. R. A. Marcus and N. Sutin, *Biochim Biophys Acta*, **811**, (1985), 265-322.
35. M. Naoi and W. Maruyama, *Mech Ageing Dev*, **111**, (1999), 175-188.
36. F. N. Rein, R. C. Rocha, and H. E. Toma, *J Inorg Biochem*, **85**, (2001), 155-166.
37. E. Winter, L. Codognoto, and S. Rath, *Anal Lett*, **40**, (2007), 1197-1208.
38. S. Shinkai, K. Araki, and O. Manabe, *J Am Chem Soc*, **110**, (1988), 7214-7215.
39. W. Misiuk and M. Zalewska, *Anal Lett*, **41**, (2008), 543-560.
40. A. Bernini, O. Spiga, A. Ciutti, M. Scarselli, G. Bottoni, P. Mascagni, and N. Niccolai, *Eur J Pharm Sci*, **22**, (2004), 445-450.
41. H. Dodzuik, Cyclodextrins and Their Complexes, Wiley-VCH, 2006.
42. I. Bratu, J. M. Gavira-Vallejo, A. Hernanz, M. Bogdan, and G. Bora, *Biopolymers*, **73**, (2004), 451-456.
43. J. B. Chao, H. B. Tong, Y. F. Li, L. W. Zhang, and B. T. Zhang, *Supramol Chem*, **20**, (2008), 461-466.
44. L. Fielding, *Tetrahedron*, **56**, (2000), 6151-6170.

45. V. M. S. Gil and N. C. Oliveira, *Journal of Chemical Education*, **67**, (1990), 473-478.
46. G. Wenz, C. Strassnig, C. Thiele, A. Engelke, B. Morgenstern, and K. Hegetschweiler, *Chem-Eur J*, **14**, (2008), 7202-7211.
47. L. Liu and Q. X. Guo, *J Incl Phenom Macro*, **42**, (2002), 1-14.
48. The Columbia Encyclopedia, Bartleby, 2008.
49. T. Luczak, *Electroanal*, **20**, (2008), 1639-1646.
50. Y. X. Sun and S. F. Wang, *Microchim Acta*, **154**, (2006), 115-121.
51. X. S. Li, L. Liu, T. W. Mu, and Q. X. Guo, *Monatsh Chem*, **131**, (2000), 849-855.
52. V. Zia, R. A. Rajewski, and V. J. Stella, *Pharmaceut Res*, **18**, (2001), 667-673.
53. K. Okimoto, R. A. Rajewski, K. Uekama, J. A. Jona, and V. J. Stella, *Pharmaceut Res*, **13**, (1996), 256-264.
54. M. T. Record, C. F. Anderson, and T. M. Lohman, *Q Rev Biophys*, **11**, (1978), 103-178.
55. X. P. Wang, J. H. Pan, W. H. Li, and Y. Zhang, *Talanta*, **54**, (2001), 805-810.
56. W. Saenger, *Angew Chem Int Edit*, **19**, (1980), 344-362.
57. I. Tabushi, Y. I. Kiyosuke, T. Sugimoto, and K. Yamamura, *J Am Chem Soc*, **100**, (1978), 916-919.
58. T. Loftsson and M. E. Brewster, *J Pharm Sci*, **85**, (1996), 1017-1025.
59. J. Mosinger, V. Tomankova, I. Nemcova, and J. Zyka, *Anal Lett*, **34**, (2001), 1979-2004.
60. J. J. Wang, G. J. Zheng, L. Yang, and W. R. Sun, *Analyst*, **126**, (2001), 438-440.
61. I. V. Terekhova, R. S. Kumeev, and G. A. Alper, *J Incl Phenom Macro*, **59**, (2007), 301-306.
62. R. Malcolm, C. Dawson, D. C. Elliott, W. H. Elliott, and K. M. Jones, Data for Biochemical Research Oxford University Press, 1986.
63. X. F. Chen, J. Y. Zhang, H. L. Zhai, X. G. Chen, and Z. D. Hu, *Food Chem*, **92**, (2005), 381-386.

## 6.1 Introduction

It is well known that Poly($_{D,L}$ – lactide-*co*-glycolide) (PLGA) copolymers can facilitate tissue engineering and, in particular, the electrospun nanofiber mat has been reported to be an excellent tissue engineering mat.[1-4] PLGA was also chosen for this study because it, firstly, has been studied extensively for biomedical applications due to its biocompatibility and biodegradability properties and, secondly, its rate of degradation can be controlled by adjusting the ratio of lactic to glycolic acid units.[5] However, in the interest of drug delivery the use of PLGA offers a great potential, either as a drug delivery system itself [6-8] or in conjunction with a controlled release device.[9]

In Chapter 4, the use of polypyrrole (PPy) as a drug delivery system was investigated; in this chapter the influence of introducing biodegradable PLGA nanofibers under the PPy matrix is explored. Nanostructures offer an increase in the surface area compared to their bulk counterparts. For this reason, the introduction of the nanofibers was investigated for a potential improvement on the uptake and release of dopamine (DA).

The aim of this chapter was to introduce nanotechnology by the formation of nanofibers, using the technique of electrospinning. The work presented here describes the fabrication and characterisation of the electrospun PLGA fibers and the electrochemical deposition of PPy onto the formed substrates. These PLGA/PPy electrodes were then used for application in a drug delivery system for the controlled release of DA. The PLGA nanofibers were electrospun onto Au mylar. The structures were examined using both SEM and optical microscopy. PPy was electrochemically and chemically deposited onto the PLGA Au coated mylar electrodes which were then characterised using electrochemical measurements. The uptake and release of DA was performed using the same parameters as previously described in Chapter 3. The release of the drug was monitored using UV-visible spectroscopy.

## 6.2 Experimental

### 6.2.1 Materials

#### *6.2.1.1 Reagents*

Poly($_{D,L}$ – lactide-*co*-glycolide) (PLGA 50:50) copolymer with an inherent viscosity (the ratio of the natural logarithm of the relative viscosity, to the mass concentration of the polymer) of 0.59 dL $g^{-1}$ was kindly donated by Dr. Kerry Gilmore, from the IPRI, in the University of Wollongong. The solvents, chloroform ($CHCl_3$), N, N dimethylforamide (DMF) and 1,1,1,3,3,3 hexafluroisopropanol (HFIP) and analytical reagents sodium sulfate ($Na_2SO_4$), sulfonated β-cyclodextrin (Sβ-CD) and dopamine hydrochloride salt were purchased from Aldrich and used as received. Pyrrole (Py) and para-toluene-4-sulfonic acid sodium salt (PTS, $C_7H_7NaO_3S$) were obtained from Merck and distilled prior to experimental use. Distilled Py was stored in the fridge at low temperature in the dark. Potassium ferricyanide ($K_3FeCN_6$) was obtained from Ajax. 40% Fe(III)/PTS in ethanol was obtained from Dr.Jun Chen from the IPRI, in the University of Wollongong.

#### *6.2.1.2 Electrodes and Instruments*

The electrospinning apparatus consisted of a number of pieces of equipment: a high voltage power source which was connected to the metallic needle, a digital syringe pump and an electrically grounded collector plate made of galvanised iron mounted on a stand. A schematic of the experimental set up is shown in Figure 6.1. The fibers were electrospun onto 5 x 5 cm cut squares of Au mylar. Au mylar was purchased from CPFilms Inc (USA). This material was selected for these studies as it is a good conducting substrate, easy to use, and a specific area of the deposited fibers can be cut into the dimensions needed for experimental analysis. A digital syringe pump (Kd Scientific Pump) and high voltage power supply (Gamma High Voltage) were used.

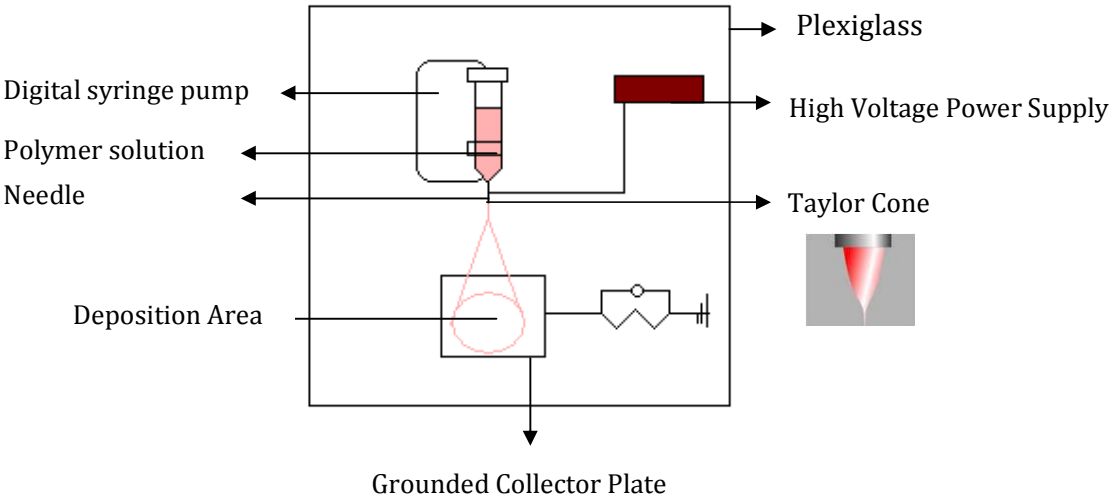


**Figure 6.1:** Schematic diagram of the electrospinning set-up.

Optical Microscopy and SEM were used to study the morphology of the fibers obtained and were preformed on a Leica DMEP DFC-280 and a Leica Stereoscan 440 SEM. The SEM samples were sputtered using an Emitech K550x Gold Sputter Coater. These electrospun samples were then cut into strips and an area of 5 x 5 mm of the PLGA fibers was exposed. Electrochemical analysis of the samples, as well as electropolymerisation of Py using galvanostatic (constant current), potentiostatic (constant potential) and cyclic voltammetry (CV) was carried out using an Electrochemical EDAQ Potentiostat Model EA160 and a Solartron Model SI 1285 potentiostat. UV studies on the release of the DA were carried out on a Shimadzu UV – 1601 and a Varian Instruments Cary 50 Conc UV-visible spectrophotometer using a 1 cm path length quartz crystal cuvette. Finally, a study on the vapour phase deposition of PPy onto the electrospun PLGA fibers was performed using a Model WS-400B-6NPP/LITE Spinning machine.

## 6.2.2 Procedures

### *6.2.2.1 Formation of PLGA nanofibers by electrospinning*

For the formation of PLGA fibers, the structure of which is illustrated in Figure 6.2; solutions of 50:50 PLGA at various concentrations, in the range of 12% to

25% by weight, with different ratios of the organic solvents, $CHCl_3$, DMF and HFIP (neat $CHCl_3$, $CHCl_3$:DMF at 70:30, neat HFIP by vol%) were prepared and left to stir overnight to dissolve. The polymer solution was then placed in the syringe and delivered by the syringe pump at various flow rates in the range of 0.1 – 1.0 mL $h^{-1}$. The distance from the needle to the collector plate (ground electrode) was in the range of 3 – 15 cm; while the positive voltage applied to the polymer solution was in the range of 5 – 20 kV. The amount of time used for the electrospinning process was varied from 1 to 10 min. A flow of dry air was also turned on during electrospinning to minimise bead formation. All experiments were carried out at room temperature. For the electrospinning of the PLGA fibers onto the Au mylar substrate, a metal iron template was welded to the collector plate and 5 x 5 cm samples of Au coated mylar were cut out, washed with acetone, dried, and clipped onto the template with the conducting side facing the needle. It is also important to note that the electrospun PLGA fibers are non-conducting.

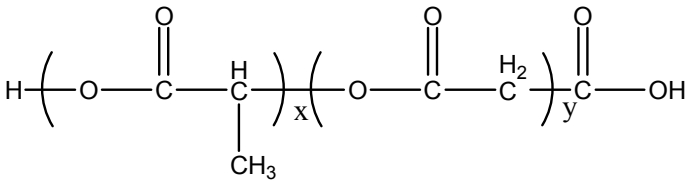


**Figure 6.2:** Structure of PLGA.

### *6.2.2.2 Formation of electrospun fibers containing DA*

From a 20% PLGA in HFIP solution, 1 mL was transferred to a clean vile and 1 wt % (0.01 g) DA was added and left to stir on heat for ~ 24 hr to dissolve. This solution was then placed in the electrospinning set up, and using a flow rate of 0.2 mL $h^{-1}$ at a distance of 7 cm from the needle to the collector plate (ground electrode), a positive voltage of 20 kV was applied to the polymer solution. The samples were then cut into 5 x 5 mm areas and placed in a 1 mL artificial cerebrospinal fluid (CSF) and left at 22 $^0$C. The solution was monitored over time using UV-visible spectroscopy, for the presence of DA.

#### *6.2.2.3 Optical microscopy and SEM sample preparation and imaging*

The image processing and analysis to study the formation of fibers as a function of the various parameters applied were performed using optical and SEM imaging techniques. Samples were electrospun where a variety of parameters were altered and images were taken using both techniques. For the optical images, PLGA fibers were electrospun onto both glass slides and Au mylar. In the case of SEM, the Au mylar substrate was sputtered with a thin coat of gold prior to analysis. Images were also taken before and after the polymerisation of Py onto the fibers.

#### *6.2.2.4 Electrochemical analysis*

Electrochemical experiments were preformed using an EDAQ system, with a conventional three-electrode system. An Ag/AgCl (3.0 mol $dm^{-3}$ NaCl) and a platinum wire mesh electrode were used as reference and auxiliary electrode, respectively. Electrospun samples mounted on the Au mylar substrate were used as the working electrode. These samples were electrospun from a 20 % PLGA in HFIP solution at a distance of 7 cm, diameter of the needle of 0.49 mm, at a feeding rate of 0.2 and 0.8 mL $h^{-1}$ and at potentials of 5, 10, 15 and 20 kV. In addition, the difference between fibers spun for 1 min and for 15 min was examined. The nanofibers on Au coated mylar were cut into strips with a diameter of 5 mm. A surface area of 5 x 5 mm was subjected to the solution and the samples were swept through a potential of –0.600 to 0.600 V vs. Ag/AgCl at a scan rate of 100 mV $s^{-1}$. For comparative studies, bare Au mylar was used. CV was used to investigate the electrochemical properties of the PLGA fibers. In all cases, a 0.25 $cm^2$ surface area of the sample was immersed in the electrolyte solution, 0.01 mol $dm^{-3}$ $K_3FeCN_6$ in 0.10 mol $dm^{-3}$ KCl, where the potential was swept from -0.600 to 0.600 V vs. Ag/AgCl at 100 mV $s^{-1}$. In order to determine the stability of the substrate, electrospun PLGA fiber samples were cycled between -0.300 to 0.900 V vs. Ag/AgCl for 100 cycles in 0.01 mol $dm^{-3}$ $K_3FeCN_6$ in a 0.10 mol $dm^{-3}$ KCl, supporting electrolyte.

### *6.2.2.5 Polymerisation of pyrrole*

The synthesis of PPy was carried out using an electro-synthesis method, which deposited the polymer film at the working electrode. In order to investigate which polymerisation technique maintained the greatest nanofiber morphology on the PLGA fiber mat, polymers were prepared using different electrochemical deposition approaches in a 0.10 mol $dm^{-3}$ para-toluene-4-sulfonic (PTS) acid sodium salt solution containing 0.20 mol $dm^{-3}$ Py. PPy was grown in a conventional three-electrode cell where a Ag/AgCl (3.0 mol $dm^{-3}$ NaCl) and a platinum wire mesh electrode were used as reference and auxiliary electrode, respectively, and the working electrode was bare Au coated mylar or Au coated mylar with electrospun PLGA fibers, with an electrode surface area of 0.25 $cm^2$. The various techniques employed included constant potential (V), constant current (I) and CV. For constant potential polymerisation, 0.700 V vs. Ag/AgCl was applied until a sufficient charge was passed. In the constant current experiments a current of 1 mA $cm^{-2}$ was applied, and for CV, the potential was swept between 0.000 to 0.800 V vs. Ag/AgCl at 50 mV $s^{-1}$, where the cycle number was varied. For the uptake and release of DA, the polymers were prepared using 1.00 x $10^{-2}$ mol $dm^{-3}$ sulfonated β–cyclodextrin solution containing 0.20 mol $dm^{-3}$ Py using various parameters depending on the technique used.

The vapourisation phase polymerisation of Py was also investigated. In using this method two systems were studied. The first was where the oxidant was added to the polymer solution prior to electrospinning. In this case, 0.5 mL of 20% PLGA in HFIP and 0.02 mL of the oxidant, 40% Fe(III)/PTS in ethanol, were mixed and left to stand for 60 min before electrospinning. Then, the fibers were electrospun using the same conditions outlined in Section 6.2.2.1. The second method involved previously electrospun 20 % PLGA samples from HFIP at a flow rate of 0.2 mL $h^{-1}$, at 20 kV and at a distance of 7 cm for 1 min. These samples were subjected to two drops of the oxidant and spin coated at 1000 rpm for 5 s; the oxidant was then flashed off using a hot plate and placed in a chamber containing 5 mL of the Py monomer. After 20 min the samples were removed and left to dry for 60 min. The samples were then placed in ethanol for

20 min in order to wash off any of the oxidant remaining on the sample and were allowed to dry prior to analysis using optical microscopy.

#### *6.2.2.6 Incorporation and release of DA*

The samples electrospun for use in these experiments are as follows: 20 % PLGA in 1,1,1,3,3,3 hexafluroisopropanol (HFIP) and electrospun onto Au mylar at 0.2 mL $h^{-1}$ at 20 kV at a diameter of 0.49 mm and a distance of ~ 7 cm for 1 min. In all cases, a 5 x 5 mm sample dimension was used giving a 0.25 $cm^2$ surface area. The electrochemical deposition of PPy was achieved using cyclic voltammetry, where the potential was swept in a 0.2 mol $dm^{-3}$ Py and 0.01 mol $dm^{-3}$ Sβ-CD solutions, from 0.000 to 0.800 V vs. Ag/AgCl, at various scan rates, for a numerous number of cycles ranging from 5 to 100 cycles.

These prepared polymers were then immersed in a 0.10 mol $dm^{-3}$ DA solution in a supporting electrolyte of 0.10 mol $dm^{-3}$ $Na_2SO_4$ solution and reduced at a potential of –0.900 V vs. Ag/AgCl for 30 min. This gave rise to the incorporation of DA, as detailed in Chapter 4. The sample was then transferred to a 0.10 mol $dm^{-3}$ $Na_2SO_4$ solution and held at a reduction potential, –0.900 V vs. Ag/AgCl, in order to remove any excess DA on the surface. The sample was finally transferred to an electrochemical cell, containing 25 mL of 0.10 mol $dm^{-3}$ $Na_2SO_4$ solution and a stirring bead, and an oxidation potential of 0.100 V vs. Ag/AgCl was applied to stimulate the release of the incorporated DA. A sample of the solution was removed every 10 min for the 60 min and monitored using UV-visible spectroscopy to give the concentration of DA released from the polymer/fiber sample.

## 6.3 Results and Discussion

### 6.3.1 Electrospinning of PLGA fibers

Over the past 20 years extensive efforts have been made to develop a controlled drug release system using biocompatible polymers. In this study, as well as using PPy which is biocompatible[10], the use of poly(lactide-co-glycolide) (PLGA)

was chosen for its biodegradability properties, its biocompatibility and its approval by the Food and Drug Administration (FDA).[11-13]

Electrospinning involves the application of an applied voltage to a needle or capillary connected to a syringe or reservoir containing the polymer solution. Upon application of an electric field, a conical shaped cone develops at the needle tip which is known as the Taylor cone. A schematic is shown in Figure 6.1. After a critical point, the electrostatic forces overcome the surface tension and a charged jet is ejected. This charged jet then undergoes a whipping process, leading to the formation of a fiber at the grounded electrode collector.

In order to obtain a uniform film, a stable continuous flow is required. In the formation of the electrospun PLGA fibers, a number of parameters were varied in order to achieve the optimum electrospinning system and to yield uniform nanofibers. The parameters that were varied included the solvent system, the applied voltage, the flow rate and the distance from the needle to the collector and the substrate. The main defect that is common and undesirable is beading.[14-16] The formation of beads reduces the otherwise large surface area, which is the desired feature, in the creation of nanoscale structures.

Here, results are presented on the influence of varying the solvent, the applied voltage, the flow rate, and the distance from the needle to the collector and the substrate, as well as elimination of the bead formation.

#### *6.3.1.1 Varying the voltage applied*

When a high voltage is subjected to the polymer solution, which is retained by its surface tension, repulsion charges opposite to the surface tension give rise to what is well known as the Taylor cone.[17-20] After a critical point, where the surface tension is overcome, a charged jet of the polymer solution is ejected from the needle tip of the cone. Generally, it has been established that increasing the applied voltage increases the deposition rate due to the higher mass flow from the needle tip.[21]

A 25% PLGA (50:50) polymer solution in 70:30 $CHCl_3$:DMF solvent mix was prepared and placed in the syringe. The diameter of the syringe was 0.49 mm and the distance from the syringe tip to the collector plate was ~ 8 cm. In each case the sample was electrospun for 1 min on a glass slide, in the presence of air, and analysed under an optical microscope. In Figure 6.3 images were attained at a feeding rate of 0.2 mL $h^{-1}$, where the voltage was varied from 5-20 kV. On analysing the images it was observed that as the voltage was increased there was a significant increase in the amount of fibers collected on the sample. It is also significant that as the voltage increased the diameter of the fibers decreased. The formation of beads also changed as evident from image (B) and image (D) of Figure 6.3. As the voltage was increased the fiber diameter decreased due to the simultaneous stretching effect of the charged fibers. This also affected the shape of the bead as the stretching of the jet revealed a spindle shape. At these higher voltages the surface tension is no longer dominant in the fiber formation shape. It is also reported that the application of higher voltages leads to a higher electrostatic repulsion force between the needle tip and the collector, which serves to increase the drawing tension and thus decreases the beading size.[22] It is evident from Figure 6.3 that as the voltage was increased the extent of the bead formation decreased.

These results are in good agreement with literature reports as it is well documented that increasing the applied voltage in the electrospinning process produces thinner fibers.[23-26] Li *et al.*[26] reported that initially with an increase of applied voltage, the nanofiber diameter of Polyvinylalcohol (PVA) decreased but at a certain point, began to increase again. Deitzel *et al.*[23] investigated the parameters involved in electrospinning poly(ethylene oxide) (PEO). They reported that the flow rate, voltage, solution concentration, and surface tension were all major factors in the electrospinning process of this polymer solution. In the case of applied voltage they found that as the voltage was increased a change in the originating droplet shape was observed. This change corresponded to a decrease in the stability of the liquid jet, and therefore increasing the applied voltage lead to an increase in the number of bead defects that formed along the fibers.

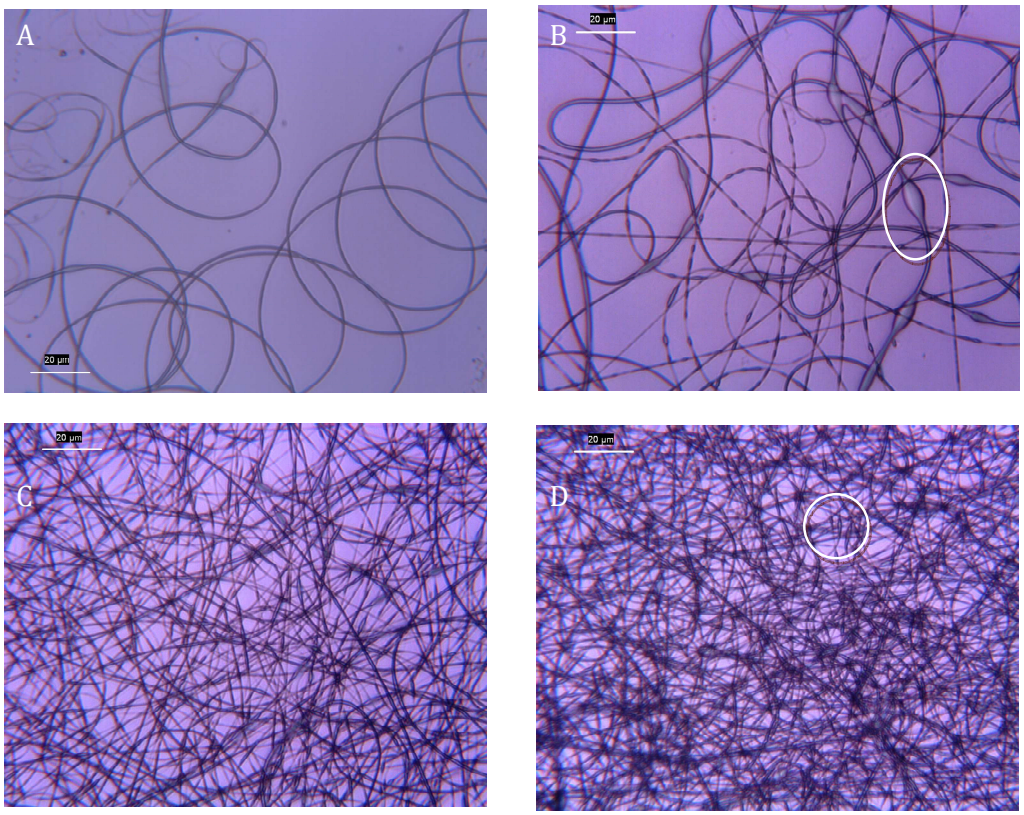


**Figure 6.3:** Optical images of 1 min electrospun 25 % PLGA (50:50) in 70:30 $CHCl_3$:DMF on a glass slide at 0.2 mL $h^{-1}$, diameter of 0.49 mm and a distance of ~ 8 cm at an applied voltage of A) 5 kV B) 10 kV C) 15 kV D) 20 kV. Highlighted areas mark beading.

The authors overcame the presence of beading by creating more viscous solutions (i.e. higher concentrations of PEO). Contrary to Dietzel and co-workers, Zuo and colleagues reported that increasing the applied voltage leads to smaller beads and at a critical point elimination of beading altogether.[14] Baumgart[27] while electrospinning acrylic fibers observed an increase in fiber length with an increase in applied voltage, while Zong and co-workers confirmed that an increase in the applied electrospinning voltage altered the shape of the initial droplet.[28]

### *6.3.1.2 Varying the solvent and solution concentration*

The solvent must be a volatile liquid, as when the process is taking place, the solvent must evaporate in order to form the solid fiber on the collector plate.[25] As the charged jet leaves the needle tip the increase in surface area enhances the rate of evaporation of the volatile solvent which results in a charged, solid polymer fiber. However, if the rate of evaporation is too high, i.e., the solvent is very volatile, the evaporation process occurs too fast on the outer surface of the polymer jet. This gives rise to a fixed outer polymer surface before the solvent content is entirely lost.[29]

A 20% PLGA solution in chloroform was used for the electrospinning process. However, in this case at no point was a continuous jet of fiber obtained. You *et al.*[30] suggest that the viscosity of PLGA is important. The authors state that at ~15 % PLGA, the viscosity stabilises the polymer solution expelled and allows the fibers to form as the solvent disperses. In light of this, the polymer solution was diluted down to ~17 % PLGA with chloroform, but once again no fibers were formed. Contrary to You and co-workers[30], this suggests that chloroform was not a suitable solvent for this PLGA system.

Another solvent was introduced, N, N dimethylforamide (DMF), which has a lower vapour pressure than chloroform (3.7 mm Hg compared to 190.2 mm Hg for chloroform). Shawon and Sung[31] believe that the vapour pressure of the solvent is important as it is an indication of a liquid's evaporation rate. The higher the vapour pressure at normal temperature the greater the evaporation rate of the solvent. They found that in the electrospinning process of polycarbonate the higher ratios of THF to DMF solvent mixtures gave rise to rapid solvent evaporation. This was attributed to the vapour pressure of THF, and the authors reported that the capability to generate more fibers than beads, was lost.

Subsequently, with evaporation rates taken into account, a 12 % PLGA (50:50) polymer solution in 70:30 $CHCl_3$:DMF was prepared. This time the electrospinning observed was promising and a continuous uniform flow of the

polymer material was observed which yielded the formation of fibers, as shown in Figure 6.4. This sample was achieved using a feeding rate of 0.6 mL $h^{-1}$, a distance ~ 10 cm, diameter of 0.49 mm and a voltage of 15 kV on a glass slide. When the sample was examined under the optical microscope, particles were observed. The observation of particles on the optical image has been well documented and indicated that the polymer concentration, and therefore the viscosity, was still not high enough.[15, 30]

Consequently, the concentration of the polymer solution was increased to 25 % PLGA (50:50) in 70:30 $CHCl_3$:DMF. This polymer solution was electrospun under the following conditions: the feeding rate was varied from 1.0 to 0.15 mL $h^{-1}$, distance ~ 10 cm, diameter 0.49 mm and a voltage of 15 kV. Although fibers were formed there was a significant amount of beading, as shown in Figure 6.5 (A). Another sample was obtained at a higher flow rate of 0.3 mL $h^{-1}$ at 15 kV in the presence of air, Figure 6.5 (B), where the formation of beading was reduced slightly.

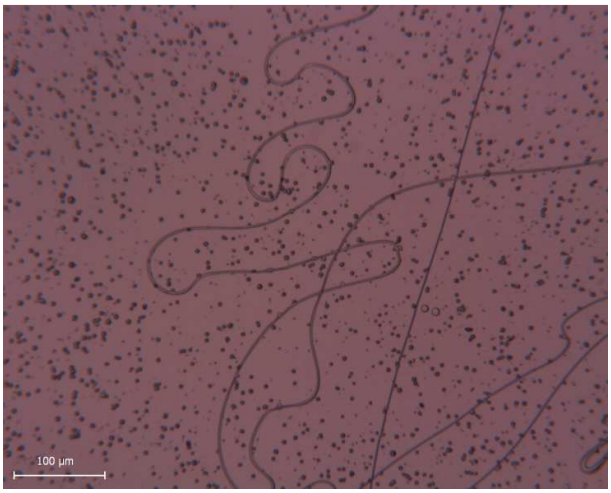


**Figure 6.4:** An optical image taken of 12% PLGA in 70:30 $CHCl_3$:DMF on glass at a flow rate of of 0.6 mL $h^{-1}$, at 15 kV.

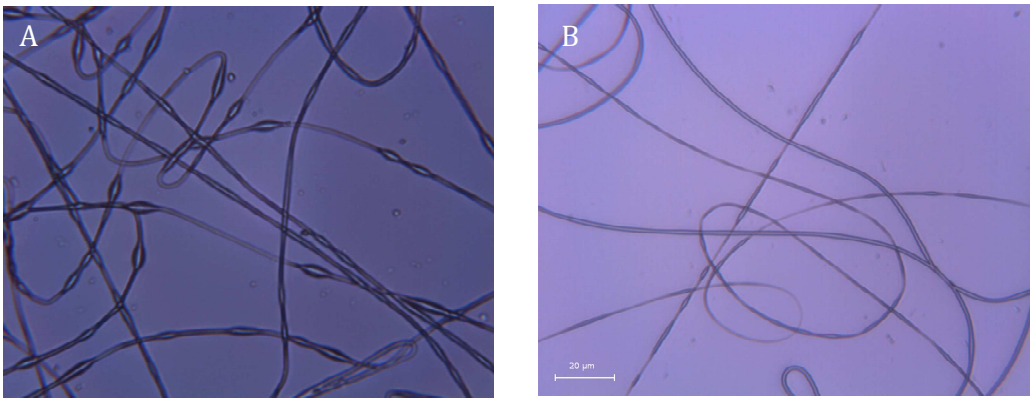


**Figure 6.5:** Optical images of 25 % PLGA in 70:30 $CHCl_3$:DMF on a glass slide, A) at a flow rate of 0.15 mL $h^{-1}$ at 15 kV. B) at a flow rate of 0.3 mL $h^{-1}$ in the presence of air at 15 kV.

As beading was still present with all the electrospun fibers, a third solvent system was chosen. In this case, the solvent, HFIP, was used to prepare a 15 % PLGA (50:50) solution. HFIP was chosen as a fellow colleague was working on a similar electrospinning process and found this solvent system formed the optimum fibers. Fibers were electrospun at a flow rate of 0.4 mL $h^{-1}$ at a distance of 8 cm, diameter 0.49 mm at 15 kV in the presence of air. However, particles were observed once again, as seen in Figure 6.6, and so the concentration was increased to 20 % PLGA (50:50) in HFIP. From the 20 % PLGA (50:50) in HFIP, samples were obtained as shown in Figure 6.7. In this instance a constant flow rate of 0.4 mL $h^{-1}$ was used and the voltage applied was varied. In all circumstances beading was observed. However, as the applied voltage was increased the extent of bead formation decreased, as shown from a comparison of images (A) and (D) in Figure 6.7. The reason for this has been previously discussed in Section 6.3.1.1.

It is evident in the literature that the concentration of the polymer solution influences the morphology and structure of the electrospun fibers.[23, 28] Taking a look at the difference between 15% and 20% PLGA in HFIP using the same parameters, Figure 6.6 (B) and Figure 6.7 (C), respectively it is evident that a considerable change in the morphology is observed.

Similar to the results obtained here by varying the concentration of the PLGA polymer solution, Zong *et al.*[28] observed extreme morphology changes as the concentration of poly(D,L-lactic acid) (PDLA) was increased. They found that the concentration or viscosity was the most effective parameter in controlling the morphology of the electrospun fibers.

Beading is a common problem in the electrospinning of fibers.[15, 23] Fong *et al.*[15] also found that viscosity, surface tension and the net charges all influenced the morphology of electrospun PEO fibers. The authors demonstrated that an increase in the net charge density favours formation of small diameter fibers.

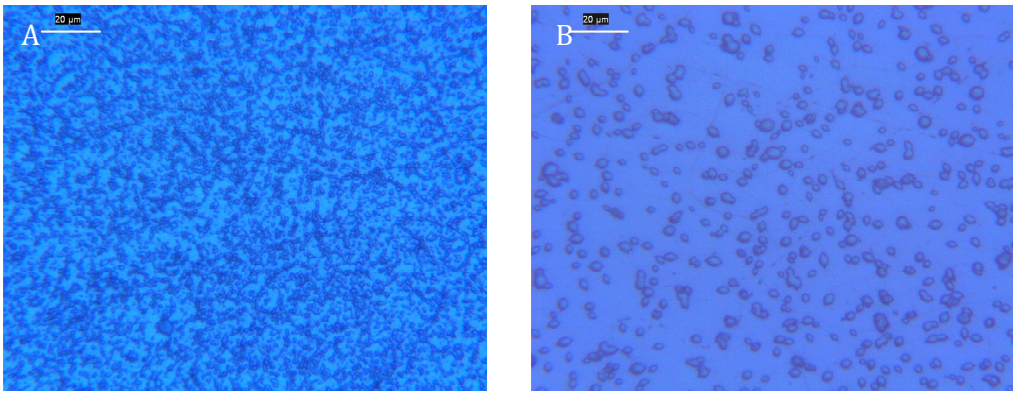


**Figure 6.6:** Optical images for 1 min of electrospun 15 % PLGA (50:50) in HFIP on glass at 15 kV and a distance of 8 cm and a feeding rate of A) 0.2 mL $h^{-1}$ B) 0.4 mL $h^{-1}$.

However, further work on the HFIP solvent system gave rise to bead-free fibers. Figure 6.8 shows SEM images of both 70:30 $CHCl_3$:DMF and HFIP solvent systems. Beading is prominent in the case of the 70:30 $CHCl_3$:DMF solvent mix, where as in the presence of HFIP, an improved fiber mat was obtained. In these cases a high applied voltage of 20 kV was used with a flow rate of 0.2 mL $h^{-1}$. It appears that the HFIP solvent system at low flow rates gives rise to the optimum conditions (viscosity, volatility, surface tension etc,) needed to generate the bead free fibers.

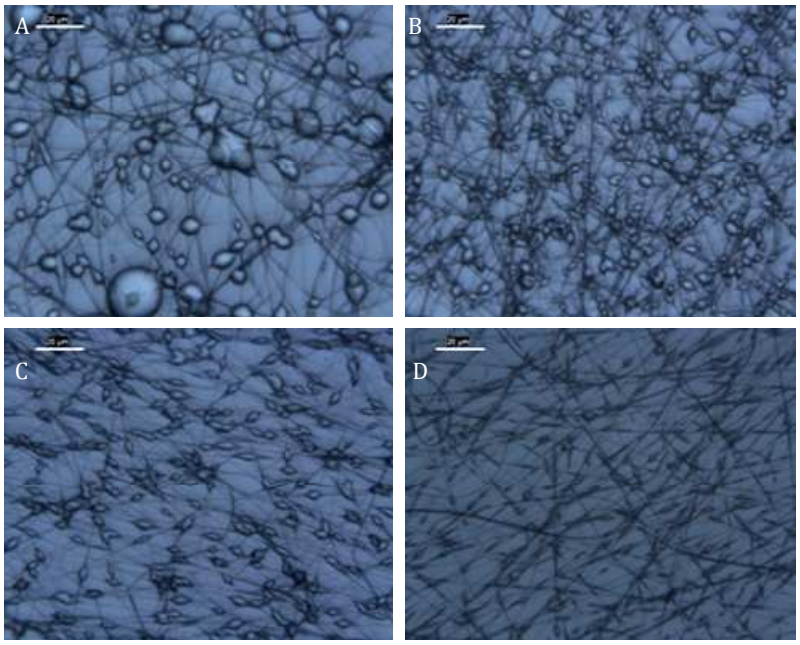


**Figure 6.7:** Optical images for 1 min of electrospun 20 % PLGA (50:50) in HFIP on glass at a constant feeding rate of 0.4 mL $h^{-1}$, a distance of 8 cm and a voltage of A) 5 kV B) 10 kV C) 15 kV D) 20 kV.

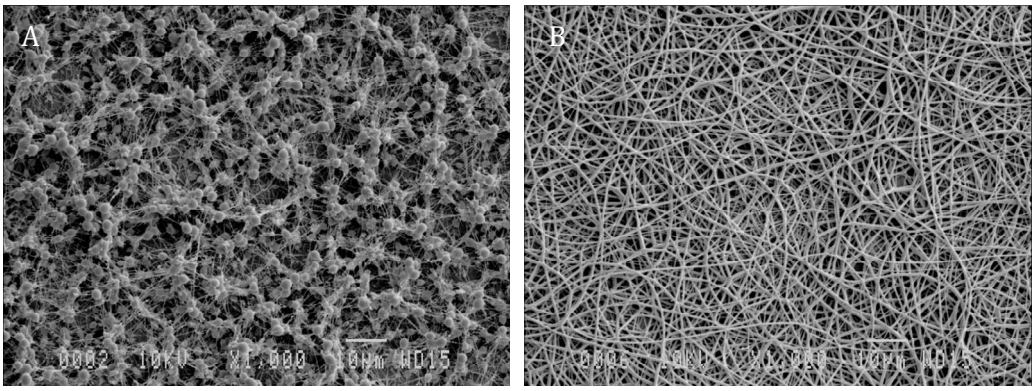


**Figure 6.8:** SEM images of 1 min electrospun 20 % PLGA (50:50) on a Au coated mylar at 7 cm distance, applied potential of 20 kV and a flow rate of 0.2 mL $h^{-1}$, A) 70:30 $CHCl_3$:DMF, B) HFIP.

With this new solvent system the feeding rate, the distance between the tip and collector and the substrate at which the fibers were collected was investigated.

#### *6.3.1.3 Varying the feeding rate*

In order to form a Taylor cone a certain minimum volume of solution is required at the tip of the needle.[28] Variation of the solution volume facilitates the generation of polymer fibers with different morphologies. In keeping with the applied voltage of 20 kV, fibers were electrospun from a 20 % PLGA (50:50) in HFIP solution on a glass slide at a diameter of 0.49 mm and a distance of ~ 7 cm, the flow rate was varied from 0.2 mL $h^{-1}$ to 0.8 mL $h^{-1}$. Figure 6.9 shows representative images for each sample generated. At a feeding rate of 0.2 mL $h^{-1}$, a fiber diameter of < 0.8 μm was obtained while at a feeding rate of 0.8 mL $h^{-1}$, a fiber diameter of ~ 1.0 μm was generated. Also, an increase in the amount of beading as the flow rate was increased was evident. Significant beading at 0.4 mL $h^{-1}$ was observed. Overall, a feeding rate of 0.2 mL $h^{-1}$ achieved the best fibrous network, with a high density of fibers.

It is well documented in the literature that the flow rate has an influence on the diameter of the fibers produced. Son and co-workers[32] investigated many parameters in the electrospinning of cellulose acetate (CA). They found in the case of varying the flow rate that the average fiber diameter increased with increasing flow rate. Li *et al*.[25] also stated that the higher the feeding rate, the greater the thickness of the fibers formed.

These experiments were a good way of optimising the fiber formation; however, beading was still present. In examining the applied voltage and the feeding rate it appears that an applied voltage in the range of 15 to 20 kV and the feeding or flow rate of 0.2 mL $h^{-1}$ produces the best fibrous mat.

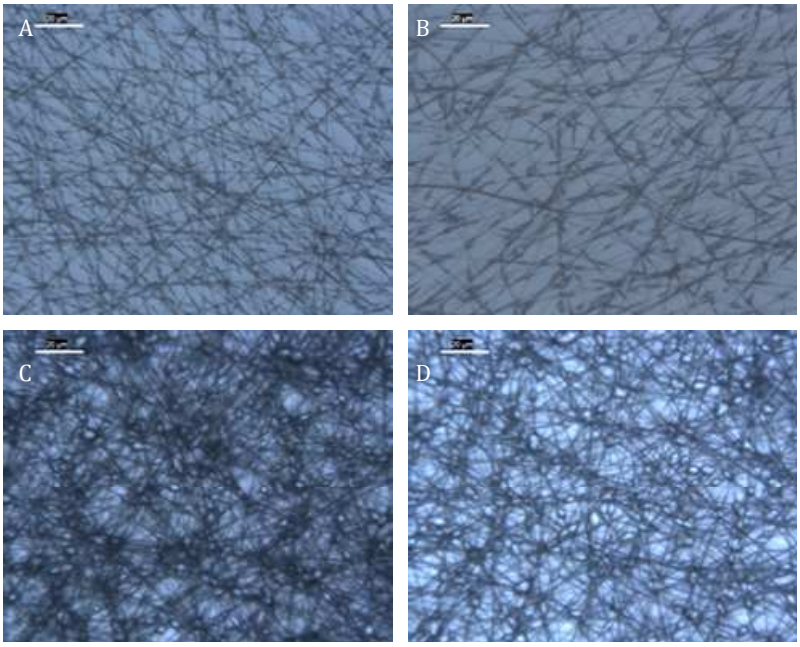


**Figure 6.9:** Optical images of 1 min electrospun 20 % PLGA (50:50) in HFIP on a glass slide at 20 kV, diameter of 0.49 mm and a distance of ~ 7 cm at a flow rate of A) 0.2 mL $h^{-1}$ B) 0.4 mL $h^{-1}$ C) 0.6 mL $h^{-1}$ D) 0.8 mL $h^{-1}$.

### *6.3.1.4 Varying the distance from needle tip to collector*

To continue on in the variation of parameters, Figure 6.10 shows the influence of the distance from the needle to the collector plate on fiber formation. Samples were electrospun at a constant flow rate of 0.2 mL $h^{-1}$ at 15 kV. In terms of these results a significant difference was observed. As the distance between the collector plate and the needle tip was decreased to 3 cm, a thicker film was acquired. A significant amount of beading was observed at needle to collector distances of 14 and 10 cm, while more fibers and less beading were evident at 7 cm. This result is consistent with the results obtained by Zuo and co-workers[14,] and Lee and colleagues[22] in the electrospinning of poly(hydroxybutyrate-co-valerate) (PHBV) and polystyrene (PS), respectively. As the tip to collector distance, is increased the electrostatic force decreases, giving rise to a higher bead formation.[22]

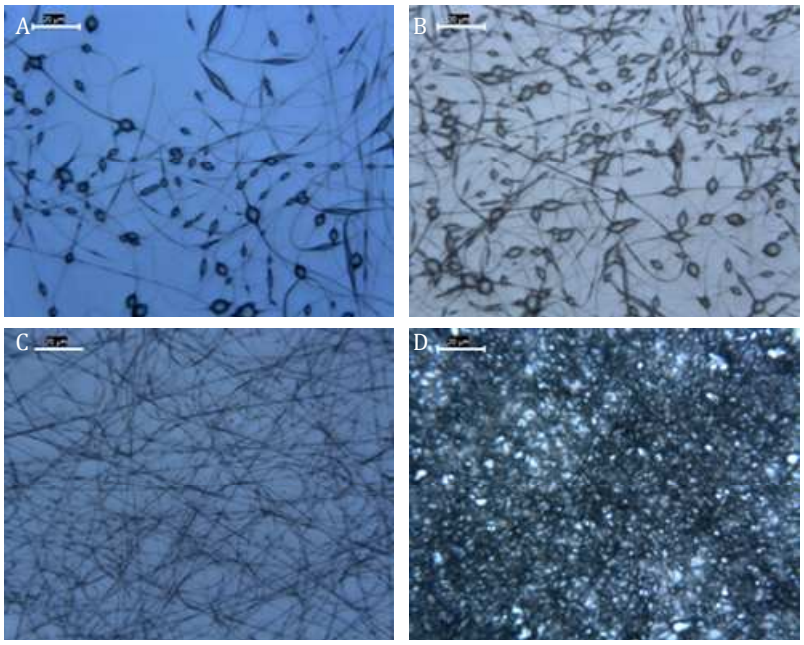


**Figure 6.10:** Optical images for 1 min of electrospun 20 % PLGA (50:50) in HFIP on glass at a constant flow rate of 0.2 mL $h^{-1}$ at 15 kV where the distance was A) 14 cm B) 10 cm C) 7 cm D) 3 cm.

### *6.3.1.5 Varying the substrate*

Finally, an investigation into the substrate on which the fibers were collected was examined. Initially samples were collected on glass slides. In order to achieve electrochemical polymerisation of Py and uptake and release of DA, a conductive substrate was needed. In this case Au coated mylar was chosen as the substrate. In comparing the samples obtained on glass slides, which are non-conducting, to the Au coated mylar which is conducting, 20 % PLGA (50:50) in HFIP polymer solution electrospun samples were obtained and analysed. Figure 6.11 show the optical images of 1 min electrospun 20 % PLGA in HFIP at a distance of 7 cm and at an applied potential of 20 kV on glass and Au mylar. No beading was observed at the Au mylar substrate. Figure 6.11 (A) and (C) show electrospun fibers on glass slides at different flow rates, and it is clear that the beading persists; it is also evident that at the higher flow rate, the presence of beading in more prominent. Again, this feature was previously discussed in Section 6.3.1.2.

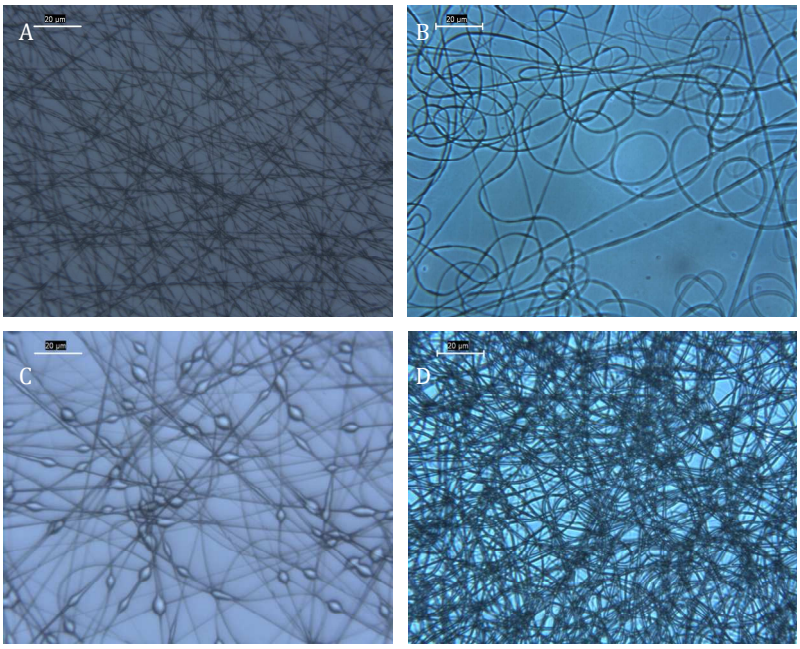


**Figure 6.11:** Optical images of 1 min electrospun 20 % PLGA in HFIP at a distance of 7 cm at 0.2 mL $h^{-1}$ at an applied potential of 20 kV on A) glass and B) Au mylar, and 0.8 mL $h^{-1}$ on C) glass and D) Au mylar.

The absence of the beading on the electrospun Au mylar samples clearly demonstrate that the substrate has a significant affect on the nature of the fibers formed. This feature correlates with results obtained by Liu *et al.*[33], who examined the effect of the collectors (substrates) on the nature of the fibers formed when electrospinning cellulose acetate (CA). The authors reported that the nature of the collector can affect the diffusion and evaporation of the residual solvent which influences the fiber structure. They also state that an electrically conducting collector is more favourable than a non-conducting substrate as it leads to a more tightly packed and thick membrane structure. Conducting substrates provide a sink for generated electric charges, which reduces inter-fiber repulsion and yields a more loosely packed fibrous network. Similar interpretations have been reported in the electrospinning of PEO, that is, more fibers are collected when a metal screen is used as a collector in comparison to those collected on cloth.[18] These results demonstrate that the fiber morphology and arrangement can be controlled by varying the

conductivity and geometry of the collector and they are consistent with the data presented here for the PLGA system. Figure 6.12 shows SEM images of 20 % PLGA in HFIP electrospun onto Au coated mylar at a distance of 7 cm, at a feeding rate of 0.8 mL $h^{-1}$, and a potential of 20 kV for 15 min. In the case of Figure 6.12 (B) the diameter of the fiber was calculated using the SEM software to be approximately 300 nm.

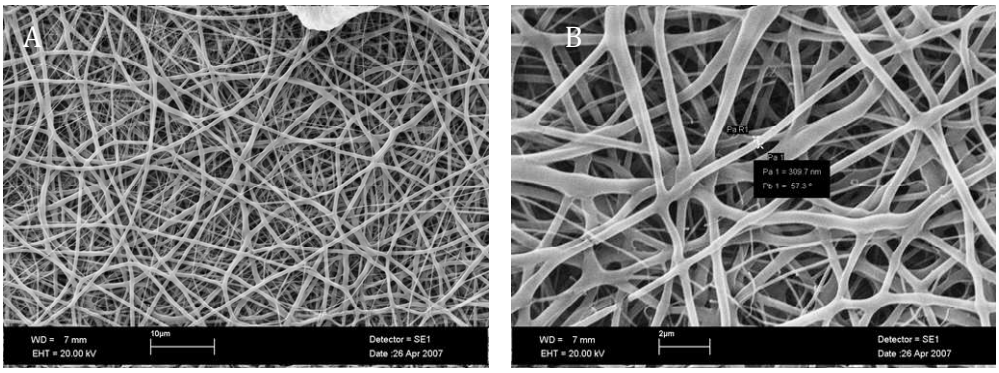


**Figure 6.12:** SEM micrographs of 20 % PLGA in HFIP electrospun onto Au coated mylar at a distance of 7 cm, at a feeding rate of 0.8 mL $h^{-1}$, and a potential of 20 kV, for 15 min.

### 6.3.2 Incorporation of DA into the polymer solution prior to electrospinning

In the past decade electrospinning has been used to prepare membranes for biomedical applications, such as tissue engineering, drug delivery and wound healing. [34-38]

The initial aim of these experiments was to, (i) compare the fibers formed *via* electrospinning of 20% PLGA in HFIP in the absence and presence of 5 wt % DA hydrochloride salt and, (ii) to monitor the natural degradation of the electrospun polymer mat to establish if the DA is incorporated during the electrospinning process. Figure 6.13 shows the optical images taken after 20% PLGA in HFIP was electrospun at a feeding rate of 0.2 mL $h^{-1}$ at 20 kV in the absence and presence of 5 wt % DA hydrochloride salt. Figure 6.14 shows the corresponding SEM images. From the image presented in Figure 6.14 (B), a

coating was observed in various areas around the sample. After analysis of the electrospun samples it was concluded that these observations were from the change in the composition of the polymer solution due to the addition of the salt, which decreased the stability of the fiber spinning process.[30]

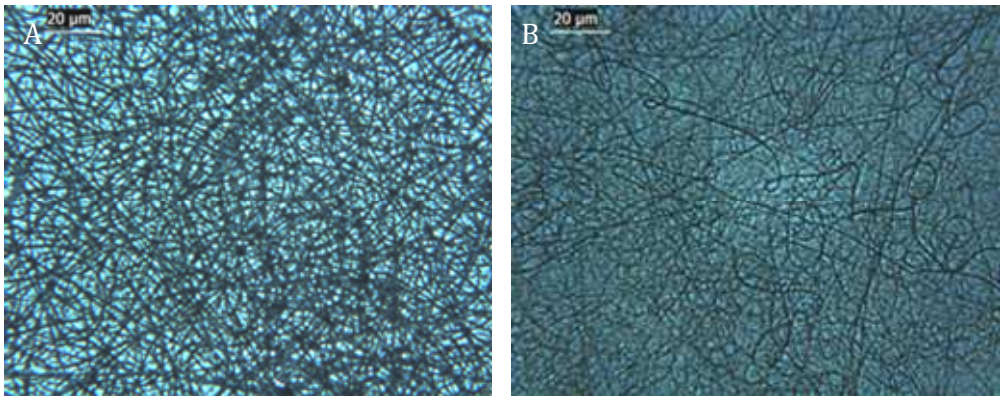


**Figure 6.13:** Optical images of electrospun 20 % PLGA in HFIP electrospun at a feeding rate of 0.2 mL $h^{-1}$ at 20 kV on Au mylar for 1 min. A) in the absence and B) presence of 5 wt % DA.

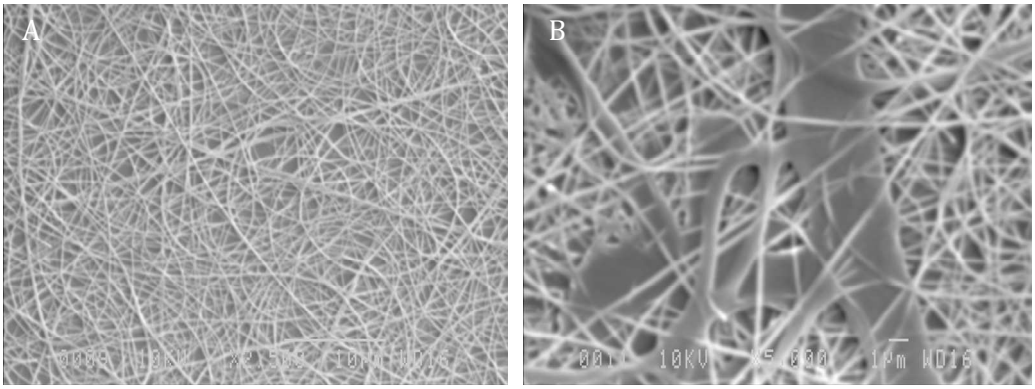


**Figure 6.14:** SEM images of electrospun 20 % PLGA in HFIP at a feeding rate of 0.2 mL $h^{-1}$ at 20 kV shown in A) absence and B) presence of 5 wt % DA hydrochloride salt.

Nevertheless, an experiment monitoring the degradation of the fibers over one month was conducted. The degradation of the polymer was monitored using

UV-visible spectroscopy. As shown previously, in Chapter 4, DA absorbs in the UV region and has a $\lambda_{max}$ = 280 nm. Figure 6.15 shows the UV data obtained for DL Lactic acid, a degradation product of the PLGA polymer, which also shows absorbance in the same region as DA. Figure 6.16 is the absorbance as a function of time observed from the samples at 256 nm. From this figure it is evident that the degradation process of the fibers was initiated. Figure 6.17 is the absorbance as a function of time observed from the samples at 280 nm. From this figure, the absorbance observed over time is due to the degradation of the electrospun PLGA fibers; there was no evidence to suggest any DA was encapsulated in the electrospun fibers. Contrary, to these results, it is well documented in the literature that encapsulation and release of drug-loaded electrospun samples is a promising field.[28, 35, 39]

The incorporation of DA during the electrospinning process may not be a viable option. This can be attributed to the fact that DA is highly soluble in water and, consequently, insoluble in non-polar organic solvents. The PLGA polymer solution is dissolved in HFIP and after addition of the solid DA, remnants of undissolved DA powder is evident in the solution.

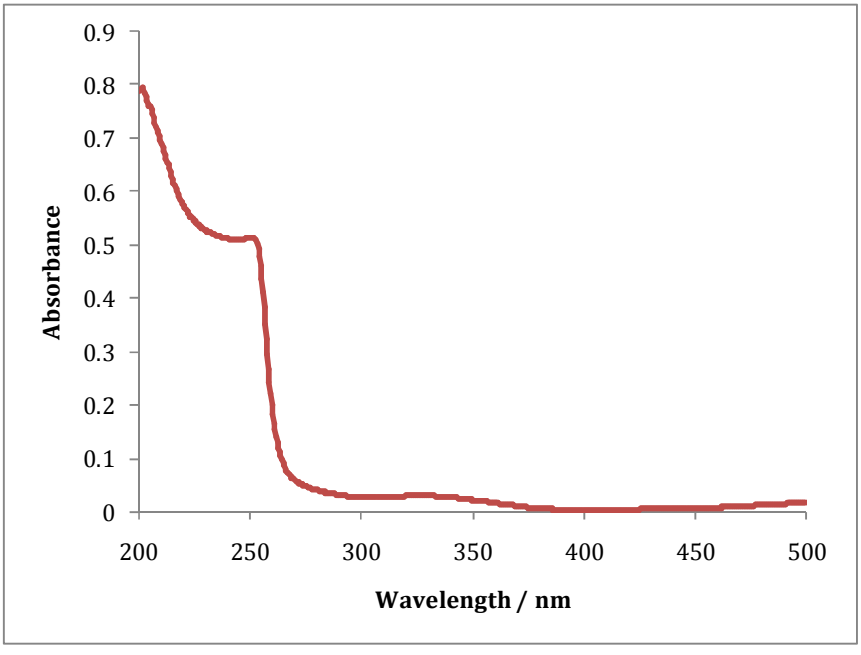


**Figure 6.15:** UV spectrum of DL Lactic acid.

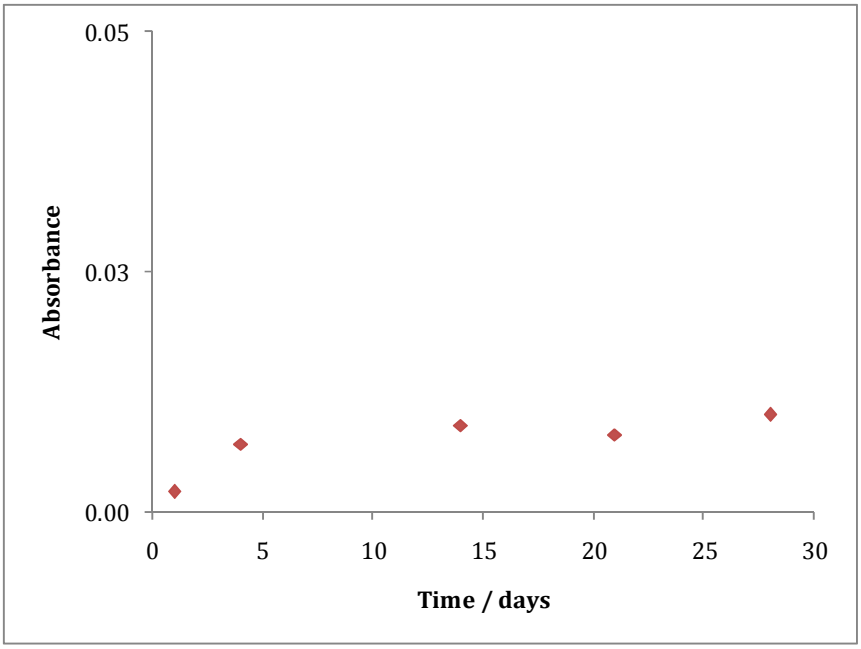


**Figure 6.16:** Absorbance recorded at 256 nm for an electrospun sample of 20 % PLGA in HFIP. The samples were immersed in 1 mL of CSF where the UV spectra were taken over a number of days.

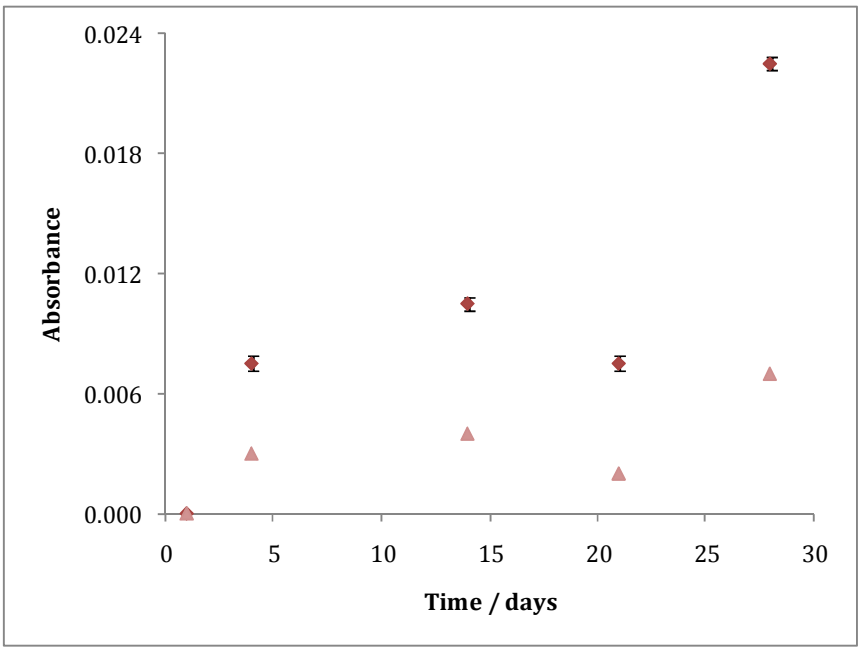


**Figure 6.17:** Absorbance as a function of time for an electrospun sample of 20 % PLGA in HFIP in the absence and presence of DA. The samples were immersed in 1 mL of CSF where the UV spectra were taken over a number of days. ♦ is PLGA in the absence and ▲ in the presence of DA.

Liao *et al.*[40] studied the encapsulation and release studies of rhodamine B in electrospun PLGA fiber mats. Rhodamine B was dissolved firstly in distilled water then added dropwise to the solvent mixture of $CHCl_3$:DMF with stirring. The authors successfully monitored rhodamine B release using fluorescence, and thus, a type of tissue engineering scaffold was created with desirable and controllable drug encapsulation/release properties. Kenawy and co-workers also achieved release of tetracycline from electrospun mats of PEVA, PLA and blends of these polymers. Tetracycline was solubilised in methanol and added to the polymer solutions prior to electrospinning. They achieved drug release over 5 days.[39]

All of the above mentioned literature reports focused on the drug loaded composite nanofibers electrospun using a mixture of the drug and the polymer, both of which were dissolved in the same solvent. This method can lead to problems in the release of the drug, as the drug particles tend to situate on the fiber surface due to rapid evaporation of the solvent.[6] In contrast, a technique involving the electrochemical deposition of PPy onto the electrospun fibers was investigated. It has previously been shown in Chapter 3, as well as in the literature, that PPy is an appropriate material for the uptake and release of compounds due to its redox properties.[41, 42] This can stimulate more effective drug release. The presence of the electrospun nanofiber matrix should enhance the surface area which, in turn, may increase the amount of drug released. Firstly, electrochemical characterisation on the PLGA nanofiber mats was carried out in order to clarify if the electrochemical deposition of PPy would be possible, at these non-conducting fibers.

### 6.3.3 Electrochemical Characterisation

CV is a technique commonly used to study the electrochemical behaviour and properties of many new materials. Once the parameters of the electrospun samples had been optimised, the electrochemical behaviour of the Au mylar with the electrospun PLGA nanofibers were studied using the voltammetric response of potassium ferricyanide. The one electron reduction of ferricyanide

to ferrocyanide is a standard used to demonstrate the electrochemical properties of many substrates, as reported in the literature. This redox couple demonstrates nearly reversible electrode kinetics, without any complications. CV in 0.01 mol $dm^{-3}$ $K_3FeCN_6$ solution was performed to characterise the electrochemical reactivity of the films. In Figure 6.18, the CV data for the reduction of ferricyanide (0.01 mol $dm^{-3}$) to ferrocyanide in the supporting electrolyte solution of KCl (0.10 mol $dm^{-3}$) at a Au mylar substrate with electrospun PLGA nanofibers are shown. The resistance or conductivity of the working electrode will determine the position of the oxidation and reduction peaks. As evident from the data shown in this figure, this material holds good electronic properties. This voltammogram in the potential range of -0.600 to 0.600 V vs. Ag/AgCl shows a well defined pair of redox peaks. The $I_{p(a)}/I_{p(c)}$ was almost unity and the anodic peak, $E_{pa}$, appears at ~ 0.26 V vs. Ag/AgCl which corresponds to the oxidation of the ferrocyanide to ferricyanide. Upon reversal of the potential, a cathodic peak, $E_{pc}$, at ~ 0.15 V vs. Ag/AgCl is observed and is associated with the reduction of ferricyanide back to ferrocyanide, as shown in Scheme 6.1. The $\Delta E_p$ value of 112 mV is somewhat higher than the value of 95 and 99 mV which has been reported for the ferricyanide/ferrocyanide system at bare and modified gold electrodes, respectively.[43, 44] Nevertheless, the Au mylar/electrospun fiber substrate shows good reversibility for the ferricyanide/ferrocyanide system.

$$[Fe(CN)_6]^{3-} + e^- \longrightarrow [Fe(CN)_6]^{4-}$$

ferricyanide Fe(III) ferrocyanide Fe(II)

**Scheme 6.1:** Reduction of ferricyanide to ferrocyanide.

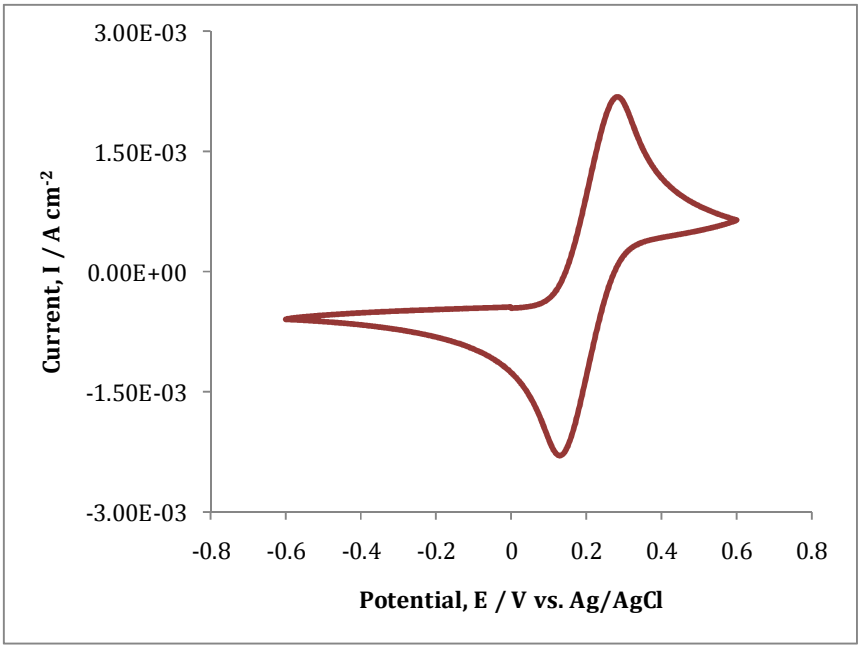


**Figure 6.18:** Cyclic voltammogram of $K_3FeCN_6$ (1.0 x $10^{-2}$ mol $dm^{-3}$) on electrospun PLGA fibers on Au mylar. The potential was swept from –0.600 to 0.600 V vs. Ag/AgCl at a scan rate 100 mV $s^{-1}$.

Figure 6.19 shows the affect of the thickness of the PLGA electrospun fibers, on the Au mylar. This figure shows results of CV data for two samples which were electrospun for 1 and 15 min. As seen in this figure, there is a significant drop in the current between a sample electrospun for 1 min and one electrospun for 15 min. For example, the anodic peak current has dropped from 1.156 x $10^{-3}$ to 3.458 x $10^{-4}$ A $cm^{-2}$ on changing from a 1 to 15 min electrospun sample, respectively. These data confirm that time has a significant influence on the thickness of the fibers obtained on the substrate, and the more time subjected to electrospinning process, the thicker the PLGA fibrous mat. Longer spinning periods increase the thickness of the fibers and decrease the porosity of the mat. This inhibits the electrochemical activity of the fiber coated Au mylar and the insulating properties of the PLGA fibers are accentuated.

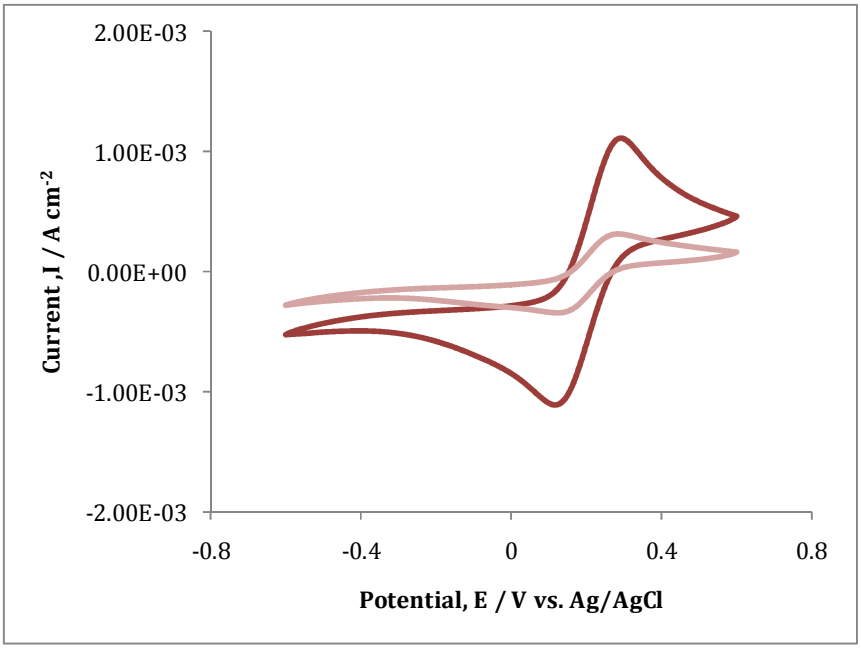


**Figure 6.19:** Cyclic voltammograms of $K_3FeCN_6$ (1.0 x $10^{-2}$ mol $dm^{-3}$) in KCl (0.1 mol $dm^{-3}$). The potential was swept from –0.600 to 0.600 V vs. Ag/AgCl at a scan rate 100 mV $s^{-1}$. Samples were electrospun at 0.8 mL $h^{-1}$ at 20 kV for —1 min — 15 min.

In order to verify experimental reproducibility, a number of samples were fabricated and investigated. Figure 6.20 shows CV data for two separate samples of electrospun PLGA onto Au mylar at 0.2 mL $h^{-1}$ at 20 kV for 1 min. The samples were subsequently cycled in 1.0 x $10^{-2}$ mol $dm^{-3}$ $K_3FeCN_6$ in 0.10 mol $dm^{-3}$ KCl where the potential was swept from –0.600 to 0.600 V vs. Ag/AgCl at a scan rate 100 mV $s^{-1}$. As evident from this figure similar results were obtained for each sample. However, in some cases CV data were found to deviate when electrospun samples were taken from different electrode areas. Therefore, care was taken in all subsequent experiments and an appropriate area from the centre of the electrospun fibers was cut.

In order to determine the stability of the substrate, a sample was cycled between -0.300 to 0.900 V vs. Ag/AgCl for 100 cycles at a scan rate 100 mV $s^{-1}$. Figure 6.21 shows an electrospun sample cycled in 1.0 x $10^{-2}$ mol $dm^{-3}$ $K_3FeCN_6$ in 0.10 mol $dm^{-3}$ KCl. In this figure, cycle 10 and 90 are shown; no change in redox properties was observed.

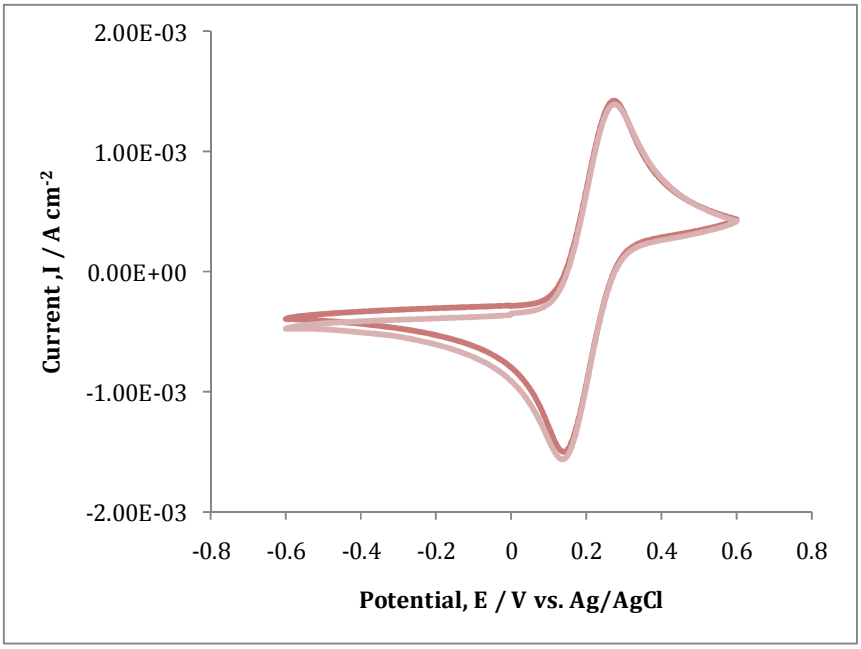


**Figure 6.20:** Cyclic voltammograms of $K_3FeCN_6$ (1.0 x $10^{-2}$ mol $dm^{-3}$) in KCl (0.10 mol $dm^{-3}$). The potential was swept from –0.600 to 0.600 V vs. Ag/AgCl at a scan rate 100 mV $s^{-1}$. Both samples were electrospun at 0.2 mL $h^{-1}$ at 20 kV for 1 min.

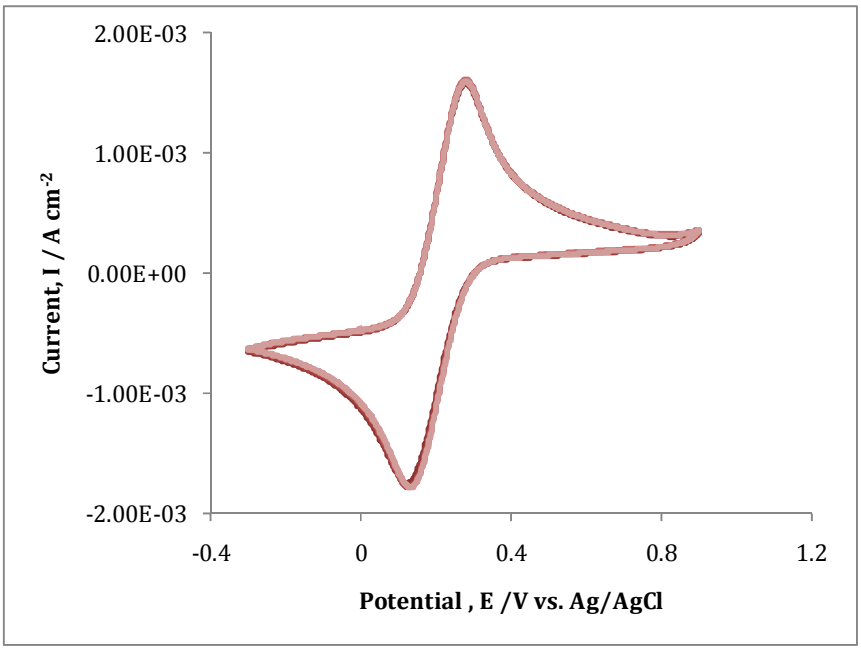


**Figure 6.21:** Cyclic voltammograms of $K_3FeCN_6$ (1.0 x $10^{-2}$ mol $dm^{-3}$) in KCl (1.0 x $10^{-1}$ mol $dm^{-3}$). The potential was swept from –0.300 to 0.900 V vs. Ag/AgCl at a scan rate of 100 mV $s^{-1}$ for 100 cycles. Samples were electrospun from 20 % PLGA in HFIP at 0.2 mL $h^{-1}$ at 20 kV for 1 min. — Cycle 10 — Cycle 90.

In increasing the potential window however, as shown in Figure 6.22, where a sample was swept between -0.300 to 1.100 V vs. Ag/AgCl for 20 cycles at a scan rate of 100 mV $s^{-1}$, all electrochemical activity was lost after 5 cycles. If the nanofibers degraded after 5 cycles, we would expect a corresponding increase in the $FeCN_6^{3-/4-}$ peak currents. This is justified in that a larger surface area of Au mylar should be available for the electrochemical reaction to take place. However, the peak current diminishes until it disappears suggesting that at these high oxidation potentials there is oxidation at the gold and loss of the gold surface from the mylar. This is probably due to the oxygen evolution at the electrode surface affecting the Au coated layer on the mylar. Indeed, this is consistent with the sharp increase in current at potentials higher than about 0.900 V vs. Ag/AgCl, Figure 6.22.

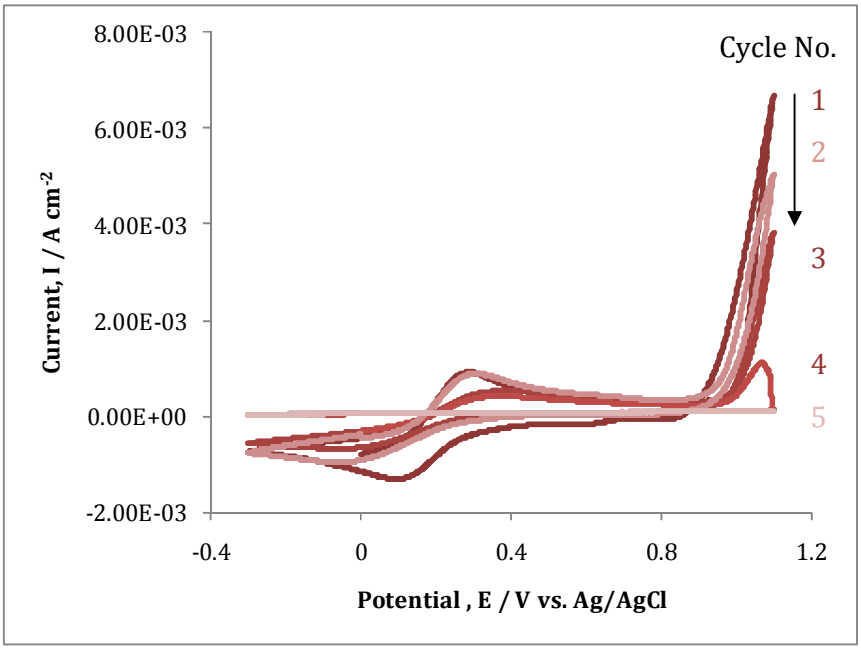


**Figure 6.22:** Cyclic voltammograms of $K_3FeCN_6$ (1.0 x $10^{-2}$ mol $dm^{-3}$) in KCl (1.0 x $10^{-1}$ mol $dm^{-3}$). The potential was swept from –0.300 to 1.100 V vs. Ag/AgCl at a scan rate of 100 mV $s^{-1}$ for 20 cycles. Samples were electrospun from 20 % PLGA in HFIP at 0.2 mL $h^{-1}$ at 20 kV for 1 min.

In Figure 6.23 the influence of the reduction potential is considered where the potential was swept from –1.100 to 0.600 V vs. Ag/AgCl at a scan rate of 100 mV $s^{-1}$ for 20 cycles. This figure shows as the cycle number increases the peak currents also increase. This is possibly due to the occurrence of the hydrogen evolution reaction at more negative potentials which takes place at the electrode surface and destroys the electrospun fibers, therefore giving rise to a greater gold coated surface area which accounts for the increase in the peak currents. Alternatively, the electro-reduction of gold oxides at these negative potentials and the detachment of the fibers may take place leading to a higher surface area of gold.

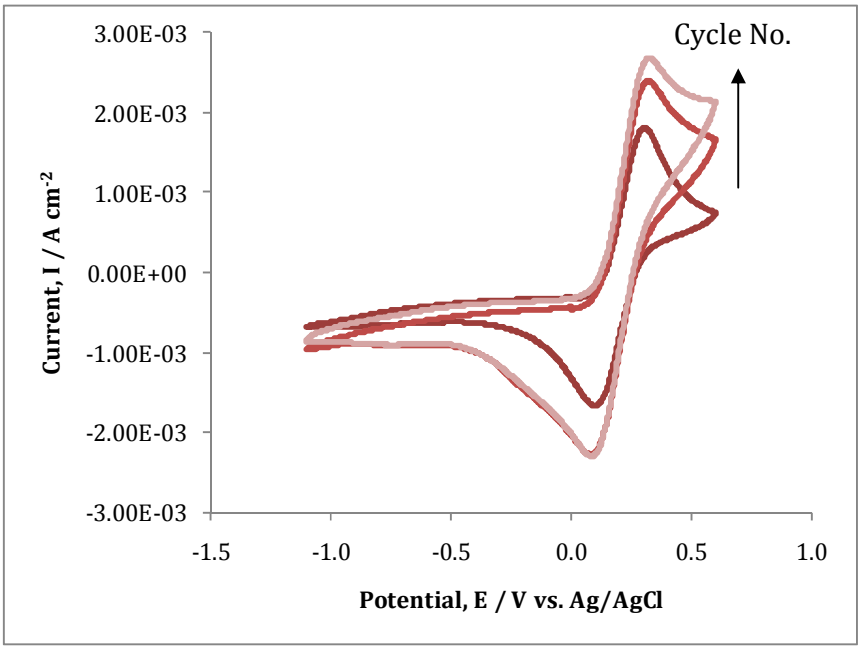


**Figure 6.23:** Cyclic voltammograms of $K_3FeCN_6$ (1.0 x $10^{-2}$ mol $dm^{-3}$) in KCl (0.10 mol $dm^{-3}$). corresponds to cycle 2, cycle 7 and cycle 18. The potential was swept from –1.100 to 0.600 V vs. Ag/AgCl at a scan rate of 100 mV $s^{-1}$ for 20 cycles. Samples were electrospun from 20 % PLGA in HFIP at 0.2 mL $h^{-1}$ at 20 kV for 1 min.

The final analysis was performed to assess the stability of the nanofibers in a 1.0 x $10^{-2}$ mol $dm^{-3}$ ferrocyanide in 0.10 mol $dm^{-3}$ KCl solution over a number of minutes. Samples were prepared and immersed in the solution and the potential

was swept from –0.300 to 0.600 V vs. Ag/AgCl at a scan rate of 100 mV $s^{-1}$ for 20 cycles every 60 min for 480 min. Figure 6.24 presents the results of the peak currents obtained as a function of time. The peak current observed after 60 min is lower than that observed in previous experiments, because a thicker sample was used to monitor the sample over a long period of time. An increase in the peak currents was observed the longer the fibers were left in the solution; this suggests that the adherence of the fibers to the Au mylar is lost as time elapses. The greatest increase in current is observed during the first 180 min of immersion.

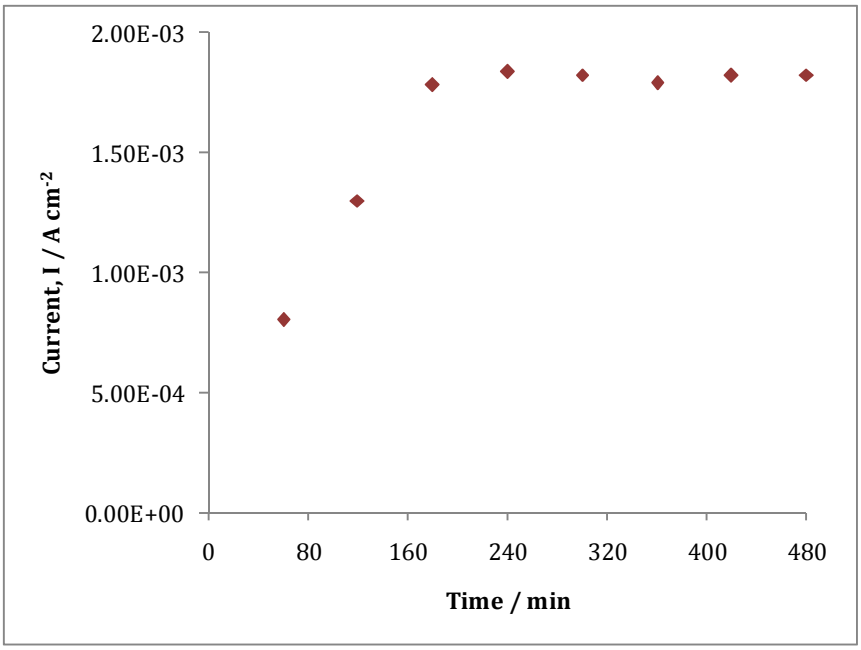


**Figure 6.24:** Peak current as a function of time for electrospun samples immersed and cycled every hour in 1.0 x $10^{-2}$ mol $dm^{-3}$ ferrocyanide in 0.10 mol $dm^{-3}$ KCl. The potential was swept from –0.300 to 0.600 V at a scan rate of 100 mV $s^{-1}$ for 20 cycles.

Overall, the Au mylar substrates with PLGA electrospun fibers are stable in the potential window where Py can be polymerised and the uptake and release of DA can be achieved. The current profiles also show that the non conducting fibers do not inhibit the redox behaviour of the ferrocyanide/ferricyanide system allowing electron transfer to occur at the Au substrate. However, fibers

degrade with time; therefore, the amount of time the fibers are immersed in solution should be kept to a minimum. An investigation into the best technique for the polymerisation of Py onto the fiber mats was performed.

## 6.3.4 Polymerisation of pyrrole onto the nanofibers

### *6.3.4.1 Polymerisation using electrochemical methods*

Many groups have used conducting polymers for a variety of applications, including drug delivery.[9, 45] Conducting polymers are of substantial interest for many biomedical applications and PPy in particular has been shown to be biocompatible and has been used for several of these applications.[9, 46-49] However, polymerisation of Py onto electrospun PLGA fibers is a new approach with only one other group reporting this.[9]

In this section a range of techniques were employed for the electrochemical polymerisation of Py onto the electrospun fibers including CV, galvanostatic and potentiostatic depositions. As shown in Section 6.3.3, there is enough conducting gold interface for the standard redox couple of ferricyanide to occur and therefore enough to electrochemically deposit PPy. The effects of various deposition methods on maintaining the fibrous structure of the PLGA substrates were investigated. All experimental work in this section was performed using electropsun PLGA fiber samples on Au coated mylar, these samples were fabricated from a 20% PLGA in HFIP solution, at a flow rate of 0.2 mL $h^{-1}$, at a distance of 7 cm from the needle to the collector plate and the positive voltage applied to the polymer solution was 20 kV for 1 min. After the preparation of the PLGA fibers, PPy doped with PTS was electrochemically formed on the electrode surfaces. It was observed during the electrochemical polymerisation that PPy nucleated from the Au mylar and grew around the PLGA nanoscale fibers creating a 3D mesh of PPy nanoscale fibers. The polymer formed around the fibrous mat and not from the insulating PLGA electrospun fibers.

Figure 6.25 shows optical images obtained when each technique was employed on the electrospun samples. The corresponding SEM micrographs are shown in

Figure 6.25. In the case of constant current, a current of 1 mA $cm^{-2}$ was applied until 0.5 C was passed. For the constant potential deposition, 0.700 V vs. Ag/AgCl was applied until a sufficient charge of 0.5 C $cm^{-2}$ was passed and for CV deposition, the potential was swept between 0.000 - 0.800 V vs. Ag/AgCl at 50 mV $s^{-1}$, and the cycle number was varied in the range of 5 to 100 cycles. After some preliminary experiments and observations from the optical and SEM analysis of various polymer samples, polymer growth using CV was shown to maintain, to a large extent, the underlying nanofiber structure. Constant potential and constant current methods are known to promote aggressive nucleation of the polymer leading to rapid polymer growth, as shown in Figure 6.26 (B) and (D). Accordingly, the CV method was chosen and used to deposit PPy onto the electrospun fibers in the subsequent experiments.

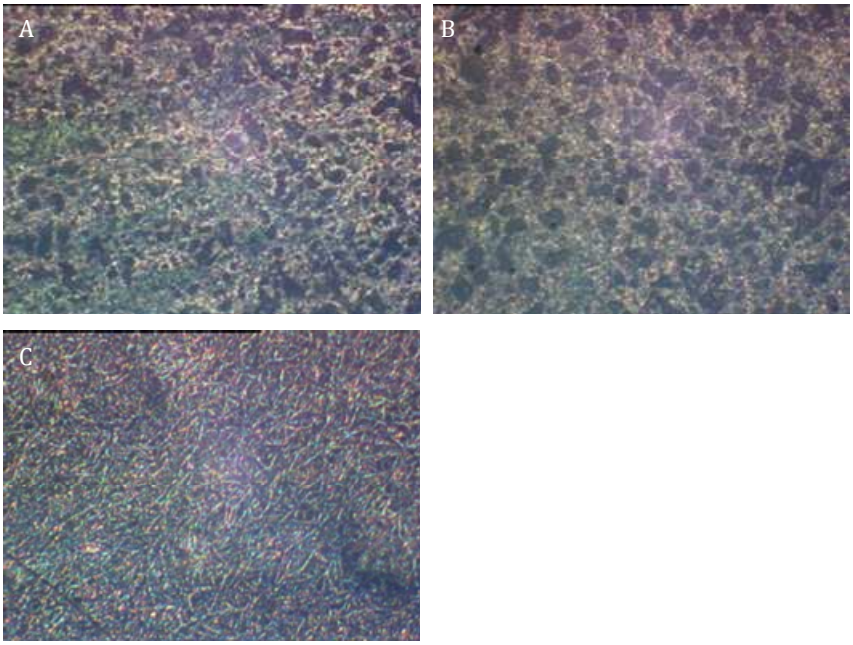


**Figure 6.25:** Optical images obtained from a sample electrospun at 0.2 mL $h^{-1}$ at 20 kV on Au mylar where various electrochemical polymerisation techniques were employed in the presence of 0.2 mol $dm^{-3}$ Py and 0.1 mol $dm^{-3}$ PTS. A) constant current 1 mA $cm^{-2}$ to 0.5 C, B) constant potential of 0.700 V vs. Ag/AgCl to 0.5 C and C) CV growth for 10 cycles where the potential was swept from 0.000 to 0.800 V vs. Ag/AgCl.

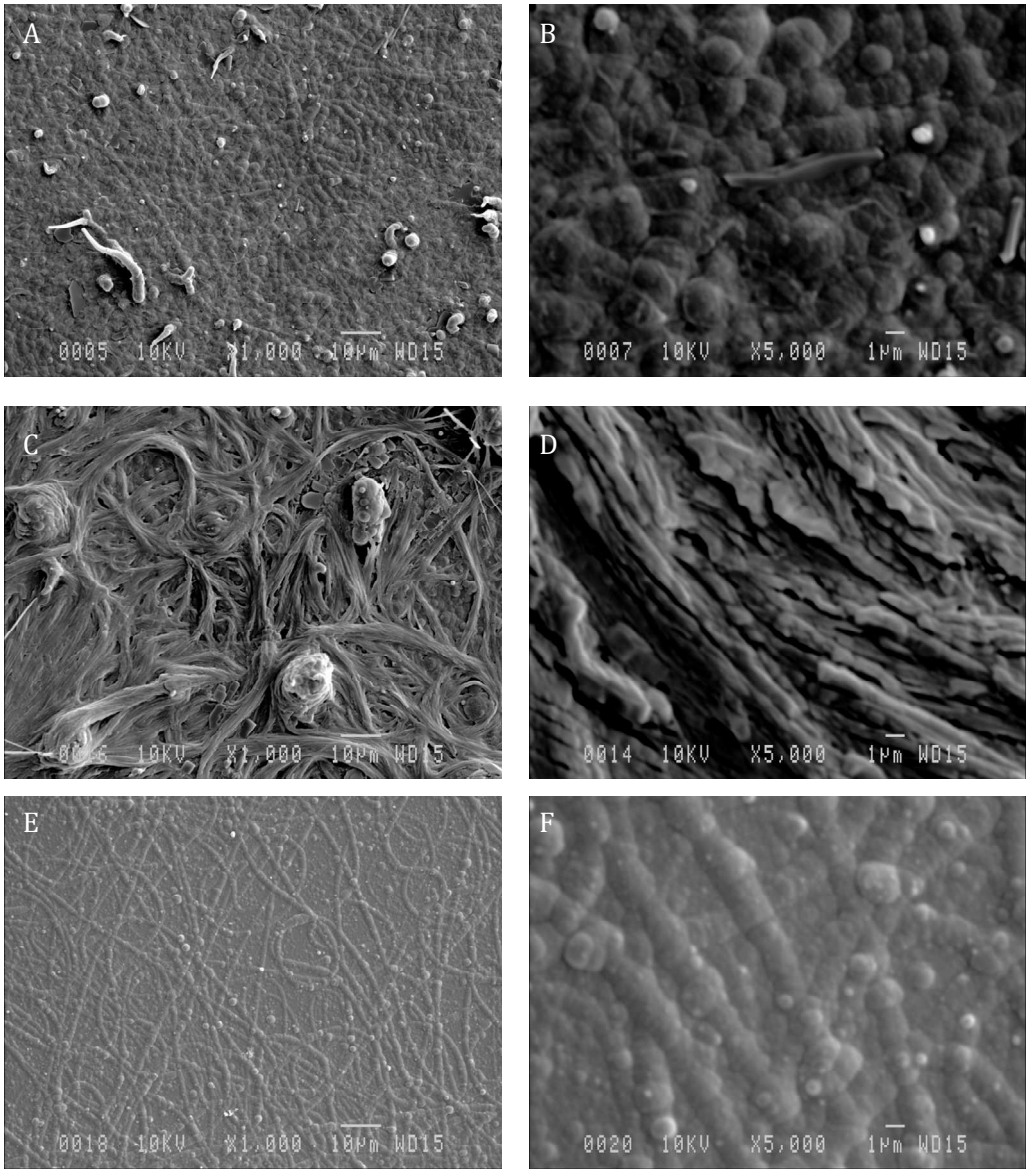


**Figure 6.26:** SEM images of PPy electrochemically deposited on electrospun PLGA fibers using 0.2 mol $dm^{-3}$ Py and 0.1 mol $dm^{-3}$ PTS A) –B) Constant current of 1 mA $cm^{-2}$ to 0.5 C, C) – D) Constant potential of 0.700 V vs. Ag/AgCl to 0.5 C and E) - F) CV growth for 10 cycles where the potential was swept from 0.000 to 0.800 V vs. Ag/AgCl.

### *6.3.4.2 Polymerisation using CV*

To ensure the nanofiber network was maintained PPy was deposited using CV. For the uptake and release of DA, sulfonated β-cyclodextrin was used as the dopant. Figure 6.27 shows a typical plot of current as a function of potential for

the CV polymerisation of Py in the presence of 0.01 mol $dm^{-3}$ Sβ-CD on a sample of electrospun PLGA fibers. The increase of the anodic current at approximately 0.500 V vs. Ag/AgCl is associated with the oxidation of the Py monomer. The current increases with increasing cycle number, indicating the formation of a conducting film, even though the underlying fibers are insulating.

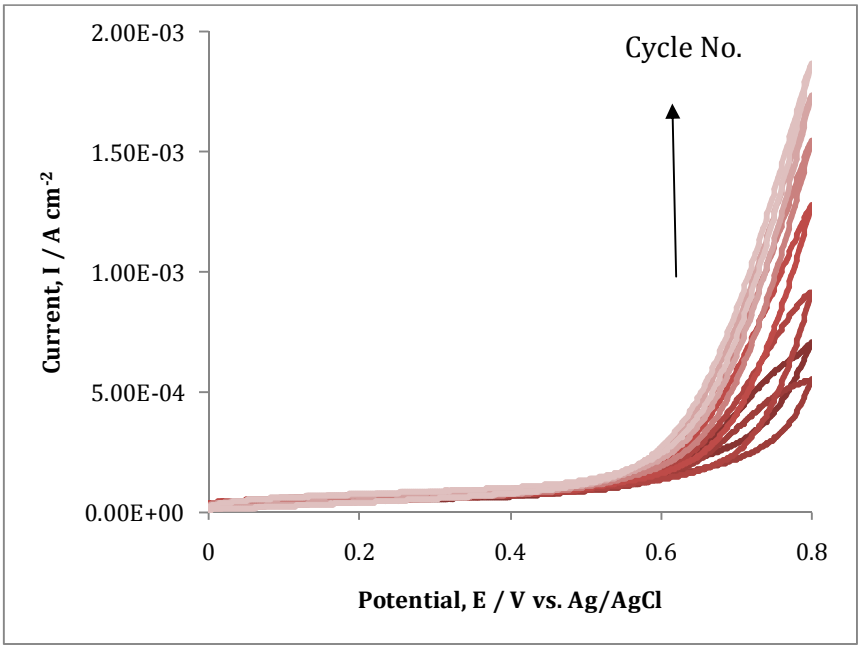


**Figure 6.27:** CV growth of PPy on a sample of PLGA fibers in HFIP electrospun at 0.2 mL $h^{-1}$ at 20 kV on Au mylar in the presence of 0.20 mol $dm^{-3}$ Py and 0.01 mol $dm^{-3}$ Sβ-CD. The potential was swept from 0.000-0.800 V vs. Ag/AgCl at a scan rate of 50 mV $s^{-1}$ for 20 cycles.

Various electrospun samples were taken where PPy was electrodeposited onto the substrates as a function of the cycle number. Optical images were taken before polymerisation and after each subsequent amount of CV growth. Figure 6.28 shows an electrospun sample which was imaged prior to 10 cycles of CV growth and then subsequently imaged again. The sample was further subjected to another 5 cycles of CV growth and imaged. This method was repeated in increments of 5 cycles until 25 cycles of CV growth were obtained. It is clear from these images that the deposition of PPy increases with increasing cycle

number. It is also evident that the nanofiber structure becomes less dominant with increasing amounts of deposited PPy, as highlighted in Figure 6.28 (E).

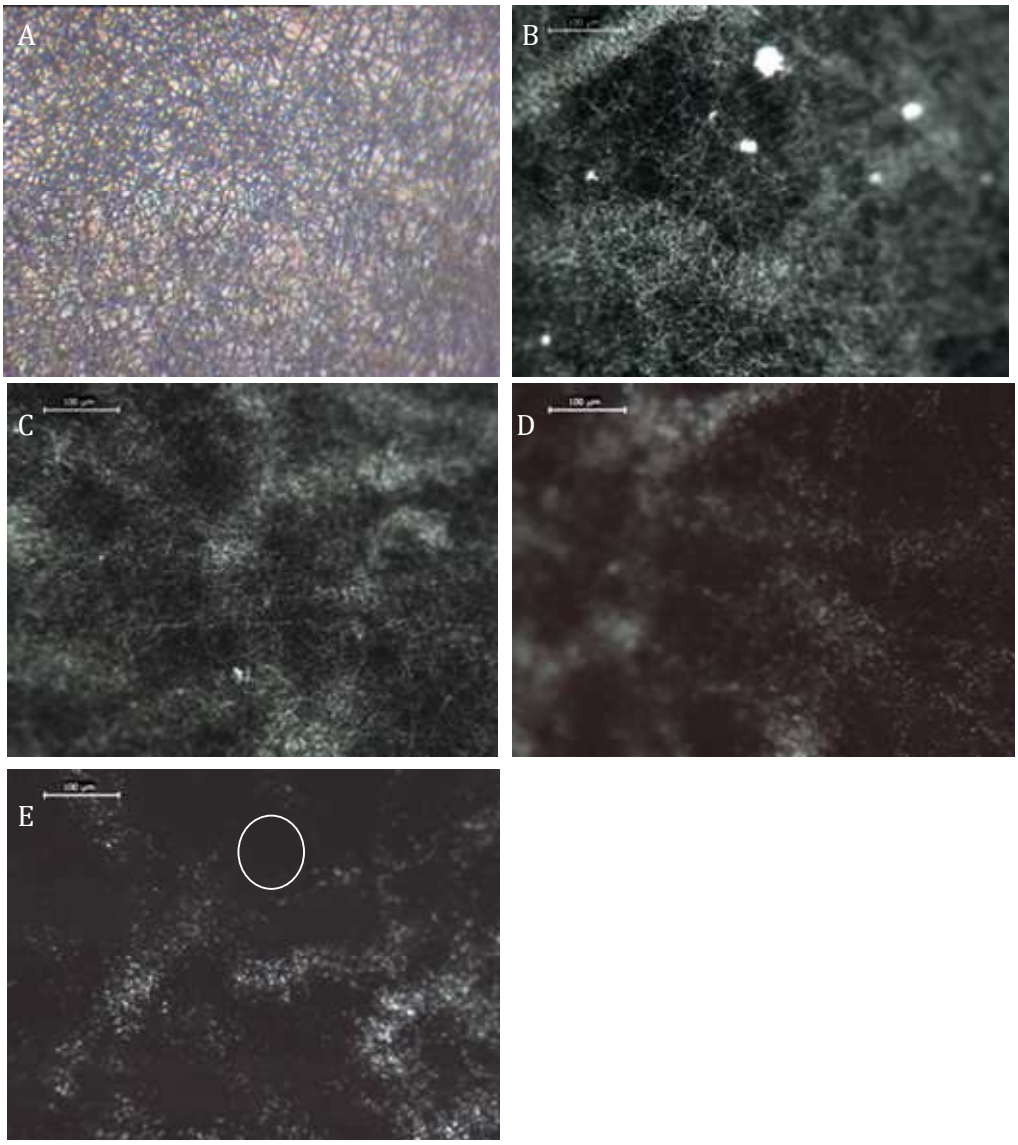


**Figure 6.28:** Optical images of a sample electrospun at 0.2 mL $h^{-1}$ at 20 kV for 1 min on Au mylar where CV growth was obtained in the presence of 0.2 mol $dm^{-3}$ Py and 0.01 mol $dm^{-3}$ Sβ-CD. A) prior to CV growth B) after 10 cycles C) 15 cycles D) 20 cycles and E) 25 cycles of polymer growth and the potential was swept from 0.000 to 0.800 V vs. Ag/AgCl at 50 mV $s^{-1}$.

SEM images of samples of electrospun PLGA with and without PPy are shown in Figure 6.29 and 6.30, respectively. CV growth was performed for a total of 20 cycles using a potential window of 0.000 to 0.800 V vs. Ag/AgCl at 50 mV $s^{-1}$. From the images it can be clearly observed that the nanofiber structure is being maintained, as highlighted in Figure 6.30 (B). The polymer is growing over the fibers. The cauliflower morphology of the PPy was also evident, as highlighted in Figure 6.30 (E).

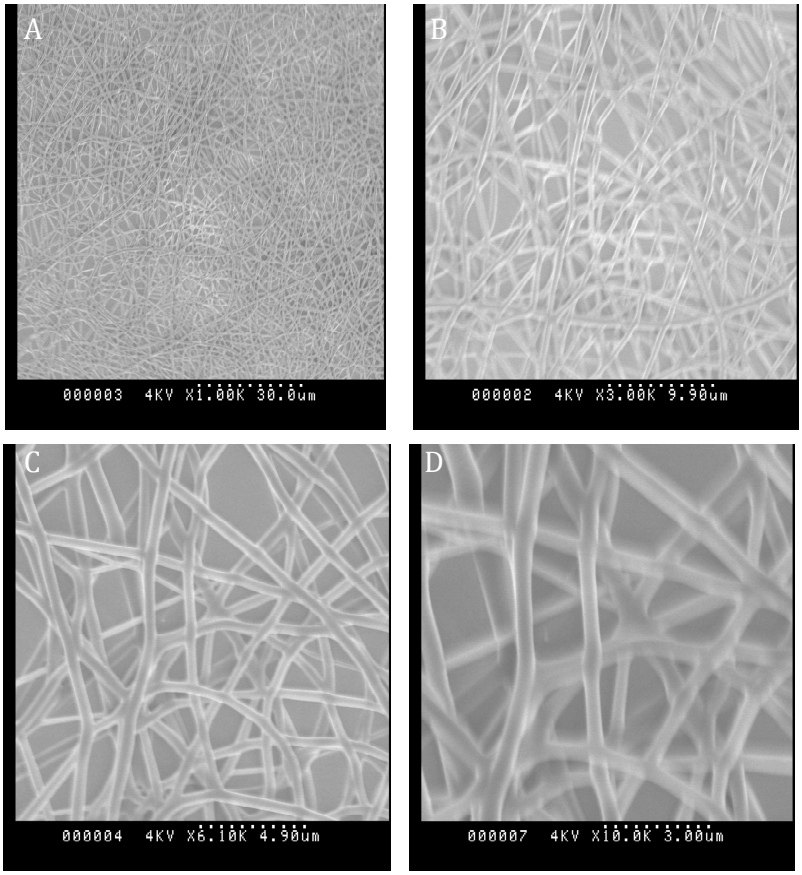


**Figure 6.29:** SEM images at various magnification of electrospun 20% PLGA (50:50) in HFIP at a feeding rate of 0.2 mL $h^{-1}$ at 20 kV for 1 min. A) 1000 B) 3000 C) 6000 D) 10000 magnification.

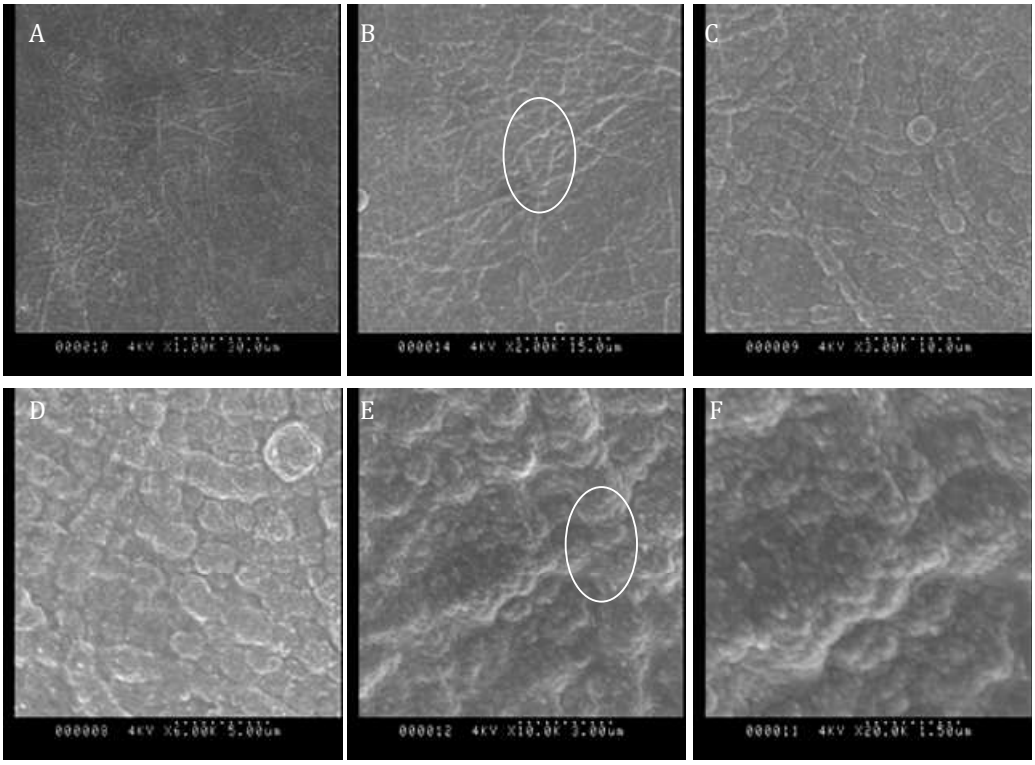


**Figure 6.30:** SEM images at various magnification of electrospun 20% PLGA (50:50) in HFIP at a feeding rate of 0.2 mL $h^{-1}$ at 20 kV for 1 min where PPy was electrodeposited using CV for 20 cycles swept between 0.000-0.800 V vs. Ag/AgCl at 50 mV $s^{-1}$. a) 1000 b) 2000 c) 3000 d) 6000 e) 10000 f) 20000 magnification.

Abidian *et al.*[9] produced conducting polymer nanotubes using PLGA nanofibers as a template. Once the polymers were electropolymerised onto the surface the electrospun fibers were removed by soaking them in DMF.

After investigating three electrochemical methods for the deposition of PPy onto the electrospun mats; another method known as vapour phase polymerisation was examined and compared to the electrochemical approaches.

### *6.3.4.3 Vapour phase polymerisation of pyrrole*

The most common approach in the incorporation of molecules into PPy is during the electrochemical polymerisation process. However, some reports have shown that in industry this can be a slow process and so chemical deposition using vapour phase polymerisation of Py has been investigated.[50] Vapour phase polymerisation was investigated for the chemical deposition of Py. This technique was tried in two ways: (i) the oxidant was added to the electrospinning polymer solution and once the fibers were successfully electrospun, the samples were placed in a chamber containing the monomer solution; (ii) the fibers were electrospun and the oxidant was spin coated onto the sample and the samples were once again placed into the Py monomer chamber.

#### 6.3.4.3.1 Incorporation of the oxidant prior to electrospinning

As outlined in Section 6.2.2.5, 0.5 mL of 20% PLGA (50:50) in HFIP was added to 0.02 mL of the oxidant, 40% Fe(III)/PTS in ethanol. The solution was placed in the syringe and samples were electrospun onto Au mylar. Figure 6.31 shows two optical images; both samples were electrospun at a distance of ~7 cm, image (A) was electrospun at 0.5 mL $h^{-1}$ at 15 kV and image (B) was electrospun at 1 mL $h^{-1}$ at an applied voltage of 18 kV.

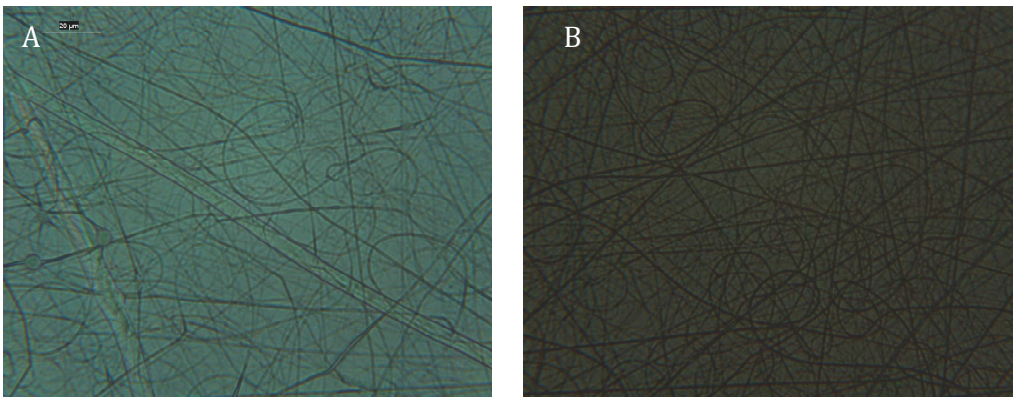


**Figure 6.31:** Optical images of electrospun PLGA in HFIP in the presence of the oxidant 40% Fe(III)/PTS in ethanol A) at 0.5 mL $h^{-1}$ at 15 kV B) 1 mL $h^{-1}$ at 18 kV.

These electrospun samples were then placed in a monomer chamber containing 3 mL of the Py monomer for 30 min to allow vapour phase polymerisation of Py to occur. After polymerisation the samples were washed in ethanol for 20 min to eliminate any excess oxidant. Figure 6.32 shows SEM micrographs of the samples. Figure 6.32 (A) shows a SEM of the electrospun fibers from the PLGA/oxidant solution at 0.5 mL $h^{-1}$ at 15 kV prior to vapour phase polymerisation. Figure 6.33 (B) shows a SEM image after 30 min of vapour phase and washing in ethanol for 20 min. There are particles present which represent the crystals formed from the evaporation of the oxidant. It is essential that once the fibers are electrospun they are placed straight into the monomer chamber. From Figure 6.32 (A) the electrospun fibers obtained are extremely promising especially after the addition of the oxidant. These images were used to try to confirm the growth of PPy. However, from these preliminary experiments it was hard to say if PPy was present, or if only shorter chain oligomers were formed.

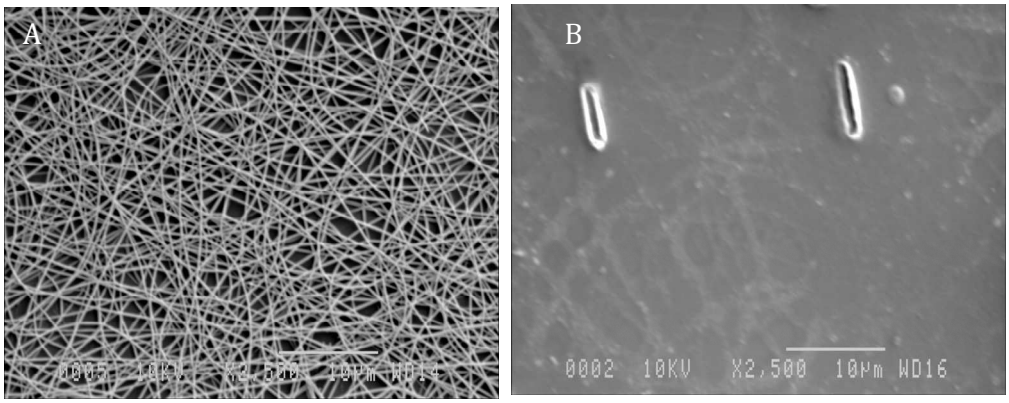


**Figure 6.32:** SEM image of electrospun PLGA in HFIP with the oxidant at 0.5 mL $h^{-1}$ at 15 kV A) prior to vapor phase polymerisation. B) after 30 min vapor phase polymerisation and 20 min washing with ethanol.

#### 6.3.4.3.2 Vapour phase polymerisation on previously electrospun PLGA fibers

The second attempt of vapour phase polymerisation of Py included the spin coating of the oxidant, 40% Fe(III)/PTS in ethanol, onto previously electrospun samples of 20 % PLGA in HFIP. The samples were then placed into the monomer chamber containing Py for 20 min, removed and left to dry before washing with ethanol for 20 min.

Figure 6.33 shows optical images of 5 min electrospun PLGA fibers before and after 20 min vapour phase polymerisation and washing in ethanol. It is evident that the fibers are not present after the vapour phase process. A valid reason for this is the fact that at a rotation speed of 1000 rpm during the spin coating of the oxidant, the adherence of the fibers on the Au mylar substrate is lost and all that is left is the flat Au mylar surface. This is also evident in the sample shown in Figure 6.34. This sample was electrospun for 10 min and the same procedures were carried out. In Figure 6.34 (B) the presence of some fibers are highlighted however, the SEM image (C) shows lines of crystal structures which could be attributed to the crystallisation of the oxidant.

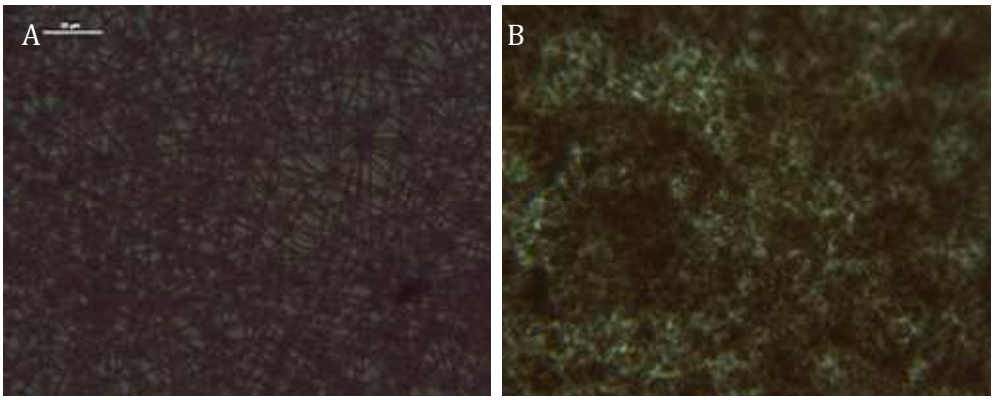


**Figure 6.33:** Optical images of an electrospun 20 % PLGA fiber sample in HFIP for 5 min at a feeding rate of 0.2 mL $h^{-1}$ and an applied potential of 20 kV and a distance of ~ 7 cm (A) prior to and (B) after 20 min vapour phase polymerisation and 20 min washing with ethanol.

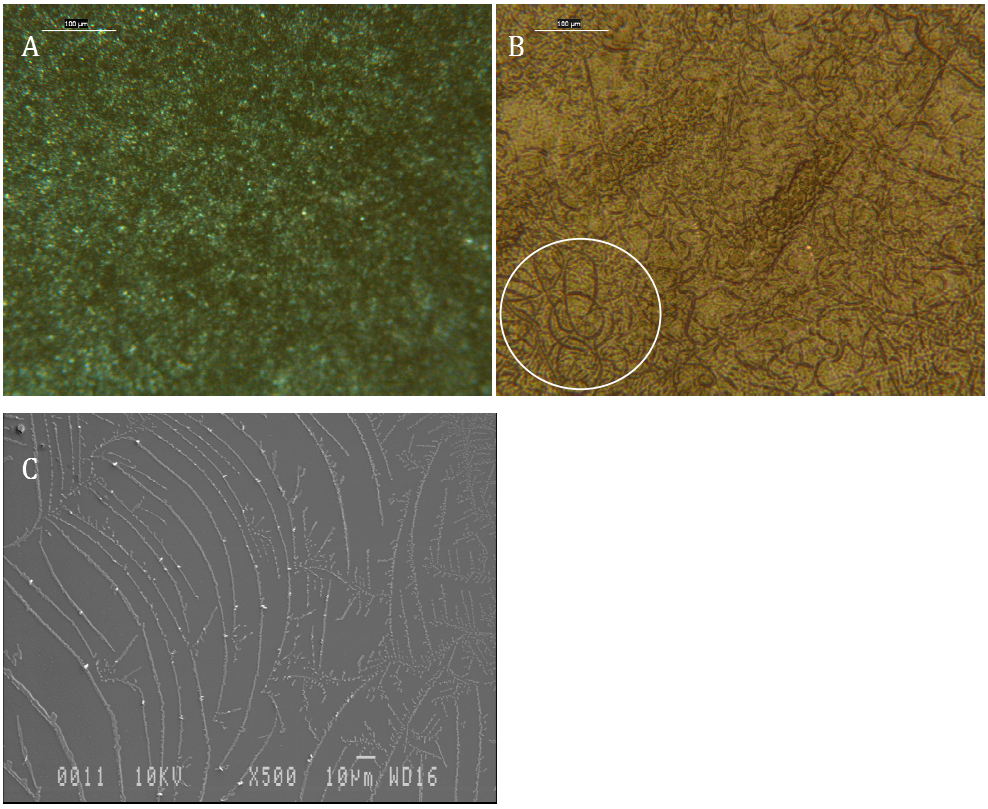


**Figure 6.34:** Optical and SEM images of an electrospun 20 % PLGA fiber sample in HFIP for 10 min at a feeding rate of 0.2 mL $h^{-1}$ and an applied potential of 20 kV and a distance of ~ 7 cm (A) prior to and (B) after 20 min vapour phase polymerisation and 20 min washing with ethanol. (C) SEM image after 20 min vapour phase polymerisation of Py and washing in ethanol.

Cyclic voltammetry is often used to study conducting polymer films. This technique is widely used for investigating the electroactivity of conducting polymers as it follows the electron transfer.[51] Therefore, the CV technique was used to determine if PPy was formed during the vapour phase polymerisation. Electrospun samples after the vapour phase polymerisation step were placed in a three electrode set up in the presence of 0.1 mol $dm^{-3}$ $Na_2SO_4$. In order to observe the redox potentials of PPy the potential was swept from -0.800 to 0.800 V vs. Ag/AgCl at 50 mV $s^{-1}$ for 20 cycles. In Figure 6.35, the CV shows two redox peaks, an oxidation peak at 0.094 V vs. Ag/AgCl and a reduction peak at -0.496 V vs. Ag/AgCl which can be related to the PPy matrix. These values are

similar to values obtained in the literature. However, the signals were lost as the cycle number increased. This indicates a loss in the conducting properties of the deposited PPy. However, these data confirm the presence of polypyrrole.

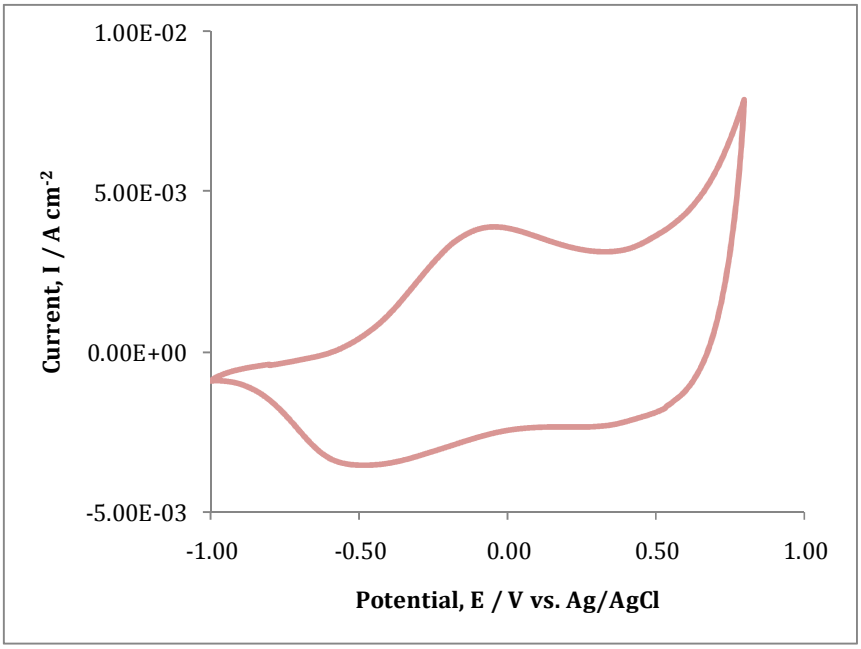


**Figure 6.35:** CV data of an electrospun 20 % PLGA fiber sample in HFIP at a feeding rate of 0.2 mL $h^{-1}$ and an applied potential of 20 kV and a distance of ~ 7 cm after 20 min vapour phase polymerisation washing in ethanol. Samples were cycled in 0.1 mol $dm^{-3}$ $Na_2SO_4$ from -0.800 to 0.800 V vs. Ag/AgCl at 50 mV $s^{-1}$.

Clearly, this vapour phase technique has the potential to deposit the polymer either prior to or after electrospinning. However, one significant problem was loss of the fibers upon spin coating of the oxidant at the high rotation speeds. As well as that, the amount of polymer deposited was not consistent. Due to the inconsistency of this method, PPy polymers used in the uptake and release of DA were generated using cyclic voltammetry from a pyrrole-sulfonated β-cyclodextrin solution. All parameters were kept as described in Section 6.3.4.2 where the number of cycles was varied. For comparative studies polymers were electrochemically synthesised on bare Au mylar to investigate if the presence of the electrospun PLGA nanofibers had an influence on the amount of DA released from the system.

### 6.3.5 Incorporation and release of DA

It has been documented that a promising characteristic of conducting polymers is their ability to use their redox properties to incorporate and release ions under applied potentials.[50, 52-54] Due to this characteristic the polymer films can be used to deliver small amounts of DA as described in Chapter 4. With the addition of the PLGA nanofibers two types of delivery could be achieved, firstly through degradation of the PLGA network which could potentially lead to the overall degradation of the polymer matrix and subsequent release of the DA. Secondly, and the technique that was examined here, by actively applying the redox properties to the drug loaded polymer matrices using an applied potential. Using UV-visible spectroscopy, the release profile of DA was monitored. As previously demonstrated in Chapter 4, DA absorbs at $\lambda_{max}$ = 280 nm.

Once the electrospun fibers with deposited PPy doped with Sβ-CD had been prepared, these polymers were investigated for the uptake and release of DA. As illustrated in Figure 6.36 during the reduction of the PPy-CD polymer matrix the cationic DA is injected into the polymer and the negative charges of the immobilised cyclodextrin are compensated. Here, overall charge neutrality is maintained. Upon application of a positive potential the positively charged DA molecules are expelled into the solution. [55, 56]

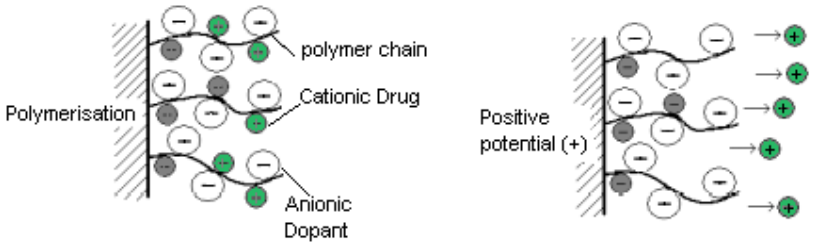


**Figure 6.36:** Schematic of the concept of the DA uptake and release.

### *6.3.5.1 Uptake and release of DA using electrochemical means*

Figure 6.37, shows UV spectra for the release of DA from a sample where PPy was deposited onto the electrospun PLGA nanofibers using CV for 30 cycles. In this case a potential of 0.100 V vs. Ag/AgCl was applied to the sample in order to release the DA. This figure illustrates that the amount of DA released increases over time upon an application of an oxidation potential.

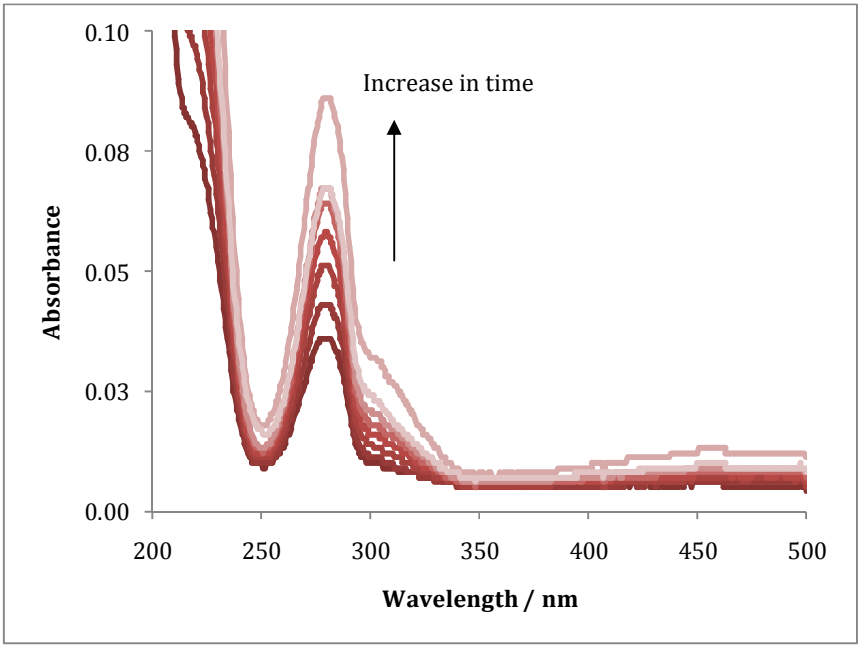


**Figure 6.37:** Absorbance as a function of wavelength of the release of DA upon application of 0.100 V vs. Ag/AgCl over a 2 h period on a sample where PLGA was electrospun at 0.2 mL $h^{-1}$ at 20 kV for 1 min and PPy was electrochemically deposited using CV for 30 cycles.

In Figure 6.38 the release profiles are expressed as a function of time. In all cases, PPy was electrochemically formed using CV growth swept between 0.000-0.800 V vs. Ag/AgCl at 50 mV $s^{-1}$ for 30 cycles. PPy was also deposited onto a bare Au mylar electrode for comparison. From the results it can be clearly seen that the presence of the nanofibers on the substrate increases the amount of DA incorporated and subsequently released.

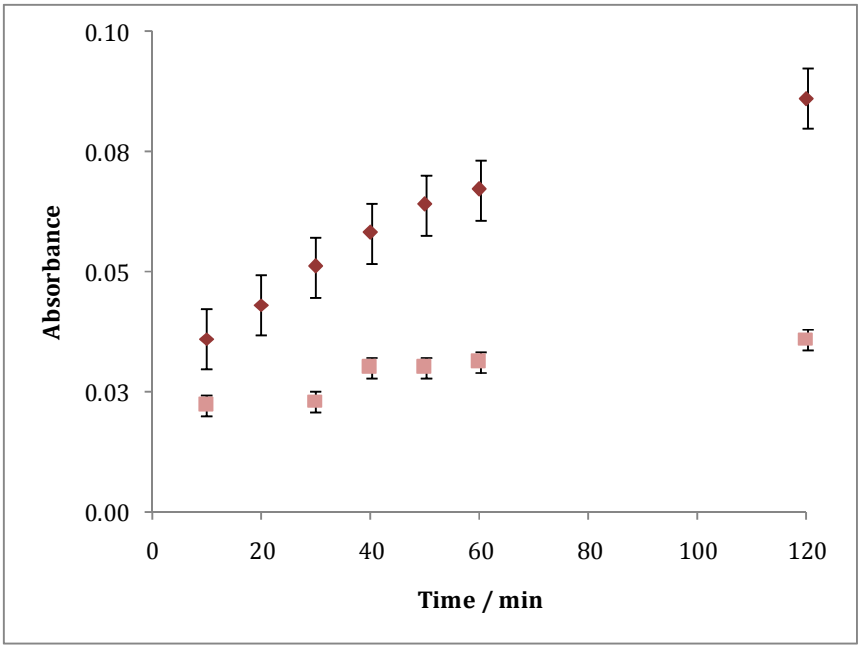


**Figure 6.38:** Absorbance as a function of time for the release of DA at 0.100 V vs. Ag/AgCl for 2 h where PPy was electrodeposited in the presence of 0.2 mol $dm^{-3}$ Py and 0.01 mol $dm^{-3}$ Sβ-CD for 30 cycles of CV growth at a potential of 0.000-0.800 V vs. Ag/AgCl and at a scan rate of 50 mV $s^{-1}$ on ♦ Electrospun PLGA present ■ Bare Au.

In Figure 6.39 the maximum absorbance of DA at 280 nm after 120 min of applying an oxidation potential was recorded and plotted as a function of the number of cycles applied during polymerisation. In each case all the parameters were the same except for the number of cycles applied during CV growth. An application of an oxidation potential of 0.100 V vs. Ag/AgCl over 120 min was applied in order to release the DA. Again in all cases the samples where PLGA fibers were present show a greater release for DA. For some reason the polymer grown to 30 cycles observed the best release profile. This is probably related to the fact that with further cycles more PPy is electrochemically deposited and the nanofiber structure is lost. At this point the deposited polymer has the characteristic cauliflower structure and gives a DA release profile similar to pure PPy, as shown at 50 cycles, Figure 6.39.

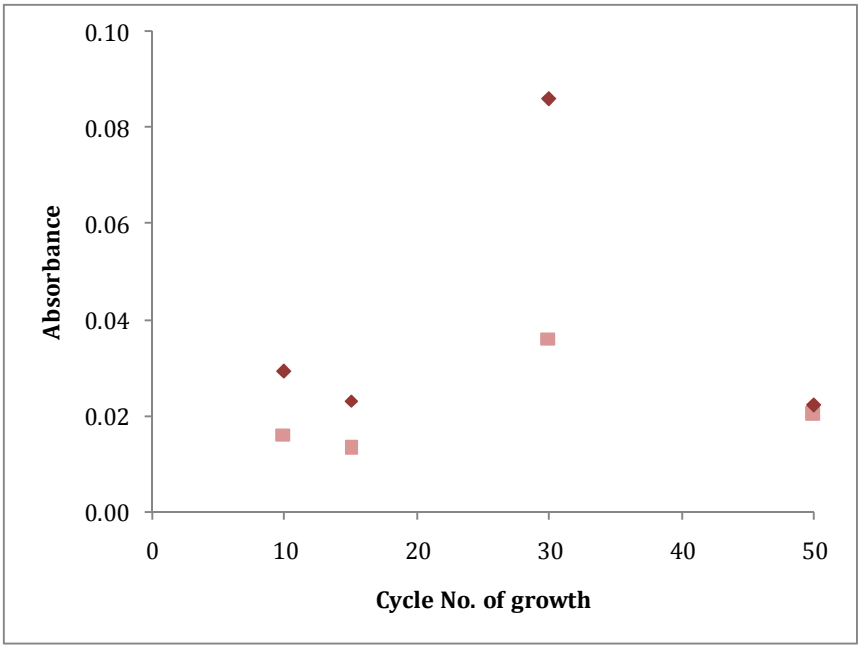


**Figure 6.39:** The absorbance of DA at 280 nm as a function of the number of cycles applied during polymerisation of PPy. PPy was electrodeposited in the presence of 0.2 mol $dm^{-3}$ Py and 0.01 mol $dm^{-3}$ Sβ-CD on ♦ Electrospun PLGA present ■ Bare Au.

It is interesting to note that the release profile at 50 cycles for PPy deposited onto both the bare Au mylar and the PLGA fiber coated substrate give very similar release profiles. This is more clearly shown in Figure 6.40 where the PPy gold and PPy fiber gold electrodes are compared for the release of DA. In both cases the polymer was grown using 50 cycles between 0.000 and 0.800 V vs. Ag/AgCl. Similar absorbance values are recorded for both electrodes, showing no difference between the release profiles.

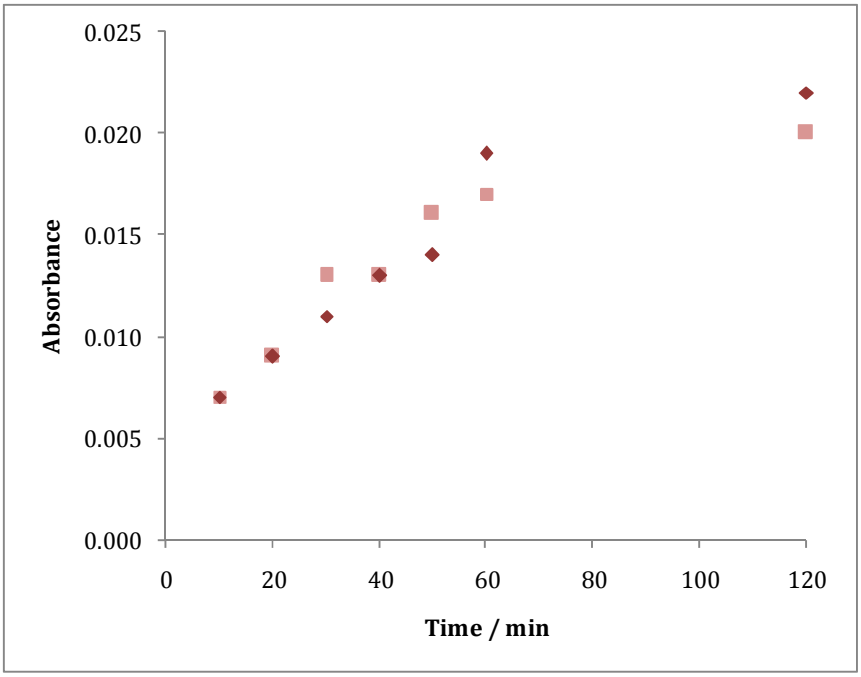


**Figure 6.40:** Absorbance as a function of time for the release of DA at 0.100 V vs. Ag/AgCl for 120 min where PPy was electrodeposited in the presence of 0.2 mol $dm^{-3}$ Py and 0.01 mol $dm^{-3}$ Sβ-CD for 50 cycles of CV growth at a potential of 0.000-0.800 V and a scan rate of 50 mV $s^{-1}$ on ♦ Electrospun PLGA present ■ Bare Au.

### *6.3.5.2 Comparison of applying a potential for release*

Another experiment attempted was the release of DA over time without the use of electrochemical stimulation in order to evaluate how much more DA is being released with the application of an oxidation potential.

In the results shown in Figure 6.41 both polymers were grown on electrospun fibers using CV growth for 30 cycles where once again the potential was swept between 0.000-0.800 V vs. Ag/AgCl at 50 mV $s^{-1}$. The normal incorporation and washing procedures were applied in both cases, however, in terms of release the results shown are where an applied potential of 0.100 V vs. Ag/AgCl and no electrical stimulation was applied over 120 min. From these data, the significance of the electrical stimulation is apparent and it clearly shows the benefit in applying stimulation instead of relying on slow release to take place, confirming that electrical stimulation is an important factor in the release of the

drug from the polymer. It is also interesting to note that the rate of release is slower in when no potential is applied in comparison to the application of an electrical stimulation. This result was also observed in the bulk system discussed in Chapter 4, Section 4.3.4.3.

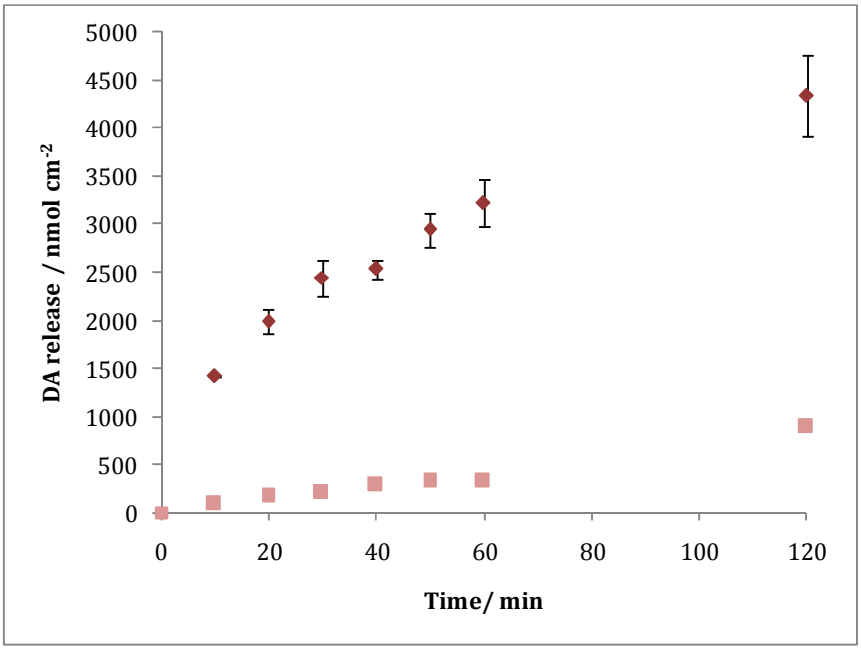


**Figure 6.41:** The release of DA monitored at 280 nm as a function time. The DA was released using ♦ 0.100 V vs. Ag/AgCl ▪ no electrochemical stimulation over 120 min.

In order to calculate the amount of DA being released the calibration curve and subsequent equation demonstrated in Chapter 2 was used. The concentration of DA was evaluated and expressed in nmol $cm^{-2}$. The amount of DA released upon applying a potential in comparison to no potential was 4335 to 887 nmol $cm^{-2}$, respectively. This corresponds to a 79.52 % increase in the release of the drug when the electrical stimulation was applied. As shown in Chapter 4, similar results were obtained for the bulk system.

Abidan *et al.*[9] demonstrated the release of dexamethasone (DEX) from electrospun PLGA nanofibers covered with an electroactive polymer, poly(3,4-

rthylenedioxythiophene), (PEDOT). In monitoring the drug release of the DEX, the electrospun fibers were removed or allowed to slowly degrade, where, the PEDOT maintained its nanofibrous structure. They observed a significant increase in the amount of drug released when an electrical stimulation was applied in comparison to no potential. This verifies the point made in Chapter 4 and by other authors[53], that the application of an applied potential presents a way of controlling the release of the drug.

### *6.3.5.3 Comparing the release of DA*

It is clear from Figure 6.38 that the nanofiber substrate provides better release of DA. However, with the increasing amounts of PPy, this enhancement is lost, as observed from the data shown in Figure 6.40, where DA release was monitored from PPy films electrochemically deposited for 50 cycles in the presence and absence of electrospun fibers substrates. Figure 6.42 summaries data obtained from bare Au coated mylar samples (no electrospun PLGA), where PPy was electrochemically deposited using CV at 50 mV $s^{-1}$.

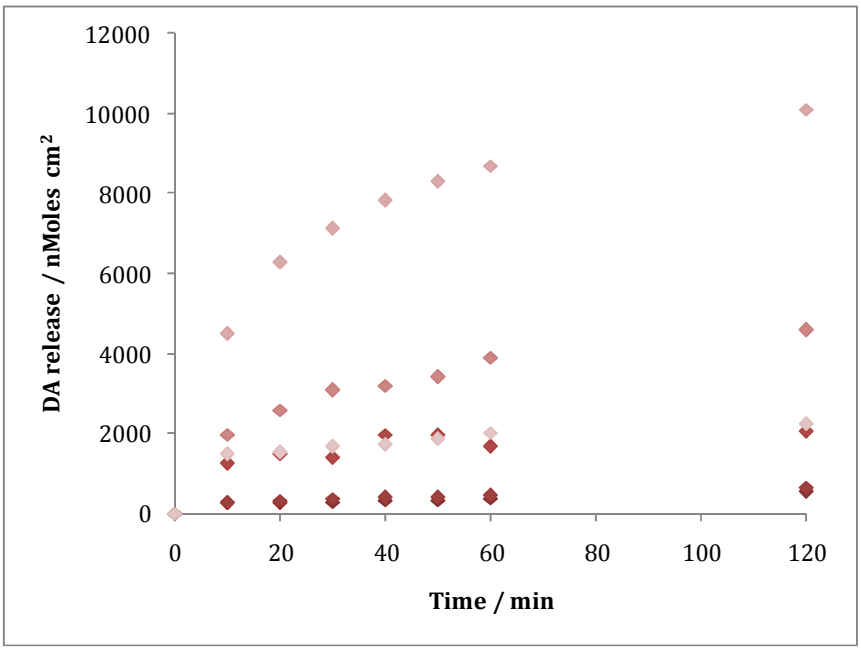


**Figure 6.42:** The amount of DA release upon applying 0.100 V vs. Ag/AgCl for 120 min as a function of time from polymers generated using CV where the amount of cycles was varied. Cycles of PPy growth were ♦5, ♦10, ♦20, ♦30, ♦and 50 at 50 mV $s^{-1}$.

This figure demonstrates what was shown, previously, in Chapter 4 that as the thickness, or the amount, of polymer on the working electrode increased; an increase in the amount of DA released was obtained. This makes a direct comparison of the results obtained in this chapter with Chapter 4 impossible. However, it can be concluded that the PLGA nanofibers give rise to a higher release of DA.

## 6.4 Summary of results

Neat chloroform is not a suitable solvent for the electrospinning of PLGA (50:50). The voltage applied during the formation of fibers has a significant affect on the amount of fibers produced. As the voltage is increased more fibers are formed therefore giving thicker films on the substrate. Also, if an increase in flow rate is applied during electrospinning more beading is observed. The collector plate has a significant affect on the samples taken in terms of beading. In the case of the 20 % PLGA in HFIP beading was observed when samples were collected on a glass slide but when samples were collected on Au coated mylar bead formation was reduced substantially.

Investigation by CV of PLGA fibers indicates that this material exhibits good electronic properties. Film thickness and voltage applied in forming the nanostructured material have a significant affect on the electrochemistry of the samples. The application of oxidation potentials above 1.100 V shows a significant affect on the redox properties of the substrate and leads to the loss of gold from the gold coated mylar substrate. The application of low reduction potentials increases the amount of hydrogen evolution and therefore, an increase in the oxidation peak currents were observed due to the loss of the fibers from the electrode surface. The stability of the PLGA fibers on the Au mylar decreases significantly over time when left immersed in the electrolyte solution.

PPy can successfully be electrochemically polymerised onto the nanofibers using various techniques; however, it was confirmed that CV growth was the

best technique in maintaining the nanostructured material. DA was successfully incorporated and released from the polymer composite of nanofibers and PPy. UV-visible spectroscopy was a feasible technique to monitor the release. It was also confirmed that the application of an electrical stimulation to the drug-incorporated polymers released ~80 % more drug than allowing the drug to undergo slow release. Electrospun PLGA nanofibers have been successfully used as substrates for the polymerisation of PPy and subsequently the uptake and release of DA. It is also evident that an increase of the DA release was obtained in the presence of the electrospun PLGA fiber/PPy matrix.

## 6.5 References


1. A. Greiner and J. H. Wendorff, *Angew Chem Int Edit*, **46**, (2007), 5670-5703.
2. W. J. Li, C. T. Laurencin, E. J. Caterson, R. S. Tuan, and F. K. Ko, *J Biomed Mater Res*, **60**, (2002), 613-621.
3. H. Yoshimoto, Y. M. Shin, H. Terai, and J. P. Vacanti, *Biomaterials*, **24**, (2003), 2077-2082.
4. Y. You, B. M. Min, S. J. Lee, T. S. Lee, and W. H. Park, *J Appl Polym Sci*, **95**, (2005), 193-200.
5. J. M. Anderson and M. S. Shive, *Adv Drug Deliver Rev*, **28**, (1997), 5-24.
6. C. L. He, Z. M. Huang, X. J. Han, L. Liu, H. S. Zhang, and L. S. Chen, *J Macromol Sci B*, **45**, (2006), 515-524.
7. H. L. Jiang, D. F. Fang, B. J. Hsiao, B. J. Chu, and W. L. Chen, *J Biomat Sci-Polym E*, **15**, (2004), 279-296.
8. K. Kim, Y. K. Luu, C. Chang, D. F. Fang, B. S. Hsiao, B. Chu, and M. Hadjiargyrou, *J Control Release*, **98**, (2004), 47-56.
9. M. R. Abidian, D. H. Kim, and D. C. Martin, *Adv Mater*, **18**, (2006), 405-409.
10. Z. Zhang, R. Roy, F. J. Dugre, D. Tessier, and L. H. Dao, *J Biomed Mater Res*, **57**, (2001), 63-71.
11. M. Garinot, V. Fievez, V. Pourcelle, F. Stoffelbach, A. des Rieux, L. Plapied, I. Theate, H. Freichels, C. Jerome, J. Marchand-Brynaert, Y. J. Schneider, and V. Preat, *J Control Release*, **120**, (2007), 195-204.
12. D. Luo, K. Woodrow-Mumford, N. Belcheva, and W. M. Saltzman, *Pharmaceut Res*, **16**, (1999), 1300-1308.

13. X. H. Zong, S. Li, E. Chen, B. Garlick, K. S. Kim, D. F. Fang, J. Chiu, T. Zimmerman, C. Brathwaite, B. S. Hsiao, and B. Chu, *Ann Surg*, **240**, (2004), 910-915.
14. W. W. Zuo, M. F. Zhu, W. Yang, H. Yu, Y. M. Chen, and Y. Zhang, *Polym. Eng. Sci.*, **45**, (2005), 704-709.
15. H. Fong, I. Chun, and D. H. Reneker, *Polymer*, **40**, (1999), 4585-4592.
16. F. Vollrath and D. T. Edmonds, *Nature*, **340**, (1989), 305-307.
17. J. Doshi and D. H. Reneker, *J Electrostat*, **35**, (1995), 151-160.
18. D. H. Reneker, A. L. Yarin, H. Fong, and S. Koombhongse, *J Appl Phys*, **87**, (2000), 4531-4547.
19. Y. M. Shin, M. M. Hohman, M. P. Brenner, and G. C. Rutledge, *Appl Phys Lett*, **78**, (2001), 1149-1151.
20. G. I. Taylor, *Proc. Roy. Soc. Lond.*, **A313**, (1969), 453-475.
21. T. Subbiah, G. S. Bhat, R. W. Tock, S. Pararneswaran, and S. S. Ramkumar, *J Appl Polym Sci*, **96**, (2005), 557-569.
22. K. H. Lee, H. Y. Kim, H. J. Bang, Y. H. Jung, and S. G. Lee, *Polymer*, **44**, (2003), 4029-4034.
23. J. M. Deitzel, J. Kleinmeyer, D. Harris, and N. C. B. Tan, *Polymer*, **42**, (2001), 261-272.
24. X. Y. Geng, O. H. Kwon, and J. H. Jang, *Biomaterials*, **26**, (2005), 5427-5432.
25. D. Li and Y. N. Xia, *Adv Mater*, **16**, (2004), 1151-1170.
26. N. Li, X.-H. Qin, L. Lin, and S.-Y. Wang, *Polym. Eng. Sci.*, **48**, (2008), 2362-2366.
27. P. Baumgart, *J Colloid Interf Sci*, **36**, (1971), 71-&.
28. X. H. Zong, K. Kim, D. F. Fang, S. F. Ran, B. S. Hsiao, and B. Chu, *Polymer*, **43**, (2002), 4403-4412.
29. R. V. N. Krishnappa, K. Desai, and C. M. Sung, *J Mater Sci*, **38**, (2003), 2357-2365.
30. Y. You, S. J. Lee, B. M. Min, and W. H. Park, *J Appl Polym Sci*, **99**, (2006), 1214-1221.
31. J. Shawon and C. M. Sung, *J Mater Sci*, **39**, (2004), 4605-4613.
32. W. K. Son, J. H. Youk, T. S. Lee, and W. H. Park, *J Polym Sci Pol Phys*, **42**, (2004), 5-11.
33. H. Q. Liu and Y. L. Hsieh, *J Polym Sci Pol Phys*, **40**, (2002), 2119-2129.
34. Z. Jing, X. Y. Xu, X. S. Chen, Q. Z. Liang, X. C. Bian, L. X. Yang, and X. B. Jing, *J Control Release*, **92**, (2003), 227-231.
35. E. R. Kenawy, F. I. Abdel-Hay, M. H. El-Newehy, and G. E. Wnek, *Mat Sci Eng a-Struct*, **459**, (2007), 390-396.

36. M. Y. Li, Y. Guo, Y. Wei, A. G. MacDiarmid, and P. I. Lelkes, *Biomaterials*, **27**, (2006), 2705-2715.
37. Y. Z. Zhang, C. T. Lim, S. Ramakrishna, and Z. M. Huang, *J Mater Sci-Mater M*, **16**, (2005), 933-946.
38. M. S. Khil, D. I. Cha, H. Y. Kim, I. S. Kim, and N. Bhattarai, *J Biomed Mater Res B*, **67B**, (2003), 675-679.
39. E. R. Kenawy, G. L. Bowlin, K. Mansfield, J. Layman, D. G. Simpson, E. H. Sanders, and G. E. Wnek, *J Control Release*, **81**, (2002), 57-64.
40. Y. L. Liao, L. F. Zhang, Y. Gao, Z. T. Zhu, and H. Fong, *Polymer*, **49**, (2008), 5294-5299.
41. S. Geetha, C. R. K. Rao, M. Vijayan, and D. C. Trivedi, *Anal Chim Acta*, **568**, (2006), 119-125.
42. R. Wadhwa, C. F. Lagenaur, and X. T. Cui, *J Control Release*, **110**, (2006), 531-541.
43. J. Wang, B. Z. Zeng, C. Fang, and X. Y. Zhou, *J Electroanal Chem*, **484**, (2000), 88-92.
44. J. Q. Liu, A. Chou, W. Rahmat, M. N. Paddon-Row, and J. J. Gooding, *Electroanal*, **17**, (2005), 38-46.
45. R. Gref, Y. Minamitake, M. T. Peracchia, V. Trubetskoy, V. Torchilin, and R. Langer, *Science*, **263**, (1994), 1600-1603.
46. D. H. Kim, S. M. Richardson-Burns, J. L. Hendricks, C. Sequera, and D. C. Martin, *Adv Funct Mater*, **17**, (2007), 79-86.
47. C. E. Schmidt, V. R. Shastri, J. P. Vacanti, and R. Langer, *P Natl Acad Sci USA*, **94**, (1997), 8948-8953.
48. B. C. Thompson, S. E. Moulton, J. Ding, R. Richardson, A. Cameron, S. O'Leary, G. G. Wallace, and G. M. Clark, *J Control Release*, **116**, (2006), 285-294.
49. X. D. Wang, X. S. Gu, C. W. Yuan, S. J. Chen, P. Y. Zhang, T. Y. Zhang, J. Yao, F. Chen, and G. Chen, *J Biomed Mater Res A*, **68A**, (2004), 411-422.
50. B. Winther-Jensen and N. B. Clark, *React Funct Polym*, **68**, (2008), 742-750.
51. J. Heinze, *Synthetic Met*, **43**, (1991), 2805-2823.
52. L. L. Miller and Q. X. Zhou, *Macromolecules*, **20**, (1987), 1594-1597.
53. J. M. Pernaut and J. R. Reynolds, *J Phys Chem B*, **104**, (2000), 4080-4090.
54. J. R. Reynolds and P. J. Kinlen, *Abstr Pap Am Chem S*, **217**, (1999), U565-U565.
55. M. R. Gandhi, P. Murray, G. M. Spinks, and G. G. Wallace, *Synthetic Met*, **73**, (1995), 247-256.
56. E. W. H. Jager, O. Inganas, and I. Lundstrom, *Science*, **288**, (2000), 2335-2338.

## 7.1 Conclusions

The work described in this thesis addressed the need to develop a controllable device, for a cationic species. PPy, a conducting polymer, is an attractive material extensively researched in the area of biomedical devices. In the studies presented in this research, it successfully served as a controllable material for delivery of dopamine, DA, a cationic species.

The results obtained in Chapter 3, described the formation and characterisation of the polymers in the presence of various electrolytes. Attention was focused on the large sulfonated β-cyclodextrin (Sβ-CD) for the doping of the PPy films. Due to their large size, these dopants were found to remain immobilised in the polymer matrix and act predominantly as cation exchangers. Conductivity measurements performed on the Sβ-CD in water, confirmed that the Sβ-CD was a sufficiently strong electrolyte for the polymerisation of pyrrole. Moreover, no other supporting electrolyte was required, contrary to reports by other research groups.[1-3] The growth, morphology and doping levels of these films were also examined and showed that the PPy-Sβ-CD films could successfully be prepared electrochemically using both potentiostatic and potentiodynamic methods. The CV experiments demonstrated that the pyrrole monomer oxidised at lower potentials in the presence of the Sβ-CD, in comparison to other dopants like the $Cl^-$ anion. Additionally, the growth kinetics demonstrated a 4-fold increase in the rate of oxidation of PPy-Sβ-CD films, contrary to PPy-Cl films. Simultaneous, EQCM and CV experiments were used to measure the redox properties of these films and demonstrated not only the well defined redox properties of the PPy-Sβ-CD films, but the main cationic movement associated with the electroactivity of these films. SEM confirmed polymer growth and illustrated an oriented and organised manner in which the polymer was deposited, while EDAX measurements confirmed the presence of the Sβ-CD anion. The influence of the fluxes, cation and solvent, as a function of the potential, were also explored during CV measurements. EQCM measurements showed that a considerable amount of solvent, water was taken up into the film during redox switching.

We also report for the first time, the application of this simple modified electrode for the drug delivery of DA. Chapter 4 demonstrated the impressive release of DA from polymers synthesised in the presence of Sβ-CD in comparison to smaller, more mobile, dopants. Various parameters, including, the application of potential during the incorporation and release process of the drug, as well as, polymer thickness were optimised. The electrochemical stimulated release of DA from these films was successfully obtained. The release was shown to be dependent on the potential as, at open-circuit potentials, the polymer film does not reach the potentials required, over the time monitored, for oxidation of the polymer film and subsequent release of the DA. Results also provided some limitations in these systems, the first, that the application of anodic potentials higher than 0.100 V vs. SCE, to the electrochemical system, resulted in the oxidation of DA. Secondly, polymers synthesised to a charge $\geq$ 4.0 C $cm^{-2}$ resulted in the oxidation of the DA.

The question of inclusion phenomena was introduced and exhaustively examined in Chapter 5 and showed that indeed the DA was forming an inclusion complex with the CD in solution. This can be attributed to the significant increase in the release of DA. Although, there is a difference in analysing the complexation properties of CDs in solution and on the surface, many papers have examined both these processes and have attained similar observations.[4, 5] Damos *et al*.[4] demonstrated the simple process of self assembled monolayer's (SAM) of CDs on gold. They showed that when the CDs are immobilised onto the surface they retain their strong inclusion complexation properties with $[Fe(CN)_6]^{3-/4-}$. In Chapter 3, it was shown that the pyrrole monomer did not form an inclusion complex with the Sβ-CD. If the radical cations and the CD formed an inclusion complex, a decrease in the rate of polymerisation would be evident; however, in this case the opposite was observed. Therefore, there is no evidence to suggest an inclusion complex with the PPy, leaving a large number of cavities available for complexation of DA. We can safely say that the DA is forming an inclusion complex with the Sβ-CD. Also, in the analysis performed in Chapter 3 on the doping levels of the CD with the polymer, it was presented that if all of the negative sulfonated groups were involved with the polymerisation for the

polymer, it could lead to a considerable strain on the polymer system. Therefore, it can be assumed that there are free negative groups around the ring. Chapter 5 revealed that the presence of the sulfonated groups enhanced complexation. In the case of the polymer, if some of the sulfonate groups are not involved in the doping then this would favour the complexation of the DA and, therefore, include more DA.

The inclusion complexation of DA with Sβ-CD was dealt with in Chapter 5. Techniques including UV, NMR, CV and RDV were all used to demonstrate not only the 1:1 stoichiometry but evaluate the apparent formation constants. UV spectra showed a distinct shift in the wavelength and an increase in the intensity of the DA, in the presence of excess Sβ–CD, confirming a change in the environment of the DA and verifying complexation. In the electrochemical studies, the DA oxidation potentials shifted to higher potentials, while, the peak current decreased upon the addition of Sβ-CD. These traits were once more attributed to the formation of an inclusion complex due to the DA being harder to oxidise inside the cavity and the decrease in the diffusion coefficient of DA due to the less mobile bulky complex. Structural information on the inclusion complex was obtained from NMR studies and concluded that the aromatic DA ring was included inside the cavity, while the protonated amine was bound through electrostatic interactions to the sulfonated groups on the rim of the CD.

In all techniques the formation constants evaluated were in very close agreement, which not only validated the results, but confirmed that the methods examined for the complexation could be recommended as a reliable option in determining the formation constants of the inclusion complex of Sβ–CD, with other guest molecules. In comparing the data obtained in these experiments to data found in the literature for the neutral β-CD, 95.06,[6] it can be concluded that the negatively charged sulfonate groups on the CD play an important role in the complexation and increase the binding affinities in the case of protonated DA. Examinations on the influence of supporting electrolyte established that a change in the anion had an influence on the DA-Sβ-CD complexation while no change was observed for the cation. Complexation of DA with a smaller CD,

sulfonated α-CD showed no complexation and it was concluded that this was due to the size of the DA being too large to fit inside the cavity of the Sα-CD but it is sufficient in size for most of it to fit inside the Sβ-CD cavity.

Finally, poly($_{D,L}$ – lactide-*co*-glycolide) (PLGA) nanofibers were successfully deposited onto a Au mylar substrate using a technique known as electrospinning. During the electrospinning process a number of parameters were varied in order to form bead free nanofibers, including solvent, polymer concentration, potential and feeding rate. After successful fibers were attained, PPy films were both chemically and electrochemically deposited using vapour phase polymerisation and potentiostatic, galvanostatic and potentiodynamic methods, respectively. From SEM images, it was established that the electrochemical technique, CV, was the best technique employed enabling the formation of uniform conducting films, while still maintaining the nano-fibrous structure of the PLGA fibers. DA was again effectively incorporated and delivered from these new materials using electrical stimulation.

## 7.2 Conference presentations

- Gillian M. Hendy, Bernadette E. Alcock and Carmel B. Breslin 'Drug Release from Polypyrrole'. NUI Maynooth Postgraduate Open Day, Maynooth, 1st March (2006). [Oral Presentation].

- Gillian M. Hendy, Claire C. Harley, Bernadette E. Alcock and Carmel B. Breslin, 'Application of Polypyrrole in Drug Delivery' International Conference on Materials-Energy-Design (MED06), Dublin, 14–17th March (2006). [Oral Presentation].

- Gillian M. Hendy and Carmel B. Breslin, 'Studies on the binding and release of dopamine from a polypyrrole film: Applications in drug delivery' Irish Universities Research Colloquium, NUI Galway, 14-16th June (2006). [Poster Presentation].

- Gillian M. Hendy and Carmel B. Breslin, 'Using the redox chemistry of conducting polymers to bind and release cationic and anionic species: applications in the controlled delivery of drugs' Analytical Research Forum, University College, Cork 17-19th July (2006). [Poster Presentation].

- Gillian M. Hendy and Carmel B. Breslin, 'Polypyrrole for the Controlled Delivery of Anionic and Cationic Drugs' 57th Annual Meeting of the International Society of Electrochemistry, 27th August – 1st September, Edinburgh, Scotland, (2006). [Poster Presentation].

- Gillian M. Hendy and Carmel B. Breslin, 'Using the redox chemistry of polypyrrole to bind and release dopamine and epinephrine: applications in drug delivery' International Conference on Science and Technology of Synthetic Metals (ICSM) 2-7th July, Dublin (2006). [Poster Presentation].

- Gillian M. Hendy, Dan Li, Simon E. Moulton, Gordon G. Wallace and Carmel B. Breslin, 'Polypyrrole: Applications in Drug Delivery', Alan MacDiarmid Symposium, University of Wollongong, Australia, 16th May (2007). [Oral Presentation].

- Gillian M. Hendy, Claire Harley, Dan Li, Simon E. Moulton, Gordon G. Wallace and Carmel B. Breslin, 'The Application of Nanofibers in Biological Sensors and Drug Delivery Systems' NCSR/IPRI symposium, DCU, Dublin, 24th Sept (2007). [Poster Presentation].

- Gillian M. Hendy and Carmel B. Breslin, 'Studies of the Incorporation and Release of Dopamine using Polypyrrole'. 212th ECS Meeting, Washington DC, 7–12th Oct 2007. [Poster Presentation].

- Gillian M. Hendy and Carmel B. Breslin, Polypyrrole, Its application in the drug delivery of dopamine. ISE, 1st Regional Symposium on

Electrochemistry of South-East Europe, Rovinj, Croatia, 4–8th May 2008. [Poster Presentation].

- Gillian M. Hendy and Carmel B. Breslin, Polypyrrole, Its application in the delivery of dopamine. 215th ECS Meeting, San Francisco, 24-29th May 2009. [Poster Presentation].

- Gillian M. Hendy and Carmel B. Breslin, An electrochemical and spectrophotometric analysis on the inclusion complexation of dopamine and an anionic β-cyclodextrin. 215th ECS Meeting, San Francisco, 24-29th May 2009. [Oral Presentation].

## 7.3 Papers in preparation/submitted

- Controlled release of dopamine from sulfonated β-cyclodextrin doped polypyrrole.

- An Electrochemical Study in Aqueous Solutions on the Binding of Dopamine to a Sulfonated Cyclodextrin Host.

- A Spectrophotometric and NMR Study on the Formation of an Inclusion Complex between Dopamine and a Sulfonated Cyclodextrin Host.

- Electrochemical polymerisation of a sulfonated β-cyclodextrin doped polypyrrole film onto electrospun poly(D,L – lactide-*co*-glycolide) (PLGA) nanofibers.

## 7.4 References

1. N. Izaoumen, D. Bouchta, H. Zejli, M. El Kaoutit, A. M. Stalcup, and K. R. Temsamani, *Talanta*, 66, (2005), 111-117.

2. K. R. Temsamani, O. Ceylan, B. J. Yates, S. Oztemiz, T. P. Gbatu, A. M. Stalcup, H. B. Mark, and W. Kutner, *J Solid State Electr*, 6, (2002), 494-497.

3. K. R. Temsamani, H. B. Mark, W. Kutner, and A. M. Stalcup, *J Solid State Electr*, 6, (2002), 391-395.

4. F. S. Damos, R. C. S. Luz, A. A. Sabino, M. N. Eberlin, R. A. Pilli, and L. T. Kubota, *J Electroanal Chem*, 601, (2007), 181-193.

5. J. G. Zhi, X. L. Tian, W. Zhao, J. B. Shen, B. Tong, and Y. P. Dong, *J Colloid Interf Sci*, 319, (2008), 270-276.

6. Y. Y. Zhou, C. Liu, H. P. Yu, H. W. Xu, Q. Lu, and L. Wang, *Spectrosc Lett*, 39, (2006), 409-420.

## 7.1 Conclusions

The work described in this thesis addressed the need to develop a controllable device, for a cationic species. PPy, a conducting polymer, is an attractive material extensively researched in the area of biomedical devices. In the studies presented in this research, it successfully served as a controllable material for delivery of dopamine, DA, a cationic species.

The results obtained in Chapter 3, described the formation and characterisation of the polymers in the presence of various electrolytes. Attention was focused on the large sulfonated β-cyclodextrin (Sβ-CD) for the doping of the PPy films. Due to their large size, these dopants were found to remain immobilised in the polymer matrix and act predominantly as cation exchangers. Conductivity measurements performed on the Sβ-CD in water, confirmed that the Sβ-CD was a sufficiently strong electrolyte for the polymerisation of pyrrole. Moreover, no other supporting electrolyte was required, contrary to reports by other research groups.[1-3] The growth, morphology and doping levels of these films were also examined and showed that the PPy-Sβ-CD films could successfully be prepared electrochemically using both potentiostatic and potentiodynamic methods. The CV experiments demonstrated that the pyrrole monomer oxidised at lower potentials in the presence of the Sβ-CD, in comparison to other dopants like the $Cl^-$ anion. Additionally, the growth kinetics demonstrated a 4-fold increase in the rate of oxidation of PPy-Sβ-CD films, contrary to PPy-Cl films. Simultaneous, EQCM and CV experiments were used to measure the redox properties of these films and demonstrated not only the well defined redox properties of the PPy-Sβ-CD films, but the main cationic movement associated with the electroactivity of these films. SEM confirmed polymer growth and illustrated an oriented and organised manner in which the polymer was deposited, while EDAX measurements confirmed the presence of the Sβ-CD anion. The influence of the fluxes, cation and solvent, as a function of the potential, were also explored during CV measurements. EQCM measurements showed that a considerable amount of solvent, water was taken up into the film during redox switching.

We also report for the first time, the application of this simple modified electrode for the drug delivery of DA. Chapter 4 demonstrated the impressive release of DA from polymers synthesised in the presence of Sβ-CD in comparison to smaller, more mobile, dopants. Various parameters, including, the application of potential during the incorporation and release process of the drug, as well as, polymer thickness were optimised. The electrochemical stimulated release of DA from these films was successfully obtained. The release was shown to be dependent on the potential as, at open-circuit potentials, the polymer film does not reach the potentials required, over the time monitored, for oxidation of the polymer film and subsequent release of the DA. Results also provided some limitations in these systems, the first, that the application of anodic potentials higher than 0.100 V vs. SCE, to the electrochemical system, resulted in the oxidation of DA. Secondly, polymers synthesised to a charge $\geq$ 4.0 C $cm^{-2}$ resulted in the oxidation of the DA.

The question of inclusion phenomena was introduced and exhaustively examined in Chapter 5 and showed that indeed the DA was forming an inclusion complex with the CD in solution. This can be attributed to the significant increase in the release of DA. Although, there is a difference in analysing the complexation properties of CDs in solution and on the surface, many papers have examined both these processes and have attained similar observations.[4, 5] Damos *et al*.[4] demonstrated the simple process of self assembled monolayer's (SAM) of CDs on gold. They showed that when the CDs are immobilised onto the surface they retain their strong inclusion complexation properties with $[Fe(CN)_6]^{3-/4-}$. In Chapter 3, it was shown that the pyrrole monomer did not form an inclusion complex with the Sβ-CD. If the radical cations and the CD formed an inclusion complex, a decrease in the rate of polymerisation would be evident; however, in this case the opposite was observed. Therefore, there is no evidence to suggest an inclusion complex with the PPy, leaving a large number of cavities available for complexation of DA. We can safely say that the DA is forming an inclusion complex with the Sβ-CD. Also, in the analysis performed in Chapter 3 on the doping levels of the CD with the polymer, it was presented that if all of the negative sulfonated groups were involved with the polymerisation for the

polymer, it could lead to a considerable strain on the polymer system. Therefore, it can be assumed that there are free negative groups around the ring. Chapter 5 revealed that the presence of the sulfonated groups enhanced complexation. In the case of the polymer, if some of the sulfonate groups are not involved in the doping then this would favour the complexation of the DA and, therefore, include more DA.

The inclusion complexation of DA with Sβ-CD was dealt with in Chapter 5. Techniques including UV, NMR, CV and RDV were all used to demonstrate not only the 1:1 stoichiometry but evaluate the apparent formation constants. UV spectra showed a distinct shift in the wavelength and an increase in the intensity of the DA, in the presence of excess Sβ–CD, confirming a change in the environment of the DA and verifying complexation. In the electrochemical studies, the DA oxidation potentials shifted to higher potentials, while, the peak current decreased upon the addition of Sβ-CD. These traits were once more attributed to the formation of an inclusion complex due to the DA being harder to oxidise inside the cavity and the decrease in the diffusion coefficient of DA due to the less mobile bulky complex. Structural information on the inclusion complex was obtained from NMR studies and concluded that the aromatic DA ring was included inside the cavity, while the protonated amine was bound through electrostatic interactions to the sulfonated groups on the rim of the CD.

In all techniques the formation constants evaluated were in very close agreement, which not only validated the results, but confirmed that the methods examined for the complexation could be recommended as a reliable option in determining the formation constants of the inclusion complex of Sβ–CD, with other guest molecules. In comparing the data obtained in these experiments to data found in the literature for the neutral β-CD, 95.06,[6] it can be concluded that the negatively charged sulfonate groups on the CD play an important role in the complexation and increase the binding affinities in the case of protonated DA. Examinations on the influence of supporting electrolyte established that a change in the anion had an influence on the DA-Sβ-CD complexation while no change was observed for the cation. Complexation of DA with a smaller CD,

sulfonated α-CD showed no complexation and it was concluded that this was due to the size of the DA being too large to fit inside the cavity of the Sα-CD but it is sufficient in size for most of it to fit inside the Sβ-CD cavity.

Finally, poly($_{D,L}$ – lactide-*co*-glycolide) (PLGA) nanofibers were successfully deposited onto a Au mylar substrate using a technique known as electrospinning. During the electrospinning process a number of parameters were varied in order to form bead free nanofibers, including solvent, polymer concentration, potential and feeding rate. After successful fibers were attained, PPy films were both chemically and electrochemically deposited using vapour phase polymerisation and potentiostatic, galvanostatic and potentiodynamic methods, respectively. From SEM images, it was established that the electrochemical technique, CV, was the best technique employed enabling the formation of uniform conducting films, while still maintaining the nano-fibrous structure of the PLGA fibers. DA was again effectively incorporated and delivered from these new materials using electrical stimulation.

## 7.2 Conference presentations

- Gillian M. Hendy, Bernadette E. Alcock and Carmel B. Breslin 'Drug Release from Polypyrrole'. NUI Maynooth Postgraduate Open Day, Maynooth, 1st March (2006). [Oral Presentation].

- Gillian M. Hendy, Claire C. Harley, Bernadette E. Alcock and Carmel B. Breslin, 'Application of Polypyrrole in Drug Delivery' International Conference on Materials-Energy-Design (MED06), Dublin, 14–17th March (2006). [Oral Presentation].

- Gillian M. Hendy and Carmel B. Breslin, 'Studies on the binding and release of dopamine from a polypyrrole film: Applications in drug delivery' Irish Universities Research Colloquium, NUI Galway, 14-16th June (2006). [Poster Presentation].

- Gillian M. Hendy and Carmel B. Breslin, 'Using the redox chemistry of conducting polymers to bind and release cationic and anionic species: applications in the controlled delivery of drugs' Analytical Research Forum, University College, Cork 17-19th July (2006). [Poster Presentation].

- Gillian M. Hendy and Carmel B. Breslin, 'Polypyrrole for the Controlled Delivery of Anionic and Cationic Drugs' 57th Annual Meeting of the International Society of Electrochemistry, 27th August – 1st September, Edinburgh, Scotland, (2006). [Poster Presentation].

- Gillian M. Hendy and Carmel B. Breslin, 'Using the redox chemistry of polypyrrole to bind and release dopamine and epinephrine: applications in drug delivery' International Conference on Science and Technology of Synthetic Metals (ICSM) 2-7th July, Dublin (2006). [Poster Presentation].

- Gillian M. Hendy, Dan Li, Simon E. Moulton, Gordon G. Wallace and Carmel B. Breslin, 'Polypyrrole: Applications in Drug Delivery', Alan MacDiarmid Symposium, University of Wollongong, Australia, 16th May (2007). [Oral Presentation].

- Gillian M. Hendy, Claire Harley, Dan Li, Simon E. Moulton, Gordon G. Wallace and Carmel B. Breslin, 'The Application of Nanofibers in Biological Sensors and Drug Delivery Systems' NCSR/IPRI symposium, DCU, Dublin, 24th Sept (2007). [Poster Presentation].

- Gillian M. Hendy and Carmel B. Breslin, 'Studies of the Incorporation and Release of Dopamine using Polypyrrole'. 212th ECS Meeting, Washington DC, 7–12th Oct 2007. [Poster Presentation].

- Gillian M. Hendy and Carmel B. Breslin, Polypyrrole, Its application in the drug delivery of dopamine. ISE, 1st Regional Symposium on

Electrochemistry of South-East Europe, Rovinj, Croatia, 4–8th May 2008. [Poster Presentation].

- Gillian M. Hendy and Carmel B. Breslin, Polypyrrole, Its application in the delivery of dopamine. 215th ECS Meeting, San Francisco, 24-29th May 2009. [Poster Presentation].

- Gillian M. Hendy and Carmel B. Breslin, An electrochemical and spectrophotometric analysis on the inclusion complexation of dopamine and an anionic β-cyclodextrin. 215th ECS Meeting, San Francisco, 24-29th May 2009. [Oral Presentation].

## 7.3 Papers in preparation/submitted

- Controlled release of dopamine from sulfonated β-cyclodextrin doped polypyrrole.

- An Electrochemical Study in Aqueous Solutions on the Binding of Dopamine to a Sulfonated Cyclodextrin Host.

- A Spectrophotometric and NMR Study on the Formation of an Inclusion Complex between Dopamine and a Sulfonated Cyclodextrin Host.

- Electrochemical polymerisation of a sulfonated β-cyclodextrin doped polypyrrole film onto electrospun poly(D,L – lactide-*co*-glycolide) (PLGA) nanofibers.

## 7.4 References

1. N. Izaoumen, D. Bouchta, H. Zejli, M. El Kaoutit, A. M. Stalcup, and K. R. Temsamani, *Talanta*, 66, (2005), 111-117.

2. K. R. Temsamani, O. Ceylan, B. J. Yates, S. Oztemiz, T. P. Gbatu, A. M. Stalcup, H. B. Mark, and W. Kutner, *J Solid State Electr*, 6, (2002), 494-497.

3. K. R. Temsamani, H. B. Mark, W. Kutner, and A. M. Stalcup, *J Solid State Electr*, 6, (2002), 391-395.

4. F. S. Damos, R. C. S. Luz, A. A. Sabino, M. N. Eberlin, R. A. Pilli, and L. T. Kubota, *J Electroanal Chem*, 601, (2007), 181-193.

5. J. G. Zhi, X. L. Tian, W. Zhao, J. B. Shen, B. Tong, and Y. P. Dong, *J Colloid Interf Sci*, 319, (2008), 270-276.

6. Y. Y. Zhou, C. Liu, H. P. Yu, H. W. Xu, Q. Lu, and L. Wang, *Spectrosc Lett*, 39, (2006), 409-420.

## 7.1 Conclusions

The work described in this thesis addressed the need to develop a controllable device, for a cationic species. PPy, a conducting polymer, is an attractive material extensively researched in the area of biomedical devices. In the studies presented in this research, it successfully served as a controllable material for delivery of dopamine, DA, a cationic species.

The results obtained in Chapter 3, described the formation and characterisation of the polymers in the presence of various electrolytes. Attention was focused on the large sulfonated β-cyclodextrin (Sβ-CD) for the doping of the PPy films. Due to their large size, these dopants were found to remain immobilised in the polymer matrix and act predominantly as cation exchangers. Conductivity measurements performed on the Sβ-CD in water, confirmed that the Sβ-CD was a sufficiently strong electrolyte for the polymerisation of pyrrole. Moreover, no other supporting electrolyte was required, contrary to reports by other research groups.[1-3] The growth, morphology and doping levels of these films were also examined and showed that the PPy-Sβ-CD films could successfully be prepared electrochemically using both potentiostatic and potentiodynamic methods. The CV experiments demonstrated that the pyrrole monomer oxidised at lower potentials in the presence of the Sβ-CD, in comparison to other dopants like the $Cl^-$ anion. Additionally, the growth kinetics demonstrated a 4-fold increase in the rate of oxidation of PPy-Sβ-CD films, contrary to PPy-Cl films. Simultaneous, EQCM and CV experiments were used to measure the redox properties of these films and demonstrated not only the well defined redox properties of the PPy-Sβ-CD films, but the main cationic movement associated with the electroactivity of these films. SEM confirmed polymer growth and illustrated an oriented and organised manner in which the polymer was deposited, while EDAX measurements confirmed the presence of the Sβ-CD anion. The influence of the fluxes, cation and solvent, as a function of the potential, were also explored during CV measurements. EQCM measurements showed that a considerable amount of solvent, water was taken up into the film during redox switching.

We also report for the first time, the application of this simple modified electrode for the drug delivery of DA. Chapter 4 demonstrated the impressive release of DA from polymers synthesised in the presence of Sβ-CD in comparison to smaller, more mobile, dopants. Various parameters, including, the application of potential during the incorporation and release process of the drug, as well as, polymer thickness were optimised. The electrochemical stimulated release of DA from these films was successfully obtained. The release was shown to be dependent on the potential as, at open-circuit potentials, the polymer film does not reach the potentials required, over the time monitored, for oxidation of the polymer film and subsequent release of the DA. Results also provided some limitations in these systems, the first, that the application of anodic potentials higher than 0.100 V vs. SCE, to the electrochemical system, resulted in the oxidation of DA. Secondly, polymers synthesised to a charge $\geq$ 4.0 C $cm^{-2}$ resulted in the oxidation of the DA.

The question of inclusion phenomena was introduced and exhaustively examined in Chapter 5 and showed that indeed the DA was forming an inclusion complex with the CD in solution. This can be attributed to the significant increase in the release of DA. Although, there is a difference in analysing the complexation properties of CDs in solution and on the surface, many papers have examined both these processes and have attained similar observations.[4, 5] Damos *et al*.[4] demonstrated the simple process of self assembled monolayer's (SAM) of CDs on gold. They showed that when the CDs are immobilised onto the surface they retain their strong inclusion complexation properties with $[Fe(CN)_6]^{3-/4-}$. In Chapter 3, it was shown that the pyrrole monomer did not form an inclusion complex with the Sβ-CD. If the radical cations and the CD formed an inclusion complex, a decrease in the rate of polymerisation would be evident; however, in this case the opposite was observed. Therefore, there is no evidence to suggest an inclusion complex with the PPy, leaving a large number of cavities available for complexation of DA. We can safely say that the DA is forming an inclusion complex with the Sβ-CD. Also, in the analysis performed in Chapter 3 on the doping levels of the CD with the polymer, it was presented that if all of the negative sulfonated groups were involved with the polymerisation for the

polymer, it could lead to a considerable strain on the polymer system. Therefore, it can be assumed that there are free negative groups around the ring. Chapter 5 revealed that the presence of the sulfonated groups enhanced complexation. In the case of the polymer, if some of the sulfonate groups are not involved in the doping then this would favour the complexation of the DA and, therefore, include more DA.

The inclusion complexation of DA with Sβ-CD was dealt with in Chapter 5. Techniques including UV, NMR, CV and RDV were all used to demonstrate not only the 1:1 stoichiometry but evaluate the apparent formation constants. UV spectra showed a distinct shift in the wavelength and an increase in the intensity of the DA, in the presence of excess Sβ–CD, confirming a change in the environment of the DA and verifying complexation. In the electrochemical studies, the DA oxidation potentials shifted to higher potentials, while, the peak current decreased upon the addition of Sβ-CD. These traits were once more attributed to the formation of an inclusion complex due to the DA being harder to oxidise inside the cavity and the decrease in the diffusion coefficient of DA due to the less mobile bulky complex. Structural information on the inclusion complex was obtained from NMR studies and concluded that the aromatic DA ring was included inside the cavity, while the protonated amine was bound through electrostatic interactions to the sulfonated groups on the rim of the CD.

In all techniques the formation constants evaluated were in very close agreement, which not only validated the results, but confirmed that the methods examined for the complexation could be recommended as a reliable option in determining the formation constants of the inclusion complex of Sβ–CD, with other guest molecules. In comparing the data obtained in these experiments to data found in the literature for the neutral β-CD, 95.06,[6] it can be concluded that the negatively charged sulfonate groups on the CD play an important role in the complexation and increase the binding affinities in the case of protonated DA. Examinations on the influence of supporting electrolyte established that a change in the anion had an influence on the DA-Sβ-CD complexation while no change was observed for the cation. Complexation of DA with a smaller CD,

sulfonated α-CD showed no complexation and it was concluded that this was due to the size of the DA being too large to fit inside the cavity of the Sα-CD but it is sufficient in size for most of it to fit inside the Sβ-CD cavity.

Finally, poly($_{D,L}$ – lactide-*co*-glycolide) (PLGA) nanofibers were successfully deposited onto a Au mylar substrate using a technique known as electrospinning. During the electrospinning process a number of parameters were varied in order to form bead free nanofibers, including solvent, polymer concentration, potential and feeding rate. After successful fibers were attained, PPy films were both chemically and electrochemically deposited using vapour phase polymerisation and potentiostatic, galvanostatic and potentiodynamic methods, respectively. From SEM images, it was established that the electrochemical technique, CV, was the best technique employed enabling the formation of uniform conducting films, while still maintaining the nano-fibrous structure of the PLGA fibers. DA was again effectively incorporated and delivered from these new materials using electrical stimulation.

## 7.2 Conference presentations

- Gillian M. Hendy, Bernadette E. Alcock and Carmel B. Breslin 'Drug Release from Polypyrrole'. NUI Maynooth Postgraduate Open Day, Maynooth, 1st March (2006). [Oral Presentation].

- Gillian M. Hendy, Claire C. Harley, Bernadette E. Alcock and Carmel B. Breslin, 'Application of Polypyrrole in Drug Delivery' International Conference on Materials-Energy-Design (MED06), Dublin, 14–17th March (2006). [Oral Presentation].

- Gillian M. Hendy and Carmel B. Breslin, 'Studies on the binding and release of dopamine from a polypyrrole film: Applications in drug delivery' Irish Universities Research Colloquium, NUI Galway, 14-16th June (2006). [Poster Presentation].

- Gillian M. Hendy and Carmel B. Breslin, 'Using the redox chemistry of conducting polymers to bind and release cationic and anionic species: applications in the controlled delivery of drugs' Analytical Research Forum, University College, Cork 17-19th July (2006). [Poster Presentation].

- Gillian M. Hendy and Carmel B. Breslin, 'Polypyrrole for the Controlled Delivery of Anionic and Cationic Drugs' 57th Annual Meeting of the International Society of Electrochemistry, 27th August – 1st September, Edinburgh, Scotland, (2006). [Poster Presentation].

- Gillian M. Hendy and Carmel B. Breslin, 'Using the redox chemistry of polypyrrole to bind and release dopamine and epinephrine: applications in drug delivery' International Conference on Science and Technology of Synthetic Metals (ICSM) 2-7th July, Dublin (2006). [Poster Presentation].

- Gillian M. Hendy, Dan Li, Simon E. Moulton, Gordon G. Wallace and Carmel B. Breslin, 'Polypyrrole: Applications in Drug Delivery', Alan MacDiarmid Symposium, University of Wollongong, Australia, 16th May (2007). [Oral Presentation].

- Gillian M. Hendy, Claire Harley, Dan Li, Simon E. Moulton, Gordon G. Wallace and Carmel B. Breslin, 'The Application of Nanofibers in Biological Sensors and Drug Delivery Systems' NCSR/IPRI symposium, DCU, Dublin, 24th Sept (2007). [Poster Presentation].

- Gillian M. Hendy and Carmel B. Breslin, 'Studies of the Incorporation and Release of Dopamine using Polypyrrole'. 212th ECS Meeting, Washington DC, 7–12th Oct 2007. [Poster Presentation].

- Gillian M. Hendy and Carmel B. Breslin, Polypyrrole, Its application in the drug delivery of dopamine. ISE, 1st Regional Symposium on

Electrochemistry of South-East Europe, Rovinj, Croatia, 4–8th May 2008. [Poster Presentation].

- Gillian M. Hendy and Carmel B. Breslin, Polypyrrole, Its application in the delivery of dopamine. 215th ECS Meeting, San Francisco, 24-29th May 2009. [Poster Presentation].

- Gillian M. Hendy and Carmel B. Breslin, An electrochemical and spectrophotometric analysis on the inclusion complexation of dopamine and an anionic β-cyclodextrin. 215th ECS Meeting, San Francisco, 24-29th May 2009. [Oral Presentation].

## 7.3 Papers in preparation/submitted

- Controlled release of dopamine from sulfonated β-cyclodextrin doped polypyrrole.

- An Electrochemical Study in Aqueous Solutions on the Binding of Dopamine to a Sulfonated Cyclodextrin Host.

- A Spectrophotometric and NMR Study on the Formation of an Inclusion Complex between Dopamine and a Sulfonated Cyclodextrin Host.

- Electrochemical polymerisation of a sulfonated β-cyclodextrin doped polypyrrole film onto electrospun poly(D,L – lactide-*co*-glycolide) (PLGA) nanofibers.

## 7.4 References

1. N. Izaoumen, D. Bouchta, H. Zejli, M. El Kaoutit, A. M. Stalcup, and K. R. Temsamani, *Talanta*, 66, (2005), 111-117.

2. K. R. Temsamani, O. Ceylan, B. J. Yates, S. Oztemiz, T. P. Gbatu, A. M. Stalcup, H. B. Mark, and W. Kutner, *J Solid State Electr*, 6, (2002), 494-497.

3. K. R. Temsamani, H. B. Mark, W. Kutner, and A. M. Stalcup, *J Solid State Electr*, 6, (2002), 391-395.

4. F. S. Damos, R. C. S. Luz, A. A. Sabino, M. N. Eberlin, R. A. Pilli, and L. T. Kubota, *J Electroanal Chem*, 601, (2007), 181-193.

5. J. G. Zhi, X. L. Tian, W. Zhao, J. B. Shen, B. Tong, and Y. P. Dong, *J Colloid Interf Sci*, 319, (2008), 270-276.

6. Y. Y. Zhou, C. Liu, H. P. Yu, H. W. Xu, Q. Lu, and L. Wang, *Spectrosc Lett*, 39, (2006), 409-420.

## 7.1 Conclusions

The work described in this thesis addressed the need to develop a controllable device, for a cationic species. PPy, a conducting polymer, is an attractive material extensively researched in the area of biomedical devices. In the studies presented in this research, it successfully served as a controllable material for delivery of dopamine, DA, a cationic species.

The results obtained in Chapter 3, described the formation and characterisation of the polymers in the presence of various electrolytes. Attention was focused on the large sulfonated β-cyclodextrin (Sβ-CD) for the doping of the PPy films. Due to their large size, these dopants were found to remain immobilised in the polymer matrix and act predominantly as cation exchangers. Conductivity measurements performed on the Sβ-CD in water, confirmed that the Sβ-CD was a sufficiently strong electrolyte for the polymerisation of pyrrole. Moreover, no other supporting electrolyte was required, contrary to reports by other research groups.[1-3] The growth, morphology and doping levels of these films were also examined and showed that the PPy-Sβ-CD films could successfully be prepared electrochemically using both potentiostatic and potentiodynamic methods. The CV experiments demonstrated that the pyrrole monomer oxidised at lower potentials in the presence of the Sβ-CD, in comparison to other dopants like the $Cl^-$ anion. Additionally, the growth kinetics demonstrated a 4-fold increase in the rate of oxidation of PPy-Sβ-CD films, contrary to PPy-Cl films. Simultaneous, EQCM and CV experiments were used to measure the redox properties of these films and demonstrated not only the well defined redox properties of the PPy-Sβ-CD films, but the main cationic movement associated with the electroactivity of these films. SEM confirmed polymer growth and illustrated an oriented and organised manner in which the polymer was deposited, while EDAX measurements confirmed the presence of the Sβ-CD anion. The influence of the fluxes, cation and solvent, as a function of the potential, were also explored during CV measurements. EQCM measurements showed that a considerable amount of solvent, water was taken up into the film during redox switching.

We also report for the first time, the application of this simple modified electrode for the drug delivery of DA. Chapter 4 demonstrated the impressive release of DA from polymers synthesised in the presence of Sβ-CD in comparison to smaller, more mobile, dopants. Various parameters, including, the application of potential during the incorporation and release process of the drug, as well as, polymer thickness were optimised. The electrochemical stimulated release of DA from these films was successfully obtained. The release was shown to be dependent on the potential as, at open-circuit potentials, the polymer film does not reach the potentials required, over the time monitored, for oxidation of the polymer film and subsequent release of the DA. Results also provided some limitations in these systems, the first, that the application of anodic potentials higher than 0.100 V vs. SCE, to the electrochemical system, resulted in the oxidation of DA. Secondly, polymers synthesised to a charge $\geq$ 4.0 C $cm^{-2}$ resulted in the oxidation of the DA.

The question of inclusion phenomena was introduced and exhaustively examined in Chapter 5 and showed that indeed the DA was forming an inclusion complex with the CD in solution. This can be attributed to the significant increase in the release of DA. Although, there is a difference in analysing the complexation properties of CDs in solution and on the surface, many papers have examined both these processes and have attained similar observations.[4, 5] Damos *et al*.[4] demonstrated the simple process of self assembled monolayer's (SAM) of CDs on gold. They showed that when the CDs are immobilised onto the surface they retain their strong inclusion complexation properties with $[Fe(CN)_6]^{3-/4-}$. In Chapter 3, it was shown that the pyrrole monomer did not form an inclusion complex with the Sβ-CD. If the radical cations and the CD formed an inclusion complex, a decrease in the rate of polymerisation would be evident; however, in this case the opposite was observed. Therefore, there is no evidence to suggest an inclusion complex with the PPy, leaving a large number of cavities available for complexation of DA. We can safely say that the DA is forming an inclusion complex with the Sβ-CD. Also, in the analysis performed in Chapter 3 on the doping levels of the CD with the polymer, it was presented that if all of the negative sulfonated groups were involved with the polymerisation for the

polymer, it could lead to a considerable strain on the polymer system. Therefore, it can be assumed that there are free negative groups around the ring. Chapter 5 revealed that the presence of the sulfonated groups enhanced complexation. In the case of the polymer, if some of the sulfonate groups are not involved in the doping then this would favour the complexation of the DA and, therefore, include more DA.

The inclusion complexation of DA with Sβ-CD was dealt with in Chapter 5. Techniques including UV, NMR, CV and RDV were all used to demonstrate not only the 1:1 stoichiometry but evaluate the apparent formation constants. UV spectra showed a distinct shift in the wavelength and an increase in the intensity of the DA, in the presence of excess Sβ–CD, confirming a change in the environment of the DA and verifying complexation. In the electrochemical studies, the DA oxidation potentials shifted to higher potentials, while, the peak current decreased upon the addition of Sβ-CD. These traits were once more attributed to the formation of an inclusion complex due to the DA being harder to oxidise inside the cavity and the decrease in the diffusion coefficient of DA due to the less mobile bulky complex. Structural information on the inclusion complex was obtained from NMR studies and concluded that the aromatic DA ring was included inside the cavity, while the protonated amine was bound through electrostatic interactions to the sulfonated groups on the rim of the CD.

In all techniques the formation constants evaluated were in very close agreement, which not only validated the results, but confirmed that the methods examined for the complexation could be recommended as a reliable option in determining the formation constants of the inclusion complex of Sβ–CD, with other guest molecules. In comparing the data obtained in these experiments to data found in the literature for the neutral β-CD, 95.06,[6] it can be concluded that the negatively charged sulfonate groups on the CD play an important role in the complexation and increase the binding affinities in the case of protonated DA. Examinations on the influence of supporting electrolyte established that a change in the anion had an influence on the DA-Sβ-CD complexation while no change was observed for the cation. Complexation of DA with a smaller CD,

sulfonated α-CD showed no complexation and it was concluded that this was due to the size of the DA being too large to fit inside the cavity of the Sα-CD but it is sufficient in size for most of it to fit inside the Sβ-CD cavity.

Finally, poly($_{D,L}$ – lactide-*co*-glycolide) (PLGA) nanofibers were successfully deposited onto a Au mylar substrate using a technique known as electrospinning. During the electrospinning process a number of parameters were varied in order to form bead free nanofibers, including solvent, polymer concentration, potential and feeding rate. After successful fibers were attained, PPy films were both chemically and electrochemically deposited using vapour phase polymerisation and potentiostatic, galvanostatic and potentiodynamic methods, respectively. From SEM images, it was established that the electrochemical technique, CV, was the best technique employed enabling the formation of uniform conducting films, while still maintaining the nano-fibrous structure of the PLGA fibers. DA was again effectively incorporated and delivered from these new materials using electrical stimulation.

## 7.2 Conference presentations

- Gillian M. Hendy, Bernadette E. Alcock and Carmel B. Breslin 'Drug Release from Polypyrrole'. NUI Maynooth Postgraduate Open Day, Maynooth, 1st March (2006). [Oral Presentation].

- Gillian M. Hendy, Claire C. Harley, Bernadette E. Alcock and Carmel B. Breslin, 'Application of Polypyrrole in Drug Delivery' International Conference on Materials-Energy-Design (MED06), Dublin, 14–17th March (2006). [Oral Presentation].

- Gillian M. Hendy and Carmel B. Breslin, 'Studies on the binding and release of dopamine from a polypyrrole film: Applications in drug delivery' Irish Universities Research Colloquium, NUI Galway, 14-16th June (2006). [Poster Presentation].

- Gillian M. Hendy and Carmel B. Breslin, 'Using the redox chemistry of conducting polymers to bind and release cationic and anionic species: applications in the controlled delivery of drugs' Analytical Research Forum, University College, Cork 17-19th July (2006). [Poster Presentation].

- Gillian M. Hendy and Carmel B. Breslin, 'Polypyrrole for the Controlled Delivery of Anionic and Cationic Drugs' 57th Annual Meeting of the International Society of Electrochemistry, 27th August – 1st September, Edinburgh, Scotland, (2006). [Poster Presentation].

- Gillian M. Hendy and Carmel B. Breslin, 'Using the redox chemistry of polypyrrole to bind and release dopamine and epinephrine: applications in drug delivery' International Conference on Science and Technology of Synthetic Metals (ICSM) 2-7th July, Dublin (2006). [Poster Presentation].

- Gillian M. Hendy, Dan Li, Simon E. Moulton, Gordon G. Wallace and Carmel B. Breslin, 'Polypyrrole: Applications in Drug Delivery', Alan MacDiarmid Symposium, University of Wollongong, Australia, 16th May (2007). [Oral Presentation].

- Gillian M. Hendy, Claire Harley, Dan Li, Simon E. Moulton, Gordon G. Wallace and Carmel B. Breslin, 'The Application of Nanofibers in Biological Sensors and Drug Delivery Systems' NCSR/IPRI symposium, DCU, Dublin, 24th Sept (2007). [Poster Presentation].

- Gillian M. Hendy and Carmel B. Breslin, 'Studies of the Incorporation and Release of Dopamine using Polypyrrole'. 212th ECS Meeting, Washington DC, 7–12th Oct 2007. [Poster Presentation].

- Gillian M. Hendy and Carmel B. Breslin, Polypyrrole, Its application in the drug delivery of dopamine. ISE, 1st Regional Symposium on

Electrochemistry of South-East Europe, Rovinj, Croatia, 4–8th May 2008. [Poster Presentation].

- Gillian M. Hendy and Carmel B. Breslin, Polypyrrole, Its application in the delivery of dopamine. 215th ECS Meeting, San Francisco, 24-29th May 2009. [Poster Presentation].

- Gillian M. Hendy and Carmel B. Breslin, An electrochemical and spectrophotometric analysis on the inclusion complexation of dopamine and an anionic β-cyclodextrin. 215th ECS Meeting, San Francisco, 24-29th May 2009. [Oral Presentation].

## 7.3 Papers in preparation/submitted

- Controlled release of dopamine from sulfonated β-cyclodextrin doped polypyrrole.

- An Electrochemical Study in Aqueous Solutions on the Binding of Dopamine to a Sulfonated Cyclodextrin Host.

- A Spectrophotometric and NMR Study on the Formation of an Inclusion Complex between Dopamine and a Sulfonated Cyclodextrin Host.

- Electrochemical polymerisation of a sulfonated β-cyclodextrin doped polypyrrole film onto electrospun poly(D,L – lactide-*co*-glycolide) (PLGA) nanofibers.

## 7.4 References

1. N. Izaoumen, D. Bouchta, H. Zejli, M. El Kaoutit, A. M. Stalcup, and K. R. Temsamani, *Talanta*, 66, (2005), 111-117.

2. K. R. Temsamani, O. Ceylan, B. J. Yates, S. Oztemiz, T. P. Gbatu, A. M. Stalcup, H. B. Mark, and W. Kutner, *J Solid State Electr*, 6, (2002), 494-497.

3. K. R. Temsamani, H. B. Mark, W. Kutner, and A. M. Stalcup, *J Solid State Electr*, 6, (2002), 391-395.

4. F. S. Damos, R. C. S. Luz, A. A. Sabino, M. N. Eberlin, R. A. Pilli, and L. T. Kubota, *J Electroanal Chem*, 601, (2007), 181-193.

5. J. G. Zhi, X. L. Tian, W. Zhao, J. B. Shen, B. Tong, and Y. P. Dong, *J Colloid Interf Sci*, 319, (2008), 270-276.

6. Y. Y. Zhou, C. Liu, H. P. Yu, H. W. Xu, Q. Lu, and L. Wang, *Spectrosc Lett*, 39, (2006), 409-420.